

A11100 985909

NATL INST OF STANDARDS & TECH R.I.C.



A11100985909

/Applications of phase diagrams in metal
QC100 .U57 V496;V1:1978 C.1 NBS-PUB-C 19



NBS SPECIAL PUBLICATION 496

U.S. DEPARTMENT OF COMMERCE / National Bureau of Standards

National Bureau of Standards
Library, E-01 Admin. Bldg.

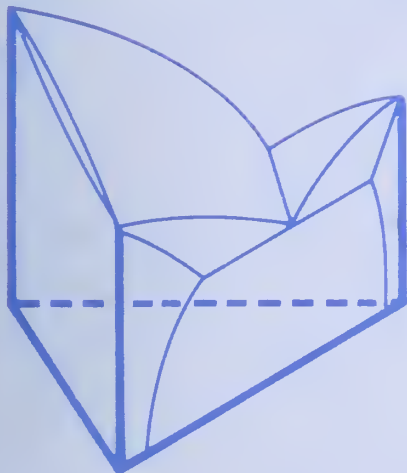
OCT 1 1981

191050

QC

100

.457



Applications of Phase Diagrams in Metallurgy and Ceramics

Volume 1

NATIONAL BUREAU OF STANDARDS

The National Bureau of Standards¹ was established by an act of Congress March 3, 1901. The Bureau's overall goal is to strengthen and advance the Nation's science and technology and facilitate their effective application for public benefit. To this end, the Bureau conducts research and provides: (1) a basis for the Nation's physical measurement system, (2) scientific and technological services for industry and government, (3) a technical basis for equity in trade, and (4) technical services to promote public safety. The Bureau consists of the Institute for Basic Standards, the Institute for Materials Research, the Institute for Applied Technology, the Institute for Computer Sciences and Technology, the Office for Information Programs, and the Office of Experimental Technology Incentives Program.

THE INSTITUTE FOR BASIC STANDARDS provides the central basis within the United States of a complete and consistent system of physical measurement; coordinates that system with measurement systems of other nations; and furnishes essential services leading to accurate and uniform physical measurements throughout the Nation's scientific community, industry, and commerce. The Institute consists of the Office of Measurement Services, and the following center and divisions:

Applied Mathematics — Electricity — Mechanics — Heat — Optical Physics — Center for Radiation Research — Laboratory Astrophysics² — Cryogenics² — Electromagnetics² — Time and Frequency².

THE INSTITUTE FOR MATERIALS RESEARCH conducts materials research leading to improved methods of measurement, standards, and data on the properties of well-characterized materials needed by industry, commerce, educational institutions, and Government; provides advisory and research services to other Government agencies; and develops, produces, and distributes standard reference materials. The Institute consists of the Office of Standard Reference Materials, the Office of Air and Water Measurement, and the following divisions:

Analytical Chemistry — Polymers — Metallurgy — Inorganic Materials — Reactor Radiation — Physical Chemistry.

THE INSTITUTE FOR APPLIED TECHNOLOGY provides technical services developing and promoting the use of available technology; cooperates with public and private organizations in developing technological standards, codes, and test methods; and provides technical advice services, and information to Government agencies and the public. The Institute consists of the following divisions and centers:

Standards Application and Analysis — Electronic Technology — Center for Consumer Product Technology: Product Systems Analysis; Product Engineering — Center for Building Technology: Structures, Materials, and Safety; Building Environment; Technical Evaluation and Application — Center for Fire Research: Fire Science; Fire Safety Engineering.

THE INSTITUTE FOR COMPUTER SCIENCES AND TECHNOLOGY conducts research and provides technical services designed to aid Government agencies in improving cost effectiveness in the conduct of their programs through the selection, acquisition, and effective utilization of automatic data processing equipment; and serves as the principal focus within the executive branch for the development of Federal standards for automatic data processing equipment, techniques, and computer languages. The Institute consist of the following divisions:

Computer Services — Systems and Software — Computer Systems Engineering — Information Technology.

THE OFFICE OF EXPERIMENTAL TECHNOLOGY INCENTIVES PROGRAM seeks to affect public policy and process to facilitate technological change in the private sector by examining and experimenting with Government policies and practices in order to identify and remove Government-related barriers and to correct inherent market imperfections that impede the innovation process.

THE OFFICE FOR INFORMATION PROGRAMS promotes optimum dissemination and accessibility of scientific information generated within NBS; promotes the development of the National Standard Reference Data System and a system of information analysis centers dealing with the broader aspects of the National Measurement System; provides appropriate services to ensure that the NBS staff has optimum accessibility to the scientific information of the world. The Office consists of the following organizational units:

Office of Standard Reference Data — Office of Information Activities — Office of Technical Publications — Library — Office of International Standards — Office of International Relations.

¹ Headquarters and Laboratories at Gaithersburg, Maryland, unless otherwise noted; mailing address Washington, D.C. 20234.

² Located at Boulder, Colorado 80302.



APR 26 1978
7103-000-

Applications of Phase Diagrams in Metallurgy and Ceramics

Volume 1

Proceedings of a Workshop Held at the
National Bureau of Standards
Gaithersburg, Maryland, January 10-12, 1977

Edited by

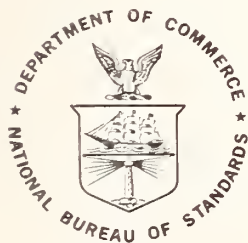
G.C. Carter

Institute for Materials Research
National Bureau of Standards
Washington, D.C. 20234

Sponsored by:

Institute for Materials Research and
Office of Standard Reference Data, NBS
and by

- National Science Foundation
- Defense Advanced Research Projects Agency
- Office of Naval Research
- National Aeronautics and Space Administration
- Energy Research and Development Administration
- U.S. Army Research Office



U.S. DEPARTMENT OF COMMERCE, Juanita M. Kreps, Secretary

Dr. Sidney Harman, Under Secretary

Jordan J. Baruch, Assistant Secretary for Science and Technology

NATIONAL BUREAU OF STANDARDS, Ernest Ambler, Director

Issued March 1978

21108
JCT
1978
C.2

to Special Publications (NBS-SP-300) V.1

Library of Congress Catalog Card Number: 78-2201

National Bureau of Standards Special Publication 496/1

Nat. Bur. Stand. (U.S.) Spec. Publ. 496/1, 767 pages (March 1978)

CODEN: XNBSAV

U.S. GOVERNMENT PRINTING OFFICE
WASHINGTON: 1978

For sale by the Superintendent of Documents, U.S. Government Printing Office, Washington, D.C. 20402

Stock No. 003-003-01895-3

2-volume set; sold in sets only.

(Add 25 percent additional for other than U.S. mailing).

General Abstract

The proceedings of a Workshop on Applications of Phase Diagrams in Metallurgy and Ceramics, held at the National Bureau of Standards, Gaithersburg, Maryland, on January 10-12, 1977, is presented in this NBS Special Publication. The Workshop was co-sponsored by the Institute for Materials Research and the Office of Standard Reference Data, NBS, and the National Science Foundation, the Defense Advanced Research Projects Agency, the Office of Naval Research, the National Aeronautics and Space Administration, the Energy Research and Development Administration, and the U. S. Army Research Office.

The purpose of the Workshop was to assess the current national and international status of phase diagram determinations and evaluations for alloys, ceramics and semiconductors; to determine the needs and priorities, especially technological, for phase diagram determinations and evaluations; and to estimate the resources being used and potentially available for phase diagram evaluation. These proceedings reflect the detailed contents of the Workshop for both the tutorial and review sessions as well as four poster sessions and four panel sessions covering the subjects; critical phase diagram availability, user needs of phase diagrams, experimental methods of determination, theoretical methods of calculation and prediction, methods of phase diagram representations of calculation and prediction, methods of phase diagram representations (especially multicomponent) and distribution to the user. Three of the panels addressed the subject of phase diagram needs in industrial applications.

These proceedings represent documentation of this assessment, and constitute a valuable resource to workers in these areas, especially those planning to initiate phase diagram programs. Most subjects within the overall scope have been dealt with substantially in these proceedings; a few specialized topics such as surface and small particle phases, needed for the study of catalysis, have not been treated in detail. As the Alloy Data Center maintains a continuing phase diagram program, we would like to receive suggestions for similar topics of current and future interest, descriptions of new needs, or addenda and corrigenda to these proceedings. A tear-off sheet has been provided at the end of these proceedings for this purpose to be sent to the NBS Alloy Data Center.

KEY WORDS: Ceramics; computer predictions; critical evaluations; data compilations; electronic materials; industrial needs; metallurgy; phase diagrams; theory of phase diagrams; thermodynamics.

Foreword

Quantitative data on physical and chemical properties of materials form a key resource of modern technology. In the past a few dedicated scientists and engineers have performed an important service by compiling and evaluating such data for use by the technical community; an outstanding example is the work of Hansen on alloy phase diagrams. With the rapid growth of science and technology, this task has become too large and complex for a single individual. Organized programs with proper funding and continuity are essential if the technical community is to have the reliable data needed to solve the problems of modern society.

This Workshop represents an effort to coordinate and reinforce the current efforts on compilation of phase diagrams of alloys and ceramics. Many research groups and individual scientists throughout the world are concerned with phase equilibrium data.

Specialized expertise exists in small institutions as well as large laboratories. If this talent can be effectively utilized through a cooperative effort, the needs for such data can be met. The Office of Standard Reference Data, which serves as the program management office for the National Standard Reference Data System, is eager to work with all groups concerned with this problem. Through a cooperative international effort we can carry out a task which has become too large for an individual.

David R. Lide, Jr.
Chief
Office of Standard Reference Data
National Bureau of Standards

CONTENTS

	Page
General Abstract.....	iii
Foreword.....	v
Welcome - E. Ambler.....	xv
Overview of the Workshop - G.C. Carter.....	xvii
Workshop Organizing Committee	xviii

VOLUME 1

Present Status of Phase Diagram Compilation Activities

Phase Diagram Compilation Activities in Ceramics R.S. Roth, L.P. Cook, T. Negas, G.W. Cleek, and J.B. Wachtman, Jr.	1
Discussion	22

Present Status of Phase Diagram Compilation Activity for Semiconductors

C.D. Thurmond.....	23
--------------------	----

Phase Diagram Compilations for Metallic Systems - An Assessment of Ongoing Activities

G.C. Carter.....	36
------------------	----

Organization of Phase Diagram Information in the Soviet Union

N.V. Ageev, D.L. Ageeva, T.P. Kolesnikova, and L.A. Petrova.....	90
Discussion.....	95

A Survey of High Pressure Phases of Materials

L. Merrill.....	100
Discussion (Jan. 10 - AM Session)	121

Phase Diagram Information from Computer Banks

I. Ansara.....	123
----------------	-----

An Overview of the Determination of Phase Diagrams

F.N. Rhines.....	142
Discussion.....	163

Phase Diagram Compilation and Data Evaluation Activities

Proposal for a Comprehensive Handbook on "Ternary Phase Diagrams of Metals"

F. Aldinger, E.-Th. Henig, H.L. Lukas, and G. Petzow	164
------------------------------------------------------	-----

Phases and Phase Relations in the Binary Oxide Systems Containing WO₃

Luke L.Y. Chang.....	165
----------------------	-----

RIC in Phase with Rare-Earth Constitutional Diagrams K.A. Gschneidner, Jr., M.E. Verkade and B.L. Evans.....	226
Evaluations of Phase Diagrams and Thermodynamic Properties of Ternary Copper Alloy Systems Y.A. Chang, J.P. Neumann, U.V. Choudary.....	229
Phase Equilibria in Variable Valence Oxide Systems W.B. White.....	251
Phase Diagrams for Ceramists L.P. Cook, R.S. Roth, T. Negas and G.W. Cleek.....	257
NBS Crystal-Data Center A. Mighell, H. Ondik, J. Stalick, R. Boreni.....	259
The NBS Alloy Data Center G.C. Carter, D.J. Kahan, and L.H. Bennett.....	261
A Review of Phase Equilibria in the $\text{Na}_3\text{AlF}_6\text{-LiF-CaF}_2\text{-AlF}_3\text{-Al}_2\text{O}_3$ System D.F. Craig, R.T. Cassidy, and J.J. Brown, Jr.	272
Methods of Compiling and Editing "Structure and Properties of Binary Metallic Systems" A.E. Vol and I.K. Kagan.....	346
English Translation	351
Experimental Techniques in Phase Diagram Determinations	
The Determination of Phase Diagrams for Liquid Oxides and Metallurgical Slags by Hot-Wire Microscopy H.A. Fine.....	355
Experimental Techniques in Phase Diagram Determination of Superconducting Compounds Containing Volatile Components at Temperatures up to 2200°C R. Flükiger and J.-L. Jorda	375
Application of Experimental Techniques and the Critical Determination of Phase Equilibria in Oxide Systems F.P. Glasser.....	407
Protective Coatings for Superalloys and the Use of Phase Diagrams M.R. Jackson and J.R. Rairden	423
Application of the Scanning Electron Microscope to the Study of High Temperature Oxide Phase Equilibria L.P. Cook and D.B. Minor.....	440

Hyperfine Techniques and the Determination of Phase Diagrams R.C. Reno, L.J. Swartzendruber, G.C. Carter , and L.H. Bennett.....	450
Experimental Determination of Phase Diagrams with the Electron Microprobe and Scanning Transmission Electron Microscope A.D. Romig, Jr. and J.I. Goldstein.....	462
Interrelations Between Phase Diagrams and Hydriding Properties for Alloys Based on the Intermetallic Compound FeTi G.D. Sandrock, J.J. Reilly, and J.R. Johnson.....	483
Phase Equilibria in the System MgO-RCl (R=Li, Na and K) Solution Under Hydrothermal Conditions by Means of a Capsule Bursting Method Shigeyuki Sōmiya, Kazuo Nakamura, Shin-ichi Hirano and Shinroku Saito	508
High-Energy Ion Beams in Phase Diagram Determination J.E. Smugeresky, and S.M. Myers.....	516
Phase Equilibrium Diagrams in Terms of Electronic Structure F. E. Wang.....	545
Use of Segregation Phenomena in Solid Solutions as a Method for Determining Solidification Diagrams. Application to some Sc ₂ O ₃ - Ho ₂ O ₃ and Sc ₂ O ₃ - Dy ₂ O ₃ Systems J.M. Badie.....	550
Studies of the Fe-C-B Phase Diagram by Autoradiography T.B. Cameron and J.E. Morral.....	566
User Needs for Phase Diagrams P. J. Fopiano.....	567
Phase Diagram of a Specimen at High Temperatures Under External Tensile or Shear Stress or Both K.M. Khanna.....	575
Phase Diagram of a Metal-Gas System V.K. Sinha.....	578
Methods of Phase Diagram Calculations	
Theory of Alloy Phases R.E. Watson, H.Ehrenreich and L.H.Bennett.....	592
Discussion.....	620

Computation and Prediction of Phase Diagrams (Panel I)

Estimation of Conjugate γ and γ' Compositions in Ni-Base Superalloys R.L. Dreshfield.....	624
Discussion (Panel I - Jan. 11).....	658

Review of Phase Diagram Representations, Format, and Distribution

The Representation of Phase Equilibria A. Prince.....	660
Phase-Diagram Compilations - A User's View J.D. Livingston.....	703
Some Thoughts on the Distribution of Reference Data H. J. White, Jr.....	709
Remarks on Producing and Publishing Critically Evaluated Data W.B. Pearson.....	720
Discussion (Jan. 11 - PM Session).....	725
AUTHOR INDEX	725-A
SUBJECT INDEX	725-C
MATERIALS INDEX	725-J

VOLUME 2

Computational Techniques for Phase Diagram Construction

Computerized Characterization of the Au-Cu-Ni Ternary System S.K. Tarby, C.J. Van Tyne, and M.L. Boyle.....	726
Correlations and Predictions of Metal-Boron Phase Equilibria K.E. Spear.....	744
A Valence Bond Test for the Validity of Intermetallic and Semiconducting Structures F.L. Carter.....	763
Computation of the Component Activities from Ternary Miscibility Gap Data: The Cu-Ag-S and Cu-Ag-Se Systems U.V. Choudary and Y.A. Chang.....	774
The Mathematical Representation of Activity Data in Three Component Systems I. Eliezer and R.A. Howald.....	803
A Program for Binary Phase Equilibria Using the Redlich- Kister Equations I. Eliezer and R. A. Howald.....	846
Polynomial Representation of the Excess Free Energy of Multicomponent Systems and Their Use in Phase Diagram Calculations H. Gaye and C.H. P. Lupis	907

Thermodynamic Data for the Fe-O System Evaluated Using a New Computer-Aided Strategy J.L. Haas, Jr. and J.R. Fisher.....	909
Analysis and Synthesis of Phase Diagrams of the Fe-Cr-Ni, Fe-Cu-Mn and Fe-Cu-Ni Systems M. Hasebe and T. Nishizawa.....	911
Optimization of Phase Diagrams by a Least Squares Method Using Simultaneously Different Types of Data E.-Th. Henig, H.L. Lukas, B. Zimmermann and G. Petzow ..	955
Theoretical Calculation of Phase Diagrams Using the Cluster Variation Method R. Kikuchi and D. de Fontaine	967
Fundamental Calculations of Coherent Phase Diagrams D. de Fontaine and R. Kikuchi..... Discussion.....	999 1017
Generation of Self-Consistent Gibbs Energy Functions for Binary Systems: The Fe-Cu System as an Example J.F. Smith, D.M. Bailey and O. Kubaschewski.....	1027
Characteristics and Calculation of Stability Diagrams S. McCormick and Y. Bilimoria.....	1047
The Effect of Irradiation on Phase Stability L. Kaufman, J.S. Watkin, J.H. Gittus and A.P. Miodownik	1065
Facility for the Analysis of Chemical Thermodynamics (F*A*C*T) - A Computerized Canadian Thermodynamic Data Treatment Centre A.D. Pelton, C.W. Bale, and W.T. Thompson.....	1077
The Calculation of Pourbaix Diagrams Using a Modified Linear Programming Technique B.H. Rosof.....	1090
Theoretical Concepts Useful in the Calculation or Storage of Phase Diagrams of Ionic Systems M.-L. Saboungi and M. Blander.....	1093
Estimation of Isothermal Sections of Ternary Phase Diagrams of Lithium Containing Systems: The Al-Li-Mg System M.-L. Saboungi and C.C. Hsu.....	1109
Cybernetic Prediction of the Formation of Chemical Compounds in Uninvestigated Systems E.M. Savitskii, V.P. Gribulya, and N.N. Kiselyeva	1139
English Translation.....	1151

The Determination and Representation of Metastable Phase Diagram Features and Other Thermal Characteristics of Metastable Alloys, Especially Amorphous Metals	
B.C. Giessen.....	1161
Discussion.....	1183
 The Calculation of Multicomponent Alloy Phase Diagrams at the National Physical Laboratory	
T.G. Chart.....	1186
 Synthesis of Binary Metallic Systems I. Isomorphous Systems II. Simple Eutectic Systems	
S.S. Balakrishna, and A. K. Mallik.....	1200
 Quantitative Fits to Phase Lines and High Temperature Thermodynamic Data for Systems Forming Semiconductor Compounds	
R.F. Brebrick.....	1220
 Format and Distribution of Phase Diagram Data	
 Table of Contents and Cumulative Subject Index for "Phase Diagrams of Metallic Systems," N.V. Ageev, editor, Volumes 1-19	
C.M. Scheuermann	1237
 Standards for Publication of Phase Equilibrium Studies	
E.R. Kreidler.....	1307
 Formatting and Distributing Evaluated Reference Data: The Office of Standard Reference Data at the National Bureau of Standards	
S.P. Fivozinsky and G.B. Sherwood.....	1325
 User Needs for Phase Diagram Information (Panel II)	
 Panel Discussion: Primary Metal Production	
J.F. Elliott.....	1332
 Needs for Phase Diagram Information in Non-Ferrous Industry	
P.R. Ammann.....	1334
Discussion.....	1353
 Primary Metals Production	
H.R. Larson.....	1354
Discussion.....	1357
 Use of Phase Diagrams in Iron and Steelmaking	
R.D. Pehlke.....	1360
Discussion.....	1371

Materials Processing (Fabricating, Machining, Heat Treating, etc.)
 (Panel III)

User Needs for Phase Diagrams for Materials Processing:
 Glasses

R.C. Doman, and R.N. McNally 1378

Equilibrium Diagrams in Non-Ferrous Alloys

L.F. Mondolfo..... 1382

Phase Equilibria in the Development of High Temperature
 Structural Ceramics

S. Prochazka..... 1409

Phase Diagram Information for Processing of Superconductors

D. Dew-Hughes..... 1411

Product Applications (User Needs for Phase Diagram Information)
 (Panel IV)

Panel Discussion: Product Applications

F.L. VerSnyder..... 1418

Importance of Phase Diagrams in the Electric Power Industry

R.I. Jaffee..... 1420

Summary of Presentation on User Needs of Phase Diagrams:
 The Solar Energy Field

A.I. Mlavsky..... 1426

The Use of Phase Equilibria in the Manufacture of Spinel
 Ferrites

P. Slick..... 1427

The Application of the Phase Diagram to Thermal Energy
 Storage Technology

J.E. Beam and J.E. Davison..... 1428

The Needs for Phase Equilibria Data in the Development
 of Magnetohydrodynamics

R.A. Howald and I. Eliezer..... 1440

Discussion..... 1451

Summary Remarks

J. F. Elliott..... 1453

Evaluation of Conference

R.A. Howald..... 1470

Evaluation of Conference

J.E. Selle..... 1471

Comments on the Phase Diagram Workshop	
D. de Fontaine.....	1472
Additional Contributed Papers to the Workshop	
The Relation Between Bond Length and Crystal Structures in Metals	
A.P. Miodownik.....	1479
On Computerized Construction of Multidimensional Phase Diagrams in a Factographic IRS	
I.V. Tulupova and V.S. Stein.....	1506
REGISTRATION LIST.....	1520
AUTHOR INDEX.....	1529
SUBJECT INDEX.....	1531
MATERIALS INDEX.....	1538

Disclaimer

Certain commercial products and instruments are identified in this publication in order to specify adequately the experimental procedure. In no case does such identification imply recommendation or endorsement by the National Bureau of Standards, nor does it imply that the products or equipment identified are necessarily the best available for the purpose.

Welcome to the Workshop on Applications of
Phase Diagrams in Metallurgy and Ceramics

E. Ambler

Good morning. It is my pleasure to welcome you this morning to the National Bureau of Standards and this Workshop on Applications of Phase Diagrams in Metallurgy and Ceramics. Evidence of the broad interest in and importance of this subject matter is seen when one notes that the National Science Foundation, Defense Advance Research Project Agency, Office of Naval Research, National Aeronautics and Space Administration, and U. S. Army Research Office have joined with the NBS Institute for Materials Research and NBS Office of Standard Reference Data in the sponsorship of this workshop.

As I looked over the material for this workshop, I found this group to be truly international and interdisciplinary in scope. There are participants here from Canada, France, Germany, India, Japan, the United Kingdom, Switzerland, the Union of Soviet Socialist Republics, and our own United States. You include representatives from data compilation groups, major industries and trade associations, and scientists from industry, government and university laboratories.

Of special interest to me is your banquet speaker, W. Dale Compton, who is the Vice President for Scientific Research at the Ford Motor Company. In addition, Dale is also a member of the NBS Visiting Committee - our Board of Directors so to speak - and the former chairman of the National Science Foundation Numerical Advisory Board. I look forward to joining you for the banquet and Dale's presentation.

For more than 100 years, phase diagrams have been a recognized and important tool in the development of science and technology. As one example, phase diagrams formed the basis for the development of new alloys and the respective heat treatments for these alloys. This resulted in new materials highly characterized and tailored to a host of specific uses. Today, phase diagrams are increasingly relevant to the development of new and substitute materials.

Now, as we stand at the threshold of this Workshop, it seems an appropriate time to spend a brief moment clarifying our perspective concerning the development of phase diagrams. Where do we stand in the study of phase diagrams and the compilation of phase diagram data? Clearly, the studies of and the techniques used today are vastly different than those of yesterday.

The optical microscope was used 100 years ago to study the character of alloys and minerals. By 1914, x-rays were used to confirm the crystalline structure of materials. The 1930's brought the advent of the electron microscope and a higher resolution of the materials being studied. From that evolved the electron microprobe which allowed us to determine the chemical composition of an individual phase on a spatial resolution of two to three μm in diameter. More recently, we have seen the development of the scanning electron microscope, the field ion microscope, and the Auger electron spectrometer.

Over the past 30 - 35 years, we have witnessed and participated in an evolution in experimental techniques. Today, we are able to determine phase diagrams to a high level and detail of accuracy. Certainly, our techniques are vastly improved. But the task we face is still enormous. Just consider the study of alloys. In the study of binaries, there are 1770 possible diagrams; with ternaries, there are 34,200 possible phase diagrams; and with quaternaries, there are many, many possible diagrams. To compound this task is the fact that it is the multicomponent materials which are of the greatest interest today.

To meet this problem, new techniques are now being developed which are based on a theoretical understanding of materials. We find that we can achieve "paper calculations" through theoretical prediction of phase diagrams. In addition, we can develop mathematical models that are predictive. However, the validity of these models is dependent on the availability of accurate data. Thus, while we strive to predict complicated phenomena, we do so with the clear understanding that we must first develop a simple, accurate data base.

An assessment of today's environment then shows that although we possess many new and improved tools, they are still not sufficient to perform the task that faces us. Therefore, we stand in a position where our first order of business should be an assessment of priorities. The goals of this workshop:

- To assess the current national and international status of phase diagram determination and evaluation for alloys, ceramics and semi-conductors;
- To determine the needs and priorities, especially technological, for phase diagram determinations and evaluations; and
- To estimate the resources being used and potentially available for phase diagram evaluation;

are quite timely. In fact, I think that the key statement for this workshop is found on page 1 of your program: "It is hoped that the workshop will provide the stimulus for the production of more relevant more useful, and more useable phase diagram data."

I concur with that statement and heartily endorse the goals of this workshop. Moreover, it is my personal belief that communication, such as this workshop is intended to foster, is a critical component to all scientific and technological ventures.

In closing, again let me welcome you to NBS. Our facilities are at your disposal and we would invite any inquiries about our specific programs that are of interest to you. I look forward to joining you Tuesday evening and I hope that your workshop is both stimulating and productive.

Overview of the Workshop

G. C. Carter

Knowledge of the structure of materials is important in understanding several industrially significant phenomena and applications such as aging, hardness, occurrence of brittle intermetallic compounds, magnetic transition temperatures, high-temperature solubility of impurities, corrosion resistance, solid electrolytes and non-crystalline solids. The study of a phase diagram appropriate to a particular material can often provide information important to its scientific and technical application.

Wide participation by industry, government, and university representatives was achieved at the Workshop. International participation was particularly successful among the data evaluation groups including important representations from the Soviet Union, Germany, France, the UK, Japan, and Canada. Other countries were represented; experimentalists and theorists determining phase diagrams were among the participants, as were a substantial fraction of phase diagram users from industry.

Specific subjects of investigation were:

- ... to assess the current national and international status of phase diagram determinations and evaluations for alloys, ceramics and semiconductors; to identify resources being expended that could be made more useful by appropriate coordination; to recognize unnecessarily overlapping efforts in determining phase diagrams; to suggest areas of international cooperation.
- ... to determine the needs and priorities, especially technological, for phase diagram determinations and evaluations; to gauge the relative importance of depth of coverage and range of materials including factors such as a) high precision, b) metastable phases, c) binary and higher order systems, d) magnetic, metal nonmetal and other phase transitions, e) high pressure data, f) integration of collateral information, and g) the role of impurities or trace additions.
- ... to review the strengths and limitations of various experimental techniques for determining phase diagrams,
- ... to briefly survey the status and merits of various predictive methods (CALPHAD, PHACOMP, pseudopotential, etc.),
- ... to discuss diverse presentation methods, and
- ... to discuss effective and alternative means for dissemination of phase diagram data.

The workshop program was designed to stimulate interactions between (i) phase diagram data providers and users, (ii) metallurgists, geochemists, thermochemists, ceramics, solid state chemists, physicists, and scientists in other disciplines, (iii) representatives from industry, government, and the academia, (iv) phase diagram data centers throughout the world.

Plenary lectures introduced the subjects of present status of data availability from reference books, data centers and computerized files, the status of experimental data and theory of alloy phases. A panel on computation and prediction gave a more thorough introduction to that subject, and short reviews introduced the subjects of phase diagram representations and methods of distribution. Lively poster sessions followed these introductions. Three panel sessions were devoted to industrial needs in (i) Primary Metals Production, (ii) Materials Processing, and (iii) Product Applications. Discussion covered needs for multicomponent diagrams (up to 9 or 10 components) for industrial applications down to binary equilibrium diagrams, for various R & D programs, theoretical and prediction models, and other applications.

Four on-line demonstrations of computer-data handling systems related to phase diagrams were held and short instructional movies were shown during the poster session.

The workshop was organized by the Alloy Data Center and the group compiling "Phase Diagrams for Ceramists". The success of the Workshop program could not have been realized without invaluable assistance received from our very able organizing committee.

WORKSHOP ORGANIZING COMMITTEE

Members from NBS

L. H. Bennett, chairman
G. T. Armstrong, C. J. Bechtoldt, D. B. Butrymowicz, G. C. Carter, L. P. Cook, J. R. Cuthill, P. R. deBruyn, D. J. Kahan, M. B. McNeil, R. L. Parker, R. M. Waterstrat, H. J. White

Members from other Organizations

N. Ault, Norton Co., Worcester, MA
J. Elliott, M.I.T., Cambridge, MA
S. G. Epstein, Aluminum Association, New York, NY
L. Kaufman, ManLabs, Cambridge, MA
R. Laudise, Bell Telephone Laboratories, Murray Hill, NJ
J. D. Livingston, General Electric, Schenectady, NY
E. S. Osborne, Carnegie Geophysical Lab., Washington, DC
E. C. Van Reuth, Defense Advanced Res. Projects Agency, Arlington, VA
Schrade F. Radtke, Intl. Lead-Zinc Research Organization, New York, NY
R. Reynik, National Science Foundation, Washington, DC
E. Salkovitz, Office of Naval Research, Arlington, VA
L. M. Schetky, International Copper Research Assoc., New York, NY
C. Scheuermann, NASA Lewis Research Center, Cleveland, OH
M. Semchyschen, Climax Molybdenum Corp., Ann Arbor, MI
J. Swisher, Energy Research & Development Admin., Washington, DC

ARRANGEMENTS COMMITTEE

Ronald B. Johnson, Chairman
Sara R. Torrence



PHASE DIAGRAM COMPILATION ACTIVITIES IN CERAMICS

R.S. Roth, L.P. Cook, T. Negas, G.W. Cleek, and J.B. Wachtman, Jr.

National Bureau of Standards
Institute for Materials Research
Washington, D.C. 20234

1.0 Introduction

Phase diagrams play an important role in the development of ceramic materials. Phase equilibria data are essential in meeting the expanding needs for refractories, electronic components, non-crystalline solids, and various other applications of interest to ceramic scientists and engineers. The chemical information generally summarized as a phase equilibrium diagram is extremely useful in many industrial processes. However, the necessary research involved in obtaining such information is often very costly. The average binary phase diagram can be estimated to take about one man year and a ternary diagram may take five times that effort. To avoid duplication, it is advantageous to have all existing diagrams compiled and distributed for easy access.

2.0 Compilation Activities in Ceramics

2.1 General Phase Diagrams

The major references in English for phase equilibria data are:

- E. M. Levin, et al., "Phase Diagrams for Ceramists" (3 volumes)
- G. J. Janz, et al., "Molten Salts" (4 volumes)

There is some duplication of compilation activity in the ceramic sciences but this is largely an international problem. The principal compilations in addition to "Phase Diagrams for Ceramists" are Russian. Such duplication is not necessarily wasteful, since any publication would have to be made available in both languages. Also, the two groups of publications, which are partly independent, can be cross-checked for inclusion of references otherwise missed.

The U.S.S.R. publications include:

- N. A. Toropov, et al., "Handbook of Phase Diagrams of Silicate Systems" (English translations available from NTIS)
- V. P. Barzanovskii, et al., "Phase Diagrams of the Silicate Systems", 2 volumes (in Russian)
- D. L. Ageeva, "Phase Diagrams of Non-Metallic Systems", 10 volumes (in Russian)
- F. V. Chukov, "Minerals: Phase Diagrams of Importance to Mineral Formation" (2 volumes - in Russian)

In Japan compilation activities have, so far, been confined mainly to refractories. These include:

- S. Somiya, "Zirconia Bearing Refractories" (in Japanese)

2.2 Compilation Activities - Metal Oxygen Systems

The link between metallurgy and ceramics is found in the equilibria data for the binary metal-oxygen systems. Special compilation activities in the United States for these systems began in 1961 with a group of reports by J. H. Westbrook, R. L. Carter and R. C. DeVries:

- I. Rare Earth Metal - Oxygen Systems
- II. Alkaline Earth - Oxygen Systems
- III. Precious Metal - Oxygen Systems

Another compilation has been published in India by B. K. Rajput, A. M. George and M. D. Karkhanavala and pertinent portions will be extracted in the next supplement to "Phase Diagrams for Ceramists". The proceedings of this meeting contain a report of a more ambitious compilation attempt by W. B. White for the metal-oxygen systems (paper MPSI-5).

3.0 Phase Diagrams for Ceramists

The history of the compilation of Phase Diagrams for Ceramists dates back to 1933, when 157 diagrams collected by F. P. Hall and Herbert Insley were published in the October issue of the Journal of the American Ceramic Society. A supplement was published in the April 1938 issue of the same journal. A complete compilation of the diagrams appeared as Part II of the November 1947 Journal and contained 485 diagrams. In December 1949, H. F. McMurdie and F. P. Hall were authors of a supplement to the 1947 edition. In January 1956, the American Ceramic Society published a separate volume of phase diagrams edited by E. M. Levin, H. F. McMurdie and F. P. Hall. Part II of this volume appeared in 1959 authored by E. M. Levin and H. F. McMurdie. In 1964, a new complete compilation containing 2066 diagrams was published with E. M. Levin, H. F. McMurdie, and C. R. Robbins as authors. A supplement to the 1964 volume appeared in 1969 and contained another 2183 diagrams.

A third supplement, published in 1975 (850 diagrams), includes a discussion of the methods, data and interpretations made in the construction of each diagram. Since the death of E. M. Levin in 1974, this effort is being continued by a team of scientists actively engaged in phase equilibria studies in research centers in this country and abroad. This group is led by researchers at NBS who are assuming the responsibility for collecting data from the literature, distributing it among the group for evaluation, coordinating preparation of the publication, and preparing evaluations of systems in their own areas of expertise.

This latest supplement will include critical commentaries discussing preparation of starting materials, experimental methods, characterization of products, accuracy and precision of data and of diagram. The following experts in various fields are serving as Contributing Editors for the 1978 Supplement:

- J. J. Brown, Jr., Virginia Polytechnic Inst.
Fluoride containing systems
- L. L. Y. Chang, Miami Univ.
Tungstates, molybdates, carbonates
- R. C. DeVries, General Electric Co.
High pressure studies
- F. P. Glasser, Univ. Aberdeen
Alkali oxide containing systems
- F. A. Hummel, Pennsylvania State Univ.
Sulfides, phosphates
- K. H. Jack, Univ. Newcastle Upon Tyne
Nitrides, oxynitrides
- A. Muan, Pennsylvania State Univ.
First row transition metal oxide containing systems
- C. Semler, Ohio State Univ.
Anhydrous silicate - oxide systems
- C. A. Sorrell, Univ. Missouri-Rolla
Aqueous salt systems
- K. H. Stern, Naval Research Laboratory
Binary systems with halides only
- R. E. Thoma, Oak Ridge National Laboratory
Fused salts
- D. R. Wilder and M. F. Berard, Iowa State Univ.
R.E. oxide bearing systems
- H. S. Yoder, Jr., Carnegie Inst. Washington
Hydrous silicate systems, high pressure silicate studies

Scientists at NBS (L. Cook, R. Roth and T. Negas) with the help of the American Ceramic Society (G. Cleek) are assuming much of the responsibility for gathering the data from the literature and coordinating the preparation of evaluations and final editing of diagrams.

Coverage according to chemical system for the various editions is as follows:

	<u>1964</u>	<u>1969</u>	<u>1975</u>	<u>1978</u>
Metal-oxygen systems	146	202	104	~205
Metal oxide systems	855	408	401	~655
Systems with oxygen containing radicals	172	228	68	~120
Systems with halides only	483	718	145	~365
Systems containing halides with other substances	214	273	72	~160
Systems containing cyanides, sulfides, etc.	43	82	20	~140
Systems containing water	151	131	40	~250

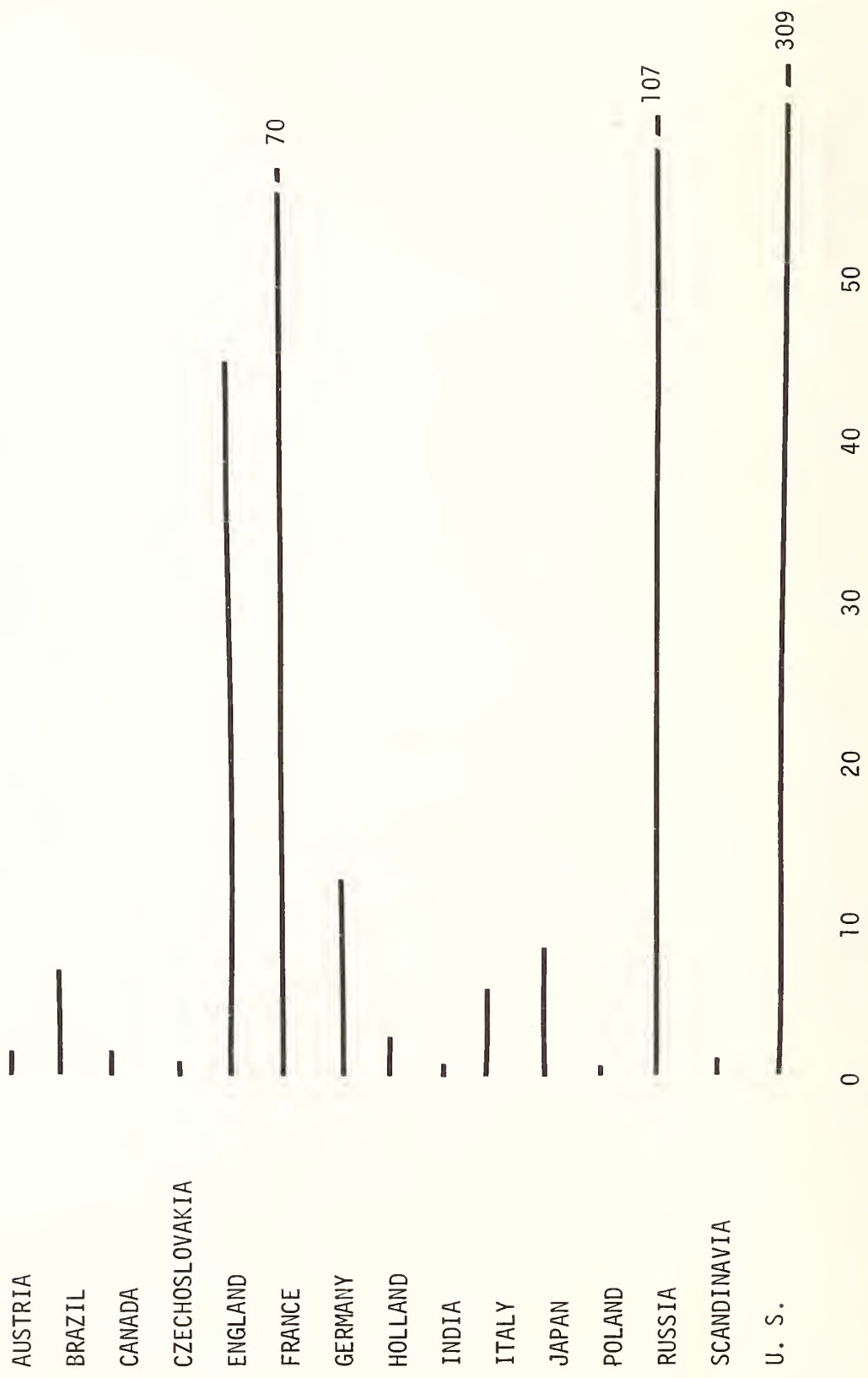


Figure 1. Publication of Oxide Systems by Country - 1975 Supplement.

A summary of the countries of publication of the phase diagrams reviewed in the 1975 Supplement is shown in Figures 1 and 2. The oxide systems by country are shown in a bar graph in Figure 1. It is evident that England, France, USSR and US are the major publishers of the diagrams. Figure 2 illustrates the distribution of the origin of other systems. The large number from the Soviet Union are mostly fused salt systems. It is highly probable that the distribution illustrated by these figures is biased by the techniques used to obtain the references and the reviewers' personal interests. It is hoped that any such bias will be eliminated in future supplements as greater attempts are made to make the compilation more complete and up-to-date.

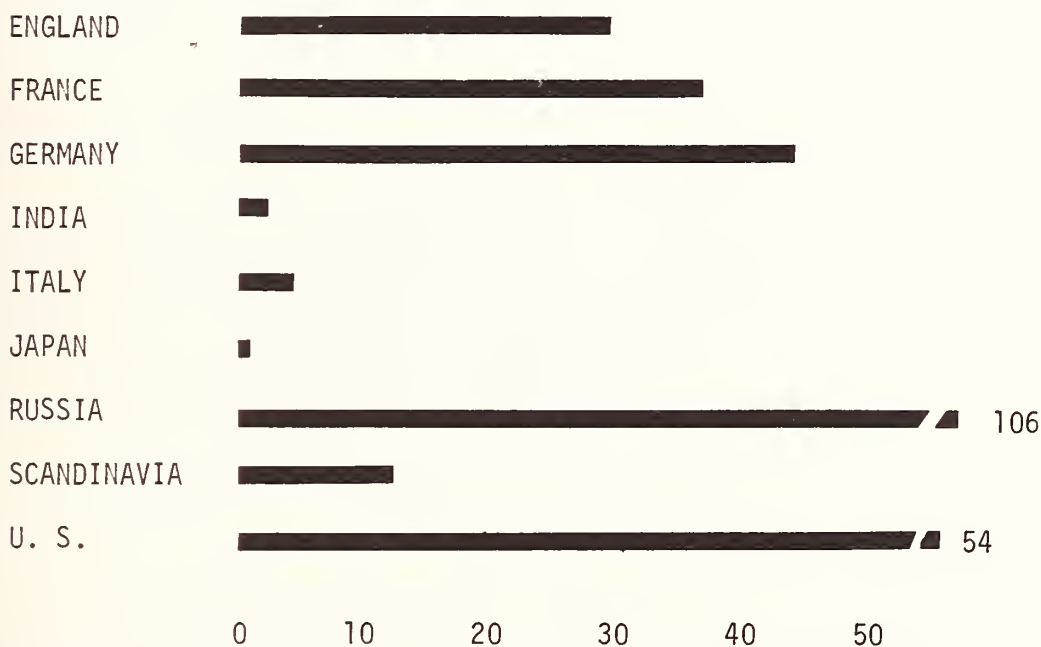


Figure 2. Publication of Other Systems by Country - 1975 Supplement.

4.0 Phase Diagrams for Ceramists - Survey of Users

A questionnaire was distributed by the American Ceramic Society in July 1976 to purchasers of the 1975 Supplement of "Phase Diagrams for Ceramists". The total number of questionnaires distributed was 460. The total number returned in the first three months was 186. This is a response of 40%, a remarkably large percent return, illustrating the great interest in the user community in this compilation. Table 1 gives the statistical breakdown of the origin of the returns. It should be noted that 81 or 44% of these are of domestic industrial users. The large response allows a determination of user needs in phase equilibria with a reasonably high statistical probability of success.

Table 1. PHASE DIAGRAMS FOR CERAMISTS PRELIMINARY RESULTS OF SURVEY OF USERS

Total Number Distributed - 460

Total Number Returned in First Three Months - 186

Response - 40%

- Unidentified - 25 (13%)

- Foreign - 37 (20%)

- Domestic

1. Government and National Laboratories - 5 (3%)

2. University and Non-Profit Laboratories - 38 (20%)

3. Industrial - 81 (44%)

In this questionnaire, twenty-one questions were asked covering the four major categories:

- I. Description of Respondent (1-7)
- II. Uses of Phase Equilibria Data and Principles (8-10)
- III. Evaluation of Phase Diagrams for Ceramists as a Publication of the American Ceramic Society (11-18)
- IV. Important Needs for Experimental and/or Theoretical Work (not now being done) (19-21)

4.1 Description of Respondent (I) *

4.1.1 Personal Data

The first seven questions requested personal data and nature of employment. Under Type of Training 127 individuals (68%) identified themselves as scientists while 71 (38%) refer to themselves as engineers, with only four (or 2%) belonging to the "other" category. As scientists and engineers add up to more than 100% obviously some identify themselves with both groups. This breakdown along with the highest degree of the respondent is shown in Table 2. Note that 62% have a Ph.D. or equivalent. Their highest degree was generally in the fields of ceramics, chemistry, materials or geology (Table 3). In Table 4 the present type of work checked by the respondent is summarized by total number and percent. As the respondent was asked to check as many as appropriate, the totals again are greater than 100%. By far the largest group is in research and development although technical management and education activities are well represented. As shown in Table 5, 83% identify themselves as members of the American Ceramic Society and their division affiliations are mostly Basic Science, Refractories, Glass and Electronics.

* Roman numeral in parenthesis indicates Major Category.

Table 2. DESCRIPTION OF RESPONDENT (I)

Type of Training (1)

- Scientist - 127 (68%)
- Engineer - 71 (38%)
- Other - 4 (2%)

Highest Degree (2)

- BS or BA - 31 (17%)
- MS or MA - 30 (16%)
- PhD or ScD - 115 (62%)
- OTHER - 10 (5%)

Table 3. SPECIFIC FIELD OF HIGHEST DEGREE (2)

1. Ceramics (Technology, Engineering, Science) - 56 (30%)
2. Chemistry (Physical, Inorganic, Engineering, Industrial, Electrochemistry, etc.) - 40 (22%)
3. Materials Science (Engineering) - 17 (9%)
4. Geology - Mineralogy - 16 (9%)
5. Metallurgy - 12 (6%)
6. Physics - 5
7. Engineering - 4
8. Crystallography - 1
9. Natural Sciences - 1
10. No Identification - 33 (18%)

Table 4. PRESENT TYPE OF WORK (3)

- Research - 143 (77%)
- Development - 85 (46%)
- Production - 18 (10%)
- Technical Management - 40 (22%)
- Education - 46 (25%)
- Other - 9

Table 5. MEMBERSHIP IN THE AMERICAN CERAMIC SOCIETY (4a)

- Yes - 155 (83%)
 - No - 28 (15%)

DIVISION AFFILIATION (4b)

1) Basic Science - 56	Nuclear - 5
Cement - 4	2) Refractories - 29
Ceramic-Metal Systems - 5	Structural Clay Products - 1
4) Electronics - 21	White Wares - 1
3) Glass - 23	No Division - 12
Materials and Equipment - 4	

4.1.2 Standard Industrial Categories of Employer (5) **

The respondents were requested to check one or more of a group of listed Standard Industrial Categories (SIC) which best describe their employer. Those categories receiving ten or more entries are listed in Table 6. The major industrial categories include stone, clay and glass products, electrical and electronic equipment, chemicals and non-metallic minerals. The name and address of the employer was given by 150 respondents and 174 listed their own name and address indicating a (conditional) willingness to be contacted for further information.

Table 6. STANDARD INDUSTRIAL CATEGORIES OF EMPLOYER (5)

(10 or more checked)

<u>SIC NO.</u>	<u>CATEGORY</u>	<u>NO. OF TIMES CHECKED</u>
32	Stone, Clay and Glass Products	50
82	Educational Services	46
36	Electrical and Electronic Equipment	26
28	Chemicals and Allied Products	20
14	Nonmetallic Minerals, Except Fuels	19
33	Primary Metal Industries	15
34	Fabricated Metal Products	13
38	Instruments and Related Products	10
	Other	35

** Arabic numeral in parenthesis indicates Question Number.

4.2 Uses of Phase Equilibria Data and Principles (II)

4.2.1 Applications (8-9)

Question eight asked for areas of application of phase equilibria in the respondent's organization (check as many as possible). Fifteen categories were listed while the sixteenth, entitled "Other", requested specifics. Table 7 lists these categories rearranged according to decreasing number of responses.

Table 7. USES OF PHASE EQUILIBRIA DATA (8)

AREAS OF APPLICATION:

- | | |
|------------------------------------|----------------------------|
| - Sintering of Ceramics - 117 | - Geology - 33 |
| - Search for New Compounds - 93 | - Energy Conversion - 31 |
| - Glass Processing - 63 | - Optical Materials - 29 |
| - Education - 57 | - Magnetic Materials - 29 |
| - Electronic Materials - 54 | - Building Materials - 23 |
| - Crystal Growing - 51 | - Environment Effects - 17 |
| - Metal Coating or Processing - 41 | - Nuclear Materials - 15 |
| - Smelting and Refining - 39 | - Other - 19 |

Question nine, requesting specific application of phase equilibria data, elicited 127 responses. This may perhaps be the most important point in the questionnaire and will be treated in detail in a later publication. Table 8 summarizes these answers according to the type of material, the property of interest and the industry involved. One typical quote suffices to illustrate the simple yet very important uses which can be made by easy access to phase equilibria data:

"Refractory attack occurred at bottom of furnace when metal temperature was lowered 50°C. Analysis of phase diagram showed that 50°C drop lowered bottom of furnace operating temperature below melting point of anorthite which built up during low end of temperature cycle. Upon heating to upper end of metal melting temperature, corrosive liquid was formed which ate the SiO₂ lining of the induction furnace. Bottom end of temperature range was raised 50°C and problem was eliminated."

Table 8. SPECIFIC APPLICATION OF PHASE EQUILIBRIA DATA (9)

Total Number of Answers - (127)

Industrial - (67)

MATERIAL

Oxide Ceramics (12)	Silicates (4)
Glass or Slag Plus Refractory (10)	Alumina (3)
Glass or Slag (9)	Metal + Slag (3)
Refractories (6)	Titanates, Etc. (2)
	Raw Materials (2)

PROPERTY

Identification of Phases (17)	Corrosion (4)
Glass Forming Regions (9)	Homogeneity (4)
Melting Points (6)	Chemical Reaction (4)
Liquidus (5)	Primary Phases (3)
Sintering (4)	Refractory Nature (3)

INDUSTRY

Glass (12)	Chemical (4)
Electronics (9)	Refining and Smelting (4)
Refractories (7)	Ceramics (2)
Electro-Optics (5)	Communications (2)
Iron and Steel (5)	Abrasives (2)

4.2.2 Classes of Systems of High Interest (10)

Question ten asked, "Which classes of systems are of high interest to you? Please indicate by 3 = High interest, 2 = Moderate interest, 1 = Some interest, 0 = No interest." Most respondents listed only 3 and 2. Table 9 lists the classes of systems divided into oxides, halides and general with the number of (3) answers given for each class, rearranged according to those of most interest in each category. Metal oxides and silicates are obviously of the highest interest with oxides in general being the most important. In the general category there is a significantly large vote for carbides and borides which are not covered in the present compilation, nor are there plans for inclusion of them. At the bottom of this list are arsenides, phosphides, selenides, and tellurides which are also not intended for coverage in the near future.

Table 9. CLASSES OF SYSTEMS OF HIGH INTEREST (10)

<u>OXIDES</u>	<u>NO.</u>	<u>(%)</u>	<u>GENERAL</u>	<u>NO.</u>	<u>(%)</u>
Metal Oxides	144	(77)	Carbides, Borides	43	(23)
Silicates	107	(58)	Oxynitrides, Nitrides	32	(17)
Alkali Oxides	77	(41)	Sulfates, Sulfides	32	(17)
Alkaline Earths	53	(28)	Carbonates	31	(17)
Rare Earths	40	(22)	Nitrates and Nitrites	18	(10)
Phosphates	35	(19)	Aqueous Systems at 1 atm	14	(8)
Borates	34	(18)	Hydrothermal Systems	12	(6)
			Arsenides, Phosphides	10	(5)
<u>HALIDES</u>	<u>NO.</u>	<u>(%)</u>	Selenides, Tellurides	6	(3)
Fluorides	25	(13)			
Chlorides	24	(13)			
Bromides	1				
Iodides	1				
			Other - 15	(8)	

4.3 Evaluation of Phase Diagrams for Ceramists as a Publication of the American Ceramic Society (III)

In general the tone of evaluation in this section was very favorable, although it might be argued that the audience was biased in favor of the book as they had just ordered the latest supplement.

4.3.1 Value of Phase Diagrams for Ceramists as a Publication (11)

As shown in Table 10, an overwhelming majority (87%) considered "Phase Diagrams for Ceramists" very valuable; defined as "in the top priority category among special publications [Note: The Journal, Bulletin and Ceramic Abstracts are not special publications]". There were no votes for the category "No Value; should be discontinued".

Table 10. EVALUATION OF PHASE DIAGRAMS FOR CERAMISTS (11)

- Very Valuable - 162 (87%)
- Moderately Valuable - 20 (11%)
- Marginal Value - 1
- No Value - 0

4.3.2 Does Range of Systems Treated Span Range of Interest (12)

Question (12) asked: Considering the 1975 Supplement together with the 1969 Supplement and the 1964 volume, does the range of systems treated span your range of interests? This question elicited answers similar to those of question 10. Indeed, there was a large amount of redundancy deliberately built into the questionnaire specifically to obtain that opinion which most interested or bothered the respondent. In this category 126 or 68% of the respondents checked YES, indicating they were quite happy with the range of coverage. Only 38 or ~20% answered NO and bothered to describe other systems which should be covered. These results are summarized in Table 11. Some of the suggested systems summarized under "not covered" are of course found in other non-ceramic compilations. Also note the similarity to the answers for question 19.

In Table 11 and succeeding tables the figures in brackets after the information refers to the number of times it was suggested. No number means it was only mentioned once. Unfortunately, the answers reflect the systems which the respondents want studied rather than compiled. There is very little published data in many of the categories listed. Many of the desired categories are outside the field of present coverage. Indeed some of them are outside the field of ceramics entirely. Other answers have nothing to do with the question; for instance, the comments "total coverage not adequate" and "time lag too great". These later points will be covered in the conclusion section.

Table 11. OTHER SYSTEMS WHICH SHOULD BE COVERED (12)

<u>ALREADY COVERED</u>	<u>NOT COVERED</u>
Glass Forming Systems (4)	Carbides, Borides, Nitrides (7)
Refractories (3)	Mixed Systems (5)
High Pressure (2)	Selenides, Tellurides (2)
Sulfides (2)	Silicides
Electronic Oxide Materials	Simple Metal Systems (2)
Oxyfluorides	Intermetallics
Hydrates	Metal-Gas Systems
Minerals	Refractories with Molten Metal
	Non-Oxide Containing Systems

IMPORTANT COMMENTS:

Systems with Variable P_{O_2} (8)

Total Coverage Not Adequate

Time Lag Too Great

4.3.3 Evaluation of Phase Diagrams for Ceramists (13-16)

In this section the respondent was asked to comment on (13) Gaps in Coverage, (14) More Attention During Experiment, (15) Is Information in Useful Format and (16) Are (1975) Commentaries Useful and of Right Length. The completely satisfied respondent would answer No, No, Yes, Yes, About Right to these questions. Table 12 shows the statistical summary of these answers and again it is evident that most people are fairly satisfied with the book as presently published.

4.3.3.1 Gaps in Coverage (13)

Table 13 shows that 67 answers considered that there were gaps in coverage. Again their written descriptions summarized in this table show that the gaps are mostly in the availability of experimental data rather than in the compilation of published data.

Table 12. EVALUATION OF PHASE DIAGRAMS FOR CERAMISTS (III)

(Completely Satisfied Checks No, No, Yes, Yes, About Right)

(13)	Gaps in Coverage -	No - 93
		Yes - 67
(14)	More Attention During Experiment -	No - 89
		Yes - 69
		I Don't Know - 1
(15)	Information in Useful Format -	Yes - 165
		No - 10
(16)	(1975) Commentaries Useful -	No - 7
		Yes - 153
	LENGTH: Too Long -	7
		About Right - 129
		Too Short - 9

Table 13. ARE THERE GAPS IN COVERAGE OR COMPILATION (13)

No - 93
Yes - 67

Summary of Answers

- Multicomponent Oxides - 34
- Systems with Variable P_{O_2} - 17
- Non Oxides - 14
- Hydrous, Hydrothermal and High Pressure - 5
- Metastable and Non-Equilibrium Phases - 3
- Commentaries for Important Systems from Vol I and II
- Compilation not Complete Because Some Published Diagrams not Included

Table 14. ARE THERE FEATURES WHICH NEED MORE ATTENTION DURING EXPERIMENTAL STUDIES? (14)

No - 89 (48%)
 Yes - 69 (37%)

APPLICATIONS:

<u>PRIMARY</u>	<u>EITHER</u>	<u>SECONDARY</u>
Glass Forming Regions (3)	Ranges of Homogeneity (5)	Effect of P _{O₂} on Equilibria (5)
Viscosity (Even Qualitative)	Impurity Effects (5)	P-T-X Equilibria and Vapor Pressure (2)
SO ₄ ⁻² in Glass	Kinetics (3)	Phase Changes
Molten Metals vs Refractories and Slag	Metastability (2)	Crystallographic Information
Slag and/or Other Wastes Plus Feldspar, Clay, etc.	Lattice Parameters vs Composition	Magnelli-Type Phases
More Property Measurements	Immiscibility Regions	Nonstoichiometry
	Exsolution	Methods of Detection of Solid Solution

"Opinions from Experts on Relative Accuracy of Conflicting Published Data"

4.3.3.2 Experimental Needs (14)

Question 14 asked "Are there features of the systems to which more attention should be given during experimental studies [such as solid solution below the one percent level]?" Only 18 people, or about 10%, specifically agreed with the suggestion concerning solid solution below the one percent level. They were about equally divided between industrial and university representatives. As pointed out by one individual in charge of the Materials Research Laboratory of a leading U.S. university, "This is very difficult data to get." The descriptions to the Yes answers of 69 individuals (37%) are summarized in Table 14, according to the type of applications of the features. Once again the answers are not necessarily those which have much relation to the question.

4.3.3.3 Useful Format (15)

A total of 165 respondents agreed that "the information given in the diagrams (was) presented in a useful format." Although only 10 persons indicated a No answer there were considerably more suggestions made for possible improvements. These are summarized in Table 15.

Table 15. IS INFORMATION IN PHASE DIAGRAMS IN USEFUL FORMAT (15)

1. The 1975 Format is Well Done (6)
2. State Whether Mole or Weight Percent (4)
3. Axes Should Always be Mole % not Wt %
(Axes Should Always be Wt % not Mole %)
4. More Isothermal Sections (2)
5. Better Cross Referencing
i.e. Ternary Liquidus to Binary Subsolidus
6. Exotic Formats Should Have Simplified Formats as Well
7. More Use of Descriptive Methods
8. P_{O_2} Assumed to be Air
9. All Diagrams Should be Reviewed for Theoretical Correctness

4.3.3.4 Information in Commentaries (17)

The respondents were asked to check four informational points (purity, accuracy, method and reference) as to their usefulness in the commentaries by using 3 = High value, 2 = Moderate, 1 = Marginal, 0 = No value. No one bothered to indicate zero value although certain portions were often without an entry. Table 16 indicates the number of times each of these points were given a 3 (High value). Purity of starting materials was considered to be the most important single factor to be included.

Table 16. IS IT USEFUL TO HAVE INFORMATION IN COMMENTARIES ON THE FOLLOWING:
(17)

High Value:

Purity of Starting Materials - 103 (55%)
Information on Accuracy - 88 (47%)
Description of Method - 85 (46%)
References to Earlier Work - 61 (33%)

4.3.4 Additional Information for Commentaries (18)

Question 18 asked "What additional information, if any, would you suggest be included in the diagrams and/or the commentaries" and gave four blank lines for an answer. Only 43 people (23%) bothered to answer this question, and again, many answers had little bearing on the question. Tables 17 and 18 summarize the answers according to those possibly within the scope of the compilation, and those probably outside the scope of the compilation. In Table 19 four comments are given from answers to question 18 which are well worth considering, if not for inclusion in the commentaries, at least as a starting point for discussion.

Table 17. WHAT ADDITIONAL INFORMATION SHOULD BE INCLUDED? (18)

Return to '69 Format - (1)
Keep '75 Format - (9)

Answers Possibly Within Scope of Compilation

References (with titles) to Earlier Work (5)
Reaction Kinetics (4)
Purity (3)
References to X-Ray Diffraction Data (2)
Accuracy (2)
Stoichiometry
Metastable Phases (2)
Volatilization (2)
Comments on Possible Errors

More Complete Coverage

Table 18. WHAT ADDITIONAL INFORMATION SHOULD BE INCLUDED (18)

Answers Probably Outside Scope of Compilation

- Glass Forming Properties (3)
- Optical Properties (2)
- Vapor Pressure
- Electrical Resistivity
- Dielectric Constant
- Mechanical Properties
- Free Energy Data
- Electronic Properties
- Viscosity of Liquidus

"Useful Data"

Table 19. WHAT ADDITIONAL INFORMATION SHOULD BE INCLUDED (18)

Noteworthy Comments:

1. Same Information in Same Order for Commentaries
2. A List of What Kind of Optical-Structural-Physical Data are Available in the Source Reference
3. Identify Which Part of Diagram is Theoretical and Which is Experimental
4. Comment on Rate of Volatilization and Attainment of Equilibrium to Indicate Probability of Real System Attaining Equilibrium Phase Composition

4.4 Important Needs for Experimental and/or Theoretical Work (IV)

In section IV of the questionnaire the respondent was asked to comment on "important needs for experimental and/or theoretical work not now being done". It was pointed out that "Compilers are usually also research workers and influence other workers. Your indication of the relative importance of certain research gaps might lead to filling some of these gaps". In general the response was very good. In fact, one respondent eloquently answered, "General increase in information on phase diagrams is needed. This is basic information of lasting value".

Table 20. NEEDS FOR EXPERIMENTAL OR THEORETICAL WORK NOT NOW BEING DONE (IV)

SPECIFIC SYSTEMS FOR WHICH DIAGRAMS ARE NEEDED (19)

TYPES:

Silicates (9)	Carbides and Nitrides (9)
Aluminates (5)	Oxynitrides (6)
Zincates (5)	Sulfides, Selenides, Tellurides (3)
Rare Earths (4)	Fluorides, Oxyfluorides (3)
Phosphates (3)	Oxyhydroxides (2)
Zirconates (3)	Sulfates
Titanates (2)	Metal-Oxygen Systems
Stannates (2)	Ferrites
Vanadates (2)	Actinides
Borates	

APPLICATIONS:

Glass (7)
 Magnetics (3)
 Refractories (3)
 Steel Making (2)
 Cement
 Abrasives
 Semiconductors
 Ferroelectrics
 Electronics
 Optics

SPECIAL CATEGORIES:

Ore Minerals
 Low PO_2
 High Pressure Systems
 High Pressure Silicates
 Very Complex Systems
 (Five or More Components of Mixed Types)
 Oxy-Nitro-Carbides
 Oxide-Carbonate-Sulfates

4.4.1 Specific Systems for Which Diagrams are Needed (19)

Question 19 asked "Are there specific systems for which diagrams are needed and not available?" There were 44 No answers and 90 Yes answers. In describing their Yes answers the respondents were generally quite specific. However, for the purposes of this paper these answers can be summarized (Table 20) either by types of systems, by applications or in special categories. Note that the types of systems include most of those listed in question 10 and the applications cover most of those mentioned in question 8.

4.4.2 Existing Diagrams Which Need Updating or Correction (20)

Question 20 asked "Are there parts of existing diagrams for which more detailed data are needed or which you suspect of being in error?" There were 68 No answers and 42 Yes. The description of the Yes answers are summarized by categories in Table 21. Many of these were silicates, aluminates or zirconates.

Table 21. EXISTING DIAGRAMS WHICH NEED UPDATING OR CORRECTING (20)

No - (68)

Yes - (42)

CATEGORIES:

Silicates (14)	Sulfides
Aluminates (3)	Oxyfluoride
Zirconates (3)	Garnets
Titanates	Non-Stoichiometric Oxides
Chromates	Refractories
Phosphates	Ultra High Temperatures (>1800°C)
Uranates	

- Many Based on Assumed Equilibrium

- Many Determined Accurately Only if Need Arises

4.4.3 Aspects of Phase Equilibria Needed but Inadequately Explored (21)

Question 21 was worded, "Are there aspects of phase equilibria which are needed and generally inadequately explored in most studies? [for example, solid solution below one percent]" There were 61 No answers and 51 Yes. The Yes respondent was asked to "please describe the problem and, if possible, suggest experimental methods for obtaining such data". Fifteen people agreed with the example of solid solution below the one percent level as shown in Table 22, which also lists some other aspects given in the answers. In Table 23 a summary is given of some of the suggested experimental methods which might be used to obtain some of these hard to get data.

Table 22. ASPECTS OF PHASE EQUILIBRIA NEEDED BUT INADEQUATELY EXPLORED (21)

No - 63

Yes - 51

Example Given: Solid Solution Below One Percent (15)

Other Aspects:

- Explore Systems as a Function of P_{O_2} (6)
- Kinetics of Attainment of Equilibrium (5)
- Vapor Pressure (5)
- Immiscibility (Liquid and Solid) (3)
- Application of Phase Diagrams to Metastable or Non-Equilibrium Systems (2)

Table 23. ASPECTS OF PHASE EQUILIBRIA NEEDED BUT INADEQUATELY EXPLORED (21)

Experimental Methods for Obtaining Such Data

- Transmission Electron Microscopy
- Electron Diffraction
(High Resolution Lattice Images)
- Vapor Pressure Measurements Across S.S. Region
- High Temperature X-Ray Diffraction in Mixed Gases
- Resistivity vs Temperature
- Scanning Electron Microscope
- Etch Techniques
- Neutron Diffraction
- IR Spectroscopy
- Neutron Activation Analyses

4.4.4 Some Conclusions from the Questionnaire

Several important points are worth summarizing as a result of the analyses of the answers received from this questionnaire. With regard to needed experimental data, there are two areas of experimental research which are apparently badly needed. The first involves the study of various elements and oxides capable of oxidation/reduction under conditions of variable P_{O_2} . There is very little such data available for compilation. Only the simplest² systems have so far been studied. The second area needed involves mixed systems containing refractories with slag or melt plus metal. Such mixed ternary or more complex systems are not primarily the classical concern of either ceramists or metallurgists. Consequently very few "academic" studies of such nature have been

published. Probably a large amount of such data has been accumulated by individual industrial laboratories. Such data is generally considered proprietary and is very seldom published.

Regarding the compilation itself, there were several justified complaints which are worth reemphasizing. The first problem mentioned was that the time lag was too great between publication of the data and publication of the compilation. Attempting to supply a commentary for each diagram only increased the time lag. In answer to this criticism, the present technique utilizing guest editors for the commentaries has been established. It is obvious that 12 editors can produce more commentaries than one or two in the same amount of time. It remains to be proven that the system will work, but the coordinating editors presently hope to publish a new up-to-date supplement every three years with the next due in 1978.

The second comment is that the total coverage is not adequate. No matter how the editors try to find all published diagrams they are bound to miss some which were published in obscure journals or reports. Individuals have always been encouraged to submit references which they find have been missed, but this has never amounted to a large percentage. It is proposed that an advertisement for the publications be published several times a year in the trade journal(s) requesting readers to submit missed references from any date preceding some fixed value. Hopefully this will increase the probability of obtaining responses from the large community of users.

Another problem which will eventually have to be faced by the editors involves commentaries for the diagrams published in the 1964 and 1969 editions. It seems most likely that only the more important systems would require commentaries. The decision as to which diagrams should be republished with commentaries will have to be faced in the near future.

DISCUSSION

F. P. Glasser - The audience should be aware that compilers frequently have difficulties determining in their evaluation, which information is estimated and which is determined. This question often prevents the possibility of a decision. Given the information as it exists in the literature, often the best a compiler can do is to point out the discrepancies to the reader, and let them make up their minds.

R. S. Roth - Dr. Glasser is speaking from experience. You most often cannot tell what was experimental and what was theoretical, and furthermore, that you usually do not question the experimenter's interpretation of his data according to the phase rule until you do experiments on the system yourself.



PRESENT STATUS OF PHASE DIAGRAM COMPILATION
ACTIVITY FOR SEMICONDUCTORS

by

C. D. Thurmond
Bell Laboratories
Murray Hill, New Jersey 07974

I. INTRODUCTION

There is no single compilation of semiconductor phase diagrams. There are, however, 3 principal compilations among which many of the important semiconductor phase diagrams are included. The phase diagrams compiled are for semiconductors belonging to the diamond-like class all having tetrahedral coordination with 4 valence electrons per atom. These semiconductors have proven to be important both because of their technologically important properties and because those properties have become understood at a fundamental level.

The class of elements and compounds that are tetrahedrally coordinated and average 4 valence electrons per atom is summarized in Table 1. Binary and ternary compounds are included.

In addition to 3 major compilations, certain other compilations will be mentioned. Brief mention will also be given to other semiconductors and some comments about other types of phase diagrams of interest to those in the semiconductor field.

II. PRINCIPAL COMPILATIONS

The most extensive compilation of semiconductor phase diagrams is contained in "Constitution of Binary Alloys," by Hansen, Elliott and Shunk.¹ These phase diagrams are only a small fraction of the total binary temperature-composition diagrams included in this work. Nevertheless, it contains more binary diagrams of semiconductors than any other compilation.

There are 76 diagrams for which 1 component is either Ge or Si. There are 8 diagrams containing a 3-5 compound and 7 containing a 2-6 compound (Table 2).

Panish and Ilegems² have critically reviewed a number of 3-5 compound binary and ternary phase diagrams. This includes a number of pseudobinary solid solutions of the types $A_x^3B_{1-x}^3C^5$ and $A_x^3B_x^5C_{1-x}^5$, i.e., with common "anion" and with common cation. There are 7 binary diagrams, 8 ternaries with common anion and 3 ternaries with common cation (Table 3).

Shay and Wernick³ have included 26 phase diagrams in their book on "Ternary Chalcopyrites". Most are pseudobinaries that include the chalcopyrite (Table 4). They include much information on the lattice parameters of the chalcopyrites and their composition dependence in solid solutions.

The level of evaluation of the phase diagrams in the 3 compilations is estimated in Table 5.

III. OTHER COMPILATIONS

Berezhnoi⁴ has brought together silicon binary phase diagrams in a book published in Russia in 1958 and published in an English translation in 1960. The convenience of having silicon phase diagrams in 1 volume is offset by the volume now being somewhat out-of-date. The volumes of Hansen, et al.¹ contain, in general, the most up-to-date information on the binary silicon diagrams.

Goryunova⁵ has expressly devoted her attention to the diamond-like, tetrahedrally coordinated semiconductors. Discussion of quaternary and higher systems is included. Few phase diagrams are given but there is useful related information and references.

IV. OTHER SEMICONDUCTORS

There are several classes of semiconductors not included among the tetrahedrally coordinated semiconductors described in Table 1 that should be mentioned. The most important of these is the class of 4-6 compounds, A^4B^6 , for example, PbSe and the solid solutions formed between them, for example, $Pb_{1-x}Sn_xSe$. These semiconductors have the NaCl structure. A number of 4-6 phase diagrams are included in Hansen, et al.¹ Harman⁶ has discussed the phase diagrams of 3 of the more important 4-6 ternary solid solutions.

There are two subclasses of semiconductors not previously mentioned that are usually thought to be members

of the diamond-like, tetrahedrally coordinated class of semiconductors. They are called defect semiconductors and excess semiconductors. The former can be thought of as tetrahedrally coordinated but with some fraction of one kind of site vacant. The semiconductor Ga_2S_3 is an example with 1/3 of its cation sites vacant. The excess semiconductors also have tetrahedral coordination but some fraction of normally vacant sites are occupied.

V. OTHER PHASE DIAGRAMS

The phase diagrams of Hansen, et al.,¹ Panish and Ilegems² and Shay and Wenick³ by and large depict liquid-solid and solid-solid phase equilibria. There are other types of phase diagrams of special usefulness to those interested in semiconductor phase diagrams.

The technological importance of semiconductors arises primarily from the properties given to the semiconductor by donor and acceptor impurities. The maximum amount of impurity that can be added is of special interest. The solidus curves of impurities in Ge and Si have been compiled by Trumbore.⁷ In order to display the characteristic low concentrations, a plot of T vs. log C is used. The solidus curve near the semiconductor melting point is of particular importance. It is described in terms of the ratio of the impurity concentration in the solid phase to its concentration in the liquid phase.

This ratio is the distribution coefficient $k = C_s/C_l$ and is constant for temperatures in a range near the melting point. Values of k have been included by Trumbore⁷ for impurities in Ge and Si. Milnes⁸ has compiled distribution coefficients for impurities in Ge and Si as well as for a number of 3-5 compounds.

Another type of phase diagram of particular significance for semiconductors is the Brouwer diagram. The dilute solution concentrations of impurities and defects as functions of temperature, concentration or partial pressure of particular components can be represented with considerable simplicity on $\log C-1/T$ or $\log C_1$ vs. $\log C_2$ or $\log P$ plots. Brouwer⁹ has pointed out that such relationships for each component would be well approximated by a series of connected straight lines the slopes of which gave important information. A number of these diagrams may be found in "The Chemistry of Imperfect Crystals" by Kröger.¹⁰

An important class of semiconductor phase diagrams not included in Refs. 2 and 3 are the ternary diagrams giving the liquidus and solidus curves for an impurity in a compound semiconductor. As examples, Zn in GaAs and in GaP have received the most attention. Jordan¹¹ has considered these systems in some detail and gives critically evaluated liquidus and solidus information.

Other phase diagrams not included are the partial pressure-temperature diagrams giving the pressures of components of compound semiconductors for vapor-liquid-solid equilibria. Two examples are the GaAs and the GaP systems discussed by Thurmond.¹² In addition, the P-T diagrams for the pure semiconductor are of interest. Examples can be found in the paper by Jayaraman and Cohen.¹³ A last example of phase diagrams not included in the principal compilations cited above is the solid-vapor equilibria of the multicomponent systems used to grow semiconductors from the vapor phase. Examples of such systems may be found in Shaw.¹⁴

SUMMARY

There is no compilation of phase diagram devoted exclusively to semiconductors. There are 3 compilations containing the most up-to-date information on binary and ternary tetrahedrally coordinated, 4 electrons per atom semiconductors. This is the largest and most important class of semiconductors. Phase diagrams of other semiconductors are mentioned. Some comments are included about other kinds of phase diagrams than the T-X diagram that are used for semiconductors.

REFERENCES

1. M. Hansen, Constitution of Binary Alloys, 2nd Ed., prepared in cooperation with K. Anderko, (McGraw Hill), 1958; R. P. Elliott, First Supplement, 1965; F. A. Shunk, Second Supplement, 1969.
2. M. B. Panish and M. Ilegems, Phase Equilibria in Ternary III-V Systems, in Progress in Solid State Chemistry, eds., H. Reiss and J. O. McCaldin (Pergamon Press, New York) 1972, Vol. 7, p. 39-83.
3. J. L. Shay and J. H. Wernick, Ternary Chalcopyrite Semiconductors; Growth, Electronic Properties and Applications, (Pergamon Press, 1975).
4. A. S. Bereznoi, Silicon and its Binary Systems, (Consultants Bureau, N. Y., 1960); Russian Edition, 1958.
5. N. A. Goryunova, The Chemistry of Diamond-Like Semiconductors, published in English (MIT Press, 1965); first published in Russian, 1963.
6. T. C. Harman, "Control of Imperfection in Crystals of $Pb_{1-x}Sn_xTe$, $Pb_{1-x}Sn_xSe$ and $PbS_{1-x}Se_x$," Physics of IV-VI Compounds and Alloys, (Gordon and Breach, N. Y.), S. Rabi Ed., p. 141, 1974.
7. F. A. Trumbore, "Solid Solubilities of Impurity Elements in Germanium and Silicon," Bell System Technical Journal 39, 205 (1960).

8. A. G. Milnes, Deep Impurities in Semiconductors, (John Wiley and Sons, 1973).
9. G. Brouwer, Philips Res. Rep. 9, 366 (1954).
10. F. A. Kröger, The Chemistry of Imperfect Crystals, Vol. 1, Preparation, Purification, Crystal Growth and Phase Theory, and Vol. 2, Imperfection Chemistry of Crystalline Solids, 2nd revised edition, 1974.
11. A. S. Jordan, "The Solid Solubility Isotherms of Zn in GaP and GaAs," J. Electrochem. Soc. 118, 781 (1971), and "The Liquidus Surfaces of Ternary Systems Involving Compound Semiconductors: Calculation of the Liquidus Isotherms and Component Partial Pressures in the Ga-As-Zn and Ga-P-Zn Systems. Met. Trans., 2, 1965 (1971).
12. C. D. Thurmond, "Phase Equilibria in the GaAs and the GaP Systems, J. Phys. Chem. Solids 26, 785 (1965).
13. A. Jayaraman and L. H. Cohen, "Phase Diagrams," Vol. 1 A. M. Alper Ed. (Academic Press, 1970).
14. D. W. Shaw, "Mechanisms of Vapor Epitaxy in Semiconductors," in Crystal Growth, Vol. 1, pp. 1-48 (1974). C. H. L. Goodman, Ed., (Plenum Press).

TABLE 1

Tetrahedrally Coordinated Semiconductors
4 Electrons per Atom

<u>Symbol</u>	<u>Example</u>	<u>Structure</u>
A^4	Si	diamond
A^3B^5	GaAs	sphalerite (zincblende), wurtzite
A^2B^6	ZnS	sphalerite (zincblende), wurtzite
$A^2B^4C^5_2$	ZnSiAs ₂	chalcopyrite, sphalerite, wurtzite
$A^1B^3C^6_2$	AgGaSe ₂	chalcopyrite, sphalerite, wurtzite

TABLE 2

Number of Semiconductor Phase Diagrams in
Hansen, Elliott and Shunk¹

<u>System</u>	<u>Number</u>
A^4-B^n	76
A^3-B^5	8
A^2-B^6	7

TABLE 3

Number of Phase Diagrams in
Panish and Ilegems²

<u>Systems</u>	<u>Number</u>
A^3-B^5	7
$A^3-B^3-C^5$	8
$A^3-B^5-C^5$	3

TABLE 4

Number of Phase Diagrams in
Shay and Wernick³

<u>Systems</u>	<u>Number</u>
$A^1-B^3-C^6$	14
$A^2-B^4-C^5$	7
$A^2-B^3-C^4-D^5$ ($A^2C^4D_2^5+B^3D^5$)	4
$A^2-B^2-C^4-D^5$ ($A^2C^4D_2^5-B^2C^4D_2^5$)	1

TABLE 5

Depth of Treatment	
Hansen, Elliott and Shunk ¹	2, 3, 4
Panish and Ilegems ²	4
Shay and Wernick ³	3, 4

1. Bibliography
2. Annotated Bibliography
3. Unevaluated Phase Diagrams and Bibliography
4. Critical Evaluation



Phase Diagram Compilations for Metallic Systems - an Assessment of Ongoing Activities

G. C. Carter
Alloy Data Center
Metallurgy Division
Institute for Materials Research
National Bureau of Standards
Washington, D.C. 20234

Alloy phase diagrams provide a basis for solving many industrial problems. It is, therefore, not surprising to find critical phase diagram data compilation activities generally concentrated in the more industrialized countries. Large compilation projects are being carried out in Germany, France, the USSR, and the UK. Several notable projects are also carried out in other countries. Concise descriptions of all data centers we are aware of are given in Appendix A of this paper.

Historically, too, metallurgy was performed by the more culturally developed peoples, at first only creating ornamental objects, starting more than 10,000 years ago, with practical applications following at a much later date (1): Nearly all the industrially useful properties of matter, and shaping material, had their origins in decorative arts, writes Prof. C. S. Smith, the noted metallurgical historian. "The making of ornaments from copper and iron certainly precedes their use in weapons ..." Although metallurgical information was not quantified or documented accurately, a substantial amount must have been known in order to produce the fine artwork created in many cultures. Rather, metallurgical findings and fiction were relayed orally in a rather qualitative manner from master to apprentice.*

An early major quantitative physical property compilation for virtually every alloy known at the time was prepared by Achard in the 18th century in Germany, and is described in a review by C. S. Smith (3). It covered over 900 compositions, some with as many as seven components. Unfortunately, the compilation was written in the language of the Berlin Academy, which was French at that time (i.e. not the language of the German blacksmith), though the Academy's language was changed soon after. Another shortcoming described by Smith was that the compilation was devoid of theoretical speculation, and yet was not in a format attractive to engineers or artisans. It was noted that consequently, as far as could be determined, the compilation was never used. That is, user orientation of the compilation was important then, as much as it is today.

*as, for example, by the Samurai swordsmiths (2), giving the following data: "Heat the steel at final forging until it turns to the color of the moon about to set out on its journey across the heavens on a June or July evening (old calendar)", or, "After the final forging, place the sword in water which has a temperature of water in February or August (old calendar). They believed that water temperature in February or August was the same. Thus, when a swordsmith inscribed the month of manufacture on the sword, he generally used either February or August, regardless of the time of year the sword was actually made". This information, of course, states something semi-quantitatively about an Fe-C based alloy phase diagram, but was not interpreted in that perspective.

In the early 20th century, critical compilations were produced in Germany (this time in German) for binary (4) and "all" (5) phase diagrams, for which complete bibliographies of experimental determinations were collected and subsequently critical evaluations produced. This method of approach has been continued successfully in many smaller compilations up to today. The work by Hansen (6) (published in 1958 in English) was the last successfully produced complete critical compilation of all binary alloys. While two supplements to this volume were feasible (Elliott, 1965; Shunk, 1969) (7), a full re-working of these three volumes plus more recent literature, into a single reference book proved to be impracticable for a single group; the amount of literature to be evaluated has grown to prohibitive proportions.

This problem becomes amplified for ternaries and higher multicomponent alloys. However, methods of preparing critical phase diagram compilations have undergone substantial changes since large products such as the "Hansen" series (6,7) were produced. The reason is that in the past there existed an ample, though not excessive, amount of classical metallurgical data on the one hand, while, on the other hand, theoretical models and computerized methods to obtain phase diagrams from thermodynamic data were not yet adequate. In recent years tremendous progress has been made in this latter approach to phase diagram determination: improved computer facilities and increasingly sophisticated models either integrate existing experimental data with evaluated thermodynamic data, from which equilibrium diagrams can be calculated, or simply use the thermodynamic data to predict equilibrium diagrams. This latter method becomes invaluable for alloys for which classical phase diagram determination experiments are cumbersome, difficult, and lengthy (i.e. expensive), as is often the case for multicomponent alloys utilized in industrial applications. Especially for these alloys, specific groups of phase diagrams only in certain ranges of composition need to be evaluated, and comprehensive phase diagram compilations are not always a desired product for such specific needs. For example, Co-base and Ni-base superalloys tend to exhibit certain hard intermetallic phases precipitating after solidification (8), and data are only needed in those composition ranges in which the superalloys form (e.g. p. 624, Dreshfield).

An excellent review on the general topic of obtaining phase diagram information from thermodynamic data for various applications is given in reference (9). As a result of these computational developments, a large number of small projects are now underway in various countries. Several of these projects collaborate with each other, forming larger groups such as CALPHAD (see Appendix B for a listing of its members).

There are several other international collaborative programs. A prominent one is the Scientific Group of Thermodata Europe (SGTE), a thermochemical data bank, of which THERMODATA (10) represents very active french subgroup. THERMODATA is a bank of critically evaluated data including metallurgical thermodynamics for elements, stoichiometric compounds, alloys and non-stoichiometric phases. European scientific institutions from several countries, highly qualified in thermodynamics, select and critically evaluate the data, and review each other's evaluations before entering the data on an on-line accessible computer data bank.

Another international collaborative program is that organized by the International Atomic Energy Agency, Vienna. The IAEA has coordinated compilation and critical evaluation projects for thermodynamic and phase diagram data for the actinides on an international scale (Oetting et al. general editors), to be published in eleven parts (see under Oetting, Appendix A and C for further details), and a Special Issue series on elements and their alloys and compounds, for elements used heavily in the nuclear industry, with O. Kubaschewski as general editor (see under O. Knacke, and O. Kubaschewski, Appendix A and C for further details).

It is hoped that all compilation and critical evaluation projects for metallic phase diagrams will partake in yet increased international collaborative efforts in order to minimize costly and time consuming duplication of efforts, and to maximize availability of urgently needed reliable phase diagram data, not only for bulk equilibrium phases, but also for other phase diagram needs such as metastable phases, high pressure, small particle, surface phases, etc. Responses to this suggestion have been overwhelmingly favorable, although details of a large-scale collaborative effort must yet be developed.

As a preliminary start to the development of collaboration, a list has been prepared (see Appendix A) of all alloy phase diagram data compilation activities currently underway. This list represents an update to the one given in reference (11). The products of these compilation activities are included in a complete list of phase diagram compilations and handbooks as prepared by the Alloy Data Center (12), with the most recent edition given in Appendix C of this paper.

References

- (1) P. Knauth, "The Metalsmith", in "The Emergence of Man" series, Time-Life Books, NY (1974).
- (2) J. M. Yumoto, "The Samurai Sword - A Handbook", C. E. Tuttle Co., Rutland, VT., and Tokyo, Japan (1958).
- (3) K. F. Achard, "Properties of Alloys" Berlin (1788), described by C. S. Smith, "Four Outstanding Researchers in Metallurgical History", American Society for Testing and Materials, Philadelphia (1963).
- (4) M. Hansen, "Der Aufbau der Zweistofflegierungen" Springer-Verlag, Berlin (1936).
- (5) E. Jänecke, "Kurzgefasstes Handbuch Aller Legierungen", Verlag von Robert Kiepert, Berlin-Charlottenburg (1940).
- (6) M. Hansen and K. Anderko, "Constitution of Binary Alloys", McGraw-Hill, NY (1958).
- (7) Supplements to ref (6): R. P. Elliott, Supplement I (1965), and F. A. Shunk, Supplement II (1969), McGraw-Hill, NY.
- (8) L. R. Woodyatt, C. T. Sims, and H. J. Beattie, Trans AIME 218, 277 (1960), and W. J. Boesch and J. S. Slaney, Met. Prog. 86, 109 (1964).
- (9) T. G. Chart, J. F. Counsell, G. P. Jones, W. Slough, and P. J. Spencer, Review 195 in "International Metallurgical Reviews" 20, 57 (1975).
- (10) Y. Deniel, dir., Bibliotheque Universitaire des Sciences, Domaine Universitaire, B.P. 22, F-38402 Saint Martin d'Heres (Grenoble) France.
- (11) L. H. Bennett, G. C. Carter, and D. J. Kahan, CODATA Conference, Boulder, Colo., June 1976.
- (12) L. H. Bennett, D. J. Kahan, and G. C. Carter, Mat. Sci. and Eng. 24, 1 (1976).

Appendix A

Alloy Phase Diagram Compilation Activities

Prepared by G. C. Carter, D. J. Kahan, and L. H. Bennett

Persons or Centers conducting continuing phase diagram data programs as of January 1977 are listed below. Additional phase diagram calculation groups some of which also compile and critically evaluate phase diagram data are listed under CALPHAD Members, Appendix B. Generally, projects involved in computational techniques without specific compilation outputs are not included in this list. It is a natural activity for research scientists to collect their own data files on their own subjects of specialty. Unless specific efforts in compilation outputs are produced by such scientists, their activities are generally not included in this Appendix.

N. Ageev, President of the Scientific Council, and
O. S. Ivanov et al.
Physical & Chemical Bases of Metallurgical Processes
Academy of Sciences of the USSR
Leninski Prospekt 49
17334 Moscow, USSR

(unevaluated comprehensive data compilation for binary, ternary, and a few higher-order phase diagrams are published approximately annually; cumulative indices available, with the most recent one translated in English, and given in these proceedings by C. M. Scheuermann, TPSII-1; also see paper p. 90; to obtain, see under Mikhailov, VINITI).

I. Ansara and C. Bernard
Laboratoire de Thermodynamique et Physico-Chimie Metallurgiques
associe au CNRS
Institut National Polytechnique
B.P. 44-38401 St. Martin d'Herès
Grenoble, France

(computer prediction of phase equilibria from computer stored critical thermodynamic data; also see paper p. 123).

B. B. Argent
University of Sheffield
Sheffield S10 2TN S. Yorkshire
England

(experimental thermodynamic verification of Fe-based multicomponent systems, as a check on models used in phase diagram calculations).

T. I. Barry
National Physical Laboratory
Teddington, Middlesex, UK

(ceramic and glass pressure/temperature/composition diagrams are evaluated for specific customers).

L. Brewer
Inorganic Materials Research Div.
University of California
Berkeley, CA 94720

(prediction of high-temperature equilibria for binary and higher-order systems, presented in useful, two-dimensional, Brewer projection diagrams; review of all Mo binary alloy phase diagrams in preparation as part of the IAEA series; La alloys, Ac alloys, Fe alloys; surface phases in collaboration with G. A. Somorjai).

G. C. Carter
Alloy Data Center
Metallurgy Division
National Bureau of Standards
Washington, DC 20234

(coordination of phase diagram evaluation projects; evaluation of selected phase diagrams; automated, annotated bibliography of phase diagrams and physical properties; also see paper p. 909).

Y. A. Chang
Materials Department
College of Engineering and Applied Science
University of Wisconsin
Milwaukee, WI 53211

(ternary copper alloy phase diagrams are being critically evaluated see paper MPSI-4).

T. G. Chart
National Physical Lab.
Teddington, Middlesex, England

(bibliography being compiled on phase diagrams of binary and multi-component systems of technologically important elements; critically evaluated thermochemical computer data file available through L. Kaufman's service (see below); evaluation of diagrams selected for use in prediction of multicomponent systems, currently mainly B-X, Si-X binaries upon which multicomponent superalloys are based; see paper p. 1186).

T. F. Connolly
Research Materials Information Center
Bldg 2,000, Oak Ridge Natl. Laboratory
P.O. Box X
Oak Ridge, TN 37830

(bibliography on all inorganic research materials (~4,000) for preparation of high quality research samples; unevaluated diagrams or abstracts thereof, stored in the systems, to prepare responses to specific queries).

R. Ferro
Istituto di Chimica Generale
University of Genoa
Genoa, Italy

(evaluated crystal structures for the IAEA series; see under O. Knacke, and under F. L. Oetting, below).

K. A. Gschneidner, Jr.
Rare Earth Information Center
Iowa State University
Ames, IA 50010

(the Center maintains a bibliographic file of papers dealing with many aspects of rare earths, including phase equilibria, crystallographic and thermodynamic data of rare earth alloys; reviews of rare earth alloy phase diagrams and other properties are published; see paper p. 226).

R. Hultgren, Prof. Emeritus
Dept. of Metallurgy
Lawrence Radiation Laboratory, Univ. of Calif.
Berkeley, CA 94720

(comprehensive data files of thermodynamic data and critical evaluations up to 1972; a small effort continues towards maintaining the bibliographic files of the center current).

International Atomic Energy Agency

(see under O. Knacke and under F. L. Oetting et al. of this appendix; for more details see Appendix C, under O. Kubaschewski, ed., of the phase diagram data section, and under F. L. Oetting, ed., of the thermodynamic data section).

L. Kaufman
ManLabs, Inc.
21 Erie St.
Cambridge, MA 02139

(computer prediction of phase equilibria from stored thermodynamic data; available to subscribers is an on-line file of critical thermodynamic data from the National Physical Laboratory (U.K.) and ManLabs, together with software for computation of binary and ternary phase diagrams, derived from the component metals Fe, Cr, Ni, Co, Al, Nb, Mo, Ti, C, and W).

K. M. Khanna
Materials Science Department
National Institute of Foundry and Forge Technology
P.O. Box Hatia
Ranchi 834003, India

(new program on phase diagrams of ferromagnetic materials).

Prof. Mats. Hillert
Dept. of Metallurgy, Division of Physical Metallurgy
10044 Stockholm 70, Sweden

(phase equilibria for iron-rich alloys)

O. Knacke and O. Kubaschewski
Institut für Theoretische Huttenkunde
Technische Hochschule
Aachen, Germany

(critically evaluated thermodynamic data, from which phase diagrams are deduced (see paper TPSI-13). Among the phase diagram evaluators are O. von Goldbeck; P. Spencer and others. Critical evaluation of Be, Hf, Nb, Pu, Ta, Th, and Zr-base alloy phase diagrams, begun in 1966, have been edited by O. Kubaschewski and published as Special Issues of the "Atomic Energy Review" (Vienna) (also see Appendix C, the phase diagram data section). Evaluations planned are Mo (see under Brewer, above), Hf, and Ta. In this series much of the phase diagram evaluations have been carried out by O. von Goldbeck. R. Ferro of the University of Genoa has contributed evaluations of crystal structures. P. T. Spencer: critical evaluations of mostly transition metal alloys, especially Fe).

D. J. Lam
Argonne National Laboratory
Argonne, IL 60439

(formation and crystal structures of binary and ternary actinide alloys; a publication in "The Actinides: Electronic Structure and Related Properties": II (1974), edited by A. J. Freeman and J. B. Darby, entitled "The Crystal Chemistry of Actinide Compounds").

V. C. Marcotte
IBM East Fishkill Facility
D/45k B/300-95
Hopewell Junction, NY 12533

(small scale compilation for the immediate area of liquid solder-solid metal interactions; file currently in the form of internal IBM reports, literature, and in-house research results).

L. Merrill
High Pressure Data Center
Brigham Young University
Provo, UT 84602

(the Center maintains a bibliographic file of papers dealing with properties of materials under high pressure, including phase transformations in metals; also see paper p. 100).

A. I. Mikhailov, Dir.
Institute for Scientific Information (VINITI)
Academy of Sciences of the USSR
Baltiyskaya ul. 14
Moscow, USSR

(products include an Abstracts journal Metallurgy (Referativniy Zhurnal Metallurgiya) a Current Awareness Bulletin Metallurgia, magnetic data tapes starting 1977, "Phase Diagrams of Metallic Systems", editor N. V. Ageev et al., described in Appendix C under Ageev. Outputs are formatted as bound volumes, microfiche, and, recently, magnetic tapes. Subscriptions to the Ageev series must be applied for, in the several months preceding the year for which the subscription is intended. This and the other VINITI material can be obtained through "Mezhdunarodnaya Kniga", Moscow, USSR, or through Prof. A. I. Mikhailov.

A. P. Miodownik
University of Surrey
Guildford, Surrey, England

(critical evaluation of Fe-Co and Fe-Ni phase diagrams, and reference to work on other Fe-base alloys exhibiting magnetic effects; bibliography on a wider range of alloys; effect of irradiation on phase diagrams; see paper p. 1065).

W. G. Moffatt
Metallurgy and Ceramics Laboratory
General Electric Research and Development Lab.
Schenectady, NY 12301

(compilation of mostly unevaluated binary phase diagrams, intended to complement the Hansen-Elliott-Shunk series, "Constitution of Binary Alloys" and supplements; also see Appendix C under his name).

F. L. Oetting
Div. of Research & Labs.
IAEA, Vienna, Austria

V. Medvedev
Inst. High Temp.
Moscow, USSR

M. H. Rand
Atomic Energy Res. Est.
Harwell, Oxfordshire OX11 0RA, UK

(the International Atomic Energy Agency has initiated an interational program of compilation for the Actinides. The above constitute the Advisory board. Eleven volumes are planned in this series. Further details are described in the thermodynamic data section of Appendix C).

A. D. Pelton and C. W. Bale
Dept de Genie Metallurgique
Ecole Polytechnique
Universite de Montreal
Montreal, Quebec H3C 3A7, Canada

and

W. T. Thompson
Dept. of Met. & Mining Eng.
McGill University
Montreal, Quebec, Canada

(a comprehensive critical computerized thermodynamic data treatment bank is being established; on-line capabilities are available with software packages; one for generalized predominance area diagrams, and one for the calculation of binary and ternary phase diagrams. This software can be applied to stored or user-supplied thermodynamic data; see paper p. 1077).

G. Petzow
Max-Planck-Institut fur Metallforschung
Institut fur Werkstoffwissenschaften
Stuttgart-80, Busnauerstr. 175
Germany

(a phase diagram data center is being established; a monumental compilation of ternary phase diagrams is being planned (see paper p. 164); currently experimental thermodynamic data are determined and CALPHAD-type computerized methods used to determine ternary phase diagrams; see paper p. 955).

A. Prince
Hirst Research Centre
General Electric Co. Ltd.
East Lane, Wembley, Middlesex, HA9 7PP
England

(critical evaluation of phase diagram data on Au-based alloys is in progress; compilation of a bibliography on multicomponent alloy constitution to update the 1956 bibliography by Haughton and Prince is being finalized (see Appendix C).

M. H. Rand
Atomic Energy Research Establishment
Harwell, Oxfordshire OX11 0RA, UK

(critical evaluation of phase diagrams of multicomponent alloys of some transuranic elements, including predictive methods from thermodynamic data. See Appendix C, under O. Kubaschewski, ed., in the phase diagram data section, and under F. L. Oetting, ed. in the thermodynamic data section, for listing of some of the compilations).

G. Raynor
Dept. of Physical Metallurgy and Science of Materials
University of Birmingham
Birmingham, B15 2TT
England

(critical evaluation of ternary and quaternary phase diagram data on Mg-based alloys is to be published shortly in Int. Metals Rev.; similar work for Be alloys may be planned).

R. S. Roth
Inorganic Materials Division
National Bureau of Standards
Washington, DC 20234

("Phase Diagrams for Ceramists" is prepared by this group; though dealing mainly with ceramic systems, some metal-metal-oxygen and metal-metal-sulfur diagrams are included).

E. Rudy
Materials Science Department
Oregon Graduate Center
Beaverton, OR 97705

(evaluated phase diagrams of refractory carbide and boride systems; see Appendix C).

E. M. Savitsky
A. A. Baikov Inst. of Metallurgy
Academy of Sciences of the USSR
Leninski Prospect 49
117334 Moscow USSR

(data compilations on metals and their applications are produced; see various entries of Appendix C).

C. M. Scheuermann
Alloys Branch
NASA Lewis Research Center
Cleveland, OH 44135

(compile binary and higher-order phase diagrams of Fe, Co, or Ni with Al, B, C, Ce, Hf, Mo, N, Nb, O, Re, Si, Ta, Ti, U, W, Y, or Zr; started in 1974; output in loose-leaf format).

S. P. Singhal
College of Engineering
State University of New York
Stonybrook, NY 11794

(critically evaluated phase diagrams of Au-Pt, Ag-Pt, and some mixed oxide systems exhibiting metal-non metal transitions).

C. Smithells
Butterworths Publishers, Ltd.
London, England

(edits "Metals Reference Book" (5th ed., 1976) containing phase diagrams of many binary and some hydrogen-metal alloys, and a bibliography on ternary, quaternary, and higher-order alloy diagrams).

K. Spear
Materials Research Laboratory
Pennsylvania State University
University Park, PA 16802

(critical compilation of binary B-X diagrams, including predictions from electronic considerations, where experimental data are lacking; also see paper p. 744).

VINITI (see under A. I. Mikhailov)

A. E. Vol
Novocherkaskiy Prospekt Dom 20, Kvartia 31
Leningrad K-272
USSR

(has prepared three volumes of critically evaluated phase diagrams and other physical properties for binary systems. Volumes 4 and 5 are in preparation; see p. 346, and see entries in Appendix C).

R. W. Waterstrat (American Dental Association)
Polymers Division
National Bureau of Standards
Washington, DC 20234

(evaluates binary phase diagrams of Pt-group alloys with V, Cr, Nb and Ta metals, begun in 1969; a chart of certain transition metal combinations to be published).

N. Yukawa
Dept. of Metallurgy
Nagoya University
Nagoya, Japan

(have critically evaluated phase diagram of Cr-Ni to be applied to evaluation of up to quaternary Cr and Ni systems; results will appear in J. Inst. Met. Jap.).

Appendix B

CALPHAD Members: This group (CALculations of PHase Diagrams) does computer predictions of phase diagrams using thermodynamic data bases. They meet about once a year and are currently producing a journal "CALPHAD", L. Kaufman general editor (see Appendix C for a complete citation).

- B. S. Achar; P. O. Research Stn., London, England
- I. Ansara; Inst. Nat. Polytechnique, Grenoble, France
- C. Bernard; Inst. Nat. Polytechnique, Grenoble, France
- T. G. Chart; Nat. Phys. Lab., Teddington, England
- J. Counsell; Tech. Hochschule, Aachen, Germany
- M. Hillert; Royal Inst. of Technology, Stockholm, Sweden
- G. Inden; Max-Planck Inst. für Eisenforschung, Düsseldorf, Germany
- L. Kaufman; ManLabs, Inc., Cambridge, MA, USA
- G. Kirchner; Metallwerk Berndorf, Berndorf, Austria
- O. Kubaschewski; Tech. Hochschule, Aachen, Germany
- C. Lupis, Carnegie-Mellon University, Pittsburgh, PA, USA
- A. P. Miodownik; University of Surrey, Guilford, England
- H. Nesor; ManLabs, Inc., Cambridge, MA, USA
- W. Pitsch; Max-Planck Inst. für Eisenforschung, Düsseldorf, Germany
- M. Rand; Atomic Energy Agency, AERE Harwell, England
- D. Spencer; Tech. Hochschule, Aachen, Germany

Appendix C

Compilations of Phase Diagram and Related Data

Prepared by D. J. Kahan, G. C. Carter, and L. H. Bennett

Alloy Data Center, NBS

(April 1977)

This compilation of existing phase diagram data compilations is prepared to be comprehensive for the subject of alloy phase diagrams only. Any suggested additions to this listing would be gratefully received. At the end of this compilation, a separate list of several thermodynamic tables is given, followed by a list of several crystallographic data compilations and a short list of some textbook treatments, theory and review. One of these latter lists are intended to be complete, nor do they repeat any of the pertinent entries that already appear in the phase diagram compilation list.

References are grouped into four sections: I (Phase Diagram Data Compilations), II (Thermodynamic Data Compilations), III (Crystallographic Data Compilations) and IV (Phase Diagrams - Theory and Review).

Assistance from our colleagues in bringing several compilations to our attention is gratefully acknowledged. Among these contributions are J. H. Westbrook, E. M. Savitskii, and I. Ansara.

I. Phase Diagram Data Compilations

Ageev, N. V., editor

Phase Diagrams of Metallic Systems

(A non-critical, comprehensive compilation of binary and ternary phase diagrams issued annually from Volume 1, for the 1955 literature (published in 1959) through Volume 20, for the 1974 literature (published in 1976); Volumes 21 and 22 in preparation; text in Russian; available from Prof. A. I. Mikhailov, Director, 125219 Institute for Scientific Information (VINITI) Academy of Sciences of the U.S.S.R. Baltijskaya UL, No. 14 Moscow, USSR.

Subscriptions must be applied for in the several months preceding the year for which the subscription is intended. A cumulative index translated in English is included into these workshop proceedings on p. 1237.

Phase Diagram Data Compilations

- Ageev, N. V.
Ivanov, O. S., editors
- Phase Diagrams of Metallic Systems, published by "Nauka", Moscow, 1971. Text in Russian.
(Several review papers cover data on a large number of binary and ternary diagrams.)
- Ageeva, D. L.
Shvedov, L. V.
- Phase Diagrams of Non-Metallic Systems (Oxides and Silicides of Metallic Elements), published by VINITI, Moscow, approximately annually since 1966 (most recent issue = 11, 1976). Text in Russian. Availability as in first entry.
(Phase diagrams for ternary metal-metal-oxygen systems, and for mixed oxide and oxide-silicide systems.)
- Alisova, A. P.
Budberg, P. B.
- Constitutional Diagrams of Metal Systems, English translation of Vol. 13 (1970) of Ageev's compilation (see above); available from NTIS as document AD 746,792.
- American Society for Metals
- Aluminum (A 3-volume set edited by K. R. van Horn and published by the American Society for Metals, Metals Park, Ohio, 1967.)
(28 binary, 19 ternary, and 4 quaternary diagrams are collected in an appendix; all are taken from other compendia.)
- American Society for Metals
- Metals Handbook (8th edition), Vol. 8: Metallography, Structures, and Phase Diagrams, edited by D. T. Hawkins and R. Hultgren (binaries) and by L. Brewer and S.-G. Chang (ternaries) and published by the American Society for Metals, Metals Park, Ohio, 1973.
(Approximately 400 binary and 50 ternary phase diagrams.)
- Badaeva, T. A.
- The Structure of Thorium Alloys, published by "Nauka", Moscow, 1968. Text in Russian.
(A compilation of phase diagrams, sometimes accompanied by crystallographic, metallographic, or hardness information, for 64 binary and 30 ternary Th alloy systems. A periodic chart on a large fold-out page summarizes the binary alloy diagrams.)

Phase Diagram Data Compilations

- Baikov Institute Diagrams of Ternary Metallic Systems (reference bibliography, 1972), published by the Institute of Metallurgy, Baikov Institute (Moscow), 1972. Text in Russian. (This bibliography covers papers published from 1910 to 1969; references are printed in their source language, mostly English and Russian, and listed by system; systems covered are listed in both Russian and English indexes; no diagrams.)
- Battelle Memorial Institute Cobalt Monograph, Battelle Memorial Institute, Columbus, Ohio, 1960. (Phase diagrams of 18 binary, 19 ternary, and a few higher order Co alloys; all of the binary diagrams are taken from Hansen.)
- Berezhnoi, A. S. Silicon and Its Binary Systems, published in Russian by Academy of Sciences of the Ukrainian SSR, Kiev (1958) and available in English translation from Consultants Bureau, New York, 1960. (Phase diagram and crystallographic structure data are systematically presented for most of the binary silicon alloys.)
- Brewer, L. Metals Handbook. (See under American Society for Metals.)
- Brewer, L. Molybdenum: Physico-Chemical Properties of Its Compounds and Alloys. (See under Kubaschewski.)
- Butts, A.
Coxe, C. D. Silver - Economics, Metallurgy, and Use, (Van Nostrand, New York, 1967) (21 binary and 14 ternary phase diagrams of Ag alloys; most of the binary diagrams have been taken from Hansen.)
- Campbell, I. E.
Sherwood, E. M., editors High-Temperature Materials and Technology (J. Wiley, New York, 1967) (A chapter on carbides includes a discussion of their crystallography and a small compilation of binary and ternary diagrams.)

Phase Diagram Data Compilations

- Cannon, J. F. Behavior of the Elements at High Pressures, an article in J. Phys. Chem. Ref. Data 3, 781, 1974.
(A critical compilation of P-T phase diagrams and crystal structure data for the elements; 431 references to the literature.)
- Carlson, O. N.
Stevens, E. R. A Compilation of Thorium Binary Phase Diagrams (published by Iowa State University as report No. IS-1752, 1968).
(phase relationships are discussed for 60 binary Th alloys; phase diagrams are given for most).
- Carter, G. C.
Bennett, L. H.
Kahan, D. J. Metallic Shifts In NMR, published in "Progress in Materials Science" 20, 1-2350 by Pergamon Press, Elmsford, N.Y. (1977).
(Phase diagrams are included for those binary systems for which critical NMR Knight shift evaluations have been prepared. The ~ 800 binary diagrams have mostly been taken from the Hansen, Elliott and Shunk compilations (q.v.) and, occasionally, from other compilations, or original papers. Where diagram sections were available from different sources, these are condensed into a single diagram; all diagrams redrawn in a uniform format.)
- Centre Nationale de la Recherche Scientifique Index Thermochimique (Issued monthly since 1964 by the Centre d'Information de Thermodynamique Chimique Minerale, Grenoble.) Text in French.
(Bibliography of thermodynamic papers, including some on phase diagrams.)
- Chang, S.-G. Metals Handbook. (See under American Society for Metals.)
- Diehl, J.
Schilling, W.
Schumacher, D., organizing comm. International Conference on Vacancies and Interstitials in Metals, a 2-volume set of preprints of papers contributed to the conference (Sept. 1968), and available from the central library of the Kernforschungsanlage Jülich GmbH, Jülich, Germany. All papers are in English.
(A substantial amount of constitution-related data on vacancies and interstitials in metals is given; more than 900 pages.)

Phase Diagram Data Compilations

Supplement: "Gases and Carbon In Metals" (Fromm, E., Jehn, H. and Horz, G.) published by ZAED (Center for Atomic Energy Documentation Karlsruhe, Germany) as data compilation 5-1 (1976).

Giessen, B. C., editor

Developments in the Structural Chemistry of Alloy Phases, based on AIME Symposium held in 1967 (Published by Plenum Press, New York, 1969). (Several articles review the crystallography, packing, and other properties of metallic phases; one article reviews the occurrence of metastable phases in binary alloys, and presentation of this information.)

Gittus, J. H.

Uranium (A volume in the "Metallurgy of the Rarer Metals" series, Butterworths and Co., London, 1963.) (More than 40 binary phase diagrams and 5 ternary phase diagrams of U alloys are compiled from various papers and evaluations.)

Gmelin, L., first editor

Gmelins Handbuch der Anorganischen Chemie (many volumes published, starting in 1817), available from Springer-Verlag, New York. Text in German. (Single elements, or groups of similar elements, are treated in separate volumes; evaluated data include thermodynamic properties of the elements and their compounds and, in some volumes, phase diagrams.)

Gmelin, L., first editor

Gmelins Handbuch der Anorganischen Chemie - Zinn (Teil D, Legierungen, 1974), available from Springer-Verlag, New York. Text in German. (Data on a wide spectrum of physical properties, including crystallographic and thermodynamic, are compiled for binary, ternary, and some higher-order Sn alloys; phase diagrams are presented for many alloy systems; references cited throughout the text.)

Phase Diagram Data Compilations

- Gmelin, L., first editor Gmelins Handbuch der Anorganischen Chemie - Zirkonium (1958), available from Springer-Verlag, New York. Text in German.
(The compilation of data on the physical, chemical, mechanical, and thermodynamic properties of Zr alloys and compounds occupies a major portion of the book. Phase diagrams and crystallographic information are presented for many binary Zr-metal and Zr-metalloid systems. References cited throughout the text.)
- Gschneidner, K. A., Jr. Rare Earth Alloys (Van Nostrand, New York, 1961).
(Contains binary and ternary phase diagrams for some systems containing at least one lanthanide).
- Gschneidner, K. A., Jr. Selected Cerium Phase Diagrams (Published by Iowa State University as report no. IS-RIC-7, 1974.)
(An up-to-date compilation of 19 binary phase diagrams, with bibliographies for each system.)
- Gschneidner, K. A., Jr. Inorganic Compounds and Alloys and Intermetallic Compounds, chapters 8 and 9, respectively, in "Scandium, its Occurrence, Chemistry, Physics, Metallurgy, Biology and Technology (edited by C. T. Horovitz, et al.); published by Academic Press, New York, 1975.
(Thermodynamic properties and phase diagrams are presented for several dozen binary and ternary hydrides, borides, carbides, nitrides, oxides, phosphides, arsenides, sulfides, halides, chalcogenides, and alloys; several hundred references cited).
- Guertler, W.
Guertler, M.
Anastasidas, E. A Compendium of Constitutional Ternary Diagrams of Metallic Systems; original German published in 1958; English translation (1969) available from NTIS as document TT 69-55069.
(A major compilation of ternary systems, containing more than 100 phase diagrams.)
- Hansen, M. Constitution of Binary Alloys (McGraw-Hill, New York, 1958)
(This volume, together with its supplements, constitutes one of the major critical data compilations on binary phase diagrams.)

Phase Diagram Data Compilations

- Haughton, J. L.
Prince, A., editors
- The Constitutional Diagrams of Alloys: A Bibliography (2nd edition), published by the Institute of Metals, London, 1956; a 3rd edition, by A. Prince, (for ternaries only) is nearing completion.
(The bibliography covers the literature (including Soviet work) through the end of 1954, with some 1955 citations included; while the greater portion of the bibliography refers to binary and ternary systems, references are given for alloys with up to 6 components.)
- Hawkins, D. T.
- Metals Handbook. (See under American Society for Metals.)
- Hellwege, K. H. and A. M.
- Landolt-Börnstein Tables (See under Landolt-Börnstein.)
- Hoffman, W.
- Lead and Lead Alloys - Properties and Technology, Springer-Verlag, New York, 1970.
(An extensive treatment of binary and ternary Pb alloys, including mechanical properties, crystallography, and more than 20 binary and more than 20 ternary phase diagrams.)
- Hultgren, R.
Desai, P. D.
Hawkins, D. T.
Gleiser, M.
Kelley, K. K.
Wagman, D. D.
- Selected Values of the Thermodynamic Properties of the Elements and Binary Alloys (in 2 volumes), (American Society for Metals, Park, Ohio, 1973).
(Evaluated thermodynamic data and phase diagrams, sometimes not found in other compilations, are included for the elements and for many binary alloys.)
- Hultgren, R.
Desai, P. D.
Hawkins, D. T.
Gleiser, M.
- The Metallurgy of Copper, published by INCRA and NSRDS, 1971; available from International Copper Research Assn., New York.
(Approximately 30 phase diagrams, and crystallographic and evaluated thermodynamic data, are given for Cu binary alloys.)
- Hultgren, R.
- Metals Handbook (See under American Society for Metals.)

Phase Diagram Data Compilations

- Int'l. Atomic Energy Agency Atomic Energy Review: Special Issues. The physico-chemical properties of metals and their compounds and alloys.
(On metals important in nuclear reactor technology; see under the general editor, O. Kubaschewski, for complete listing.)
- Int'l. Atomic Energy Agency An 11-volume series presenting critically evaluated thermodynamic data and estimates where data are unavailable (see under the executive editor, F. L. Oetting, in the following section; Thermodynamic Data Compilations).
- Ivanov, O. S. Physical Chemistry of Alloys and Refractory Compounds of Thorium and Uranium, published in Russian by "Nauka", Moscow, 1968; English translation (1972) available from NTIS as document TT 71-50053 or AEC-TR-7212.
(Phase diagrams for some binary Th and binary and ternary U alloys are scattered throughout the text; a bibliography is given for each system.)
- Ivanov, O. S.
Badaeva, T. A.
Sofronova, R. M.
Kishenevskii, V. B.
Kushnir, N. P. Phase Diagrams and Phase Transformations of Uranium Alloys, published by "Nauka", Moscow, 1972. Text in Russian.
(Phase diagrams of more than 60 binary, more than 90 ternary, and about dozen higher-order uranium alloy systems are collected from the literature. Crystallographic information is frequently given, and a bibliography is included.)
- Jänecke, E. Kurzgefasstes Handbuch Aller Legierungen (Published by R. Kiepert, Berlin-Charlottenburg, 1940.) Text in German.
(A systematized treatment of ternary and higher-order alloys is given, including over 800 phase diagrams and 80 tables.)
- Jones, H.
Suryanarayana, C. Rapid Quenching from the Melt: An Annotated Bibliography 1958-72, an article in J. Matl. Sci. 8, 705-753, 1973.
(This comprehensive bibliography lists several hundred papers on the subject, together with an index by alloy.)

Phase Diagram Data Compilations

- Klement, W. Phase Relations and Structures of Solids at High Pressures (A chapter in "Progress in Solid State Chemistry" 3, 289-376, 1967, edited by H. Reiss.) (Review of high-pressure phases of the elements and phase diagrams for elements at high pressures.)
- Kornilov, I. I. Physico-Chemical Basis of Heat Resistant Alloys, published by Izdatel'stvo Akad. Nauk, Moscow, 1961. Text in Russian. (Phase diagram information on systems with up to 7 components is scattered throughout the text.)
- Kornilov, I. I. The Chemistry of Metallides, published in Russian by "Nauka", Moscow, 1964; available in translation (1966) from Consultants Bureau, New York. (Data on the chemical properties and phase equilibria of metal-metallide compounds are tabulated and reviewed; phase diagrams of many ternary and higher-order systems are shown; 267 references cited.)
- Kornilov, I. I.
Matveeva, N. M. Metallides, published by "Nauka", Moscow, 1971. Text in Russian. (This collection of review papers includes a considerable amount of phase diagram and crystallographic data, especially for light metal systems.)
- Kotel'nikov, R. B.
Bashl'kov, S. N.
Galiakborov, E. G.
Kashtanov, A. I. Especially High-Melting Elements and Compounds, published by "Metal-lurgiya", Moscow, 1969. Text in Russian. (Data on crystallographic, thermo-dynamic, electron transport, diffusion and other properties of transition elements, their alloys and metalloid intermetallic compounds are summarized; additional data, including phase diagrams for binary and ternary systems, comprises the greater portion of the book.)

Phase Diagram Data Compilations

Kubaschewski, O., editor

Atomic Energy Review: Special Issues, published by the International Atomic Energy Agency and available from UNIPUB, Inc., New York.

Plutonium: Physico-Chemical Properties of its Compounds and Alloys, by M. H. Rand, D. T. Livey, P. Feschotte, H. Nowotny, K. Seifert and R. Ferro; Special Issue No. 1 (1966).

(13 phase diagrams, plus crystallographic data and thermodynamic information, are compiled for binary Pu alloys.)

Niobium: Physico-Chemical Properties of its Compounds and Alloys, by V. I. Lavrentev, Ya. I. Gerassimov, P. Feschotte, D. T. Livey, O. Von Goldbeck, H. Nowotny, K. Seifert, R. Ferro and A. Dragoo; Special Issue No. 2 (1968).

(Phase diagrams, crystallographic data and thermodynamic information are compiled for approximately 20 binary and some ternary Nb alloys.)

Tantalum: Physico-Chemical Properties of its Compounds and Alloys, by Ya. I. Gerassimov, V. I. Lavrentev, O. Von Goldbeck, D. T. Livey, R. Ferro, and A. L. Dragoo; Special Issue No. 3 (1972).

(17 phase diagrams, plus crystallographic data and thermodynamic information, are compiled for binary Ta alloys.)

Beryllium: Physico-Chemical Properties of its Compounds and Alloys, by P. J. Spencer, O. Von Goldbeck, R. Ferro, K. Girgis, and A. L. Dragoo; Special Issue No. 4 (1973).

(16 phase diagrams, plus crystallographic data and thermodynamic information, are compiled for binary Be alloys.)

Phase Diagram Data Compilations

Kubaschewski, O., editor
(continued)

Thorium: Physico-Chemical Properties of its Compounds and Alloys, by M. H. Rand, O. Von Goldbeck, R. Ferro, K. Girgis and A. L. Dragoo; Special Issue No. 5 (1975).

(Phase diagrams, crystallographic data and thermodynamic information are compiled for approximately 50 binary Th alloys.)

Zirconium: Physico-Chemical Properties of its Compounds and Alloys, by C. B. Alcock, K. T. Jacob, S. Zador, O. Von Goldbeck, H. Nowothy, K. Seifert, and O. Kubaschewski; Special Issue No. 6 (1976).

(Review of 65 binary systems, including 46 phase diagrams; chemical, thermodynamic, diffusion and crystallographic data for Zr binary alloys and compounds are compiled.)

Molybdenum: Physico-Chemical Properties of its Compounds and Alloys, by L. Brewer; Special Issue No. 7 (to be published). Future compilations in this series are planned for Hafnium and Titanium.

Landolt-Börnstein

Landolt-Börnstein Tables - Zahlenwerte und Functionen aus Physik, Chemie, Astronomie, Geophysik und Technik; available from Springer-Verlag, New York.

Relevant data are contained in the following volumes:

I Band 4. Teil: Kristalle, 1955 (in German). (Includes data on crystal structures and lattice parameters of metals, alloys (mainly binary) and intermetallic compounds.)

II Band 2. Teil: Eigenschaften der Materie in Ihren Aggregatzuständen.
a) Gleichgewichte Dampft - Kondensat und Osmotische Phänomene, 1960 (in German).

(Includes data on vapor pressures for the metals and some binary alloys, phase diagrams for binary alloys (also as a function of pressure) with information on some of the thermodynamic quantities related to phase transitions.)

Phase Diagram Data Compilations

b) Lösungsgleichgewichte I, 1962
(in German).
(Thermodynamic properties, such as solubilities of gases in metals and alloys, are given in this volume; also for the liquid phase.)

II Band 3. Teil: Schmelzgleichgewichte und Grenzflächenerscheinungen, 1959
(in German).
(Includes a section on binary and ternary phase diagrams; lattice constants and discussions are not given.)

Levin, E. M.
Robbins, C. R.
McMurdie, H. F.

Phase Diagrams for Ceramists (1964), first supplement (1969), and second supplement (1975); third supplement envisioned; all published by the American Ceramic Society, Columbus, Ohio 43214.
(Evaluated phase diagrams are given for approximately 5,000 oxide, halide, salt and other ceramic systems, ranging from binaries to systems with six components; literature references cited for each diagram.)

Levinskii, Yu. V.

Phase Diagrams of Metals with Gases, published by "Metallurgiya", Moscow (1975). Text in Russian.
(Metal-gas equilibria as functions of temperature and pressure are reviewed; phase diagrams are given for 23 metal-hydrogen, 7 metal-nitrogen, and 6 metal-oxygen systems; more than 300 references cited.)

Ludwick, M. T.

Indium, published by Indium Corporation of America, Utica, New York, 1959.
(Contains phase diagrams for binary, ternary, and higher order In systems.)

Miller, G. L.

Zirconium (A volume in the "Metallurgy of the Rarer Metals" series, Butterworths & Co., London, 1975.)
(Approximately 30 phase diagrams of Zr alloys are compiled from various papers and evaluations.)

Miller, G. L.

Tantalum and Niobium (A volume in the "Metallurgy of the Rarer Metals" series, Butterworths & Co., London, 1959).
(Approximately 40 phase diagrams of Ta alloys and of Nb alloys are compiled from various papers and evaluations.)

Phase Diagram Data Compilations

- Moffatt, W. G., editor
Handbook of Binary Phase Diagrams, 1970 and 1972, published in 1976 and available from Business Growth Services, General Electric Co., 1 River Road, Schenectady, NY 12345.
(This 2-volume loose-leaf compilation includes phase diagrams for more than 600 binary alloys not contained in or updated from the Hansen-Elliott-Shunk series; no crystallographic data are noted; references cited; includes a permuted alloy index indicating coverage of each system in Hansen, Elliott, Shunk and this compilation; semi-annual updating is projected.)
- Molchanov, Y. K.
Atlas of Diagrams of State of Titanium Alloys, Translated from the Russian (1964) and available from NTIS as document AD 670,090 (1967); also available as Phase Diagram of Titanium Alloys, E. K. Molchanova, edited by G. S. Glazunov. (Translated by the Israel Program for Scientific Translations, Jerusalem, 1965.)
(Extensive compilation of binary and ternary Ti phase diagrams.)
- Mondolfo, L. F.
Metallography of Aluminum Alloys (J. Wiley and Sons, New York, 1943.)
(Many binary, ternary and quaternary phase diagrams are given, with references to the original literature.)
- Mondolfo, L. F.
Aluminum Alloys: Structure and Properties (Butterworths & Co., Boston and London, 1976.) (A major data compilation on Al metal and its binary and higher order alloys; evaluated phase diagrams, together with some chemical, physical and technological properties are reviewed; more details are presented for pure and commercial Al metal than the alloys. Evaluated phase diagram and crystallographic, mechanical, physical and corrosion behavior for approximately 70 binary Al alloys are given; crystallographic and (sometimes) phase diagram data for several hundred ternary and well-characterized higher order alloys are given; literature references are included throughout the text; a 971 page handbook.)

Phase Diagram Data Compilations

- Mieller, W. M.
Blackledge, J. P.
Libowitz, G. G. Metal Hydrides, published by Academic Press, New York, 1968. (Phase diagrams are presented for many binary and some ternary metal-hydrogen systems. Several pressure-composition isotherms, solubilities and other property data are tabulated throughout the text.)
- Newkirk, H. A Literature Survey of Metallic Ternary and Quaternary Hydrides, available from NTIS as document number UCRL-51244, Revision 1 (1975). (Several figures of pressure-composition and pressure-temperature relations and some phase diagrams are given.)
- Northcott, L. Molybdenum (A volume in the "Metallurgy of the Rarer Metals" series, Butterworths & Co., London, 1956.) (Phase diagrams of 13 binary and a few ternary Mo alloys are compiled from various papers and evaluations.)
- Pascal, P., editor Nouveau Traité de Chimie Minérale Vol. 20, in 3 parts; published by Maison & Cie, Paris, 1962-64. Text in French. (Both binary and ternary phase diagrams are discussed; liberal reference listings; Part I: alloys of alkali, alkaline earth and light metals, and light metal - refractory metal alloys. Part II: alloys of Cu, Ag, Au and precious metal, refractory transition metal, and low melting alloys. Part III: alloys of Co, Fe, Mn, Ni, Th, U and transuranium metal, refractory transition metal and rare earth metal alloys.)
- Prince, A. Constitutional Diagrams of Alloys: Bibliography. (See under Haughton.)
- Prokoshkin, D. A.
Vasil'eva, E. V. Alloys of Niobium, edited by A. M. Samarian; published in Russian by "Nauka", Moscow (1964) and available in translation from the Israel Program for Scientific Translations, Jerusalem, 1965. (Phase diagrams, crystallography and thermodynamic data are found throughout the book.)

Phase Diagrams Data Compilations

- Rajput, B. K.
George, A. M.
Karkhanavala, M. D.
- Binary Metal-Oxygen Phase Equilibrium Diagrams and Crystallographic Data, published by the Indian Atomic Energy Commission, Bombay, as document BARC-653 (1972) and available from the Bhabha Atomic Research Centre, Bombay. (A compilation of phase equilibrium and crystallographic data.)
- Raynor, G. V.
- Compilation of Mg Alloy Phase Diagrams (not exact title); to be published in Int'l. Met. Rev. (1977). (A phase diagram compilation of binary, ternary and quaternary Mg alloys.)
- Reed, R. P.
Breedis, J. F.
- Low-Temperature Phase Transformations, (published by ASTM as STP No. 387 (1966); available from the American Society for Testing Materials, Philadelphia. (Low-temperature phase transformations are reviewed for alloys, including some ternary and higher-order systems.)
- Rough, F. A.
Bauer, A. A.
- Constitutional Diagrams of Uranium and Thorium Alloys, prepared at Battelle Memorial Institute and published by Addison-Wesley, Reading, MA (1958). (Phase diagrams and descriptive text are given, together with crystallographic data for more than 100 binary and 18 ternary systems.)
- Rudy, E.
- Ternary Phase Equilibria in Transition Metal-Boron-Carbon-Silicon Systems - Part V. Compendium of Phase Diagram Data (originally published as Technical Report AD 689,843, 1969), available from NTIS as document no. AFML-TR-65-2, Part V. (Phase diagrams and, in most cases, lattice parameters are compiled for over 50 binary, 36 ternary and four quaternary Ta₂C-X-Y alloys; a bibliography is included for each system; 689 pages.)
- Samsonov, G. V.
- Refractory Compounds, published by "Metallurgizdat", Moscow (1963). Text in Russian. (Data for crystallographic, physical, thermodynamic and mechanical properties are compiled; about 60 binary phase diagrams presented; 1100 references.)

Phase Diagram Data Compilations

- Samsonov, G. V., editor Aluminides, published by "Naukova Dumka", Kiev (1965). Text in Russian. (Phase equilibria data are presented for most binary, 69 ternary, 12 quaternary and 4 quintary alloy systems; copy not received by ADC - annotation by J. Westbrook.)
- Samsonov, G. V. Beryllides, published in Russian (1966), English translation available from NTIS as document no. JPRS 43,479 (1967). (Lattice constants are given for metal-beryllium compounds, and some phase diagrams are included.)
- Samsonov, G. V. The Oxide Handbook, published in Russian by "Metallurgiya", Moscow (1969); English translation (1973) available from Plenum Press, New York. (One chapter is devoted to presentation of metal-oxygen phase diagrams.)
- Samsonov, G. V. Nitrides, published by "Naukova Dumka", Kiev (1969). Text in Russian. (Crystallographic and thermodynamic data and many phase diagrams scattered throughout the text; more than 1,100 references.)
- Samsonov, G. V., editor Refractory Carbides, published in Russian by "Naukova Dumka", Kiev (1970); English translation (1974) available from Plenum Press, New York. (Preparation, properties and uses of refractory carbides are reviewed; crystallographic and thermodynamic properties for several (binary) carbides are compiled; phase diagrams of C-Mo-Ti, C-Ta-V, and C-Nb-Re are described.)
- Samsonov, G. V. Magnesides, published by "Naukova Dumka", Kiev (1971). Text in Russian. (A comprehensive review of both binary and ternary systems, including crystallographic data and phase diagrams; more than 1,400 references.)

Phase Diagram Data Compilations

Samsonov, G. V.
Bondarev, V. N.

Germanides, published in Russian by "Metallurgiya", Moscow (1968); English translation (1969) available from Plenum Publishing Corp., New York. (A comprehensive review of binary and ternary Ge alloys includes data on phase diagrams, crystallographic and thermodynamic properties; nearly 500 references are cited.)

Samsonov, G. V.
Markovskii, L. Ya.
Zhigach, A. F.
Valyashko, M. G.

Boron, Its Compounds and Alloys, published by the Academy of Sciences of the Ukrainian SSR, Kiev (1960) and available, in English translation, in 2 volumes, from NTIS as document no. AEC-TR-5032, Books I and II. (Constitutional and physical properties of binary, ternary and a few higher-order metal-boron alloys and compounds; phase diagrams and tables of various physical properties are scattered throughout the text; a bibliography cites over 500 references.)

Samsonov, G. V.
Portnov, K. I.

Alloys Based On High-Melting Compounds, published in Russian by "Oborongiz", Moscow (1961); translation available from NTIS as document no. AD 283,859 (1962). (Phase diagrams, crystallographic, physical and engineering properties are reviewed for binary alloys of metals with B, C, N or Si and for higher-order systems based on these alloys; binary systems formed between the non-metallic elements are also discussed; more than 316 references cited.)

Samsonov, G. V.
Serebryakova, T. I.
Neronov, V. A.

Borides, published by "Atomizdat", Moscow (1975). Text in Russian. (Phase diagrams of many binary boron systems and tables summarizing physical and thermodynamic properties for selected boron compounds are scattered throughout the text; a bibliography cites over 1,000 references.)

Samsonov, G. V.
Upadkhaya, G. Sh.
Neronov, V. S.

Physical Metallurgy of Carbides, published by "Naukova Dumka", Kiev (1974). Text in Russian. (Crystallographic data and many binary and ternary phase diagrams are scattered throughout the text.)

Phase Diagram Data Compilations

- Savitskii, E. M., editor Phase Diagrams of Metallic Systems, published by "Nauka", Moscow (1968). Text in Russian.
(Phase diagram and crystallographic data are reviewed for binary and ternary systems between IVA, VA and VIA group metals; systems based on these metals, but including an element from elsewhere in the periodic table, are presented, also.)
- Savitskii, E. M.
Baron, V. V.
Efimov, Yu. V.
Bychkova, M. I.
Myzenkova, L. F. Superconducting Materials, published in Russian by "Nauka", Moscow (1969); English translation (1973) available from Plenum Press, New York.
(Phase diagrams and crystallographic data for binary and ternary alloys showing superconducting behavior are reviewed in a chapter; 309 references.)
- Savitskii, E. M.
Burkhanov, G. S. Physical Metallurgy of Refractory Metals and Alloys, published by "Nauka", Moscow (1967); English translation (1970) available from Plenum Press, New York.
(Phase diagrams, crystallographic, some thermodynamic and other physical property data are given; most of the phase diagram data are found in Chapters II and III, largely for binary diagrams, some ternary diagrams and a quaternary Mo-Nb-W-Zr diagram; bibliographies follow each chapter, 287 pages.)
- Savitskii, E. M.
Polyakova, V. P.
Tylkina, M. A. Palladium Alloys (1967), translated from the Russian and published by Primary Sources, New York, 1969.
(Most of this book is devoted to a review of Pd metal and its binary and ternary alloys; assorted mechanical and physical property data are also given for many systems.)
- Savitskii, E. M.
Polyakova, V. P.
Gorina, N. B.
Roshan, N. R. Physical Metallurgy of the Platinum Metals, published by "Metallurgiya", Moscow (1975). Text in Russian; English translation to be published by "MIR", Moscow (1977).
(Several Pt metal phase diagrams are collected in one section of the book.)

Phase Diagram Data Compilations

- Savitskii, E. M.
Terekhova, V. F.
Burov, I. V.
Markov, I. A.
Naumkin, O. P.
- Rare Earth Alloys, published in Russian by the Academy of Sciences of the USSR, Moscow (1962); English translation available from NTIS as document AEC-TR-6151.
(Binary and ternary phase diagrams of alloys containing a rare earth component are reviewed; tables of physical, chemical and mechanical property data are given; extensive bibliographies follow each chapter.)
- Savitskii, E. M.
Tylkina, M. A.
Povarova, K. B.
- Rhenium Alloys, published in Russian by "Nauka", Moscow (1965); English translation available from NTIS as document no. 69-55081.
(26 binary and 15 ternary Re phase diagrams are compiled, together with a general discussion of the Re diagrams.)
- Schwartzkopf, P.
- Refractory Hard Metals; Borides, Carbides, Nitrides, (and) Silicides, (Macmillan, New York, 1953).
(Phase diagram and crystallographic information is given for some of these materials.)
- Selle, J.
- Summary of Binary Phase Diagrams, prepared at the Mound Laboratory of Monsanto Research Corporation (1970).
(This large color wall chart shows the degree of solubility, number of intermetallic compounds, number of eutectics and other information for binary alloys.)
- Shunk, F. A.
- Constitution of Binary Alloys, Second Supplement (McGraw-Hill, New York, 1969)
(Continuation of Hansen's compilation; see under Hansen.)
- Shunk, F. A.
- Constitution of Alloys, a series of IIT reports (May 1972) updating sections of the Hansen series: Vols. 1A (systems Ac-H through Ag-Zr), 1B (Al-Am through Ar-U), 1C (As-Au through Au-Zr) and 2 (miscellaneous systems from B-Hg through Ge-Re); available from the Illinois Institute of Technology, Chicago.

Phase Diagram Data Compilations

Smithellas, C. J., editor
Brandes, E. A. asst. ed.

Metals Reference Book (5th edition, Butterworths & Co., Boston and London, 1976.)

(This summary of various data on alloys includes more than 300 binary phase diagrams (with literature references), bibliographies on more than 500 ternary and more than 50 quaternary alloy systems, and data on the solubility of gases in metals.)

Sōmiya, S.

Zirconia Bearing Refractories, published in "Kogyo Zairyo no Shinpo" (Progress of Engineering Materials): pages 201-234 (1964). Text in Japanese. (23 phase diagrams, and 7 liquidus curves for binary and/or pseudo-binary systems and 29 phase diagrams and phase relation figures for ternary systems of zirconia or zircon are described.)

Sōmiya, S.
Hashimoto, K.-I.

Glossary for the Phase Diagrams, published in "Seramikkus" (Ceramics Japan) 2 (10), 817-827 (1967). Text in Japanese.

Smith, J. F.
Carlson, O. N.
Peterson, D. T.
Scott, T. E.

Thorium: Preparation and Properties (Iowa State University Press, Ames, Iowa, 1975.)

(Phase diagrams, crystallography and thermodynamics of several binary Th alloys are given in one of chapters.)

Sōmiya, S. editor

Application of Phase Diagrams in Refractories, published by the Ceramic Society of Japan (1968). Text in Japanese.
(A 119-page textbook.)

Spedding, F. H.
Daane, A. H.

The Rare Earths, published in 1961; reprinted in 1971 by R. E. Krieger Publishing Co., Huntington, N. Y. (Phase diagrams of nearly 100 binary rare earth-metal alloys are presented; many are taken from Hansen.)

Phase Diagram Data Compilations

- Spear, K. E. Phase Behavior and Related Properties of Rare-Earth Borides, a chapter in "Phase Diagrams: Materials Science and Technology": IV, 91-159, 1976 (A. M. Alper, editor); published by Academic Press, New York.
(Evaluated binary phase diagrams, including predictions from electronic considerations, where experimental data are lacking, are presented for Sc, Y and all of the lanthanide-boron systems; crystal chemistry and electronic structure are reviewed; approximately 150 references cited.)
- Staudhammer, K. P.
Murr, L. E. Atlas of Binary Alloys (Marcel Dekker, New York, 1973)
(This book presents periodic tables of the elements, giving the characteristics of binary phase diagrams between each element in turn and all the other elements (e.g., Co with each of the other elements); information is given on degree of solubility, number of compounds, temperatures of lowest melting eutectic or peritectic and number of eutectics or peritectics; no diagrams are given.)
- Storms, E. K. The Refractory Carbides (Academic Press, New York, 1967)
(Phase diagrams, crystallography and thermodynamic properties, among others, are described for several refractory metal-carbon systems.)
- Sully, A. H. Manganese (A volume in the "Metallurgy of the Rarer Metals" series, Butterworths & Co., London, 1955.)
(Phase diagrams of approximately 30 binary and a few ternary Mn alloys are compiled from various papers and evaluations.)
- Sully, A. H.
Brandes, E. A. Chromium (A volume in the "Metallurgy of the Rarer Metals" series, 2nd edition, Plenum Press, New York, 1967.)
(Phase diagrams of 24 binary and 5 ternary Cr alloys are compiled from various papers and evaluations.)

Phase Diagram Data Compilations

Tananaev, I. V., editor

Physico-Chemistry of Rare Metals, published in Russian by "Nauka", Moscow (1972); English translation (1974) available from NTIS as document TT 73-58025 or AEC-TR-7409.

(Review chapters on the theory and application of metals and alloys have been contributed by different authors; electrical, thermodynamic and other properties are treated; one chapter is devoted to computer prediction of phase diagrams. Phase data are scattered throughout the text of 324 pages. This collection is in dedication to E. M. Savitskii, and represents the subjects in physico-chemistry and physical metallurgy he has investigated throughout his career.)

Terekhova, V. F.
Savitskii, E. M.

Yttrium - Properties, Phase Diagrams, Industrial Applications, published in Russian by "Nauka", Moscow (1967); English translation available from NTIS as document no. AEC-TR-6980 (1970).

(Phase diagrams, crystallographic, physical and mechanical property data are compiled for many binary and a few ternary Y alloys. Elemental Y metal is treated in great detail; 280 literature references cited.)

Thoma, R. E., editor

Phase Diagrams of Nuclear Reactor Materials, available from NTIS as ORNL report 2548 (15th edition, 1959.)

(Phase diagram compilation giving Zr-rich binary diagrams with Ag, In, Sb and Pb as minority component, five alkali-metal-halide systems, and many non-metallic binary and multicomponent diagrams.)

Toth, L. E.

Transitional Metal Carbides and Nitrides (Academic Press, New York, 1971.)

(One chapter is devoted to phase diagrams; other chapters include crystallography, thermodynamic and other physical and engineering properties.)

Phase Diagram Data Compilations

- Valignat, N. Bibliographie Nb 2. Diagrammes de Phases et Structure des Systemes a base de Niobium, published by the Laboratoire de Thermodynamique et Physico-Chimie Metallurgiques de Grenoble, 1970. Text in French. (This bibliography lists references to work on phase diagrams and crystallography in a large number of binary and ternary Nb alloys.)
- van Horn, K. R. Aluminum (See under American Society for Metals.)
- Vines, R. F. The Platinum Metals and Their Alloys (Edited by E. M. Wise; published by the Intl. Nickel Co., New York, 1941.) (Phase diagrams for a few of these alloys are given.)
- Vol, A. E. Handbook of Binary Metallic Systems - Structures and Properties, Vol. 1 (1959) and Vol. 2 (1962), available in English translation from NTIS as documents TT-66 51149 and TT-66 51150 (1966), respectively; Vol. 3 (co-authored with I. K. Kagan) published by "Nauka", Moscow (1976), translation requested by the ADC; Volumes 4 and 5 in preparation. (A major compilation of phase diagrams and data on physical, mechanical and chemical properties of binary alloys; Vol. 1: alloys of Ac, Al, Am, B, Ba, Be and N. Vol. 2: alloys of Bi, Dy, Eu, Fe, Ga, Gd, Ge, H, Hf, Ho, V and W. Vol. 3: alloys of Au, In, Ir, Y and Yb. Vol. 4: alloys of Ca, Cd and K. Vol. 5: alloys of Co, O and Si.)
- Vol'skii, A. N.
Sterlin, Y. M. The Metallurgy of Plutonium, published in Russian by "Nauka", Moscow (1967) and available in English translation from NTIS as document no. TT-70-500004. (Pu binary and ternary alloy phase diagrams are compiled in this book.)
- Wang, F. E. Superconducting Critical Temperature, T_c , and Phase Equilibrium Diagram of A_3B (β -W) Type Compounds, an article in J. Phys. Chem. Sol. 35, 273-278, 1974.

Phase Diagram Data Compilations

(Phase diagrams (copied from the Hansen series) are presented for 23 systems in which a superconducting A_3B type compound is formed; superconducting transition temperatures are correlated with the solid solubility ranges of the A_3B compounds.)

Zhavoronkov, N. M., editor

Chemistry of Metallurgical Alloys,
published by "Nauka", Moscow (1973).
Text in Russian.

(Phase diagrams, crystallography and data on physical properties of binary and ternary systems are reviewed in several chapters.)

II. Thermodynamic Data Compilations

Bayanov, A. P.

Thermodynamics of the Interaction of the Lanthanides With Other Elements, an article in Russ. Chem. Rev.: 44, #2, 122, 1975.

(Thermodynamic characteristics (Gibbs free energies, enthalpies and entropies) for the interaction of the lanthanides with various elements to form hydrides, borides, carbides, silicides, pnictides, halides, chalcogenides and intermetallic compounds are reviewed.)

Blank, H.

Lindner, R., editors

Plutonium 1975 and other Actinides, Proceedings of the 5th International Conference on Plutonium and other Actinides 1975; published by North-Holland (1976) and available from American Elsevier, New York.

(Papers are presented on thermodynamic and other physical properties; many contributions relate to phase equilibria, though few phase diagrams are presented; nearly 1,000 pages.)

Brewer, L.

The Cohesive Energies of the Elements, published by Lawrence Berkeley Laboratory of the University of California at Berkeley as report LBL-3720 (1975).

(A tabulation of heats of atomization for the elements, extending the earlier work of Hultgren, et al., "Selected Values of the Thermodynamic Properties of the Elements", 1973.)

Eklund, S., editor

Thermodynamics of Nuclear Materials (Proceedings of a Symposium sponsored by the International Atomic Energy Agency in Vienna, 1962 and available from UNIPUB, Inc., New York.)

(Contributed papers on theory and experimental results on thermodynamic properties and phase diagrams of actinide metals and alloys; papers often include binary or multicomponent phase diagrams; especially to be noted is a paper by E. Rudy giving 19 ternary diagrams.)

Elliott, R. P.

Alloying Characteristics of the Rare Earth Elements with the Transition Elements (see in Crystallographic Data Compilations list).

Thermodynamic Data Compilations

- Gluchko, V. P. Thermodynamic Constants of Matter, Vol. VII (for Mn, Tc, Re, Cr, Mo, W, V, Nb, Ta, Ti, Zr and Hf metals and their compounds), published by the Academy of Science of the USSR, VINITI, Moscow (1974).
(Data are tabulated for enthalpies and free energies of formation, room temperature entropies and specific heats and enthalpies and entropies of phase transformations and the temperatures and pressures at which the transformations occur; bibliography not included.)
- Gschneidner, K. A., Jr.
Kippenhan, N. Thermochemistry of the Rare Earth Carbides, Nitrides and Sulfides for Steelmaking (published by Iowa State University as report no. IS-RIC-5, 1971.)
(Heats of formation and free energies for selected rare earth compounds are compiled, in both tabular form (up to 2500 °K) and graphical form (up to 4000 °K); data sources are given in bibliography of 65 references.)
- Gschneidner, K. A., Jr.
Kippenhan, N.
McMasters, O. D. Thermochemistry of the Rare Earths: Part 1 (rare earth oxides), Part 2 (rare earth oxysulfides) and Part 3 (rare earth compounds with B, Sn, Pb, P, As, Sb, Bi, Cu and Ag), (published by Iowa State University as report no. IS-RIC-6, 1973.)
(This report continues report no. IS-RIC-5 (1971) by Gschneidner and Kippenhan (see previous entry); heats of formation and free energies for many rare earth compounds are given in both tabular form (up to 2000-2700 °K) and graphical form (up to 4000 °K); a bibliography cites almost 100 references.)
- Gschneidner, K. A., Jr. Thermodynamic Stability and Physical Properties of Metallic Sulfides and Oxysulfides, a chapter in "Sulfide Inclusions in Steel" (edited by J. J. DeBarbadillo and E. Shape); published by the American Society for Metals, Metals Park, Ohio, 1975.

Thermodynamic Data Compilations

Müller, W.
Blank, H., editors

Heavy Element Properties, Proceedings of the Joint Sessions of the 4th International Transplutonium Element Symposium and the 5th International Conference on Plutonium and other Actinides 1975; published by North-Holland (1976) and available from American Elsevier, New York. (Nuclear, electronic, chemical and thermodynamic properties of the actinide and transplutonium metals and their alloys are reviewed; many data relating to alloy phase stability are presented, though phase diagrams, themselves, are not shown; 125 pages.)

Müller, W.
Lindner, R., editors

Transplutonium 1975, Proceedings of the 4th International Transplutonium Element Symposium (1975); published by North-Holland (1976) and available from American Elsevier, New York. (Papers are presented on nuclear, chemical and physical properties of the transplutonium elements; many contributions relate to thermodynamics of the elements and their compounds; no phase diagrams are presented; nearly 500 pages.)

Oetting, F. L.

The Chemical Thermodynamic Properties of Plutonium Compounds, an article in Chem. Revs. 67, 261-297, 1967. (An evaluation of data for hydrides, carbides, nitrides, oxides, sulfides, sulfates, halides and oxyhalides.)

Oetting, F. L., executive editor
Medvedev, V.
Rand, M. H.
Westrum, E. F., Jr., editors

The Chemical Thermodynamics of Actinide Elements and Compounds, published by the International Atomic Energy Agency and available from UNIPUB, Inc., New York. Volumes within the scope of this compilation are listed below:

Part 1. The Actinide Elements (1976), by F. L. Oetting, M. H. Rand and R. J. Ackermann,

Part 3. Miscellaneous Actinide Materials, by E. H. P. Cordfunke and P. A. G. O'Hare,

Thermodynamic Data Compilations

Part 4. The Actinide Carbides, by C. E. Holley, M. H. Rand and E. K. Storms,

Part 5. The Actinide Pnictides, by K. C. Mills, P. E. Potter and Y. Takahashi,

Part 6. The Actinide Chalcogenides, by J. Drowart, F. Grønvold and E. F. Westrum, Jr.,

Part 7. The Actinide Hydrides, by H. E. Flotow and S. Yamaguchi,

Part 8. The Actinide Alloys, by V. V. Akhachinskij, I. Ansara, P. Chiotti and M. H. Rand,

Part 9. Selected Ternary Systems, by H. Holleck, P. E. Potter and K. E. Spear,

Part 11. The Actinide Oxides, by R. J. Ackermann, F. Grønvold, F. L. Oetting, A. Pattoret and M. H. Rand.

Rand, M. H.
Kubaschewski, O.

The Thermochemical Properties of Uranium Compounds, published by Interscience, New York, 1963. (Thermochemical data are compiled for alloys, hydrides, carbides, oxides, sulfides, halides and uranyl compounds; phase diagrams almost totally absent.)

Reed, T. B.

Free Energy of Formation of Binary Compounds: An Atlas of Charts for High - Temperature Chemical Calculations, published by the MIT Press, Cambridge, MA, 1974.

(Free energies of formation and enthalpy and entropy changes on formation of binary compounds are compiled for metallic hydrides, nitrides, oxides, sulfides, selenides, telurides and halides; data are compiled in both tabular and graphical form; plastic overlays are provided to enable the reader to determine the composition of reacting gases, equilibrium constants, EMF and other thermodynamic quantities directly from the data graphs; data are also

Thermodynamic Data Compilations

compiled for the free energies of ionization of some elements and changes in free energy, enthalpy and entropy of the elements upon condensation. Sources and accuracy of the data are noted in appendices; 35 references cited.)

Stull, D. R.
Prophet, H.

JANAF Thermochemical Tables, 2nd edition, 1971, published as NSRDS-NBS 37 and available from the Government Printing Office, Washington, D. C.; 1974 and 1975 Supplements, edited by M. W. Chase, et al., published in J. Phys. Chem. Ref. Data 3, 311-480, 1974 and 4, 1-175, 1975, respectively; reprints available from the American Chemical Society, Washington, D. C. (Thermodynamic data, including heat capacities, enthalpies and entropies, are tabulated mainly for compounds, but also for some metals.)

Teatum, E. T.
Gschneidner, K. A., Jr.

Compilation of Calculated Data Useful in Predicting Metallurgical Behavior of the Elements in Binary Alloy Systems, available from NTIS as document no. LA-4003 (1968); supersedes LA-2345. (Radii for coordination number 12, atomic volumes, heats of sublimation, electronegativities, melting points and solubility parameters for the elements are tabulated; radius ratios, energy ratios, Mott numbers, Hildebrand factors and electronegativity differences are tabulated for elements as impurities in elemental hosts; 39 references to the literature.)

Voitovich, R. F.

Refractory Compounds (Thermodynamic Characteristics), published by "Naukova Dumka", Kiev (1971). Text in Russian. (Graphical and tabular presentations of the temperature dependences of various thermodynamic quantities.)

Wagman, D. D.
Evans, W. H.
Parker, V. B.
Halow, I.
Bailey, S. M.
Schumm, R. H.

Selected Values of Chemical Thermodynamic Properties (NBS Tech Note 270, sections 3 (Jan. 1968) through 7 (Apr. 1973), sections 1 and 2 superseded; available from NTIS. (Evaluated thermodynamic data for the elements.)

Thermodynamic Data Compilations

- Wagner, C. Thermodynamics of Alloys (Addison-Wesley, New York, 1952).
(Thermodynamic properties are given for some alloys in a chapter of this book.)
- Weibke, F.
Kubaschewski, O. Thermochemistry of Alloys (Thermochemie der Legierungen), published by Springer-Verlag, Berlin, 1943. Text in German.
(Review of experimental and theoretical treatment of the subject; critical compilation of thermochemical properties and often phase diagrams for some 250 binary alloy systems.)
- Westrum, E. F. Bulletin of Thermodynamics and Thermochemistry (Prepared under the auspices of IUPAC and published at the University of Michigan, Ann Arbor.)
(A monthly index to publications on metallic materials, among others.)
- Wicks, C. E.
Block, F. E. Thermodynamic Properties of 65 Elements - Their Oxides, Halides, Carbides, and Nitrides, available from the Government Printing Office, Washington, D.C. as Bureau of Mines Bulletin 605 (1963).
(A data book giving specific heats, enthalpies, entropies, free energies and other thermodynamic functions for about 50 metals and their compounds; 141 references cited.)

III. Crystallographic Data Compilations

- Lam, D. J.
Darby, J. B., Jr.
Nevitt, M. V.
- The Crystal Chemistry of Actinide Compounds, a chapter in "the Actinides: Electronic Structure and Related Properties," edited by A. J. Freeman and J. B. Darby, Jr. II, 119-184, 1974.
(Crystal structure data, lattice parameters, symmetries and atomic positions are compiled for actinide intermetallic compounds; about 80 references cited.)
- Landolt-Börnstein
- Landolt-Börnstein Tables - Zahlenwerte und Functionen aus Physik, Chemie, Astronomie, Geophysik und Technik; available from Springer-Verlag, New York.
Selected Data of Elements and Intermetallic Phases, New Series, Group III, Vol. 6, 1971.
(Tabular compilation of evaluated data on space groups, lattice constants, and (sometimes) magnetic transition temperatures.)
- McMasters, O. D.
Gschneidner, K. A., Jr.
- Rare Earth Intermetallic Compounds, a chapter in the Proceedings of the International Symposium on Compounds of Interest in Nuclear Reactor Technology, 1964 (J. T. Waber, P. Chiotti and W. N. Miner, editors); published by the AIME as Nuclear Metallurgy 10, 93-158, 1964.
(Crystallographic data for rare earth intermetallic compounds are reviewed and tabulated; 164 references cited.)
- Pearson, W. B.
- Handbook of Lattice Spacings and Structures of Metals: Vol. I (1958) and Vol. II (1967); published by Pergamon Press, New York.
(Critical evaluation of space groups and lattice parameters for metals, alloys and intermetallic compounds.)
- Pearson, W. B.
- The Crystal Chemistry and Physics of Metals and Alloys (J. Wiley, New York, 1972)
(600 types of metallic structures are described and their crystal chemistry is discussed.)
- Schubert, K.
- Kristallstrukturen Zweikomponentiger Phasen, published by Springer-Verlag, New York, 1964. Text in German.
(Includes tables of lattice parameters for intermetallic compounds and binary compounds between a metal and a non-metal.)

IV. Phase Diagrams - Theory and Review

- Alper, A. M., editor
Phase Diagrams: Materials Science and Technology, (Academic Press, New York)
(This series is directed towards reviews of phase diagrams as applied to specific practical areas, such as solidification, joining and extractive metallurgy, as well as some more basic considerations. Some reviews of special interest in this list are entered separately; volumes published from 1970 to 1976.)
- American Society for Metals
Theory of Alloy Phases, proceedings of a seminar (1955); published by the American Society for Metals, Metals Park, Ohio, 1956. (A collection of contributed papers on the electronic structure of metals and alloys and its relation to crystallography and phase stability.)
- Bokii, G. B.
Introduction to Crystal Chemistry, published by Moscow University, 1954. Text in Russian. (Alloy crystallography and phase diagrams are reviewed.)
- Brewer, L.
Prediction of High Temperature Metallic Phase Diagrams (proceedings of the Second Berkeley International Materials Conference, edited by V. F. Zackay, 1964), pgs. 12 - 103 (J. Wiley, New York, 1965).
- Cahn, R. W., editor
Physical Metallurgy, North-Holland Publishing Co., Amsterdam, 1970.
(A chapter on "Phase Diagrams and Their Determination," by G. V. Raynor, gives an overview of the subject.)
- Chart, T. G.
Counsell, J. F.
Jones, G. P.
Slough, W.
Spencer, P. J.
Provision and Use of Thermodynamic Data for the Solution of High-Temperature Practical Problems, an article in Intl. Met. Revs. 20, 57, 1975.
(Description and use of the NPL metallurgical data bank, including examples of phase diagram prediction and more than 200 references.)
- Chernov, A. N.
Evtyanova, E. N., editors
General Review of Phase Diagrams for Metallic Systems, published by "Nauka", Moscow (1973). Text in Russian.
(Structural and crystallographic properties, among others, are reviewed for binary and ternary alloys.)
- Darken, L. S.
Gurry, R. W.
Physical Chemistry of Metals (McGraw-Hill, New York, 1953)
(A textbook treatment of the subject.)

Phase Diagrams - Theory and Review

- Findlay, A. Phase Rule (Dover Publications, New York, 1951) (Development and use of the phase rule.)
- Giessen, B. C.
Willens, R. H. Rapidly Quenched (Splat-Cooled) Metastable Alloy Phases; their Phase-Diagram Representation, Preparation Methods, Occurrence and Properties, a chapter in "Phase Diagrams: Materials Science and Technology" III, 103-141, 1970 (A. M. Alper, editor), published by Academic Press, New York. (Equilibrium and metastable phase diagrams for several binary alloys are compared and the representation of metastable compounds or phases together with the equilibrium diagram discussed; about 90 references cited.)
- Gordon, P. Principles of Phase Diagrams in Materials Systems (McGraw-Hill, New York, 1968) (Largely on the theory of phase diagrams.)
- Gould, R. F., editor Nonstoichiometric Compounds, published by the American Chemical Society in the "Advances in Chemistry" series, 39, 1963. (Contributed chapters treat the problem of nonstoichiometry in metal compounds; phase diagrams and related subjects are discussed; 253 pages.)
- Hume-Rothery, W.
Christian, J. W.
Pearson, W. B. Metallurgical Equilibrium Diagrams Institute of Physics, London, 1952) (Textbook-type treatment on the methodology of determining phase diagrams.)
- Hume-Rothery, W. The Engel-Brewer Theories of Metals and Alloys, a review in "Progress in Materials Science" 13 (#5), 1967, published by Pergamon Press, New York.
- Ivanov, O. S.
Aleksseev, Z. M., editors Structure of Phases, Phase Transformations, and Phase Diagrams of Metallurgical Systems, Proceedings of the 6th All-Union Conference on Research on the Structure of Phases, Phase Transformations and Phase Diagrams and Problems in the use of new Metallurgical Alloys (18-21 Sept. 1972, Baikov Inst., Moscow), published by "Nauka", Moscow (1974). Text in Russian. (Contributed papers deal with the subjects cited in the title; proceedings treat many ternary systems.)

Phase Diagrams - Theory and Review

- Kaufman, L. Computer Calculations of Phase Diagrams, With Special Reference to Refractory Metals (Academic Press, New York, 1970).
(A how-to-do it book).
- Kaufman, L. The Stability of Metallic Phases, an article in Progress in Materials Science 14 (1971), edited by B. Chalmers and W. Hume-Rothery.
(Discussion of phase diagram predictions based mainly on thermodynamic data.)
- Kaufman, L., editor CALPHAD: Computer Coupling of Phase Diagrams and Thermochemistry, a journal published quarterly beginning Jan. 1977, by Pergamon Press, New York.
(A journal addressed to techniques and results of computer prediction of phase equilibria from thermodynamic data.)
- Kubaschewski, O., editor Metallurgical Chemistry, proceedings of a symposium held at Brunel University and NPL (July, 1971) and published by H.M.S.O. (London), 1972.
(The proceedings include both review papers and reports of new experimental data. The prediction and determination of phase equilibria, lattice structures and thermodynamic data and the presentation of phase diagrams comprise the major portion of the proceedings. One session is devoted to the problem of data compilation and computer storage.)
- Kubaschewski, O.
Barin, I. Phase Equilibria in Condensed Systems, an article in Pure and Appl. Chem. 38, 469-494, 1974.
(Construction of phase diagrams from thermochemical data is reviewed and the results compared to experimentally determined diagrams.)
- Lumsden, J. Thermodynamics of Alloys (Academic Press, New York, 1966).
(Textbook treatment on the thermodynamics of phase equilibria in metals and alloys.)
- Masing, G. Ternary Systems, Introduction to the theory of three component systems, published by Dover Publications, New York, 1960).
(Easy-to-follow text; no data.)

Phase Diagrams - Theory and Review

- Massalski, T. B., editor
Alloying Behavior and Effects in Concentrated Solid Solutions, published as the Proceedings of an AIME Metallurgical Society Conference, Vol. 29 (1965) by Gordon and Breach Science Publishers, New York.
(Invited conference papers dealing with the electronic structure and other aspects of alloy behavior are presented.)
- Massalski, T. B.
Pops, H.
Intermediate Phases in Metallic Phase Diagrams, a chapter in "Phase Diagrams: Materials Science and Technology" II, 221-263, 1970 (A. M. Alper, editor); published by Academic Press, New York.
(Electronic and thermodynamic parameters which determine phase stability are reviewed, with a few binary phase diagrams and ternary sections given as illustrations; more than 50 references cited.)
- Palatnik, L. S.
Landau, A. I.
Phase Equilibria in Multicomponent Systems (Holt, Rinehart and Winston, New York, 1964).
(Theory of phase diagrams, mostly for binary systems.)
- Perel'man, F. M.
Phase Diagrams of Multicomponent Systems - Geometrical Methods, published in Russian by "Nauka", Moscow (1965); English translation (1966) available from Consultants Bureau, New York.
(The problems of representing multicomponent phase diagrams on a flat surface are discussed; representations for equilibria in two 6-component alloys are given; 59 references cited.)
- Prince, A.
Alloy Phase Equilibria (Elsevier Publishing Corp., New York, 1966).
(Theory of binary, ternary and higher-order phase diagrams; descriptions of most phase diagram forms and topologies.)
- Reisman, A.
Phase Equilibria (Academic Press, New York, 1970).
(Thermodynamics, applications, experimental determinations and graphical representations of alloy and non-metal phase equilibria are reviewed.)
- Rhines, F. N.
Phase Diagrams in Metallurgy - their Development and Application (McGraw-Hill, New York, 1956).
(Textbook describing interpretation of both binary and ternary phase diagrams.)

Phase Diagrams - Theory and Review

- Ricci, J. E. The Phase Rule and Heterogenous Equilibrium (Peter Smith Publisher, Inc., Magnolia, Gloucester, MA, 1951). (Application of the phase rule to binary, ternary and quaternary systems.)
- Rudman, P. S.
Stringer, J.
Jaffee, R. I., editors Phase Stability in Metals and Alloys, proceedings of a conference held in 1966; (McGraw-Hill, New York, 1967).
- Salli, I. V. Structure Formation in Alloys, published in Russian by "Metallurgizdat", Moscow (1963) and available in English translation (1964) from Consultants Bureau, New York. (Theoretical survey of thermodynamics and kinetics of equilibrium and non-equilibrium phase transformations.)
- Savitskii, E. M.
Gribulya, V. B. A series of papers on the computer prediction of intermetallic phases in binary systems includes the following:
- a. Dokl. Acad. Sci. USSR 178, #1, 79-81, 1968 (in Russian), on recognizing binary phase diagrams,
 - b. Dokl. Acad. Sci. USSR 183, #5, 1110-1112, 1968 (in Russian), on prediction of solubility ranges of A_3B type intermetallic compounds,
 - c. Dokl. Acad. Sci. USSR 185, #3, 561-563, 1969 (in Russian), on prediction of peritectic type reactions and solubility ranges,
 - d. Dokl. Acad. Sci. USSR 206, #4, 848-851, 1972 (in Russian), on prediction of phase stability,
 - e. Metallofizika: 46, 52-62, 1973 (in Russian), on prediction of laves phase occurrence,
 - f. Dokl. Acad. Sci. USSR 214, #5, 1059-1062, 1974 (in Russian), on prediction of occurrence of $CaCu_5$ -type structures,
 - g. Metallofizika: 52, 84-86, 1974 (in Russian), on prediction of laves phase occurrence, and
 - h. Dokl. Acad. Sci. USSR 220, #6, 1066-1069, 1975 (in Russian), on prediction of solubility range and sigma phases.

Phase Diagrams - Theory and Review

- Savitskii, E. M.
Devingtal', Yu. V.
Gribulya, V. B. Superconducting Alloys and Compounds,
published by "Nauka", Moscow (1972).
Text in Russian.
(A 14-page paper in this volume; super-
conducting critical temperatures for
binary compounds are predicted; annotation
by J. H. Westbrook; copy not received
by ADC.)
- Savitskii, E. M.
Gribulya, V. B. Structures and Properties of Heat-Resistant
Metallurgical Materials, published by
"Nauka", Moscow (1973). Text in Russian.
(An 8-page paper in this volume; melting
points for binary compounds are predicted;
annotation by J. H. Westbrook; copy not
received by ADC.)
- Swalin, R. A. Thermodynamics of Solids, 2nd edition
(J. Wiley, New York, 1972).
(This theoretical treatment includes,
among other topics, discussions of
defects and ordering in metals and
alloys.)
- Vozdvizhenskii, V. M. Prediction of Binary Phase Diagrams,
published by "Metallurgiya", Moscow
(1975). Text in Russian.
(Thermodynamics of binary alloys,
with emphasis on construction of
phase diagrams, is reviewed.)
- Zhavoronkov, N. M., editor Chemistry of Metallurgical Alloys,
published by "Nauka", Moscow (1973).
Text in Russian.
(This volume, published as a tribute
to N. V. Ageev, consists of many
articles reviewing the field.)

(NTIS publications may be ordered from the National Technical Information Service at 5286 Port Royal Road, Springfield, VA 22161).



Organization of Phase Diagram Information in the Soviet Union

N. V. Ageev, D. L. Ageeva, T. P. Kolesnikova, and L. A. Petrova

Baikov Institute of Metallurgy
USSR Academy of Sciences
Institute of Scientific Information
Moscow, USSR

Over two and a half centuries ago, in 1724, the Academy of Sciences was set up at St Petersburg by an edict of Peter the Great. From its early days, the Academy was paying unflinching attention to metallurgical problems [1]. In 1829, academician A. J. Kupfer published a study [2] on the congelation temperatures of a system of two metals - tin and lead. Towards the end of the 19th century, N. S. Kurnakov [3] began his famous research into phase diagrams and properties of metal alloys. His studies were markable for their systemic character, with the underlying principle being an analysis of relationships between the nature of alloy's phases, the phase diagram pattern, and the position of the respective components in the Periodic Table. All findings unequivocally pointed to Mendeleev's Periodic Law as a sound basis for understanding the nature of metal alloys and their phase diagram patterns [4].

The study of phase diagrams of metal systems is important, not just for theory of metals, but also for many major practical issues of physical metallurgy and metals engineering. No less significant is the study of phase diagrams of nonmetal, both oxide and silicate systems. The present-day technological progress largely depends on development of new high-quality materials, their production and processing to endow them with properties needed for use in up-to-date technologies.

An efficient organisation of phase diagram studies and their theoretic and practical use requires that information supply on all publications in this field, be well in hand.

Studies by N. S. Kurnakov and his disciples (S. F. Zhemchuzhny, N. A. Pushin, N. S. Konstantinov, N. I. Stepanov, G. G. Urazov, V. A. Nemilov, and others) were carried in the Journal of the Russian Physico-Chemical Society, Transactions of the St Petersburg Polytechnical Institute, Transactions of the Institute for Platinum Studies, and also in foreign journals - Zeitschrift für anorganische Chemie and Journal of the Institute of Metals.

The first handbook on phase diagrams to appear in the Soviet Union was the translation of a comprehensive reference monograph by M. Hansen "Structure of Binary Metal Alloys" [5] published in 1941. In 1956, "Bibliography of Soviet Studies concerning Phase Diagrams of Metal Systems", edited by I. I. Kornilov, was published [6]. In 1959, the first volume of the reference book "Structure and Properties of Binary Metal Systems" by A. E. Vol appeared [7], followed by the second volume in 1962; subsequent volumes are ready for print and will appear within a few years' time. In 1962, a Russian translation of the two-volume handbook by M. Hansen and K. Anderko "Structure of Binary Alloys" [8] came off the press, and in 1970, another handbook by R. Elliott appeared under the same title and also in two volumes [9], and in 1973 - handbook by F. Schunk [10] under the same title.

In 1972, a bibliographic reference book "Phase Diagrams of Ternary Metal Systems, 1910-1969" (Ed. by N. V. Ageev) was published [11].

Along with emerging interest in particular metals used as alloy components, monographs and handbooks of phase diagrams of the respective systems were appearing. For example, in 1964 "Atlas of Phase Diagrams of Titanium Alloys", compiled by E. K. Molchanova and edited by S. G. Glazunov [12], was printed. In 1964, D. A. Prokoshin and E. V. Vasil'eva published a monograph on "Niobium Alloys". In 1968, T. A. Badaeva published a monograph on "Binary and Ternary Phase Diagrams of Thorium-Based Alloys. Structure of Thorium Alloys" [14]. The monograph by O. S. Ivanov, T. A. Badaeva, R. M. Safronova, V. B. Kishinevsky, and N. P. Kushnir "Phase Diagrams and Phase Transitions of Uranium Alloys: appeared in 1972 [15].

In 1973, O. S. Ivanov, A. S. Adamova, E. M. Tararyeva, and I. A. Tregubov published the monograph "Structure of Zirconium Alloys. Binary and Ternary Phase Diagrams" [16].

Since 1956, the All-Union Institute of Scientific Information of the USSR Academy of Sciences (VINITI) has been issuing an abstract journal "Chemistry" and since 1956 "Metallurgy". The former journal includes a section for "Physico-Chemical Analysis" and the latter, sections for "Phase Equilibrium" and "Theory of Metallurgical Processes" covering studies on phase diagrams published in the USSR and elsewhere. Since 1959, VINITI has been publishing a yearbook titled "Phase Diagrams of Metal Systems", edited by N. V. Ageev. Thus far, twenty issues have appeared, which cover metal system diagrams described in 1955-1974 [17-35,52]. Issues XXI (1975) and XXII (1976) are being compiled. Each issue carries phase diagrams investigated and reported in the literature in a respective year. The yearbook covers papers describing or containing graphic images of complete phase diagrams or parts thereof (phase boundaries, solubility lines). Sources describing studies of crystal structures, physical and chemical properties and other features of individual phases are not included. Phase diagrams of metals with nonmetal elements are given only if the study has been conducted starting from 100 percent metal component. Diagrams are arranged according to increasing number of components, viz.: binary, ternary, quaternary, and so on; within each group, entries are ordered by Roman alphabet of component names. Roman alphabet has been adopted beginning with XVIII issue, for the benefit of users who are not familiar with the Russian language. All phase diagrams are described in accord with the following entry format: (1) materials used in the study; (2) methods of preparing and studying the alloy; (3) description of the diagram and its points and lines; (4) description of phases; (5) bibliographic details; and (6) note. Complete phase diagrams and sections of ternary or more complex systems are always reproduced from the original publication without any modification or a critical assessment of their reliability. Composition is mostly given in weight percentages, unless

otherwise indicated. Temperatures are centigrade, unless otherwise indicated. Each issue ends up with a table of contents indicating the pages containing phase diagrams. A cumulative index is compiled every ten years and inserted into the current issue. The first cumulation to issues I-X (1955-1964) of the "Phase Diagrams of Metal Systems" was printed in 1964 [26]. The second cumulation for twenty years (issues I-XX) is inserted in issue XX.

Since 1966, VINITI has been issuing a series of handbooks under the general title - "Phase Diagrams of Nonmetal Systems", edited by D. L. Ageeva. So far, issues I to X have appeared, covering diagrams of oxide systems published from 1963 through 1974 [36-45,53]. The entry format is the same as described above for metal systems, but illustrations from originals are reproduced selectively.

On phase diagrams of silicate systems, three volumes of the reference book "Phase Diagrams of Silicate Systems" edited by V. P. Barzakovsky [46-48] were published in 1969, 1970 and 1972.

Primary publications dealing with study of phase diagrams in the Soviet Union are carried in the following main sources: Izvestia Akademii Nauk ("Metals" series); Doklady Akademii Nauk SSSR; Dopovidi Akademii Nauk URSS; Fizika metallov i metallovedenie; Izvestia Akademii Nauk SSSR (Non-Organic Materials series); Poroshkovaya metallurgia; Vestnik Moskovskogo Universiteta (Chemistry" series); Zhurnal neorganicheskoi khimii, as well as special subject compendia which are issued by various publishers.

A critical overview of the phase diagram information in the Soviet Union suggests that:

- (1) information on phase diagrams covers not just binary, but also ternary and more complex systems;
- (2) handbooks reproduce phase diagrams from original publications without any modification;
- (3) regular published information on phase diagrams of metal and oxide systems is produced;
- (4) primary publications dealing with studies of phase diagrams are not concentrated in any single source, but scattered over several journals and serials;

(5) times spent on bringing information to user's notice are: through VINITI's abstract journal - for Soviet publications, 3 to 5 months; for foreign publications, 4 to 8 months; through VINITI's handbooks, three years;

(6) no works on critical review of experimental data, such as the handbook of M. Hansen et al., are available;

(7) those handbooks that are being published are sold out too soon; and

(8) despite definite phase diagram description formats sanctioned by practice, there are no strict standard requirements, so that original publications often lack essential data for a judgement about reliability and quality of the phase diagrams.

From data covered by handbooks, one can conclude (see Figures 1, 2) that the Soviet Union holds a major place in studies of metal systems' phase diagrams. The work is under way in many research organisations across the country and coordinated by the USSR Academy of Sciences Scientific Council on Physico-Chemical Principles of Metallurgical Processes (117334, Moscow, Leninski prospekt, 49), which scrutinises the research programmes and the plans for conducting scientific conferences and meetings. Phase diagrams today are a product of experimental research. Phase diagrams calculated from thermodynamic data thus far only serve for reciprocal tests of computations and experiments, but as yet are no substitute for experiment. During experimental studies of phase diagrams, Soviet authors have been trying to improve the methods by studying samples of a variable composition which are produced by condensing films on a base [49] or by the diffusion layer method, which issued in studying phases formed by diffusion [50-51]. With these methods the sample is not in equilibrium state, so they are no adequate substitute for the study of particular samples of a definite composition brought into equilibrium state by thermal treatment.

It may be said in conclusion that cooperation between the researchers concerned with phase diagrams and the information officers is bound to improve and accelerate the work in the phase diagram field.

Research on computerized modelling of phase diagrams is also conducted in the Institute of Scientific Information (VINITI, USSR) [54-65].

DISCUSSION

W. B. Pearson - How many copies of each Ageev volume are printed?

T. Kolesinkova - 3,000 to 4,000 copies. These can be obtained through "International Books" [editor's note: see also description under Mikhailov (VINITI), p 44, in listing of international data compilation activities].

A. Navrotsky - Would you be able to tell us what publications on thermodynamic data are available in the Soviet Union?

T. Kolesnikova - There are many publications. We publish each year handbooks by a center of standard data. Eleven volumes have now been issued.

References

* Figures 1 and 2 may be obtained by contacting the authors.

1. Lomonosov, M. V., "The Basic Foundations of Metallurgy and Mining" (1763).
2. Kupfer, A. J., Ann. Chim., 40, 285, 1829.
3. Kurnakov, N. S., selected works, 611 pages, published by Izdatel'stvo Akademiia Nauk, Moscow (1961).
4. Ageev, N. V., Compt. Rend. (Chim. Phys.): 281, 287, 1952.
5. Hansen, M., "Structure of Binary Alloys", 2 volumes on the literature of ferrous and non-ferrous metallurgy, 1050 pages, published by the State Scientific-Technical Publishing House, Leningrad, 1941.
6. "Bibliography of Soviet Studies concerning Phase Diagrams of Metal Systems", edited by I. I. Kornilov, 38 pages, published by the Institute for Technical and Experimental Information, Academy of Sciences of the USSR, Moscow, 1956.
7. Vol, A. E., "Structure and Properties of Binary Metal Systems";¹ reference series, in 4 volumes, including physico-chemical properties of the elements; systems of Ac, Al, Am, B, Ba, Be, and N are treated in volume 1 (755 pages, 1959) systems of Bi, Dy, Eu, Fe, Ga, Gd, Ge, H, Hf, Ho, V, and W in volume 2 (982 pages, 1962) and systems of Au, In, Ir, Y, and Yb in volume 3 (814 pages, 1976); published by "Izdatel'stvo Fiziko-Matematicheskii Literatur" (Moscow).
8. Hansen, M. and Anderko, K., "Structure of Binary Alloys", translated from English and published by "Metallurgizdat," Moscow, 1962.
9. Elliott, R. P., "Structure of Binary Alloys, First Supplement", volumes 1 (455 pages) and 2(472 pages), translated from English and published by "Metallurgizdat", Moscow, 1970.
10. Shunk, F. A., "Structure of Binary Alloys, Second Supplement" 760 pages, translated from English and published by "Metallurgizdat," Moscow, 1973.

11. "Phase Diagrams of Ternary Metal Systems, 1910-1969" (bibliographic reference book), Ageev, N. V., editor, 189 pages, produced by the Institute of Metallurgy, Academy of Sciences of the U.S.S.R., and published by "Nauka", Moscow, 1972.
12. Molchanova, E. K., "Atlas of Phase Diagrams of Titanium Alloys",² 392 pages, published by "Izdatel'stvo Mashinostroenie," Moscow, 1964.
13. Prokoshkin, D. A. and Vasil'eva, E. V., "Niobium Alloys", 332 pages, published by "Nauka", Moscow, 1964.
14. Badaeva, T. A., "Structure of Thorium Alloys. Binary and Ternary Phase Diagrams of Thorium-Based Alloys," 177 pages, published by "Nauka," Moscow, 1968.
15. Ivanov, O. S., Badaeva, T. A., Sofronova, R. M., Kishinevsky, V. B., and Kushnir, N. P. (edited by Ivanov, O. S.), "Phase Diagrams and Phase Transitions of Uranium Alloys", 252 pages, published by "Nauka," Moscow, 1972.
16. Ivanov, O. S., Adamova, A. S., Tararyeva, E. M., and Tregubov, I. A., "Structure of Zirconium Alloys. Binary and Ternary Phase Diagrams", 199 pages, published by "Nauka," Moscow, 1973.
17. Alisova, S. P., Vul'f, L. B., Markovich, K. M., Novik, P. K., Petrova, L. A., and Rogachevskaya, Z. M. (edited by Ageev, N. V.), "Phase Diagrams of Metal Systems," vol. 1 (covering information published in 1955), 138 pages, published by VINITI, Moscow, 1960.
18. *ibid.*, vol. 2 (covering information published in 1956), 280 pages, published by VINITI, Moscow, 1960.
19. *ibid.*, vol. 3 (covering information published in 1957), 128 pages, published by VINITI, Moscow, 1960.
20. *ibid.*, vol. 4 (covering information published in 1958) 403 pages, published by VINITI, Moscow, 1961.
21. Rogachevskaya, Z. M. [edited by Ageev, N. V.], "Phase Diagrams of Metal Systems", vol. 5 (covering information published in 1959), 168 pages, published by VINITI, Moscow, 1962.
22. *ibid.*, vol. 6 (covering information published in 1960), 168 pages, published by VINITI, Moscow, 1962.
23. *ibid.*, vol. 7 (covering information published in 1961), 263 pages, published by VINITI, Moscow, 1963.
24. *ibid.*, vol. 8 (covering information published in 1962), 232 pages, published by VINITI, 1964.
25. Grankova, L. P., Mints, R. S., and Petrova, L. A. [edited by Ageev, N. V.] "Phase Diagrams of Metal Systems", vol. 9 (covering information published in 1963), 277 pages, published by VINITI, Moscow, 1966.
26. Alisova, S. P. and Budberg, P. B. [edited by Ageev, N. V.], "Phase Diagrams of Metal Systems", vol. 10 (covering information published in 1964), 240 pages, published by VINITI, Moscow, 1966.

27. *ibid.*, vol. 11 (covering information published in 1965), 270 pages, published by VINITI, Moscow, 1968.
28. *ibid.*, vol. 12 (covering information published in 1966), 272 pages, published by VINITI, Moscow, 1968.
29. *ibid.*, vol. 13 (covering information published in 1967), 277 pages, published by VINITI, Moscow, 1970.
30. *ibid.*, vol. 14 (covering information published in 1968), 272 pages, published by VINITI, Moscow, 1970.
31. *ibid.*, vol. 15 (covering information published in 1969), 264 pages, published by VINITI, Moscow, 1971.
32. *ibid.*, vol. 16 (covering information published in 1970), 308 pages, published by VINITI, Moscow, 1972.
33. *ibid.*, vol. 17 (covering information published in 1971), 420 pages, published by VINITI, Moscow, 1973.
34. *ibid.*, vol. 18 (covering information published in 1972), 268 pages, published by VINITI, Moscow, 1975.
35. *ibid.*, vol. 19 (covering information published in 1973), 268 pages, published by VINITI, Moscow, 1976.
36. Ageeva, D. L., "Phase Diagrams of Non-Metallic Systems. Oxides and Silicides", vol. 1, 123 pages, published by VINITI, Moscow, 1966.
37. *ibid.*, vol. 2, 224 pages, published by VINITI, Moscow, 1966.
38. *ibid.*, vol. 3, 143 pages, published by VINITI, Moscow, 1968.
39. Dobroshvetov, B. L., *ibid.*, vol. 4, 276 pages, published by VINITI, Moscow, 1969.
40. Ageeva, D. L. and Shvedov, L. V., *ibid.*, vol. 5, 199 pages, published by VINITI, Moscow, 1970.
41. Ageeva, D. L., *ibid.*, vol. 6, 232 pages, published by VINITI, Moscow, 1971.
42. Ageeva, D. L. and Shvedov, L. V., *ibid.*, vol. 7, 161 pages, published by VINITI, Moscow, 1972.
43. Ageeva, D. L. and Shvedov, L. V., *ibid.*, vol. 8, 155 pages, published by VINITI, Moscow, 1973.
44. Ageeva, D. L. and Shvedov, L. V., *ibid.*, vol. 9, 155 pages, published by VINITI, Moscow, 1974.
45. Ageeva, D. L. and Shvedov, L. V., *ibid.*, vol. 10, 115 pages, published by VINITI, Moscow, 1975.
46. Toropov, N. A., Barzakovskii, V. P., Lapin, V. V. and Kursheva, N. N., "Phase Diagrams of Silicide Systems" (part I, Binary Systems), 822 pages, published by "Nauka", Leningrad, 1969.

47. Toropov, N. A., Barzakovskii, V. P., Bondar, I. A., Udalov, Yu. P., *ibid.* (part II, Metal-Oxygen Phases in Silicide Systems), 372 pages, published by "Nauka", Leningrad, 1970.
48. Toropov, N. A., Barzakovskii, V. P., Lapin, V. V., Kurtseva, N. N., and Boikova, A. I., "Phase Diagrams of Silicide Systems" (reference book), vol. 3 (Ternary Systems), 448 pages, published by "Nauka", Leningrad, 1972.
49. Vekshchinskii, S. A., "Novel Method for Metallographic Study of Alloys," 252 pages, published by State Publishing House, Moscow, 1944.
50. Ivanov, O. S., et al., "Theoretical and Experimental Methods of studying Phase Diagrams of Metal Systems", pages 160-166, published by "Nauka", Moscow, 1969.
51. Tregubov, I. A., Kuzina, L. N., and Ivanov, O. S., Russian Metallurgy (English translation of *Izvestiia Akademii Nauk SSSR - Metally*): no. 4, 104-108, 1967.
52. Eroshchenkova, I. G., Olenicheva, V. G., and Petrova, L. A. [edited by Ageev, N. V.], "Phase Diagrams of Metallurgical Systems", vol. 20 (covering information published in 1974), 360 pages, published by VINITI, Moscow, 1976.
53. Ageeva, D. L., Shvedov, L. V., "Phase Diagrams of Non-Metal Systems. Oxide Systems", vol. 11, 110 pages, published by VINITI, Moscow, 1976.
54. Seifer, A. L., Stein, V. S., The topology of composition-property diagrams for binary systems. "Zhurnal Neorganicheskoi Khimii" (Journal of Inorganic Chemistry), 1961, 6, No. 12, p. 2719.
55. Seifer, A. L., Kleinermann, G. I., Stein, V. S., The principles of construction of a machine language for physico-chemical analysis. "Information Storage and Retrieval", 1963, No. 1, p. 13-18.
56. Stein, V. S., Principles of computer recording of phase regions in phase diagrams as exemplified by binary metallic systems. "Nauchno-Tekhnicheskaya Informatsiya" (Scientific and Technical Information), 1963, No. 3, p. 31-35.
57. Novik, P. K., Stein, V. S., Unification of names of regions of binary metallic systems. "Nauchno-Tekhnicheskaya Informatsiya" (Scientific and Technical Information), 1964, No. 5, p. 25-28.
58. Stein, V. S., Solution of some information problems of physico-chemical analysis by computers (in Russian). Dissertation, VINITI, USSR Academy of Sciences, 1966.
59. Stein, V. S., Design of an information retrieval system for physico-chemical analysis. In the book: "Prikladnaya dokumentatsiya" (Applied documentation), Moscow, "Nauka" Publishers, 1968, (in Russian).

60. Adler, Iu. P., Stein, V. S., Composition-property diagrams: representation of information for computers. "Information Storage and Retrieval", 1969, 4, p. No. 4, p. 329-332.
61. Stein, V. S., Information language for representation of binary and ternary phase diagrams in computer memory for solving certain problems of physico-chemical analysis. In the book: "Diagrammy sostoyaniya metallicheskih system" (Phase diagrams of metallic systems), "Nauka" Publishers, Moscow, 1968, (in Russian).
62. Stein, V. S., On certain methods of computer processing and retrieval of scientific information in diagrams of physico-chemical analysis. In the book: Teoreticheskiye i eksperimentalniye metody issledovaniya diagram sostoyaniya (Theoretical and experimental methods of research into phase diagrams), "Nauka" Publishers, Moscow, 1969, (in Russian).
63. Stein, V. S., Possibilities and problems of developing an information retrieval system for metallurgy. "Izvestiya Akademii Nauk SSSR", "Metally" (Metals), 1969, No. 2, (in Russian).
64. Tulupova, I. V., Stein, V. S., Topology of equilibrium diagrams of multicomponent systems and formal methods of their description. In the book: Struktura faz, fazoviye prevrashcheniya i diagrammy sostoyaniya metallicheskih system. (Phase structure, phase conversion and phase diagrams of metallic systems). "Nauka" Publishers, Moscow, 1974, (in Russian).
65. Tulupova, I. V., Stein, V. S., Topology of equilibrium diagrams of multicomponent systems with a critical phase and formal methods of their description. Deposited at VINITI, N 2454-74, on 9 September, 1974, (in Russian).

Reference Notes

1. ref. 7 (Vol, A. E.): volumes 1, 2, and 3 have been published; volumes 4 and 5 are in press; see paper by Vol and Kagan (p.) for details, including the binary systems treated volumes 4 and 5.
2. ref. 12 (Molchanova, E. K.): English translation available from the National Technical Information Service, Springfield, VA 22161 as document AD 670,090 (1967).



A SURVEY OF HIGH PRESSURE PHASES OF MATERIALS

Leo Merrill

High Pressure Data Center
5093 HBLL
Brigham Young University
Provo, Utah 84602 USA

A survey of polymorphic phase diagrams as a function of pressure and temperature is presented for the elements and simple inorganic compounds. Historically, the preparation and study of material phase were carried out as a function of temperature and composition. In 1955 with the successful synthesis of diamond¹, the importance of the use of high pressure in the synthesis of new materials became evident. In a few years a large number of new dense phases of the elements and compounds had been discovered and characterized. High pressure-high temperature phase studies of materials include the following formula types: elements (69)*, AB (87), AB₂ (78), AB₃ (8), ABO₂ (11), A₂B₃ (67), ABO₄ (54), and miscellaneous types (58) mainly of mineral systems or mineral analogs. All materials in this survey are those for which crystallographic data are available.

The preparation of high pressure phases falls into three principle categories: (1) pressure and temperature induced structural transformations of known elements or compounds, (2) synthesis of new compounds and (3) disproportionation reactions. In pressure induced structural phase transitions, materials proceed to structures with higher densities and generally to more efficient packing arrangements or higher cation coordination numbers. It would be impossible to discuss all the pressure induced phases, so reviews and compilations will be referenced and only the more interesting groups discussed. Since all successful theory of physical and transport properties are related to lattice symmetries, phase transformations will be discussed in terms of the crystal structures of the particular phases.

Why is high pressure useful in the preparation of new phases. Generally, the major effect of pressure is to force cations to adopt a higher coordination and to occupy sites in which they do not go naturally because of the unfavorable empirical radius ratio or their particular electronic configuration. Many compounds and/or phases of materials have no equilibrium configuration which can be prepared at atmospheric pressure. Compounds which cannot be formed due to high vapor pressure of one of its constituents are often synthesized at high pressure. In alloy systems pressure produces a change in solubility of one or both end members.

Elements. There are two excellent reviews of the high pressure-high temperature phases of the elements. Young² compiled phase diagrams of all the reported solid-solid and solid-liquid phase boundaries, which include approximately 80 phase diagrams. Cannon³ published a similar report which is restricted to those materials for which the crystal structures of the high pressure phases have been identified by either x-ray or neutron diffraction techniques. This latter report, which contains 60 phase diagrams, is a critical evaluation of the phase boundaries and contains tables of the crystallographic data of the individual phases.

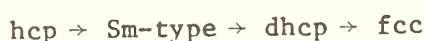
In an attempt to find some empirical relation which would predict which elements had pressure induced phase transformation Liu⁴ plotted the room temperature densities of the elements with solid and liquid phases against atomic number. It was found that pressure induced polymorphic phase transformations of the solid elements appear to be closely correlated to the density periodicity. With the exception of Fe, all the solids with pressure induced phase transition lie below a straight line

$$\rho = 2.8 + 0.12Z$$

By using this correlation, Liu was able to predict new high pressure phases in Se, Tm, and Lu.

In general, the crystal structures of the metals are relatively simple as are their high pressure phases. In the phase diagrams of the metals it is very common for the bcc structure to be stable at high temperature adjacent to the melting curve. Starting in the first column of the period table Cs(fcc) undergoes a number of interesting transformations. Bridgmann⁵ originally had observed two transitions at 23 and 43 kb which were detected by ΔV and electrical resistance anomalies. It was later shown that the resistance trace at 43 kb was not a cusp but two sharp discontinuities spaced about 0.5 kbar apart indicating the pressure of two closely spaced transitions at 42.2 and 42.7 kb. At 23 kb the transition is from bcc to fcc while at 42.2 kb the fcc phase transforms to a collapsed fcc' phase. The crystal structure above 42.7 kb could not be resolved.⁶ An analogous transition occurs in Ce at 6 kb (fcc \rightarrow fcc) and apparently involves an electronic transition. In cerium a critical point exists in the vicinity of 21.5 kb and 340°C. These transitions and others for the group B metals are summarized in Appendix A.

The rare earth metals form an interesting group and are structurally divided into two regions. The heavier elements from Gd have the hcp structure except Yb which is bcc. The lighter rare earth elements have more complicated structures as a result of different stacking sequences of close packed layers. The high temperature phases of the rare earth metals are mainly bcc. Jayaraman⁷ has shown that the trend of the pressure induced structural phase transitions in the rare earth metals follow the sequence



which is in the direction of increasing cubic character. (Table I).

This is not true, however, for Eu and Yb which are divalent. Eu has no known high pressure phase while Yb undergoes a transition from fcc \rightarrow bcc at 40 kb. The phase boundary of Eu has a negative slope and intersects the temperature axis near 800°C. The details of the phase diagrams and phases of Yb and Sr are almost identical.

The group IIIA through VIIA elements generally exhibit more complexity in both phase diagrams and the associated crystal structures. The phases of these elements are summarized in App. A. It should be noted that many of the polymorphic transitions of the elements do not undergo an increase in coordination as is particularly well illustrated in the transitions of the trivalent rare earth elements in which all the phases have coordination number 12.

AB Type Compounds. A recent review of the high pressure phases of the AB-type compounds⁸ covers approximately 85 compounds with tables of crystallographic data and phase diagrams. The high pressure transitions in this group of compounds will in general be associated with an increase in cation coordination number. Experimentally, equilibrium values of the room temperature transitions are difficult to obtain due to poor kinetic effects in these compounds.

After the synthesis of diamond, the next significant discovery was the synthesis of the cubic form of boron nitride which is a high pressure analogue to diamond and also an abrasive. The principal groups of the AB type compounds which have been studied at high pressure are compounds of the halides, Group VA, and the chalcogenides. All the alkali halides with the exception of CsCl, CsBr and CsI crystallize in the 6 coordinated NaCl-type structure and have very simple phase diagrams. At high pressure the NaCl-type alkali halides transform to the 8 coordination CsCl-type structure.

Phase transitions in the ammonium halides, as well as their deuterium analogues, have been widely studied by a variety of methods. While a λ -transition at low temperatures is common to all these compounds, a pressure induced Fm3m (NaCl) to Pm3m (CsCl) transition is exhibited by ammonium chloride, bromide and iodide and their deuterated analogues at high temperature. Much of the theoretical work has been devoted to the λ transition in ammonium halides. In NH_4Br this transition is attributed to an order-disorder rotational orientation of the NH_4 groups.

AB-type compounds of the Group VA and VIA elements and Group 1B halides within the scope of this report have as the stable phases the αAgI , wurtzite, PbO, NaCl, ZnS or NiAs-type structure. The high pressure phases have the same or increased coordination (Appendix B) and consist mainly of HgS , CsCl, PbO, Wurtzite, NaCl, beta-Sn and HgS structure types.

Rare Earth Compounds. One of the particularly interesting areas where high pressure has been successful is with compounds of the rare earth elements. On the basis of high temperature synthesis it is usually found that there are regions where a particular structure cannot be formed (Table II). An empirical explanation is that in the higher rare earths the size of the ion is too small to form a stable compound. If as in the case of LuTe_2 the tellurium is more compressible than the rare earth member, high pressure can produce a favorable radius ratio for the formation of the particular series of compounds. Although this has been successful in synthesizing many new rare earth compounds, it is evident that other factors such as 4-f bonding play an important role.

The rare earth trialuminides⁹ have layered type structures which have the Ni_3Sn , BaPb_3 , TiNi_3 , HoAl_3 , and Cu_3Au type structures as shown in Table

III. These structure types are arranged according to increasing cubic character. The effect of high pressure on these layered compounds produces structures with greater cubic character.

Geological Studies. The use of high pressure has been extremely useful in studying the structure within the earth. The basis for dividing the earth's interior into various regions comes from seismic velocity data. From a knowledge of the ultrasonic properties of known minerals, the mineralogy can be predicted to approximately 200 km. In the region of the upper mantle known as the transition zone there are two major seismic discontinuities at about 400 km and 600 km. The discontinuity at 400 km is due to a transition of olivine to the spinel type structure and below 600 km silicon is in six fold coordination. Evidence for these phase changes comes principally from laboratory high pressure studies.

Of particular interest in this work was the discovery of new dense forms of quartz. Coesite containing Si in four fold coordination was prepared by Coes.¹⁰ The synthesis of stishovite first prepared by Stishov and Popova¹¹ has the rutile structure with Si in octahedral coordination. A solution of the mineralogy of the lower mantle is not as straight forward as with the upper mantle. Present theory points to close packed oxide structures. One possible solution would be the existence of silicon in 8 fold coordination.

In order to test this possibility, the geologists began to look for analogue materials with rutile (octahedral coordination) type structures to see if pressure and temperature would favor the CaF_2 -type structure. The use of analogue structure in the study of the structure of the earth's mantle has been a very productive technique.

Goldschmidt predicted that PbO_2 and MnF_2 would be the most likely rutile-type structures to undergo a transition to a CaF_2 -type structure since their radius ratios are very close to critical value for the fluorite structure derived from simple geometrical considerations.

Experimental investigations confirmed PbO_2 and MnF_2 , as well as CoF_2 and NiF_2 , transform to the 8 coordinated fluorite structure. MnF_2 goes through a series of transformations; first to a 7-8 coordinated distorted fluorite, then to a 9 coordinated PbCl_2 phase and finally to the fluorite phase at high P and T. Fluorite phases of Ba, Sr, Cd, and Ca difluorides all transform to a 9 coordinated αPbCl_2 structure.

In a recent experiment natural ilmenite $(\text{Fe,Mg})\text{TiO}_3$ (pyroxene) was found to transform to the perovskite structure at high pressure and then to disproportionate into its component oxides $(\text{Fe,Mg})\text{O}$ and a cubic phase¹² of TiO_2 in which Ti is in 8 fold coordination. Other important transformations are those of olivine which transforms first to the spinel phase and finally to dense oxide phases. The pyroxenes at high pressure transform to spinel phases plus stishovite, etc. The success of this work has resulted from laboratory high pressure experiments.

(p-T-x) Phase Diagrams. While most of the high pressure studies have been devoted to the preparation of stoichiometric compounds, a number of researchers have investigated binary and ternary systems as a function of pressure, temperature and composition (p,T,x). Systems which have been reported in the literature include W-C, NiC, FeC, Fe-V, Fe-Cr, Fe-Si, Bi-Su, Bi-Tl, Bi-Pb, Bi-S, InS, Tl-In, Al-Si, Cu-Al, Ag-In and Au-Ga.

One of the best illustrations of the usefulness of phase diagrams at high pressure is the Ni-C system important in the production of synthetic

diamond (Fig. 1). At pressure less than 54 kbar there is no liquid - diamond region in the phase diagram which is necessary for the nucleation and growth of diamond crystals.¹³ In connection with diamond production the Fe-C and Fe-Ni-C phase diagrams have been thoroughly investigated. The BN-Li₃BN₂ phase diagram is important for the production of the high pressure cubic BN. Relatively new products of commercial significance which are presently being developed are the sintered or polycrystalline forms of diamond and cubic boron nitride.

Considerable work is being done in the USSR on phase diagrams at high pressure. A review of this work has recently been published by Shinyaev (in Russian) of the Baikov Institute of Metallurgy.¹⁴

Displacive Transformations. Displacive phase transitions which are classified as second order or nearly second order are of particular interest in high pressure investigations. These are the soft mode type transitions in which the symmetry of the new phase can be related to either a temperature or volume dependent lattice instability in a mode of low energy. These transitions are important because they enable study of the basic physics of phase transitions.

In TeO₂ the elastic modulus ($C_{11}-C_{12}$) goes continuously to zero with pressure. NaNO₃ undergoes a paraelectric-ferroelectric ($R\bar{3}c - R3c$) transition at 49 kbar. KH₂PO₄ (KDP) has a tricritical point at approximately 2 kbar. In CaCo₃, which has a displacive paraelectric-antiferroelectric ($R\bar{3}c - P2_1/c$) transition, by the use of group theoretical calculations, a lattice mode has been identified which accounts for the observed displacements of the transition. Transitions of this type also occur in Sn at 90 kbar, KNO₃, SrTiO₃, the ammonium halides and others. Lattice dynamical

studies of the soft mode type phase transformation holds great promise in the development of basic theory of phase stability and structural phase transformations,

REFERENCES

* The number in parentheses is the number of materials which have been tabulated in each formula type.

1. H. T. Hall, *Synthesis of Diamonds*, J. Chem. Ed. 38, 484-489 (1961).
2. D. A. Young, *Phase Diagrams of the Elements*, UCRL 51902 Lawrence Livermore Laboratory (September 11, 1975).
3. J. F. Cannon, *Behavior of the Elements at High Pressure*, J. Phys. Chem. Ref. Data 3, 781-824 (1974).
4. L. G. Liu, *Correlation of density periodicity to pressure induced polymorphic transformations in solid elements*, J. Appl. Phys., 44, 2470-2474 (1973).
5. P. Bridgman, *Proc. Am. Acad. Arts Sci.*, 76, 55-70 (1948).
6. H. T. Hall, L. Merrill, J. D. Barnett, *High Pressure Polymorphism in Cesium*, *Science* 146, 1297-1299 (1964).
7. A. Jayaraman, *Solid-Liquid and solid-solid transformations in the Rare Earth Metals at High Pressure*, *Phys. Rev.* 139A, 690-696 (1965).
8. L. Merrill, *Behavior of the AB-Type compounds at High Pressure*. (In press)
9. J. F. Cannon, H. T. Hall, *Effect of High Pressure on the Crystal Structures of Lanthanide Trialuminides*, *J. Less Common Metals*, 40, 313-328 (1975).
10. L. Coes, *A new dense crystalline silica*. *Science* 118, 131-133 (1953).
11. S. M. Stishov, S. V. Popova, *New dense polymorphic modification of silica*. *Geokhimiya* 8, 649-659 (1962).
12. L. G. Liu, *High Pressure Phase Transformations and Compressions of Ilmenite and Rutile, I. Experimental Results*, *Phys. of the Earth and Planetary Interiors* 10, 167-176 (1975).
13. H. M. Strong, R. E. Hanneman, *Crystallization of Diamond and Graphite*, *J. Chem. Phys.* 46, 3668-3676 (1967).
14. A. Ya. Shinyaev, *Phase diagrams and properties of alloys at high pressure*, *Baikov Institute of Metallurgy of the Academy of Sciences USSR*, 154p., 1973 Moscow.

Table I. Pressure Induced Phase Transformations for the Rare Earth Elements.

Metal	hcp	Sm-Type	dhcp	fcc
Gd, Tb, Dy, Ho, Tm, Lu	I	→	II	
Er	I	→		II
Sm		I	→	II
La, Pr, Nd				I → II

Table II.

Rare Earth Series Compounds Showing Regions Where the Synthesis Range has been Extended by the use of Pressure.

R. E. Compound	La	Ce	Pr	Nd	Sm	Eu	Gd	Tb	Dy	Y	Ho	Er	Tm	Yb	Lu
RSb ₂ (LaSb ₂ Type)	*	*	P	*	*	-	P	P	-	-	-	-	-	-	-
RSb ₂ (HoSb ₂ Type)	-	-	-	-	-	-	P	P	P	P	P	P	P	-	-
RS ₂ (LaTe ₂ Type)	*	*	*	*	*	-	*	-	*	-	*	*	P	P	P
RTe _{2-x} (0 < x < 0.3)	*	*	*	*	*	-	*	*	*	P	P	P	P	*	P
RTe ₃ (P4/nmm)	*	*	*	*	*	-	*	*	*	*	*	*	*	-	P
RCo ₂ (MgCu ₂ Type)	P														
RFe ₂ (MgCu ₂ Type)	-	-	P	P	*	-	*	*	-	*	P	-	-	P	*
RSn ₃ (AuCu ₃ Type)	*	*	*	*	*	*	*	P	P	P	P	P	-	*	-
RPb ₃ (AuCu ₃ Type)	*	*	*	*	*	-	*	*	*	*	*	*	*	*	P
RB ₂	-	-	-	-	P	-	*	*	*	-	*	*	*	*	*
RB ₁₂	-	-	-	-	-	-	P	*	*	-	*	*	*	*	*

Key: (-) Compound is unknown.

(*) Compound is prepared at atmospheric pressure and high temperature.

(P) Compound is prepared at high pressure and high temperature.

Table III. Pressure Induced Phase Transformations in the Rare Earth Trialuminides.

Compound	Ni ₃ Sn ⁽¹⁾	BaPb ₃ ⁽²⁾	TiNi ₃ ⁽³⁾	HoAl ₃ ⁽⁴⁾	Cu ₃ Au ⁽⁵⁾	
GdAl ₃	I	→	II			
TbAl ₃		I	→	II		
DyAl ₃			I	→	II	
HoAl ₃				I	→	II

Key:	Structure Type	Crystal Lattice	Space Group	Hexagonal Character (ABAB)	Cubic Character (ABCA)
(1)	Ni ₃ Sn	hex	P6 ₃ /mmc	100%	0%
(2)	BaPb ₃	rhomb	R3m	67%	33%
(3)	TiNi ₃	hex	P6 ₃ /mmc	50%	50%
(4)	HoAl ₃	rhomb	R3m	40%	60%
(5)	Cu ₃ Au	cubic	Pm3m	0%	100%

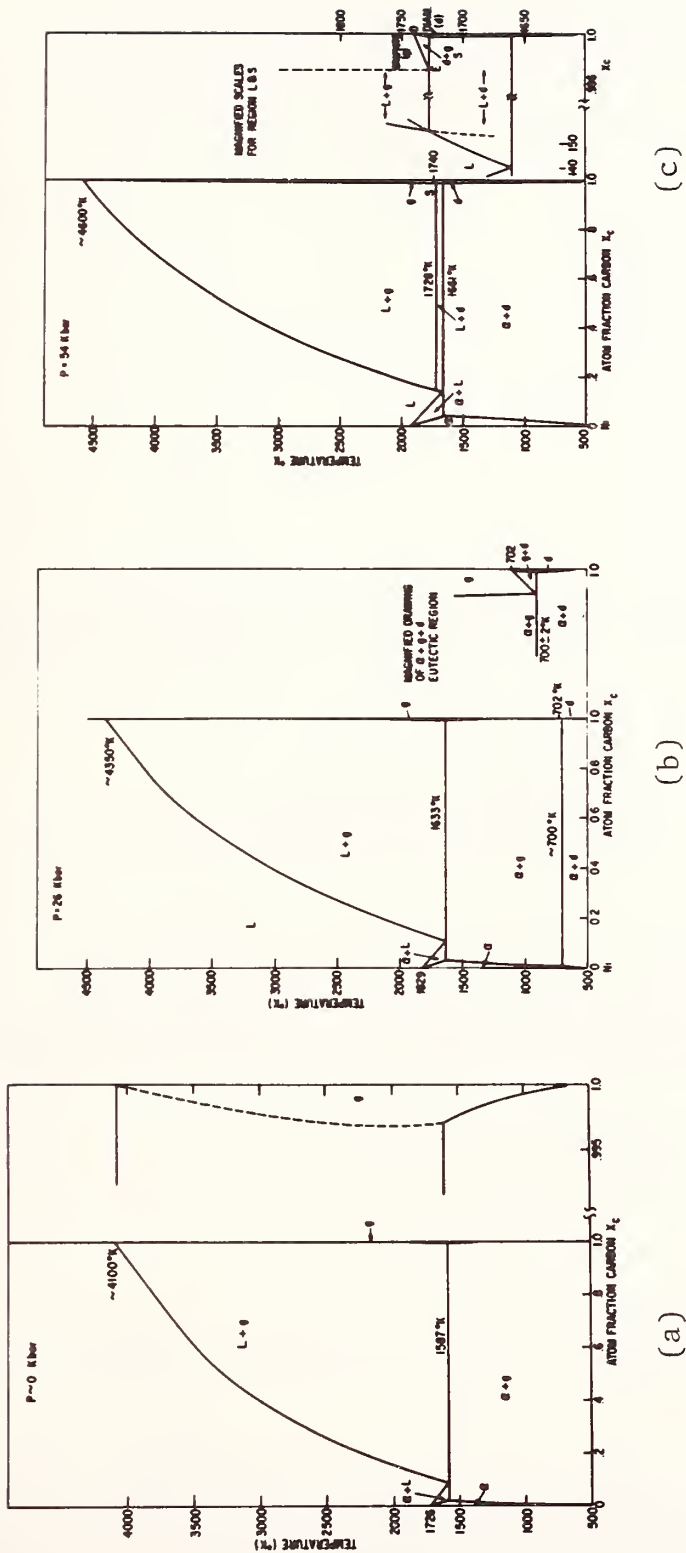


Figure 1. Isobaric sections of the Ni-C system equilibrium phase diagrams at (a) atmospheric pressure, (b) 26 kilobars, and (c) 54 kilobars.

Appendix A. Crystallographic data for the Elements.

Element	Pressure (kbar)	Temperature (°C)	Crystal System	Structure Type	a (Å)	b (Å)	c (Å)	Angle (°)	Z	Space Group
Cs(I)	R	25	cubic	bcc	6.141				2	Im3m
Cs(II)	25	R	cubic	fcc	6.465				4	Fm3m
Cs(III)	41.7	27	cubic	fcc	5.800				4	Fm3m
Sr(I)	R	25	cubic	fcc	6.0849				4	Fm3m
Ba(I)	R	25	cubic	bcc	5.013				2	Im3m
Ba(II)	58	R	hexagonal	hcp	3.901		6.154		2	P6 ₃ /mmc
Ga(I)	R	24	orthorhombic		4.5197	4.5260	7.6633		8	Cmca
Ga(II)	>20	R	tetragonal	bct	2.808		4.458		2	I4/mmm
Tl(I)	R	18	hexagonal	hcp	3.4566		5.5248		2	P6 ₃ /mmc
Tl(II)	R	262	cubic	bcc	3.882				2	Im3m
Tl(III)	60	R	cubic	fcc	4.778				4	Fm3m
C(I)	R	R	hexagonal	graphite	2.456		6.696		4	P6 ₃ mc
C(II)	R	20	cubic	diamond	3.56679				8	Fd3m
Si(I)	R	25	cubic	diamond	5.4307				8	Fd3m
Si(II)	134	R	tetragonal	white-Sn	4.686		2.585		4	I4 ₁ /amd
Si(III)	R	R	cubic		6.636				16	Ia3
Ge(I)	r	25	cubic	diamond	5.6575				8	Fd3m
Ge(II)	R	R	tetragonal		5.93		6.98		12	P4 ₃ 2 ₁ 2
Ge(III)	100	R	tetragonal	white-Sn	4.884		2.696		4	I4 ₁ /amd
Sn(I)	R	25	tetragonal	white-Sn	4.8315		3.1814		4	I4 ₁ /amd
Sn(III)	39	314	tetragonal	bct	3.81		3.48		2	I4 ₁ /mmm
Pb(I)	R	25	cubic	fcc	4.9502				4	Fm3m
Pb(II)	139	R	hexagonal	hcp	3.265		5.387		2	P6 ₃ /mmc
P(Black I)	R	22	orthorhombic		3.3136	10.478	4.3763	57.25	8	Cmca
P(Black II)	86	R	rhombohedral	As	3.524				2	R3m
P(Black III)	101	R	cubic	sc	2.377				1	
As(I)	R	23	rhombohedral	As	4.1318			54.13	2	R3m
As(II)	R	R	tetragonal		8.691		6.363		2	
Sb(I)	R	25	rhombohedral	As	4.5067			57.107	2	R3m
Sb(II)	64	R	cubic	sc	2.986				1	
Bi(I)	R	25	rhombohedral	As	4.746			57.23	2	R3m
Bi(II)	26	R	monoclinic		6.674	6.117	3.304	110.33	4	C2/m
Bi(V)	90	R	cubic	bcc	3.800				2	Im3m
Fe(I)	R	25	hexagonal	Sc	4.3656		4.9590		3	P3 ₁ 21
Se(II)										
Te(I)	R	25	hexagonal		4.4566		5.9268		3	P3 ₁ 21
Te(III)	115	R	rhombohedral	β-Po	3.002			103.3	1	R3m
Ti(I)	R	25	hexagonal	hcp	2.9511		4.6843		2	P6 ₃ /mmc

Element	Pressure (kbar)	Temperature (°C)	Crystal System	Structure Type	a(Å)	b(Å)	c(Å)	Angle (°)	Z	Space Group
Tl(II)	R	900	cubic	bcc	3.3065				2	Im3m
Tl(III)	R	R	hexagonal		4.625		2.813		3	
Tl(IV)?	R	R	cubic	bcc	3.276				2	Im3m
Zr(I)	R	25	hexagonal	hcp	3.2312		5.1477		2	P6 ₃ /mmc
Zr(II)	R	862	cubic	bcc	3.6090				2	Im3m
Zr(III)	R	R	hexagonal		5.036		3.109		3	
Zr(IV)?	R	R	cubic	bcc	3.568				2	Im3m
Fe(I)	R	20	cubic	bcc	2.8664				2	Im3m
Fe(II)	R	916	cubic	fcc	3.6468				4	Fm3m
Fe(III)	R	1394	cubic	bcc	2.9322				2	Im3m
Fe(IV)	151	R	hexagonal	hcp	2.461		3.952		2	P6 ₃ /mmc
Rh	R	20	cubic	fcc	3.8044				4	Fm3m
Hg(I)	R	-46	rhombohedral	Hg	3.005			70.53	1	R3m
Hg(II)	R	-196	tetragonal	bct	3.995		2.825		2	I4/mmm
La(I)	R	R	hexagonal	dhcp	3.770		12.159		4	P6 ₃ /mmc
La(II)	R	R	cubic	fcc	5.296				4	Fm3m
La(III)	R	887	cubic	bcc	4.26				2	Im3m
Ce(I)	R	23	cubic	fcc	5.1601				4	Fm3m
Ce(II)	R	25	hexagonal	dhcp	3.673		11.802		4	P6 ₃ /mmc
Ce(III)	R	-196	cubic	fcc	4.85				4	Fm3m
Pr(I)	R	R	hexagonal	dhcp	3.6725		11.8354		4	P6 ₃ /mmc
Pr(II)	R	821	cubic	bcc	4.13				2	Im3m
Pr(III)	40	R	cubic	fcc	4.88				4	Fm3m
Nd(I)	R	R	hexagonal	dhcp	3.6579		11.7992		4	P6 ₃ /mmc
Nd(II)	R	883	cubic	bcc	4.13				2	Im3m
Nd(III)	50	R	cubic	fcc	4.80				4	Fm3m
Sm(I)	R	R	rhombohedral	Sm	8.996			23.22	3	R3m
Sm(III)	R	R	hexagonal	dhcp	3.618		11.66		4	P6 ₃ /mmc
Gd(I)	R	20	hexagonal	hcp	3.6360		5.7826		2	P6 ₃ /mmc
Gd(II)	R	R	cubic	bcc	4.06				2	Im3m
Gd(III)	R	R	rhombohedral	Sm	8.92			23.3	3	R3m
Tb(I)	R	R	hexagonal	hcp	3.6010		5.6936		2	P6 ₃ /mmc
Tb(II)	R	R	cubic	bcc					2	Im3m
Tb(III)	R	R	rhombohedral	Sm	8.83			23.42	3	R3m
Dy(I)	R	R	hexagonal	hcp	3.5903		5.6475		2	P6 ₃ /mmc
Dy(II)	R	R	cubic	bcc					2	Im3m

Appendix A. Crystallographic data for the Elements.

Element	Pressure (kbar)	Temperature (°C)	Crystal System	Structure Type	a (Å)	b (Å)	c (Å)	Angle (°)	Z	Space Group
Dy(III)	75	R	rhombohedral	Sm	8.39			23.0	3	R3m
Ho(I)	R	R	hexagonal	hcp	3.5773		5.6158		2	P6 ₃ /mmc
Ho(II)	R	R	cubic	bcc					2	Im3m
Ho(III)	85	R	rhombohedral	Sm	8.26			23.3	3	R3m
Er(I)	R	R	hexagonal	hcp	3.5588		5.5874		2	P6 ₃ /mmc
Er(II)	R	R	cubic	bcc					2	Im3m
Tm(I)	R	R	hexagonal	hcp	3.5375		5.5546		2	P6 ₃ /mmc
Tm(II)	116	R	rhombohedral	Sm	3.327		23.48		3	R3m
Yb(I)	R	R	cubic	fcc	5.4862				4	Fm3m
Yb(II)	R	23	hexagonal	hcp	3.8799		6.3859		2	P6 ₃ /mmc
Yb(III)	39.5	R	cubic	bcc	4.02				2	Im3m
Lu(I)	R	R	hexagonal	hcp	3.5031		5.5509		2	P6 ₃ /mmc
Lu(II)	230	R	rhombohedral	Sm	3.176		21.77		3	R3m
Th(I)	R	R	cubic	fcc	5.0845				4	Fm3m
Th(II)	R	1450	cubic	bcc	4.11				2	Im3m
U(I)	R	25	orthorhombic	U	2.8537	5.8695	4.9548		4	Cmcm
U(II)	R	720	tetragonal		10.759		5.656		30	P4 ₂ /mmm
U(III)	R	805	cubic	bcc	3.524				2	Im3m
Np(I)	R	20	orthorhombic		6.633	4.723	4.887		8	Pnma
Np(II)	R	313	tetragonal		4.897		3.388		4	P4 ₂ 12
Np(III)	R	600	cubic	bcc	3.52				2	Im3m
Pu(I)	R	21	monoclinic		6.183	4.822	10.963	101.79	16	P2 ₁ /m
Pu(II)	R	190	monoclinic		9.284	10.463	7.859	92.13	34	I2/m
Pu(III)	R	235	orthorhombic		3.1587	5.7682	10.162		8	Fddd
Pu(IV)	R	320	cubic	fcc	4.6370				4	Fm3m
Pu(V)	R	500	cubic	bcc	3.638				2	Im3m
Am(I)	R	20	hexagonal	dhcp	3.4680		11.240		4	P6 ₃ /mmc
Am(II)	R	22	cubic	fcc	4.894				4	Fm3m

Element	Pressure (kbar)	Temperature (°C)	Crystal System	Structure Type	a(Å)	b(Å)	c(Å)	Angle (°)	Z	Space Group
CsCl(I)	N	R	Cubic	CsCl	4.123				1	Pm3m
CsCl(II)	N	500	Cubic	NaCl	7.09				4	Fm3m
KBr(I)	N	R	Cubic	NaCl	6.599				4	Fm3m
KBr(II)	22		Cubic	CsCl	3.74				1	Pm3m
KCl(I)	N	R	Cubic	NaCl	6.2929				4	Fm3m
KCl(II)	22		Cubic	CsCl	3.58				1	Pm3m
KF(I)	N	R	Cubic	NaCl	5.344				4	Fm3m
KF(II)	35		Cubic	CsCl	3.06				1	Pm3m
KI(I)	N	R	Cubic	NaCl	6.0655				4	Fm3m
KI(II)	19		Cubic	CsCl	3.94				1	Pm3m
LiCl(I)	N	R	Cubic	NaCl	5.1399				4	Fm3m
NaCl(I)	N	R	Cubic	NaCl	5.6402				4	Fm3m
NaCl(II)	290		Cubic	CsCl	2.997				1	Pm3m
NaF(I)	N	R	Cubic	NaCl	4.628				4	Fm3m
NaI(I)	N	R	Cubic	NaCl	6.475				4	Fm3m
NH ₄ Br(I)	N	250	Cubic	NaCl	6.90				4	Fm3m
NH ₄ Br(II)	N	26	Cubic	NaCl	4.059				1	Pm3m
NH ₄ Br(III)	N	-73	Tetragonal	CsCl	5.713	4.055			2	P4/nmm
NH ₄ Br(IV)	N	-170	*							
NH ₄ Cl(I)	N	250	Cubic	NaCl	6.52				4	Fm3m
NH ₄ Cl(II)	N	26	Cubic	CsCl	3.8758				1	Pm3m
NH ₄ Cl(III)	N	-185	Cubic		3.8200				1	P43m
NH ₄ F(I)	N	23	Hexagonal	Wurtzite	4.4385		7.1635		2	P6 ₃ mc
NH ₄ F(II)	4	23	Tetragonal		10.2		3.37		8	
NH ₄ F(III)	11.5	23								
NH ₄ F(IV)	4	178	Cubic	NaCl	5.77				4	Fm3m
NH ₄ I(I)	N	R	Cubic	NaCl	7.259				4	Fm3m
NH ₄ I(II)	N	-17	Cubic	CsCl	4.38				1	Pm3m
NH ₄ I(III)	N	-100	Tetragonal		6.18		4.37		2	P4/nmm
NH ₄ I(IV)	10	-100	*							
ND ₄ Br(I)	N	-30	Cubic	CsCl	4.034				1	Pm3m
ND ₄ Br(II)	N	-71.5	Tetragonal		5.713		4.055		2	P4/nmm
ND ₄ Br(III)	N	-140	Cubic	4.010					1	P43m
ND ₄ F(I)	N	23	Hexagonal	Wurtzite	4.4378		7.1635		2	P6 ₃ mc
ND ₄ F(II)	4	23	Tetragonal		10.2		3.37		8	
RbBr(I)	N	R	Cubic	NaCl	6.868				4	Fm3m

Element	Pressure (kbar)	Temperature (°C)	Crystal System	Structure Type	a (Å)	b (Å)	c (Å)	Angle (°)	Z	Space Group
RbBr(II)	5	R	Cubic	CsCl	4.09				1	Pm3m
RbCl(I)	N	R	Cubic	NaCl	6.590				4	Fm3m
RbCl(II)	5	R	Cubic	CsCl	3.91				1	Pm3m
RbF(I)	N	R	Cubic	NaCl	5.64				4	Fm3m
RbF(II)	5	R	Cubic	CsCl	3.29				1	Pm3m
RbI(I)	N	R	Cubic	NaCl	7.34				4	Fm3m
TlBr	N	R	Cubic	CsCl	3.838				1	Pm3m
TlCl	N	R	Cubic	CsCl	3.9846				1	Pm3m
TlF(I)	N	82	Tetragonal	Distorted NaCl	3.771	6.115			2	I4/mmm
TlF(II)	N	R	Orthorhombic		5.180	5.495	6.080		4	Fmmm
TlF(III)	12	R	*							
TlI(I)	N	R	Orthorhombic		5.24	4.57	12.92		4	Cmcm
TlI(II)	5	R	Cubic	CsCl	4.10				1	Pm3m
AgCN(I)	N	R	Rhombohedral		3.99		5.26		3	R3c
AgCN(II)	12	R	*							
AuCN(I)	N	25	Hexagonal		3.40		5.09		1	P6mm
AuCN(II)			*							
CsCN(I)	N	20	Cubic	CsCl	4.29				1	Pm3m
CsCN(II)	N	-80	Rhombohedral		5.79		7.78		3	R3m
KCN(I)	N	25	Cubic	NaCl	6.527				4	Fm3m
KCN(III)	30	100	Cubic	CsCl	3.808				1	Pm3m
KCN(IV)	25	23	Monoclinic		5.530	5.209	3.743	95	2	Cm
KCN(V)	N	-80	Monoclinic		8.04	4.53	7.47	109.4	4	Cc
KSCN(I)	N	160	Tetragonal		6.70		7.73		4	I4/mcm
KSCN(II)	N	20	Orthorhombic		6.66	7.58	6.635		4	Pcmb
KSCN(III)	20	450	*							
KSCN(IV)	28	500	*							
NaCN(I)	N	20	Cubic	NaCl	5.88				4	Fm3m
NaCN(II)	N	-10	Orthorhombic		4.71	5.61	3.74		2	Immm
NaSCN	N	R	Orthorhombic		13.45	4.10	5.66		8	Pnma or Pn21a
RbCN(I)	N	R	Cubic		6.834				4	P2 ₁
RbCN(II)	N	-182	Monoclinic		6.66	4.87	4.77	94.3	2	P6 ₃ /mmc
PtB	N	R	Hexagonal		3.36		4.06		1	
MoC(I)	N	R	Hexagonal		2.898		2.809		1	

Element	Pressure (kbar)	Temperature (°C)	Crystal System	Structure Type	a (Å)	b (Å)	c (Å)	Angle (°)	Z	Space Group
MoC(I)	N	R	Hexagonal		3.00		14.58		6	P6 ₃ /mmc
MoC(I)	N	R	Hexagonal		2.932		10.97		4	Fm3m
MoC(II)	N	R	Cubic	NaCl	4.27				4	Fm3m
ReC	60	800	Hexagonal	γ-MoC	2.840		9.85		4	P6 ₃ /mmc
BN(I)	N	35	Hexagonal	BN	2.502		6.661		6	P6 ₃ /mmc
BN(II)	N	R	Cubic	ZnS	3.62				4	F43m
BN(III)	N	R	Hexagonal	Wurtzite	2.55		4.20		2	P6 ₃ mc
BaO(I)	N	R	Cubic	NaCl	5.542				4	Fm3m
BaO(II)	100	R	Tetragonal		4.549		3.606		2	P4/mmm
BaO(III)	180	R	Tetragonal	PbO	4.397		3.196		2	P4/mmm
EuO(I)	N	R	Cubic	NaCl	5.143				4	Fm3m
EuO(II)	310	R	Cubic	NaCl	4.743				4	Fm3m
EuO(III)	400	R	Cubic	CsCl	2.92				1	Pm3m
FeO	N	R	Cubic	NaCl	4.312				4	Fm3m
SnO(I)	N	R	Tetragonal	PbO	3.796		4.816		2	P4/mmm
SnO(II)	60	R	Hexagonal	Wurtzite	3.42		5.62		2	P6 ₃ mc
SrO(I)	N	R	Cubic	NaCl	5.142				4	Fm3m
SrO(II)	175	R	Tetragonal		4.912		4.949		4	Fm3m
ZnO(I)	N	R	Hexagonal	Wurtzite	3.242		5.176		2	P6 ₃ mc
ZnO(II)	N	R	Cubic	NaCl	4.28				4	Fm3m
NaOH(II)	N	R	Orthorhombic	TlI	3.397	11.32	3.397		4	Amam
NaOH(I)	N	300	Monoclinic		3.434	3.428	6.068	109.8	2	P2 ₁ /m
NaOH(III)			*							
NaOH(IV)			*							
NaOH(V)			*							
BP	N	R	Cubic	ZnS	4.54				4	F43m
GaP(I)	N	10	Cubic	ZnS	5.447				4	F43m
GaP(II)	220	R	*							
GeP(I)	N	R	Tetragonal		3.544		5.581		2	I4mm
InP(I)	N	1	Cubic	ZnS	5.868				4	F43m
InP(II)	N	R	Cubic	NaCl	5.71				4	Fm3m
SiP(I)	N	R	Orthorhombic		6.90	9.40	7.68		12	
SiP(II)	N	R	Cubic	ZnS	5.241				4	F43m
SnP(I)	N	R	Hexagonal		8.78		5.98		8	
SnP(II)	N	R	Tetragonal		3.831		5.963		2	
SnP(III)	N	K	Cubic	NaCl	5.536				4	Fm3m
CdS(I)	N	R	Hexagonal	Wurtzite	4.134		6.713		2	P6 ₃ mc

Appendix B. Crystallographic data for the AB Type Compounds

Element	Pressure (kbar)	Temperature (°C)	Crystal System	Structure Type	a(Å)	b(Å)	c(Å)	Angle (°)	Z	Space Group
CdS(I)	N	R	Cubic	ZnS	5.835				4	F43m
CdS(II)	77	R	Cubic	NaCl	5.27				4	Fm3m
FeS(I)	N	R	Hexagonal	Triolite	5.946		11.72		12	P62c
FeS(II)	100	22	**							
FeS(III)	N	R	Hexagonal	NIAs	3.426		5.687		2	P63/mmc
HgS(I)	N	R	Cubic	ZnS	5.858				4	F43m
HgS(II)	N	R	Hexagonal	HgS	4.149		9.149		3	Pe121
NiS(I)	N	R	Hexagonal	NIAs	3.428		5.340		2	P63/mmc
NiS(II)	20	R	Hexagonal	Wurtzite	**				2	P63mc
SmS(I)	N	R	Cubic	NaCl	5.863				4	Fm3m
SmS(II)	6.5	R	Cubic	NaCl'	5.70				4	Fm3m
ZnS(I)	N	R	Cubic	ZnS	5.406				4	F43,
ZnS(II)	N	R	Hexagonal	Wurtzite	3.811		6.234		2	P63mc
ZnS(III)	190	R	*							
ZnS(IV)	420	R	*							
BAs	N	R	Cubic	ZnS	4.777				4	F43m
GaAs(I)	N	R	Cubic	ZnS	5.654				4	F43m
GaAs(II)	190	R	*							
GaAs(III)	200	R	*							
GeAs(I)	N	R	Tetragonal		3.715		5.832		2	
InAs(I)	N	R	Cubic	ZnS	6.036				4	F43m
InAs(II)	100	R	Cubic	NaCl	5.514				4	Fm3m
MnAs(I)	N	R	Hexagonal	NIAs	3.710		5.691		2	P63/mmc
MnAs(II)	N	50	Orthorhombic	MnP	6.39	5.64	3.63		4	Pbmm
AlSb(I)	N	R	Cubic	ZnS	5.985				4	F43m
AlSb(II)	120	R	Tetragonal	β-Sn	5.375		5.911		2	I41/amd
GaSb(I)	N	R	Cubic	ZnS	6.135				4	F43m
GaSb(II)	90	R	Tetragonal	β-Sn	5.348		2.973		2	I41/amd
	1 atm.	90 K			5.47		3.06		2	
InSb(I)	N	R	Cubic	ZnS	6.474				4	F43m
InSb(II)	.26	R	Tetragonal	β-Sn	5.862		3.105		2	I41/amd
InSb(III)	125	R	Hexagonal		6.099		5.708		2	
InSb(IV)	70	R	Orthorhombic		2.921	5.56	3.06		1	
CdSe(I)	N	R	Hexagonal	Wurtzite	4.30		6.02		2	P63mc
CdSe(II)	32	R	Cubic	NaCl	5.49				4	Fm3m
HgSe(I)	N	R	Cubic	ZnS	6.09				4	F43m
HgSe(II)	15	R	Hexagonal	HgS	4.32		9.62		3	P3121

Element	Pressure (kbar)	Temperature (°C)	Crystal System	Structure Type	a(Å) °	b(Å) °	c(Å) °	Angle (°)	Z	Space Group
InSe(I)	N	R	Hexagonal		4.05		16.93		4	P6 ₃ /mmc
InSe(II)	40	520	*							
PbSe(I)	N	R	Cubic	NaCl	6.122				4	Fm3m
PbSe(II)	42	R	Orthorhombic		11.71	4.36	4.42		4	Pnma
CdTe(I)	N	R	Cubic	ZnS	6.478				4	F43m
CdTe(II)	30	R	Cubic	NaCl	5.92				4	Fm3m
CdTe(III)	100	R	Tetragonal		5.86		2.94		2	I4 ₁ /amd
CdTe(III)	200	R	Tetragonal		5.62		2.96		2	I4 ₁ /amd
EuTe(I)	N	R	Cubic	NaCl	6.591				4	Fm3m
EuTe(II)	100	R	Cubic	CsCl	3.755				1	Pm3m
GeTe(I)	N	R	Rhombohedral	As	4.171				3	
GeTe(II)	40	R	Cubic	NaCl	5.80		10.661		4	Fm3m
GeTe(II)	N	60	Cubic	NaCl	5.998				4	Fm3m
HgTe(I)	N	R	Cubic	ZnS	6.37				4	F43m
HgTe(II)	20	R	Hexagonal	HgS	4.51		10.13		3	P3 ₁ 21
InTe(I)	N	R	Tetragonal	TlSe	8.437		7.139		8	I4/mcm
InTe(II)	30	R	Cubic	NaCl	6.160				4	Fm3m
InTe(II')	N	R	Tetragonal		6.06				2	P6 ₃ /mmc
MnTe(I)	N	R	Hexagonal		4.148		6.710		4	Fm3m
MnTe(II)	N	R	Cubic		6.003				4	Fm3m
PbTe(I)	N	R	Cubic	NaCl	6.36				4	Fm3m
PbTe(II)	43	R	Orthorhombic		11.61	4.00	4.39		4	Pnma
PrTe(I)	N	R	Cubic	NaCl	6.315				4	Fm3m
PrTe(II)	90	R	Cubic	CsCl	3.761				1	Pm3m
SmTe(I)	N	R	Cubic	NaCl	6.595				4	Fm3m
SmTe(II)	110	R	Cubic	CsCl	3.656				1	Pm3m
SnTe(I)	N	R	Cubic	NaCl	6.2956				4	Fm3m
SnTe(II)	20	R	Orthorhombic		11.59	4.37	4.48		4	Pnma
YbTe(I)	N	R	Cubic	NaCl	6.353				4	Fm3m
ZnTe(I)	N	R	Cubic	ZnS	6.101				4	F43m
ZnTe(II)			*							

Appendix B. Crystallographic data for the AB Type Compounds

Element	Pressure (kbar)	Temperature (°C)	Crystal System	Structure Type	a(Å)	b(Å)	c(Å)	Angle (°)	Z	Space Group
AgBr(I)	N	R	Cubic	NaCl	5.7745				4	Fm3m
AgBr(II)	70	R	Hexagonal	HgS	4.0		7.15		3	P3121
AgCl(I)	N	R	Cubic	NaCl	5.547				4	Fm3m
AgCl(II)	74	R	Hexagonal	B9 (HgS)	4.06		7.02		3	P3121
AgCl(III)	74	R	Orthorhombic		6.90	5.08	4.05		4	Pnma
AgF(I)	N	R	Cubic	NaCl	4.932				4	Fm3m
AgF(II)	25	R	Cubic	CsCl	2.945				1	Pm3m
AgF(III)		R	Hexagonal		3.246		6.226		2	
AgI(I)	N	145.8	Cubic	5.044					2	Im3m
AgI(II)	N	R	Hexagonal	Wurtzite	4.58		7.494		2	P63mc
AgI(II')	N	R	Cubic	ZnS	6.486				4	F43m
AgI(III)	4	R	Cubic	NaCl	6.07				4	Fm3m
AgI(IV)	3	R	Tetragonal		4.58		6.00		2	
AgI(V)	100	R	Tetragonal		4.615		5.020		4	
CsF(I)	N	R	Cubic	NaCl	6.008				4	Fm3m
CsF(II)	48	R	Cubic	CsCl	3.39				1	Pm3m
CuBr(I)	N	480	Cubic	αAgI	4.56				2	Im3m
CuBr(II)	N	430	Hexagonal	Wurtzite	4.06		6.66		2	P63mc
CuBr(III)	N	R	Cubic	ZnS	5.691				4	F43m
CuBr(IV)	50	R	*							
CuBr(V)	55	R	Tetragonal		5.40		4.75		4	
CuBr(VI)	75	R	Cubic	NaCl	5.14				4	Fm3m
CuCl(I)	N	410	Hexagonal	Wurtzite	3.91		6.42		2	P63mc
CuCl(II)	N	25	Cubic	ZnS	5.416				4	F43m
CuCl(III)	10	450	*							
CuCl(IV)	55	R	Tetragonal		5.21		4.61		4	
CuCl(V)	70	R	Cubic	NaCl	4.93				4	Fm3m
CuI(I)	N	440	Cubic	Disordered	6.14				4	F43m
CuI(II)	N	390	Hexagonal	Wurtzite	4.31		7.09		2	P63mc
CuI(III)	N	R	Cubic	ZnS	6.059				4	F43m
CuI(IV)	16	R	Rhombohedral		4.164		20.41		6	
CuI(V)	65	R	Tetragonal	Red PbO	4.02		5.70		2	P4/mmm
CuI(VI')	77	120	Cubic	S. C.	5.627				4	
CuI(VII)	20	800	*							
CuI(VIII)	120	R	Cubic	NaCl	5.15				4	Fm3m

DISCUSSION (Jan. 10 - AM Session)

T. B. Massalski, chairman - I would like to invite any further discussion on the subject of phase diagram compilations for which there exists a great need, and for which agencies should give financial assistance to projects carried out by qualified users.

Barry Rosof - I have one observation about the compilation, "Phase Diagrams for Ceramists". I have the feeling that metallurgists should look a little bit more carefully after their phase diagram needs in areas other than metallic systems. That is, perhaps we need more metallurgical input into the areas such as slags, oxides, oxichlorides, etc., that some of Dr. Roth's respondents alluded to. I'm sure that several of the diagrams in the areas that "Phase Diagrams for Ceramists" does not do a complete job on, are in areas of great interest to metallurgists.

P. Gallagher - I am a little concerned with Dr. Roth's removal of the vapor pressure on the phase diagram, treating it more as a physical property. I find it difficult to divorce vapor pressure from the study of phase diagrams. I would be interested to know whether other people felt the same way.

L. Kaufman - I believe that the integration of the vapor pressure and other thermochemistry, as it were, is an integral part of the phase diagram picture. I think only with the coupling of these two types of information that we begin to unscramble the different types of equilibria that can be observed experimentally and make some sense for example, out of the copper-lead system. Although, the job may be a lot more complicated, I think that's what will evolve over the next period of 5 to 10 years as an activity that will help bring some order to this field. I think it will be a costly activity, but I think the means to fund such efforts in this country and overseas will be found, because the needs for such information is really quite acute.

W. White - I think we have identified an interesting "gap problem" this morning, which is actually related to the band gap. If you have materials with band gaps 2 1/2 to 3 electron volts, there're called ceramics, and Dr. Roth described quite a wide range of such materials for which compilations exist. If the gap is zero or small, it is a metal or a semiconductor and several groups are working on that. In between, from about 0.5 to 2.5 electron volts, is a very large range of particular chalcogenide and pnictide systems, such as sulfides and selenides, for which, as near as I can tell, there are no systematic compilations at all. Most of these, incidentally, are P-T-X systems and not simply T-X type systems.

L. Bennett - I'd like to respond to that. I do agree exactly with what you've said. I want to emphasize that one of the reasons for the organization of this meeting as a joint organization between Dr. Roth's group in ceramics and our own for metallic system, was to be sure that this in between part does not fall into the cracks. There will be some cases of overlap, but that is better than exclusion. The problem of gaps and overlap is something we will continue to pay attention to, and we plan to work together on that aspect.

R. Roth - I'll take this opportunity to answer some of these questions. First of all vapor pressure: I have worked for 25 years with the condensed phase rule and I tend to ignore not only vapor pressure but also partial pressures. However, I am just one voice in quite a large compilation effort. I think that any published phase equilibrium diagram in which vapor pressure is taken into account experimentally and properly will be included in "Phase Diagram for Ceramists". The other question is that which Bill White raised. The new editions of "Phase Diagrams for Ceramists" will make a chance to include all sulfides and all nitrides and oxinitrides in mixed materials of the Sialon type. We made a judgment based largely on consultation with Dr. Thurmond not to include semiconductors. So nobody is covering selenides and tellurides of the semiconducting type.

A. Navrotsky - In addition to interrelation between phase diagrams and thermodynamic data (and I agree with Larry Kaufman's comments), we also have to integrate phase diagrams, thermodynamic data and crystal structures. It's very important to characterize the phases that are being formed and realize what is going on in a structural scale and to let this tell us what is possible or impossible in terms of phase relations and what is sensible or nonsense in terms of thermodynamic parameters and thermodynamic equations we use.



PHASE DIAGRAM INFORMATION FROM COMPUTER BANKS

BY

I. ANSARA

LABORATOIRE DE THERMODYNAMIQUE ET PHYSICO-CHIMIE METALLURGIQUES
ASSOCIE AU C.N.R.S., E.N.S.E.E.G., DOMAINE UNIVERSITAIRE, B.P. 44,
38401 - ST. MARTIN D'HERES, FRANCE.

Phase diagrams are usually determined by classical methods such as thermal analysis, N.M.R., and equilibrium techniques for relatively small composition and temperature ranges ; rather fewer are calculated from the thermodynamic properties because of the lack of experimental determinations. Although these two methods of establishing phase diagrams have been carried out independently, they can be reconciled through thermodynamic principles to ensure a complete and consistent description of the system.

The experimental data are usually presented in the literature in the form of tables, equations or graphs, the analysis of which data is always tedious. When partial quantities of the thermodynamic properties relative to multicomponent solutions are determined, different methods are used to integrate the Gibbs-Duhem equation, all of them requiring limiting binary data which are not always critically analyzed.

A feature which is rarely achieved is the consistency between the thermodynamic properties of a solution and phase equilibria. This is due not only to the lack of complete information for both of these properties but also to the complexity of the problem.

And yet the need to develop computer techniques for phase diagram calculation and storage arises from a number of major practical considerations. Firstly, since the volume of in-

formation is very large both for phase diagrams and thermodynamic properties, computers provide a simple means of handling the data. Secondly, and certainly the most expensive of all, it is necessary to achieve consistency between the phase diagram and thermodynamic data, which requires extensive computation. Thirdly, modern technology requires that information be provided rapidly on the equilibrium phase stability of the materials that it uses. The computer enables such data to be calculated for the operating conditions of interest and to be presented in a comprehensive manner to the user.

Thus the establishment of a data bank for phase diagrams necessarily implies computer programs for the numerical treatment of raw data in order to perform a critical assessment. Kirchner(1) has used a computerized mathematical optimization procedure to analyze the experimental tie-lines for the Fe-Cr-Mn system in terms of a thermodynamic model. Zimmermann (2) has developed a method based on the least squares technique in order to facilitate critical assessment for binary and ternary systems, and an account of this work is described in these proceedings. Most of these programs should be designed so as to retrieve the thermodynamic properties of the system or to be used to predict them.

Bennett (3) has recently listed both existing phase diagram data compilations and the persons and centers (4) carrying out continuing phase data programs to which should be added the monographs co-ordinated by the International Atomic Energy Agency in Vienna, the Incra series and the individual contributions of the Calphad Members.

But to my knowledge, the only organized centers for the computation of phase diagrams from thermodynamic properties are those of the S.G.T.E. (Scientific Group of Thermodynamicists, Europe), and ManLabs (U.S.A.) Such calculations are carried out in the U.S.S.R. but emphasis is put on the mathematical representation of the phase "Surfaces" or Volumes" for multicomponent systems.

The organization of a data bank relative to the thermodynamic properties and the calculation of phase diagrams is summarized in Table I. The experimental information for the binary and multicomponent systems is critically analyzed. The equilibrium conditions for phase stability involved therein can be analyzed either by considering the equality of the partial Gibbs energies of the different components in the different phases or by minimizing the Gibbs energy of the system. In the latter case, the Gibbs energy of the multiphase system is equal to :

$$\Delta G = \sum_{j=1}^{j=\phi} P_j (\Delta G^{(j)} - \sum_{i=1}^{i=m} x_i \Delta G_i^{(j \rightarrow \phi)})$$

$$\text{with } \Delta G^{(j)} = G^{(j)} - \sum_{k=1}^{k=m} x_k {}^\circ G_k^{(j)}$$

$$\text{and } \sum_{j=1}^{j=\phi} P_j = 1$$

where $\Delta G^{(j)}$ is the Gibbs energy of phase j referred to its pure elements in the same structural state and $\Delta G_i^{(j \rightarrow \phi)}$ the free energy difference due to the transformation of component i from the structural state j to that of ϕ . The number of variables, which are the composition at equilibrium for a given temperature, vary from 1 to $(m-1)$, as is seen by considering the constraints imposed by the generalized lever rule. For a ternary system, that would correspond from the simplest case of a ternary phase in equilibrium between ternary phases.

From a practical point of view and especially for higher order systems, the use of integral quantities is preferable to that of the partial quantities because it reduces the number of mathematical operations. Numerical methods which do not require the calculation of derivatives such as the simplex method described by Nelder (6) are also preferable. This method can be established for unknown compositions, where n is a variable parameter. After an iterative process, evaluated data are obtained, which can be stored and retrieved for various applications. In that framework, it is also possible to evaluate the thermodynamic properties from phase diagrams according to methods described by Wagner (7),

Hiskes (8,9,10), Rudman (11), Kaufman (12,13), Chiotti (14), Vieland (15) and Sundquist (16).

When the thermodynamic properties of a multicomponent system are not available, they can be calculated from equations which are derived from statistical thermodynamics (18 to 31) or are semi empirical (32 to 40) but always imply the knowledge of the limiting binary data. These equations have been reviewed elsewhere (17).

Apart from the quasi-chemical treatment which needs a resolution of a set of equations to derive the thermodynamic properties of mixing, all the other equations which are used to describe an excess property (for example the heat of mixing ΔH) can be written in the general form :

$$\Delta H = \sum_{i=1}^{i=m-1} \sum_{j=i+1}^{j=m} \alpha_{ij} (\Delta H_{ij}(x_i, x_j)) + \beta \prod_{k=1}^{k=m} x_k \sum_{i=1}^{i=m-1} \sum_{j=i+1}^{j=m} (\Delta \bar{H}_{i(j)}^{\infty} + \Delta \bar{H}_{j(i)}^{\infty})$$

where ΔH_{ij} represents the heat of mixing of the binary system ij , $\Delta \bar{H}_{i(j)}^{\infty}$ the partial heat of mixing of component i in the concentrated solution of j , α_{ij} and β are parameters which vary according to the model or equation which is used. Table II presents the relationship between these quantities for seven equations. A computer subroutine can automatically establish the dependence between these quantities when the name of the model is given ; the analytical form of the equations describing the thermodynamic properties of the binary system can be of any type, generally related to the structure of the data file in the computer bank.

CALCULATION OF BINARY PHASE DIAGRAMS FROM THERMODYNAMIC PROPERTIES

Let us consider a system which exhibits different solution phases and intermetallic compounds like the Ni-Ti for example. Phase boundaries have been calculated by various numerical methods (Newton Raphson or graphical methods) (9 to 12, 41, 42, 43) by considering all the possible two phase systems most of which are metastable with respect to the equilibrium phase diagram. When all the different possibilities have been assembled, the stable system can be

derived by inspection.

The other alternative is to design a computer program (44) which calculates the Gibbs energies of formation of all the different phases over the entire composition range and only those portions which have the lowest values are retained. If such curves intersect, there must be a common tangent to the two curves, whose point of contact lies on either side of the point of intersection. Thus the Gibbs energy is minimized at the point of intersection by any mathematical procedure which determines a common tangent. The phase diagram is then determined by a temperature scan. A metastable diagram can be obtained by deleting from the file the data corresponding to any given stable phase.

This procedure is similar to the method employed manually and has the advantage of considering all the phases simultaneously and of using integral quantities which may be represented either by polynomials or calculated by interpolation from tables using a spline function. In that case, a simplex method for minimization is preferable. Nevertheless, such a method can only be utilized if the thermodynamic properties of the different phases are given over the complete composition range ; thus the description of the hypothetical phases have to be included. For this, the lattice stabilities or the Gibbs energies of transformation of the pure elements have to be known. Kaufman (12) has derived these quantities for all the transition metals plus a certain number of others, and Michaels (45) has shown that Kaufman's approach could be extended to metals of group 1 to 3 and Lanthanides elements.

Similar procedures have been used by Hillert to calculate the Fe-S (46), Fe-N (47) and Mn-S (48) systems using a regular solution model. Kaestle (49) has also used simple models to calculate the binary phase diagram $T=F(x)$ of the FeO-X (X=MgO, MnO, Al_2O_3 , P_2O_5), CaO-Y (Y=MnO, MgO, SiO_2 , Al_2O_3 , P_2O_5), SiO_2 -Z (Z=MnO, MgO, Al_2O_3), MnO-MgO, MnO- Al_2O_3 systems.

Mathematical procedures can be incorporated into the organization of a bank so as to represent the phase boundaries by analytical equations. The coefficients which are then obtained are stored in a reduced manner. Figures 1 and 2 represent the phase diagrams of the Al-Mn and Ni-Ti systems published by Hansen (50) and which have been retrieved from the data bank on a graph plotter.

When computer facilities are available, the results obtained for a particular system by these two methods can be compared on a graphical or visual display. Figure 2 illustrates an on-line calculation for which the $T=F(x)$ curve is static on the screen superimposed on the calculated phase diagram, for which the user can adjust the underlying thermodynamic data.

CALCULATION OF TERNARY PHASE DIAGRAM FROM THERMODYNAMIC PROPERTIES

Extensive work has been carried out on phase diagram calculation from thermodynamic properties for ternary systems (51 to 61). Information is required not only on phase boundaries but also on tie-lines, locus of univariant points (e.g. eutectic valleys) in a ternary system, crystallization paths, etc. All these problems are in essence the same and can be resolved by minor changes in computer programs.

Different strategies of computing phase boundaries can then be considered. For example, it seems easier to calculate a univariant line by considering the three-phase equilibrium rather than to determine it by intersection of two liquidus lines at a given temperature. The number of unknowns to be calculated does not lengthen the calculation. Figure 3 shows the eutectic valley existing in the Ga-Sn-Zn calculated by this manner.

A similar strategy would be the most appropriate in quaternary and higher order systems. For example, once a three or four phase domain has been located at one temperature in such systems, it would be wise starting the calculation at other temperatures by determining the boundaries of this same region.

This strategy can be applied to the determination of the evolution of the composition of the liquid phase when a solid solution precipitates. For certain topologies of liquidus and solidus surfaces, the condition to precipitate a solid solution of fixed composition results from a straightforward calculation. Slightly different is the case where an imposed fraction of the liquid precipitates. In that case, a composition gradient in the solid may appear. Nevertheless optimum conditions can be defined. These two cases have been applied to the Ga-In-Sb system (63). Figures 4 and 5 show that below a certain temperature, a solid solution of fixed composition is obtained in both cases.

One has to be aware that if by using various models the phase boundaries differ only slightly, nevertheless the tie-line may differ appreciably. Figure 6 shows how the molar fraction of GaSb in the quasi-binary section $\text{GaSb}_x\text{-InSb}_{(1-x)}$ varies with respect to the molar fraction of gallium in the liquid solution when the regular solution (64,65) is used or when an "extended" Toop equation (54) is adjusted to agree with experimental ternary values.

The main problem in determining isothermal sections is the prediction of ternary intermetallic compounds or a limited intrusion of compound from the binary system into the ternary, for example the ternary sigma phase in the Fe-Cr-Ni system. Thus, the Gibbs energy of formation of the hypothetical sigma Ni-Cr phase must be estimated. Kaufman (60) and Rudy (66) have considered many of such cases.

Considerable work is being carried out on the use of the lattice simplex method (67 to 72). This technique was primarily used to establish a composition/property diagram in order to reduce lengthy experiments. The essence of such method, proposed by Scheffe (73) and analyzed by Gorman (74), consists in constructing mathematical models, usually polynomials, which correlate the property and composition of a test alloys. To calculate the coefficients of the equations, the properties are measured not at random, but according to a definite distribution within a simple lattice. A

possible selection of composition points for measuring responses is one that gives a uniform distribution of points over all possible mixtures of the components. Such a distribution is referred to as a quadratic, cubic or quartic lattice, depending on the number of points. For example, a cubic model in a ternary system shown in figure 7 describing the property y would be :

$$y = \beta_1 x_1 + \beta_2 x_2 + \beta_3 x_3 + \beta_{12} x_1 x_2 + \beta_{13} x_1 x_3 + \beta_{23} x_2 x_3 + \gamma_{12} x_1 x_2 (x_1 - x_2) \\ + \gamma_{13} x_1 x_3 (x_1 - x_3) + \gamma_{23} x_2 x_3 (x_2 - x_3) + \beta_{123} x_1 x_2 x_3$$

The coefficients β_i , β_{ij} , γ_{ij} and β_{123} are related to the value of property for a lattice point which may be a single determination or the average of several determinations. The solidus volume of the Nb-W-Ti-Zr was calculated by this manner by Zakharov (72) in the niobium rich corner.

CONCLUSION

Since the first attempts at determining the miscibility gap and the spinodal surface in the Cd-Pb-Sn-Zn system (75,76), not much work has been performed on quaternary phase diagrams. If the systems involving carbon, oxygen and nitrogen (77 to 81) are excluded, the only ones studied are those of the III-V or II-VI elements (82 to 86) and a system involving low melting elements (87).

The development of an a priori calculation for reciprocal systems (88,89,90), metal gas equilibria (91 to 97), slags, systems of nuclear interest, chemical vapor deposition, geochemical applications is becoming increasingly important. Thus it is important that a data bank be as complete as possible and its application adapted to the user's needs. This is not the case at present. Existing data banks relative to the thermodynamic properties are limited to inorganic substances and alloy systems, and for many

of them, it is not yet possible to calculate the phase diagram over the complete composition and wide temperature ranges. The data are scattered in the literature and a considerable task still remains to be done.

The thermodynamic description of solution phases, stable or metastable in the complete composition range or enthalpies of formation for intermetallic compounds are essential when higher order systems are to be investigated, and more and more theoretical work of increasing precision on the phase stabilities of elements and alloys (98 to 103) in particular is being published.

If this contribution is limited mainly to metallic systems, it is satisfying to see the number of contributions which are presented in these proceedings and which may bring considerable progress in the prediction, assessment and compilation of phase diagrams of systems other than those involving metals.

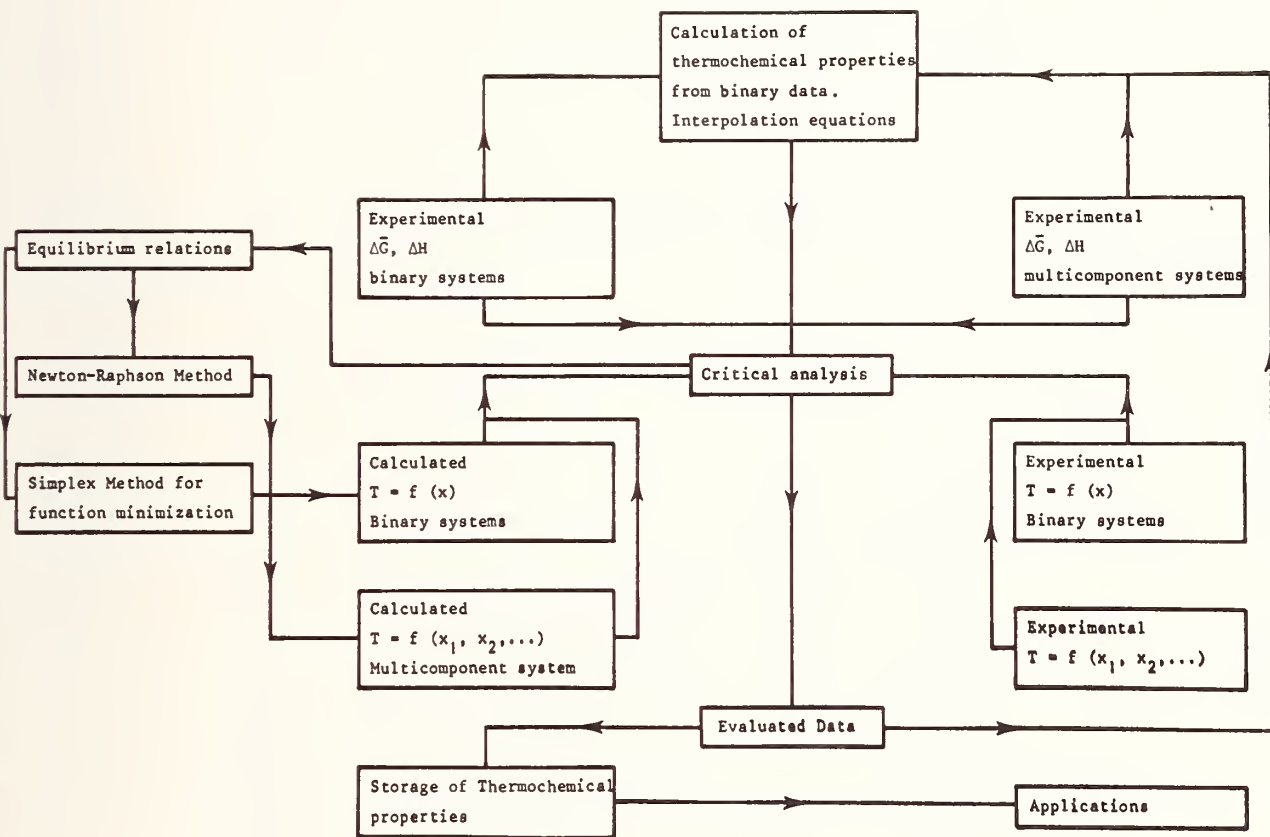
BIBLIOGRAPHY

- (1) G. Kirchner and B. Uhrenius, *Acta Met.*, 1974, 22, 523
- (2) B. Zimmermann, Dr. Rer. Nat. Thesis, Univ. Stuttgart, W.Germany, 1976.
- (3) L.H. Bennett, D.J. Kahan and G.C. Carter, *Mat. Sci. Eng.*, 1976, 24, 1.
- (4) L.H. Bennett, G.C. Carter and D.J. Kahan, *Proc. Vth Inter. Codata Conf.*, 1976, Boulder (U.S.A.).
- (5) From N.P.L. (U.K.), A.E.R.E. (Harwell, U.K.), Vrije Univ. (Brussel Belgium), Rhein-West T.H. (Aachen, W. Germany), I.R.S.I.D. (Maiziere, France), Thermodata and L.T.P.C.M. - E.N.S.E.E.G. (St Martin d'Hères, France)
- (6) J.A. Nelder and R. Mead, *Comp. J.*, 1965, 7, 308.
- (7) C. Wagner, *Acta Met.*, 1958, 6, 309.
- (8) R. Hiskes and W.A. Tiller, *Mat. Sci. Eng.*, 1967/68, 2, 320.
- (9) R. Hiskes and W.A. Tiller, *Met. Sci. Eng.*, 1969, 4, 163.
- (10) R. Hiskes and W.A. Tiller, *Mat. Sci. Eng.*, 1969, 4, 173.
- (11) P.S. Rudman, *Adv. in Materials Research*, Vol. IV, Interscience Publishers, N.Y. 1969..
- (12) L. Kaufman and H. Bernstein, "Computer Calculations of Phase Diagrams", Academic Press, N.Y. (1970).
- (13) L. Kaufman, "Metallurgical Chemistry", *Proc. Symp.* 1971, Ed. O. Kubaschewski (HMSO, London, 1972), P. 373.

- (14) P. Chiotti, M.F. Simmons and Kateley J.A., "Nuclear Metallurgy", Vol. 15, Reprocessing of Nuclear Fuels, Met. Soc. Aime., Conf. 690801, CFSTI, NBS, Spring. Virginia, 1969.
- (15) L.J. Vieland, Acta Met., 1963, 11, 137.
- (16) B.E. Sundquist, Trans. Met. Soc. Aime., 1966, 236, 1111.
- (17) I. Ansara, "Metallurgical Chemistry", Proc. Symp., 1971, Ed. O. Kubaschewski, (HMSO, London, 1972), p. 403.
- (18) J.H. Hildebrand, Proc. Nat. Acad. Sci., Wash., 1927, 13, 167.
- (19) J.H. Hildebrand, J. Amer. Chem. Soc., 1929, 51, 66.
- (20) E.A. Guggenheim, "Mixtures", Clarendon Press, Oxford, 1952.
- (21) J.C. Mathieu, F. Durand and E. Bonnier, J. Chim. Phys., 1965, 11-12, 1289.
- (22) J.C. Mathieu, F. Durand and E. Bonnier, J. Chim. Phys., 1965, 11-12, 1297.
- (23) P. Hicter, J.C. Mathieu, Durand F. and E. Bonnier, J. Chim. Phys., 1967, 2, 261.
- (24) C.H.P. Lupis, Ph.D. Thesis, M.I.T., Boston, 1965.
- (25) C.H.P. Lupis and J.F. Elliott, Acta Met., 1967, 15, 265.
- (26) B. Brion, J.C. Mathieu, P. Hicter and P. Desré, J. Chim. Phys., 1969, 66, 1238.
- (27) B. Brion, J.C. Mathieu and P. Desré, J. Chim. Phys., 1970, 67, 1745.
- (28) H.K. Hardy, Acta Met., 1953, 1, 202.
- (29) N.A. Gokcen and E.T. Chang, "Metallurgical Chemistry", Proc. Symp. 1971, Ed. O. Kubaschewski (HMSO, London, 1972), p. 219.
- (30) F. Durand, These Doctorat ès Sci. Phys., Grenoble, 1962.
- (31) E. Bonnier, F. Durand and P.J. Laurent, C.R. Acad. Sci., 1962, 254, 107.
- (32) K. Wohl, Trans. Amer. Inst. Chem. Eng., 1946, 42, 215.
- (33) J.J. Van Larr, Z. Phys. Chem., 1913, 599.
- (34) E. Bonnier and R. Caboz, C.R. Acad. Sci. 1960, 250, 527.
- (35) G.W. Toop, Trans. Met. Soc. Aime., 1965, 233, 850.
- (36) F. Kohler, Monatsch. Chemie, 1960, 91, 738.
- (37) N.J. Olson and G.W. Toop, Trans. Met. Soc. Aime, 1966, 236, 590.
- (38) H. Kehiaian, Bull. Soc. Pol. Sci. 1966, 14, 153.
- (39) C. Chatillon-Colinet, I. Ansara, P. Desré and E. Bonnier, Rev. Int. Htes. Temp. et Réfract., 1969, 6, 227.
- (40) C. Colinet, D.E.S. Fac. Sci., Univ. Grenoble, France, 1967.
- (41) O. Kubaschewski and T.G. Chart, J. Inst. Metals, 1964, 93, 329.
- (42) H. Gaye and C.H.P. Lupis, Scripta Met., 1970, 4, 685.
- (43) H. Gaye and C.H.P. Lupis, Met. Trans., 1975, 6A, 1049.
- (44) I. Ansara, J.N. Barbier and C. Bernard, Unpublished Results.
- (45) K.F. Michaels, W.F. Lange III, R. Bradley and H.I. Aaronson, Met. Trans., 1975, 6A, 1843.
- (46) M. Hillert and L. -I. Staffansson, Met. Trans., 1975, 6B, 3, 37.
- (47) M. Hillert and M. Jarl, Met. Trans., 1975, 6A, 3, 553.
- (48) L.-I. Staffansson, Met. Trans., 1976, 7B, 3, 131.
- (49) C. Kaestle and K. Koch, Report "Zur Berechnung von Phasen-Diagrammen Oxidischer Mehrstoffsysteme Mit Hilfe von Mathematischen Thermodynamischen Modellen", Inst. Für Eisenhütt., Techn. Univ., Clausthal, 1976.

- (50) M. Hansen and K. Anderko, "Constitution of Binary Alloys", McGraw-Hill Book Co. Inc., 1958, N.Y.
- (51) S.M. Carmio and J.L. Meijering, Zeit. Für Metallkde., 1973, 64, 3, 170.
- (52) M. Gaye and C.H.P. Lupis, Met. Trans. 1975, 6A, 1057.
- (53) F. Ajersch, E. Hayer, J.N. Barbier and I. Ansara, Zeit. Für Metallkde., 1975, 66, 10, 624.
- (54) I. Ansara, M. Gambino and J.P. Bros, J. Crystal Growth, 1976, 32, 101.
- (55) P.E. Potter, J. Nucl. Mat., 1973, 47, 7.
- (56) R.K. Iyengar and W.O. Philbrook, Met. Trans., 1973, 4, 2181.
- (57) P.J. Spencer and J.F. Counsell, Zeit.Für Metallkde., 1973, 64, 9, 662.
- (58) O. Kubaschewski and I. Barin, Pure and Appl. Chem., 1974, 38, 469.
- (59) L. Kaufman and H. Nesor, Zeit. Für Metallkde, 1973, 64, 4, 249.
- (60) L. Kaufman and H. Nesor, Can. Met. Quater., 1975, 14, 3, 221.
- (61) L. Kaufman and H. Nesor, Met. Trans., 1974, 5, 7, Part 1 : 1617, Part 2 : 1623.
- (62) L. Kaufman and H. Nesor, Met. Trans., 1975, 6A, Part 3 : 2115, Part 4 : 2123.
- (63) I. Ansara, J.N. Barbier, J.C. Mathieu and B. Schaub, J. Crystal Growth, 1976, 36.
- (64) G.M. Blom and T.S. Plaskett, J. Electrochem. Soc., 1971, 118, 1832.
- (65) A. Joullié, R. Dedies, J. Chevrier and F. Bougnot, Rev. Phys. Appl., 1974, 9, 455.
- (66) E. Rudy, Tech. Rep. Afml-TR-69-117, Part IX, 1970.
- (67) G.I. Silman, Obsch. Zakonomern. Str. Diagramm Sost. Met. Sist., 1973, 94.
- (68) V.N. Pervikova, F.S. Veselova, Y.U.K. Berendeev and L.I. Pryakhina, Obsch. Zakonomern. Str. Diagramm Sost. Met, Sist., 1973, 88.
- (69) G.P. Vyatkin, V. YA. Mishchenko and D. YA. Povolotskii, Izvest. Vyssh. Ucheb. Zaved., Chern. Metall., 1974, 8, 9.
- (70) V.I. Levanov, N.N. Sobolev, V.S. Mikheev and O.P. Elyutin, Fazovye Prevrashcheniya Diagrammy Sostoyaniya Metall. Sistem., Ed. O.S. Ivanov, Moscow, Izdatel'Stvo Nauka (1974).
- (71) T.D. Dzhuraev, A.V. Vakhobov and K.K. Eshonov, Zavod. Lab., 1975, 41, 3, 335.
- (72) A.M. Zhakharov, F.S. Novik and E.P. Daneliya, Izvest. Akad. Nauk SSSR, Met., 1970, 5, 212.
- (73) H. Scheffé, J. Royal Statistical Soc., Series B, 1958, 20, 344.
- (74) L.W. Gorman and J.E. Hinman, Technometrics, 1962, 4, 4, 463.
- (75) J.F. Counsell, E.B. Lees and P.J. Spencer, DCS Rep. 9, N.P.L. Teddington, U.K., 1970.
- (76) J.C. Chenavas, N. Valignat, I. Ansara and E. Bonnier, Chimie et Industrie, Génie Chimique, 1971, 104, 15, 1907.
- (77) P.E. Potter, J. Nucl. Mat., 1972, 42, 1.
- (78) H.Holleck and H. Kleykamp, J. Nucl. Mat., 1969, 32, 1.
- (79) E. Rudy, J. Less Common Metals, 1973, 33, 43.
- (80) G.G. Mikhailov and V.A. Kozheurov, SB. Nauchn. TR., Chelyab. Politekh. Inst., 1973, 118, 8.

- (81) G.G. Mihkailov, V.A. Kohzeurov, A.M. Tupikin, M.A. Ryss and V.P. Zaiko, SB. Nauchn. TR., Politekh. Inst., 1973, 118, 14.
- (82) N. Kazuo, O. Kozo and M. Yotaro, J. Electrochem. Soc., 1975, 122, 9, 1245.
- (83) A.S. Jordan and M. Ilegems, J. Phys. Chem. Solids, 1975, 36, 329.
- (84) A. Laugier, Sem. Chimie Etat Solide, (1974), Vol. 9, Masson 1975.
- (85) G.B. Stringfellow, J. Cryst. Growth, 1974, 24, 21.
- (86) A. Laugier, Rev. Phys. Appl., 1973, 8, 3, 259.
- (87) A.D. Pelton, C.W. Bale and M. Rigaud, To be published in Zeit. Für Metallkde.
- (88) M. Blander, Chem. Geol., 1968, 3, 33.
- (89) M.L. Saboungi and M. Blander, J. Amer. Ceram. Soc., 1974, 58, 1-2, 1.
- (90) H. Hillert and L.-I. Staffansson, Acta Met., 1976, 24, 1079.
- (91) J.M. Pourbaix and C.M. Rorivé-Bouté, "The Physical Chemistry of Process Metallurgy", Discussion Far. Soc., N° 4, 1948.
- (92) W. Hirschwald, O. Knacke and P. Reinitzer, Erzmetall, 1957, X, H-3, 123.
- (93) C.B. Alcock, Can. Met. Quat., 1971, 10, 4, 287.
- (94) A.S. Pashinkin, S.S. Bakeeva and M.I. Bakeev, TR. Khim.-Metall. Inst., Akad. Nauk. Kaz. SSR, 1974, 25, 142.
- (95) A.D. Pelton and H. Schmalzreid, Met. Trans., 1973, 4, 1395.
- (96) J. Sticher and H. Schmalzreid, Report "Zur Geometrischen Darstellung Thermodynamischer Zustandsgrößen in Mehrstoff-Systemen Auf Eisenbasis", Techn. Univ. Clausthal, 1975.
- (97) G. Eriksson, Chem. Src., 1975, 8, 3, 100.
- (98) J. Van Der Rest, F. Gautier and F. Brouers, J. Phys. F: Metal Phys., 1975, 5, 2283.
- (99) F. Gautier, J. Van Der Rest and F. Brouers, J. Phys F: Metal Phys., 1975B, 1884.
- (100) A.R. Miedema, R. Boom and R. De Boer, J. Less Common Metals, 1975, 41, 283.
- (101) A.R. Miedema, J. Less Common Metals, 1976, 46, 67.
- (102) R. Boom, F.R. De Boer and A.R. Miedema, J. Less Common Metals, 1976, 45, 237.
- (103) R. Boom, F.R. De Boer and A.R. Miedema, J. Less Common Metals, 1976, 46, 271.



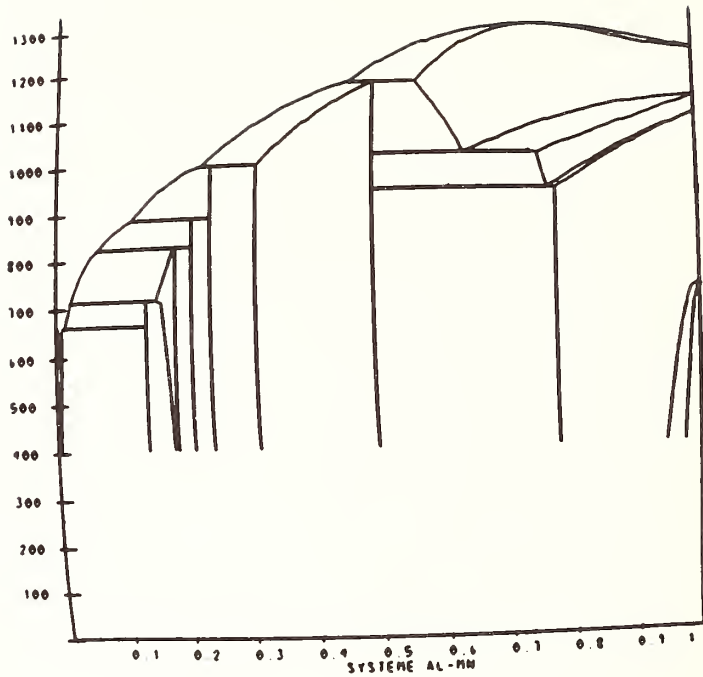


Fig. 1 : System Al-Mn from Ref, 50.

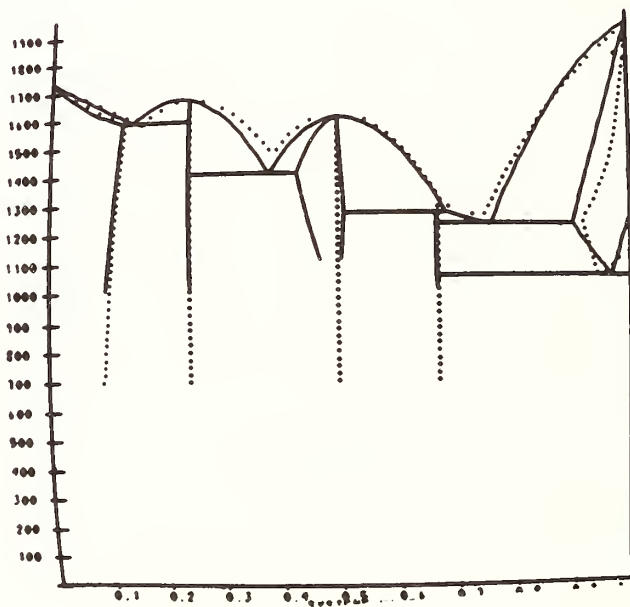


Fig. 2 : System Ni-Ti from Ref. 50 Calculated diagram in dotted lines.

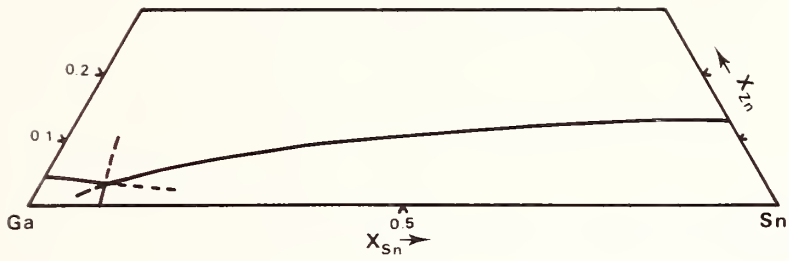


Fig. 3 : Eutectic valley in the Ga-Sn-Zn system.

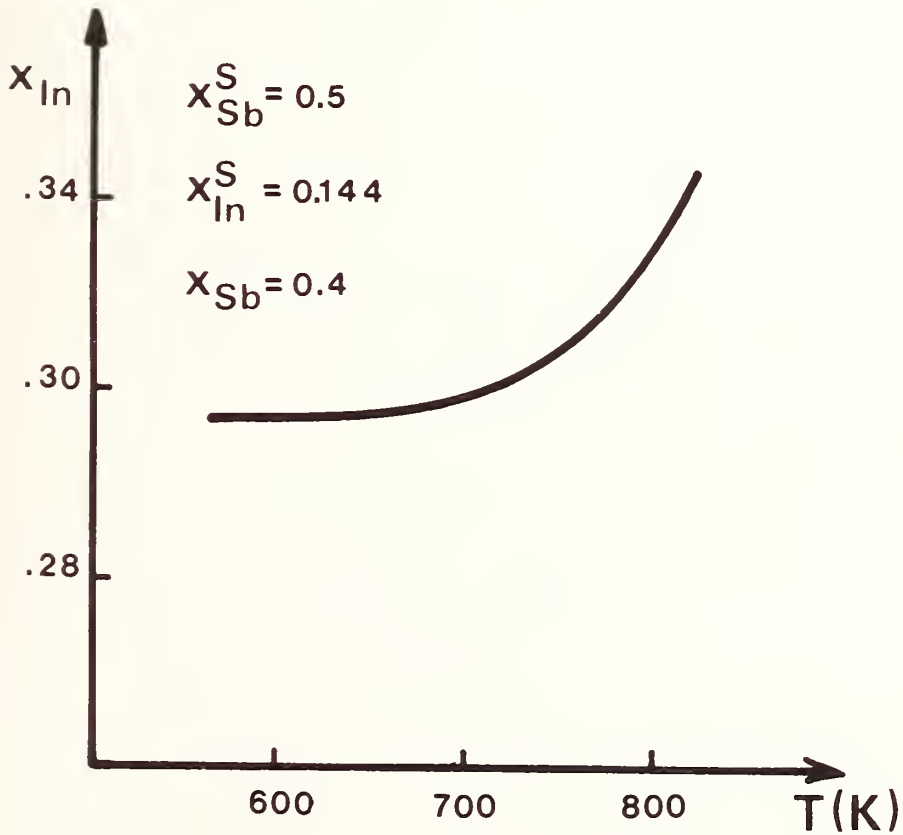


Fig. 4 : Variation of the molar fraction of In in the two phase region with respect to temperature.

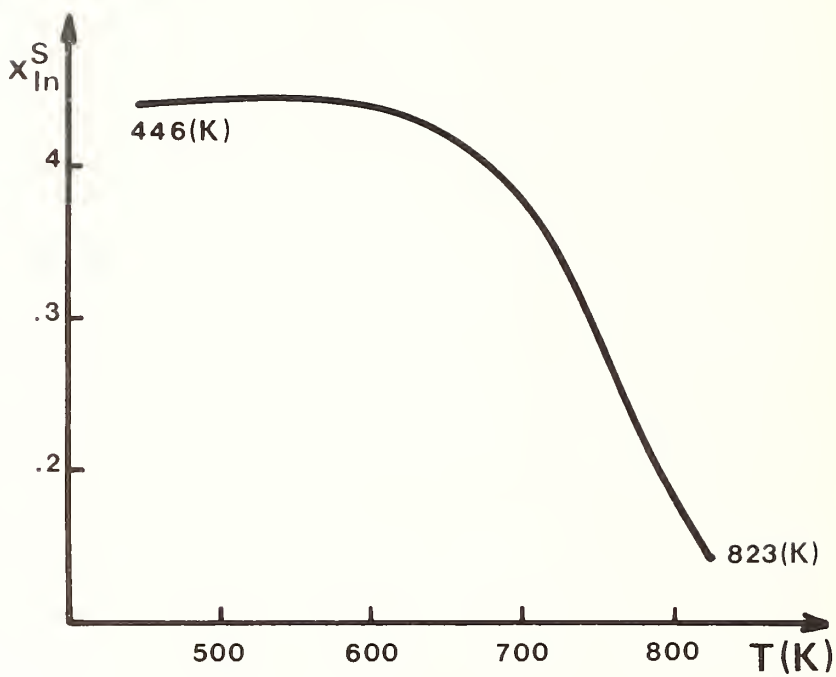


Fig. 5 : Variation of the molar fraction of In the quasi-binary solid solution with respect to temperature.

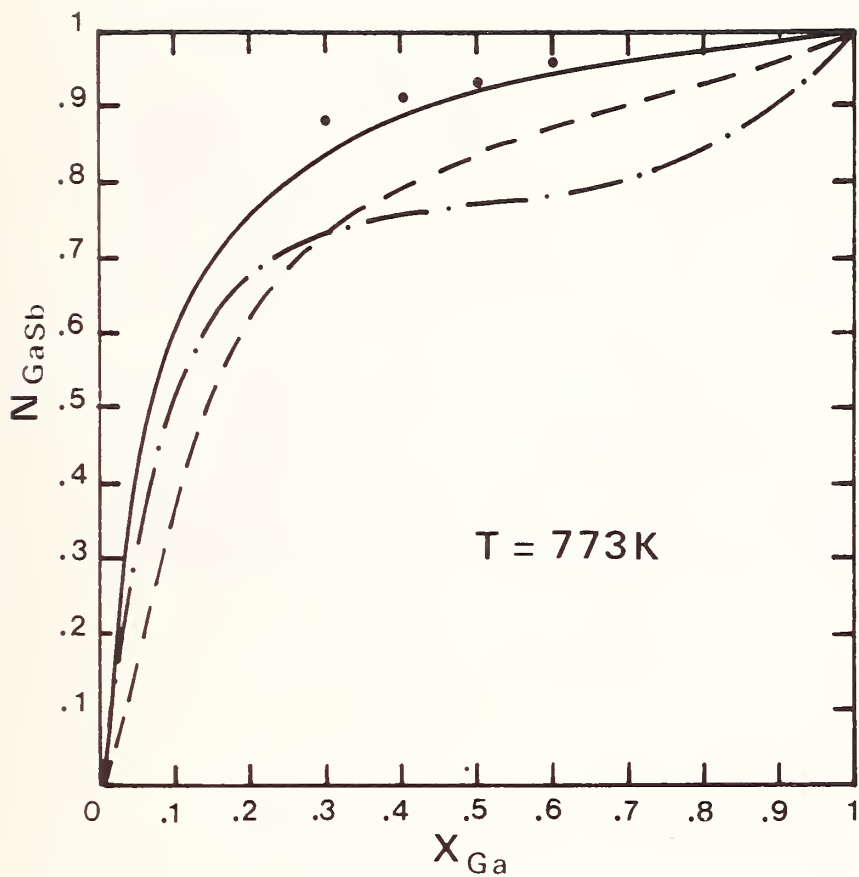


Fig. 6 : Variation of $N_{GaSb}^S = f(x_{Ga}^1)$ at 773K. • Experimental values (G.A. Antypas, J. Electrochem. Soc., 1970, 8, 3, 259)

- Calculated from experimental values in Réf. 54.
- - - Recalculated from data in Réf. 64.
- · - · - Recalculated from data in Réf. 65.

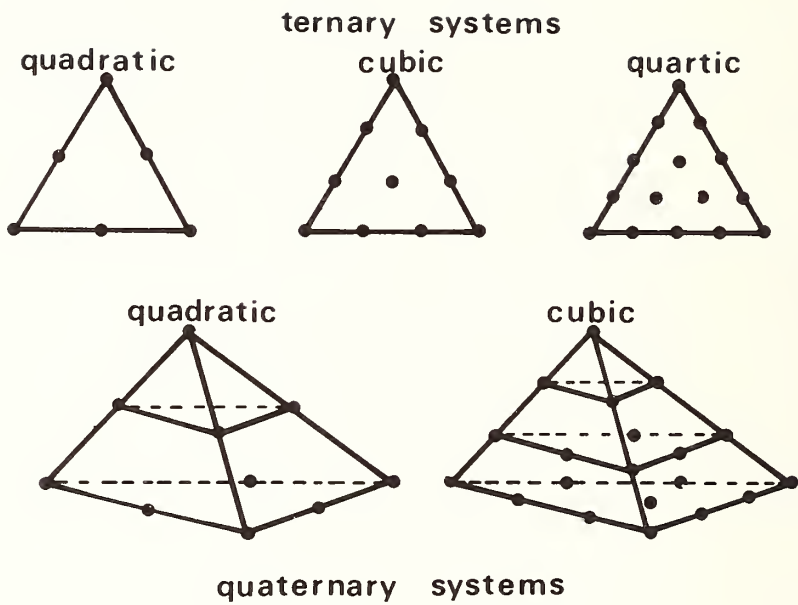


Fig. 7 : Simplex lattices.

	ΔH_{ij}	α_{ij}	RELATION BETWEEN BINARY AND TERNARY MOLAR FRACTION	β
Power series	$\sum_{n=1}^{n=m} x_i x_j^n (x_i - x_j)^n$	1	$x_i = N_i$ $x_j = N_j$	1
Power series Hardy type	$x_i x_j (\alpha + \beta(x_i - x_j))$	1	$x_i = N_i$ $x_j = N_j$	0
Power series Hardy type	$x_i x_j (\alpha' x_i + \beta' x_j)$	1	$x_i = N_i$ $x_j = N_j$	$\frac{1}{2}$
Kohler	$\Delta H_{ij} = f(x_i, x_j)$	$(N_i + N_j)^2$	$x_i = \frac{N_i}{N_i + N_j}$ $x_j = \frac{N_j}{N_i + N_j}$	0
Toop	$\Delta H_{12} = f(x_1, x_2)$ $\Delta H_{13} = f(x_1, x_3)$ $\Delta H_{23} = f(x_2, x_3)$	$\alpha_{12} = \frac{N_2}{1 - N_3}$ $\alpha_{13} = \frac{1 - N_1}{1 - N_3}$ $\alpha_{23} = (1 - N_1)^2$	$x_1 = N_1$ $x_2 = 1 - N_1$ $x_3 = 1 - N_1$ $x_2 = N_3 / (N_2 + N_3)$	0 0 0
Surrounded atom model	$x_i x_j (\alpha' x_i + \beta' x_j)$	1	$x_i = N_i$ $x_j = N_j$	1

* That equation is not symmetrical with respect to the component subscript ;

** Terms of higher order (used when experimental ternary data are available)



AN OVERVIEW OF THE DETERMINATION OF PHASE DIAGRAMS

By: F. N. Rhines

Department of Materials Science and Engineering
University of Florida, Gainesville, Florida 32611

In view of the impressive progress that has been made toward complete coverage of at least the binary systems of the elements, one may well ask why we should continue to concern ourselves with methods of phase diagram investigation. The answer cannot be that we are generally dissatisfied with the phase diagrams that are being produced, because the improvement in the quality of constitutional determinations in the years since the second World War is every bit as impressive as is the outpouring of new diagrams. Rather, I see our present interest associated, first, with the fact that the systems that remain to be undertaken have special difficulties that have prevented their being attacked earlier and, second, with problems of refinement where there is importance in determining very small solubilities, in improving the accuracy of temperature measurement, in extending phase diagrams into regions of low and high temperatures and in exploiting the pressure variable.

A survey of current activity in the determination of phase diagrams makes it clear that the preponderance of investigations, even on exotic systems, is being conducted by the use of old time-tested methods, such as thermal analysis, dilatometry, diffusion couple analysis, metallographic

analysis, chemical analysis, x-ray crystallography and lattice parameter measurement, electrical conductivity and dip sampling. These methods are so well-known and their uses so commonly understood that it does not seem appropriate to review them upon this occasion. I shall direct my remarks, instead, to the newer, more sophisticated techniques, which seem destined to see increasing use in the years to come. Upon perusing the literature dealing with new methods, I find many of the authors understandably pre-occupied with the details of the method to the near exclusion of consideration of the requirements of phase equilibrium. Since we are about to be instructed in some of the newer techniques, it may be worthwhile to begin by paying our respects to the Phase Rule and reflecting for a few minutes upon its meaning with respect to experimental methods.

A phase diagram is, of course, a graphical expression of the Phase Rule, where

$$\begin{array}{ccccccc}
 & P & + & F & = & C & + & 2 \\
 \swarrow & & & \downarrow & & \downarrow & & \searrow \\
 \text{Number of phases} & & & \text{Number of degrees} & & \text{Number of} & & \text{Number of externally} \\
 \text{participating in} & & & \text{of freedom, equal to} & & \text{components} & & \text{controlled variables} \\
 \text{each equilibrium} & & & \text{the order of the} & & \text{together} & & \text{constituting one more} \\
 & & & \text{topological simplex} & & \text{than the} & & \text{dimensionality of the} \\
 & & & \text{representing each} & & \text{phase diagram} & & \\
 & & & \text{equilibrium} & & & &
 \end{array}$$

This is a topological relationship, which means that it deals in whole numbers. It stands austerely aloof from concern with the texture of any of its numbers. Thus, the number of phases in an equilibrium is just number, nothing more. It is not necessary even to give the phases names, as long as

we can see that there are two, or three, or whatever number may be participating in the equilibrium. It is necessary and sufficient to identify phase difference at equilibrium. The same is true of each of the other factors of the Phase Rule, which is concerned with the number of components, not with what they are, and with the number of externally controlled variables, not with the specific temperature or pressure. In other words, the Phase Rule pertains to the form of the phase diagram, but not to its metric characteristics.

It is probably not widely appreciated that these distinctions intrude into the business of determining phase diagrams, where clarity of purpose and of procedure can be enhanced by recognition of the bifurcated nature of the problem. In the following, I shall preserve this distinction. I shall deal first with the topological aspects of phase diagram determination and separately with the metric aspects of the phase diagram.

Topological Aspects of Phase Diagram Determination

The concept of heterogeneous equilibrium presumes thermodynamically distinguishable states of matter in physical contact and so all at the same temperature, the same pressure and the same chemical potential. In determining the number of phases it is necessary, therefore, (1) to demonstrate physical contact, (2) to show thermodynamic difference of state and (3) to prove equilibrium. In the majority of cases these requirements are easily met. There are instances, however, in which conformity with these demands is not easily provable, or in which apparent adherence is false. Since we

are concerned here with the difficult and the special cases, some penetration into this field seems desirable.

Physical contact implies not only the existence of interface, but specifically of sharp interface, sharp in the sense that every atom in the system could be identified as belonging to one phase, or another, but never as being a shared atom. The latter provision is necessitated by the requirement of equilibrium that all of the system be at constant chemical potential, a state that could not exist if there were compositional gradients at the phase interfaces, instead of abrupt differences in composition. It is only since the development of the field-ion microscope that we have had direct evidence that such a sharply differentiated state can exist. The clear demonstration that sharpness of interface can prevail lends strength to the position that indefinite boundaries do not denote phase difference. An example exists in the case of the so-called "coherent precipitates," which must be regarded as inhomogeneities in the matrix state, rather than as members of a heterogeneous equilibrium. A related problem has long troubled the field of colloid chemistry, where there arose the question of how large a particle must be before it may be said to have a surface and, hence, be regarded as a separate phase. Perhaps the most positive resolution of the question of phase difference in cases of indefinite interface is to be had by demonstrating that the postulated equilibrium can be established by following a different experimental path. For example, if it could be shown that the coherent intermediate phase could be produced by isothermal diffusion between the terminal components, as well as by precipitation from a

supersaturated solid solution, then it would become evident that it is a phase member of an equilibrium system.

Evidently, those experimental methods which provide direct access to the physical nature of the interface can be of value in phase diagram determination. The battery of electronic microscope equipment that we now have at our disposal provides ever improving resolution of the detail of phase interface. The ultimate in this group is, of course, the field-ion microscope, especially with its adjunct, the atom probe. One of the most impressive accomplishments of this instrument, thus far, has been the demonstration that the ordered and disordered forms of Cu_3Au are separated by an atomically sharp interface and are, therefore, different phases of the Cu-Au system. No other instrument could have settled this question. Because of its experimental limitations and its newness, the field-ion microscope has not yet been broadly applied, but its future in phase diagram investigation seems to be assured.

Also highly useful, even though not capable of such great resolving power, are the transmission and reflecting electron microscopes and scanning electron microscopes. These bring within the range of observation particles of a degree of fineness that would altogether escape detection by the finest of optical instruments. In many cases, the resolution of such fine particles has been sufficient to reveal their shapes as being regularly idiomorphic. This I take as indirect evidence of sharpness of interface, because the formation of facets demands that the structure of the surface be controlled by the crystalline forces of the particle, rather than by some sort

of compromise with the matrix. Accordingly, I suggest that particle shape can give useful information in the ultra fine size range, where there is sometimes doubt concerning the reality of a second phase.

While sharpness of interface seems to be a necessary condition of phase difference, the presence of sharp interface is not alone sufficient evidence. A contrary example exists in the case of polycrystalline grain boundary, which can be seen to be atomically sharp, but which is clearly not a phase interface. Another classical case exists in the distinction between optically enantiomorphic forms of crystals, both forms (according to Ricci) constituting a single phase, although they are separated by sharp interface. The domain boundaries of long-range order fall in the same category. Evidently, something more than interface is necessary for the determination of the number of phases in an equilibrium.

Thermodynamic difference of state must also be demonstrated to prove difference of phase. In principle, this should be done with the phases in contact, at equilibrium. To accomplish this, it is necessary to make an energy sensing scan, which may be approached in any of four different ways. First, the system at equilibrium can be scanned by an energy sensing device that is responsive to localized differences and, thus, identifies phase difference in situ. Second, a composition sequence, or gradient, can be traversed with an energy sensing indicator. Third, the energy content of the system, as a whole, can be traced in the course of a temperature scan. Fourth, the same thing can be done by means of a pressure scan.

In multicomponent systems, the in situ scan is appropriate and its

simplest embodiment is to be found in optical, or electron, microscopy, where phase difference is visually apparent, although not necessarily reliably so. The element of relevance to difference in chemical state is introduced by the use of chemical etching which sometimes distinguishes between phases by their relative rates of chemical reaction. A more sophisticated application of the principle of chemical difference was once proposed by Mears and Brown who employed an electrochemical probe to associate a difference in solution potential with difference of phase. Probably the most generally reliable criterion of phase difference, however, lies in composition difference per se. Micro-chemical analysis has long been in use for this purpose, but its resolution, with respect to the subdivision of the microstructure, has been limited. This defect has been largely overcome by the development of the electron microprobe, which is useful down to a particle size of about 3 microns, and the STEM, which is said to be capable of analyzing a particle only one micron in diameter. In this connection, it should be noted that precision of analysis is not crucial where the objective is to ascertain the form of the phase diagram, as distinguished from its quantitative characteristics. All that is necessary is to show difference of phase.

Difference in crystal structure is a generally reliable means of distinguishing phases, although the absence of structural difference does not rule out phase difference. Here again, we have micro-tools such as micro x-ray diffraction and electron diffraction, which give access to a limited range of microstructures. Composition difference can sometimes be detected by the use of radioactive tracers coupled with auto-radiographic techniques.

Almost any physical property that can be measured directly upon the micro-constituent can be helpful in phase differentiation, but generally provides supplementary rather than primary phase differentiation. Included in this group are such properties as color, reflectivity, micro-indent hardness, and scratch hardness. Thermal conductivity has been used to distinguish phases by frost patterns. Osmond used micro-indentation patterns to distinguish alpha-iron from gamma-iron long before x-rays were known. Where particles are too fine to be resolved with the microscope, they have sometimes been separated from their matrix by selective chemical solution, have been concentrated by centrifuging and subsequently analyzed.

In applying such techniques, we must maintain vigilance to retain the condition of equilibrium in contact. Failure to do this has frequently been a source of error. There was a time when any compound that a chemist could make was given a place on the phase diagram. Similarly, the finding of crystal structures of transition states, as well as of compounds of subordinate stability, has intruded into the construction of phase diagrams to create confusion. Fortunately, we have been blessed with a generation of critical compilers of phase diagrams who have worked diligently to eliminate such extraneous matter.

Another very useful tool for the establishment of isothermal phase sequences is the diffusion couple. In its application to binary systems, the diffusion couple has the special advantage of displaying the phases in the order of their occurrence in the phase diagram. A suspicion that there may be a tendency for some of the proper phases to be omitted from the layers of

the diffusion couple has generally proved unfounded. This problem seems usually to have been associated with an insufficiently delicate observation of the layers. With the new high powered microscopes, this should cease to remain a problem. Lustman once provided an ingenious solution when he dissolved the couple layer by layer, using an electrolytic cell and monitoring the emf of the reaction to distinguish each phase layer from the next.

There remains, however, a legitimate question concerning the validity of the phases that form in a diffusion couple, or, for that matter, in any chemical gradient. Some have contended that equilibrium can prevail locally upon the two sides of a phase interface, even though this is embedded in a chemical gradient. Others assert that equilibrium is impossible, because the system is continuing to undergo chemical change. Concerning the concept of localized equilibrium, they contend that under the kinetic state of continuing diffusion, the energy balance at the interface will be shifted, so that the compositions on the two sides of the boundary would not be those of the stable equilibrium. This could, but does not necessarily, mean that the couple would give qualitatively wrong information. For my own part, my experience with diffusion couples has been so consistently good that I am willing to use them, with a small reservation that I am conscious that I could be misled.

Thus far, the use of diffusion couples has been limited mainly to that range of temperature within which diffusion is sensible and melting does not interfere. They have been little used in the survey of ternary and higher order systems, because the composition path of diffusion cannot be foreseen.

With regard to temperature limits, we shall shortly be hearing about methods which are capable of analyzing such shallow diffusion zones that exploration is extended to relatively low temperatures. Very thin couples can be set up by ion implant methods, then analyzing the evolving couple by ion back-scattering. As for their application to ternary systems, it is possible to make a diffusion triple by drawing wires of the three components through a die to cold weld them into a single specimen, whereupon diffusion produces a two-dimensional model of the phases of the ternary system. It is also possible to so design a set of diffusion couples as to virtually guarantee coverage of the ternary span.

The temperature scan method, best known to metallurgists in the form of cooling curves and dilatometry, differs from the isothermal chemical scan in two fundamental respects; namely, that there is no pretense of establishing equilibrium in the course of the experiment and that the total energy content of the system is monitored in order to sense phase change. It offers the very considerable advantage, not only of identifying the temperatures at which the various equilibria occur, but, most particularly, of providing recognition of the variance of otherwise undocumented equilibria over an enormous temperature range. Its principal limitations arise (1) from the need for any new phase to be nucleated and to grow forthwith and (2) from the rather large proportion of any new phase that is normally required for detection. The requirement of nucleation and growth leads to undercooling and superheating effects, to the failure of some stable phases to be observed with the appearance of meta-stable, or transition states, instead, or in

addition. These are all familiar occurrences bearing upon the problem of achieving equilibrium and will be reserved for later discussion. The matter of the detection of small quantities of a new phase is, however, one which has been largely overcome in recent years and which will be considered upon this occasion. I have reference to the magnetic detection methods, i.e. NMR and Mossbauer Effect measurements. Under favorable circumstances, these are very sensitive detectors of small quantities of a new phase. In their present form, they require expert interpretation, because there are some magnetic indications that are not connected with phase change. In proper use, however, they are capable of extending the knowledge of phase equilibria into systems that have not previously been open to study, because of their very narrow solubility limits.

The pressure scan also provides a very broad range of conditions and, like the temperature scan, depends upon the sensing of property changes in the bulk of the sample to reveal the occurrence of phase changes. The techniques that are available divide themselves naturally into two classes, the one relating to relatively high pressures at which the gas phase is absent, the other dealing with the medium to low pressure range within which the gas phase is usually present. For the high pressure range, piston type compression cells are usually employed. At a pressure where a phase change occurs, there is ordinarily a change in the specific volume of the test material, which can be sensed by an alteration in the volume/pressure ratio. For experimental reasons, this indication of phase change is often difficult to detect. It has been more common, therefore, to provide for

heating the cell and for reading the phase change by the use of a differential thermocouple implanted in the sample along with a reference material. Thus, the pressure variable and the temperature variable are scanned together. At each step in advance of the pressure, the cell is heated and cooled to explore for a phase change. Such experiments are usually conducted in a series of rising pressure steps, rather than the reverse, because the pressure seals become tighter with rising pressure, but tend to fail as the piston is retracted.

When the gas phase is present, the pressure of the system is determined by the equilibrium between the gas and the condensed phases. Thus, a temperature pressure scan is produced whenever a material is enclosed within an inert cell and is heated, or cooled. In order to define the equilibria traversed in this experiment, it is necessary to monitor both the temperature and pressure and to determine the compositions of the gas and of the condensed phases. In the field of chemistry where vapor pressures are readily measurable, such techniques are classical. The application of this method to metal systems, however, has seen less use, especially in alloy investigation. Boyle and I used it successfully for the determination of the gas-eutectic of the system Cd-Zn. We used a capsule composed of two glass bulbs joined by a capillary. The metallic sample was contained in one of the bulbs and the system was evacuated and sealed. The capsule was then held several days in a thermostat which kept the gas bulb about one degree hotter than the specimen bulb, in order to avoid condensation. At the end of the stabilization treatment, the capillary was sealed, by means of a hot wire,

the gas bulb was broken in a fixed volume of acid and the total composition of the gas thus analyzed. Knowing also the original volume of the bulb, the gas pressure was calculated. The solid phases were then analyzed separately to complete the description of the three-phase equilibrium at known temperature and pressure. This is a tedious procedure, but it does give us access to the PTX diagram of the alloy system.

Proof of thermodynamic equilibrium is probably the most uncertain factor in phase diagram determination, mainly because such proof can never be positive; it must always be based upon indirection of some kind. To prove that a system is in a state of minimum energy, one is burdened with the necessity of showing that all other states that can be attained with the same conditions of temperature, pressure and composition contain greater energy. Where the equilibrium is being approached isothermally and isobarically, it has been common simply to extend the time of stabilization until no further change can be observed. Equilibria that are intercepted in the course of temperature, or pressure, change, can be "boxed in" by traversing them in the opposite sense. Indeed, the true equilibrium temperature can be established to any desired degree of precision by taking cooling and heating scans at progressively lower rates of temperature change and extrapolating both cooling and heating indications to coincidence at long time. No matter how carefully the equilibrium is located, however, there can be a lingering doubt that the equilibrium is a true one and not some transition state, or a meta-stable state.

Probably the surest means for identifying meta-stable and unstable

states is to compare the results of two or more kinds of scan through the state. This is because most unstable states are arrived at through a specific sequence of temperature, pressure or composition change. If the equilibrium is approached so that the participating phases are formed by a different mechanism, the unstable form may not be generated. An interesting example exists in the case of carbon steels. When steel is cooled from its high temperature (γ) state, the eutectoid product is invariably α -iron and cementite (Fe_3C) and not α -iron and graphite, as it should be in the stable state. The reason seems to be that graphite is not easily nucleated, so that the saturated γ undercools, whereas Fe_3C nucleates with relative ease at only slightly lower temperature. Before any graphite has had an opportunity to form, all of the γ has been transformed to the meta-stable state. If, on the other hand, one attempts to form cementite by isothermal diffusion of carbon into iron, none forms. Below 738°C , only α and graphite appear in the diffusion zone and this is stable down to low temperatures. Diffusion between iron and carbon above 738°C produces γ iron, in addition to the α and graphite and the γ must decompose upon cooling. Here, the phase change occurs, not isothermally, but with falling temperature and the γ decomposes into α and cementite, as in any cooling cycle. Upon very long heating of the α -iron cementite alloy, the cementite gradually decomposes into α -iron and graphite. Thus, it is seen that the cementite is less stable than the graphite. This principle is capable of broad application.

Many of the kinds of experimentation that are used in phase diagram

determination are best conducted at room temperature (microscopy, for example). To accomplish this, we often resort to quenching the specimen from its equilibrium temperature, down to room temperature. The question then arises whether the quenched state is equivalent to the high temperature state. Again, it may be difficult to determine whether this is true. While increasing the rate of cooling usually secures the retention of the equilibrium state, this is not always the case. There are instances in which no diffusion is required to effect the transformation, so that the phase change may occur freely at room temperature. This is by no means confined to the martensitic transformation. It occurs also where the phases concerned are all of truly stable types. The case of the diffusionless transformation of beta to alpha brass is well-known, but widespread behavior of this type in the copper-based ternary alloys, as well as other alloys of the analogous type, is probably less widely recognized.

As with metastability, the incidence of quenching failure is not always obvious and may lead to confusion in the construction of the phase diagram. The most certain escape from this dilemma is, of course, to make all observations at the equilibrium temperature. This demands hot methods for microscopy, x-ray diffraction, microprobe analysis and so on. While methods for hot microscopy and x-ray diffraction have long been in use, they have been complicated by many difficulties and limitations, so that the development of better methods continues.

The number of components is perfectly straightforward as long as the elemental species are taken in total. This is usually done in the construc-

tion of phase diagrams of metal systems, so that the metallurgist is not commonly troubled by this factor. Where it is desired to designate compounds as components, as is commonly done in both inorganic and organic chemistry and in ceramics, it is necessary to exercise much care, because the equilibria that occur between two (or more) compounds may include compositions that cannot be described by mixtures of these compounds alone. The ceramic systems are particularly subject to this complication and the most troublesome problem facing the compiler of ceramic phase diagrams today is probably that of sorting out the true equilibrium diagrams from those that involve incompletely defined equilibria.

In principle, one is free to designate a quasi-binary system only when all tie-lines and all three-phase equilibrium lines lie in the plane of the diagram, or equivalently with the quasi-ternary or quasi-quaternary systems. Obviously, this condition cannot be guaranteed in advance of the experimental determination, so that it is prudent to examine this factor as a first order of business. All that is required is to equilibrate a composition somewhere in the middle of the system and to verify that the compositions of all of its phases lie upon the intended composition section. If this is true, then the likelihood of the system being other than the quasi-type intended is greatly diminished. If, however, one or more of the equilibrium phases proves to have a composition that lies off the intended sequence, then it is necessary to treat the system as being one of higher order. Too often, the fact of an assumed quasi-binary section not being such has come to light only when attempts were made to incorporate the section in a ternary, or higher order,

system. At such time, the failure of the section to connect properly with the rest of the diagram becomes painfully evident.

The question whether impurities should be included in the count of the components of a system is one that we tend to ignore as much as we can, because the answer is often embarrassing. We must, of necessity, handle our experimental materials in some kind of container, which is bound to enter into the equilibrium in some way and there are often other sources of contamination. Some of the more sophisticated experimental techniques, such as levitation melting and cold hearth melting, seek to minimize this problem, but to some degree it is always with us. The best that we can usually do is to select among potential contaminants those that will do the least damage. So long as we are concerned with the topological form of the phase diagram, as distinguished from its quantitative features, we can sometimes accept impurities that remain in solution and form no new phases. Where there is doubt on this score, the obvious remedy is to change the composition of the container system and compare the results for any evidence of a foreign phase. Unfortunately, it does not always follow that because an impurity remains in solution it has no influence upon the topology of the phase diagram. A memorable case is that of the effect of a small carbon impurity upon copper-iron alloys; in the presence of carbon, two-liquid immiscibility occurs, whereas the pure copper-iron system displays only liquid miscibility. Impurity effects remain one of the more difficult problems of phase diagram determination, especially because the problem is different from system to system.

The number of externally controlled variables is subject to reduction by fixing the pressure, the temperature, or both. So long as the fixed variable is maintained at constant value in a closed system, no problems arise and the phase diagram is reduced by one dimension for each variable that is held constant. For experimental reasons, and within reasonable limits of precision, the temperature variable may be fixed with no bad side effects. The same is true of relatively high pressure, because it is necessary to have the system confined. At ordinary and low pressure, however, it is common practice to handle the experimental materials in the open, upon the presumption that the pressure is being maintained at one atmosphere. This assumption is essentially correct for the mass of the specimen, but it may not apply at the surface. Unless the system is confined, so that the vapor phase is indeed in equilibrium with the rest of the sample, there is likely to be a non-equilibrium at the surface, resulting either in the loss of some of one of the components, or contamination by the ambient atmosphere. Continuously pumped vacuums are particularly damaging in this respect.

These matters have been inconsequential in much of the past experimentation, because the mass of the experiment was not affected and this was all that mattered. With the advent of some of the new techniques that involve very thin samples, either attached or not attached to a massive body, the state of the surface becomes a critical factor. We should pay heed to this matter in our deliberations at this gathering.

Quantitative Aspects of Phase Diagram Determination

From the point of view of the users of phase diagrams, the precision of the temperature and composition data, and sometimes of the pressure, are of first consideration. Justifiably, therefore, much of the effort that is devoted to phase diagram determination relates to accuracy of measurement. In approaching the sharpening of a datum point, it is generally presumed that the constitution of the system is already known qualitatively. Under such conditions, with the general characteristics of the system known and with the temperature and composition known approximately, it is possible to select a method of investigation and to tailor the experimental conditions to suit the specific case. This is a rather different situation from that which prevails in the exploratory type of experimentation.

Temperature of equilibrium measurements require first of all well-calibrated standards. This is taken for granted. The main problem then is the establishment of the equilibrium under conditions that permit an unobstructed measurement of temperature. For the majority of cases, the scheme of "boxing in" the true equilibrium temperature is usually the best solution. By this I mean approaching the equilibrium from both lower and higher temperature to identify a temperature of coincidence. The isothermal approach to equilibrium provides an excellent opportunity for exact temperature measurement, but the establishment of equilibrium may remain uncertain. The most sensitive measurement is usually obtained when the experiment is so arranged as to first encounter the appearance of a new phase, rather than its disappearance. Thus, cooling curves are best for locating liquidus points,

while heating curves are better for solidus determination; solubility limits are more readily detected through the beginning of precipitation than by the completion of solution.

The use of very thin specimens presents some problems that appear menacing. Ordinary temperature measuring techniques have to be miniaturized, or have to be replaced with less familiar methods. The small specimen is more responsive to temperature change and also is likely to support temperature gradients. Surface effects such as radiation and superficial reaction with the atmosphere must also be considered. The initiation of a phase change may also be sensitive to the mass of the specimen, where nucleation depends statistically upon the volume of the material. While the small specimen technology has much to recommend it, it behooves us to be wary of its pitfalls.

Finally, there is the problem of temperature determination at the extremes of temperature and pressure. This remains a field for the specialist. My personal experience in the use of optical and radiation methods for constitutional determination has often been less than satisfactory. The difficulties that I have met have not been so much connected with the measuring methods per se as with the maintenance of conditions under which they could be used. Fumes tend to obscure the path from the instrument to the specimen, sometimes fogging windows. Black body conditions are often awkward to arrange and radiation corrections unreliable. This seems to me to remain an area where innovation is needed.

The measurement of phase composition at equilibrium is especially sensi-

tive to the detailed characteristics of the system under consideration. Consequently, we have before us a broad array of methods, each having special advantages for certain situations. One of the most broadly applicable schemes is the physical separation of the phases to permit direct analysis by conventional means. Among chemists, this method has been exemplified by dip sampling. Eutectic liquids can sometimes be bled out of alloys during incipient melting and the beads of eutectic subsequently analyzed. Embedded particles of solid phases can sometimes be separated by selective dissolution and concentrated for analysis. Most of the general types of analytical techniques have already been discussed. Among the remainder are indirect methods, such as the measurement of the crystal lattice parameter for comparison with a composition standard. Such methods can be highly precise and reliable.

Closure

The objective of this overview has been to approach the field of phase diagram determination broadly, so as to bring out some general principles and to direct attention away from the experimental details, toward the basic requirements of the Phase Rule. If we are moved to receive the new methods, that will now be presented to us, in the light of their roles in the application of the Phase Rule, its mission will have been accomplished.



Proposal for a Comprehensive Handbook on "Ternary Phase Diagrams of Metals"

F. Aldinger, E.-Th. Henig, H.L. Lukas, and G. Petzow
Max-Planck-Institut für Metallforschung,
Institut für Werkstoffwissenschaften,
Büsnauerstr.175, D-7000 Stuttgart-80

Today, constitutional data of ternary systems are available on a large scale, but they are scattered over a large number of different reports, journals, and books. In order to use this enormous amount of knowledge more extensively, it is most desirable to summarize all informations on ternary phase diagrams in a critically evaluated compilation in which the systems are presented in the alphabetical order of the chemical symbols. In order to make such a handbook useful not only for insiders but also for technical people and students, the form of the presentation of the systems should be comparable to that of the binary phase diagrams in the well-known book of Hansen and Anderko. And also, the content of such a handbook has to include a brief presentation of the fundamentals of the ternary phase equilibria together with a proper nomenclature, enabling to "read" ternary phase diagrams. The form of the presentation of the systems should cover the following content:

1. A brief critical review of the work which has been published in the literature
2. A discussion of special features of the binary systems related to the ternary phase diagram
3. Composition and structure of solid phases
4. Pseudobinaries
5. Invariant equilibria
6. Liquidus surface
7. Isothermal sections
8. Miscellaneous (e.g. solid solutions, tie-lines, vertical sections, ordering, lattice constants as a function of composition, etc.)
9. References.

The presentation has to have a minimum in extension and a maximum in distinctness.

A literature survey covering constitutional work carried out before 1974 comprises about 18000 references on about 6000 ternary systems of metals. A rough estimate shows that about one-fourth of these systems are fully investigated and phase diagrams are available. About one-third of the systems are evaluated to some extent. Of the remaining systems constitutional data are available only on a rather limited scale.

According to the concept mentioned above this appreciable amount of results will comprise about 16000 pages in printed book form!



Phases and Phase Relations in the Binary Oxide
Systems Containing WO_3

Luke L. Y. Chang

Department of Geology, Miami University, Oxford, Ohio 45056

ABSTRACT

Phases and phase relations are reviewed in the systems of WO_3 with alkali oxides, alkaline earth oxides, scandium and yttrium oxides, rare earth oxides, titanium, zirconium and hafnium oxides, vanadium, niobium and tantalum oxides, molybdenum oxide, thorium and uranium oxides, manganese, iron, cobalt and nickel oxides, copper and silver oxides, zinc, cadmium and mercury oxides, boron, aluminum, gallium and indium oxides, tin and lead oxides, and phosphorus, arsenic, antimony and bismuth oxides.

INTRODUCTION

The purpose of this review is to summarize phases and phase relations in WO_3 -containing systems and to present a compilation of phase diagrams according to the types of chemical compounds. Fifteen tungstate groups have been selected for discussion and their phase diagrams are presented.

SYSTEMS ALKALI OXIDE - WO_3

Alkali tungstates have been studied extensively, but there are inconsistencies in the number, composition, and melting relations of reported phases. In the system $\text{Li}_2\text{O}\cdot\text{WO}_3$ - WO_3 (Fig. 1), Hoermann (1928) reported the formation of both 1:2 and 1:4 (alkali oxide/ WO_3 ratio) phases, However Spitsyn et al. (1938) and Kletsov et al. (1971) could not prepare the 1:4 phase. Recent work by Sakka (1968), Reau and Fouassier (1971), Hauck (1974), and Chang and Sachdev (1975) confirmed Hoermann's results. The marked difference among published phase relations in the system is in the nature of melting of the 1:2 phase. Hoermann (1928), Parmentier et al. (1972a), and Hauck (1974) all reported a congruent melting point at 745°C for the 1:2 phase, but Chang and Sachdev (1975), on the basis of x-ray diffraction and microscopic examination of polished sections, concluded that melting at 745°C is incongruent.

In the system $\text{Na}_2\text{O}\cdot\text{WO}_3\text{-WO}_3$ (Fig. 2), the existence of the 1:6 phase is the subject of controversy. It has been reported by Sakka (1968), and Chang and Sachdev (1975), but was not found by Hoermann (1928) or Caillet (1963). In addition, the melting point of the 1:4 phase determined by Chang and Sachdev is 50°C higher than that proposed by Hoermann and Caillet. Polymorphic relations in the 1:1 phase have been well established (Pistorius, 1966; Bottelberghs and van Buren, 1975). Three forms; α (orthorhombic), β (orthorhombic), and γ (cubic), have transition temperatures at 587.6°C (γ to β) and at 588.8°C (β to α).

In the system $\text{K}_2\text{O}\cdot\text{WO}_3\text{-WO}_3$ (Fig. 3), Hoermann (1928) and Mokhosoev et al. (1962) prepared two tungstates, 1:3 and 1:4, but Caillet (1963) reported 1:2 and 1:4 phases. Sakka (1968) and Guerin and Caillet (1970) reported the formation of 1:2, 1:3, 1:4 and 1:6 phases. Gelsing et al. (1965), who studied this system in some detail, identified 1:2, 1:3, 1:4 phases and two metastable phases (designated as X and Z). Chang and Sachdev (1975) confirmed all phases reported by Sakka and Guerin and Caillet, and also observed the formation of metastable phases. Chang and Sachdev stated that experimental evidence was not adequate to suggest the presence of two separate metastable phases, as proposed by Gelsing et al. The reported melting points of potassium tungstates show substantial variance. A comparison is shown

in Table 1.

Phase relations in the systems $\text{Rb}_2\text{O}\cdot\text{WO}_3\text{-WO}_3$ and $\text{Cs}_2\text{O}\cdot\text{WO}_3\text{-WO}_3$, as established by Chang and Sachdev, are very similar (Figs. 4 and 5). The 1:2 and 1:3 phases form a complete series of solid solution with melting points increasing and d-spacing decreasing from the 1:2 to the 1:3 phase. The 1:6 phases in both systems are the most refractory alkali tungstates. Chang and Sachdev confirmed the number and the composition of phases in the Rb-system as reported by Spitsyn and Kulesbov (1950). No other study on the Cs-system was found.

Several basic alkali tungstates have been reported. $3\text{Li}_2\text{O}\cdot 2\text{WO}_3$ is stable below 500°C (Parmentier et al., 1972b) $3\text{Li}_2\text{O}\cdot\text{WO}_3$ decomposes below 440°C , and $2\text{Li}_2\text{O}\cdot\text{WO}_3$ melts at 1350°C and is dimorphic with a transition point at 690°C (Hauck, 1974). In the Na-system, both $2\text{Na}_2\text{O}\cdot\text{WO}_3$ and $3\text{Na}_2\text{O}\cdot\text{WO}_3$ were prepared at 450°C in silver crucibles in sealed Vycor capsules (Reau et al., 1967). Reau et al. (1971) reported a 2:1 phase in the K-system, which decomposes at 650°C in dry oxygen to $\text{K}_2\text{O}\cdot\text{WO}_3$ and K_2O .

Among the alkali tungstates, crystal structures are known only for the 1:1 phases and the 1:2 phases of Li and Na. Chang and Sachdev suggested some structural relationships among them. $\text{Li}_2\text{O}\cdot\text{WO}_3$ and $\text{Na}_2\text{O}\cdot\text{WO}_3$ have phenakite (Zacharisen and Plettinger, 1961) and spinel (below 587.6°C) (Lindqvist, 1950).

structures, respectively. In both, structures are built up of isolated WO_4 tetrahedra linked together by alkali atoms. $K_2O \cdot WO_3$ and $Rb_2O \cdot WO_3$ are isostructural, a structure in which isolated WO_4 tetrahedra are linked by eight-coordinated alkali atoms to form layers (Koster et al., 1969; Kools et al., 1970). The $Cs_2O \cdot WO_3$ has β - K_2SO_4 structure (Kools et al., 1970), which also is characterized by the isolated WO_4 tetrahedra. The structures of the 1:2 phases, $Li_2O \cdot 2WO_3$ and $Na_2O \cdot 2WO_3$, are built up of continuous chains of WO_6 octahedra joined by bridging oxygen atoms and WO_4 tetrahedra (Lindqvist, 1950; Margarrill^{et al.}, 1973). Although the crystal structures of other alkali tungstates are not known, the WO_3 end member has a structure of solely WO_6 octahedra, linked by bridging oxygen atoms (Anderson, 1953), which suggests that in alkali tungstates the preference for the formation of the WO_6 octahedron increases in the direction from the 1:1 phase toward WO_3 .

SYSTEMS ALKALINE EARTH OXIDE - WO_3

Alkaline earth tungstates of the 1:1 type have long been known and are well characterized. Structurally, they can be divided into two major classes: (1) Tungstates of large divalent cations which are tetragonal, usually described as the scheelite-type, and (2) Tungstates of small divalent cations which are monoclinic, usually described as the wolframite-type.

Steward and Rooksby (1951) prepared a series of tungstates of the 3:1 type and showed that their crystal structures are related to that of $(\text{NH}_4)_3\text{FeF}_6$. Calcium, strontium, and barium all form this compound.

Phase relations in the systems have been studied in detail by Chang et al. (1966a) and have showed a simple eutectic in the system $\text{BeO}-\text{WO}_3$ (Fig. 6), and compound formation in other systems. In the system $\text{MgO}-\text{WO}_3$ (Fig. 7), the wolframite-type, 1:1 phase is stable to 1165°C , where it transforms to a high-temperature phase with unknown structure. On the basis of x-ray powder diffraction data, this high-temperature phase does not match with any of the known polymorphic forms of TiO_2 , $\alpha\text{-PbO}_2$, and FeNbO_4 (Laves et al., 1963). In addition, this phase does not have a form similar to MgMoO_4 , which transforms to a wolframite-type structure under high pressure (Young and Schwartz, 1963).

In the system $\text{CaO}-\text{WO}_3$ (Fig. 8), the 1:1 phase is the mineral scheelite, and its structure is used to describe crystal structure of other 1:1 tungstates. The 3:1 phase has a distorted $(\text{NH}_4)_3\text{FeF}_6$ -type structure. In high-temperature x-ray diffraction, the distortion in the 3:1 phase is gradually reduced as the temperature increases from 25° to 1200°C , but an ideal $(\text{NH}_4)_3\text{FeF}_6$ structure was not obtained. Nassau and Mills (1962) prepared a 6:1 phase, which apparently is metastable and is not present in equilibrium assemblages. Tokunov

and Kislyakov (1972) confirmed the phase relations determined by Chang et al. (1956a).

In the system SrO-WO₃ (Fig. 9), the 1:1 phase is isostructural with CaO·WO₃, and the 3:1 phase, as compared with 3CaO·WO₃, is less distorted from the (NH₄)₃FeF₆-type structure. DTA shows an endothermal peak at 1100°C for the 3:1 phase and high-temperature x-ray diffraction indicates that it transforms to the ideal (NH₄)₃FeF₆ structure (cubic) above that temperature. Tokunov and Kislyakov (1972) confirmed the phase relations in the system reported by Chang et al. (1966a), except that they proposed a 2:1 phase which melts incongruently at 1500°C and forms a eutectic point with SrO·WO₃ at 1470°C and 44.5 mole%WO₃.

In the system BaO-WO₃ (Fig. 10), published reports do not agree on the existence of a 2:1 phase. Scholder and Brixner (1955) first proposed such a phase and it was subsequently observed by Zhmud and Ostapchenko (1961), Kreidler (1972), and Tokunov and Kislyakov (1972). However, Purt (1962) and Chang et al. (1966a) found no evidence for the existence of a 2:1 phase. According to Kreidler, the 2:1 phase has three forms with transition temperatures at 1385°C and 1490°C.

SYSTEMS Sc₂O₃-WO₃ and Y₂O₃-WO₃

Phase relations in the system Sc₂O₃-WO₃ have not been established as only a 1:3 phase is characterized. This phase melts at about 1650°C (Nassau et al., 1965) and is

orthorhombic. Its crystal structure is similar to the scheelite-type (Abraham and Bernstein, 1966), but scandium atoms are six-coordinated, rather than taking the eight-coordinated positions of calcium in scheelite.

In the system $Y_2O_3-WO_3$ (Fig. 11), Borchardt (1963) reported five phases: 3:1, 9:4, 15:8, 1:1 and 1:3 and suggested some melting relations in the WO_3 -rich portion. The 3:1 phase has a rhombohedrally distorted fluorite structure (Borchardt, 1963; Aitken et al., 1964) below $1700^\circ C$, above which it transforms to a f.c.c. phase. The 9:4 phase reported by Borchardt was later proved to have a 5:2 composition by McCarthy et al. (1972), and it has a pseudo-tetragonal, fluorite-related structure. McCarthy et al. also suggested a 7:4 composition for the 15:8 phase reported by Borchardt. The 1:1 phase is monoclinic (Trunov et al., 1968) and has a crystal structure related to that of scheelite. The 1:3 phase is isostructural with $Sc_2O_3 \cdot 3WO_3$ (Nassau and Shieve, 1972).

A 3:2 phase was found by Borchardt (1963) at temperatures between 750° and $1000^\circ C$. This phase disappears on heating at $1100^\circ C$ and does not re-appear when any of the higher temperature phases are treated at $1000^\circ C$. As suggested by Borchardt, this phase is probably a metastable phase.

Crystal chemistry of and compound formation in rare earth tungstates have been well documented by McCarthy et al. (1972) and Naussau and Shieve (1972). Also, phase relations have been established in several systems. Among the five phases present in the system La₂O₃-WO₃ (Fig. 12) (Ivanova et al., 1970), three (3:1, 1:1 and 1:3) are common to all RE₂O₃-WO₃ systems, and their crystal structures are in most cases type structures for tungstates of large-sized rare earths (for example, Pr, Ce). 3La₂O₃·WO₃ has a distorted pyrochlore or ordered, defect fluorite structure (Chang and Phillips, 1964). Ivanova et al. (1970) suggested that this phase has three modifications, but these were not found by McCarthy et al. (1972). La₂O₃·WO₃ is probably monoclinic and its structure is scheelite-related (Polyanskaya et al., 1970a). La₂O₃·3WO₃ is dimorphic, both forms have distorted scheelite structure with La atoms in the eight-coordinated positions (Naussau and Shieve, 1972). The structure of 3La₂O₃·2WO₃ is not known, and that of La₂O₃·2WO₃ appears to be different from the rest of the RE₂O₃·2WO₃ phases (McCarthy et al., 1972).

The system Sm₂O₃-WO₃ also has five phases (Fig. 13) (Chang et al., 1966b). 3Sm₂O₃·WO₃ and Sm₂O₃·3WO₃ are considered to be isostructural with their counterparts in

the La-system (Chang and Phillips, 1964), but Trunov et al. (1968) prepared $3\text{Sm}_2\text{O}_3 \cdot \text{WO}_3$ at 1250°C showing a pseudo-tetragonal symmetry. $7\text{Sm}_2\text{O}_3 \cdot 4\text{WO}_3$ may also be indexed on the basis of a cubic cell, but shows a few extra reflection lines (Chang et al., 1966b). McCarthy et al. (1972) suggested a pseudo-rhombohedral cell for this phase, which is the type structure for all rare earth tungstates of the same $\text{RE}_2\text{O}_3/\text{WO}_3$ ratio, except those of La, Pr and Tb. $\text{Sm}_2\text{O}_3 \cdot \text{WO}_3$ is monoclinic (Trunov et al., 1968) and has a scheelite-related structure (Polyanskaya et al., 1970a). $\text{Sm}_2\text{O}_3 \cdot 2\text{WO}_3$ is also monoclinic (McCarthy et al., 1972). In this structure, distorted WO_6 octahedra share edges to form W_2O_9 zig-zag chains, producing both eight and nine coordinated structural positions for the rare earth atoms (Klevtsov et al., 1967; Borisov and Klevtsova, 1970).

Phase relations in the system $\text{Nd}_2\text{O}_3-\text{WO}_3$ were studied by Rode and Karpov (1966) showing five phases: 3:1, 2:1, 1:1, 1:2 and 1:3 (Fig. 14). They are all isostructural with their counterparts in the Sm-system (Trunov et al., 1968; Polyanskaya et al., 1970a; McCarthy et al., 1972). In addition, a 3:2 phase was prepared hydrothermally which has a tetragonal unit cell (Polyanskaya et al., 1970b).

Five phases were also found in the system $\text{Dy}_2\text{O}_3-\text{WO}_3$ (Fig. 15) (Ivanova and Reznik, 1972). $3\text{Dy}_2\text{O}_3 \cdot \text{WO}_3$ has a

rhombohedrally distorted fluorite structure (Aitken et al., 1964), a type structure for $3\text{RE}_2\text{O}_3 \cdot \text{WO}_3$ of small rare earths (Tb - Yb). The $5\text{Dy}_2\text{O}_3 \cdot 2\text{WO}_3$ structure is also related to the fluorite structure but has a pseudo-tetragonal cell (McCarthy et al., 1972). $7\text{Dy}_2\text{O}_3 \cdot 4\text{WO}_3$, $\text{Dy}_2\text{O}_3 \cdot \text{WO}_3$ and $\text{Dy}_2\text{O}_3 \cdot 3\text{WO}_3$ are all isostructural with their corresponding Sm phases (Polyanskaya et al., 1970a; Nassau and Shieve, 1972). Ivanova and Reznik (1972) reported a monoclinic $\text{Dy}_2\text{O}_3 \cdot 3\text{WO}_3$ which transforms to an orthorhombic form at 970°C .

SYSTEMS TiO_2 -, ZrO_2 -, and HfO_2 - WO_3

The system TiO_2 - WO_3 contains no binary phase, and shows a simple eutectic relationship (Fig. 16) (Chang et al., 1967a), whereas a 1:2 phase characterizes both the ZrO_2 - WO_3 and HfO_2 - WO_3 systems (Figs. 17 and 18) (Graham et al., 1959; Chang et al., 1967b).

X-ray powder diffraction data of $\text{ZrO}_2 \cdot 2\text{WO}_3$ can be indexed on the basis of a cubic unit cell with no systematic absence of reflections (Chang et al., 1967b). The crystal structure of $\text{ZrO}_2 \cdot 2\text{WO}_3$ has not been determined, but Chang (1967a) suggested that it has a defect wolframite-type structure. $\text{ZrO}_2 \cdot 2\text{WO}_3$ has a lower stability limit at 1105°C , which was determined by treating the stoichiometric composition side by side with the phase previously prepared at 1200°C in a series of runs (Chang et al., 1967b).

Phase relations in the system $\text{HfO}_2\text{-WO}_3$ are much like those in the Zr-system, and $\text{HfO}_2 \cdot 2\text{WO}_3$ is isostructural with $\text{ZrO}_2 \cdot 2\text{WO}_3$.

SYSTEM $\text{V}_2\text{O}_5\text{-WO}_3$

Several vanadium tungstates have been reported (Mondet, 1968; Launay-Mondet, 1971), but they all are mixed-valence phases and have compositions deviant from that of the fully oxidized binary join. Preliminary results obtained from a study in progress in this laboratory indicate that this system has a simple eutectic relationship with an invariant point at about 660°C and 4 mole% WO_3 .

SYSTEMS $\text{Nb}_2\text{O}_5\text{-WO}_3$ and $\text{Ta}_2\text{O}_5\text{-WO}_3$

A number of studies have been made on the system $\text{Nb}_2\text{O}_5\text{-WO}_3$. Kovba and Trunov (1962), Kovba et al. (1964), Felton (1965), and Gruehn (1965) reported the formation of several niobium tungstates. Goldschmidt (1960) and Fiegel et al. (1964) proposed extensive Nb_2O_5 solid solution, and Roth and Waring (1966) established phase relations in the system. The phase diagram shown in Fig. 19 is a modified version of Roth and Waring's (Levin et al., 1969). In it, the 9:16 and 9:17 phases replace the 6:11 phase and the 30:1 phase should be replaced by the phases 34:1, 20:1 and 13:1.

Roth and Wadsley (1965c) proposed a "Block Principle" and used it to describe crystal structures of niobium

tungstates and to predict possible compound formation in the system. The blocks are made of ReO_3 -type octahedra of niobium extending by sharing corners in certain numbers in a- and c-directions and infinite in the third direction. These blocks are joined together by the four-coordinated tungsten atoms. Generally, niobium tungstates can be classed on the basis of unit cell symmetry into two groups: monoclinic and tetragonal. Crystal structures of monoclinic phases, $\text{Nb}_{12}\text{W}_3\text{O}_{33}$ and $\text{Nb}_{16}\text{W}_5\text{O}_{55}$, and of tetragonal phases, $\text{Nb}_{14}\text{W}_3\text{O}_{44}$ and $\text{Nb}_{18}\text{W}_8\text{O}_{69}$, were determined in detail (Roth and Wadsley, 1965a, 1965b).

In $\text{Nb}_{12}\text{W}_3\text{O}_{33}$, the blocks of Nb-octahedra are three wide, four long and infinite in the third direction, and are joined with tetrahedrally coordinated W atoms, ordered at the junctions of every four blocks. With W atoms in similar positions, the blocks in $\text{Nb}_{16}\text{W}_5\text{O}_{55}$ are four wide, five long and infinite along the third direction, and in $\text{Nb}_{14}\text{W}_3\text{O}_{44}$ are four wide, four long and infinite along the direction which is the four-fold axis. In $\text{Nb}_{18}\text{W}_8\text{O}_{69}$, the blocks are five wide, five long and infinite in the third direction. W atoms occupy the four coordinated positions, and also share the octahedral positions with Nb atoms in a random arrangement.

The formation of tantalum tungstates and their relative stabilities have been studied by Gruehn (1965), Roth

and Stephenson (1969), Roth et al. (1970), and Stephenson and Roth (1973a, 1973b, 1973c). The phase diagram proposed by Roth et al. is shown in Fig. 20.

Crystal structures of several tantalum tungstates have been described by Stephenson and Roth (1973a, 1973b, 1973c) in terms of UO_3 -type subcell. The cations lie in sheets and have a h.c.p. arrangement within each sheet. Oxygen atoms form either distorted octahedra or pentagonal bipyramids around the cation to form the basic structural units. These units are linked together by edge-sharing to form chains within the (001) plane, and each chain is attached to other identical chains by corner-sharing along [001]. Each chain has a regular "herring-bone weave" and the folding causes distortions in crystal structures of tantalum tungstates as compared with the straight linkages in UO_3 . The crystal structures of $\text{Ta}_{22}\text{W}_4\text{O}_{67}$ (Stephenson and Roth, 1973a), $\text{Ta}_{30}\text{W}_2\text{O}_{81}$ (Stephenson and Roth, 1973b), and $\text{Ta}_{38}\text{WO}_{98}$ (Stephenson and Roth, 1973c) are based on, respectively, 13, 8, and 19 subcells of UO_3 -type.

SYSTEM MoO_3 - WO_3

Phase relations in this system have not been well established, although numerous studies were made. Rieck (1943) proposed a simple eutectic relationship with an invariant point at 765°C and 2 mole% WO_3 . Magneli (1949) reported a 1:1 phase

in the system, and Westman and Magneli (1958) found limited solid solutions between MoO_3 and WO_3 . Semikina and Limonov (1968) examined x-ray powder diffraction data in the system, and suggested three types of $(\text{Mo,W})\text{O}_3$ solid solution. Type I has compositions ranging between 84 and 66.5 mole% WO_3 (including both 1:2 and 1:3 phases), type II between 61.2 and 48 mole% WO_3 (including 1:1 phase), and type III between 44 and 27.5 mole% WO_3 (including both 2:1 and 3:1 phases).

The difficulty in attaining equilibrium in this system is to maintain molybdenum in its fully oxidized state at relatively high temperatures.

SYSTEMS ThO_2 - WO_3 and UO_3 - WO_3

In the system ThO_2 - WO_3 , there is a 2:1 phase (Trunov and Kovba, 1963; Spitsyn et al., 1968). This is in consistent with other systems including large tetravalent cations of Zr and Hf (Chang et al., 1967b). Unlike the 2:1 phases in Zr- and Hf-systems, this 2:1 phase of Th is polymorphic and has three forms: the α -form stable above 1360°C , the β -form between 1200° and 1360°C , and the γ -form below 1200°C . Spitsyn et al. also reported that phase assemblages of ThO_2 + $\text{ThO}_2 \cdot 2\text{WO}_3$ and $\text{ThO}_2 \cdot 2\text{WO}_3$ + WO_3 are stable at least to 1200°C .

Phase relations in the system UO_3 - WO_3 have been studied in some detail. Trunov et al. (1961), Juenke and Bartram (1964), and Cordfunke (1969) found only one binary

phase $\text{UO}_3 \cdot \text{WO}_3$, whereas Ampe et al. (1968), and Hauck (1974) reported both $\text{UO}_3 \cdot \text{WO}_3$ and $\text{UO}_3 \cdot 3\text{WO}_3$. Phase relations shown in Fig. 21 (Hauck, 1974) were studied under one atmosphere of oxygen. In the system, UO_3 is not stable at relatively high temperatures and decomposes to U_3O_8 , which has three forms with transition points at 630° and 850°C . The eutectic temperature given by Hauck is 25°C lower than that proposed by Cordfunke.

Crystal structures of both uranium tungstates are not known, although the unit cell symmetry of $\text{UO}_3 \cdot \text{WO}_3$ has been reported to be either cubic with $a = 3.805\text{\AA}$ (Trunov et al., 1961) or monoclinic with $a = 7.205$, $b = 5.482$, $c = 13.57\text{\AA}$, and $\beta = 104.35^\circ$ (Juenke and Bartram, 1964).

A phase, $5\text{UO}_2 \cdot 19\text{WO}_3$, was reported in the system uranium dioxide and tungsten trioxide by Rozanova et al. (1971). It is orthorhombic with cell dimensions, $a = 7.814$, $b = 7.271$, and $c = 38.67\text{\AA}$.

SYSTEMS Mn-, Fe-, Co-, Ni-Oxide - WO_3

Very few data have been reported on the phase relations in these systems; only that each system has a 1:1, wolframite-type phase (Keeling, 1957; Phillips et al., 1965; Ulka, 1967; Dach et al., 1967). The wolframite-type structure is made up of zig-zag strings of edge-sharing octahedra,

extending along the c-direction and these strings are linked together by sharing corners. Each string contains only one type of cation, either Mn (or Fe, Co, Ni) or W. Both octahedra are considerably distorted. Cell dimensions of $\text{MnO} \cdot \text{WO}_3$, $\text{FeO} \cdot \text{WO}_3$, $\text{CoO} \cdot \text{WO}_3$ and $\text{NiO} \cdot \text{WO}_3$ as well as other common wolframite-type 1:1 tungstates are listed in Table 2 (Sleight, 1972).

In the system $\text{Fe}_2\text{O}_3\text{-WO}_3$, a 1:1 phase was reported by Trunov and Kovba (1966). Waring (1965) proposed a 2:5 phase and suggested it to be isostructural with the 2:5 phase he found in the system $\text{Al}_2\text{O}_3\text{-WO}_3$. Determination of phase relations in this system is now in progress in this laboratory.

SYSTEMS Cu- and Ag-Oxide - WO_3

Gimelforb and Zelikman (1968) reported the formation of a phase with the composition of $\text{Cu}_2\text{O} \cdot \text{WO}_3$ in the process of oxidation of WC in the presence of copper, but its stability is unknown. In the system CuO-WO_3 , two phases, 3:1 and 1:1, were prepared (Tkachenki et al., 1975) with melting points at, respectively, 930° and 920°C . The 1:1 phase has a triclinically distorted wolframite-type structure (Gebert and Kihlborg, 1967; Kihlborg and Gebert, 1970). The Cu atoms are surrounded by six oxygens, four of which are in approximately square planar arrangement with the remaining two at a

distance completing an elongated octahedron. Van Uitert et al. (1963) reported that this 1:1 phase dissociates extensively at its melting point.

Phase relations in the system $\text{Ag}_2\text{O}-\text{WO}_3$ are not known.

SYSTEMS ZnO-, CdO-, and HgO - WO_3

All systems, $\text{ZnO}-\text{WO}_3$ (Fig. 22) (Kislyakov et al., 1973), $\text{CdO}-\text{WO}_3$ (Fig. 23) (Kislyakov and Lopatin, 1967), and $\text{HgO}-\text{WO}_3$ (Sleight and Licis, 1971), show the formation of a 1:1 phase. Both $\text{ZnO}\cdot\text{WO}_3$ and $\text{CdO}\cdot\text{WO}_3$ have the wolframite-type structure, but large distortion exists in $\text{CdO}\cdot\text{WO}_3$ (Sharp, 1960; Coing-Boyat, 1961; Chang, 1967b; Sleight, 1972). Cell dimensions of both $\text{ZnO}\cdot\text{WO}_3$ and $\text{CdO}\cdot\text{WO}_3$ are listed in Table 2.

$\text{HgO}\cdot\text{WO}_3$ is monoclinic (Sleight and Licis, 1971), and its structure has no obvious relationship with either the scheelite or wolframite structure.

SYSTEMS B_2O_3 - Al_2O_3 - Ga_2O_3 , and In_2O_3 - WO_3

Phase relations in the system B_2O_3 - WO_3 as determined by Levin (1965) (Fig. 24) are of a simple eutectic type with an S-shaped liquidus and with a solidus near $450^\circ C$. No liquid immiscibility exists because, as suggested by Levin, the B - O bonds are not strong enough to maintain a separated B_2O_3 -rich liquid phase.

A tentative phase diagram for the system Al_2O_3 - WO_3 was given by Waring (1965) (Fig. 25) showing a congruently melting phase with a composition later refined to be 1:3 rather than 2:5 as shown in his phase diagram (Levin et al., 1969). Craig and Stephenson (1968) showed that in the structure, each WO_4 tetrahedron by corner-sharing of oxygen atoms is surrounded by four AlO_6 and each AlO_6 octahedron is surrounded by six WO_4 . The 1:3 phase is orthorhombic with $a = 12.588$, $b = 9.055$, and $c = 9.127\text{\AA}$.

The system Ga_2O_3 - WO_3 has a simple eutectic relationship with no formation of a binary phase (Fig. 26), whereas a 1:3 phase exists in the system In_2O_3 - WO_3 (Fig. 27) (Karpov and Korotkerich, 1973), and is isostructural with $Al_2O_3 \cdot 3WO_3$ (Abraham and Berstein, 1966).

SYSTEMS Sn- and Pb-Oxide - WO_3

Tungstates of the Group IVA elements are known only in the tin and lead systems where the cations are in their di-

valent state. $\text{SnO}\cdot\text{WO}_3$ is dimorphic (Jeitschko and Sleight, 1972) with a transition temperature at 670°C . The low-temperature form is orthorhombic with $a = 5.627$, $b = 11.649$, and $c = 4.997\text{\AA}$, and the high-temperature form is cubic with $a = 7.299\text{\AA}$. Neither structure is related to either the scheelite or the wolframite structure (Sleight, 1972).

Phase relations in the system $\text{PbO}\cdot\text{WO}_3$ are shown in Fig. 28 (Chang, 1971). The 1:1 phase has the scheelite-type structure and is stable to its melting point. The absence of a phase transition in $\text{PbO}\cdot\text{WO}_3$ confirms the results of an earlier study (Chang, 1967b). Jaeger and Germs (1921) proposed a phase change at 877°C , but they did not characterize the difference in the high and low temperature forms. It is known that in natural occurrences (Palache et al., 1944) two minerals have this composition; the scheelite-type stolzite and the wolframite-type raspite. Attempts to synthesize raspite under high-pressure failed (Chang, 1971), although a new phase of $\text{PbO}\cdot\text{WO}_3$ was synthesized in the pressure range between 10 and 35 kbars. Using natural raspite, Shaw and Claringbull (1955) determined an apparent upper stability limit at about 400°C .

SYSTEMS P-, As-, Sb-, and Bi-Oxide - WO_3

Two phases, 1:1 and 1:2, have been reported in the system $\text{P}_2\text{O}_5\text{-WO}_3$ (Schulz, 1955; Kierkegaard, 1958, 1960, 1962; Kierkegaard and Asbrink, 1964), but only the latter was con-

firmed by a recent study of Martinek and Hummel (1970). They reported that the 1:2 phase is stable at least to 1125°C in an open system at atmospheric pressure and has a range of solid solution extended to the 1:1 composition. The 1:2 phase has a framework-type structure (Kierkegaard 1960; Kierkegaard and Asbrink, 1964) made by joining WO_6 octahedra and PO_4 tetrahedra in such a way that each WO_6 is linked to four PO_4 and one other WO_6 and each PO_4 is linked to four WO_6 . The 1:2 phase is monoclinic with $a = 7.83$, $b = 12.48$, $c = 7.76\text{\AA}$, and $\beta = 91.9^\circ$. The 1:1 phase, according to Kierkegaard (1958), has a layer structure made up of WO_6 octahedra and PO_4 tetrahedra. No arsenic tungstates have been reported.

Other members of Group VA elements, antimony and bismuth, show a trivalent state in their tungstate formation. In the system $Sb_2O_3-WO_3$, a 1:1 phase was prepared in sealed capsules under inert gas at 750°C and has a monoclinic symmetry with $a = 9.27$, $b = 9.80$, $c = 11.05\text{\AA}$, and $\beta = 100.4^\circ$ (Parmentier et al., 1975).

Phase relations in the system $Bi_2O_3-WO_3$ have been studied in detail (Sillen and Lundborg, 1943; Smalyaninov and Belyaev, 1962; Gal'perin et al., 1966; Speranakaya, 1970; Hoda and Chang, 1975). Phase relations established by Hoda and Chang are shown in Fig. 29. The 7:1 phase has a tetragonal face-centered structure below 784°C with $a = 5.52$

and $c = 17.39\text{\AA}$ and transforms to a f.c.c. structure above 784°C . The 7:2 phase has a f.c.c. structure with $a = 5.61\text{\AA}$ and forms a complete solid solution series with the high-temperature form of Bi_2O_3 above 784°C . Both 1:1 and 1:2 phases are orthorhombic and have cell dimensions, respectively, of $a = 5.45$, $b = 5.46$, $c = 16.42\text{\AA}$ and $a = 5.43$, $b = 5.41$, $c = 23.172\text{\AA}$.

Results obtained by Hoda and Chang (1974) confirm in general the limited information provided by Gal'perin et al. (1966), except for their extensive ranges of solid solution at 650°C . As Hoda and Chang stated, "it is suspected that the experimental procedure of those workers, which involved melting the samples at 900° to 1200°C , cooling them rapidly in water, annealing the quenched samples at 650°C for 2 hours, and furnace cooling before x-ray diffraction examination, could have resulted in misleading estimates of solid solution ranges". A better agreement between these two studies can be obtained when the solid solution ranges reported by Gal'perin et al. are considered to represent equilibrium at higher temperatures.

Phase relations proposed by Speranskaya (1970) resulted from annealing of nine compositions at 700°C and subsequent DTA. Neither x-ray diffraction data nor cell dimensions were reported.

REFERENCES

- Abraham, S. C., and Berstein, J. L., *J. Chem. Phys.*, 45, 2745-2752 (1966)
- Aitken, E. A., Bartram, S. F., and Juenke, E. F., *Inorg. Chem.*, 3, 949-954 (1964)
- Ampe, B., Leroy, J. M., Thomas, D., and Tridot, G., *Rev. Chim. Miner.*, 5, 789-800 (1968)
- Andersson, G., *Acta Chem. Scand.*, 7, 154-158 (1953)
- Borchardt, H. J., *Inorg. Chem.*, 2, 170-173 (1963)
- Borisov, S. V., and Klevtsova, R. F., *Kristallografiya*, 15, 38-42 (1970)
- Bottelberghs, P. H., and van Buren, R. R., *J. Solid State Chem.*, 13, 182-191 (1975)
- Caillet, P., *C.R.H. Acad. Sci.*, 256, 1869-1889 (1963)
- Chang, L. L. Y., *Mineral. Mag.*, 36, 436-437 (1967a)
- _____, *Amer. Mineral.*, 52, 427-435 (1967b)
- _____, *J. Amer. Ceramic Soc.*, 54, 357-358 (1971)
- _____, and Phillips, B., *Inorg. Chem.*, 3, 1192-1194 (1964)
- _____, and Sachdev, S., *J. Amer. Ceramic Soc.*, 58, 267-270 (1975)
- _____, Scroger, M. G., and Phillips, B., *J. Amer. Ceramic Soc.*, 49, 385-390 (1966a)
- _____, *J. Inorg. Nucl. Chem.*, 28, 1179-1184 (1966b)
- _____, *J. Less-common Metals*, 12, 51-56 (1967a)

-
- _____, J. Amer. Ceramic Soc., 50, 211-215 (1967b)
- Coing-Boyat, J., Acta Cryst., 14, 1100 (1961)
- Cordfunke, E. H. P., J. Inorg. Nucl. Chem., 31, 1542-1545 (1969)
- Craig, D. C., and Stephenson, N. C., Acta Cryst., B24, 1250-1255 (1968)
- Dach, H., Stoll, E., and Weitzel, H., Zeit. Krist., 125, 120-129 (1967)
- Felton, E. J., J. Less-common Metals, 9, 206-213 (1965)
- Fiegel, L. J., Mohanty, G. P., and Healy, J. H., J. Chem. Eng. Data, 9, 365-369 (1964)
- Gal'perin, E. L., Erman, L. Ya., Kolchin, I. K., Belov, M. A., and Chernyshev, K. S., Russ. J. Inorg. Chem., 11, 1137-1143 (1966)
- Gebert, E., and Kihlberg, L., Acta Chem. Scand., 21, 2575-2576 (1967)
- Gelsing, R. J. H., Stein, H. N., and Stevels, J. M., Rec. Trav. Chim., 84, 1452-1458 (1965)
- Gimelfarb, P. A., and Zelikman, A. N., Izv. Vyssh. Ucheb. Zaved. Tsvet. Met., 10, 63-66 (1968). Chem. Abs., 68, 71809k (1968)
- Goldschmidt, H. J., Metallurgia, 62, 211-218 and 241-250 (1960)
- Graham, J., Wadsley, A. D., Weymouth, J. H., and Williams, L. S. J. Amer. Ceramic Soc., 42, 570 (1959)

- Gruehn, R., *Mont. Chim.*, 96, 1789-1792 (1965)
- Guerin, R., and Caillet, P., *C.R. Acad. Sci., Ser. C*, 271, 814-817 (1970)
- Hauck, J., *J. Inorg. Nucl. Chem.*, 36, 291-298 (1974)
- Hoda, S. N., and Chang, L. L. Y., *J. Amer. Ceramic Soc.*, 57, 323-326 (1974)
- Hoermann, F., *Zeit. anorg. allgem. Chem.*, 177, 145-186 (1928)
- Ivanova, M. M., Balagina, G. M., and Rode, E. Ya., *Izv. Akad. Nauk SSSR, Neorg. Mater.*, 6, 914-919 (1970)
- _____, and Reznik, E. M., *Izv. Akad. Nauk SSSR, Neorg. Mater.*, 8, 981-983 (1972)
- Jaeger, R. M., and Germs, H. C., *Zeit. anorg. allgem. Chem.*, 119, 145-173 (1921)
- Jeitschko, W., and Sleight, A. W., *Acta Cryst.*, B29, 869-875 (1973)
- Juenke, E. F., and Bartram, S. F., *Acta Cryst.*, 17, 618 (1964)
- Karpov, V. N., and Korotkerich, I. B., *Zh. Neorg. Khim.*, 18, 520-521 (1973)
- Keeling, R. O., *Acta Cryst.*, 10, 209-213 (1957)
- Kierkegaard, P., *Acta Chem. Scand.*, 12, 1715-1729 (1958)
- _____, *Acta Chem. Scand.*, 14, 657-676 (1960)
- _____, *Ark. Kemi.*, 19, 51-74 (1962)
- _____, and Asbrink, S., *Acta Chem. Scand.*, 18, 2329-2336 (1964)
- Kislyakov, I. P., and Lopatin, B. P., *Zh. Neorg. Khim.*, 12, 3163-3165 (1967)

- _____, Smirnova, I. N., and Boguslavskaya, G. I.,
Izv. Vyssh. Ucheb. Zaved., Khim. Khim. Tekhnol.,
16, 1440 (1973)
- Kihlberg, L., and Gebert, E., Acta Cryst., B26, 1020-1026
(1970)
- Klevtsov, P. V., Kharchenko, L. Ya, and Klevtsova, R. F., Dokl.
Akad. Nauk SSSR, 176, 575-577 (1967). Chem. Abs.,
68, 24891w (1968)
- _____, Kozeva, L. P., and Klevtsova, R. F., Izv.
Akad. Nauk SSSR, Neorg. Mater., 7, 1461-1462 (1971)
- Kools, F. X. N. M., Koster, A. S., and Rieck, G. D., Acta
Cryst., B26, 1974-1977 (1970)
- Koster, A. S., Kools, F. X. N. M., and Rieck, G. D., Acta
Cryst., B25, 1704-1708 (1969)
- Kovba, L. M., and Trunov, V. K., Dokl. Akad. Nauk SSSR, 147,
622-624 (1962)
- _____, and Simanov, Ya. P., Zh. Neorg
Khim., 9, 1930-1933 (1964)
- Kreidler, E. R., J. Amer. Ceramic Soc., 55, 514-519 (1972)
- Launay-Mondet, S., Rev. Chim. Miner., 8, 391-422 (1971)
- Laves, F., Bayer, G., and Panagas, A., Schweiz. Mineral.
Petrog. Mitt., 43, 217-234 (1963)
- Levin, E. M., J. Amer. Ceramic Soc., 48, 491-492 (1965)
- _____, Robbins, C. R., and McMurdie, H. F., "Phase Dia-
grams for Ceramicists", Amer. Ceramic Soc., 1969
- Lindqvist, I., Acta Chem. Scand., 4, 1066-1074 (1950)

- Magneli, A., *Acta Chem. Scand.*, 3, 88-89 (1949)
- Margarill, S. A., Klevtsova, R. F., and Bakakin, V. V., *Kristallografiya*, 18, 269-276 (1973)
- Martinek, C. A., and Hummel, F. A., *J. Amer. Ceramic Soc.*, 53, 159-161 (1970)
- McCarthy, G. J., Fischer, R. D., Johnson, G. G., and Gooden, C. E., "Solid State Chemistry", NBS Spec. Publ., 364, 397-410 (1972)
- Mokhosoev, M. V., Kuleshov, I. M., and Fedorov, P. I., *Zh. Neorg. Khim.*, 7, 1628-1631 (1962)
- Mondet, S., *Acad. Soc. Paris., Sect. C*, 267, 1689-1691 (1968).
Chem. Abs., 70, 109803k (1969)
- Nassau, K., and Mills, A. D., *Acta Cryst.*, 15, 808-809 (1962)
- _____, Levinstein, H. J., and Loiacona, C. M., *J. Phys. Chem. Solids*, 26, 1805-1816 (1965)
- _____, and Shieve, J. W., "Solid State Chemistry", NBS Spec. Publ., 364, 445-456 (1972)
- Palache, C., Berman, H., and Frondel, C., "Dana's System of Mineralogy", 7th ed., vol. II, John-Wiley & Sons, New York, 1944
- Parmentier, M., Gleitzer, C., and Aubrey, J., *C.R. Acad. Sci., Ser. c*, 274, 1681-1683 (1972a)
- _____, Reau, J. M., Fouassier, C., and Gleitzer, C., *Bull. Soc. chim. Fr.*, 1743-1746 (1972b)
- _____, Courtous, A., and Gleitzer, C., *C.R. Hebd., Seances Acad. Sci., Ser. C*, 280, 985-986 (1975)
- Phillips, B., Chang, L. L. Y., and Scroger, M. G., *Trans. AIME, Metal. Soc.*, 233, 1220-1226 (1965)

- Pistorius, C. W. F. T., *J. Chem. Phys.*, 44, 4532-4537 (1966)
- Polyanskaya, T. M., Borisov, S. V., and Belov, N. V., *Dokl. Akad. Nauk SSSR*, 193, 83-86 (1970a)
-
- _____, *Kristallografiya*, 15, 1135-1139 (1970b)
- Purt, G., *Zeit. Phys. Chem.*, 35, 133-138 (1962)
- Reau, J. M., and Fouassier, C., *Bull. Soc. chim. Fr.*, 398-402 (1971)
-
- _____, and Hagenmuller, P., *Bull. Soc. chim. Fr.*, 3873-3876 (1967)
- Rieck, G. D., *Rec. Trav. Chim.*, 62, 427-430 (1943)
- Rode, E. Ya., and Karpov, V. N., *Izv. Akad. Nauk SSSR, Neorg. Mater.*, 2, 683-687 (1966)
- Roth, R. S., and Wadsley, A. D., *Acta Cryst.*, 19, 32-38 (1965a)
-
- _____, *Acta Cryst.*, 19, 38-42 (1965b)
-
- _____, *Acta Cryst.*, 19, 42-47 (1965c)
- Roth, R. S., and Waring, J. L., *J. Res. NBS*, 70A, 281-303 (1966)
-
- _____, and Parker, H. S., *J. Solid State Chem.*, 2, 445-461 (1970)
- Roth, R. S., and Stephenson, N. C., "Chem. Extended Defects, Nonmetal Solids", *Proc. Inst. Adv. Study*, 167-182 (1969)
- Rozanova, O. N., Kovba, L. M., and Trunov, V. K., *Radiokhimiya*, 13, 307-309 (1971). *Chem. Abs.*, 75, 54496h (1971)
- Sakka, S., *Bull. Inst. Chem. Res., Kyoto Univ.*, 46, 300-308 (1968)

- Scholder, R., and Brixner, L., *Zeit. Naturforsch.*, B10, 178-179 (1955)
- Schulz, I., *Zeit. anorg. allgem. Chem.*, 281, 99-112 (1955)
- Semikina, L. E., and Limonov, V. E., *Zh. Neorg. Khim.*, 13, 1932-1935 (1968)
- Sharp, W. E., *Zeit. Krist.*, 114, 151-153 (1960)
- Shaw, R., and Claringbull, G. E., *Amer. Mineral.*, 40, 933 (1955)
- Sillen, L. G., and Lundborg, K., *Ark. Kemi., Mineral. Geol.*, 17A, 1-11 (1943)
- Sleight, A. W., *Acta Cryst.*, B28, 2889-2902 (1972)
- _____, and Licis, M. S., *Mater. Res. Bull.*, 6, 365-369 (1971)
- Smolyaninov, N. P., and Belyaev, I. N., *Zh. Neorg. Khim.*, 7, 2591-2595 (1962)
- Speranskaya, E. I., *Izv. Akad. Nauk SSSR, Neorg. Mater.*, 1, 149-151 (1970)
- Spitsyn, V. I., and Kuleshov, I. M., *Zh. Fiz. Khim.*, 24, 1197-1200 (1950)
- _____, and Tikhomirov, I. I., *J. Gen. Chem., (USSR)*, 8, 1527-1533 (1938)
- _____, Pokrovskii, A. N., Afonskii, N. S., and Trunov, V. K., *Dokl. Akad. Nauk SSSR*, 188, 1065-1068 (1968)

- Stephenson, N. C., and Roth, R. S., *Acta Cryst.*, 27, 1010-1017 (1973a)
- _____, *Acta Cryst.*, 27, 1018-1024 (1973b)
- _____, *Acta Cryst.*, 27, 1031-1036 (1973c)
- Stewart, E. G., and Rooksby, H. P., *Acta Cryst.*, 4, 503-507 (1951)
- Tkachenki, E. V., Zhukovski, V. M., and Tel'nyk, T. F., *Zh. Fiz. Khim.*, 49, 809 (1975). *Chem. Abs.*, 83, 36904a (1975)
- Tokunov, O. I., and Kislyakov, I. P., *Izv. Vyssh. Ucheb. Zaved., Khim. Khim. Tekhnol.*, 15, 1609-1612 (1972)
- Trunov, V. K., and Kovba, L. M., *Vesta. Mosk. Univ., Ser. II, Khim.*, 18, 60-63 (1963). *Chem. Abs.*, 59, 5878f (1963)
- _____, *Izv. Akad. Nauk SSSR, Neorg. Mater.*, 2, 151-154 (1966)
- _____, and Spitsyn, V. I., *Dokl. Akad. Nauk SSSR*, 141, 114-116 (1961)
- _____, Tynshevskaya, V., and Afronskii, N. S., *Zh. Neorg. Khim.*, 13, 936-939 (1968)
- Van Uitert, L. G., Rubin, J. J., and Boumer, W. A., *J. Amer. Ceramic Soc.*, 46, 512 (1963)
- Ulku, D., *Zeit. Krist.*, 124, 192-219 (1967)

- Waring, J. L., J. Amer. Ceramic Soc., 48, 493-494 (1965)
- Westman, S., and Magneli, A., Acta Chem. Scand., 12, 363-364 (1958)
- Young, A. P., and Schwartz, C. M., Science, 141, 348-349 (1963)
- Zachariasen, W. H., and Plettinger, H. H., Acta Cryst., 14, 229-230 (1961)
- Zhmud, E. S., and Ostapchenko, E. P., Zh. Strukt. Khim., 2, 33-45 (1961)

Table 1. Comparison of Reported Melting Points ($^{\circ}\text{C}$) of Potassium Tungstates

Tungstate	Hoermann (1928)	Mokhosoev et al. (1962)	Gelsing et al. (1965)	Guerin and Caillet (1970)	Chang and Sachdev (1975)
$\text{K}_2\text{O}\cdot\text{WO}_3$	921 $^{\circ}$ (c)	926 $^{\circ}$ (c)	912 $^{\circ}$ (c)	921 $^{\circ}$ (c)	912 $^{\circ}$ (c)
$\text{K}_2\text{O}\cdot 2\text{WO}_3$	-	-	654 $^{\circ}$ (i)	619 $^{\circ}$ (i)	684 $^{\circ}$ (i)
$\text{K}_2\text{O}\cdot 3\text{WO}_3$	660 $^{\circ}$ (i)	715 $^{\circ}$ (i)	718 $^{\circ}$ (i)	710 $^{\circ}$ (i)	842 $^{\circ}$ (i)
$\text{K}_2\text{O}\cdot 4\text{WO}_3$	930 $^{\circ}$ (i)	930 $^{\circ}$ (i)	898 $^{\circ}$ (i)	812 $^{\circ}$ (i)	912 $^{\circ}$ (i)
$\text{K}_2\text{O}\cdot 6\text{WO}_3$	-	-	-	938 $^{\circ}$ (i)	964 $^{\circ}$ (i)

(solid solution between 1:6 and 1:8 phases)

Table 2. Cell Dimensions of Common Wolframite-Type, 1:1 Tungstates (Sleight, 1972)

Tungstate	a, \AA	b, \AA	c, \AA	β
$\text{MgO}\cdot\text{WO}_3$	4.687	5.675	4.928	90.71 $^{\circ}$
$\text{MnO}\cdot\text{WO}_3$	4.829	5.758	4.996	91.15 $^{\circ}$
$\text{FeO}\cdot\text{WO}_3$	4.724	5.705	4.961	90.00 $^{\circ}$
$\text{CoO}\cdot\text{WO}_3$	4.667	5.681	4.947	90.00 $^{\circ}$
$\text{NiO}\cdot\text{WO}_3$	4.599	5.665	4.910	90.00 $^{\circ}$
$\text{ZnO}\cdot\text{WO}_3$	4.690	5.718	4.926	90.64 $^{\circ}$
$\text{CdO}\cdot\text{WO}_3$	5.027	5.858	5.073	91.49 $^{\circ}$

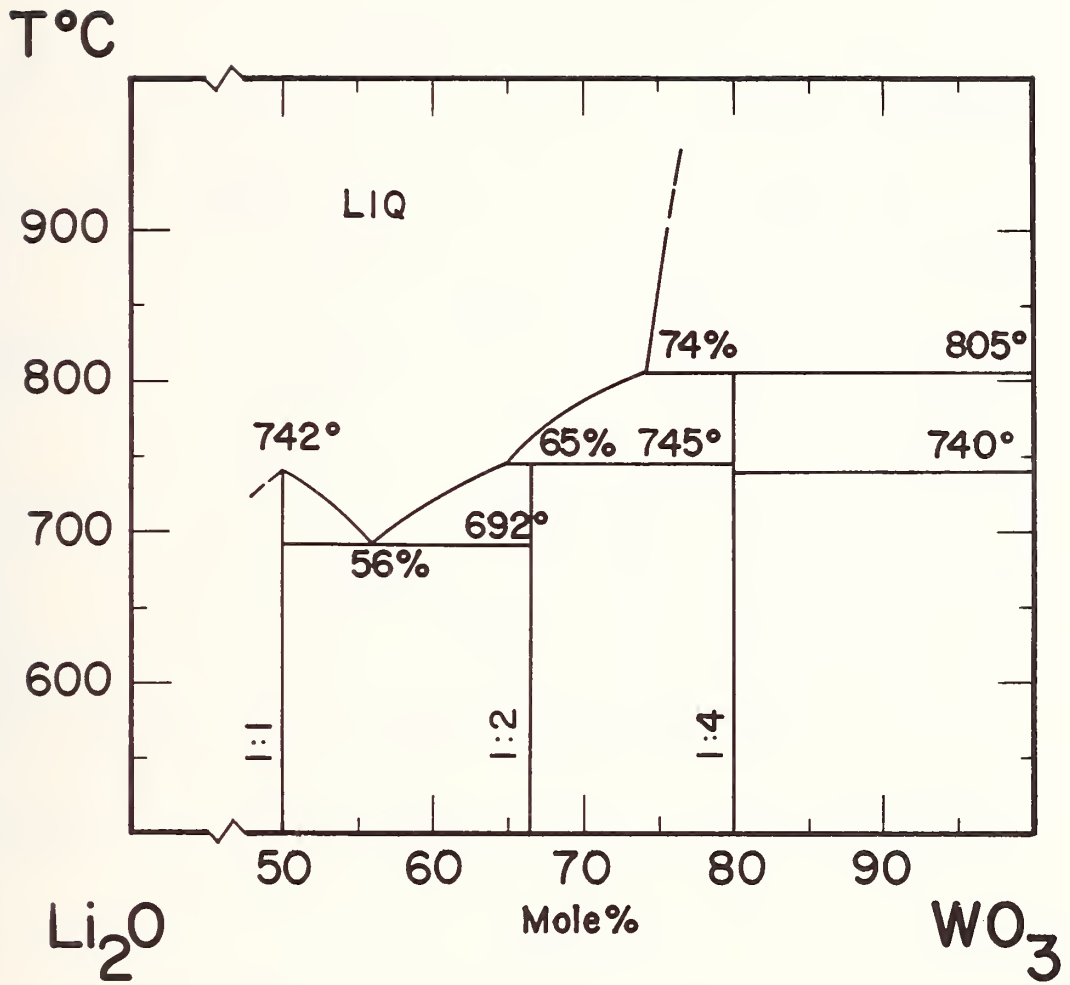


FIGURE 1. Phase relations in the system $\text{Li}_2\text{O}\cdot\text{WO}_3-\text{WO}_3$
(Chang and Sachdev, 1975)

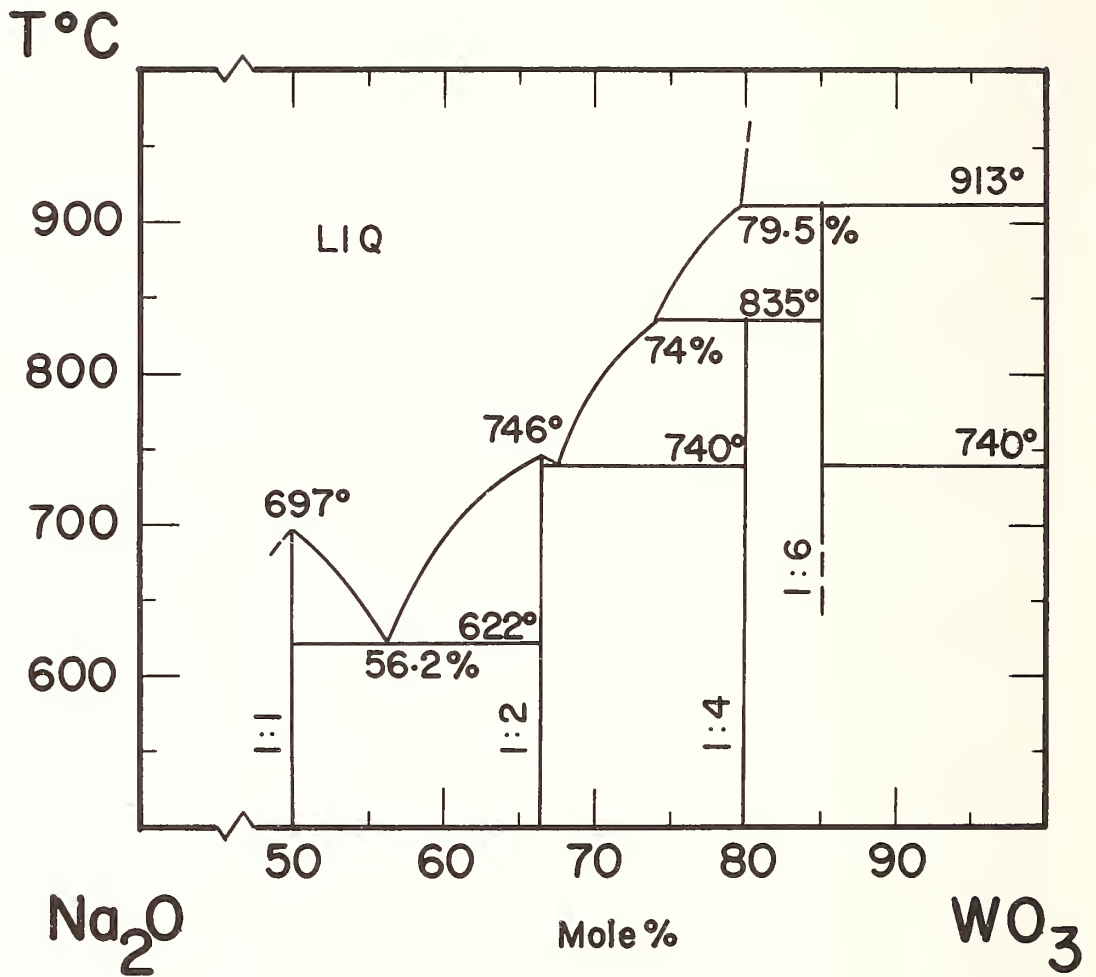


FIGURE 2. Phase relations in the system $\text{Na}_2\text{O}\cdot\text{WO}_3-\text{WO}_3$
(Chang and Sachdev, 1975)

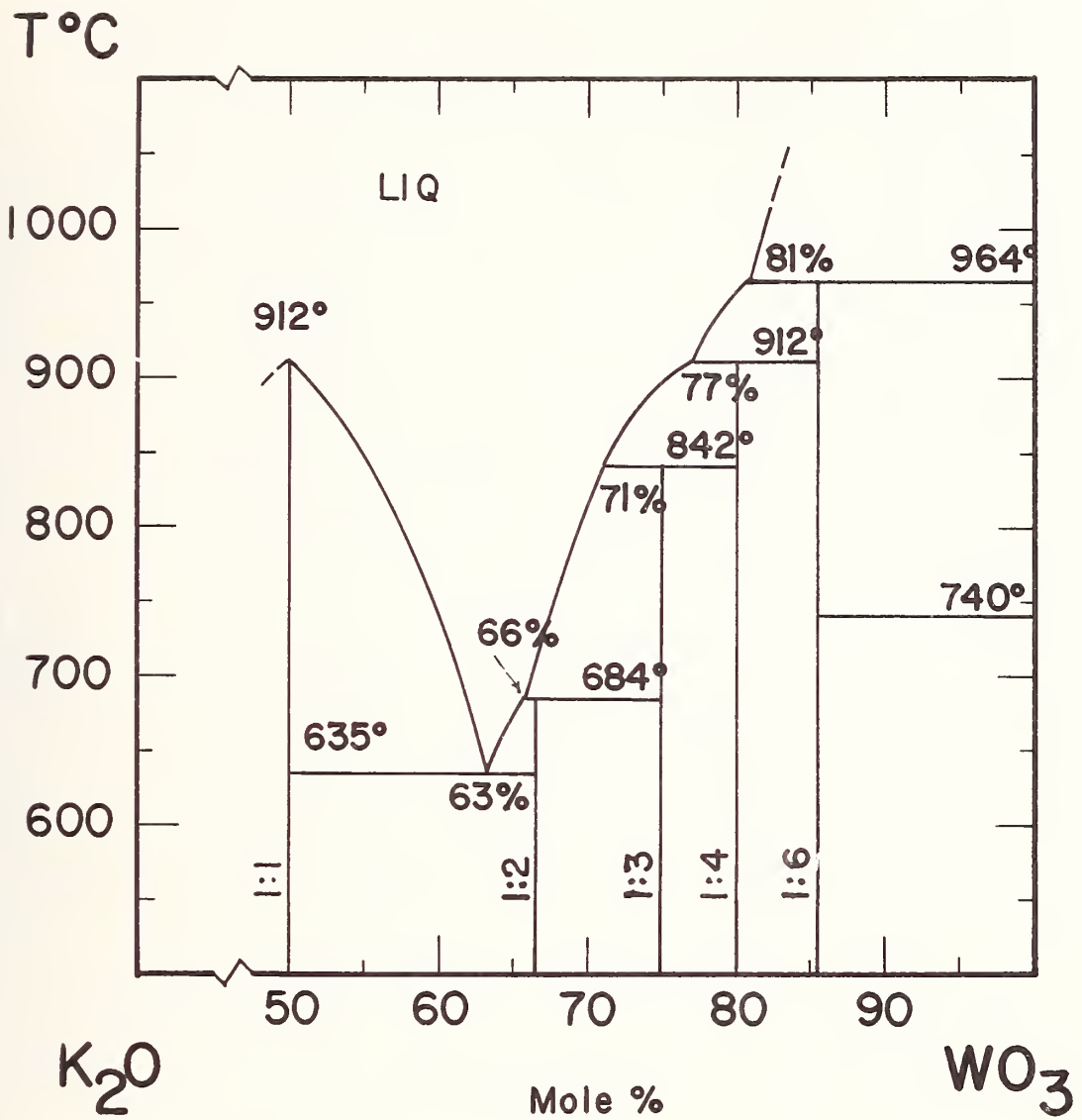


FIGURE 3. Phase relations in the system $K_2O \cdot WO_3 - WO_3$
(Chang and Sachdev, 1975)

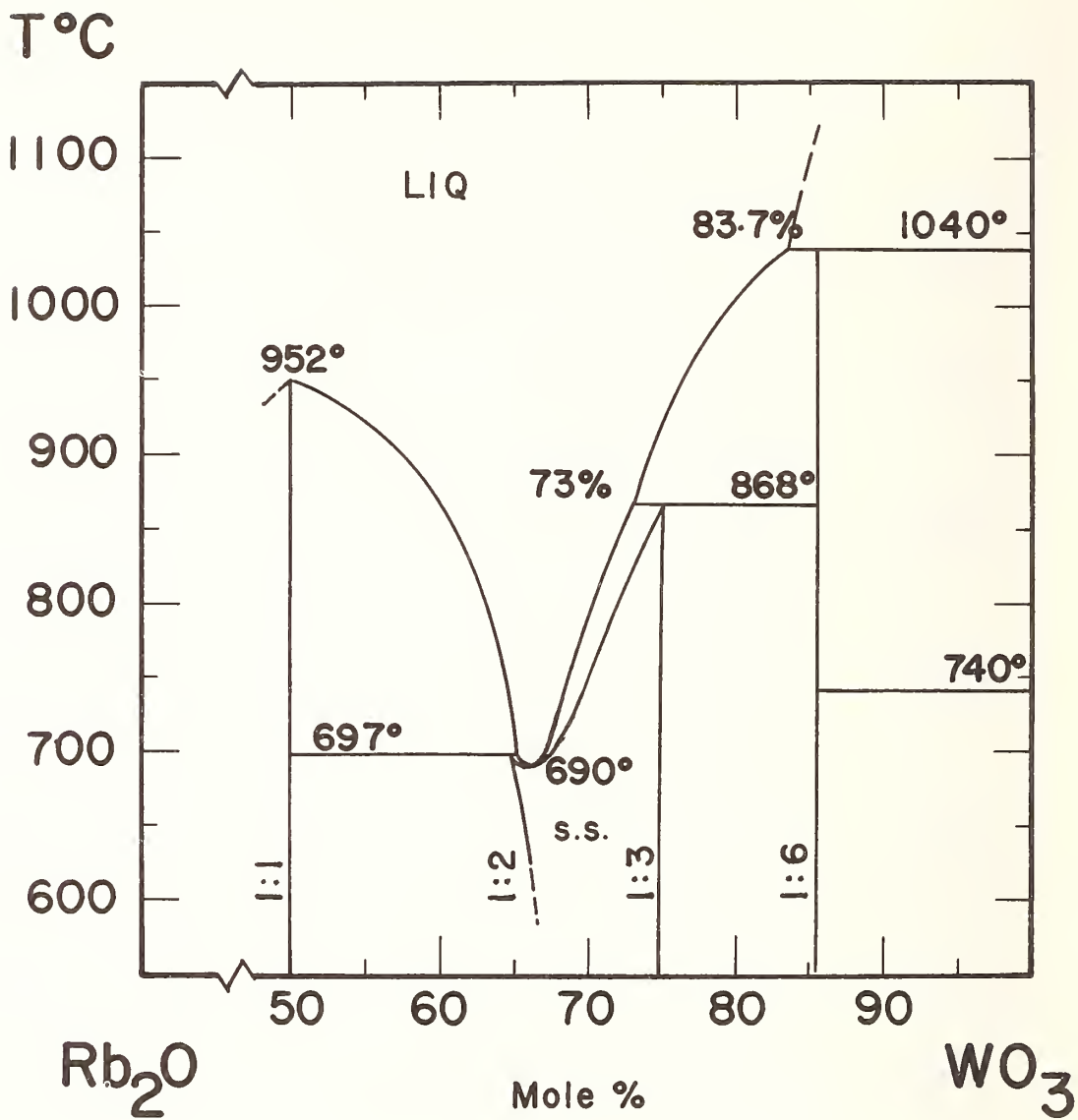


FIGURE 4. Phase relations in the system $\text{Rb}_2\text{O}\cdot\text{WO}_3-\text{WO}_3$
(Chang and Sachdev, 1975)

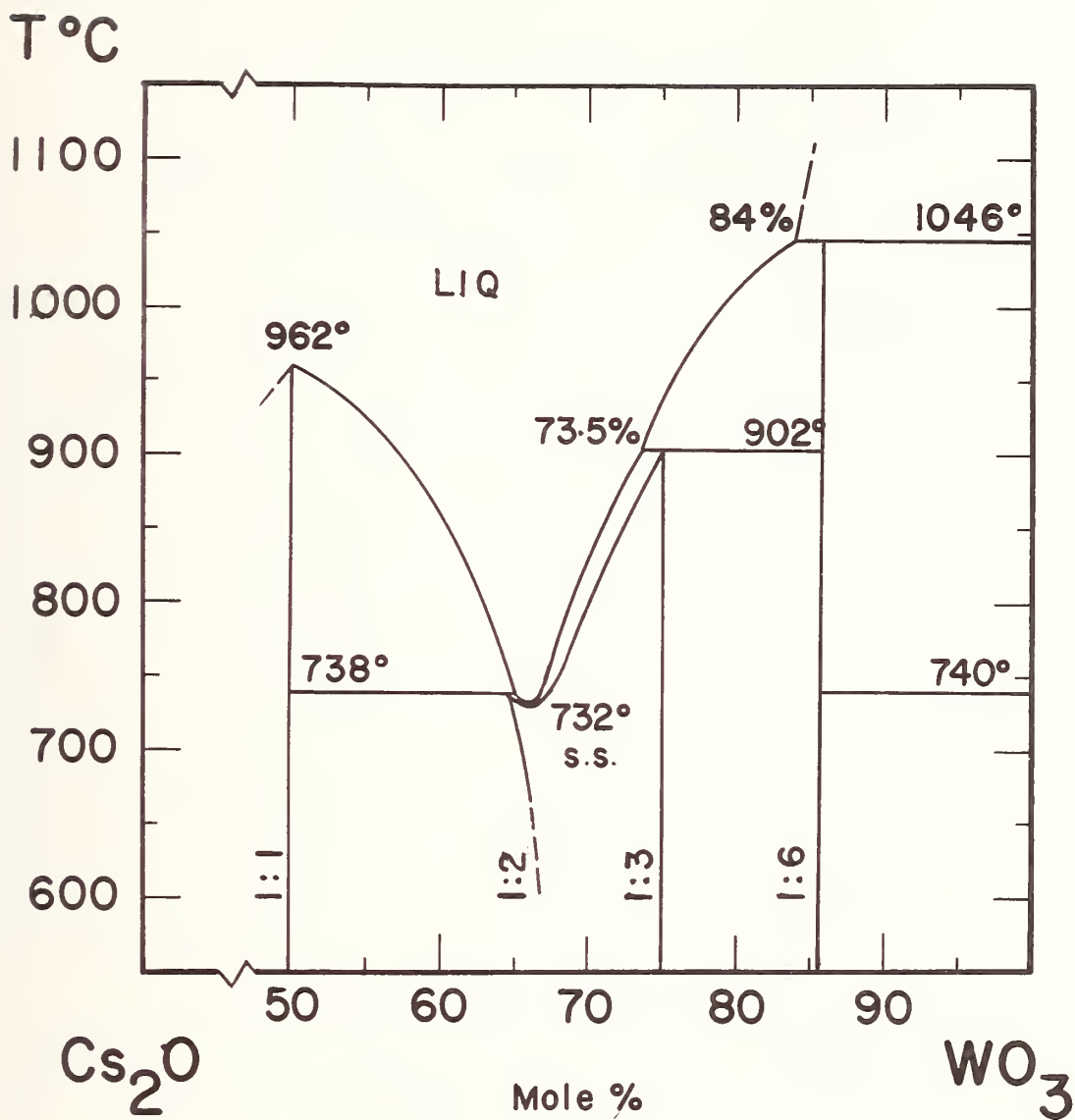


FIGURE 5. Phase relations in the system $\text{Cs}_2\text{O}\cdot\text{WO}_3-\text{WO}_3$
(Chang and Sachdev, 1975)

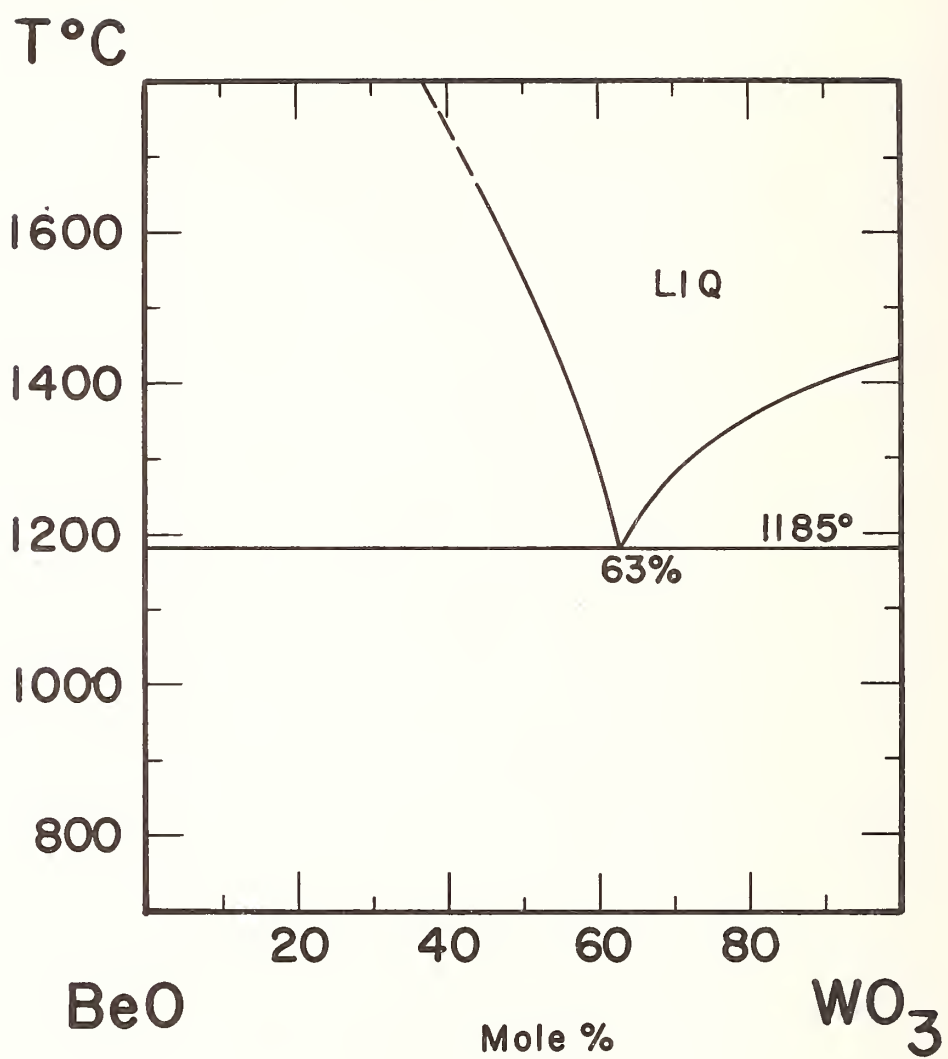


FIGURE 6. Phase relations in the system BeO-WO₃
(Chang et al., 1966a)

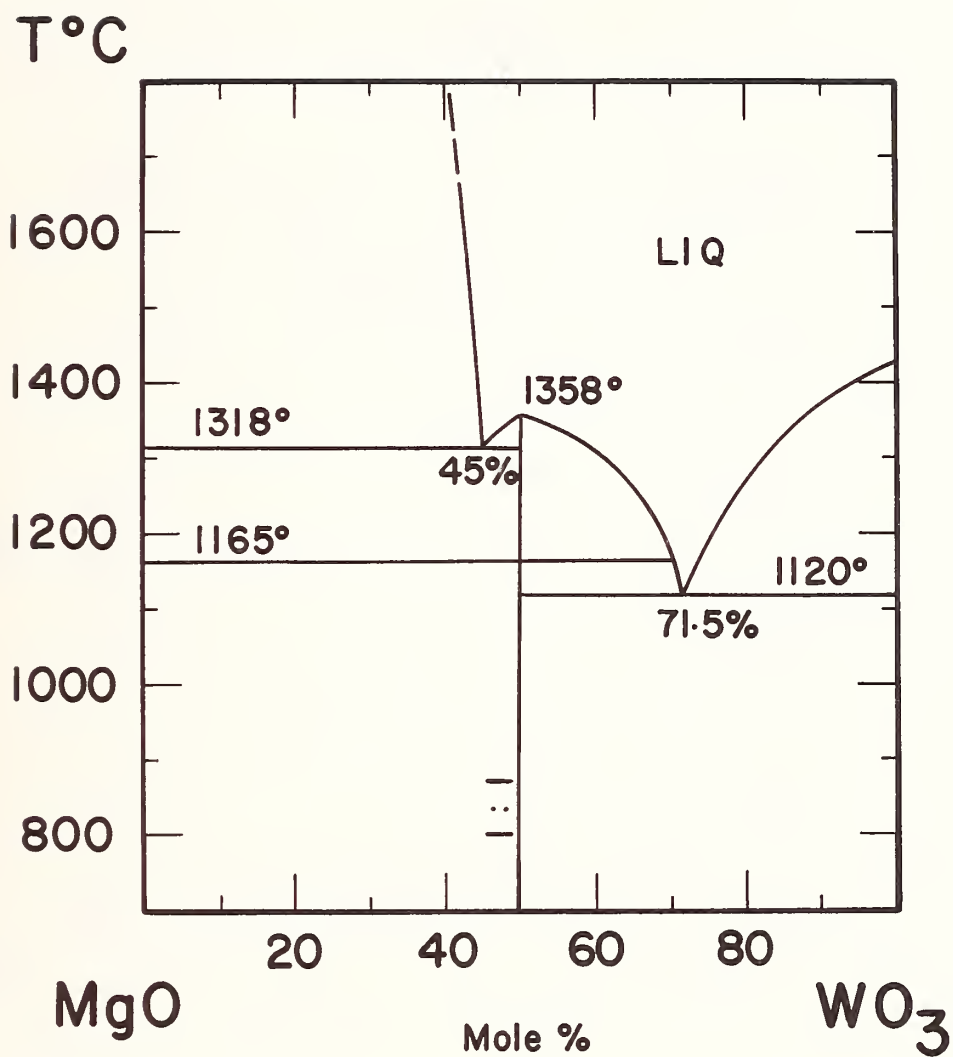


FIGURE 7. Phase relations in the system MgO-WO₃
(Chang et al., 1966a)

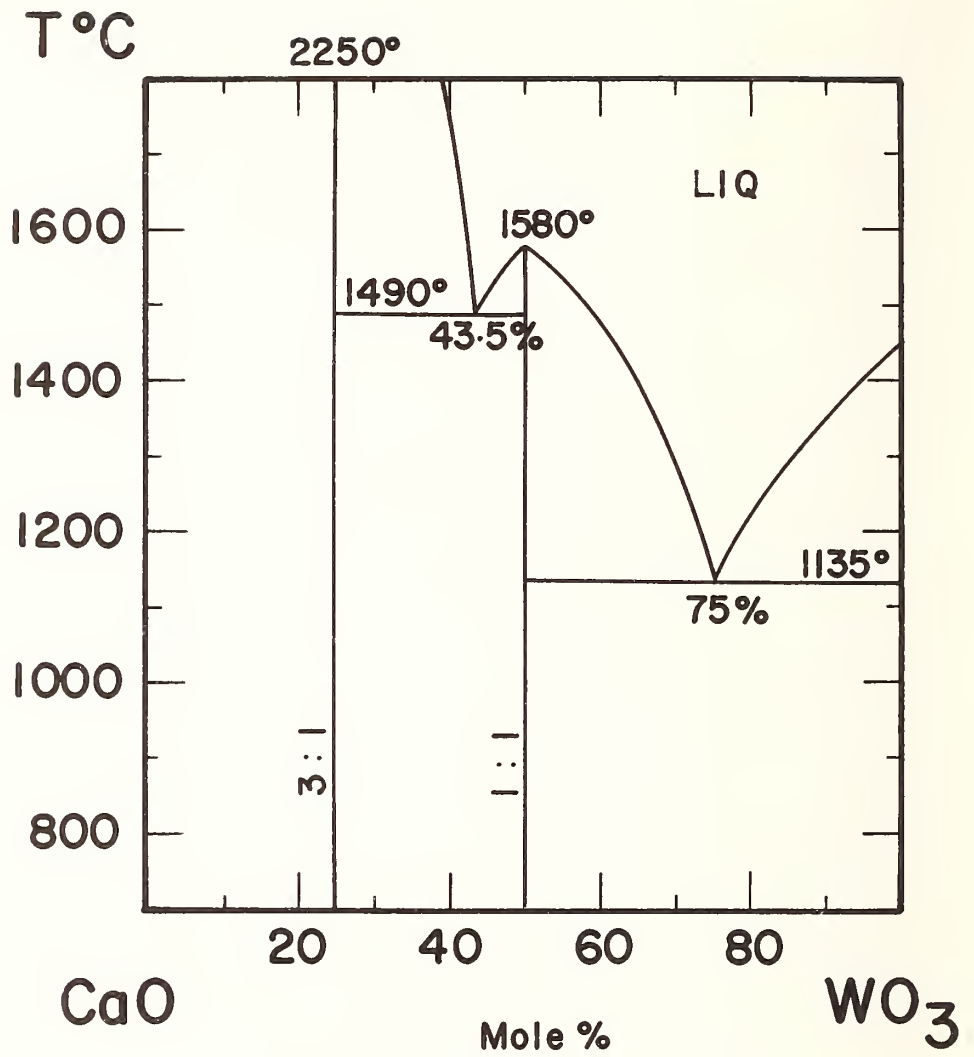


FIGURE 8. Phase relations in the system CaO-WO₃
(Chang et al., 1966a)

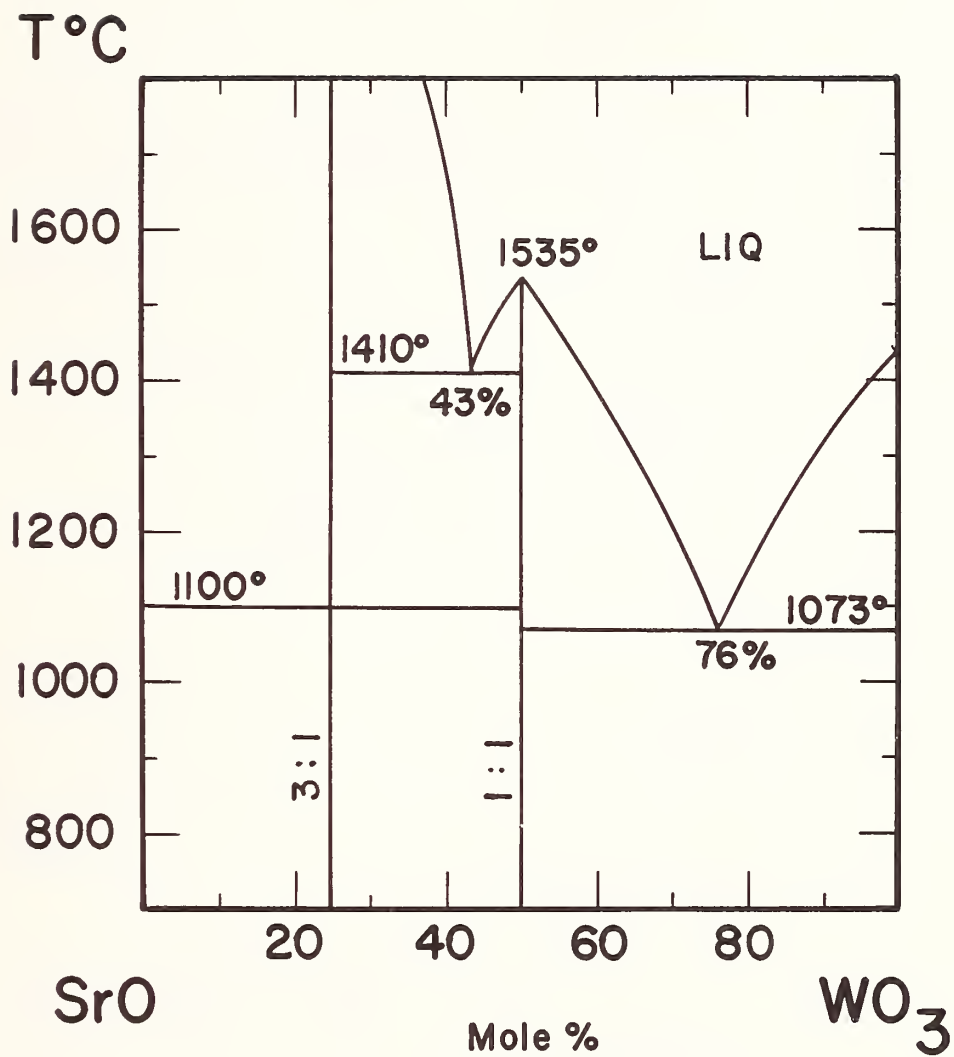


FIGURE 9. Phase relations in the system SrO-WO₃
(Chang et al., 1966a)

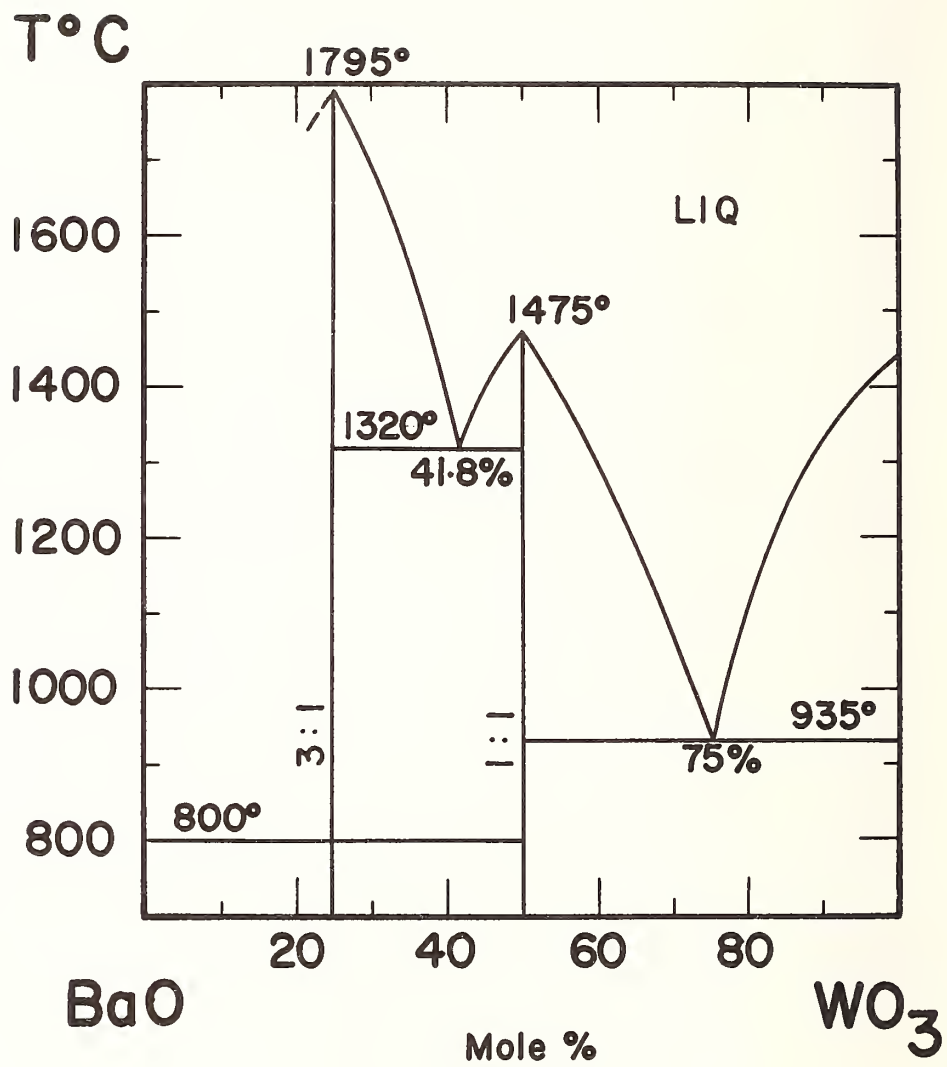


FIGURE 10. Phase relations in the system BaO-WO₃ (Chang et al., 1966a)

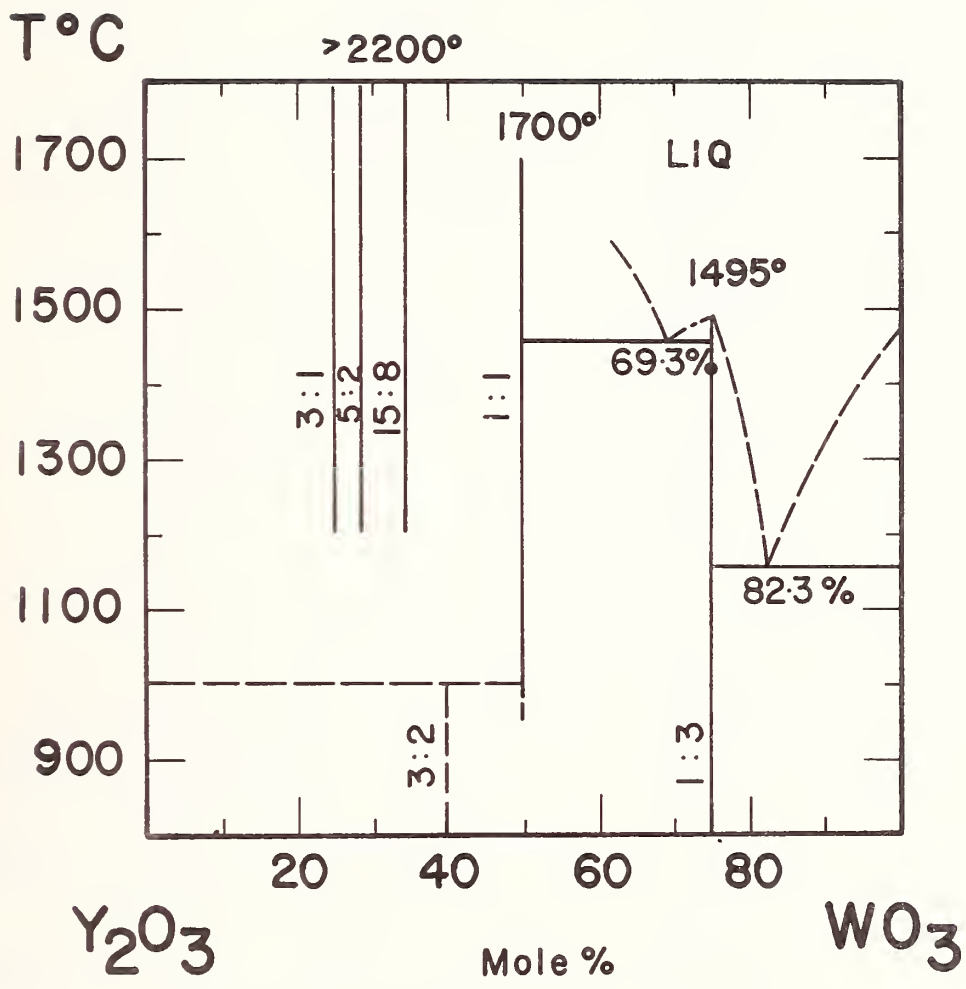


FIGURE 11. Phase relations in the system Y_2O_3 - WO_3
(Borchardt, 1963)

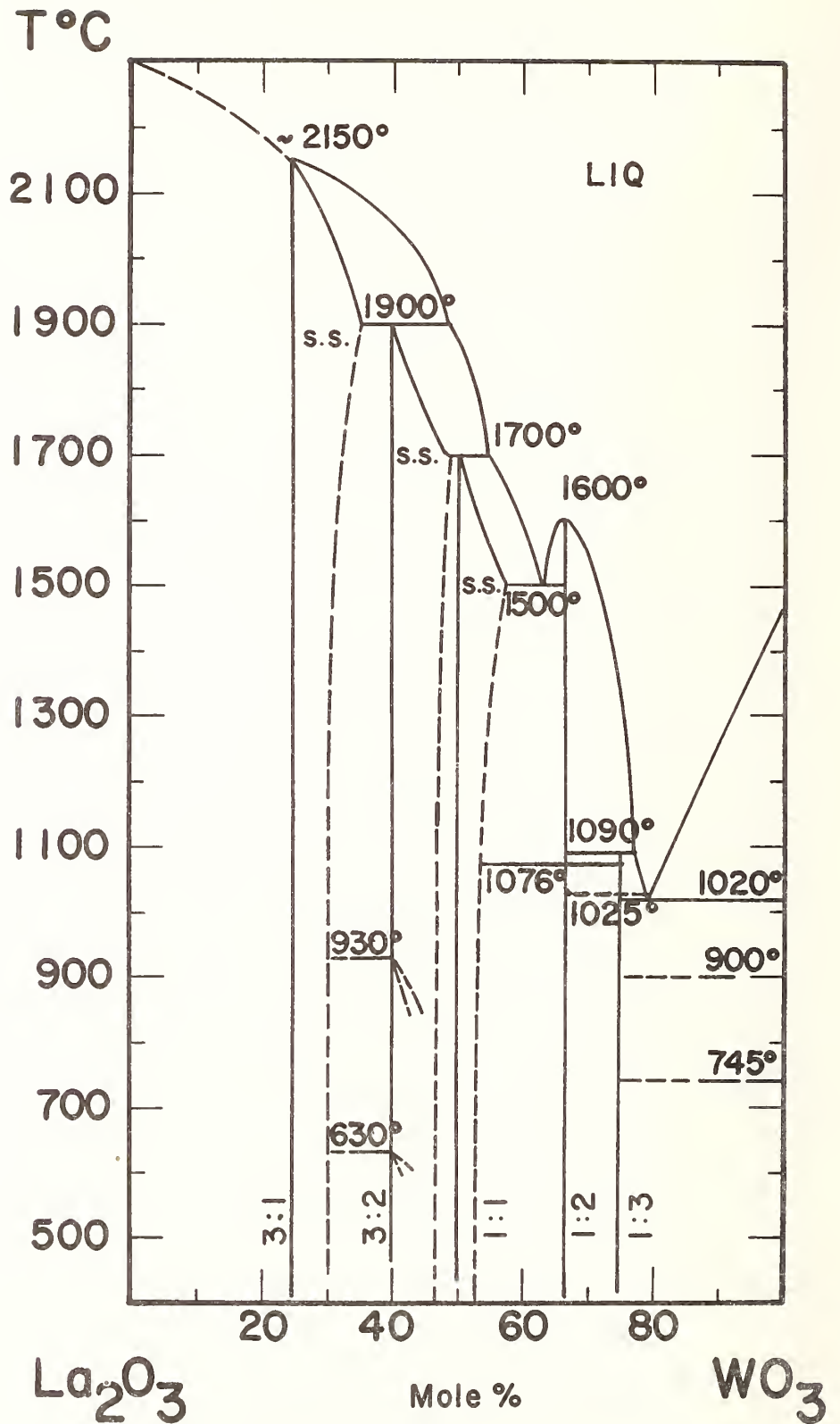


FIGURE 12. Phase relations in the system La_2O_3 - WO_3 (Ivanona et al., 1970)

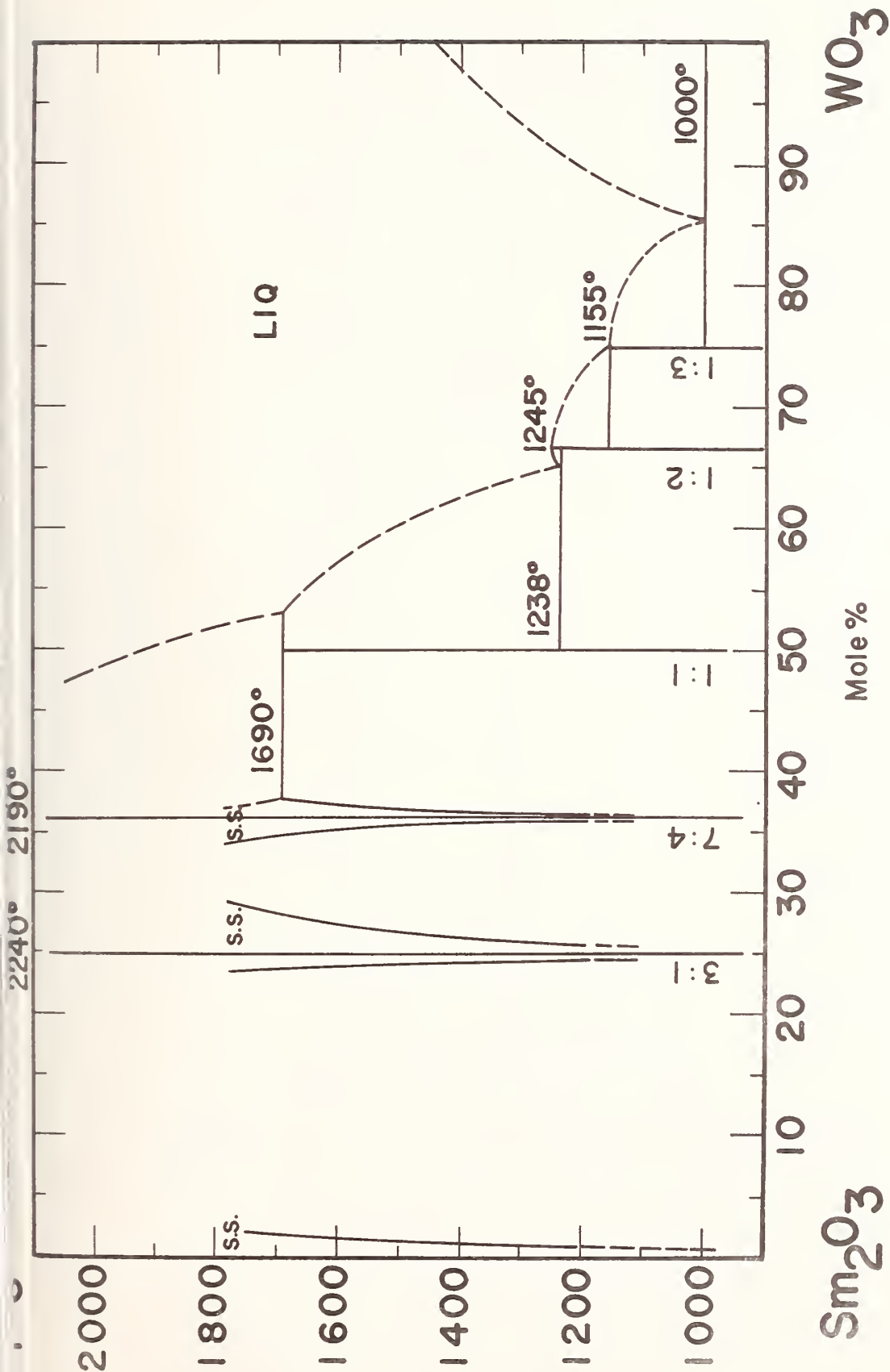


FIGURE 13. Phase relations in the system Sm_2O_3 - WO_3

(Chang et al., 1966b)

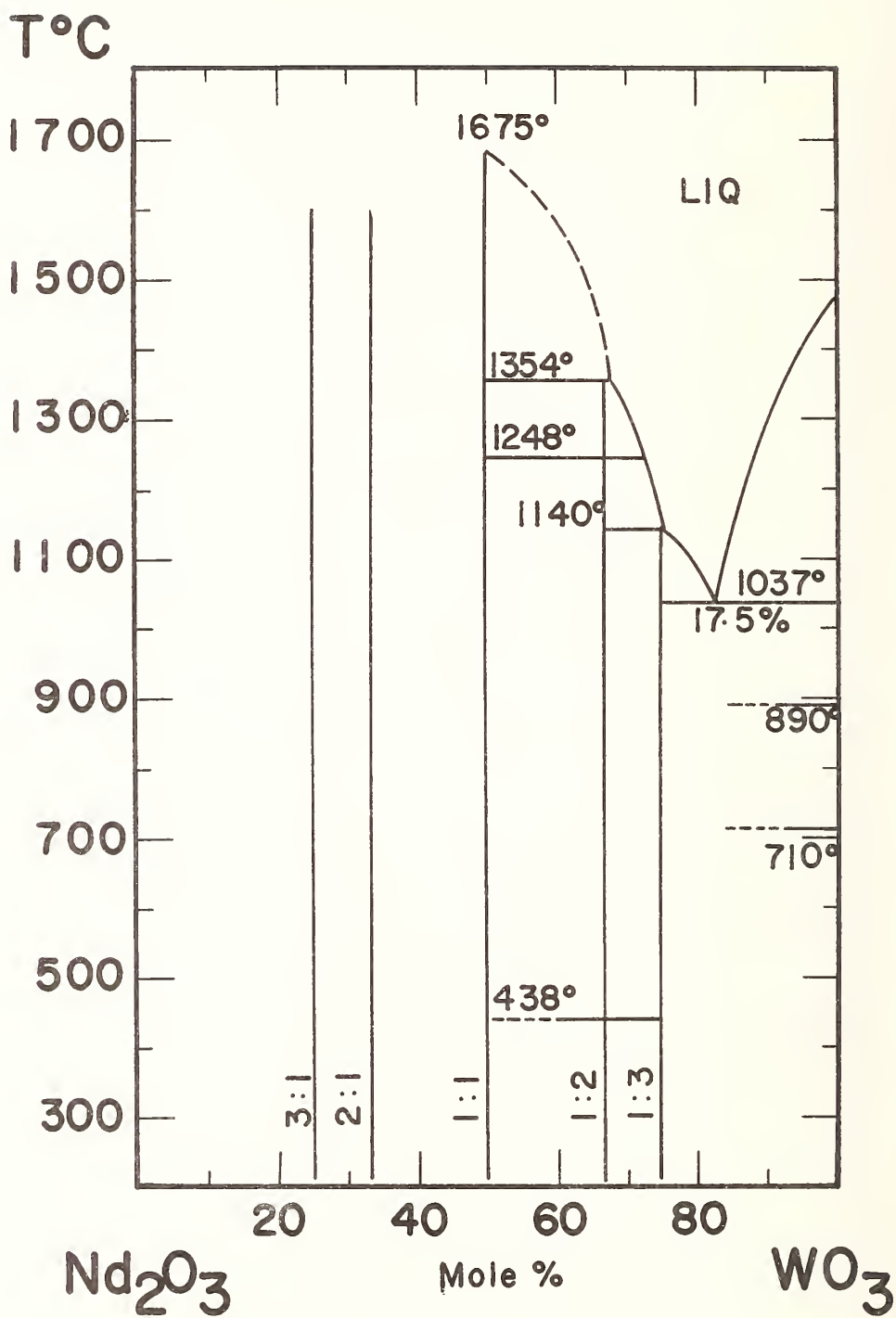


FIGURE 14. Phase relations in the system Nd_2O_3 - WO_3
(Rode and Karpov, 1966)

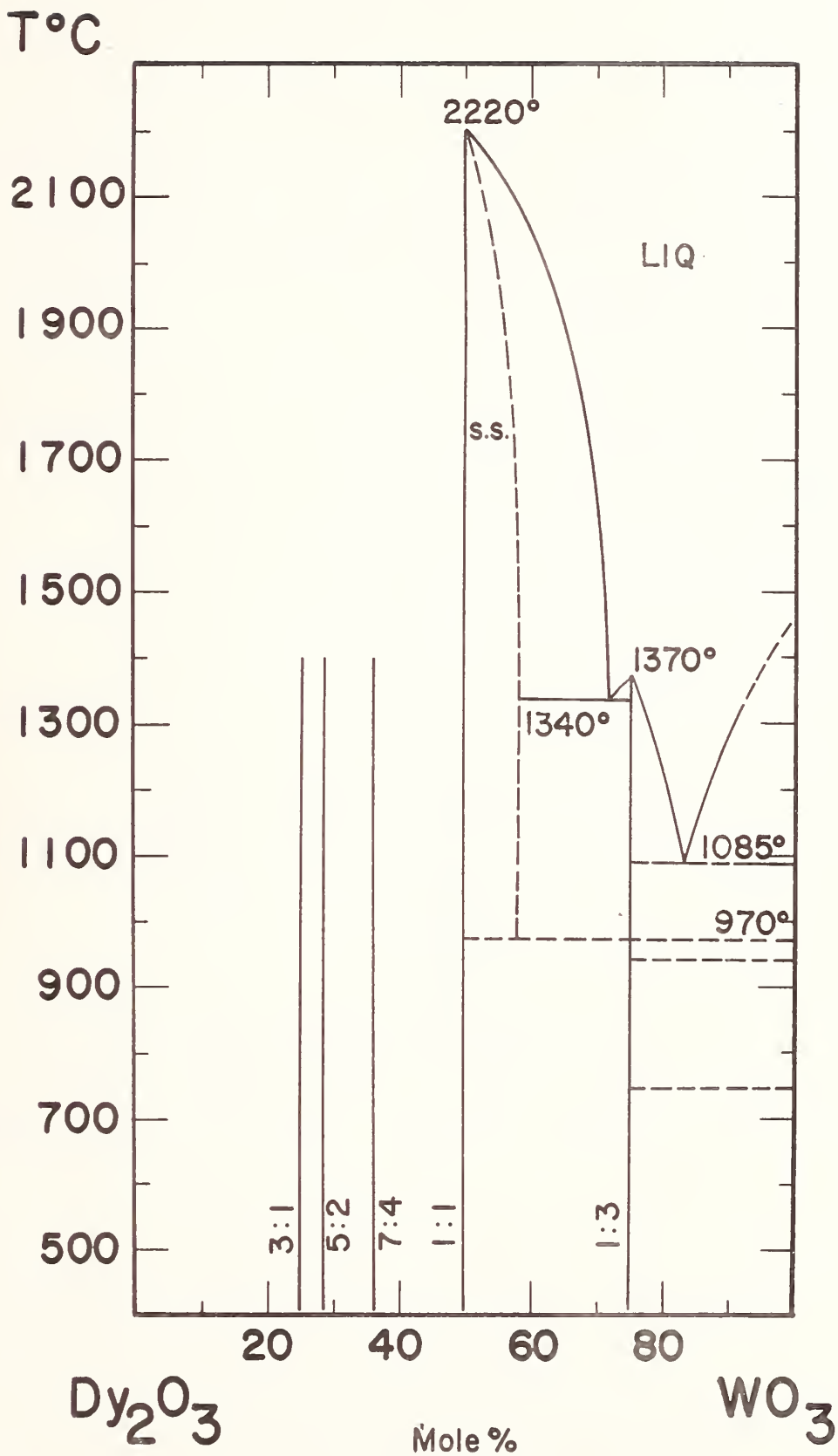


FIGURE 15. Phase relations in the system Dy_2O_3 - WO_3
(Ivanova and Reznik, 1972)

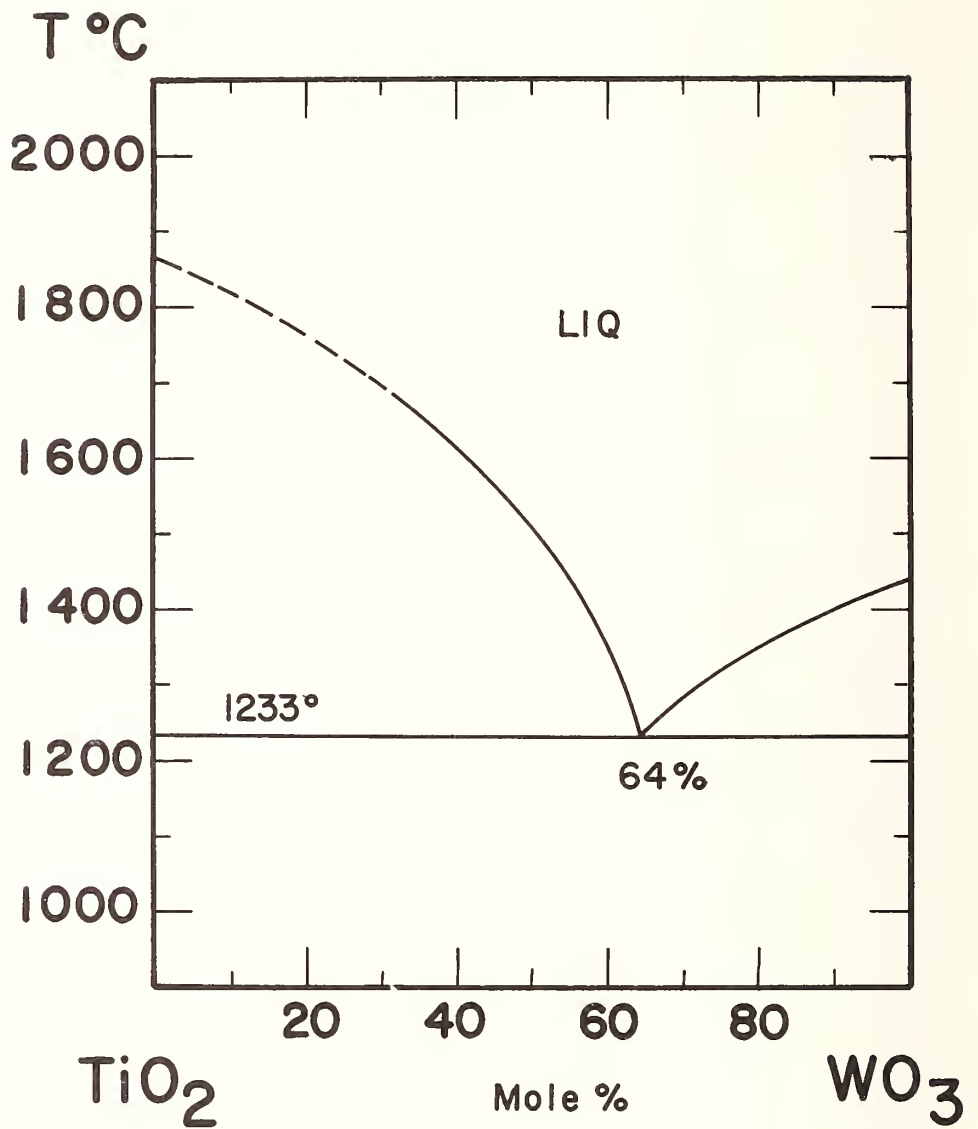


FIGURE 16. Phase relations in the system TiO_2 - WO_3
(Chang et al., 1967a)

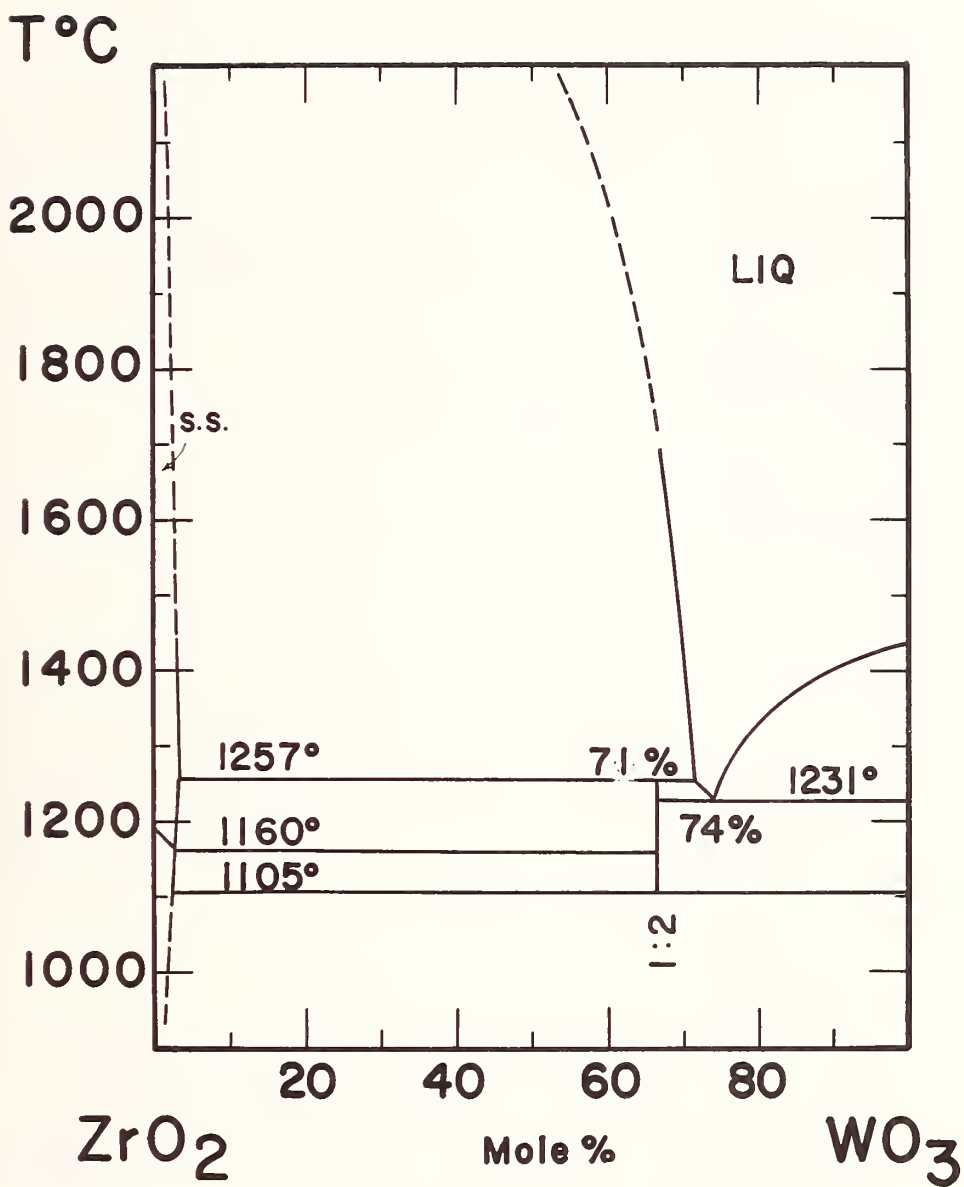


FIGURE 17. Phase relations in the system ZrO₂-WO₃
(Chang et al., 1967b)

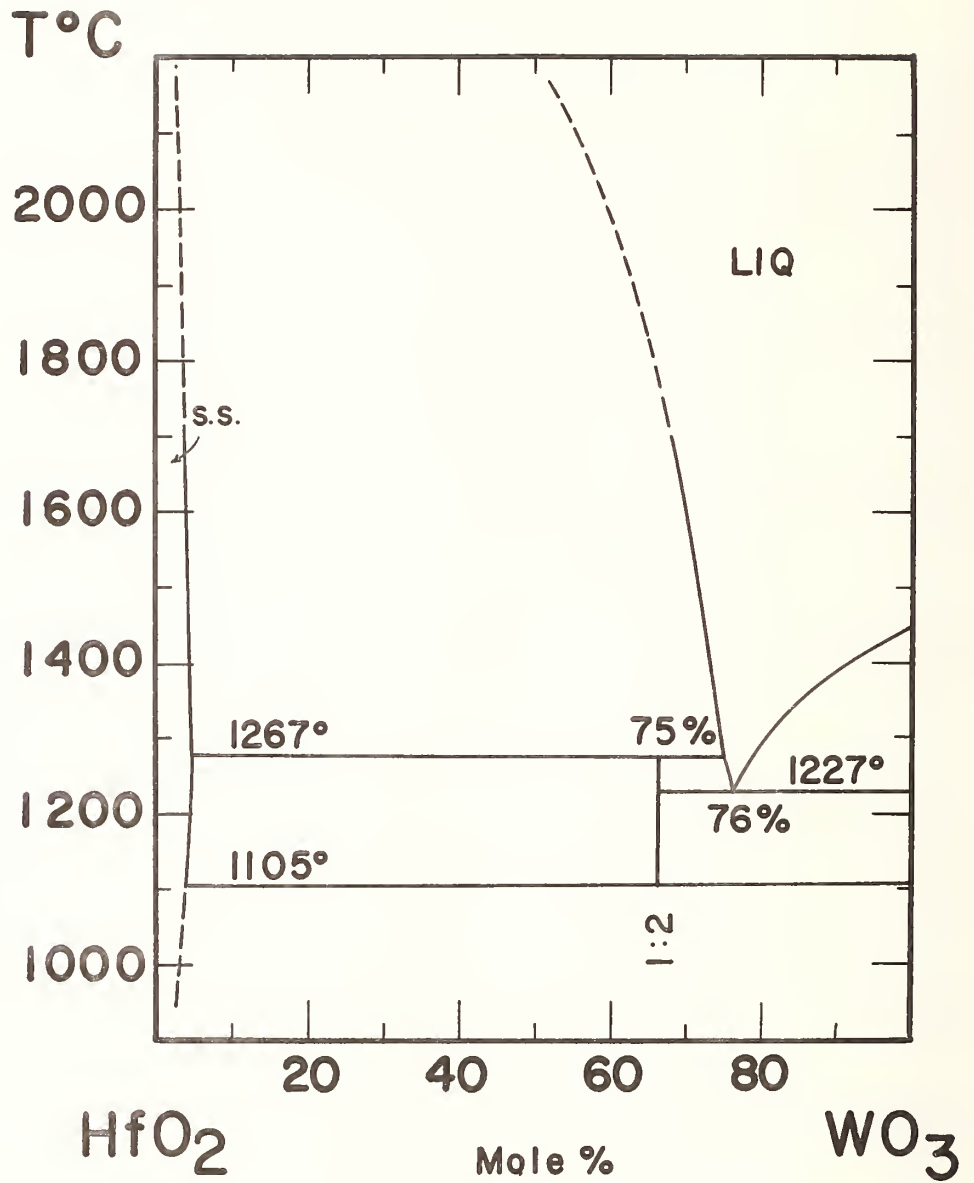


FIGURE 18. Phase relations in the system HfO₂-WO₃
(Chang et al., 1967b)

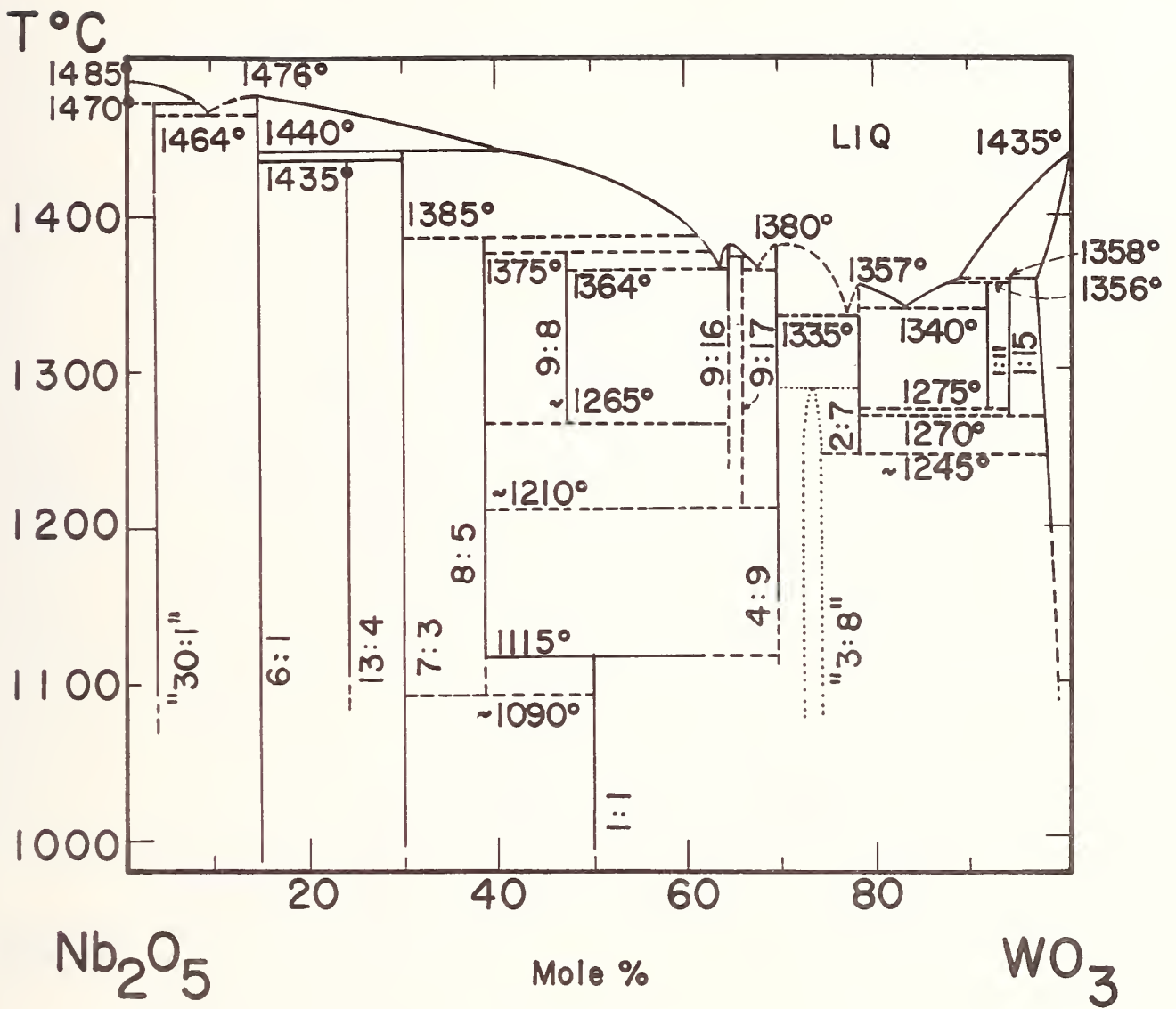


FIGURE 19. Phase relations in the system Nb_2O_5 - WO_3
 (Roth and Waring, 1966; Levin et al., 1969)

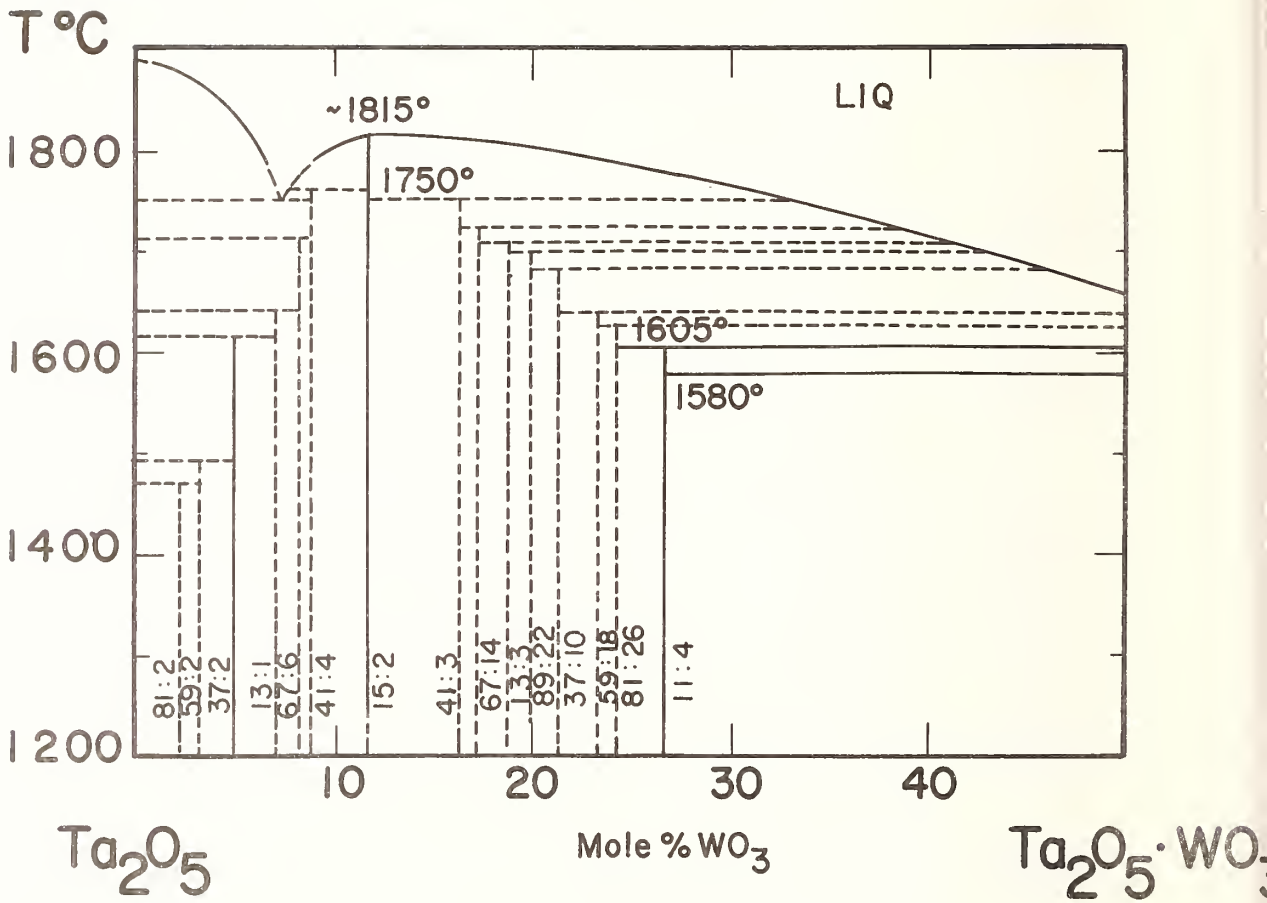


FIGURE 20. Phase relations in the system Ta_2O_5 - WO_3
(Roth et al., 1970)

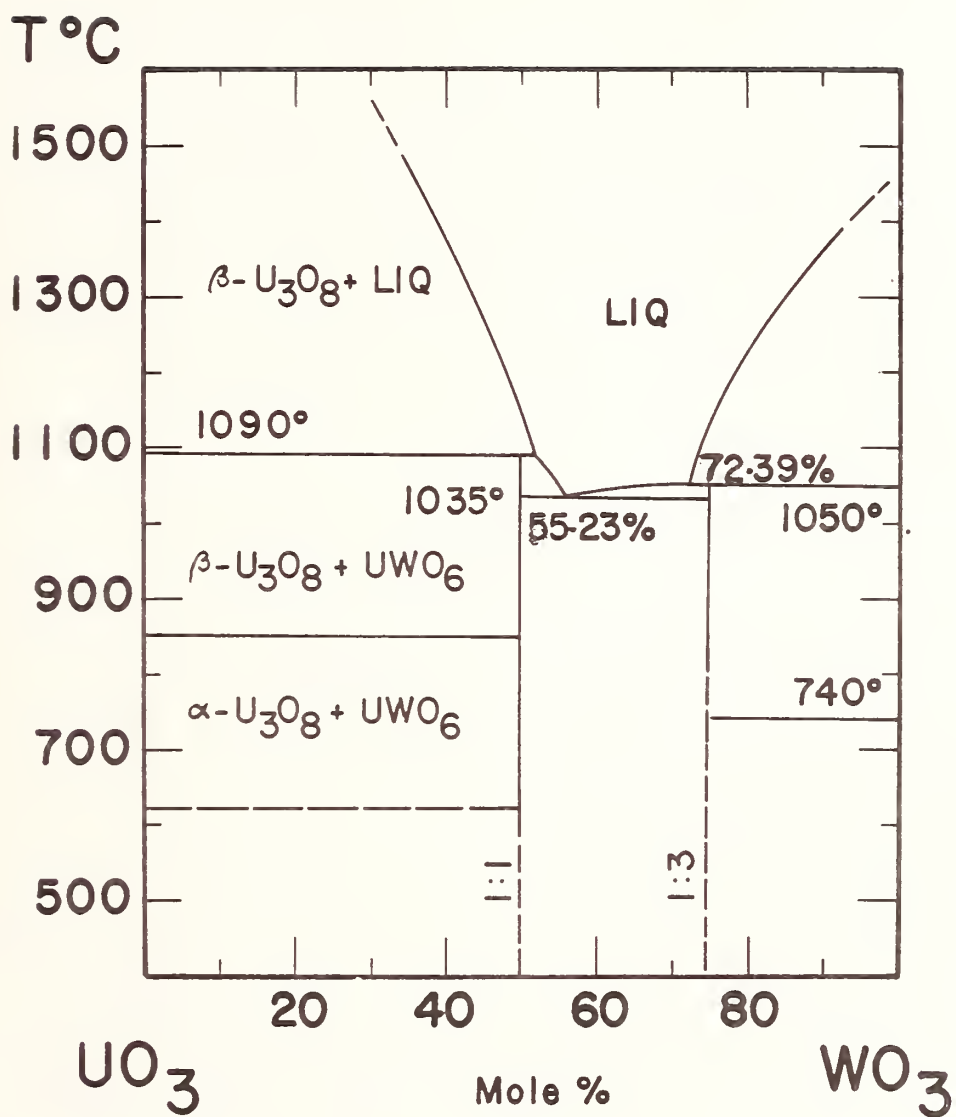


FIGURE 21. Phase relations in the system UO_3 - WO_3
(Hauck, 1974)

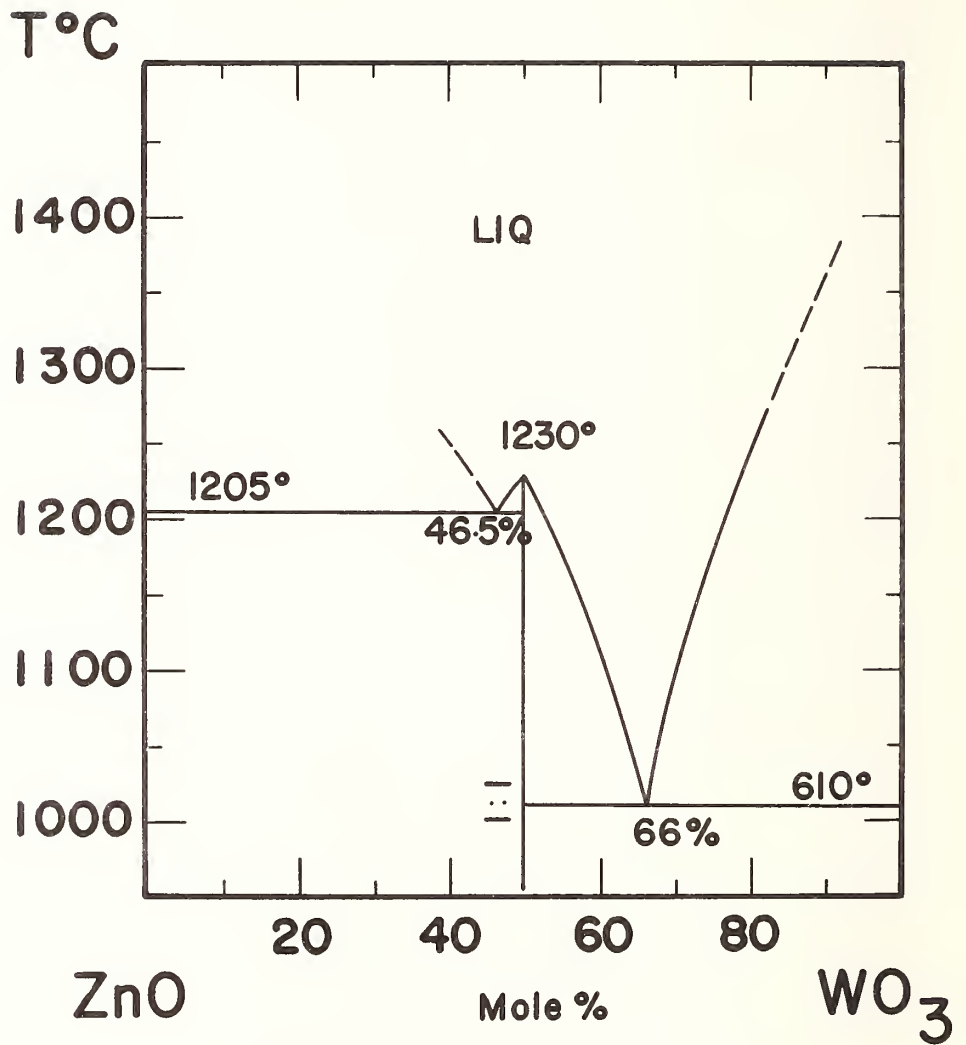


FIGURE 22. Phase relations in the system ZnO-WO₃
(Kislyakov et al., 1973)

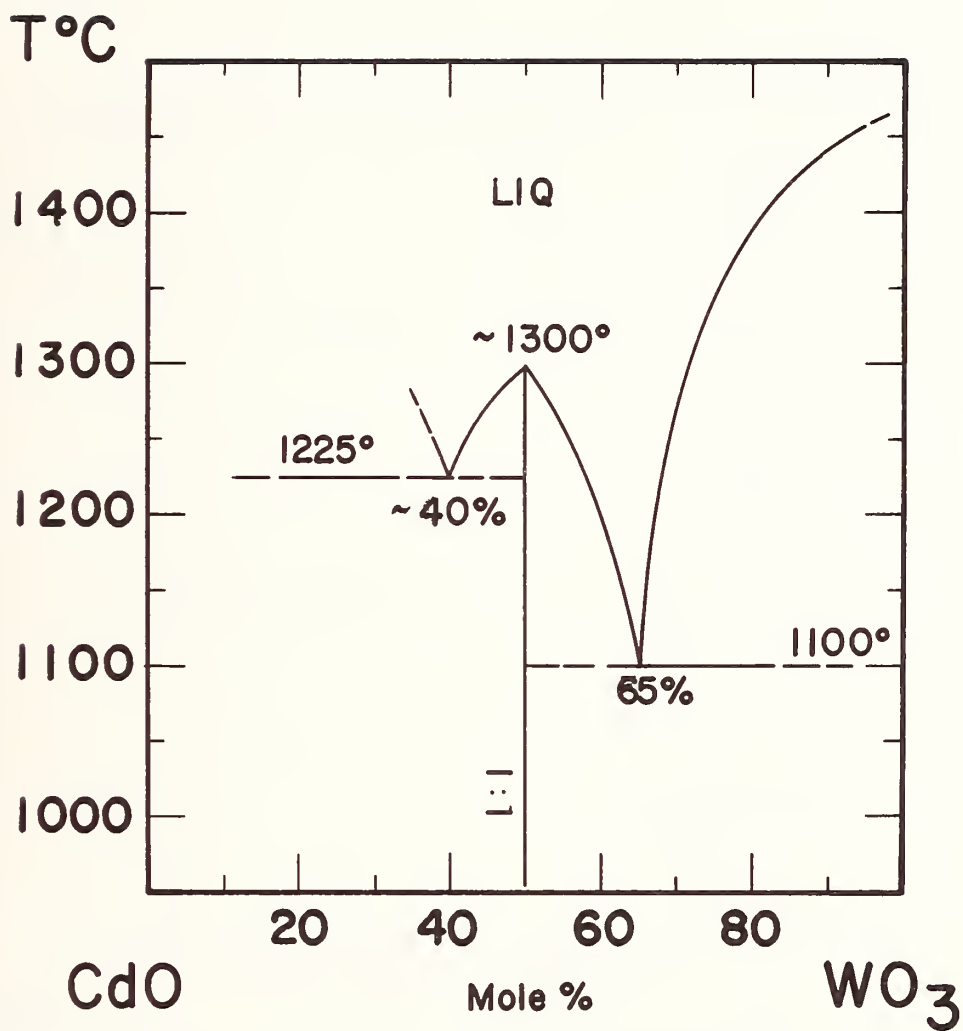


FIGURE 23. Phase relations in the system CdO-WO₃
(Kislyakov and Lopatin, 1967)

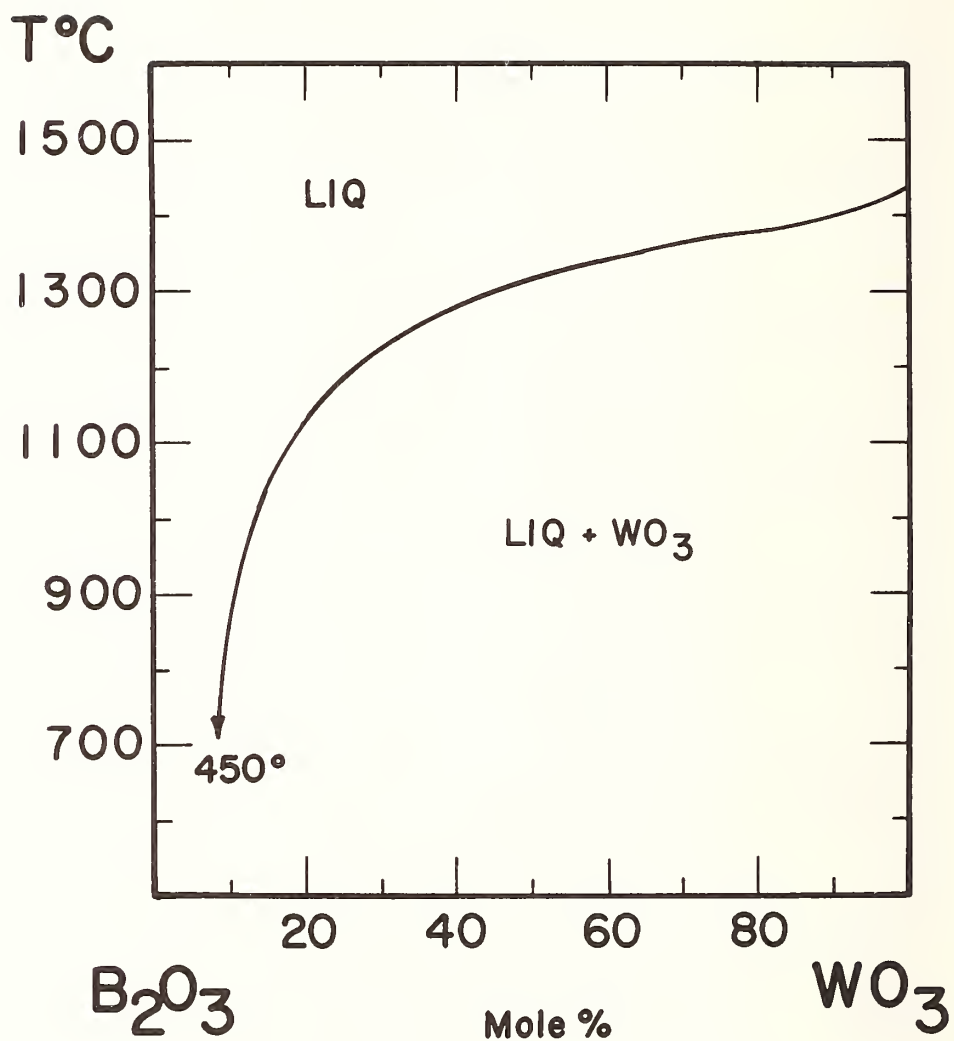


FIGURE 24. Phase relations in the system B₂O₃-WO₃
(Levin, 1965)

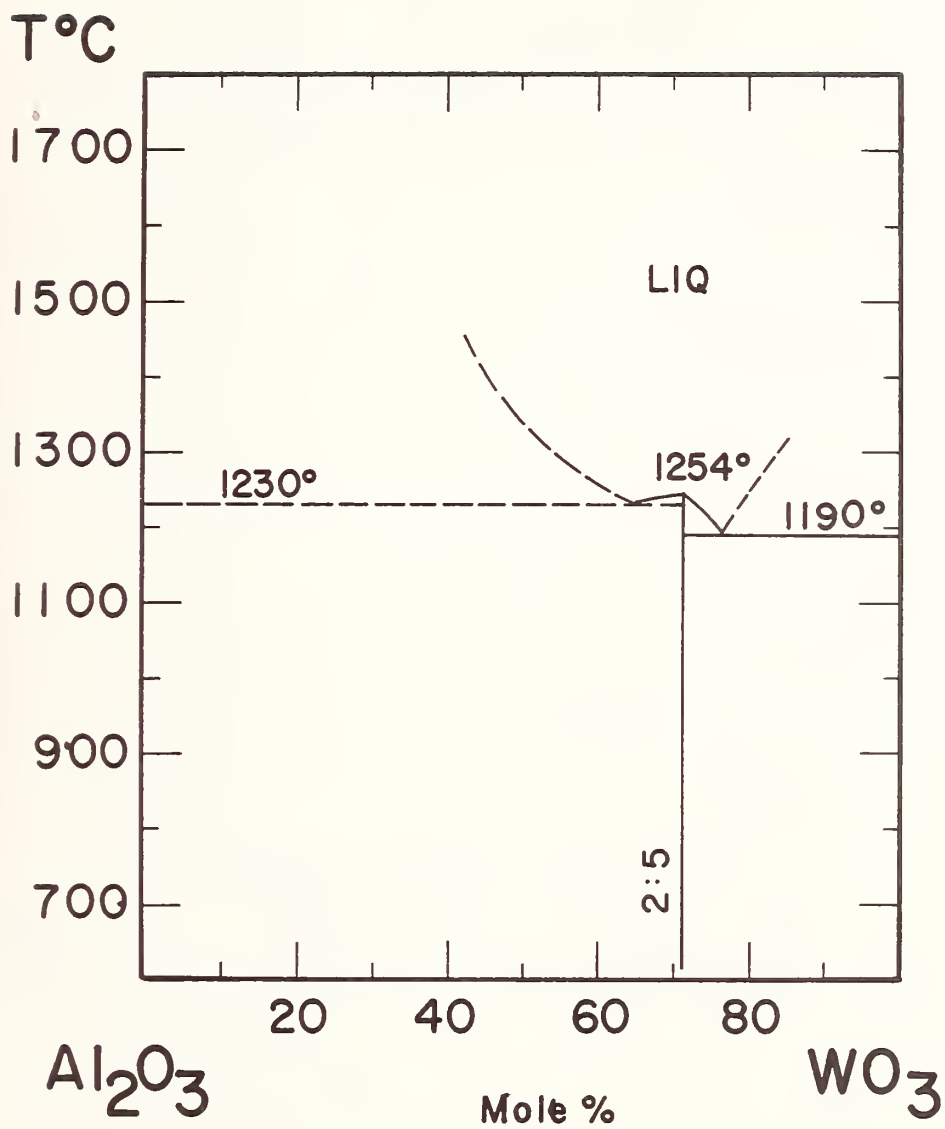


FIGURE 25. Phase relations in the system Al_2O_3 - WO_3
 (Waring, 1965; Levin et al., 1969)

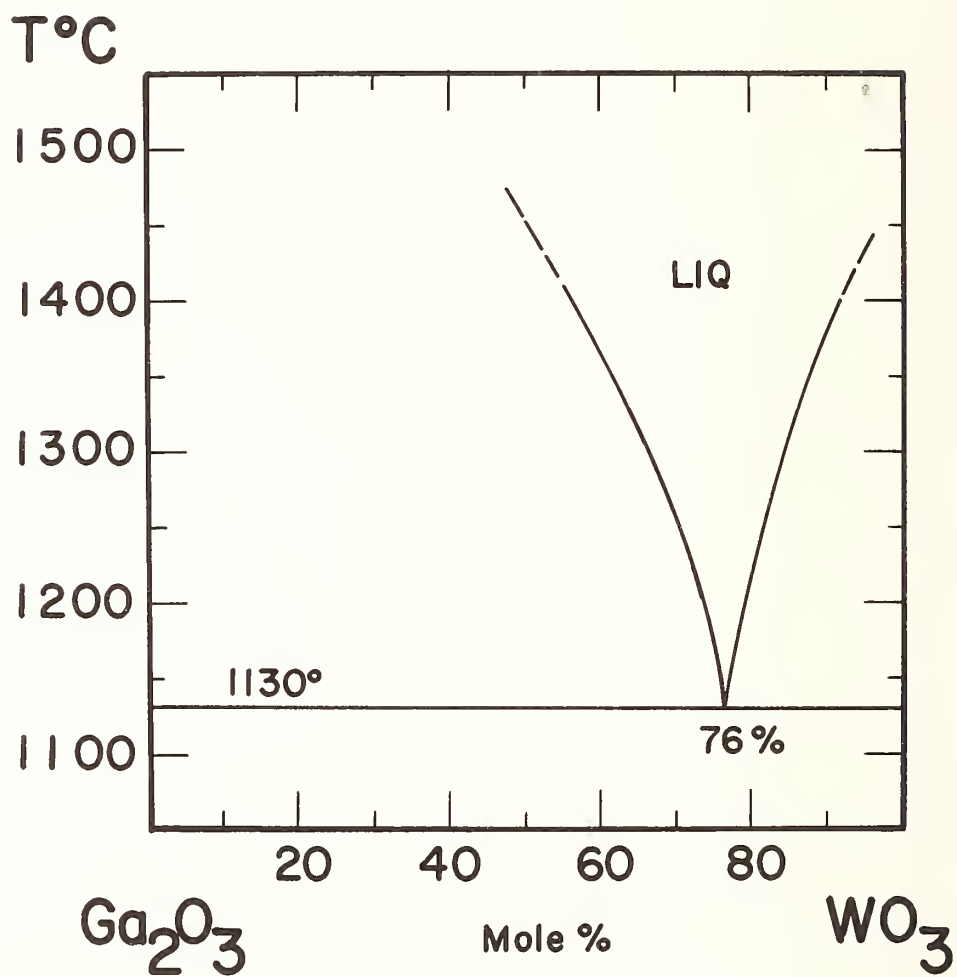


FIGURE 26. Phase relations in the system Ga₂O₃-WO₃
(Karpov and Korotkerich, 1973)

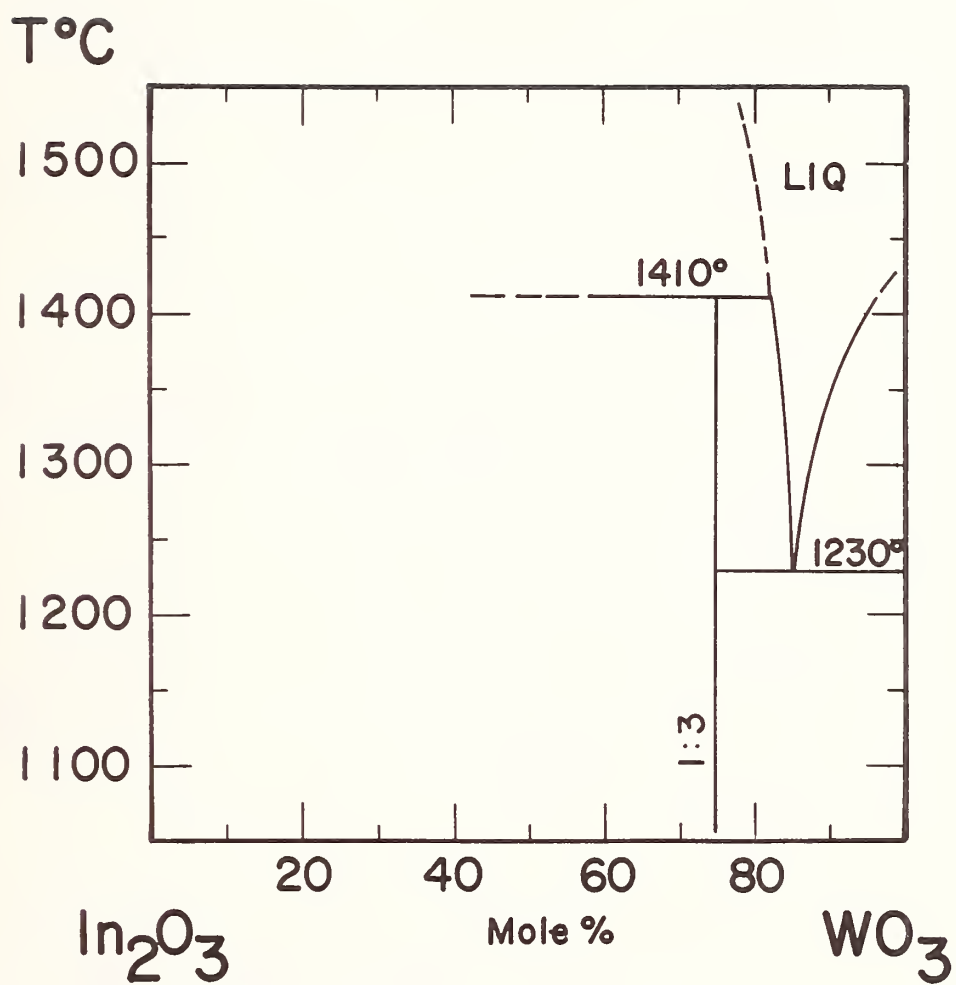


FIGURE 27. Phase relations in the system In_2O_3 - WO_3
 (Karpov and Korotkerich, 1973)

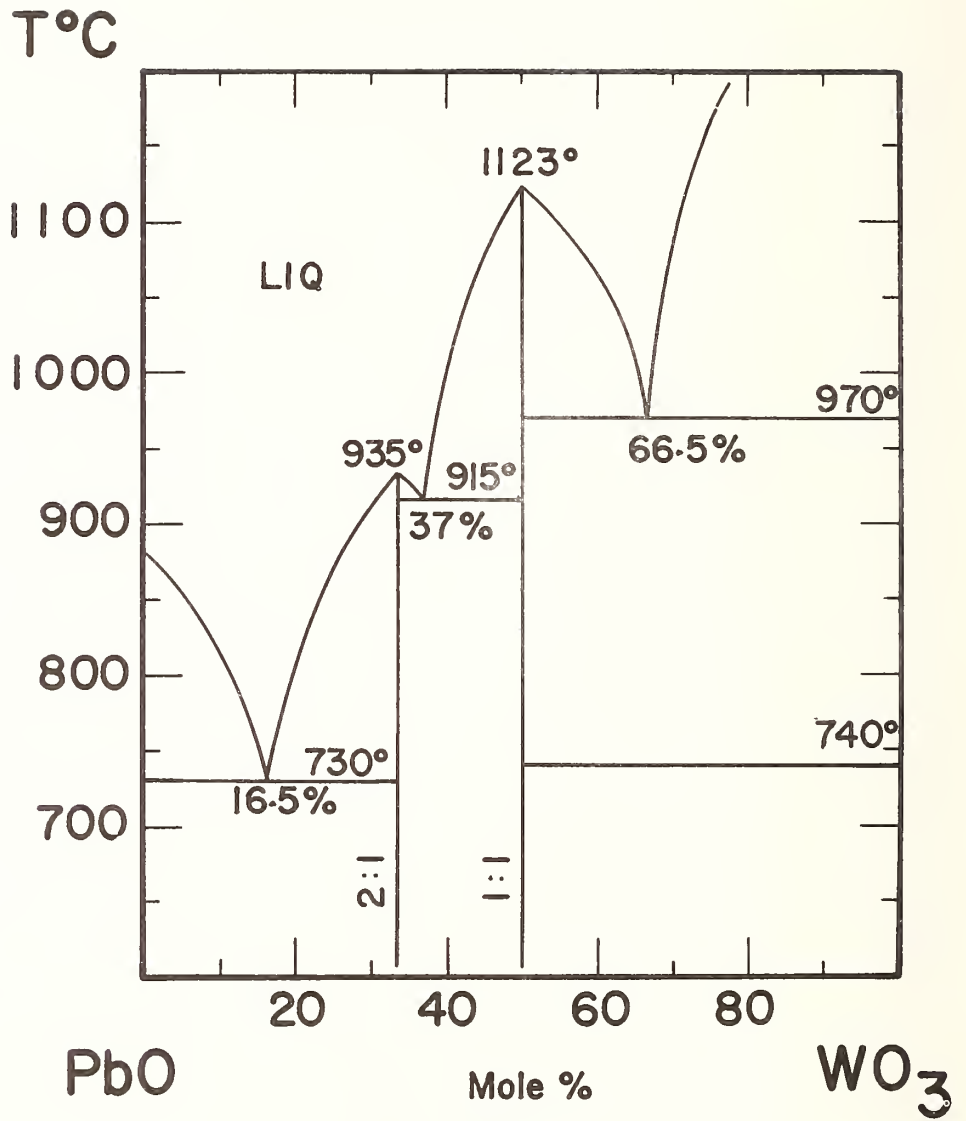


FIGURE 28. Phase relations in the system PbO-WO₃
(Chang, 1971)

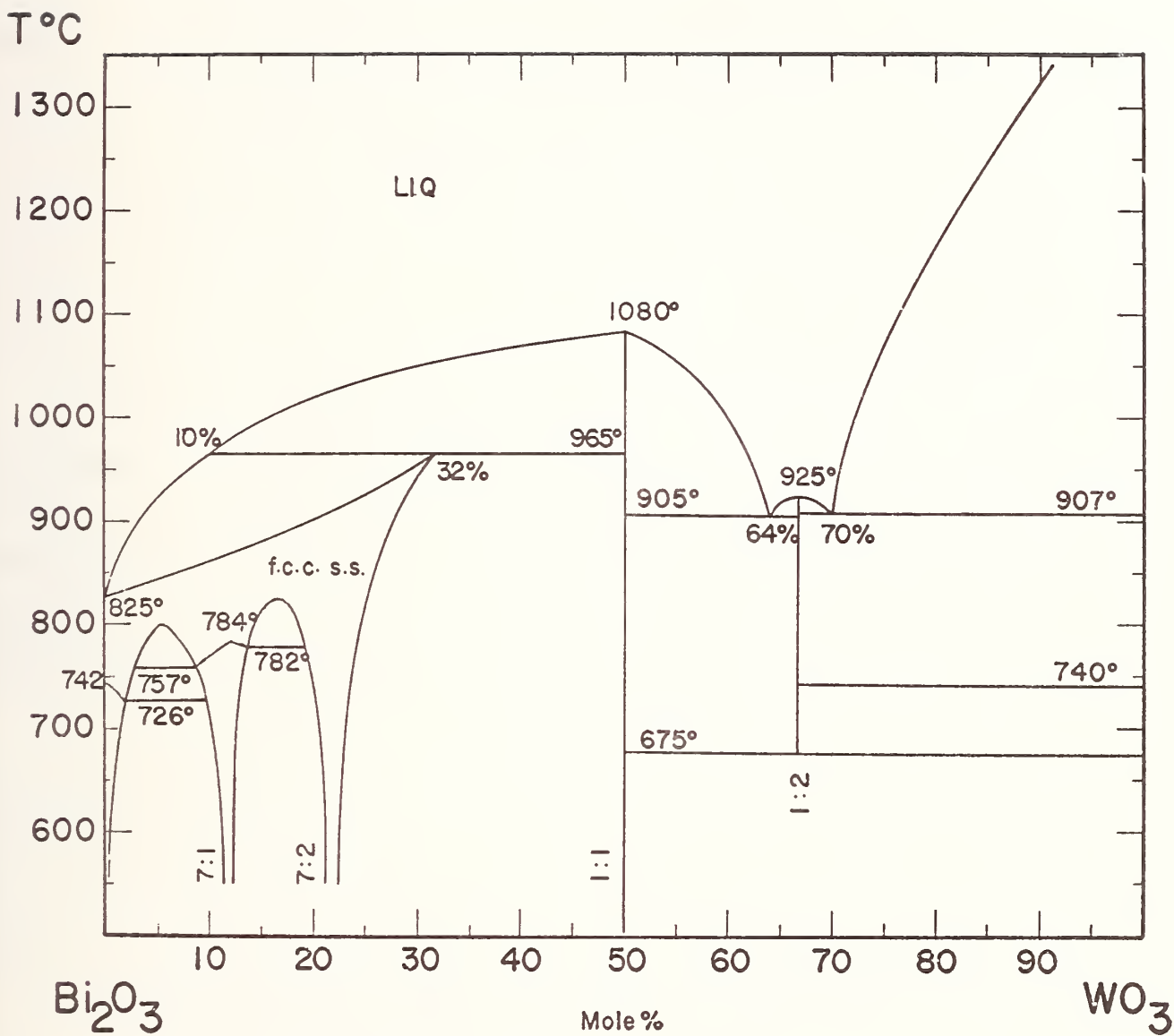


FIGURE 29. Phase relations in the system Bi_2O_3 - WO_3
(Hoda and Chang, 1974)



RIC IN PHASE WITH RARE-EARTH CONSTITUTIONAL DIAGRAMS

K. A. Gschneidner, Jr., M. E. Verkade and B. L. Evans

Rare-Earth Information Center (RIC)
Energy and Mineral Resources Research Institute
Iowa State University
Ames, Iowa 50011

Background

The Rare-Earth Information Center (RIC) was established at the Ames Laboratory by the U.S. Atomic Energy Commission's Division of Technical Information in 1966 and transferred to Iowa State University's Energy and Mineral Resources Research Institute (formerly Institute for Atomic Research) in 1968 with funding provided through grants from world-wide rare earth industries. The Center serves the scientific and technical community by collecting, storing, evaluating and disseminating rare earth information with particular emphasis on the physical metallurgy and solid state physics of the rare earth metals and their alloys.

Data Base

All available resources including books, journals, reports, conference proceedings, etc. are canvassed by the Center's technically trained staff of three (1 full time and 2 part time). Rapid and flexible retrieval of stored information is provided via a computerized system utilizing over 7400 keyword descriptors plus author indexing. Keyword descriptors are assigned following an examination of the original document rather than relying on only the title or abstract as do some indexing systems. Conversion of the information base from manually sorted punched cards to computer-read magnetic tape, begun in 1973, is about three-fourths completed and includes most of the approximately 14,000 journal articles held by the Center.

Publications

Utilizing this extensive information base, the Center engages in various publishing activities in addition to providing specialized literature searches on request. The RIC News, a quarterly newsletter containing items of current interest in science and technology of the rare earths, is distributed free

to over 3700 subscribers in the U. S. and abroad. State-of-the-art reviews, bibliographies and data compilations, prepared and published by RIC, have included a survey of rare earth metals in steel (IS-RIC-4), compilations of thermochemical data for rare earth compounds (IS-RIC-5 and IS-RIC-6), and a critical review of selected cerium binary phase diagrams (IS-RIC-7). These reports are currently available free from the Center or the sponsoring industry, Molycorp, Inc., which funded the study. Distribution of the reports is aided by publication announcements placed in appropriate scientific and trade journals, periodic notices in the RIC News and inclusion in abstracting journals.

Evaluation of Constitutional Diagrams

The staff of RIC has been involved over the past fifteen years with critical evaluation of phase equilibria, crystallographic and thermodynamic data on rare earth materials. The major effort has been primarily concerned with metallic systems. The evaluations on constitutional diagrams and crystal structures have been published as books, review articles or reports.

Rare Earth Alloys, K. A. Gschneidner, Jr., D. Van Nostrand Company, Inc., New York (1961) 449 + xiii pp.

"Rare Earth Intermetallic Compounds" by O. D. McMasters and K. A. Gschneidner, Jr., Nuclear Metallurgy 10, 93-158 (1964).

IS-RIC-7 "Selected Cerium Phase Diagrams" by K. A. Gschneidner, Jr. and M. E. Verkade (September 1974) 50 pp.

"Inorganic Compounds" by K. A. Gschneidner, Jr., and "Alloys and Intermetallic Compounds" by K. A. Gschneidner, Jr., Chapters 8 and 9 (pp. 152-251 and 252-323, respectively) of Scandium, Its Occurrence, Chemistry, Physics, Metallurgy, Biology and Technology, C. T. Horovitz, K. A. Gschneidner, Jr., G. A. Melson, D. H. Youngblood and H. H. Schock, Academic Press, New York (1975).

The RIC report on "Selected Cerium Phase Diagrams" (IS-RIC-7) contains several new innovations in addition to the standard features found in most phase diagram compilations. The new innovations are: 1. Text (discussion), phase diagram figures and crystallographic data are presented on two facing pages, and generally so are the references. Thus the reader does not need to turn pages back and forth to compare the figure while reading the text or examining the crystallographic data. If more than two pages are required the references are placed on the third page. 2. The phase

diagrams are presented twice, once in wt. % vs. temperature ($^{\circ}\text{C}$) and once in at. % vs. temperature ($^{\circ}\text{C}$). This way if the user is accustomed to phase diagrams in wt. % he (she) will find the left-hand figure more useful, but if one is more familiar with at. % the right-hand figure will be more useful.

The standard features include: 1. critical evaluation of published results, 2. composite diagram of several results (if there is more than one source of reliable information), and 3. a $^{\circ}\text{F}$ temperature scale in addition to the normal $^{\circ}\text{C}$ temperature scale.

Thermodynamic Evaluations

In addition to the above efforts the staff has also been involved in evaluating and estimating thermodynamic data for rare earth materials which are of special interest to the preparation and utilization of common metals, such as steel, ductile iron, superalloys, etc. These data compilations include:

IS-RIC-5 "Thermochemistry of the Rare Earth Carbides, Nitrides and Sulfides for Steelmaking" by Karl A. Gschneidner, Jr. and Nancy Kippenhan (August 1971) 27 pp.

IS-RIC-6 "Thermochemistry of the Rare Earths. Part 1. Rare Earth Oxides, Part 2. Rare Earth Oxysulfides, Part 3. Rare Earth Compound with B, Sn, Pb, P, As, Sb, Bi, Cu, and Ag" by Karl A. Gschneidner, Jr., Nancy Kippenhan and O. Dale McMasters, (August 1973) 67 pp.

"Thermodynamic Stability and Physical Properties of Metallic Sulfides and Oxysulfides", by Karl A. Gschneidner, Jr., pp. 159-77 in SULFIDE INCLUSIONS IN STEEL, J. J. DeBarbadillo and E. Snape, eds., American Society for Metals, Metals Park, Ohio (1975).



Evaluations of Phase Diagrams and
Thermodynamic Properties of
Ternary Copper Alloy Systems

by

Y. Austin Chang
Joachim P. Neumann
U. V. Choudary

Materials Department
College of Engineering and Applied Science
University of Wisconsin-Milwaukee
Milwaukee, Wisconsin 53201

A status report on the compilation and evaluation of phase diagrams and thermodynamic properties of ternary copper alloy systems, sponsored by INCRA, is presented. As of November 1976, 90 ternary systems have been completed. These systems contain a total of 182 diagrams, 16 general references and 421 specific references. The format of presentation is briefly discussed and the actual evaluation is demonstrated by giving two systems as typical examples, Cu-Ag-Zn and Cu-Ca-Mg.

1. Introduction

Phase diagram and thermodynamic data for copper alloy systems are of considerable fundamental and practical interest in many aspects of extractive, chemical, and physical metallurgy. These data have been reported for binary copper alloy systems in a critical evaluation by Hultgren and Desai [Gen. Ref. 8], which forms one of the monographs in the series, "The Metallurgy of Copper," sponsored by the International Copper Research Association (INCRA). Since commercial alloys usually consist of more than two components, it is imperative to extend the work of Hultgren and Desai to higher order copper alloy systems. At the suggestion of Dr. L. McDonald Schetky of INCRA, a project to compile and evaluate phase diagrams and thermodynamic properties of ternary copper alloy systems was initiated in 1972 at the University of Wisconsin-Milwaukee. A total of 39 elements in addition to copper was considered for evaluation. These 39 elements are Ag, Al, Au, B, Be, Bi, C, Ca, Cd, Ce, Co, Cr, Fe, Ga, Ge, Hg, In, Mg, Mn, Mo, Nb, Ni, O, P, Pb, Pd, Pt, Re, S, Sb, Se, Si, Sn, Ta, Te, Ti, V, W, and Zn. The non-metallic elements C, O, P and S are included because of the technological importance of systems containing these elements. A simple calculation shows that the combinations of all 39 elements yield a total of 741 ternary copper alloy systems. A literature search, mainly based on Chemical Abstracts through June 1973, indicated that data were available for approximately 300 ternary copper alloy systems. In view of this rather large number of systems and because some of these systems are of less technological interest, the total number of systems for inclusion in this project was reduced to about 180. As of November, 1976, 90 systems have been completed. These 90 systems are given in Table I. They contain a total of 182 diagrams (liquidus projections, isothermal sections, isopleths and thermodynamic properties), 16 general references and 421 specific references.

The results of the evaluations for the 20 ternary Cu-Ag systems will be published in the Journal of Physical and Chemical Reference Data. In the paper presented here, the format of presentation is briefly discussed and the actual evaluation is demonstrated by giving two systems, Cu-Ag-Zn and Cu-Ca-Mg, as typical examples.

2. Format of Presentation

The phase diagram and thermodynamic data have been evaluated for self-consistency, consistency with binary data, and consistency with known phase and thermodynamic relationships. Whenever conflicting data are reported by different groups of investigators, judgment has been made on the basis of the experimental methods used and the detailed experimental information reported by the investigators. The discussion of each system is divided into six sections: Phases and Structures, Phase Diagrams, Thermodynamic Properties, References, Tables, Figures.

2.1 Phases and Structures

Adopting the format of the Metals Handbook [Gen. Ref. 1], the following information is given for each of the binary and ternary intermediate phases: Designation, Composition, Symmetry, Symbol, and Prototype. The designations of Hansen and Anderko, Elliott, and Shunk [Gen. Refs. 3, 4, 5] are used whenever possible. If their designations cannot be used, they are given in parentheses next to the chemical formula in the composition column. For ternary intermediate phases, the designations T_1 , T_2 , T_3 ... are used. For the abbreviations of crystal symmetry, refer to pp. 243-250 of the Metals Handbook [Gen. Ref. 1]. For the structure symbols (Strukturbericht), refer to Pearson [Gen. Ref. 2]. A prototype phase is given whenever available.

2.2 Phase Diagrams

Following the notation of Rhines [Gen. Ref. 9], the three invariant four-phase equilibria are classified as types I, II, and III. If more than one four-phase equilibrium of the same type occurs, the equilibria are distinguished by

adding subscripts to the Roman numerals in order of descending temperature, I_1 , I_2 , I_3 , etc. The chemical composition is given in wt.% and the temperatures are given in degrees Celsius. Solid lines are used for known phase boundaries, dashed lines for estimated phase boundaries, and dash-dotted lines for magnetic transformations.

In the liquidus projection, the binary eutectics, peritectics and monotectics are designated by e_1 , e_2 , e_3 , ..., p_1 , p_2 , p_3 , ..., and m_1 , m_2 , m_3 , ..., respectively. The traces of the liquidus valleys, i.e., the univariant equilibria, are plotted, and the directions of their slopes toward lower temperature are indicated by arrows inscribed upon the lines. The primary phases of crystallization are given on either side of the traces of these valleys. The types of the four-phase equilibria at the intersections of the traces of the liquidus valleys are indicated by the Roman numerals I, II or III with the subscripts 1, 2, 3, etc. The melting points of congruently melting binary and ternary phases are marked with solid circles and the corresponding temperatures are given. For ternary saddle points (singular points), open circles are used.

In the isothermal sections, only the single- and two-phase regions are labelled using the designations for the phases given in the section on Phases and Structures. For the terminal solid solutions, the chemical symbol of the base element in parentheses is used. Liquid phases are designated by the letter L, with the subscripts 1, 2, etc., distinguishing different liquid phases.

In the case of isopleths, all single-, two- and three-phase regions are labelled.

2.3 Thermodynamic Properties

The Kelvin temperature scale is used to represent the temperature instead of the Celsius scale, and atom or mole fractions are used instead of weight percent. Thermodynamic activity data are generally presented in the form of iso-activity or iso-activity coefficient curves, using the Gibbs triangle.

Very often the thermodynamic properties of a particular component are known in infinitely dilute solutions. For such cases, the excess partial molar Gibbs energy is expressed in terms of the formalism suggested by Wagner [Gen. Ref. 12]:

$$\ln \gamma_i = \ln \gamma_i^0 + \epsilon_i^i x_i + \epsilon_i^j x_j \quad (1)$$

where γ_i is the activity coefficient of the solute i in a ternary dilute solution consisting of the solvent s and the solutes i and j ; γ_i^0 is the limiting activity coefficient of i in the binary system i - s ; and the terms x_i and x_j are atom fractions of the solutes i and j . The terms ϵ_i^i and ϵ_i^j are the Gibbs energy self-interaction and the Gibbs energy interaction parameters.

2.4 References

The literature references which are pertinent to each particular system are given after the discussion. A number of frequently occurring references are cited as "General References"; they are listed in section 3.

2.5 Tables

Generally, the types and temperatures of the known invariant equilibria, as well as the compositions of the coexisting phases, are given in a table.

2.6 Figures

If the information is available, figures of the phase diagrams are generally presented in the following order: liquidus projection - isothermal sections - isopleths, including quasi-binaries. Graphical representations of the thermodynamic properties are given last.

3. General References

1. Metals Handbook, 8th Ed., Vol. 8, "Metallography, Structures and Phase Diagrams," American Society for Metals, Metals Park, Ohio, 1973.
2. Pearson, W. B., A Handbook of Lattice Spacings and Structures of Metals and Alloys, Vols. 1 and 2, Pergamon Press, London, 1958 and 1967.
3. Hansen, M., and Anderko, K., Constitution of Binary Alloys, 2nd Edition, McGraw-Hill, New York, 1958.
4. Elliott, R. P., Constitution of Binary Alloys, First Supplement, McGraw-Hill, New York, 1965.
5. Shunk, F. A., Constitution of Binary Alloys, Second Supplement, McGraw-Hill, New York, 1969.
6. Hultgren, R., Desai, P. D., Hawkins, D. T., Gleiser, M., and Kelley, K. K., Selected Values of the Thermodynamic Properties of Binary Alloys, American Society for Metals, Metals Park, Ohio, 1973.
7. Hultgren, R., Desai, P. D., Hawkins, D. T., Gleiser, M., Kelley, K. K., and Wagman, D. D., Selected Values of the Thermodynamic Properties of the Elements, American Society for Metals, Metals Park, Ohio, 1973.
8. Hultgren, R., and Desai, P. D., INCRA Monograph I, Selected Thermodynamic Values and Phase Diagrams for Copper and Some of Its Binary Alloys, The International Copper Research Association, Inc., New York, 1971.
9. Rhines, F., Phase Diagrams in Metallurgy, Their Development and Application, McGraw-Hill, New York, 1956.
10. Prince, A., Alloy Phase Equilibria, Elsevier, Amsterdam-London-New York, 1966.
11. Wagner, S., and Rigney, D. A., Metall. Trans., 1974, 5, 2155.
12. Wagner, C., Thermodynamics of Alloys (Translated by Mellgren, S., and Westbrook, J. H.), Addison-Wesley, Reading, Mass., 1952.

13. Lupis, C.H.P., and Elliott, J. F., Trans. Met. Soc. AIME, 1965, 233, 829; 1200.
14. JANAF Thermochemical Tables, 2nd Ed., NSRDS-NBS 37, U.S. Department of Commerce, National Bureau of Standards, Washington, D. C., 1971.
15. King, E. G., Mah, A. D., and Pankratz, L. B., INCRA Monograph II, Thermodynamic Properties of Copper and Its Inorganic Compounds, The International Copper Research Association, Inc., New York, 1973.
16. Diaz, C., INCRA Monograph III, The Thermodynamic Properties of Copper-Slag Systems, The International Copper Research Association, Inc., New York, 1974.

4. Personnel

Personnel who have contributed to this work are Y. A. Chang (YAC), U. V. Choudary (UVC), D. Goldberg (DG), D. K. Gupta (DKG), H. Ipser (HI), and J. P. Neumann (JPN). The evaluation of each system was the primary responsibility of one of the team members, whose initials are placed on the last page of the evaluation, following the list of references.

Dr. D. Goldberg is now with Westinghouse, Plant Apparatus Division, Pittsburgh, Pennsylvania; Dr. D. K. Gupta is now with Howmet Corporation, Whitehall, Michigan; and Dr. H. Ipser is now with the Institut für Anorganische Chemie, Universität Wien, Austria.

5. Acknowledgments

Financial support for this project is being provided by INCRA. The authors wish to thank Dr. L. McDonald Schetky of INCRA for his interest in this work and his initiation of support for this project.

6. Examples of Evaluations

Two typical examples of the evaluations that are being carried out are given below, the Cu-Ag-Zn and the Cu-Ca-Mg systems.

Cu-Ag-Zn

Phases and Structures: The following intermediate phases appear in the Cu-Zn and Ag-Zn binary systems. No ternary phases have been found.

<u>Designation</u>	<u>Composition</u>	<u>Symmetry</u>	<u>Symbol</u>	<u>Prototype</u>
β_1	CuZn (HT) (β)	bcc	A2	W
β'	CuZn (LT)	ord bcc	B2	CsCl
γ_1	Cu_5Zn_8 (γ)	ord bcc	$D8_2$	γ -brass
δ	CuZn_3	ord bcc	B2	CsCl
ϵ_1	~ 83% Zn (ϵ)	hcp	A3	Mg
β_2	AgZn (HT) (β)	bcc	A2	W
ζ	AgZn (LT)	ord hex	-	-
γ_2	Ag_5Zn_8 (γ)	ord bcc	$D8_2$	γ -brass
ϵ_2	~ 70% Zn (ϵ)	hcp	A3	Mg

The crystal structures are from the Metals Handbook (Gen. Ref. 1).

Phase Diagrams: After early investigations by Ueno [1], Keinert [2], and Weigert [3], Gebhardt, Petzow, and Krauss [4] later on thoroughly re-examined the phase relations in the ternary system. The liquidus, the isotherms at 600°, 500°, and 350°C, and the isopleths at 20% Ag and 20% Zn by [4] are shown here. Gebhardt, et al. also gave isopleths at 40% Ag, 60% Ag, 40% Cu, and 60% Cu.

The liquidus diagram shows the liquidus valleys extending from the binary eutectic or peritectic points into the ternary field. Two continuous

valleys (from p_8 to p_2 and from p_4 to p_5) are formed, the other valleys meet on planes of four-phase equilibria. The invariant reaction temperatures and compositions of the co-existing phases are shown in Table I.

In the solid state, the isotherms show that continuous solid solutions, designated β , γ , and ϵ , connect the isostructural β_1 and β_2 , γ_1 and γ_2 and ϵ_1 and ϵ_2 binary phases, respectively. On the 350°C isotherm, the β and β' (ordered) regions were labelled incorrectly as β' and β , respectively, in the original paper [4]. No solid-state four-phase equilibria exist in this system.

The β' to β order-disorder transition temperature of $\text{Cu}_{.53-x}\text{Ag}_x\text{Zn}_{.47}$ alloys was investigated by Murakami, Nakanishi, and Kachi [5]. The transition temperature decreases with increasing Ag content from about 465°C at $\text{Cu}_{.53}\text{Zn}_{.47}$ to about 223°C at $\text{Ag}_{.53}\text{Zn}_{.47}$. The latter temperature is estimated from an extrapolation to 0% Cu.

Thermodynamic Data: The partial pressure of zinc over the terminal (Cu) and (Ag) solid solutions at 1000 K were measured by Argent and Lee [6]. For the terminal copper solid solution, the data yield the following values:

$$\gamma_{\text{Zn}(\ell)}^{\circ} = 0.051$$

$$\epsilon_{\text{Zn}}^{\text{Zn}} = + 6.5$$

$$\epsilon_{\text{Zn}}^{\text{Ag}} \approx 0.$$

The few data available in the terminal silver solid solution do not permit a reliable evaluation of the activity coefficients; the values given must be considered as estimates:

$$\gamma_{\text{Zn}(\ell)}^{\circ} = 0.27$$

$$\epsilon_{\text{Zn}}^{\text{Zn}} \approx 0$$

$$\epsilon_{\text{Zn}}^{\text{Cu}} \approx -3.5.$$

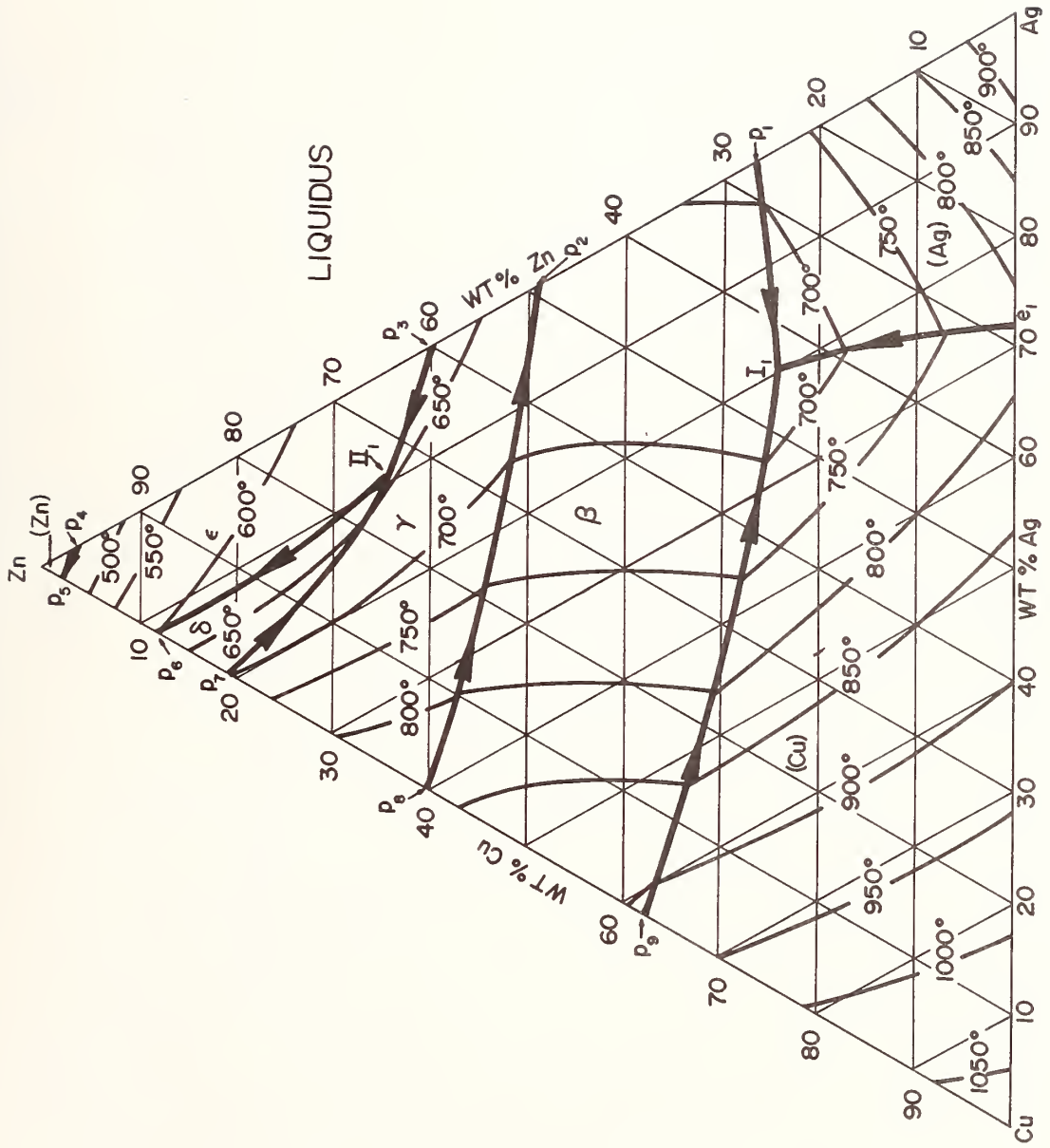
For the solid solution of zinc in copper, Hultgren (Gen. Ref. 6) reports a value of 0.014 for $\gamma_{\text{Zn(s)}}^{\circ}$ at 773 K, which corresponds to $\gamma_{\text{Zn(l)}}^{\circ} = 0.048$ at 1000 K. The data by [6] are in good agreement with this value. For the solid solution of zinc in silver, however, Hultgren (Gen. Ref. 6) reports a value of 0.199 for $\gamma_{\text{Zn(s)}}^{\circ}$ at 873 K, which corresponds to $\gamma_{\text{Zn(l)}}^{\circ} = 0.36$ at 1000 K. This value is quite different from the one obtained from the data by Argent and Lee. Values for the partial enthalpies and partial entropies of zinc are also given by [6]. An insufficient number of data was taken to calculate integral properties.

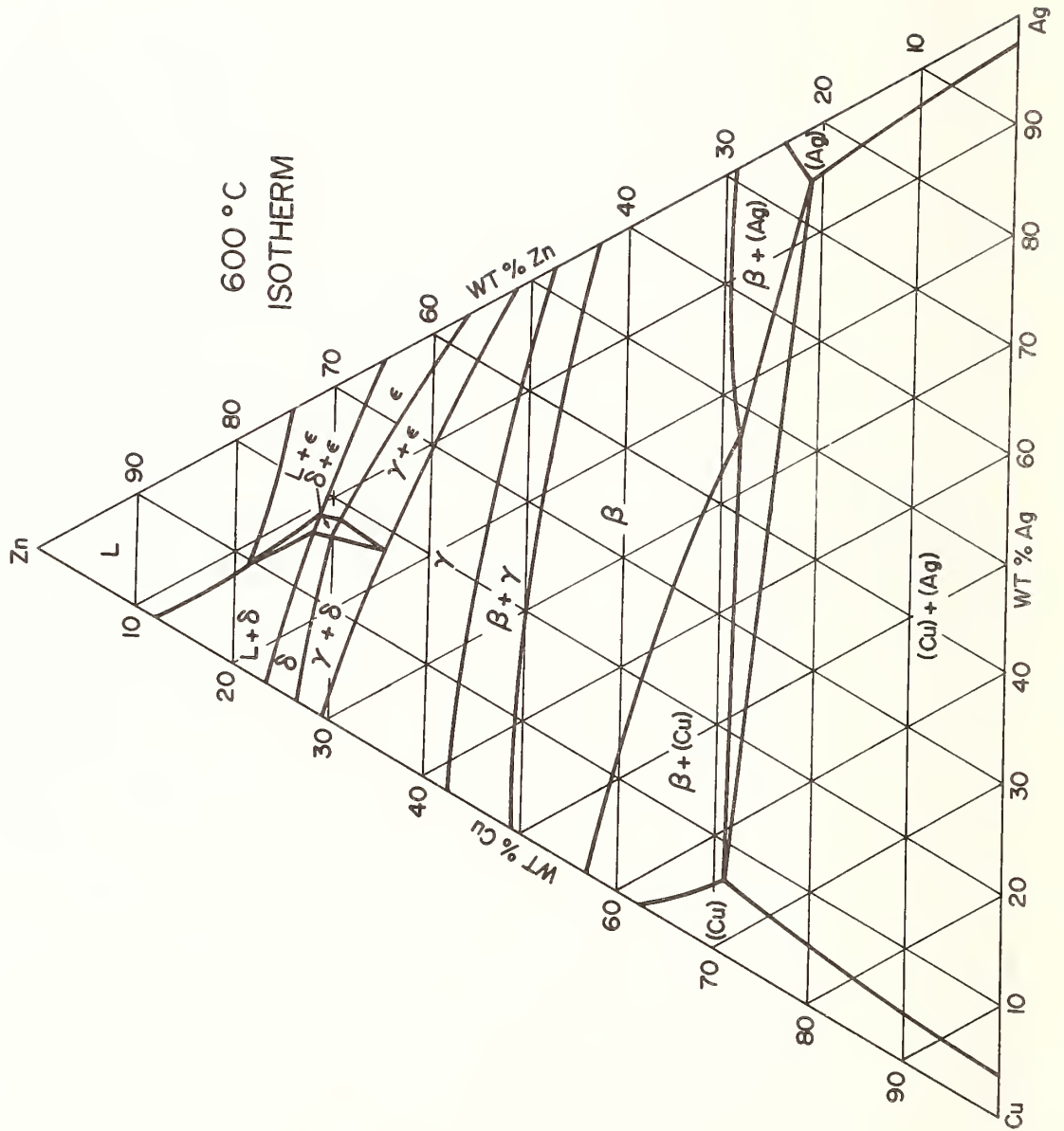
References:

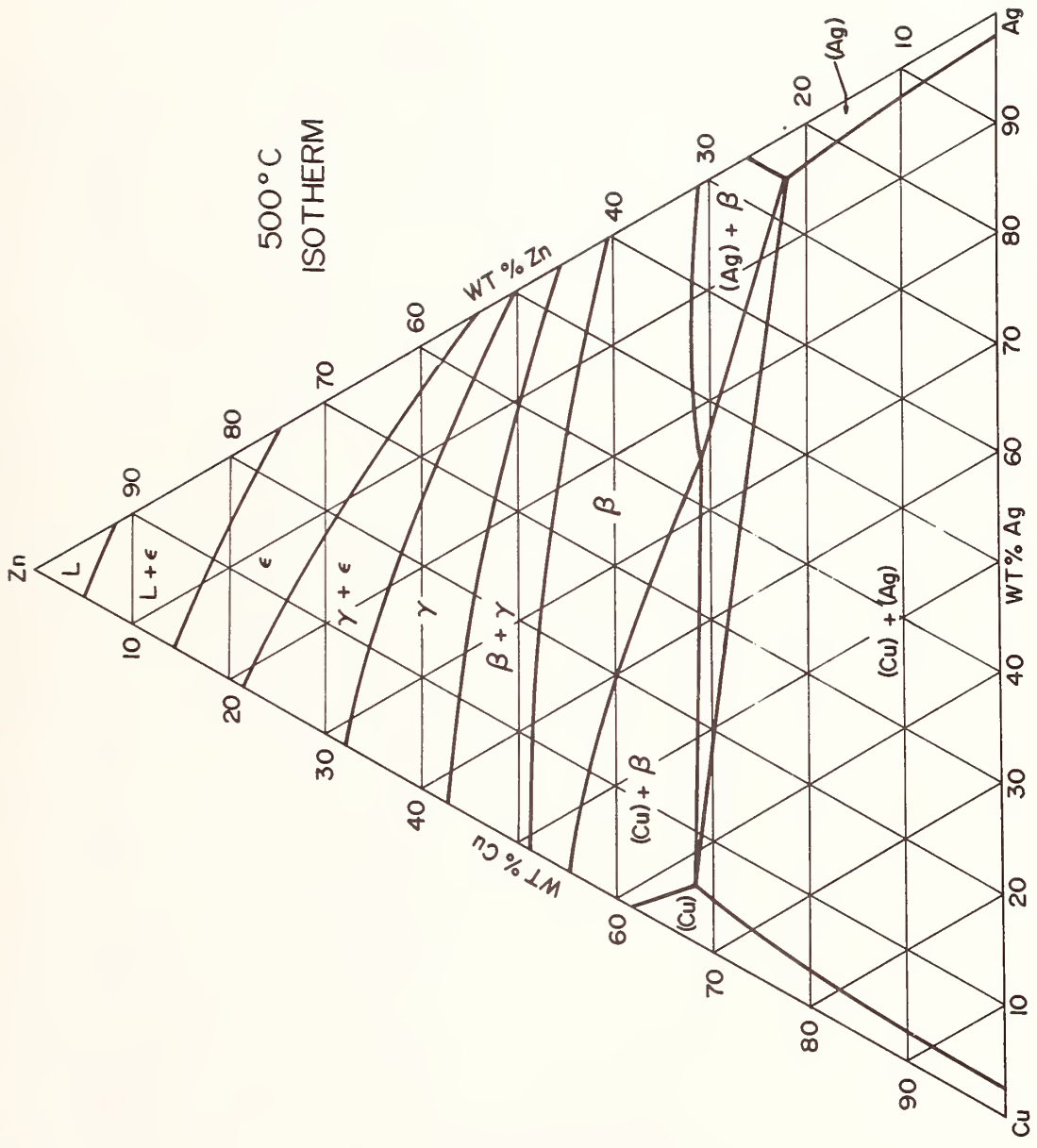
1. Ueno, S., Mem. Coll. Sci. Kyoto Imp. Univ., 1929, 12A, 347.
2. Keinert, M., Z. physik. Chem., 1932, A160, 15.
3. Weigert, K. M., Trans. AIME, 1954, 200, 233.
4. Gebhardt, E., Petzow, G., and Krauss, W., Z. Metallk., 1962, 53, 372.
5. Murakami, Y., Nakanishi, N., and Kachi, S., Acta Met., 1971, 19, 93.
6. Argent, B. B., and Lee, K. T., Trans. Faraday Soc., 1965, 61, 826.

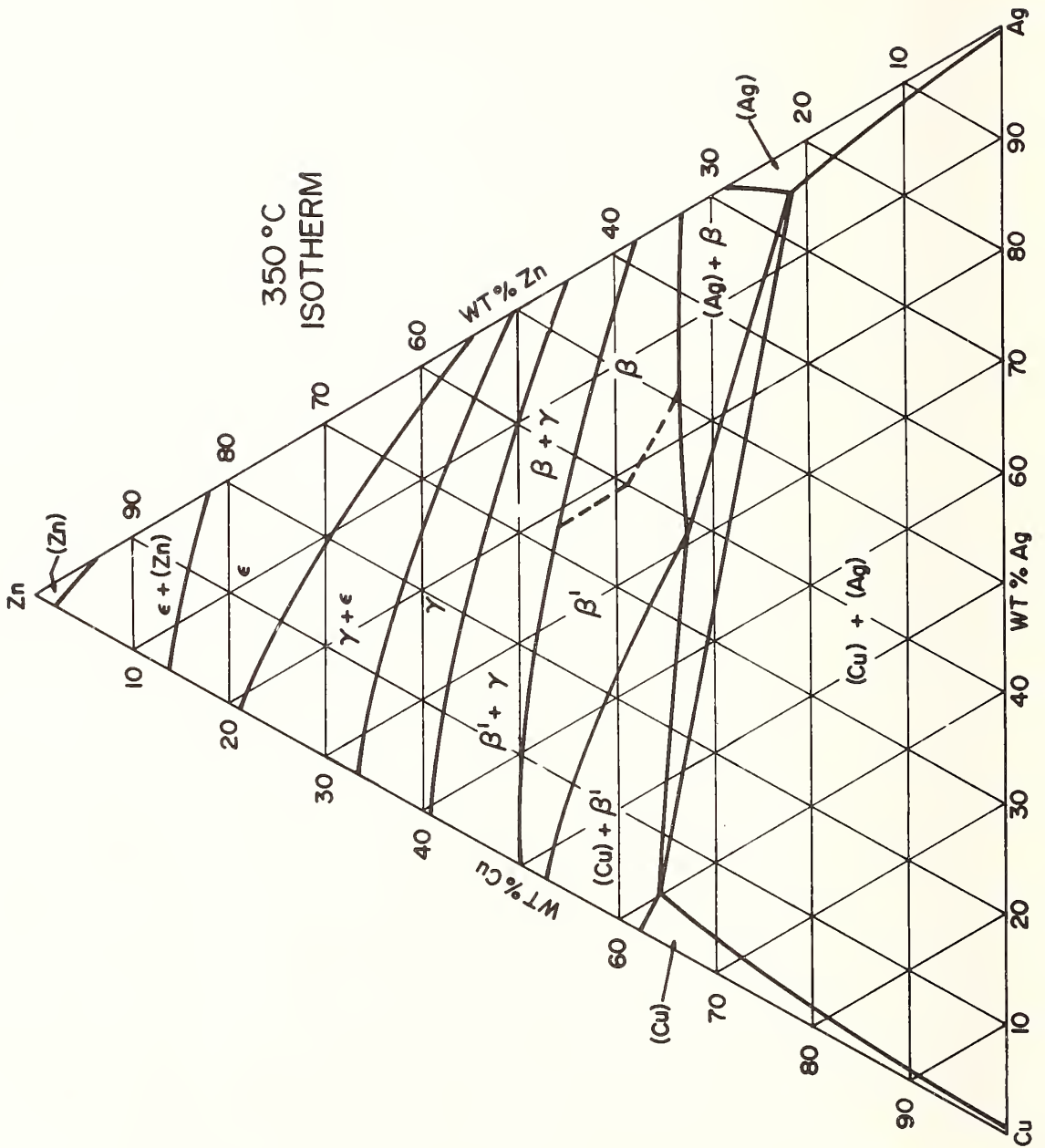
Table I. Four-phase Equilibria in the Cu-Ag-Zn System

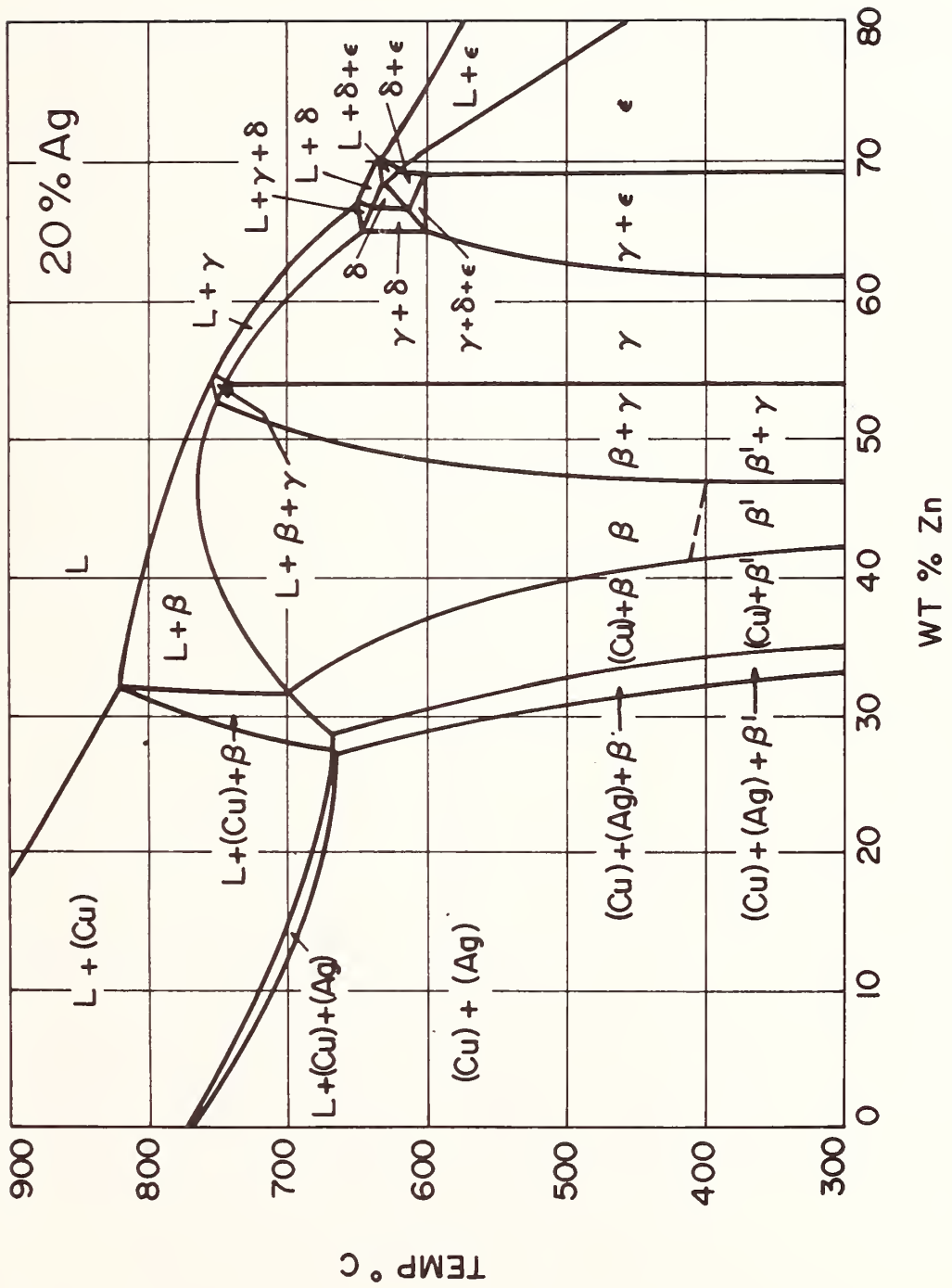
Reaction	Temp. °C	Co-existing Phases	Composition of Phases		
			Wt.% Cu	Wt.% Ag	Wt.% Zn
I ₁ : L = (Cu) + (Ag) + β	665	L	20	56	24
		(Cu)	63	9	28
		(Ag)	5	75	20
		β	23	50	27
II ₁ : L + γ = ε + δ	630	L	9.5	26	64.5
		γ	12	25	63
		ε	10.5	26	63.5
		δ	11	25	64

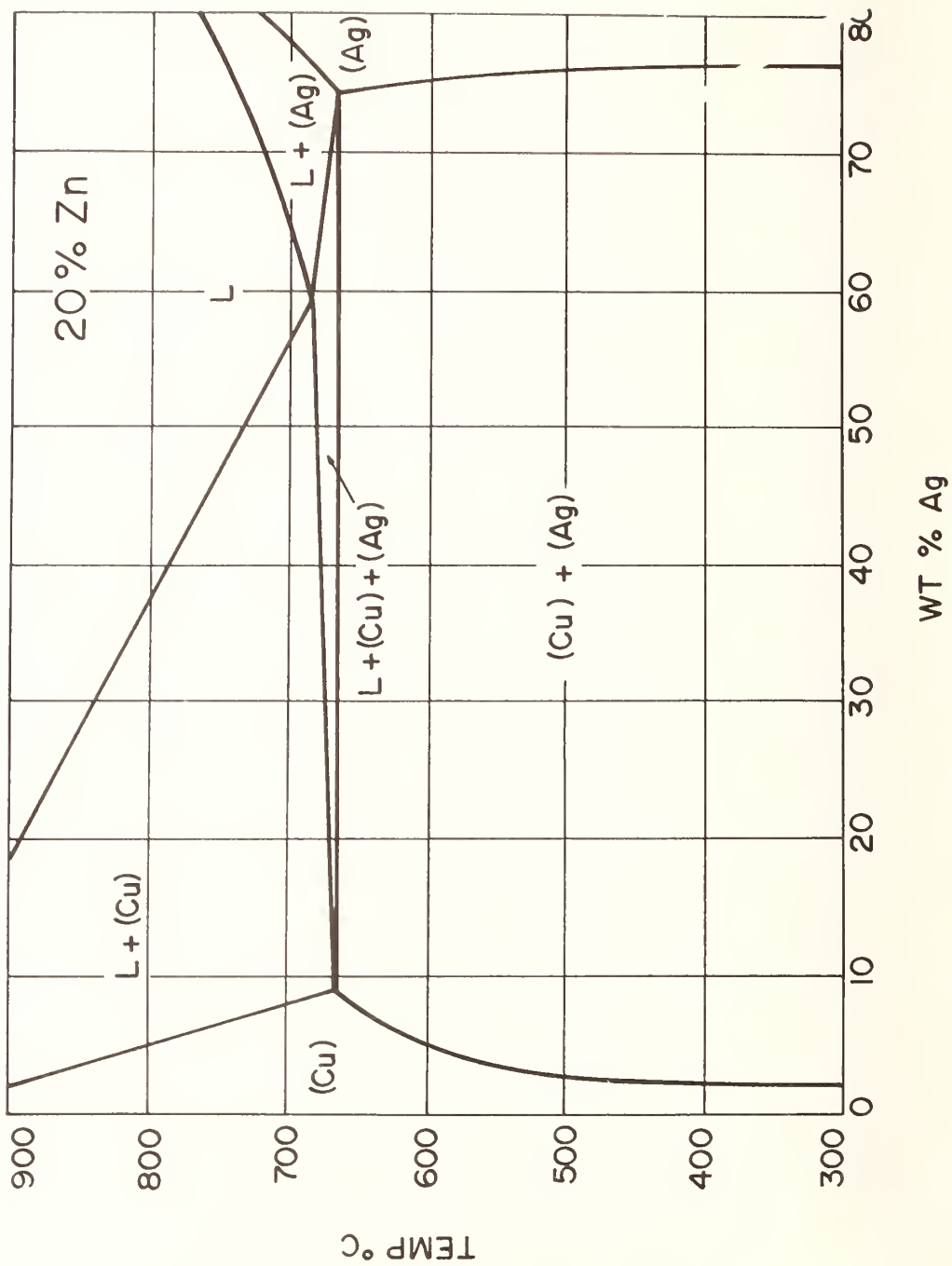












Cu-Ca-Mg

Phases and Structures: The following intermediate phases appear in the Cu-Ca, Cu-Mg, and Ca-Mg binary systems. No ternary phases have been found.

<u>Designation</u>	<u>Composition</u>	<u>Symmetry</u>	<u>Symbol</u>	<u>Prototype</u>
γ	Cu_5Ca	hex	D_{2d}^2	Cu_5Ca
η	CuCa	ortho	-	-
δ	CuCa_2	unknown	-	-
ϵ	Cu_2Mg	ord fcc	C15	Cu_2Mg
β	CuMg_2	ord ortho	-	-
ζ	CaMg_2	hex	C14	MgZn_2

The crystal structures of the Cu-Mg and Ca-Mg binary phases and the structure of the γ - Cu_5Ca phase are from the Metals Handbook (Gen. Ref. 1), whereas the structure of the η - CuCa phase is from Bruzzone [1].

Phase Diagrams: The liquidus and the 350° isotherm shown here are from the study of Myles [2]; however, the liquidus valleys have been slightly modified along the Cu-Ca binary system to bring them into agreement with the most recent data by Bruzzone [1]. This author confirmed the stoichiometry of the three Cu-Ca compounds found by Myles [2], but showed by means of a thermo-analytical investigation that η - CuCa and δ - CuCa_2 decompose peritectically instead of exhibiting congruent melting points as was assumed by Myles [2].

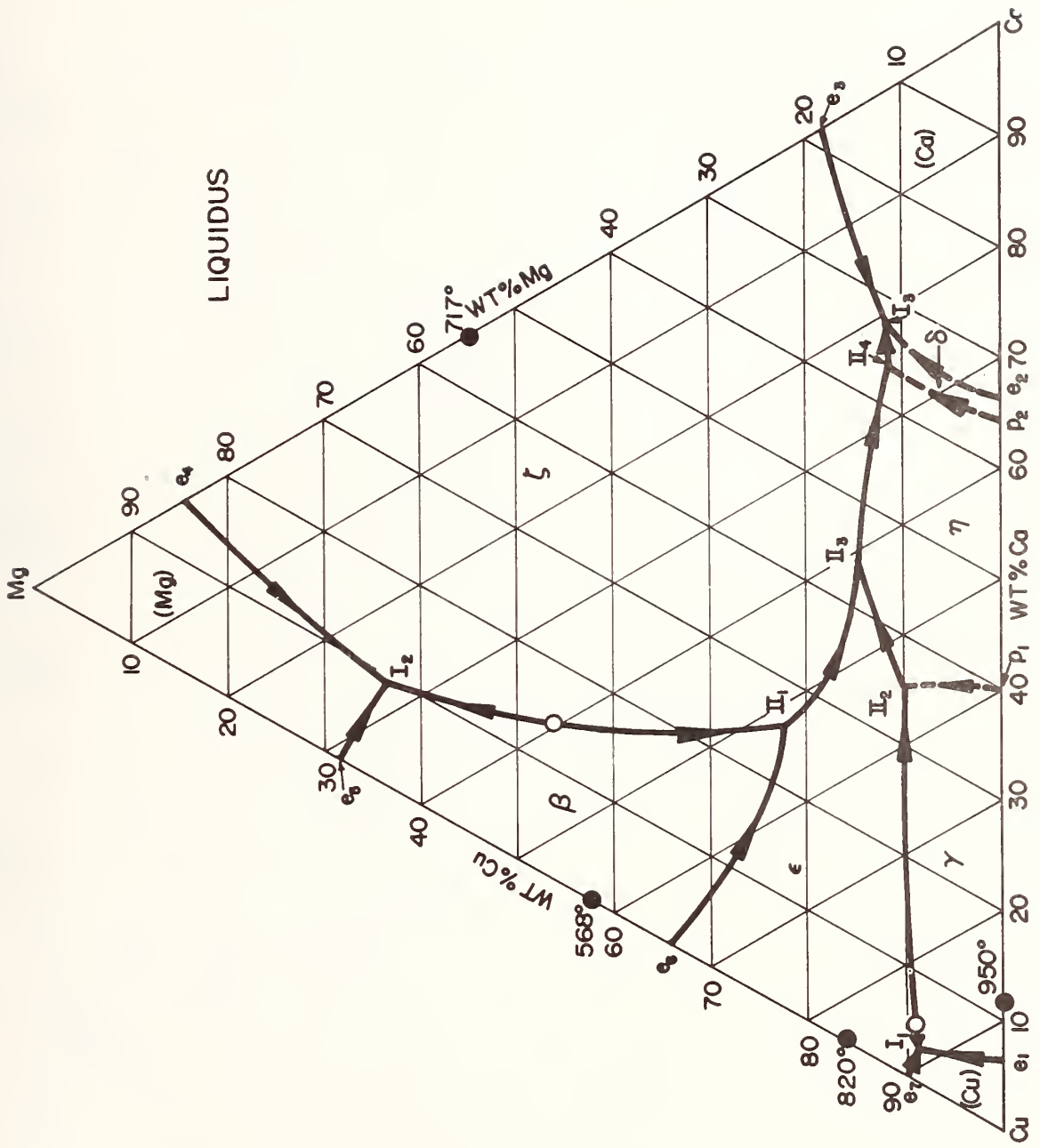
Three four-phase equilibria of type I and four of type II were found [2], they are given in Table I. The compositions of the coexisting phases are unknown as are the temperatures of the type II four-phase equilibria.

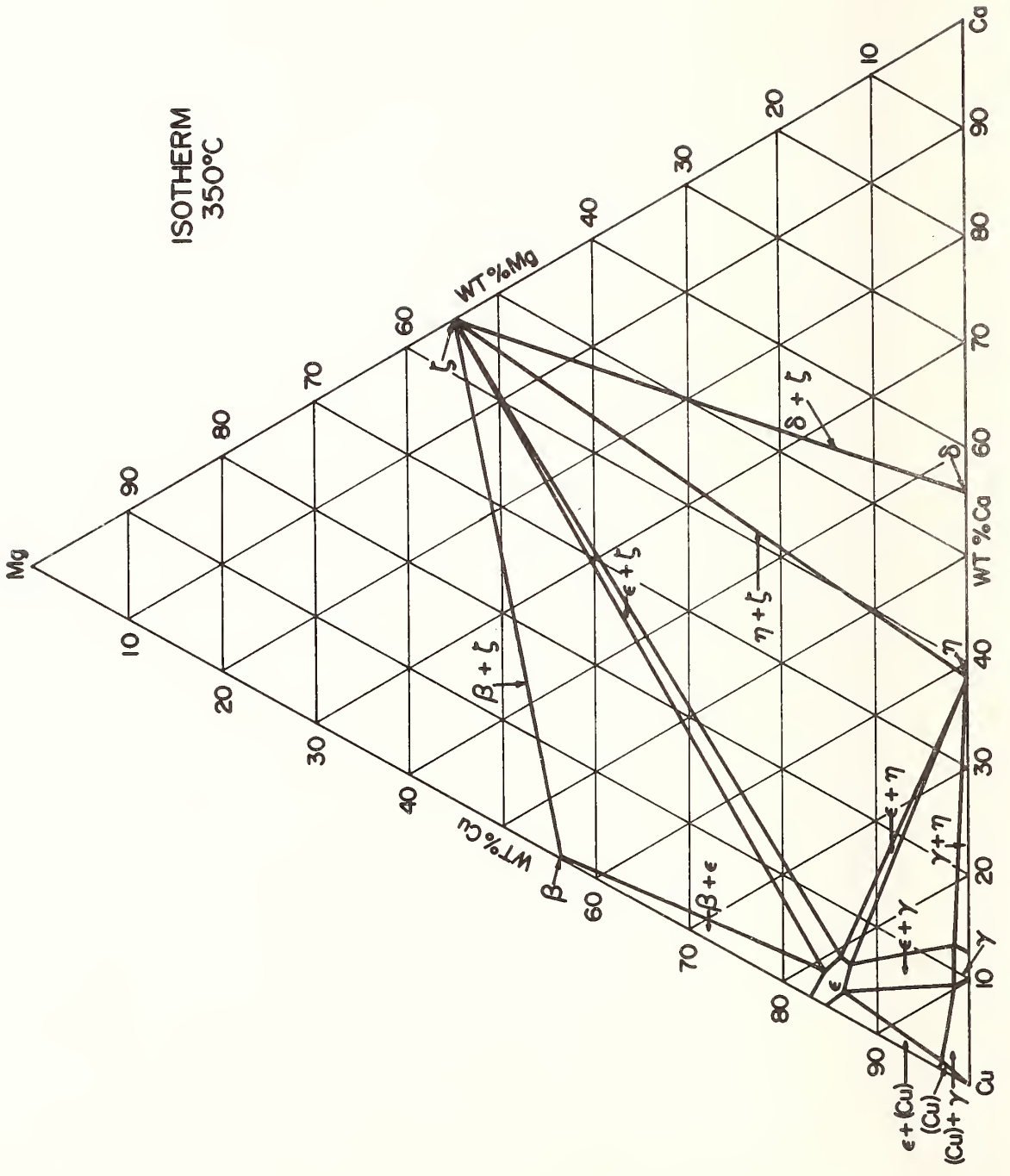
References:

1. Bruzzone, G., J. Less-Common Metals, 1971, 25, 361.
2. Myles, K. M., J. Less-Common Metals, 1970, 20, 149.

Table I. Four-phase Equilibria in the Cu-Ca-Mg System

Reaction	Temp. °C
$I_1: L = (Cu) + \epsilon + \gamma$	700
$I_2: L = (Mg) + \beta + \zeta$	430
$I_3: L = (Ca) + \zeta + \delta$	350
<hr/>	
$II_1: L + \beta = \epsilon + \zeta$	
$II_2: L + \gamma = \epsilon + \eta$	
$II_3: L + \epsilon = \eta + \zeta$	
$II_4: L + \eta = \delta + \zeta$	







PHASE EQUILIBRIA IN VARIABLE VALENCE OXIDE SYSTEMS

William B. White

Materials Research Laboratory and

Dept. of Geosciences

The Pennsylvania State University

University Park, PA 16803

Abstract

A compilation of the phase diagrams for binary metal oxygen systems is being prepared. The objectives are to reduce the available literature data to sets of internally consistent diagrams. Crystal structure information on the phases, critical discussion and explanatory text, with the diagrams are intended to be eventually published in monograph form.

Introduction

Some 40 elements react with oxygen to form compounds in which the element appears in more than one valence state. These include most of the transition elements, in which variable valence is attained by varying the number of d-electrons in the partially filled d-orbitals. It includes a group referred to as the Rydberg elements in which there are two valence states, one with a d^{10} electron configuration and one two charges smaller with an outer non-bonding lone-pair ns^2 electron configuration. The remainder include a few of the lanthanide elements and most of the actinide elements in which variable valence is achieved by varying the number of f-electrons. Finally the elements Zn, Cd, and Hg are included. Although these elements exhibit only a single oxidation state, the defect structure and electronic properties of the oxide are so dependent on oxygen fugacity that the phase equilibria become important.

Objectives

The total literature on binary metal-oxygen systems is very large but also very fragmentary. The principal objective of this work is to compile various pieces of diagrams, decomposition reactions, and other bits of information into internally consistent phase diagrams. Where possible, thermochemical data are being used to calculate missing equilibrium data.

The number of oxide phases in some systems such as Ti-O, V-O, and W-O is very large. Crystal structure and other data on the individual oxide phases is also being collected so that lists of phases can be prepared to accompany the phase diagrams. Likewise the crystallographic relations between phases related by decomposition reactions can be examined.

The ultimate objective is the publication of a monograph which will contain the best estimate of the binary metal-oxygen phase diagrams, the lists of phases with key structural information (unit cell, space group and references to full structural analyses where such exist), and an explanatory text.

Representations

Presentation of phase equilibria in these systems must take account of temperature, total pressure, and oxygen activity. Careful distinction between open and closed systems must be made. Three types of systems can be distinguished as shown below.

Conditions	Vapor Phase	Type of Diagram
I. All oxides refractory to liquidus	Oxygen fugacity less than 100 bars Vapor phase essentially pure oxygen	T-X "condensed" diagrams with superimposed isofugacity lines. Also f_{O_2} -T projections ²
II. All oxides refractory to liquidus	Oxygen fugacity greater than 100 bars Vapor phase nearly pure oxygen	P_{O_2} -T diagrams for stoichiometric oxides. P-T-X sections for non-stoichiometric oxides
III. Volatile oxides	Vapor phase of variable composition	Closed system P-T-X diagrams

Systems with volatile oxides, of which Re-O and Os-O are examples, require the use of P-T-X type diagrams and closed systems. Oxygen isofugacity lines do not coincide with SSV equilibria as is the case for the diagrams of types I and II.

Status and Progress

A large body of literature has been compiled, some 500 mostly recent references. Sweeps through the older literature by means of citation indexing

must still be done. Compilation and calculation are nearly complete on a few systems and partial compilations are in hand for a few others. Things progress, although slowly.

A listing of the systems under study (Table 1) gives the type of representation necessary and the available data base from the literature. For those systems whose status is "+++" enough data are available to prepare nearly complete phase diagrams of the solid-vapor equilibria, the compositions of non-stoichiometric compounds as a function of oxygen fugacity, and sometimes including melting behavior. Systems listed as "++" are less complete and for systems listed as "+" there are only fragmentary data.

Difficulties and Obstructions

There is a great lack of liquidus data for many systems. This includes both the two-liquid region between liquid oxide and liquid metal that exists for most systems and also the eutectic and peritectic relations between different oxides. Many diagrams will appear with only the SSV portion of the P-T-X diagram.

There is great experimental difficulty in obtaining equilibrium or even a complete set of phases at low temperatures even at fairly high oxygen pressures. Many systems contain complex oxides of high valence state that remain poorly described.

Oxygen fugacities in the metal-rich side of many binaries are extremely low. Gas buffer techniques have a lower limit at about 10^{-22} bars so that oxygen isofugacity lines are not known in the region of many oxygen-stuffed metallic phases such as occur in the system Ti-O. In absence of good thermochemical data, data for many of the intermediate phases cannot be calculated either.

Several systems, of which Ti-O and V-O are spectacular examples, exhibit one or more homologous series of shear phases, some of which occur with very small stoichiometric and stability range differences. The evidence is that many of these phases are both homogeneous and stoichiometric. However, the difference in free energy and therefore the oxygen fugacity is so small that resolution of the oxygen fugacity "stair steps" between adjacent phases is extremely difficult. There is also a very real question of whether the higher shear structure phases actually order on a macroscopic scale or whether there are domains or regions of different composition. What do we mean by a "homogeneous" phase at this level of energy resolution?

Table 1
 Status of Variable Valence Element-Oxygen
 Binary Phase Diagrams

System	Type of Representation	Status	System	Type of Representation	Status
<u>Transition Element Systems</u>			Pt-O	P-T-X	++
Ti-O	f-T-X	+++	Au-O	P-T-X	+
V-O	f-T-X	++	<u>Rydberg Systems</u>		
Cr-O	P-T-X	+++	As-O	P-T-X	++
Mn-O	f-T-X P-T-X	++	Sn-O	f-T-X	++
Fe-O	f-T-X	+++	Sb-O	P-T-X	+
Co-O	f-T-X P-T-X	++	Tl-O	f-T-X	+
Ni-O	P-T-X	+	Pb-O	P-T-X	+++
Cu-O	f-T-X	++	Bi-O	P-T-X	++
Nb-O	f-T-X	+++	<u>Lanthanide Systems</u>		
Mo-O	f-T-X	+++	Ce-O	P-T-X	+++
Tc-O	P-T-X	+	Pr-O	P-T-X f-T-X	+++
Ru-O	P-T-X	+	Eu-O	f-T-X	+++
Rh-O	P-T-X	++	Tb-O	P-T-X f-T-X	+++
Pd-O	P-T-X	++	<u>Actinide Systems</u>		
Ag-O	P-T-X	++	U-O	f-T-X	+++
Ta-O	f-T-X	+++	Np-O	f-T-X	++
W-O	f-T-X	+++	Pu-O	f-T-X	++
Re-O	P-T-X	+	Am-O	f-T-X	+
Os-O	P-T-X	+	Cm-O	f-T-X	+
Ir-O	P-T-X	++	Bk-O	f-T-X	+



PHASE DIAGRAMS FOR CERAMISTS

L.P. Cook, R.S. Roth, T. Negas and G.W. Cleek

Institute for Materials Research
National Bureau of Standards
Washington, D.C. 20234

Compilation of phase equilibria data of interest to ceramists is continuing, in accordance with the pattern established by the 1975 supplement to "Phase Diagrams for Ceramists". This latest supplement includes critical commentaries discussing preparation of starting materials, experimental methods, characterization of products, accuracy and precision of data and of diagram. The following experts in various fields are serving as Contributing Editors for the 1978 Supplement:

- J. J. Brown, Virginia Polytechnic Inst.
Fluoride containing systems
- L. L. Y. Chang, Miami Univ.
Tungstates, molybdates, carbonates
- R. C. DeVries, General Electric Co.
High pressure studies
- F. P. Glasser, Univ. Aberdeen
Alkali oxide containing systems
- F. A. Hummel, Pennsylvania State Univ.
Sulfides, phosphates
- K. A. Jack, Univ, Newcastle Upon Tyne
Nitrides, oxynitrides
- A. Muan, Pennsylvania State Univ.
First row transition metal oxide containing systems
- C. Semlar, Ohio State Univ.
Anhydrous silicate - oxide systems
- C. A. Sorrell, Univ. Missouri-Rolla
Aqueous salt systems
- K. Stern, Naval Research Laboratory
Binary systems with halides only
- R. Thoma, Oak Ridge National Laboratory
Fused salts
- D. R. Wilder and M. Berard, Iowa State Univ.
R.E. oxide bearing systems
- H. S. Yoder, Jr., Carnegie Inst. Washington
Hydrous silicate systems, high pressure silicate studies

Scientists at NBS (Cook, Roth and Negas) with the help of the American Ceramic Society (Cleek, Smith and others) are assuming much of the responsibility for gathering the data from the literature and coordinating the preparation of evaluations and final editing of diagrams.

Coverage according to chemical system for the various editions is as follows:

	<u>1964</u>	<u>1969</u>	<u>1975</u>	<u>1978</u>
Metal-oxygen systems	146	202	104	~205
Metal oxide systems	855	408	401	~655
Systems with oxygen containing radicals	172	228	68	~120
Systems with halides only	483	718	145	~365
Systems containing halides with other substances	214	273	72	~160
Systems containing cyanides, sulfides, etc.	43	82	20	~140
Systems containing water	151	131	40	~250

Results of a questionnaire are being analyzed to determine user interest as a function of chemical system and user opinion regarding the critical commentaries, in order to guide the preparation of future editions.



NBS CRYSTAL-DATA CENTER

A. Mighell, H. Ondik, J. Stalick, R. Boreni

Institute for Materials Research
National Bureau of Standards
Washington, D.C. 20234

The NBS Crystal-Data Center abstracts and critically evaluates crystallographic data. For a substance to be included in the crystal-data file, cell parameters must be reported for the material. These parameters are determined primarily by powder and single-crystal x-ray diffraction. Crystallographic data results from a variety of disciplines and, consequently, is taken from over 300 scientific journals. The total number of crystalline compounds now in the file is over 40,000.

The output of the project includes:

1. *Crystal Data Determinative Tables*: Used to identify crystalline materials via the ratios of the cell parameters. The most recent volume published is the third edition.¹ A supplement to the third edition will be issued in 1977.
2. *Crystal Data Space-Group Tables*: Materials are arranged by space group. These tables can be used to identify materials of any given space group or symmetry, and to identify isostructural materials. These tables will be consonant with the third edition of *Crystal Data*. They will be published in the *Journal of Physical and Chemical Reference Data* in the Spring of 1977.
3. NBS Magnetic Tape #9:² This tape is an abbreviated version of the third edition of *Crystal Data* and contains cell, space group, density, formula, and determinative ratios. As supplements to the third edition are published the tape will be updated.
4. Component of CIS (Chemical Information System) which is being set up by NIH/EPA: The crystal-data file will be in the CIS system along with the powder-data file, the Cambridge structural file, the mass spectroscopy file and other scientific data bases. These files are to be used primarily in the identification of unknown crystalline materials.

A principal use of the cell and chemical data is the identification of unknown crystalline materials. Several recent developments give great promise for the identification of unknown materials via single-crystal work. They include the growth of the data base, advances in lattice theory, and automation of the single-crystal x-ray diffractometer. To identify an unknown, one can start with a single crystal, mount it on a diffractometer, determine a refined primitive cell, reduce the cell, and check against a file of known reduced cells. The entire procedure can be automated. As a result, the single-crystal x-ray diffraction method can now complement the powder method for the routine analysis of crystalline materials.

A major objective of the NBS Crystal-Data Center is to establish close ties with other data efforts with common interests and to coordinate our data evaluation with these centers (e.g. Joint Committee on Powder Diffraction Standards, Cambridge Crystallographic Data Centre, The Chemical Information System).

¹ J.D.H. Donnay and Helen M. Ondik, "Crystal Data Determinative Tables," Third Edition, Vol. 1 and 2, U.S. Department of Commerce, National Bureau of Standards, and the Joint Committee on Powder Diffraction Standards (1972, 1973).

² For information about the tape and its lease, contact the National Technical Information Service (NTIS), Department of Commerce, 5285 Port Royal Road, Springfield, VA 22151.

DEMONSTRATION: The NBS magnetic tape #9 described under item 3 of this abstract will be accessed in an accompanying demonstration of "On-Line Data Retrieval and Analysis Systems Such as OMNIDATA", by B. B. Molino and J. Hilsenrath, NBS.



The NBS Alloy Data Center

G. C. Carter, D. J. Kahan, and L. H. Bennett
Metallurgy Division
Institute for Materials Research
National Bureau of Standards
Washington, D.C. 20234

Introduction

Knowledge of the structure of materials is important in understanding several industrially significant phenomena and applications such as aging, hardness, occurrence of brittle intermetallic compounds, magnetic transition temperatures, high-temperature solubility of impurities, corrosion resistance, solid electrolytes and non-crystalline solids, as well as many other physical properties. The study of a phase diagram appropriate to a particular material can often provide information important to its scientific and technical applications. In recent years it has become increasingly clear that the need for reliable phase diagrams far exceeds the availability, and the Alloy Data Center (ADC) is now addressing this problem in some detail.

Preliminary surveys concerning data availability have already been done by the ADC in the form of short reviews and compilations of existing phase diagram compilations (1) and of existing phase diagram data centers (2). Both of these are being kept current and a more extensive review together with these updated editions are given on page 36 of these proceedings. Earlier investigations on phase diagram and thermodynamic data needs had already been done via an NBS Impact study, and more recently with more specific questions by method of a questionnaire, distributed by the ADC to those showing an interest in our present phase diagram workshop.

This paper reports on the findings of the questionnaire, on general ADC activities, and on the present status and future plans of the ADC with regards to the subject of phase diagram data. Although thermodynamic data are an integral part of this subject, the present paper intends to concentrate primarily on phase diagrams.

User Needs and Data Availability - Questionnaire Results

About 150 questionnaires were sent to those persons who indicated (written or orally), an interest in the Phase Diagram Workshop. At the time of writing, 48 responses have been received. The questionnaire addressed both the topics of 1) User Needs, and 2) Data Availability. Since the papers of these workshop proceedings go into great detail in both of these areas, all results from these questionnaires will not have to be duplicated here, but rather, the results not expressed elsewhere will be described, with relation primarily to metallic alloys.

1. User Needs. The most often cited user needs were in the areas of superalloys, high temperature steels, and eutectics. Such materials are utilized in high temperature applications (e.g. turbine components), reactors, energy storage materials, etc. Other areas of needs were for coatings and their interactions with the alloys they coat, corrosion resistant alloys (e.g. Hastelloy, alloy C-267, corrosion properties versus phase diagrams), wear resistant alloys (certain carbides), impurity effects on phase diagrams in many of the instances given here, data on the effect of hot-working, heat treatments, segregation during solidification, data on materials used in ferromagnetic, mechanical, and superconducting applications (A-15 compounds and other), catalysis (metals), catalyst supports (ceramics), battery components and their corrosion properties (e.g. electrodes, high energy density batteries, lead acid batteries, etc.), memory alloys, effect of irradiation on phase transformations, dental alloys, data for specification of thermal practices, data on liquid solder-solid alloy interactions, hard steels, special steels, data on the σ -phase formation in transition metal alloys, and composite materials (e.g. refractory boride or carbide compounds with metal matrix). The occurrence of sulfur in alloys was mentioned occasionally in the questionnaires as a problem area where more data are needed, and the urgency of this subject was repeatedly mentioned during the third day of the workshop, devoted to user needs (Panels II, III, and IV). Applications of phase diagram data ranged from very specific problems such as turbines and batteries, to more general areas as materials development for materials substitution, or, in general, R & D. These needs for data on the above general categories of alloys can be rewritten in more chemical terms as needs for phase diagram data on: binary and multicomponent alloys based on Fe, Cu, Ni, Al, W, Pb, Mo, Nb, Cr, and other transition metal as well as some non-transition metal alloys, and on the carbides, sulfides, silicides, selenides, tellurides, as well as effects of impurities (O, N, C, S, and non-interstitial impurities) on all these materials.

Three tabular questions were also asked with regards to user needs (summary reproduced in Fig. 1). They query the subjects of relative needs for i) coverage in phase diagram compilations, ii) depth of evaluation (ranging from unannotated bibliographies to full critical evaluations), and iii) preferred formats of such compilations.

The urgent need for data on ternary and higher component phase diagram data is clearly demonstrated in Fig 1-i. High precision, metastable phase, impurities or trace additions, and crystallography were also of importance to many respondents. While the ADC will concern itself with all former topics, the topic of crystallography falls outside our scope. NBS' Crystal Data Center (see preceding paper, p. 259) concerns itself with this topic, and many critical compilation on crystallographic data are available (e.g. see refs 3-6, and the listing on pp. 82-83 of these proceedings).

Fig 1-ii demonstrates the preference for a full critical evaluation of binary alloys (i.e. an update of the Hansen (7) series), whereas for ternary or higher order multicomponent system, a lesser degree of evaluation will be helpful with the most weighting on unevaluated diagrams with a complete bibliography. Intermingled with this response is probably the fact that many users are accustomed to having a full evaluation for binaries and, therefore, prefer an update, whereas multicomponent data users are not so spoiled. It should be noted here that a major data project in the USSR does produce just that, giving an "unevaluated" (though some judgement has been made) phase diagram compilation with complete bibliography, issued annually (8). An English translation of a cumulative index to this Russian work has recently been completed and is enclosed in these workshop proceedings as paper TPSII-1. Other ternary phase diagram projects include the updating of the 1956 bibliography by Haughton and Prince (See p. 57, Appendix C) which is nearing completion and a new project in Germany under Petzow et al. (see p. 45, Appendix A), which plans to produce a complete, evaluated compendium of ternary diagrams.

Packaging of the output was addressed as well in tabular form in the questionnaire (Fig 1-iii). It appears that loose-leaf sheets are more popular than was anticipated. Several respondents qualified this preference noting that quick distribution was of high urgency. A bound volume could then follow at a later time. Also, insofar as many scientists have their own personal files of diagrams, loose-leaf distribution was said to be a desirable method for inclusion in private collections. Of course, bound volumes were also noted as being desirable.

Generally, the results of ii, and iii were weighted towards minimal evaluation minimal packaging in the interest of speed of distribution. To some extent the results suggest that people want new, improved versions of what they have used in the past. Very few marked magnetic tapes, microform, or on-line access as desirable forms of packaging. Although for microform there may not be much change in technology, and, therefore, popularity, the distribution of magnetic tapes, and especially the on-line access method could gain an increased popularity in the near future, since improved software is becoming available, and more and more groups are acquiring on-line terminals. Especially with the availability of software for the calculation of phase diagrams (e.g. see paper by A. D. Pelton, on p. 1077), such an alternative is becoming attractive.

2. Data Availability. The subject of data availability was also addressed in the questionnaire. As a result, a substantial amount of information was gathered, which has been added in Appendices A and C, pp. 40-80, representing a listing of on-going data activities and a listing of existing phase diagram compilations. Generally, between available books and current data projects, a fair amount of data is available. However, much of it is badly out of date, coverage is incomplete or lacking in several areas, and future products will not be out soon. For example, no comprehensive update of the critical compilation of binary phase diagrams (the old Hansen series) is being done yet; the compendium of critical ternary

phase diagrams, estimated at some 18,000 pages, is just in the initial stages (bibliography has been collected), and is not expected to be completed in the near future. Any higher order multicomponent systems are covered only very occasionally for very select systems (e.g. Raynor's Mg-alloy phase diagram compilation; see listing on p. 65). The questionnaire briefly went into the subject of experimental and calculational approaches to phase diagram determinations. Full conference papers by the respondents give a detailed account of the answers, and the present paper will not dwell on this subject.

The results of the questionnaire indicate

1. An excessively long time lag between supply and demand in those areas where data exist (this covers mostly binaries and ternaries).
2. A tremendous lack of data for multicomponent phase diagrams for alloys of immediate need, as described under User Needs, above.
3. An absence of data for multicomponent alloys in general, thereby providing no basis for materials substitution.
4. Certain gaps in coverage (as was pointed out during the workshop as well) in specific areas that lie outside the well-defined scopes of metals, ceramics, and electronic materials (e.g. semiconductors). For example, sulfur-containing materials fall in this category and tellurides were also mentioned in this context.

General ADC Activities

The Alloy Data Center is a part of the NBS' National Standard Reference Data System, under the Office of Standard Reference Data (OSRD). It maintains an awareness of about 150 physical properties in metals and alloys, evaluating only those properties for which a special need exists and for which qualified researchers are employed in the Alloy Physics Section (Metallurgy Division), in which the Alloy Data Center is located. In the past, critical compilations in soft x-ray emission spectroscopy (9) and nuclear magnetic resonance (10) were prepared (the latter including some 800 binary phase diagrams). Consequently, our current bibliographic files (11), which contain nearly all papers on the first two subjects published up to recent years are not being kept up-to-date for those subjects, while papers on phase diagrams are being annotated and entered at an increased rate for production of a comprehensive bibliographic file.

Another important function of the ADC is to maintain interactions with other existing data centers dealing with physical properties of metals and alloys, and to advise the OSRD in matters related to data activities in these areas. It is as a result of this function that the ADC has initiated its program on alloy phase diagrams, and plans to concentrate its efforts on this basic property which underlies most physical, metallurgical, or engineering properties of alloys.

ADC Phase Diagram Program

As is apparent from the compilation on pp. 40-48, several data centers throughout the world are engaged in collecting, critically evaluating, and disseminating phase diagram data. The Alloy Data Center plans to be a center of coordination and interaction for these groups and hopes to help avoid costly and time consuming duplication of efforts. It plans to continue interactions with the scientific, but more importantly the industrial, user to identify areas of greatest needs such as the four that have been identified above, and recommend programs in these areas. Other problems not yet identified by us as yet may exist today, and new ones will develop in the future. We take the task upon ourselves as a continuing data center, to continue to identify areas of needs, and to act as a liaison between the user and the data evaluation centers.

The ADC plans to assist other data centers and users in preparing bibliographies. Our currently existing computerized bibliographic files already contain many phase diagram citations and they are being entered at an increasing rate. In total, some 20,000 papers are in this system, and with the expected growth, an on-line system is being planned.

The Alloy Data Center plans to critically evaluate phase diagrams in specific areas, and has started with the metal-hydrogen systems applied to hydrogen storage, an area in which the Alloy Physics Section has expertise.

The ADC also will concern itself with the development of graphical methods in phase diagram data communication and presentation. Some preliminary considerations will be discussed below.

Interactive Graphic Demonstration

(given in conjunction with this poster presentation)

by

R. A. Kirsch and L. J. Swartzendruber
Institutes for Basic Standards and Materials Research, resp., of NBS

Introduction

Recently a considerable number of computer-based graphical display systems have become commercially available. The ease of use and sophistication of these systems have advanced to the point where it is worthwhile to consider their utility in the storage, manipulation, retrieval, and display of graphical phase diagram information.

The display of three dimensional surfaces in two dimensions is often used as an aid to visualizing the properties of ternary phase diagrams (and binary systems when pressure is also an important variable, e.g. in metal-hydrides). The use of a program which allows the surface to be plotted as it would appear to an observer when his eye is placed at any location with respect to the surface has been investigated (12). Using this program, the surface can be viewed from any number of positions, and the one position which best presents the salient features can be selected. The surface generated could then be used by a draftsman to prepare a figure for formal publication. Also, using this method, stereo pairs can be readily generated.

An example is shown in Fig. 2. To generate this figure, a mathematical formula was used to represent a surface *similar* to that found for the palladium-hydrogen system, with the vertical axis representing pressure and the other two axes representing composition and temperature. A 30 x 30 grid was used to generate the display. When using actual data such a grid would be generated using interpolation algorithms. Fig. 3 shows another view of the same surface using a 50 x 50 grid.

To illustrate the use of graphics in displaying binary phase diagrams, we have developed a system which stores the diagram information on mass storage in an abbreviated digital form. The program reads the digital information for the desired diagram from mass storage and uses it to generate a diagram using graphics software. Transformations on the temperature scale, changes between atomic and weight percent, and variations in diagrams size are readily made to obtain the diagram in desired format. Examples are shown in Fig. 4. Information for each line of the diagram is stored as follows: (1) vertical and horizontal lines are specified by their end points. (2) all other lines are specified by their end points and a fourth degree polynomial giving temperature as a function of composition. The polynomial was obtained as a least squares fit to a series of data point with a constraint requiring the curve to pass through the end points. Many other display formats, supplementary scales on each diagram, etc. are readily obtainable.

Using such a system a centralized bank of phase diagram information could be maintained, with each diagram maintained in up-to-date form. A user with access to a graphics terminal could quickly obtain any diagram in the format required. Outputs of any of all diagrams on, for example, microfilm could be supplied from such a centralized system to those without access to a graphics terminal. We have presented only a very brief glimpse at the possibilities inherent in interactive graphic display. As the problem of maintaining up to date compilations of phase diagram data becomes more extensive, such systems may offer a viable alternative.

References

- (1) L. H. Bennett, D. J. Kahan, and G. C. Carter, *Matls. Sci. Eng.* 24, 1 (1976). The compilation of phase diagram books given in this paper is being kept current and the latest edition is given as Appendix C in paper M-3 of this conference.
- (2) L. H. Bennett, "Alloy Phase Diagram Activities of the Alloy Data Center", 5th International CODATA Conference, Boulder, CO., June 28-July 1, 1976. The compilation of on-going activities given in this paper is being kept current and the latest edition is given as Appendix A in paper M-3 of this conference.
- (3) J.D.H. Donnay and H. M. Ondik, "Crystal Data Determinative Tables", Third edition, Vol 1 and 2, U.S. Dept. of Commerce, NBS, and the Joint Committee on Powder Diffraction Standards (1972, 1973). A supplement to the third edition will be issued in 1977.
- (4) W. B. Pearson, "A Handbook of Lattice Spacings and Structures of Metals and Alloys", Pergamon Press, N.Y., Vol 1 (1968), Vol. 2 (1967).
- (5) R. W. G. Wyckoff, "Crystal Structures", Interscience, N.Y., Vol. I (RX_1 , RX_2), (1963); Vol II (Inorganic Compounds, RX_n , RMX_2 , $RnMX_3$), (1964).
- (6) Landolt-Bornstein Tables, New Series, Group III, Vol 6, "Selected Data of Elements and Intermetallic Phases", Springer-Verlag, N.Y., (1971).
- (7) M. Hansen "Constitution of Binary Alloys", McGraw-Hill, N.Y. (1958) Supplement I, R. P. Elliott (1965), Supplement II, F. A. Shunk (1969).
- (8) N. V. Ageev, editor, "Phase Diagrams of Metallic Systems", issued annually in Russian (1955-1974). A cumulative index in english is available in paper TPSII-1 of this proceedings. Subscriptions to this series can be obtained by ordering only in the several months preceding the year for which the subscription is intended, from Prof. A. I. Mikhailov, Director, 125219 Institute for Scientific Information (VINITI), Academy of Sciences of the USSR, Baltijskaya UL 14, Moscow, USSR.
- (9) J. R. Cuthill, A. J. McAlister, R. C. Dobbyn, and M. L. Williams, "Soft X-ray Emission Spectra of Metallic Solids: Critical Review of Selected Systems and Annotated Spectral Index", NBS Special Publication No. 369 (1974).
- (10) G. C. Carter, L. H. Bennett, and D. J. Kahan, "Metallic Shifts in NMR", *Progress in Materials Science* 20, 1-2260, Pergamon Press (1977).
- (11) File, described in NBS Technical Note 464, by G. C. Carter et al. (1968); the file holdings up to 1970 published in "The NBS Alloy Data Center: Permuted Materials Index", by G. C. Carter et al. (1971); the file holdings through 1972 made available in NBS Magnetic Tape 3, Alloy Data Center Tape and Documentation Parcel, Natl. Tech. Info. Ser., Springfield, VA 22151.
- (12) This investigation was made by R. A. Kirsch and D. J. Orser, Applied Mathematics Division, NBS, using a program developed by T. K. Porter, LSU/CCB/DCRT/National Institutes of Health.

i) Importance of parameters (check appropriate items):

	very important	important	not important
high precision			
metastable phases			
ternary and higher order systems			
magnetic and other transitions			
high pressure			
impurities or trace additions			
surface phases			
related information: crystallography			
other (please specify): thermo data			
" (intermediate or ordered phases)			
" (tie lines sol-liq. multicomp.)			
" (high T changes under tensile and shear stress)			
" (Vapor pressure, any thermal props for x-tel growth - inorg. res. matls.)			
" (decomposition pressures)			

ii) Minimum acceptable depth (check appropriate items):

depth	binary systems	multicomponent systems	other
bibliography			
annotated bibliography			
unevaluated diagrams with bibliography			
critical evaluation			
other (coordination with evaluation of thermochem. props. of phases)			

iii) Most desirable form of "packaging" (check appropriate items):

	bibliographies	binary systems	multicomponent systems	other
loose-leaf sheets				
bound volumes				
microfilm or microfiche				
magnetic tape				
on-line computer access				
other				

Figure 1. Summary of three of the questions asked in a phase diagram data need questionnaire.

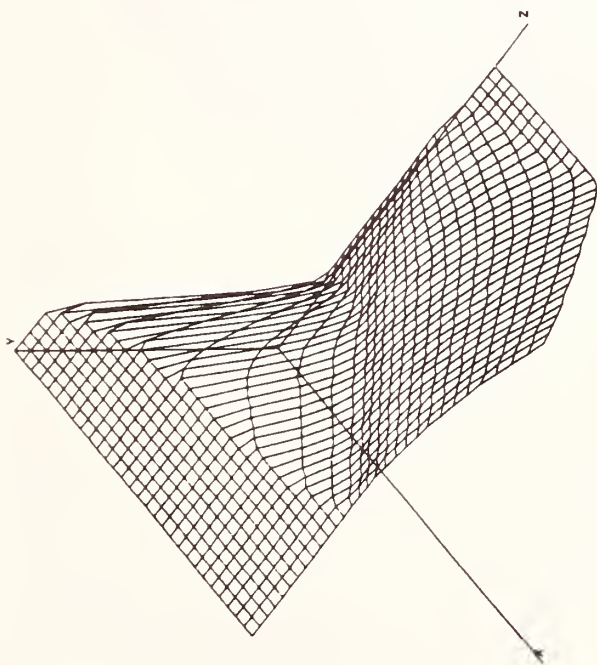
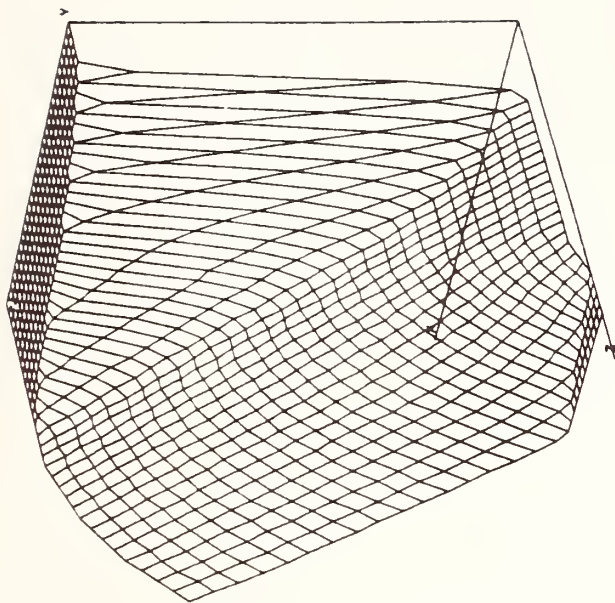


Fig. 2. Two views of a hypothetical pressure-composition-temperature plot of a metal-hydrogen system with properties similar to Pd-H. Vertical Y axis represents pressure, the Z axis composition, and the X axis temperature. The grid size is 30 points by 30 points.

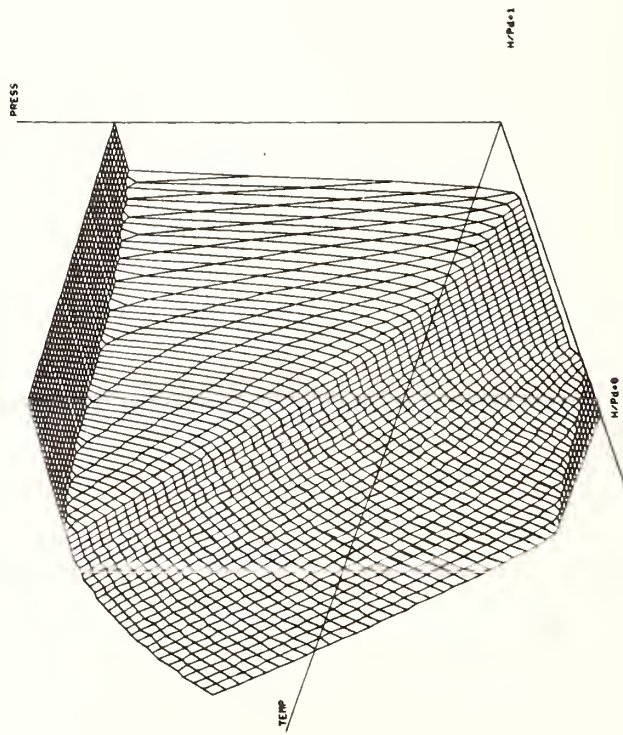
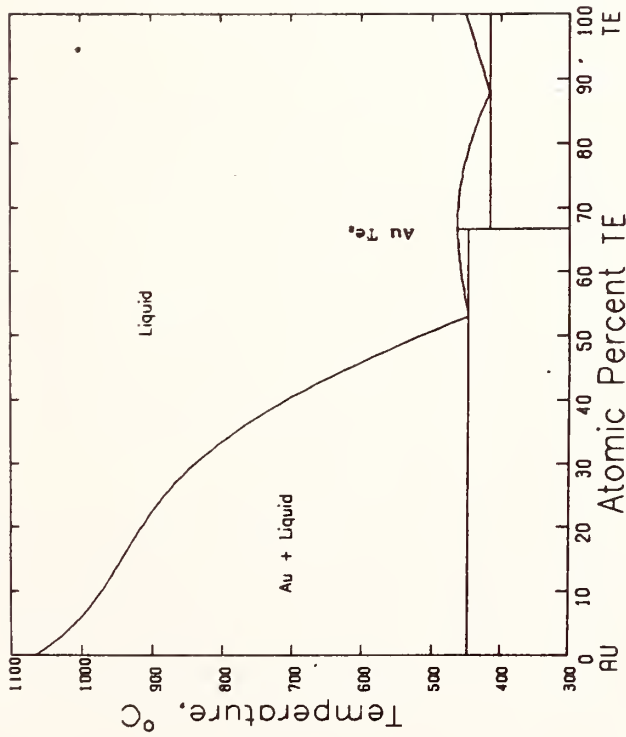


Fig. 3. Another view of the same surface shown in Fig. 2. A finer grid of 50 points by 50 points has been used.

(a)



(b)

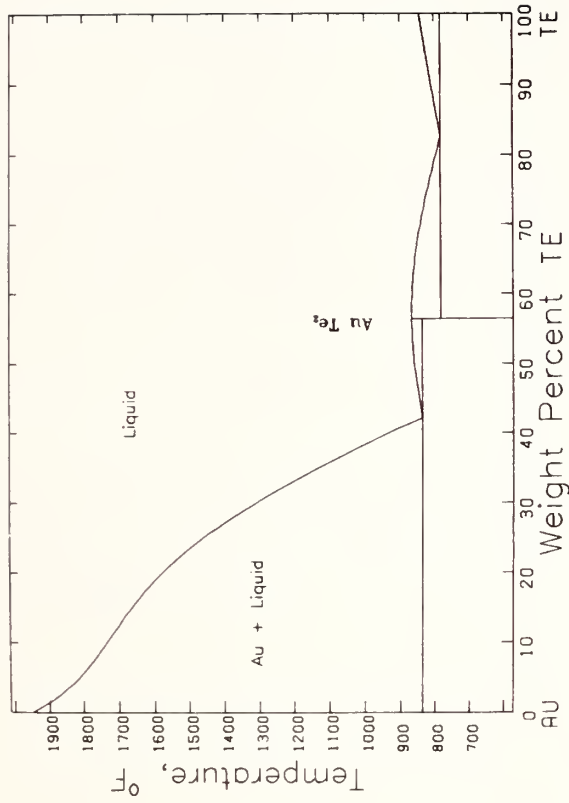


Fig. 4. (a) AuTe phase diagram as displayed on a graphics terminal, (b) AuTe diagram after software generated transformation to weight percent and degrees Fahrenheit. The scale lengths have also been altered slightly.



A Review of Phase Equilibria in the
 Na_3AlF_6 -LiF-CaF₂-AlF₃-Al₂O₃ System

Douglas F. Craig, Roger T. Cassidy, and Jesse J. Brown, Jr.
Department of Materials Engineering
College of Engineering
Virginia Polytechnic Institute and State University
Blacksburg, Virginia 24061

ABSTRACT

The electrolyte used in the Hall process for producing aluminum metal consists basically of a fused mixture of alumina (Al_2O_3) and cryolite (Na_3AlF_6). Other ingredients including AlF_3 , LiF, and CaF_2 are added to modify properties such as bath density, electrical conductivity, and freezing temperature. The electrolyte composition now used was determined largely by trial and error because of the incompleteness of available phase equilibria data.

For the past five years, a research program jointly sponsored by the Alcoa Foundation and the VPI&SU Research Division has been underway in the Materials Engineering Department at VPI&SU. This program was designed to critically review the existing phase equilibria data on systems involving cryolite and to expand upon this body of knowledge by determining the liquidus-solidus phase relationships in a portion of the Na_3AlF_6 -LiF-CaF₂-AlF₃-Al₂O₃ system.

Historically, a variety of experimental techniques have been employed to determine the phase diagrams of systems important to the Hall process. Many of the early experiments were conducted using open containers. This practice resulted in the publication of some inaccurate phase diagrams because of the decomposition of many of the fluoride

compounds at high temperatures. In more recent years, it has become standard procedure to encapsulate all samples in sealed platinum containers. Quenching and Differential Thermal Analysis (DTA) experiments using samples sealed in the platinum containers have been used to revise some of the early phase diagrams and to investigate new systems.

In this paper, the phase diagrams that are known in the Na_3AlF_6 - LiF - CaF_2 - AlF_3 - Al_2O_3 system are reviewed in a systematic manner including the diagrams that have been determined at this University over the past five years. The result is a current review of the phase equilibria knowledge of cryolite containing oxy-fluoride systems of importance to the aluminum industry.

Table of Contents

	<u>Page</u>
A. One Component Systems	277
1. Cryolite	277
2. Aluminum Fluoride	278
3. Calcium Fluoride	279
4. Aluminum Oxide	279
5. Lithium Fluoride	280
B. Two Component Systems	280
1. System $\text{CaF}_2\text{-AlF}_3$	280
2. System $\text{Na}_3\text{AlF}_6\text{-CaF}_2$	285
3. System $\text{Na}_3\text{AlF}_6\text{-AlF}_3$	289
4. System $\text{Na}_3\text{AlF}_6\text{-Al}_2\text{O}_3$	296
5. System $\text{CaF}_2\text{-Al}_2\text{O}_3$	299
6. System $\text{AlF}_3\text{-Al}_2\text{O}_3$	300
7. System LiF-AlF_3	300
8. System $\text{LiF-Na}_3\text{AlF}_6$	305
9. System $\text{Na}_3\text{AlF}_6\text{-Li}_3\text{AlF}_6$	306
10. System $\text{Li}_3\text{AlF}_6\text{-Al}_2\text{O}_3$	310
11. System LiF-CaF_2	310
12. System $\text{Li}_3\text{AlF}_6\text{-CaF}_2$	314
C. Three Component Systems	314
1. System $\text{CaF}_2\text{-AlF}_3\text{-Na}_3\text{AlF}_6$	314
2. System $\text{Na}_3\text{AlF}_6\text{-AlF}_3\text{-Al}_2\text{O}_3$	322
3. System $\text{Na}_3\text{AlF}_6\text{-CaF}_2\text{-Al}_2\text{O}_3$	325
4. System $\text{CaF}_2\text{-AlF}_3\text{-Al}_2\text{O}_3$	328
5. System $\text{Li}_3\text{AlF}_6\text{-Na}_3\text{AlF}_6\text{-Al}_2\text{O}_3$	328
6. System $\text{LiF-AlF}_3\text{-Na}_3\text{AlF}_6$	329
7. System $\text{Li}_3\text{AlF}_6\text{-LiF-CaF}_2$	329
D. Four Component Systems	333
1. System $\text{Na}_3\text{AlF}_6\text{-AlF}_3\text{-CaF}_2\text{-Al}_2\text{O}_3$	333
2. System $\text{Na}_3\text{AlF}_6\text{-AlF}_3\text{-LiF-Al}_2\text{O}_3$	336
3. System $\text{Na}_3\text{AlF}_6\text{-CaF}_2\text{-LiF-Al}_2\text{O}_3$	336

Aluminum is the most abundant metallic element in the earth's crust and ranks after oxygen and silicon as the third most abundant of all elements. Because of its strong affinity for oxygen, it is not found in nature in the elemental state but only in combined forms such as oxides, silicates, etc. In 1886 Charles Martin Hall and Paul L. T. Héroult discovered almost simultaneously the process in which alumina is dissolved in molten cryolite (Na_3AlF_6) and decomposed electrolytically. This reduction process is known as the Hall-Héroult process.

The electrolyte consists basically of a fused mixture of cryolite, aluminum fluoride, calcium fluoride, lithium fluoride, and alumina. Aluminum fluoride is added to the bath to alter the cryolite ratio ($3\text{NaF}/\text{AlF}_3$) from the stoichiometric value of 1.5 to some lower value. Calcium fluoride is added in amounts between 5 and 6 wt. % to permit lower operating temperatures with additions of approximately 0.1 wt. % LiF used to increase electrical conductivity.

While the basic process for the production of aluminum has not changed significantly since its discovery 90 years ago, the phase equilibrium diagrams involving the components of the electrolyte are in many cases contradictory and in some cases unknown. To some extent this is because of the experimental difficulties encountered in working in these systems. Cryolite decomposes on melting, AlF_3 is volatile, supercooling is often present and the primary crystallization of Al_2O_3 is difficult to detect by conventional techniques. The inter-relationships between the various fluorides in the bath and their influence on the melting temperature and alumina solubility of the electrolyte can best be understood when reliable phase diagrams for the electrolyte exist.

During the past few years an intensive study of the phase diagrams

involving the components of the electrolyte used in the smelting of aluminum has been underway in the Materials Engineering Department of the Virginia Polytechnic Institute and State University. The objectives of this study are to establish the phase equilibrium relationships in a portion of the $\text{Na}_3\text{AlF}_6\text{-LiF-CaF}_2\text{-AlF}_3\text{-Al}_2\text{O}_3$ system. This has required a critical review of the existing phase diagrams and, in some cases, experimental redeterminations of selected diagrams. Many pertinent binary and ternary systems were unknown and these were determined experimentally. The final goal of this study is to determine the invariant points in the systems $\text{Na}_3\text{AlF}_6\text{-AlF}_3\text{-CaF}_2\text{-Al}_2\text{O}_3$, $\text{Na}_3\text{AlF}_6\text{-AlF}_3\text{-LiF-Al}_2\text{O}_3$, and $\text{Na}_3\text{AlF}_6\text{-CaF}_2\text{-LiF-Al}_2\text{O}_3$. (These systems are of most interest because they contain Na_3AlF_6 and Al_2O_3 , the two primary components in the Hall electrolyte.) In this paper, the phase relationships in these systems, as known at the present time, are reviewed.

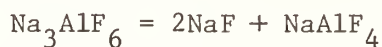
A. One Component Systems

1. Cryolite

Cryolite, Na_3AlF_6 , has been the subject of numerous investigations because of its importance in the industrial production of aluminum. The compound exists in both a low temperature (α) and high temperature (β) polymorphic form. The naturally occurring low temperature polymorph is monoclinic, space group $P2_1/n$, with cell parameters $a_0 = 5.40\text{\AA}$, $b_0 = 5.60\text{\AA}$, $c_0 = 7.78\text{\AA}$ and $\beta = 90^\circ 11'$.⁽¹⁾ Between 560 and 572°C ⁽²⁻⁶⁾ cryolite undergoes a rapid reversible transition to the high temperature cubic form, $a_0 = 7.962\text{\AA}$, with a heat of transition of 2238 cal./mole.⁽²⁾ Landon and Ubbelohde,⁽³⁾ on the basis of electrical conductance and thermal arrest data, reported the existence of a third polymorphic variety which they designated γ -cryolite. The β - γ inversion reportedly took place at 881°C with an estimated heat of transition of 200 cal./mole. Attempts by Foster⁽⁷⁾ to confirm this transition by electrical conductivity and high temperature X-ray diffraction methods were unsuccessful. More recent investigations have also failed to confirm the existence of a gamma form.

The melting point of natural cryolite has received a great deal of attention because of its importance in cryoscopic calculations. Melting points ranging from 977 to 1027°C have been reported^(3-6,8-13) with the majority of the more recent investigations yielding values close to 1009°C . Foster⁽¹⁴⁾, working with samples contained in sealed platinum tubes under carefully controlled conditions, used quenching methods to determine a melting temperature of 1009.2°C for natural Greenland cryolite. On the basis of a plot of the liquid fraction as a function of the temperature from which the samples were quenched the melting point of pure cryolite was determined as $1012 \pm 2^\circ\text{C}$.

The determination of the melting point of cryolite is complicated by the fact that the compound partially dissociates into several ionic subspecies on melting. Frank and Foster ⁽¹⁵⁾ employed calculations based on experimental densities to compare several possible reaction mechanisms. It was concluded that cryolite dissociated into NaAlF_4 and NaF on melting according to the reaction:



Foster and Frank ⁽¹⁶⁾ recognized that the calorimetric determination of the heat of fusion of cryolite (27.8 kcal./mole) included a heat effect due to partial dissociation. The true cryoscopic heat of fusion was determined to be 19.9 kcal./mole.

The refractive indices of the room temperature alpha form of cryolite are $\alpha = 1.3376$, $\beta = 1.3377$, and $\gamma = 1.3387$ ⁽¹⁷⁾.

2. Aluminum Fluoride

Aluminum fluoride is rhombohedral, space group $R\bar{3}$, with cell parameters $a_{\text{rh}} = 5.016\text{\AA}$ and $\alpha = 58^\circ 32'$ ⁽¹⁸⁾. The compound is uniaxial positive with indices of refraction of 1.3765 and 1.3767 ⁽¹⁹⁾.

O'Brien and Kelley ⁽⁴⁾, during an investigation of the heat contents of Na_3AlF_6 , AlF_3 and NaF , noted the existence of a new polymorph of AlF_3 . The transition to the high temperature form took place at 454°C and was accompanied by a weak heat effect of approximately 150 cal./mole. Holm and Holm ⁽²⁰⁾ used differential thermal analysis to confirm the existence of the polymorph, which they designated $\beta\text{-AlF}_3$, and set the transition temperature at 453°C . The new polymorph, also noted by Schultz et al. ⁽²¹⁾, could not be quenched to room temperature and no optical or X-ray diffraction data were reported. Shinn, Crocket and Haendley ⁽²²⁾ reported the existence of a third (gamma) polymorph of

AlF_3 , which could be obtained either by heating ammonium hexafluoroaluminate to 400°C or decomposing ammonium tetrafluoroaluminate. The transition to the new tetragonal form ($a_0 = 3.54\text{\AA}$ and $c_0 = 6.00$) took place at 300°C . No confirmation of the existence of this polymorph is found in the literature.

Mesrobian, Rolin and Pham ⁽²³⁾ studied mixtures of NaF and AlF_3 under pressure using thermal arrest methods. A peak at 1300°C for samples containing more than 50 wt. % AlF_3 was interpreted as resulting from a previously unknown inversion of AlF_3 . In addition, the triple point of pure AlF_3 was placed above 200 bars pressure and 1700°C . Aluminum fluoride is normally reported to sublime at 1291°C at 1 atmosphere pressure.

3. Calcium Fluoride

Calcium fluoride (fluorite) exists in only one form which has a face centered cubic structure, space group $\text{Fm}\bar{3}\text{m}$, and a cell parameter $a_0 = 5.4626$ ⁽²⁴⁾. Kojima et al. ⁽²⁵⁾ suggested that the variations in the melting point found in the literature ⁽²⁶⁾ are caused by slight hydrolysis during heating ($\text{CaF}_2 + \text{H}_2\text{O} \rightarrow \text{CaO} + 2\text{HF}$). Using anhydrous HF as a deoxidizing and purifying agent, the melting point of high purity CaF_2 was determined as 1423°C . The refractive index of the compound is 1.434 ⁽²⁷⁾.

4. Aluminum Oxide

Aluminum oxide, Al_2O_3 , exists in at least seven crystalline modifications which are arbitrarily designated as alpha, gamma, delta, eta, theta, kappa, and chi. The most common form, $\alpha\text{-Al}_2\text{O}_3$ or corundum, belongs structurally to space group $\text{R}\bar{3}\text{c}$ with cell parameters $a_{\text{hex}} = 4.758\text{\AA}$ and $c_{\text{hex}} = 12.991\text{\AA}$ ⁽²⁸⁾. Corundum is a uniaxial positive mineral with indices of refraction 1.768 and 1.760 ⁽²⁷⁾.

Eta aluminum oxide, like corundum, has been reported as the crystalline modification of Al_2O_3 present in certain areas of phase diagrams dealing with the electrolyte used in the smelting of aluminum⁽²⁹⁾. The eta form is cubic with a spinel type structure and cell parameter $a_0 = 7.94\text{\AA}$ ⁽³⁰⁾. The index of refraction is 1.670.

A metastable alumina phase designated as m-alumina by Foster⁽³¹⁾ and later as tau-alumina by Wefers and Bell⁽³²⁾ has also been reported. Tau-alumina converts first to eta- and finally to alpha-alumina on heating. The X-ray diffraction pattern is similar to mullite.

5. Lithium Fluoride

Lithium fluoride exists in one crystalline modification. It has the cubic NaCl type structure with a cell parameter of $a_0 = 4.0262$. The melting point of LiF has been reported to be between 845 and 848°C⁽³³⁻⁴²⁾.

B. Two Component Systems

1. System CaF_2 - AlF_3

The earliest investigation of the system was conducted by Fedotieff and Iljinsky⁽⁸⁾. On the basis of DTA data collected from samples heated in air, a eutectic system was identified. The invariant point was placed at 37.5 mole % AlF_3 and 820°C. Ravez and Hagenmuller⁽⁴³⁾ and Ravez et al.⁽⁴⁴⁾ reinvestigated the system using powder X-ray diffraction. Samples were encapsulated in copper and reacted at 600, 700, 800, and 840°C. One compound, CaAlF_5 , was identified and found to exist in both a low (alpha) and high (beta) temperature polymorph. Debye Sherrer patterns of α - CaAlF_5 were used to index the compound in the orthorhombic system with cell parameters $a_0 = 11.81 \pm 0.03\text{\AA}$, $b_0 = 9.16 \pm 0.02\text{\AA}$ and $c_0 = 6.35 \pm 0.01\text{\AA}$. The high temperature polymorph was found to be isotypic with CaFeF_5 and was also indexed in the orthorhombic system ($a_0 = 20.04 \pm$

0.03Å, $b_o = 9.81 \pm 0.01\text{Å}$, and $c_o = 7.31 \pm 0.01\text{Å}$). A structural analogy was noted between orthorhombic $\beta\text{-CaAlF}_5$ and tetragonal SrAlF_5 corresponding to the relationships:

$$\sqrt{2} a_{\text{SrAlF}_5} \approx a_{\beta\text{-CaAlF}_5}$$

$$b_{\text{SrAlF}_5} \approx \frac{\sqrt{2}}{2} b_{\beta\text{-CaAlF}_5}$$

$$c_{\text{SrAlF}_5} \approx c_{\beta\text{-CaAlF}_5}$$

DTA results established the transition and melting temperature of the compound at 820 and 850°C respectively. Pycnometric methods were used to determine the density of α - and $\beta\text{-CaAlF}_5$ as 3.09 and 2.96 g/cm³.

Holm⁽⁴⁵⁾ provided the first phase diagram of the system (Figure 1). He confirmed the existence of the 1:1 compound and on the basis of DTA data showed the α - β transition to take place at 740°C. The compound formed highly twinned crystals with a mean refractive index of 1.375 and a density of 2.947 g/cm³. Incongruent melting to AlF_3 and a liquid containing 44 mole % took place at 881°C. The eutectic for the system was located at 37 mole % AlF_3 and 828°C. Pronounced supercooling was noted in the area of the diagram containing 60% or more CaF_2 and DTA heating curves were therefore used to gather data in this region. No liquidus data were presented for the portion of the system richer in AlF_3 than the peritectic composition. Malinovsky, Vrbenska and Cakajdova⁽⁴⁶⁾ and Millet, Pham and Rolin⁽⁴⁷⁾ reinvestigated the system using thermal arrest methods and presented diagrams very similar to Holm's. Both studies confirmed the existence of CaAlF_5 in both a low

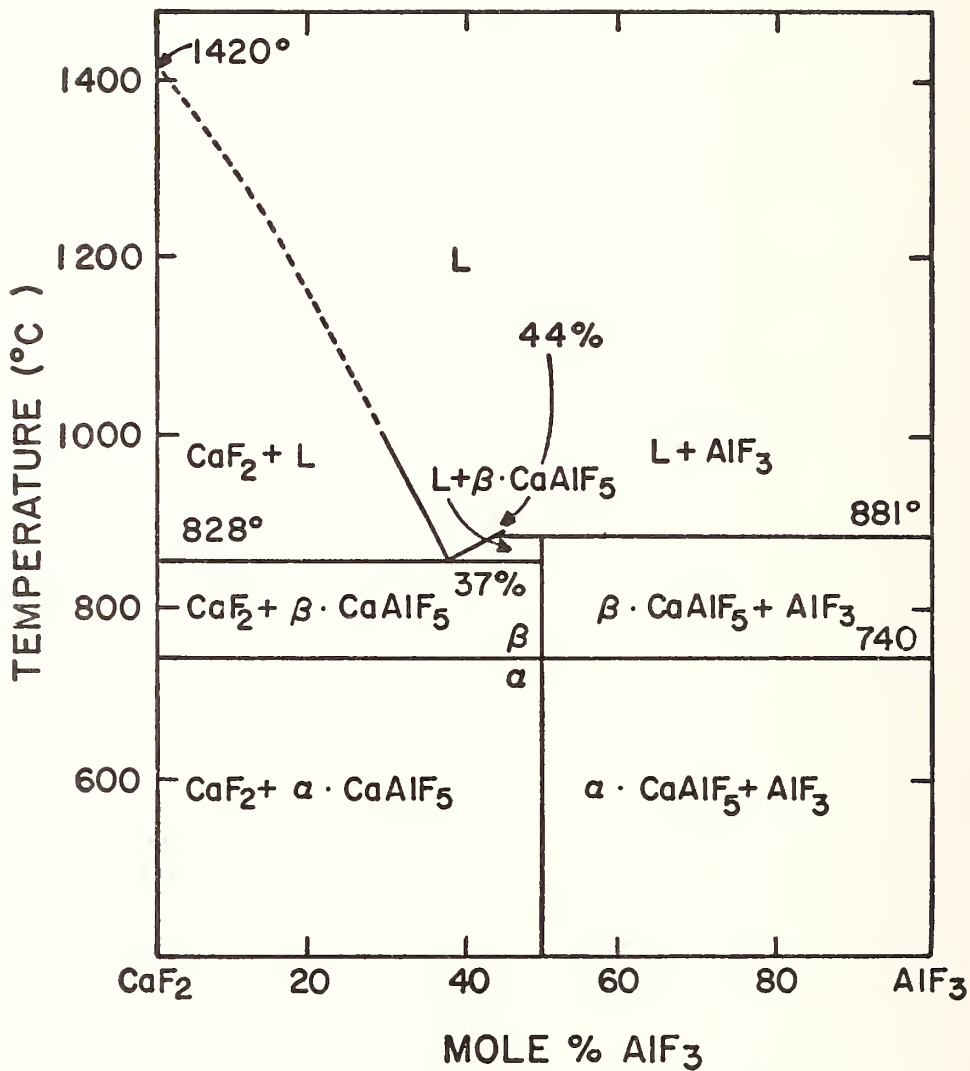


Figure 1. System CaF_2 - AlF_3 ⁽⁴⁵⁾.

and high temperature polymorphic form. Malinovsky et al. located the invariant points at 37.5 mole % AlF_3 and 829°C and 47.5 mole % AlF_3 and 893°C . Millet et al. reported slightly different compositions and temperatures (36 mole % AlF_3 and 820°C and 44 mole % AlF_3 and 880°C). The latter authors also noted that the extrapolation of the liquidus curve in the high AlF_3 end of the diagram indicated that the triple point of AlF_3 is in the neighborhood of 2250°C .

Craig and Brown⁽⁴⁸⁾, using a combination of optical microscopy, powder X-ray diffraction, quench techniques and differential thermal analysis, presented the phase diagram of the system shown in Figure 2. To prevent volatilization of AlF_3 , all heat treatments and DTA experiments were performed on samples encapsulated in sealed platinum tubes. Since pronounced supercooling existed in the system, DTA heating curves at $3^\circ\text{C}/\text{min}$ (as opposed to cooling curves) were used to obtain reaction temperatures. These temperatures were then verified by quenching experiments to insure they represented equilibrium data.

Two compounds were found to exist in the system. The 1:1 compound, noted by previous authors, melted incongruently at $873 \pm 3^\circ\text{C}$ to AlF_3 and a liquid containing 44 mole % AlF_3 . The α - β inversion remained constant at $743 \pm 3^\circ\text{C}$. A previously unreported 2:1 compound, Ca_2AlF_7 , was found to melt incongruently at $845 \pm 3^\circ\text{C}$ to CaF_2 and a liquid containing 35 mole % AlF_3 . The eutectic for the system was placed at 37.5 mole % AlF_3 and $836 \pm 3^\circ\text{C}$.

The authors noted that while Ca_2AlF_7 had not been previously reported a hydrated form $\text{Ca}_2\text{AlF}_7 \cdot 2\text{H}_2\text{O}$ and a hydrated hydroxide $\text{Ca}_4\text{Al}_2(\text{OH})_{14} \cdot 5\text{H}_2\text{O}$ ⁽⁴⁹⁾ are known to exist. The anhydrous compound was successfully formed using AlF_3 , $\text{AlF}_3 \cdot 3\text{H}_2\text{O}$ or CaAlF_5 as a starting material. The absence of

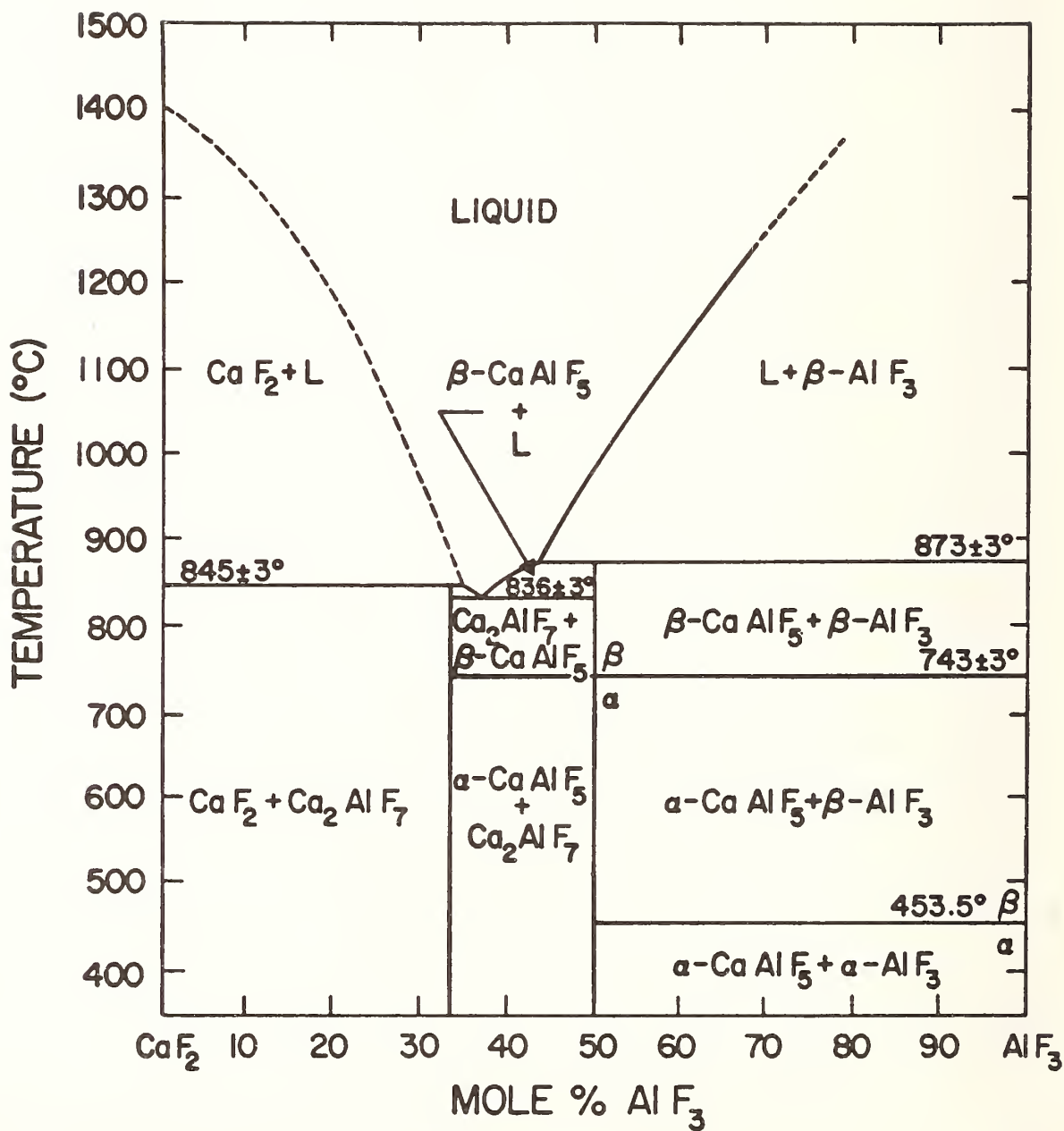


Figure 2. System CaF_2 - AlF_3 ⁽⁴⁸⁾.

any previous reports on the existence of the compound was attributed to its sluggish formation and to non-equilibrium cooling. Only the peritectic reaction was consistently observed during DTA heating experiments, but on cooling three peaks were observed. The lowest corresponded to the α - β CaAlF_5 inversion. Powder X-ray diffraction data of samples after DTA experiments showed a mixture of α - CaAlF_5 and AlF_3 which converted back to Ca_2AlF_7 on reheating.

The 2:1 compound was tentatively indexed on the basis of powder X-ray diffraction data ($\frac{1}{4}^\circ 2\theta/\text{min}-\text{CuK}\alpha$) as orthorhombic with lattice parameters $a_o = 18.22\text{\AA}$, $b_o = 9.06\text{\AA}$ and $c_o = 7.11\text{\AA}$ (Table I). A least squares cell refinement program developed by Evans, Appleman and Handwerker⁽⁵⁰⁾ was used to obtain the final cell parameters.

The structural relationships between β - CaAlF_5 and SrAlF_5 noted by Ravez et al.⁽⁴⁴⁾ were also found to exist between Ca_2AlF_7 and Sr_2AlF_7 . These suggest that the a and b parameters of the orthorhombic cell of Ca_2AlF_7 roughly coincide with the face diagonal and $\frac{1}{2}$ the face diagonal of the (001) plane of the tetragonal cell of Sr_2AlF_7 with c being common to both cells.

2. System Na_3AlF_6 - CaF_2

The first study of the Na_3AlF_6 - CaF_2 binary system was conducted by Pascal⁽¹³⁾ in 1913. He was primarily concerned with the liquidus curves reporting a eutectic at 47.8 mole % CaF_2 and 905°C . Minor modifications of the temperature and composition of the eutectic were made by Fedotieff and Iljinsky⁽⁸⁾ (48.1 mole % CaF_2 and 930°C), Matiasovský and Malinovský⁽⁵¹⁾ (50.5 mole % CaF_2 and 940°C), and Fenerty and Hollingshead⁽⁵²⁾ (48.6 mole % CaF_2 and 946°C).

TABLE I. Powder X-Ray Diffraction Data for the Compound $\text{Ca}_2\text{AlF}_7^*$

d_{obs}	d_{calc}	I/I_0	(hkl)
5.34	5.35	5	111
4.06	4.06	10	220
3.82	3.82	30	021
3.55	3.55	75	602
3.49	3.49	100	102
2.983	2.980	10	130
2.885	2.880	65	610
2.744	2.749	35	131
2.702	2.705	15	330
2.637	2.637	5	521
2.444	2.444	10	701
2.274	2.275	20	113
2.248	2.248	55	140
2.169	2.169	40	801
2.099	2.100	15	023
2.029	2.029	10	440
1.946	1.946	40	532
1.910	1.911	5	042
1.877	1.876	65	812
1.848	1.849	35	920
1.835	1.835	30	632
1.778	1.777	35	004
1.745	1.744	20	204
1.685	1.684	25	450
1.598	1.598	10	504

other reflections

$$a = 18.22\text{\AA}$$

$$b = 9.06\text{\AA}$$

$$c = 7.11\text{\AA}$$

*Evans, H. T., Appleman, D. E. and Handwerker, D. J., (1963)
Least Squares Refinement.

In 1961, Rolin⁽⁵³⁾ reported solidus data for the system. Using thermal arrest cooling curves of closely spaced compositions containing up to 53.5 mole % CaF_2 the eutectic was placed at 47.3 mole % CaF_2 and 946°C . Samples higher in Na_3AlF_6 than the eutectic composition showed a marked decrease in the eutectic temperature with increasing cryolite content. Rolin concluded that a large solid solution of CaF_2 in cryolite must exist, extending almost to the eutectic composition at 946°C . Following Rolin's suggestion that before the phase relations could be definitely established the system should be re-examined by other methods, Holm⁽⁵⁴⁾ studied the system using a combination of thermal analysis, DTA, X-ray diffraction, quenching techniques, optical microscopy and density determinations. The lack of a real eutectic halt on the high cryolite side of the diagram was again observed during DTA; however, a small exothermic peak at 785°C was also noted. Since this temperature is close to the reported eutectic temperature for the system $\text{NaF}-\text{Na}_3\text{AlF}_6-\text{CaF}_2$ ⁽⁸⁾ Holm postulated that the depression of the eutectic temperature seen by Rolin might be caused by volatilization of small amounts of AlF_3 or NaAlF_4 and not by solid solution. As further proof that solid solution of CaF_2 in Na_3AlF_6 does not exist, Holm noted that samples containing 5-90 mole % CaF_2 quenched from 950°C showed Na_3AlF_6 or CaF_2 in equilibrium with liquid. In addition, the densities of samples containing up to 60 mole % CaF_2 quenched from 970°C compared closely with calculated densities of mechanical mixtures of CaF_2 and Na_3AlF_6 . Holm's simple eutectic system showing no solid solution and a eutectic at 50 mole % CaF_2 and 945.5°C is shown in Figure 3.

Verdan and Monnier⁽⁵⁵⁾, using DTA experiments of samples contained in sealed crucibles, studied the system to resolve the controversy between

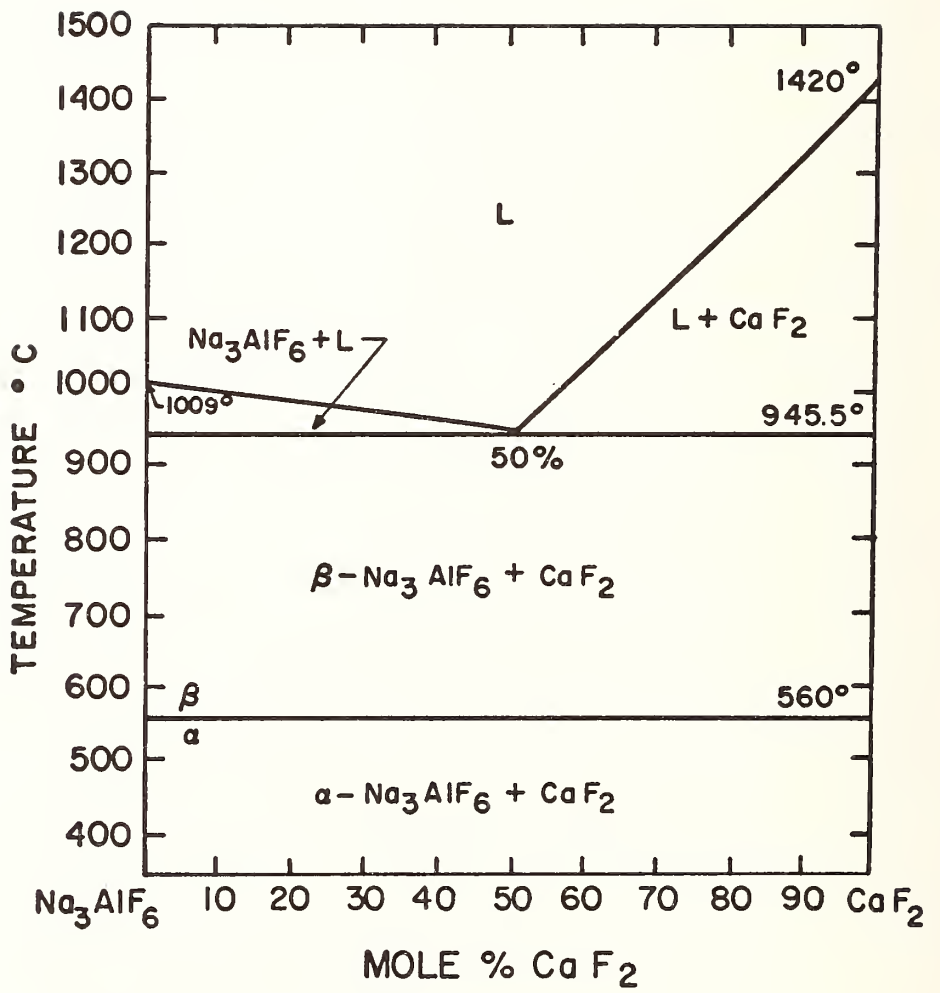


Figure 3. System Na₃AlF₆-CaF₂ ⁽⁵⁴⁾

Holm and Rolin over the existence of solid solution. They noted that the presence of a Na_3AlF_6 solid solution would explain the difficulty in purifying cryolite when CaF_2 is present. Liquidus and solidus data were obtained which indicated a solid solution of CaF_2 in Na_3AlF_6 approaching a maximum of 20 mole % CaF_2 at the eutectic temperature. A decrease in the α - β Na_3AlF_6 transition from 563°C for pure cryolite to 530°C for a sample containing between 5 and 6 mole % CaF_2 was also noted. A eutectoid reaction was, therefore, located at 5.5 mole % CaF_2 and 530°C (Figure 4).

Craig and Brown⁽⁵⁶⁾ studied samples containing 0-30 mole % CaF_2 using DTA of samples encapsulated in sealed platinum tubes. The α - β Na_3AlF_6 inversion remained constant at 567°C . No peaks corresponding to a solidus line were observed and all data agreed well with the simple eutectic diagram of the system presented by Holm.

3. System Na_3AlF_6 - AlF_3

The system Na_3AlF_6 - AlF_3 has been investigated periodically since the first published version by Fedotieff and Iljinsky⁽⁸⁾ in 1923. Foster⁽⁵⁷⁾ gives an excellent review of the more recent publications. A slightly altered version of his table of reported invariant points, compositions and temperatures is reproduced in Table II. The majority of the diagrams agree well with respect to the liquidus curve up to 30 wt. % AlF_3 ; however, there is disagreement above this value as to the location and composition of the invariant point(s), shape of the chiolite ($\text{Na}_5\text{Al}_3\text{F}_{14}$) liquidus curve and identity of the primary phase in equilibrium with liquid in the high AlF_3 end of the diagram.

A major point of contention is whether NaAlF_4 exists as a stable phase. Grjotheim⁽⁵⁾ reported NaAlF_4 to melt congruently at 731°C .

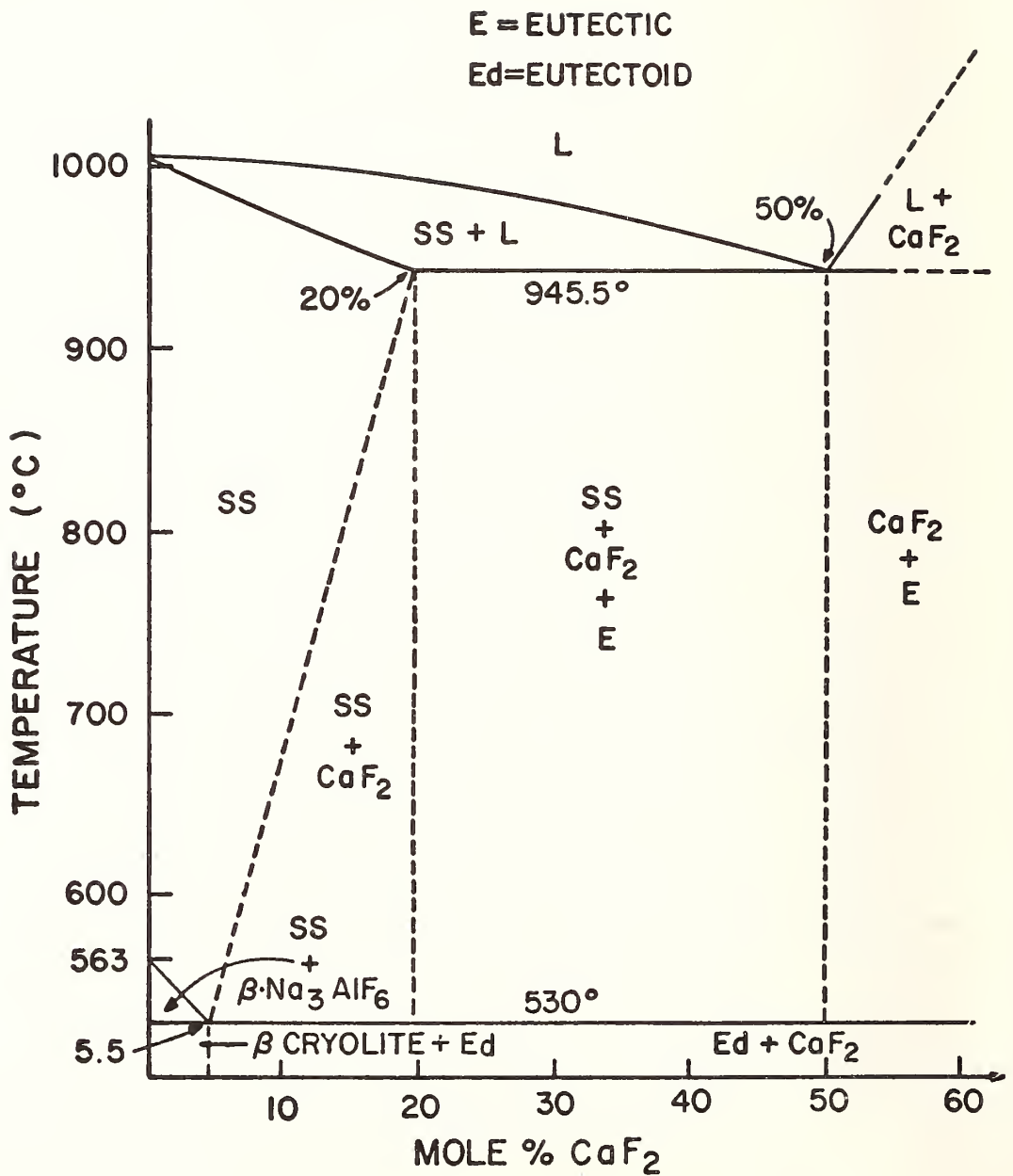


Figure 4. System $\text{Na}_3\text{AlF}_6\text{-CaF}_2$ (55).

TABLE II

Invariant Point Compositions and
Temperatures in the System Na_3AlF_6 - AlF_3

Ref.	Invariancy	Equilibrium Solid Phases	Liquid Composition (wt.%)		Temp. (°C)
			AlF_3	Na_3AlF_6	
5	Peritectic	Na_3AlF_6 $\text{Na}_5\text{Al}_3\text{F}_{14}$	28.6	71.4	734
	Eutectic (1)	$\text{Na}_5\text{Al}_3\text{F}_{14}$ NaAlF_4	35.3	64.7	690
	Eutectic (2)	NaAlF_4 AlF_3	49.8	50.2	704
10	Peritectic	Na_3AlF_6 $\text{Na}_5\text{Al}_3\text{F}_{14}$	30	70	734
	Eutectic	$\text{Na}_5\text{Al}_3\text{F}_{14}$ AlF_3	40	60	693
42	Peritectic	Na_3AlF_6 $\text{Na}_5\text{Al}_3\text{F}_{14}$	30	70	730
	Eutectic	$\text{Na}_5\text{Al}_3\text{F}_{14}$ AlF_3	38.5	61.5	684
37	Peritectic	Na_3AlF_6 $\text{Na}_5\text{Al}_3\text{F}_{14}$	30	70	739
	Eutectic	$\text{Na}_5\text{Al}_3\text{F}_{14}$ AlF_3	40	60	694
43	Peritectic	Na_3AlF_6 $\text{Na}_5\text{Al}_3\text{F}_{14}$	28.1	71.9	739
	Eutectic	$\text{Na}_5\text{Al}_3\text{F}_{14}$ AlF_3	36.6	63.4	700
44	Peritectic (1)	Na_3AlF_6 $\text{Na}_5\text{Al}_3\text{F}_{14}$	32.2	67.8	737
	Eutectic	$\text{Na}_5\text{Al}_3\text{F}_{14}$ NaAlF_6	37.5	62.5	690
	Peritectic (2)	NaAlF_4 AlF_3	38.7	61.3	710
	Eutectoid	$\text{Na}_5\text{Al}_3\text{F}_{14}$ NaAlF_4 AlF_3			680

TABLE II (Cont.)

Ref.	Invariancy	Equilibrium Solid Phases	Liquid Composition (wt.%)		Temp. (°C)
			AlF ₃	Na ₃ AlF ₆	
41	Peritectic	Na ₃ AlF ₆ Na ₅ Al ₃ F ₁₄	30	70	741
	Eutectic	Na ₅ Al ₃ F ₁₄ AlF ₃	39	61	694

Ginsberg and Wefers⁽⁵⁸⁾ agreed with Grjotheim that NaAlF_4 is a stable phase in the system but found it to melt incongruently at 710°C . In addition, a eutectoid reaction was found at 680°C with $\text{Na}_5\text{Al}_3\text{F}_{14}$ and AlF_3 forming at the expense of NaAlF_4 (Figure 5).

Several other authors^(10,52,59,60) have disagreed with the equilibrium existence of NaAlF_4 and presented diagrams showing AlF_3 as opposed to NaAlF_4 as an equilibrium solid at the eutectic. Holm⁽⁶⁰⁾ suggested that NaAlF_4 was not a stable phase since solid NaAlF_4 collected from the vapor above a melt of the same composition decomposed during differential thermal analysis at 500°C to $\text{Na}_5\text{Al}_3\text{F}_{14}$ and AlF_3 .

Foster⁽⁵⁷⁾, working with samples in sealed platinum tubes, used a combination of optical microscopy, DTA, X-ray diffraction and quench techniques to establish the diagram shown in Figure 6. It was concluded that NaAlF_4 is not a stable phase since (1) it was only found when liquid was present before quenching; (2) samples quenched from the region reported to contain NaAlF_4 and chiolite in equilibrium showed only chiolite and AlF_3 ; (3) samples quenched from the region of the diagram reported to have NaAlF_4 and liquid in equilibrium showed AlF_3 to be the primary crystalline phase; and (4) DTA (in sealed tubes) of melts that precipitated $\text{Na}_5\text{Al}_3\text{F}_{14}$ as the primary phase did not show any peaks that would indicate a phase field containing solid NaAlF_4 .

Mesrobian et al.⁽²³⁾ studied mixtures of AlF_3 and NaF and in addition to locating the triple point of AlF_3 above 200 bars pressure and 1700°C reported two new invariant lines in the system. The first was located by constant temperature peaks of thermal arrest cooling curves for compositions ranging from 45-95 wt. % AlF_3 at approximately 1300°C . It was postulated that the peaks were caused by an allotropic

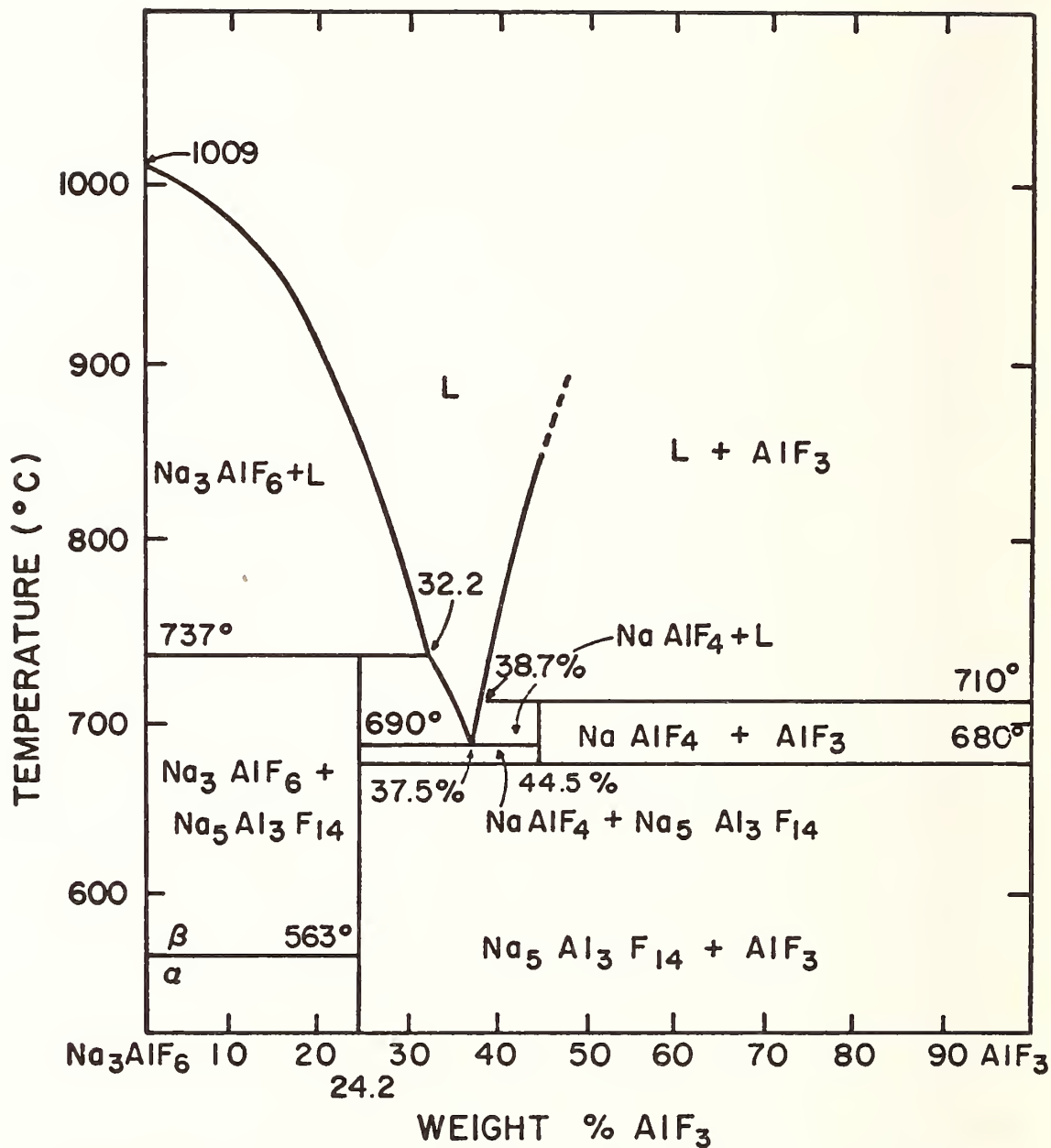


Figure 5. System NaAlF₆-AlF₃⁽⁵⁸⁾.

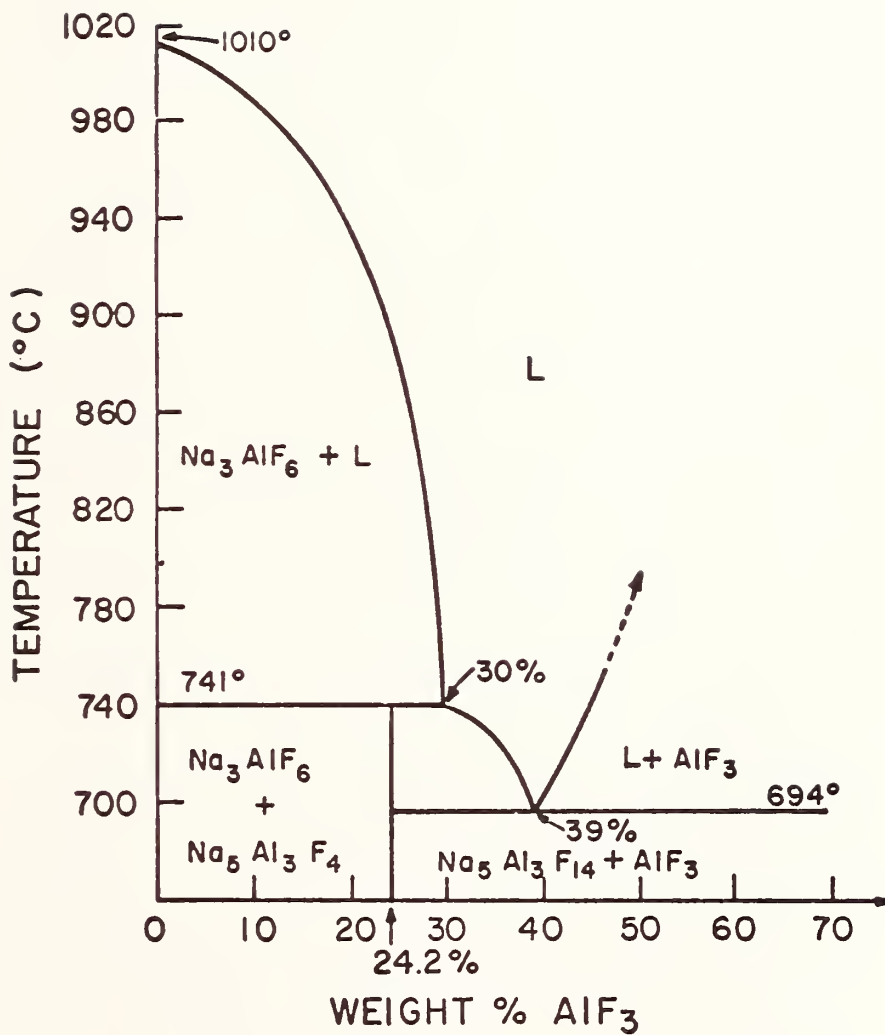


Figure 6. System Na_3AlF_6 - AlF_3 (57).

transformation of AlF_3 . A second set of peaks, measurable from 45-68 wt. % AlF_3 at 1250°C was considered to represent a peritectic line extending from an incongruently melting compound of possible composition NaAl_2F_7 . It was felt that, like NaAlF_4 , this new compound was unstable and decomposed on cooling and, therefore, is not seen in the subsolidus region.

4. System Na_3AlF_6 - Al_2O_3

A number of phase diagrams exist in the literature for the system Na_3AlF_6 - Al_2O_3 . Roush and Miyake⁽⁶¹⁾ reviewed the diagrams published up to 1925 and Phillips, Singleton and Hollingshead⁽¹⁰⁾ summarized the more recent works. There were significant differences between the various diagrams with the eutectic for the system ranging from 10 to 18.5 wt. % Al_2O_3 and 930 to 962°C . Several diagrams showed appreciable solid solubility. The possibility of solid solubility of Al_2O_3 in cryolite creates particular interest in the system because of its significance in the interpretation of the solution mechanism of Al_2O_3 in the Hall electrolyte and in the determination by cryoscopic methods of the number and structure of entities present in the molten binary mixtures.

Foster^(7,31) studied the cryolite-alumina binary using a combination of quench methods, optical microscopy and X-ray diffraction. The simple eutectic system with no solid solution and an invariant point at 10.5 wt. % Al_2O_3 and 961°C is shown in Figure 7. The primary phase on the low alumina side of the eutectic was identified by X-ray diffraction and refractive index measurements as cryolite. On the high alumina side of the eutectic the primary phase was found to be corundum. While the cryolite examined in the low-alumina end of the diagram was $\alpha\text{-Na}_3\text{AlF}_6$,

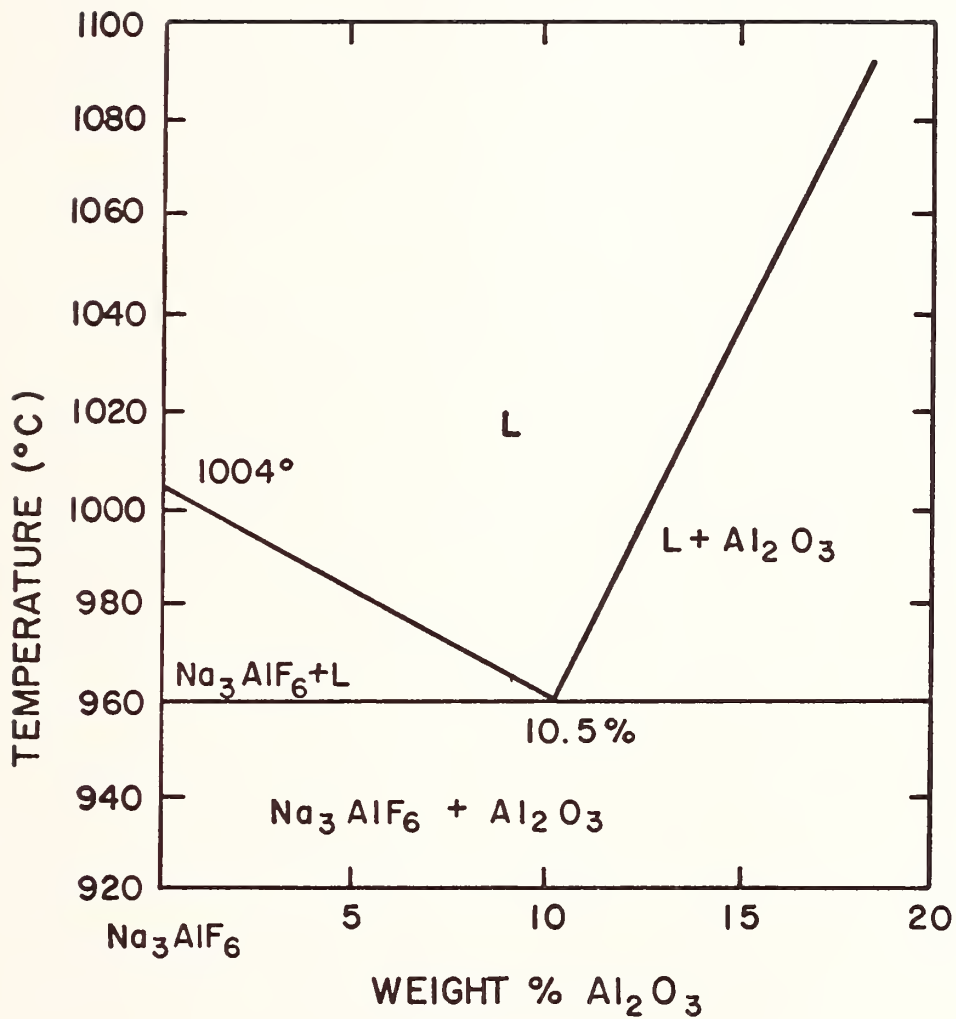


Figure 7. System Na_3AlF_6 - Al_2O_3 (7,31).

the existence of a solid solution in the high temperature form was ruled out since the alpha form did not contain polycrystalline fractures with alumina segregating at the boundaries. It was also noted that extremely rapid quenching from the liquid resulted in a new alumina phase (μ - or τ - alumina) with a diffraction pattern similar to mullite. On heating this phase transformed first to eta-alumina and then to corundum.

Rolin⁽⁶²⁾ reinvestigated the system using thermal arrest methods and arrived at the conclusion that if solid solution could not be totally disproved it was less than 1 wt. % Al_2O_3 . He presented a simple eutectic diagram with the invariant point at 11.5 wt. % Al_2O_3 and 960°C . However, the reported eutectic arrest for a sample containing 1 wt. % Al_2O_3 occurred 18°C below the established eutectic temperature. The decrease was attributed to the inability to obtain thermal equilibrium because of the large mass of solid pre-existing at the moment of eutectic crystallization. Duruz and Monnier⁽⁶³⁾ attempted to prove this assumption by investigating the system using DTA techniques. In order to avoid the problem of volatility, samples were sealed in a nickel container. Compositions containing as little as 0.5 wt. % Al_2O_3 showed a eutectic peak at the same temperature as samples containing 10 wt. % or more Al_2O_3 . Below 0.5 wt. % Al_2O_3 the sensitivity of the equipment was not sufficient to pick up the small thermal effect. A plot of the surface area of the eutectic peak versus the concentration of Al_2O_3 extrapolated through the origin indicated that no solid solution existed between 0 and 0.5 wt. % Al_2O_3 .

A substantial amount of literature is also available on the reaction mechanism for the solution of alumina in cryolite-alumina melts.

Foster and Frank⁽¹⁶⁾ reviewed the proposed reaction mechanisms and used Temkin's ionic model to calculate activities. A graph of $-\log a_c$ versus

1/T was then constructed to demonstrate that the scheme $3F^- + Al_2O_3 = 3/2AlO_2^- + 1/2AlF_6^{3-}$ was the most probable. However, considerable controversy still exists over the true reaction mechanism⁽⁶⁴⁾.

5. System $CaF_2-Al_2O_3$

The binary system $CaF_2-Al_2O_3$ was first studied in 1913 by Pascal⁽¹³⁾. Extensive solid solution at both ends of the system was noted. At the eutectic temperature 20 wt. % Al_2O_3 was soluble in CaF_2 and 71.5 wt. % CaF_2 was soluble in Al_2O_3 . The eutectic was placed at 26.5 wt. % Al_2O_3 and 1270°C.

Gunther et al.⁽⁶⁵⁾, during a study of the luminescence of phosphors of the aluminum oxide - calcium fluoride type, reported the existence of a 1:5 compound $CaAl_{10}O_{15}F_2$. The compound was obtained by heat treating CaF_2 and $NH_4(SO_4)_2 \cdot 12H_2O$ with small amounts of $MnSO_4 \cdot 4H_2O$ (added as an activator) in air at 1200-1450°C.

Using quench methods, Kuo and Yen⁽⁶⁶⁾ reported a simple eutectic diagram for the system with the invariant point at 7 mole % Al_2O_3 and 1290°C. Neither the extensive solid solution nor the compound formation reported earlier could be verified. The authors noted that, while in a closed system CaF_2 and Al_2O_3 were the stable coexisting phases, in open air under ordinary atmospheric conditions $CaAl_4O_7$ formed as the unique product according to one of the two reaction schemes shown below.

1. $CaF_2 + 2Al_2O_3 + H_2O \rightarrow CaAl_4O_7 + 2HF$
2. (a) $3CaF_2 + 7Al_2O_3 \rightarrow 3CaAl_4O_7 + 2AlF_3$
 (b) $2AlF_3 + 3H_2O \rightarrow Al_2O_4 + 6HF$

Chatterjee and Zhmoidin⁽⁶⁷⁾ reinvestigated the system by sintering samples in hermetically sealed capsules. Quenching, DTA, and optical microscopy were used to obtain data which suggested a eutectic system.

The invariant point was placed at approximately 2 wt. % Al_2O_3 and 1395°C . The liquidus curve had a pronounced "S" shape suggestive of metastable liquid phase separation.

6. System $\text{AlF}_3\text{-Al}_2\text{O}_3$

While numerous authors^(29,68-71) have reported results in ternary and quaternary systems involving the binary system $\text{AlF}_3\text{-Al}_2\text{O}_3$, their investigations have been confined to portions of the diagrams far removed from the binary system. At the present time no phase equilibrium data are available on the system.

7. System LiF-AlF_3

The numerous investigations^(69,72-78) of the LiF-AlF_3 system are summarized in Table III. Good agreement exists between the reported diagrams. One compound, lithium cryolite (Li_3AlF_6), melts congruently between 782° and 800°C and divides the system into two simple binaries ($\text{LiF-Li}_3\text{AlF}_6$ and $\text{Li}_3\text{AlF}_6\text{-AlF}_3$). The eutectic for the $\text{LiF-Li}_3\text{AlF}_6$ system has been reported between 14.5 and 16.5 mole % AlF_3 and between 705° and 715°C . The $\text{Li}_3\text{AlF}_6\text{-AlF}_3$ system has been reported to contain a eutectic between 35 and 37 mole % AlF_3 and between 690° and 711°C .

The representative diagram of the system shown in Figure 8 is that presented by Holm⁴² based on TA and DTA.

The polymorphism and structure of the compound lithium cryolite have been the subject of four studies⁽⁷⁹⁻⁸²⁾. Garton and Wanklyn⁽⁷⁹⁾ used high temperature X-ray diffraction and standard DTA methods to identify five polymorphs, α -, β -, γ -, δ -, and ϵ - Li_3AlF_6 .

The α - β transition took place at 210°C . Both forms were reported as hexagonal with cell parameters $a = 9.70\text{\AA}$ and $c = 12.32\text{\AA}$ and $a = 13.71\text{\AA}$ and $c = 12.32\text{\AA}$ respectively. The third polymorph, γ - Li_3AlF_6 was stable

TABLE III

Reported Eutectic Compositions and Temperatures in the System LiF-AlF₃ and the Melting Point of Li₃AlF₆

Author(s)	Equilibrium Solid Phases	Liquid Composition of Eutectic (Mole%)	Eutectic Temperature (C°)	M.P. Li ₃ AlF ₆
Puschin and Baskow (72)	LiF, Li ₃ AlF ₆	14.5 AlF ₃ 85.5 LiF	705	800
	Li ₃ AlF ₆ , AlF ₃	37 AlF ₃ 63 LiF	690	
Fedotieff and Timofeeff (73)	LiF, Li ₃ AlF ₆	15 AlF ₃ 85 LiF	715	790
	Li ₃ AlF ₆ , AlF ₃	36 AlF ₃ 64 LiF	710	
Dergunov (74)	LiF, Li ₃ AlF ₆	16.5 AlF ₃ 83.5 LiF	706	792
	Li ₃ AlF ₆ , AlF ₃	--- ---	---	
Thoma et al. (75)	LiF, Li ₃ AlF ₆	14.5 AlF ₃ 85.5 LiF	711	785
	Li ₃ AlF ₆ , AlF ₃	36 AlF ₃ 64 LiF	710	
Rolin et al. (69)	LiF, Li ₃ AlF ₆	--- ---	---	782
	Li ₃ AlF ₆ , AlF ₃	35.5 AlF ₃ 64.5 LiF	---	
Malinovsky et al. (76)	LiF, Li ₃ AlF ₆	15 AlF ₃ 85 LiF	711	782
	Li ₃ AlF ₆ , AlF ₃	35 AlF ₃ 65 LiF	708	
Rolin et al. (77)	LiF, Li ₃ AlF ₆	15.5 AlF ₃ 84.5 LiF	711	782
	Li ₃ AlF ₆ , AlF ₃	--- ---	---	
Matiasovsky and Malinovsky (78)	LiF, Li ₃ AlF ₆	15 AlF ₃ 85 LiF	711	782
	Li ₃ AlF ₆ , AlF ₃	35 AlF ₃ 65 LiF	708	
Holm (42)	LiF, Li ₃ AlF ₆	14.5 AlF ₃ 85.5 LiF	710	785
	Li ₃ AlF ₆ , AlF ₃	35.5 AlF ₃ 64.5 LiF	709	
Garton and Wanklyn (79)	LiF, Li ₃ AlF ₆	--- ---	---	783
	---	---	---	

TABLE III (Cont.)

Author(s)	Equilibrium Solid Phases	Liquid Composition of Eutectic (Mole%)		Eutectic Temperature (C°)	M.P. Li ₃ AlF ₆
Holm ⁽⁸⁰⁾	---	---	---	---	780
	---	---	---	---	

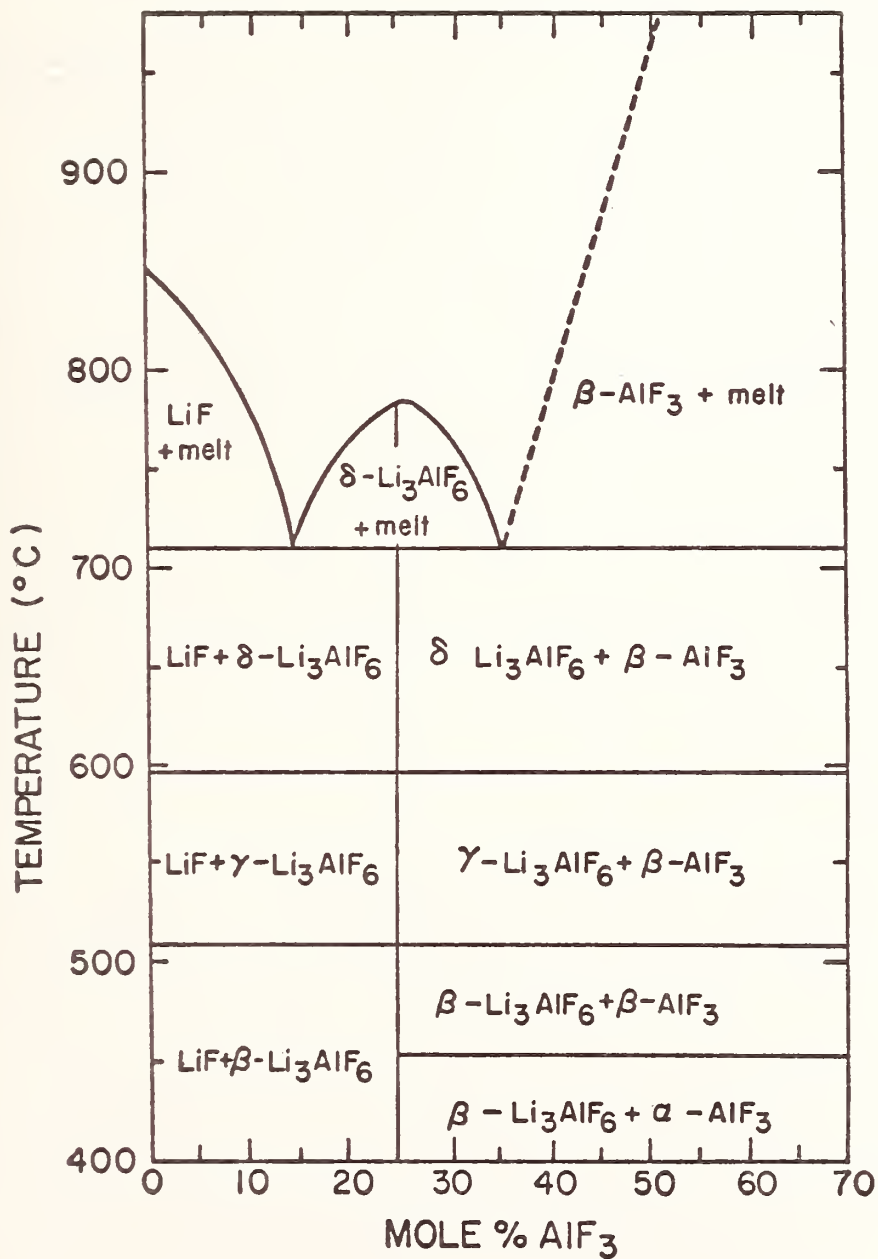


Figure 8. System $\text{LiF}-\text{AlF}_3$ ⁽⁴³⁾.

between 515°C and 604°C where it converted to δ -Li₃AlF₆. Crystallographic data on the γ polymorph conformed with a cubic unit cell, $a = 14.2\text{\AA}$ (at 596°C). The high temperature polymorph, ϵ -Li₃AlF₆, was found to be stable from 705°C to its melting point at 703°C. No crystallographic data was reported for the δ and ϵ forms.

Holm⁽⁸⁰⁾ studied lithium cryolite using DTA methods and powder X-ray diffraction. He found 3 polymorphs of Li₃AlF₆ and inversion temperatures at 505°C and 597°C. The compound was reported to melt at 780°C. The high temperature form was reported to have the garnet structure with a cubic unit cell ($a = 12.03 \pm 0.05\text{\AA}$ at $625 \pm 10^\circ\text{C}$). The low temperature form was orthorhombic with cell dimensions $a = 8.39\text{\AA}$, $b = 11.92\text{\AA}$ and $c = 7.82\text{\AA}$. No data were reported on the intermediate temperature polymorph.

Burns, Tennissen and Brunton⁽⁸¹⁾ used single crystal X-ray diffraction to study α -Li₃AlF₆. They reported an orthorhombic unit cell with parameters $a = 9.510$, $b = 8.2295$ and $c = 4.8762\text{\AA}$. Their X-ray powder pattern agreed with the pattern reported for α -Li₃AlF₆ by Garton and Wanklyn⁽⁸⁰⁾.

The discrepancies in all reported parameters lead Holm and Jenssen⁽⁸²⁾ to reinvestigate the polymorphy and structure of Li₃AlF₆. DTA heating curves resulted in transformation peaks at 510°C and 597°C. These values were reported as the $\beta \rightarrow \gamma$ -Li₃AlF₆ and $\gamma \rightarrow \delta$ -Li₃AlF₆ inversions. The α -Li₃AlF₆ polymorph was not seen after normal cooling, but was observed along with β -Li₃AlF₆ in samples quenched from 647°C and 790°C. The beta polymorph was reported to be orthorhombic with cell parameters $a = 11.78\text{\AA}$, $b = 8.43\text{\AA}$ and $c = 7.77\text{\AA}$. It was stable up to 510°C where it converted to the tetragonal gamma form with cell parameters of

$a = 11.81\text{\AA}$ and $c = 8.74\text{\AA}$. The final transformation of Li_3AlF_6 took place at 592°C when $\gamma\text{-Li}_3\text{AlF}_6$ converted to a cubic polymorph designated δ . The cell edge of $\delta\text{-Li}_3\text{AlF}_6$ is $a = 11.98\text{\AA}$.

The authors believe that the 705°C peak reported by Garton and Wanklyn⁽⁸⁰⁾ corresponded to the eutectic in the LiF-AlF_3 system reported in the literature.

8. System $\text{LiF-Na}_3\text{AlF}_6$

The system $\text{LiF-Na}_3\text{AlF}_6$ has been investigated numerous times⁽³³⁻⁴²⁾ with widely divergent results being reported. Diagrams of a simple eutectic, limited solid solubility of LiF and mutual solubility of both end members have all been reported. The reported extents of the solid solutions, in particular that of LiF in Na_3AlF_6 , differ by as much as 60 mole %.

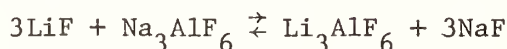
After studying the liquidus curve, Chu and Belyaev⁽³³⁾ reported the eutectic composition as 83.5 mole % LiF with a eutectic temperature of 700°C . Holm⁽³⁴⁾ reported a eutectic temperature of 693°C as did Jenssen⁽³⁵⁾. Jenssen⁽³⁵⁾ located the eutectic composition at 15.4 mole % Na_3AlF_6 .

Lewis⁽⁴⁰⁾ differed with earlier investigators and reported mutual solid solubility of the end members. Approximately 69 mole % LiF was soluble in Na_3AlF_6 and 3 mole % Na_3AlF_6 in LiF . The eutectic was located at 87 mole % LiF and 703°C .

The first investigation reporting the system to exhibit only partial solid solubility of LiF in Na_3AlF_6 was conducted by Matiasovsky and Malinovsky⁽³⁷⁾. Using TA and X-ray phase analysis the extent of solution was set at 70 mole % LiF and the eutectic was located at 14.4 mole % Na_3AlF_6 and 700°C . Holm⁽³⁸⁾ reinvestigated the system and sharply decreased the amount of LiF soluble in Na_3AlF_6 . The extent of solid solution was

12 mole % LiF and the eutectic was placed at 15 mole % Na_3AlF_6 and 694°C . Kostenska⁽³⁹⁾ further reduced the solubility of LiF to 6 mole % Na_3AlF_6 and 696°C .

Holm⁽⁴²⁾ used TA, DTA, quenching techniques and X-ray diffraction to study the system (Figure 9). He found the subsolidus region below 550°C to be a pseudobinary due to the presence of only two phases, $\alpha\text{-Na}_3\text{AlF}_6$ and LiF. He reported the solid-liquid region to be part of the ternary reciprocal system



as a result of a formation of solid solutions between Li_3AlF_6 and Na_3AlF_6 .

Foster⁽⁴¹⁾, realizing the problem of volatilization, encapsulated his samples in sealed platinum tubes. Working under carefully controlled conditions and employing both quench methods and refractive index measurements, he determined mutual solubility of both end members. By assuming Raoult behavior, the amount of LiF soluble in Na_3AlF_6 was calculated to be 14.4 mole %. Cryolite was found to be soluble in LiF up to 6.8 mole %. The eutectic was located at 85.3 mole % LiF. The diagram is shown in Figure 10.

9. System $\text{Na}_3\text{AlF}_6\text{-Li}_3\text{AlF}_6$

The $\text{Na}_3\text{AlF}_6\text{-Li}_3\text{AlF}_6$ system has been studied many times with little agreement between investigators⁽⁸³⁻⁸⁹⁾. The first study was made in 1936 by Drossbach⁽⁸³⁾. Using thermal methods he reported a continuous solid solution between the end members. Solidus temperatures ranged from 10 to 15°C below the liquidus and a thermal minimum was located at 70 mole % Li_3AlF_6 .

Mashovets and Petrov⁽⁸⁴⁾ found the system to be a simple eutectic with no solid solution. Thermal and optical studies were employed and the eutectic was found at 710°C and 62 mole % Li_3AlF_6 .

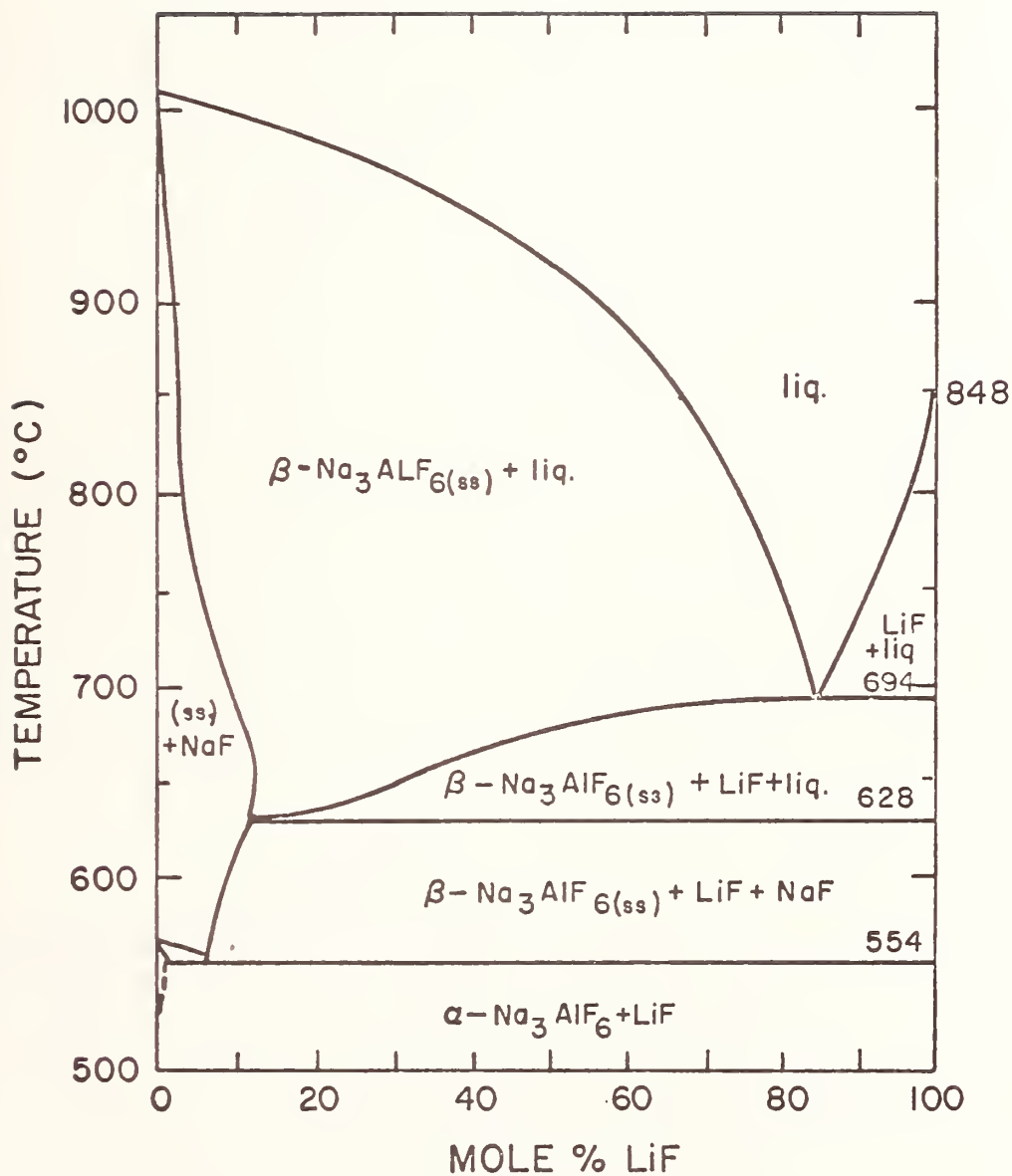


Figure 9. System Na_3AlF_6 - LiF ⁽⁴²⁾.

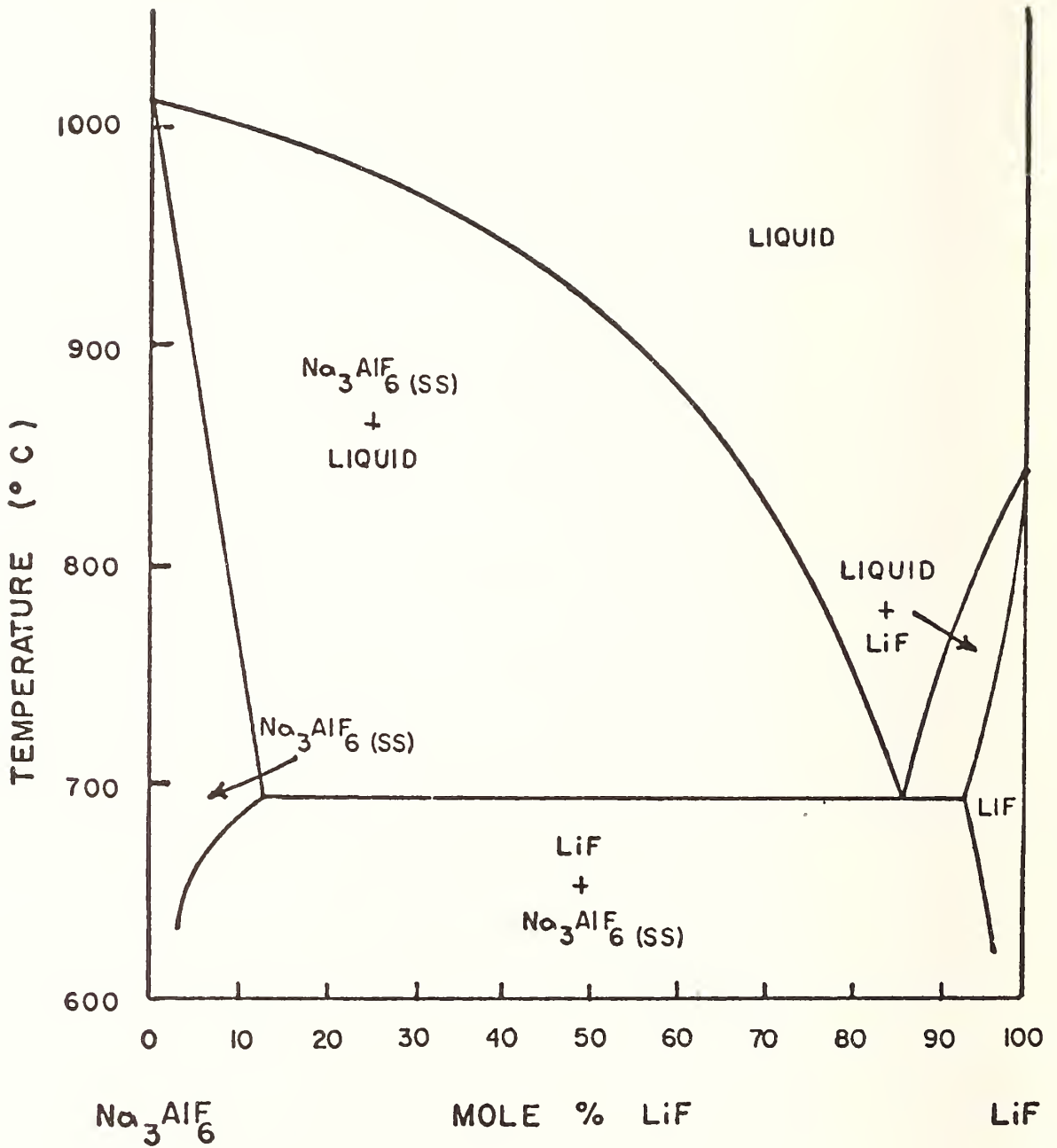


Figure 10. System Na_3AlF_6 - LiF ⁽⁴¹⁾.

Another study⁽⁸⁵⁾ reported three compounds to exist. Beletskii and Saksonov reported compounds corresponding to the formulas $\text{Li}_3\text{Na}_6\text{Al}_3\text{F}_{18}$, $\text{Li}_6\text{Na}_3\text{Al}_3\text{F}_{18}$ and $\text{Li}_{15}\text{Na}_3\text{Al}_6\text{F}_{36}$. No compound having the formula of the naturally occurring mineral cryolithionite, $\text{Na}_3\text{Li}_3\text{Al}_2\text{F}_{12}$, was reported.

Rolin and Muhlethaler⁽⁶⁹⁾ used cooling curves to examine the system. They found a continuous series of solid solutions on the Li_3AlF_6 side up to the eutectic point of 62.3 mole % Li_3AlF_6 and 713°C . Solid solution extended to 36 mole % Li_3AlF_6 on the Na_3AlF_6 side.

Garton and Wanklyn⁽⁸⁶⁾ used X-ray analysis, quenching techniques, and DTA results in studying the system. Two compounds were found, one corresponding to the natural mineral cryolithionite, $\text{Na}_3\text{Li}_3\text{Al}_2\text{F}_{12}$ and another compound of the formula $\text{Na}_2\text{LiAlF}_6$. Cryolithionite was found to exist as a nonstoichiometric solid solution which decomposed to Li_3AlF_6 and a phase of Na_3AlF_6 at 680°C . The second compound, $\text{Na}_2\text{LiAlF}_6$ was found to decompose at 500°C .

Holm and Holm⁽⁸⁷⁾ used DTA and high temperature X-ray analysis to confirm the existence of the two compounds. Each existed up to approximately 500°C . $\text{Na}_2\text{LiAlF}_6$ was found to exist in two polymorphic forms. The α polymorph was indexed on the basis of a monoclinic unit cell with parameters $a = 7.538\text{\AA}$, $b = 7.516\text{\AA}$ and $c = 7.525\text{\AA}$. On heating, $\alpha\text{-Na}_2\text{LiAlF}_6$ converted to cubic $\beta\text{-Na}_2\text{LiAlF}_6$ ($a = 7.639\text{\AA}$ at 445°C). The transformation could not be detected by DTA but high temperature X-ray diffraction showed the inversion to be complete at 420°C . $\text{Na}_3\text{Li}_3\text{Al}_2\text{F}_{12}$ was identical to naturally occurring cryolithionite ($a = 12.127\text{\AA}$ at 20°C). The study also revealed one new phase present between 560°C and 630°C from 90 to 99 mole % Li_3AlF_6 . The new phase was indexed based on a tetragonal unit cell with parameters

$a = 11.97\text{\AA}$ and $c = 8.73\text{\AA}$ (625°C). Although no solid solution was found at room temperature, an extensive amount was reported at high temperatures. The liquidus curve reached a minimum at 64 mole % Li_3AlF_6 and 710°C .

Baylor et al.⁽⁸⁸⁾ found Li_3AlF_6 to be soluble in Na_3AlF_6 up to a maximum of 18 mole %. Cryolithionite and $\text{Na}_2\text{LiAlF}_6$ were reported to decompose between 500 and 600°C . Stinton and Brown⁽⁸⁹⁾ used DTA and X-ray diffraction to study the system. Samples were sealed in platinum tubes to prevent volatilization during firing and DTA experiments. Their liquidus curve agreed well with that of Holm and Holm⁽⁸⁷⁾. The eutectic was placed at 64 mole % Li_3AlF_6 and 713°C and no solid solution was reported below 500°C . An intermediate solid solution denoted α' - Na_3AlF_6 was found to be stable between 530°C and 758°C and 10 and 38 mole % Li_3AlF_6 . Their diagram is pictured in Figure 11.

10. System Li_3AlF_6 - Al_2O_3

The first study of the system was made in 1936 by Drossbach⁽⁸³⁾ Using thermal methods he reported a simple eutectic system with the invariant point at 782°C and 1 wt. % Al_2O_3 . Mashovets and Petrov⁽⁸⁴⁾ used samples containing up to 6 wt. % Al_2O_3 to revise the eutectic location to $775 \pm 3^{\circ}\text{C}$ and 1.1 mole % Al_2O_3 . Cassidy and Brown⁽⁹⁰⁾ reexamined the system using samples encapsulated in sealed platinum tubes. Optical microscopy, X-ray diffraction, quench methods and DTA (on samples in platinum tubes) were used to place the eutectic at 773°C and 0.5 mole % Al_2O_3 . The diagram is shown in Figure 12.

11. System LiF - CaF_2

The studies of the LiF - CaF_2 system are summarized in Table IV. All investigators⁽⁹¹⁻¹⁰⁰⁾ used thermal arrest methods and reported data consistent with a simple binary eutectic system. The invariant point was

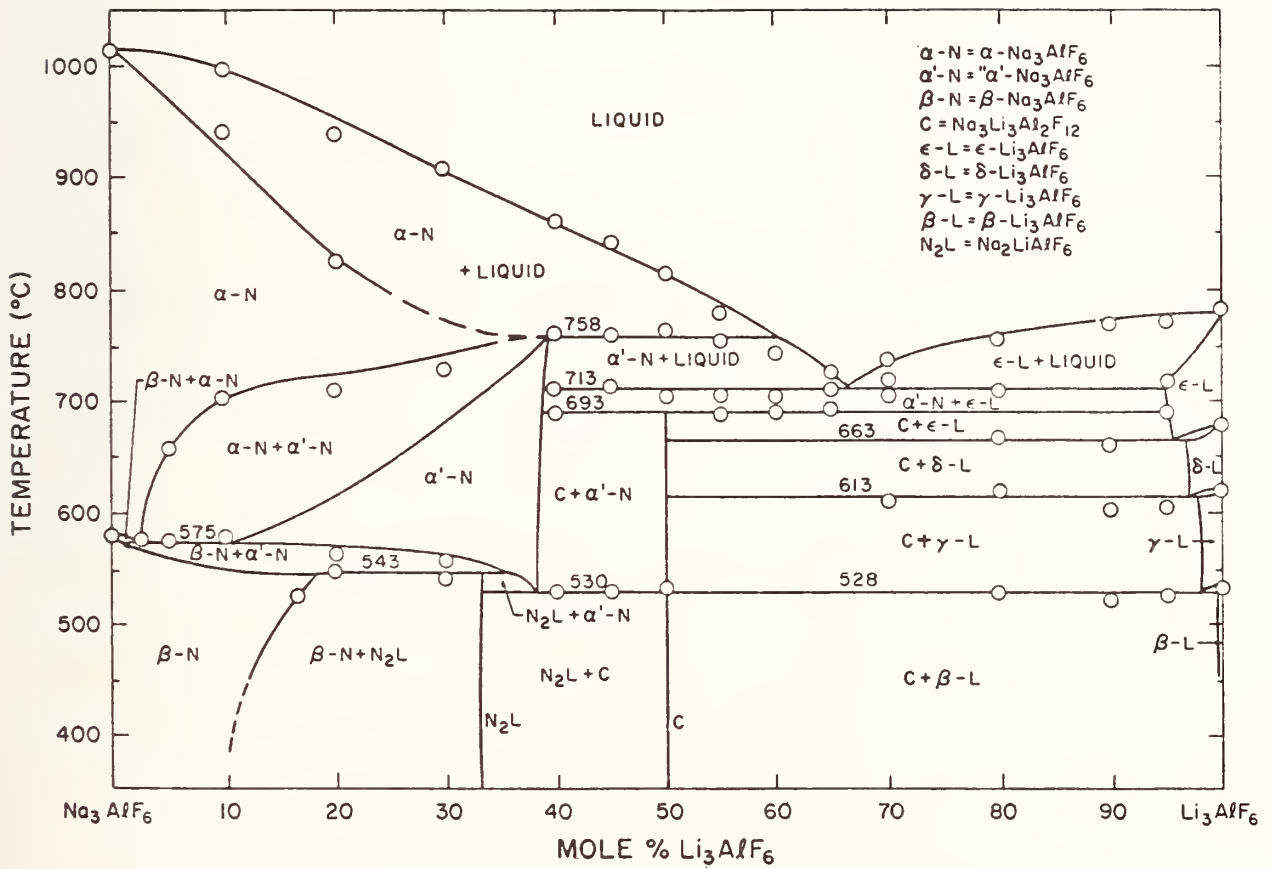


Figure 11. System $\text{Na}_3\text{AlF}_6\text{-Li}_3\text{AlF}_6$ (89).

TABLE IV

Composition and Temperature of the Eutectic
in the System LiF-CaF₂

Author(s)	Composition of Liquid (Mole %)		Temperature (°C)
	LiF	CaF ₂	
Ruff and Busch ⁽⁹¹⁾	79	21	765
Roake ⁽⁹³⁾	80.5	19.5	769
Barton, Bratcher and Grimes ⁽⁹⁵⁾	81	19	773
Bukhalova, Sulaymankulov and Bostandzhiyon ⁽⁹⁶⁾	85.5	14.5	766
Deadmore and Machin ⁽⁹⁷⁾	77	23	760
Vrbenska and Malinovsky ⁽⁹⁹⁾	79	21	755
Kostenska, Vrbenska and Malinovsky ⁽¹⁰⁰⁾	80.5	19.5	769

consistently reported to be between 77 and 85.5 mole % LiF and 755 to 773°C. The representative diagram for the system shown in Figure 13 is the most recent version reported by Kostenska et al.⁽¹⁰⁰⁾

12. System Li_3AlF_6 - CaF_2

The only study of the Li_3AlF_6 - CaF_2 system reported in the literature is by Vrbenska and Malinovsky⁽⁹⁹⁾. Based on data obtained by thermal analysis methods a simple eutectic system was presented (Figure 14). The eutectic was located at 703°C and 43 mole % CaF_2 .

C. Three Component Systems

1. System CaF_2 - AlF_3 - Na_3AlF_6

Fedotieff and Illjinsky⁽⁸⁾ presented a liquidus surface diagram of the CaF_2 - AlF_3 - NaF ternary system based on the results of differential thermal analysis experiments, performed in air, on over 100 compositions. At the time of the work no ternary compounds were known to exist and only chiolite and cryolite were identified in any of the binary systems. Two ternary eutectics were reported. The first was located at 50.2 mole % NaF, 5.0 % CaF_2 and 44.8% AlF_3 and 675°C with AlF_3 in equilibrium with Na_3AlF_6 and CaF_2 . The second eutectic was placed at approximately 73 mole % NaF, 20% CaF_2 and 7% AlF_3 and 780°C with NaF in equilibrium with Na_3AlF_6 and CaF_2 . A ternary peritectic was found at approximately 49 mole % NaF, 10% CaF_2 and 41% AlF_3 and 705°C with chiolite, cryolite and CaF_2 in equilibrium.

Rolin⁽¹⁰¹⁾, using thermal arrest methods, investigated the portion of the CaF_2 - AlF_3 - Na_3AlF_6 system containing 24 and 62.5 mole % or less CaF_2 and AlF_3 respectively. Phases precipitating from the melt were identified by the shape and sharpness of the thermal arrest peaks. A ternary eutectic was located at 35.9 mole % cryolite, 56.7% AlF_3 and 7.4% CaF_2

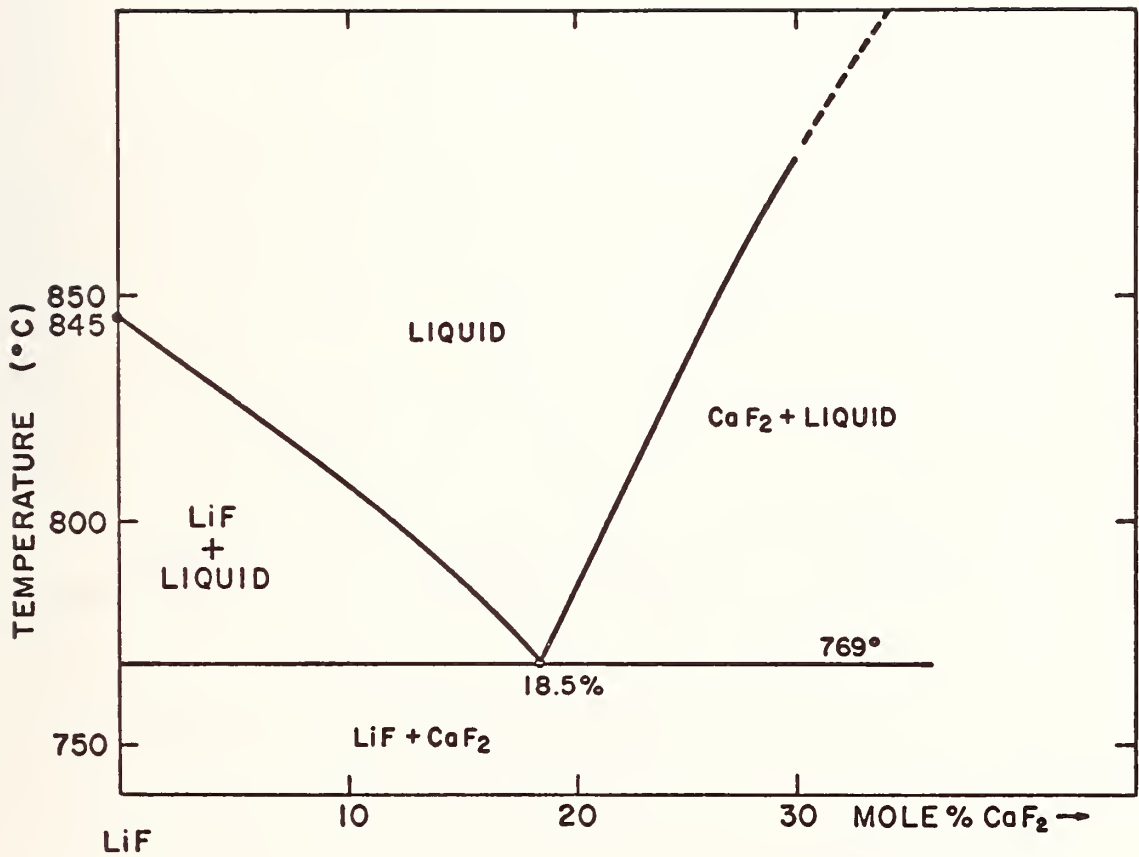


Figure 13. System LiF-CaF₂⁽¹⁰⁰⁾.

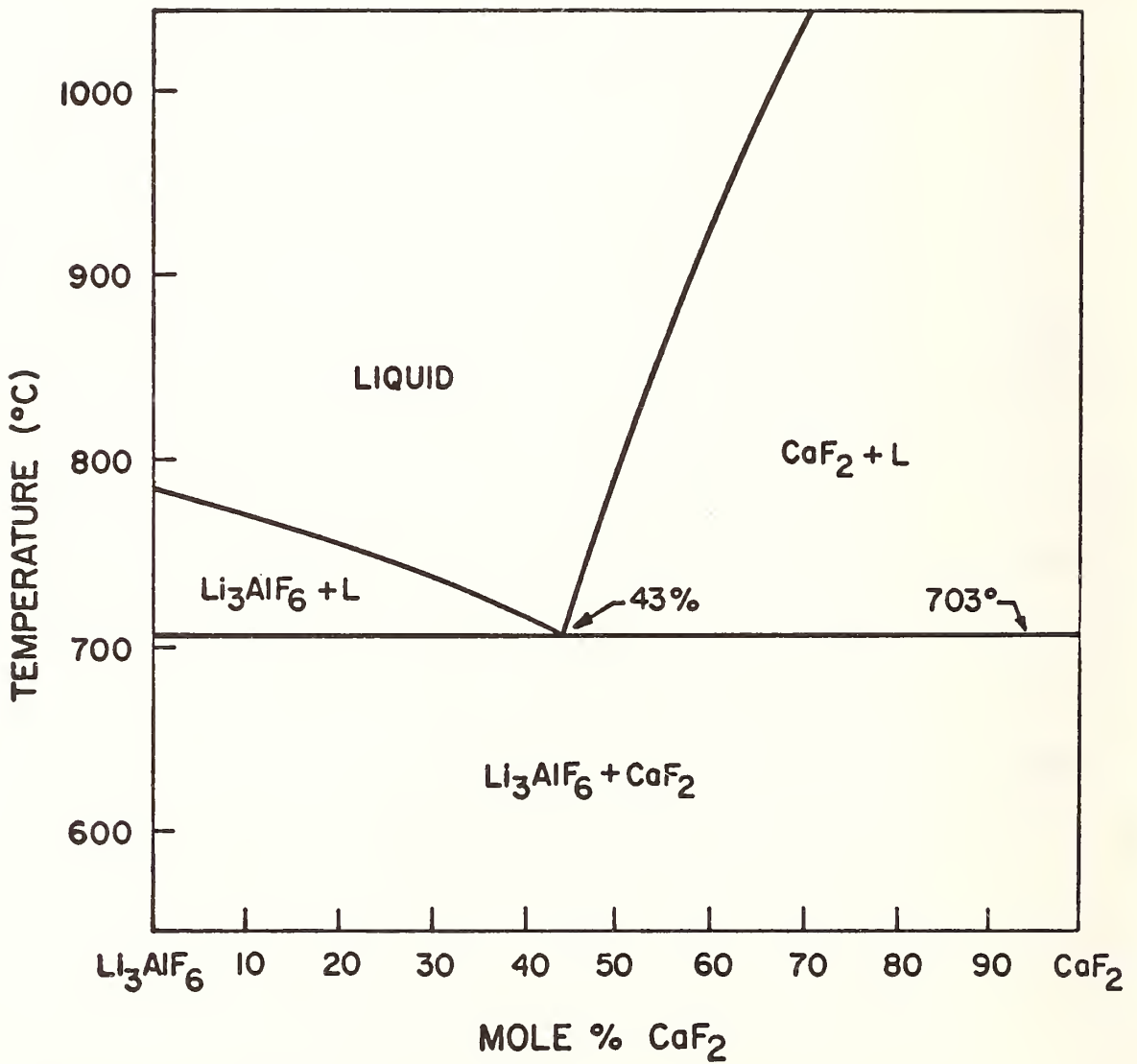


Figure 14. System Li_3AlF_6 - CaF_2 ⁽⁹⁹⁾.

and 682°C with chiolite in equilibrium with CaF_2 and AlF_3 . Two points on the chiolite- CaF_2 boundary curve were also located, the first at 32.7 mole % cryolite, 50.5% AlF_3 and 16.8% CaF_2 and 689°C and the second at 34.3 mole % Na_3AlF_6 , 52.7% AlF_3 and 13.0% CaF_2 and 688°C. A point on the CaF_2 - AlF_3 boundary was located at 28.7 mole % Na_3AlF_6 , 55.3% AlF_3 and 16.0% CaF_2 and 708°C. On the basis of these points a partial ternary diagram was present. Supercooling in the region of the diagram containing CaF_2 as the primary phase was noted. At the time of the work no compounds were known to exist either in the CaF_2 - AlF_3 binary or the ternary system.

Pfundt and Zimmermann⁽¹⁰²⁾ investigated both the ternary system and the quasi-binary system NaF - CaAlF_5 using DTA of samples contained in pressure tight nickel crucibles. They agreed with the earlier investigations that the ternary system could be divided into two subsystems, NaF - Na_3AlF_6 - CaF_2 and CaF_2 - AlF_3 - Na_3AlF_6 . The invariant temperature for the NaF containing system was placed at 780°C.

The diagram of the quasi-binary system is presented in Figure 15. One compound, NaCaAlF_6 , belonging to the system CaF_2 - AlF_3 - Na_3AlF_6 was found to melt incongruently at 740°C. The compound existed in both a low temperature (beta) and high temperature (alpha) form with the transition taking place at 653°C on heating. The beta form exhibited tetragonal symmetry with lattice parameters $a_0 = 7.32\text{\AA}$ and $c_0 = 10.18\text{\AA}$. The existence of the high temperature polymorph at room temperature was noted in both air cooled and water quenched samples but no diffraction data was reported.

Working with samples encapsulated in sealed platinum tubes and using DTA heating curves taken at 3°C/min supplemented by optical microscopy, powder X-ray diffraction and quench experiments Craig and

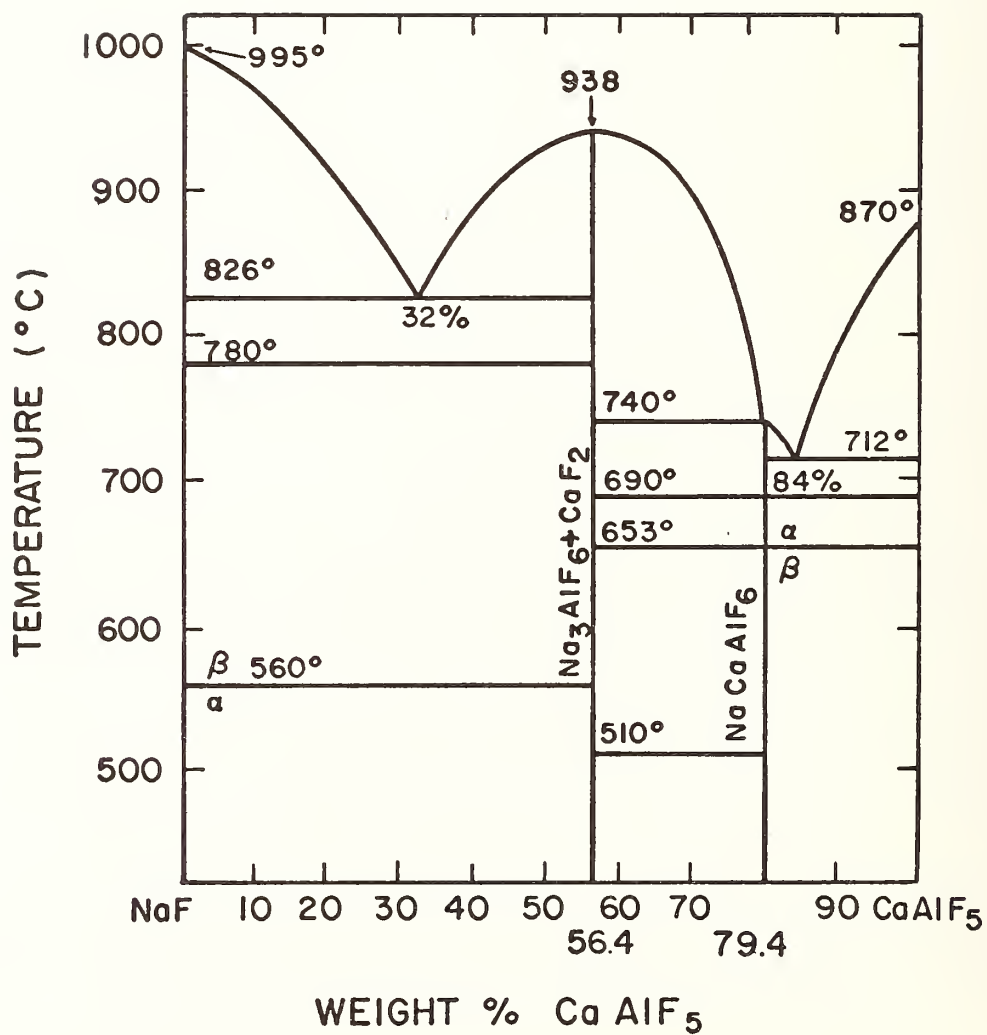


Figure 15. System NaF-CaAlF₅⁽¹⁰²⁾.

Brown⁽⁵⁶⁾ investigated the $\text{CaF}_2\text{-AlF}_3\text{-Na}_3\text{AlF}_6$ ternary system. The compound NaCaAlF_6 first noted by Pfundt and Zimmermann⁽¹⁰²⁾ was found to exist in a previously unreported γ form in addition to the α and β polymorphs. DTA showed the inversion to the new form, characterized by a sharp but small exothermic peak, to take place at 720°C . Gamma- NaCaAlF_6 was not quenchable and no diffraction data was reported. The compound melted incongruently at 737°C to CaF_2 and a liquid. In addition to NaCaAlF_6 , a previously unreported compound $\text{NaCaAl}_2\text{F}_9$ was identified. Based on powder X-ray diffraction data taken at scanning speeds of $\frac{1}{4}^\circ 2\theta/\text{min}$. using CuK_α radiation the compound was indexed as body centered cubic ($h + k + l = 2n$) with $a_0 = 10.76\text{\AA}$ (Table V). The compound melted incongruently to AlF_3 and a liquid at 715°C ; however, metastable congruent melting at 723°C was often observed.

On the basis of samples reacted for 394 hrs. in the solid state, the subsolidus compatibility relationships shown in Figure 16 were established. In the compatibility triangles containing cryolite a decrease in the α - β inversion temperature was noted. Investigation of the $\text{NaCaAlF}_6\text{-Na}_3\text{AlF}_6$ ternary join revealed that this decrease from 567 to 525°C was caused by a solubility of approximately 7 mole % NaCaAlF_6 in $\alpha\text{-Na}_3\text{AlF}_6$.

The authors noted, in support of Holm's⁽⁵⁴⁾ simple eutectic diagram for the $\text{CaF}_2\text{-Na}_3\text{AlF}_6$ system, that slight compositional errors introducing excess AlF_3 to the binary system would result in the solid solution diagrams for the system reported by Rolin⁽⁵³⁾ and Verdan and Monnier⁽⁵⁵⁾. Craig and Brown⁽⁵⁶⁾ cited as additional evidence the work of Dewing⁽¹⁰³⁾ who postulated that a 50 fold increase in the conductivity of a sample in the $\text{CaF}_2\text{-AlF}_3\text{-Na}_3\text{AlF}_6$ system (as compared to pure Na_3AlF_6) could be explained by a solid solution of CaF_2 in Na_3AlF_6 and that such a

TABLE V. X-Ray Powder Diffraction Data for the Compound $\text{NaCaAl}_2\text{F}_9$

d_{obs}	d_{calc}^*	I/I_0	(hkl)
7.59	7.61	10	110
5.37	5.38	5	200
4.40	4.39	30	211
3.80	3.81	70	220
3.40	3.40	75	310
3.11	3.11	80	222
2.873	2.877	10	321
2.691	2.691	5	400
2.538	2.537	5	511,330
2.198	2.197	15	422
2.112	2.111	50	510,431
1.966	1.965	5	521
1.904	1.903	100	440
1.845	1.846	10	530,433
1.795	1.794	30	600,442
1.747	1.746	20	611,532
1.703	1.702	55	620
1.661	1.661	5	541
1.623	1.623	15	622
1,587	1.587	10	631

Other reflections

$$a = 10.765\text{\AA}$$

*Evans, H. T., Appleman, D. E. and Handwerker, D. S., (1963) Least Squares Refinement.

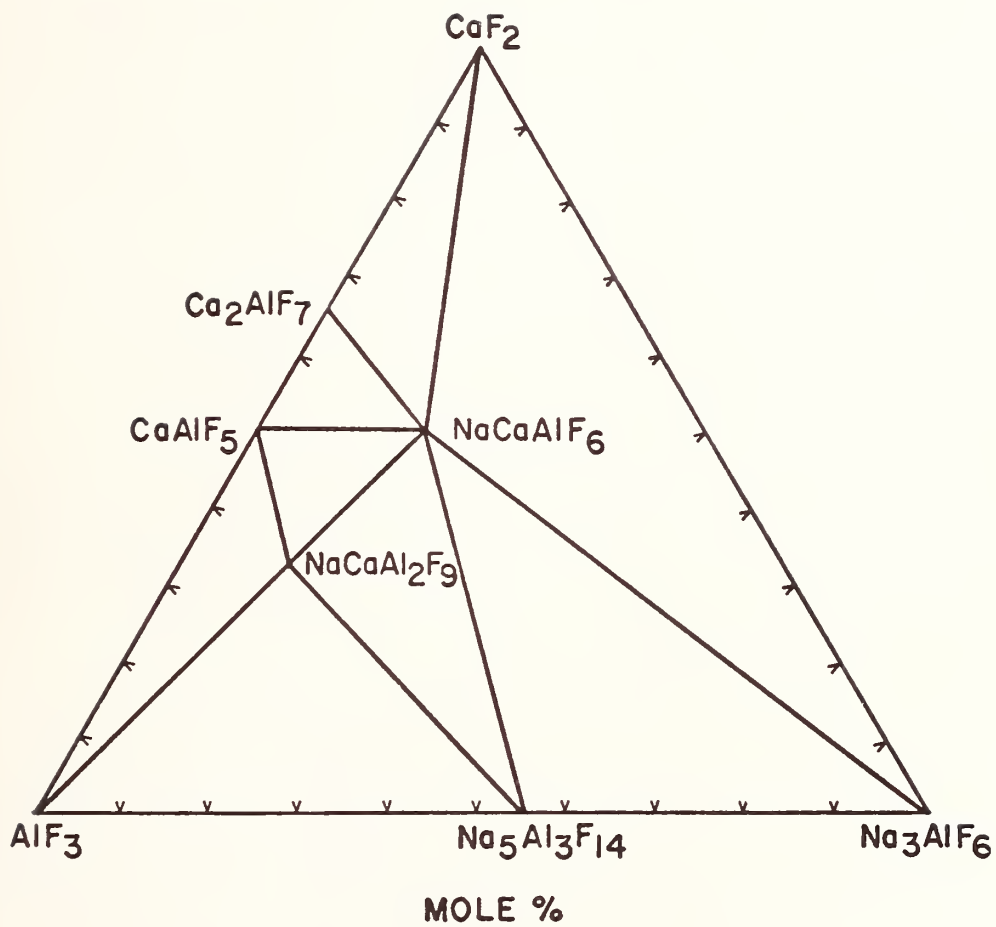


Figure 16. Subsolidus Compatibility Relationships in the System $\text{CaF}_2\text{-AlF}_3\text{-Na}_3\text{AlF}_6$ ⁽⁵⁶⁾.

solid solution was only reasonable when AlF_3 was present. It was noted that while Dewing was unaware of the existence of NaCaAlF_6 , the sample studied actually lay on the NaCaAlF_6 - Na_3AlF_6 ternary join. The conductivity increase, therefore, should be attributed to a solid solution of NaCaAlF_6 in Na_3AlF_6 and not to CaF_2 in cryolite. While firm evidence of the solubility of NaCaAlF_6 in the low temperature form of cryolite exists, the use of DTA to investigate solubility in the high form of cryolite was complicated by the dissociation of Na_3AlF_6 near its melting point. While a peak corresponding to a solidus line was often observed on cooling, the dissociation of cryolite masked its existence (if indeed it was present) on heating. The solubility of NaCaAlF_6 is, therefore, difficult to conclusively confirm.

The full phase diagram for the CaF_2 - AlF_3 - Na_3AlF_6 presented by Craig and Brown is shown in Figure 17 and the compositions, temperatures, and phase assemblages of the invariant points are given in Table VI.

2. System Na_3AlF_6 - AlF_3 - Al_2O_3 .

Fenerty and Hollingshead⁽⁵²⁾ investigated the liquidus curves in the cryolite rich portion of the system using cooling curve methods supplemented by visual observation of crystallization. The Na_3AlF_6 - Al_2O_3 phase boundary showed a gradual decrease in Al_2O_3 up to 25 wt. % AlF_3 . Above this value the boundary curved sharply with a rapid decrease in Al_2O_3 content. The ternary peritectic and eutectic were both located at alumina contents less than 1 wt. %. Rolin's⁽⁶⁸⁾ investigation of the system agreed well with the previous authors up to 25 wt. % AlF_3 . Above this value, however, the boundary curve continued a smooth approach to the ternary peritectic located at 5 wt. % Al_2O_3 , 28.5% AlF_3 and 66.5% Na_3AlF_6 and 710°C. A ternary eutectic was located at 60 wt. % Na_3AlF_6 ,

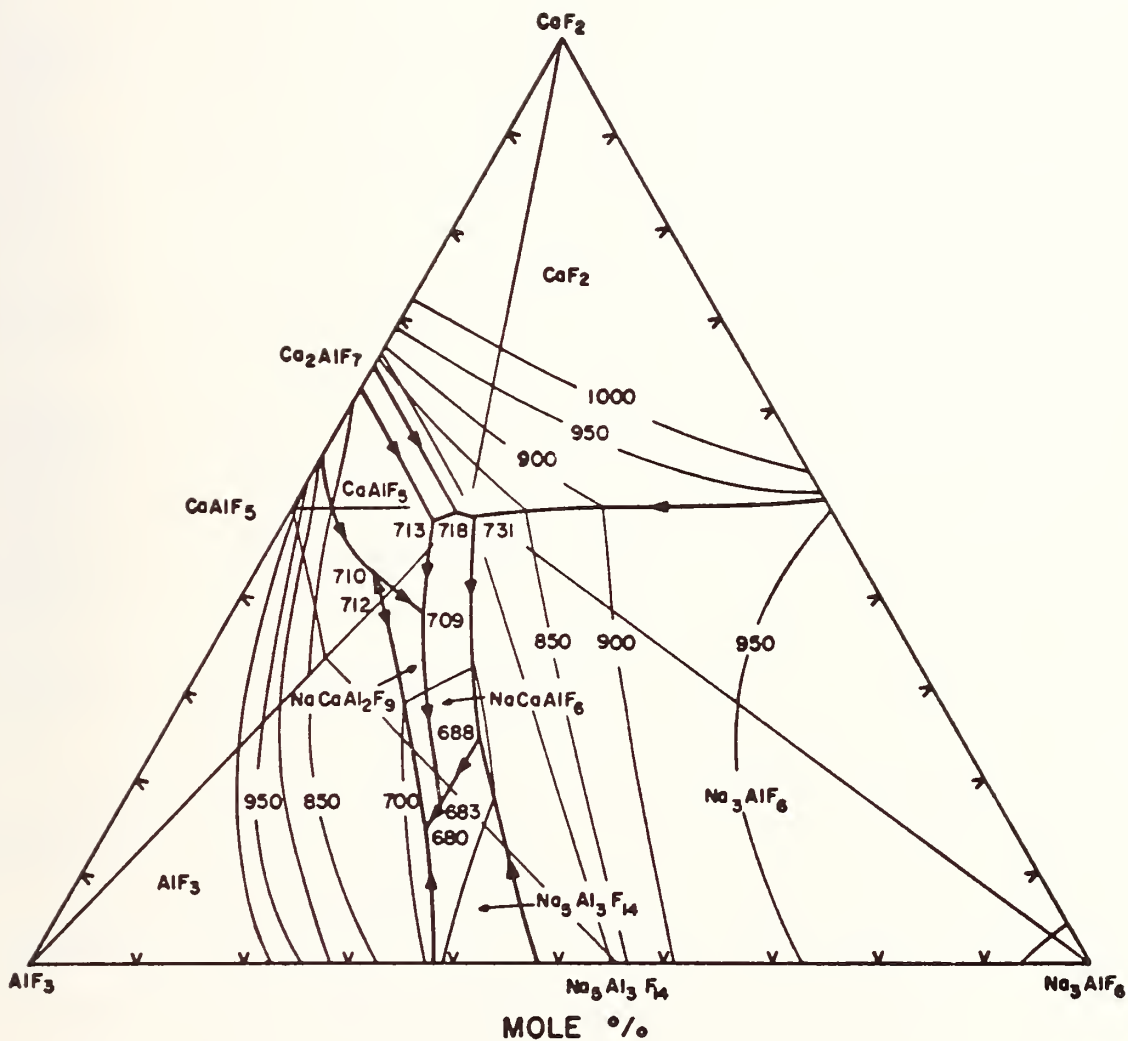


Figure 17. System CaF_2 - AlF_3 - Na_3AlF_6 (56).

TABLE VI. Invariant Points in the System $\text{CaF}_2\text{-AlF}_3\text{-Na}_3\text{AlF}_6$

<u>Point No.</u>	<u>CaF₂</u>	Mole % <u>AlF₃</u>	<u>Na₃AlF₆</u>	<u>Type</u>	<u>T (°C)</u>	<u>Equilibrium Phase Assemblage</u>
1	49.0	33.5	17.5	Peritectic	731	CaF ₂ NaCaAlF ₆ Na ₃ AlF ₆
2	49.5	35.0	15.5	Peritectic	718	CaF ₂ Ca ₂ AlF ₇ NaCaAlF ₆
3	48.5	37.5	14.0	Peritectic	713	Ca ₂ AlF ₇ CaAlF ₅ NaCaAlF ₆
4	43.0	46.0	11.0	Peritectic	710	CaAlF ₅ NaCaAl ₂ F ₉ AlF ₃
5	38.0	44.0	18.0	Peritectic	709	CaAlF ₅ NaCaAl ₂ F ₉ NaCaAlF ₆
6	25.0	45.0	30.0	Peritectic	688	Na ₃ AlF ₆ Na ₅ Al ₃ F ₁₄ NaCaAlF ₆
7	18.0	52.0	30.0	Peritectic	683	NaCaAl ₂ F ₉ Na ₅ Al ₃ F ₁₄ NaCaAlF ₆
8	15.0	55.0	30.0	Eutectic	680	AlF ₃ Na ₅ Al ₃ F ₁₄ NaCaAl ₂ F ₉
9	49.0	34.0	17.0	Saddle Point	735	CaF ₂ NaCaAlF ₆
10	39.5	47.5	13.0	Saddle Point	712	NaCaAl ₂ F ₉ AlF ₃

37% AlF_3 and 3% Al_2O_3 and 670° . Possible sources of error which could account for the previous results such as the slow dissolution of Al_2O_3 , the lack of a thermal arrest corresponding to the primary crystallization of Al_2O_3 and the purity of starting materials were noted.

Using samples contained in sealed platinum tubes, Foster⁽¹⁰⁴⁾ employed quench methods, optical microscopy and X-ray diffraction to reinvestigate the cryolite rich portion of the diagram. In support of Rolin's diagram, the Na_3AlF_6 - Al_2O_3 boundary fell regularly to the peritectic composition at 28.3 wt. % AlF_3 , 4.4% Al_2O_3 and 67.3% Na_3AlF_6 and 723°C . The ternary eutectic was located at 37.3 wt. % AlF_3 , 3.2% Al_2O_3 and 59.5% Na_3AlF_6 and 684°C (Figure 18). Compositions containing 20 wt. % or less AlF_3 precipitated α - Al_2O_3 in the primary phase field of Al_2O_3 while those containing 25 wt. % or more precipitated η - Al_2O_3 . The line defining the limits of the α - η formation (broken line, Figure 18) is not isothermal and since no solid solution exists it must define a metastable region.

3. System Na_3AlF_6 - CaF_2 - Al_2O_3

Fenerty and Hollingshead⁽⁵²⁾ investigated the Na_3AlF_6 - CaF_2 - Al_2O_3 ternary diagram using the same procedure as in their investigation of the Na_3AlF_6 - CaF_2 and Na_3AlF_6 - AlF_3 - Al_2O_3 systems. On the basis of results obtained for cuts taken at 5, 10, 15, 20, 22, 24, 25, and 26 wt. % CaF_2 a simple eutectic diagram with the ternary invariant point at 76.1 wt. % cryolite, 21% CaF_2 and 2.9% Al_2O_3 and 933°C was presented. A later investigation by Rolin⁽⁵³⁾, using the method of thermal arrest, placed the eutectic at 78 wt. % Na_3AlF_6 , 17% CaF_2 and 5% Al_2O_3 and 927°C . The major difference between the works was in the Al_2O_3 content of the cryolite-alumina phase boundary. Rolin's diagram (Figure 19) showed the boundary

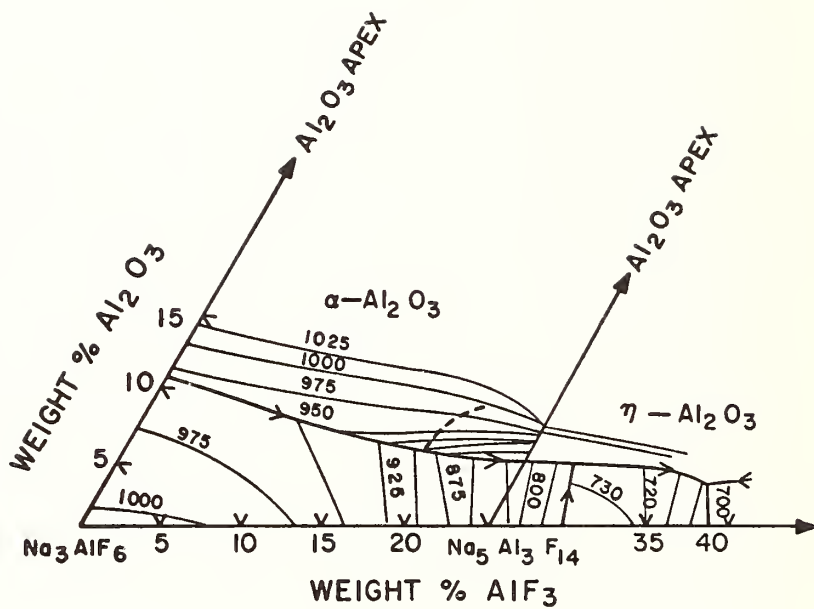


Figure 18. System Na_3AlF_6 - AlF_3 - Al_2O_3 (104).

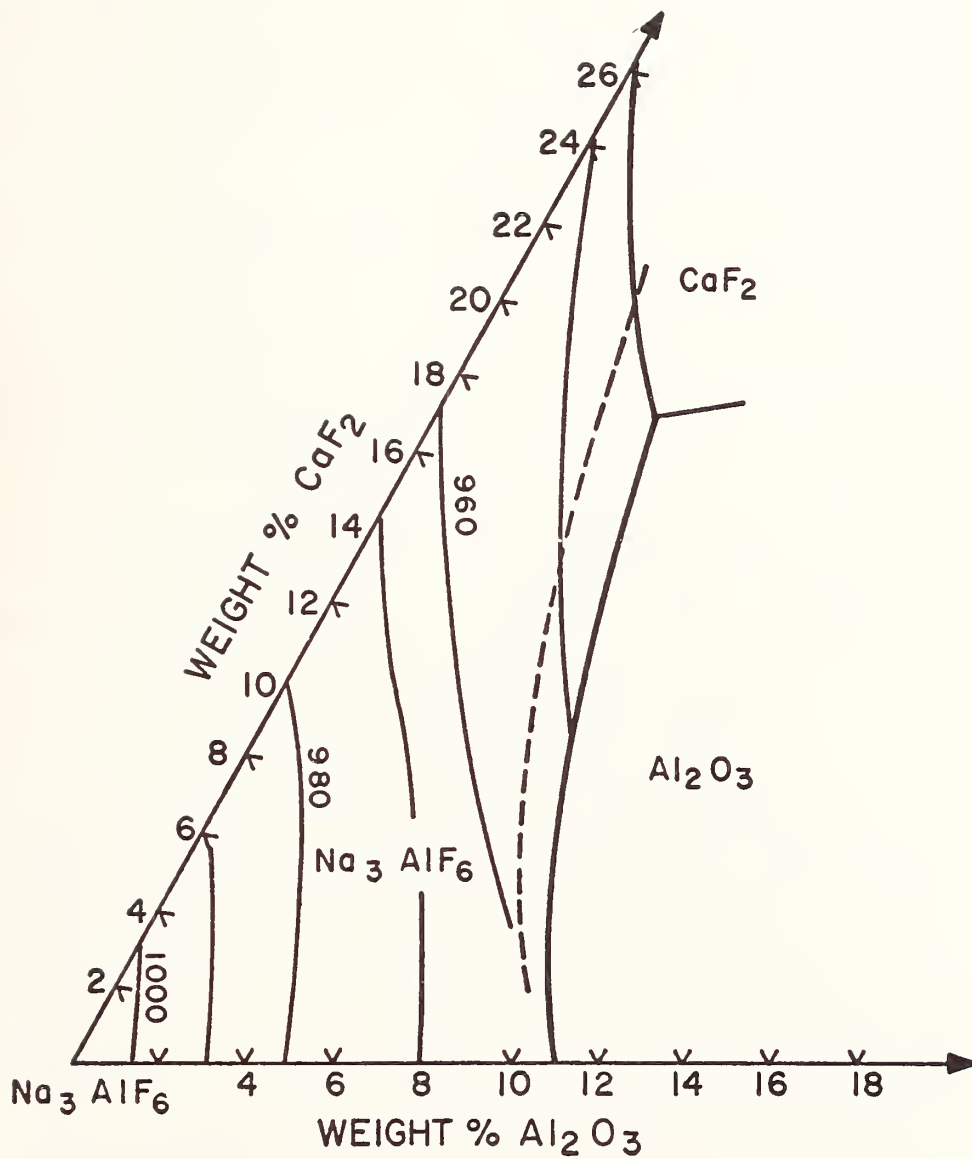


Figure 19. System Na_3AlF_6 - Al_2O_3 - CaF_2 ⁽⁵²⁾.

curve to be higher in Al_2O_3 than that of Fenerty and Hollingshead (Figure 19, dashed line).

4. System CaF_2 - AlF_3 - Al_2O_3

In the CaF_2 - AlF_3 - Al_2O_3 ternary system only the CaF_2 - AlF_3 and CaF_2 - Al_2O_3 binary systems are known. Several authors^(52,70,71,105) have investigated quaternary systems involving the ternary; however, their work has been confined to areas far removed from the ternary. At the present time no phase equilibrium data are available on the system.

5. System Li_3AlF_6 - Na_3AlF_6 - Al_2O_3

Drossbach⁽⁸³⁾ first investigated this system in 1936. Working near the Na_3AlF_6 - Li_3AlF_6 side of the ternary, he determined a boundary curve extending from 10 weight % Al_2O_3 on the Na_3AlF_6 - Al_2O_3 binary at 937°C to 38 weight % Li_3AlF_6 on the Na_3AlF_6 - Li_3AlF_6 join at 810°C . No Li_3AlF_6 primary phase field was indicated.

Mashovets and Petrov⁽⁸⁴⁾ also worked in the Na_3AlF_6 - Li_3AlF_6 side of the ternary and found a boundary curve extending from 15 weight % Al_2O_3 on the Na_3AlF_6 - Al_2O_3 join to 7 weight % Al_2O_3 on the Li_3AlF_6 - Al_2O_3 join.

Rolin and Muhlethaler⁽⁶⁹⁾ obtained similar results in their study of the diagram. Using data obtained from thermal arrest cooling curves they found a single boundary curve separating Al_2O_3 from the cryolite-lithium cryolite solid solution. The boundary curve paralleled the Na_3AlF_6 - Li_3AlF_6 binary within 1 weight % from 45 to 100 weight % Li_3AlF_6 . No ternary compounds were reported.

Cassidy and Brown⁽⁹⁰⁾ found the ternary to contain one reaction point, one peritectic point and one ternary eutectic point. Working in sealed platinum tubes and employing X-ray diffraction, DTA and

quench methods a primary phase field of the incongruently melting compound cryolithionite, $\text{Na}_3\text{Li}_3\text{Al}_2\text{F}_{12}$ was located. Three compatibility triangles were found in addition to one two phase region ($\text{Na}_3\text{AlF}_6(\text{ss}) + \text{Al}_2\text{O}_3$). The second compound on the Na_3AlF_6 - Li_3AlF_6 binary, $\text{Na}_2\text{LiAlF}_6$ which decomposes at 543°C ⁽³⁰⁾ is never in equilibrium with liquid.

The diagram is seen in Figure 20.

6. System $\text{LiF-AlF}_3\text{-Na}_3\text{AlF}_6$

Holm and Holm⁽²⁰⁾ worked in the $\text{Li}_3\text{AlF}_6\text{-Na}_3\text{AlF}_6\text{-LiF}$ portion of the ternary diagram in 1973. They found a ternary eutectic at 684°C and 83 mole % LiF , 7% AlF_3 and 10% Na_3AlF_6 . Thoma et al.⁽⁷⁵⁾ studied the NaF-LiF-AlF_3 ternary system and found the $\text{LiF-AlF}_3\text{-Na}_3\text{AlF}_6$ portion of the diagram to contain a eutectic in each of the two compatibility triangles $\text{Na}_3\text{AlF}_6\text{-AlF}_3\text{-Li}_3\text{AlF}_6$ and $\text{Na}_3\text{AlF}_6\text{-LiF-Li}_3\text{AlF}_6$. No evidence of either $\text{Na}_2\text{LiAlF}_6$ or $\text{Na}_3\text{Li}_3\text{Al}_2\text{F}_{12}$ was reported.

Rolin and Muhlethaler⁽⁶⁹⁾ presented a diagram of the $\text{Na}_3\text{AlF}_6\text{-Li}_3\text{AlF}_6\text{-AlF}_3$ ternary system (Figure 21) showing a peritectic at 647°C and 47 weight % Na_3AlF_6 , 34.5% Li_3AlF_6 and 18.5% AlF_3 and a eutectic at 36 weight % Na_3AlF_6 , 41% Li_3AlF_6 and 23% AlF_3 and 607°C .

To avoid the problem of volatilization, Stinton and Brown⁽¹⁰⁶⁾ encapsulated all samples in platinum tubes. DTA, quench methods, and X-ray analysis were employed to determine the system shown in Figure 22. Seven compatibility triangles, three eutectics, one peritectic, a reaction point and two regions of cryolite - $\text{Li}_3\text{AlF}_6(\text{ss})$ were identified.

7. System $\text{Li}_3\text{AlF}_6\text{-LiF-CaF}_2$

Only one study of the $\text{Li}_3\text{AlF}_6\text{-LiF-CaF}_2$ system exists in the literature. Using thermal arrest methods Vrbanska and Malinovsky⁽⁹⁹⁾

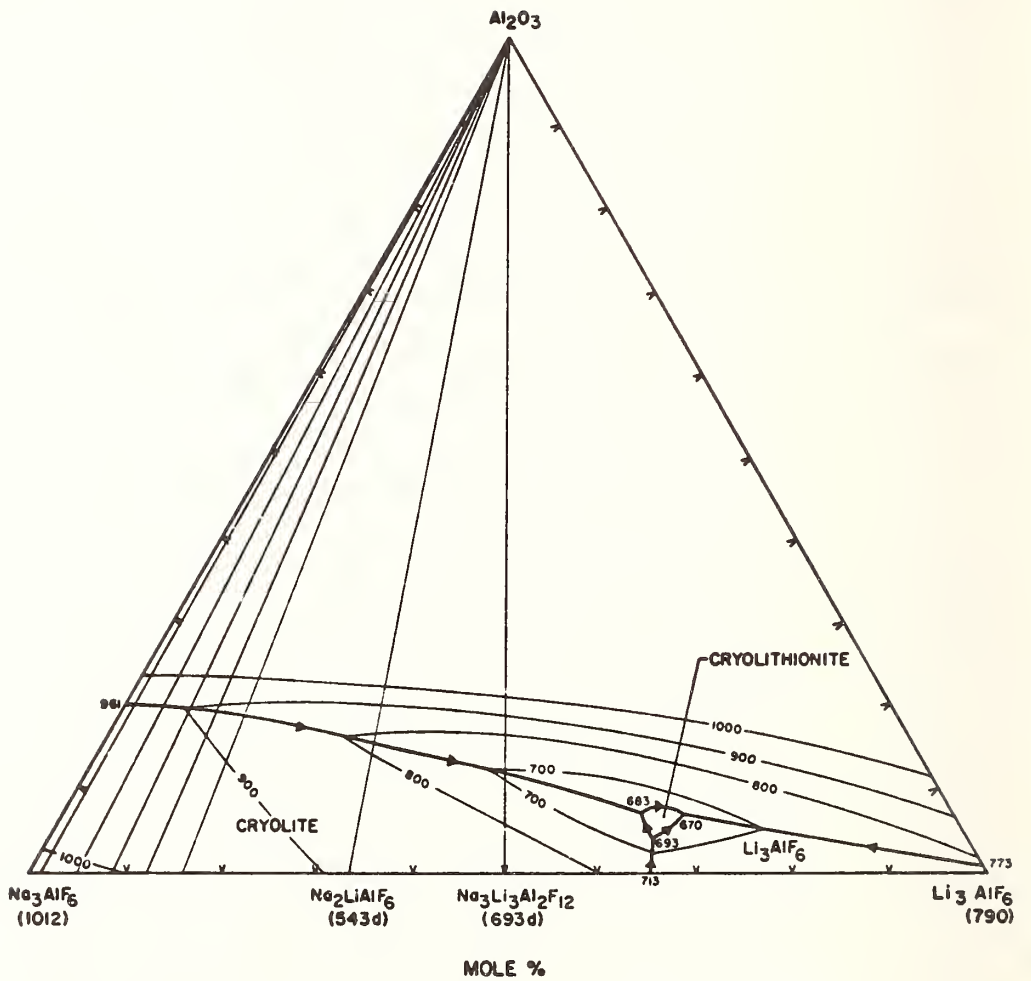


Figure 20. System Li_3AlF_6 - Na_3AlF_6 - Al_2O_3 (90).

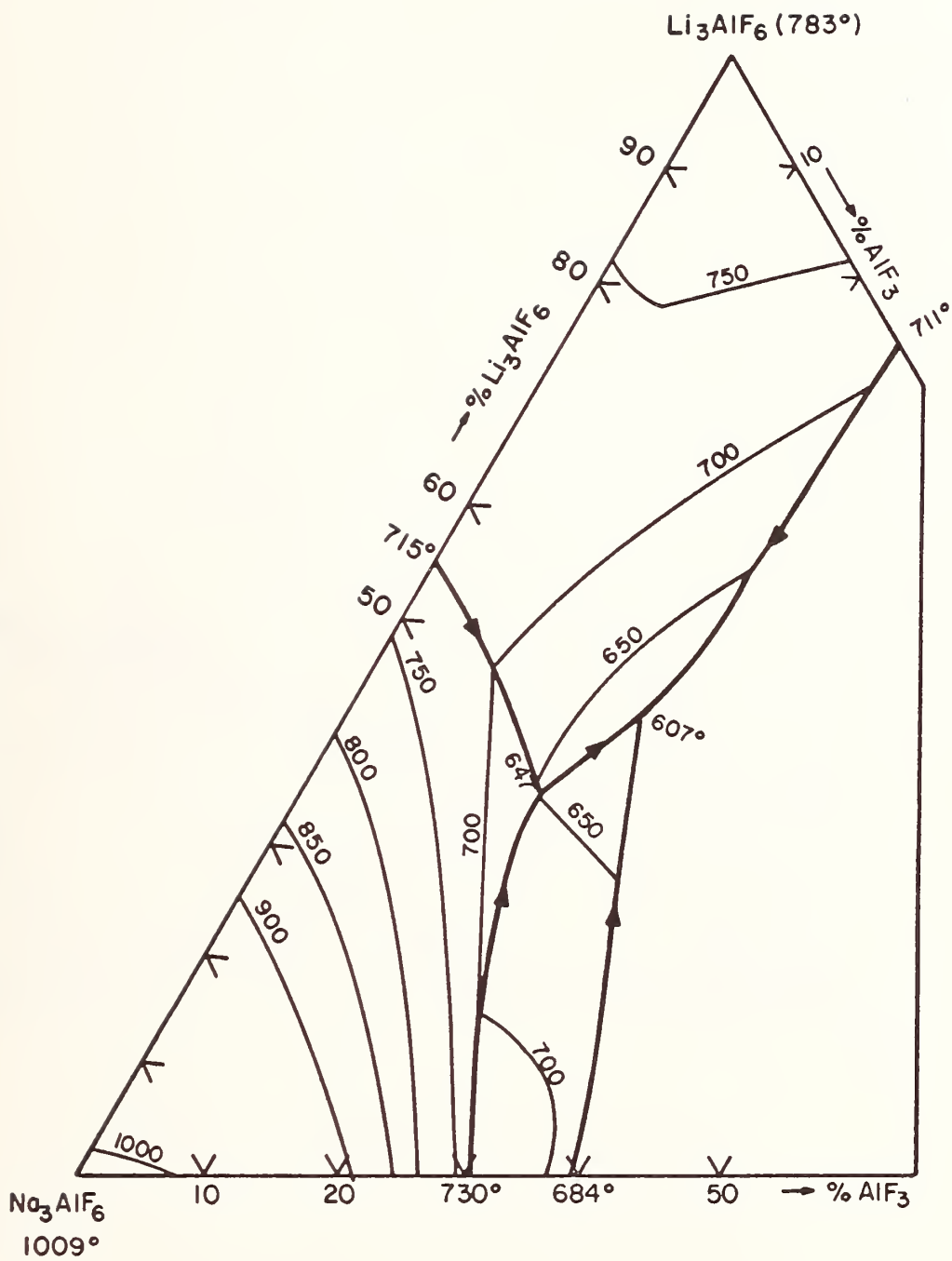


Figure 21. System Na_3AlF_6 - Li_3AlF_6 - AlF_3 (69).

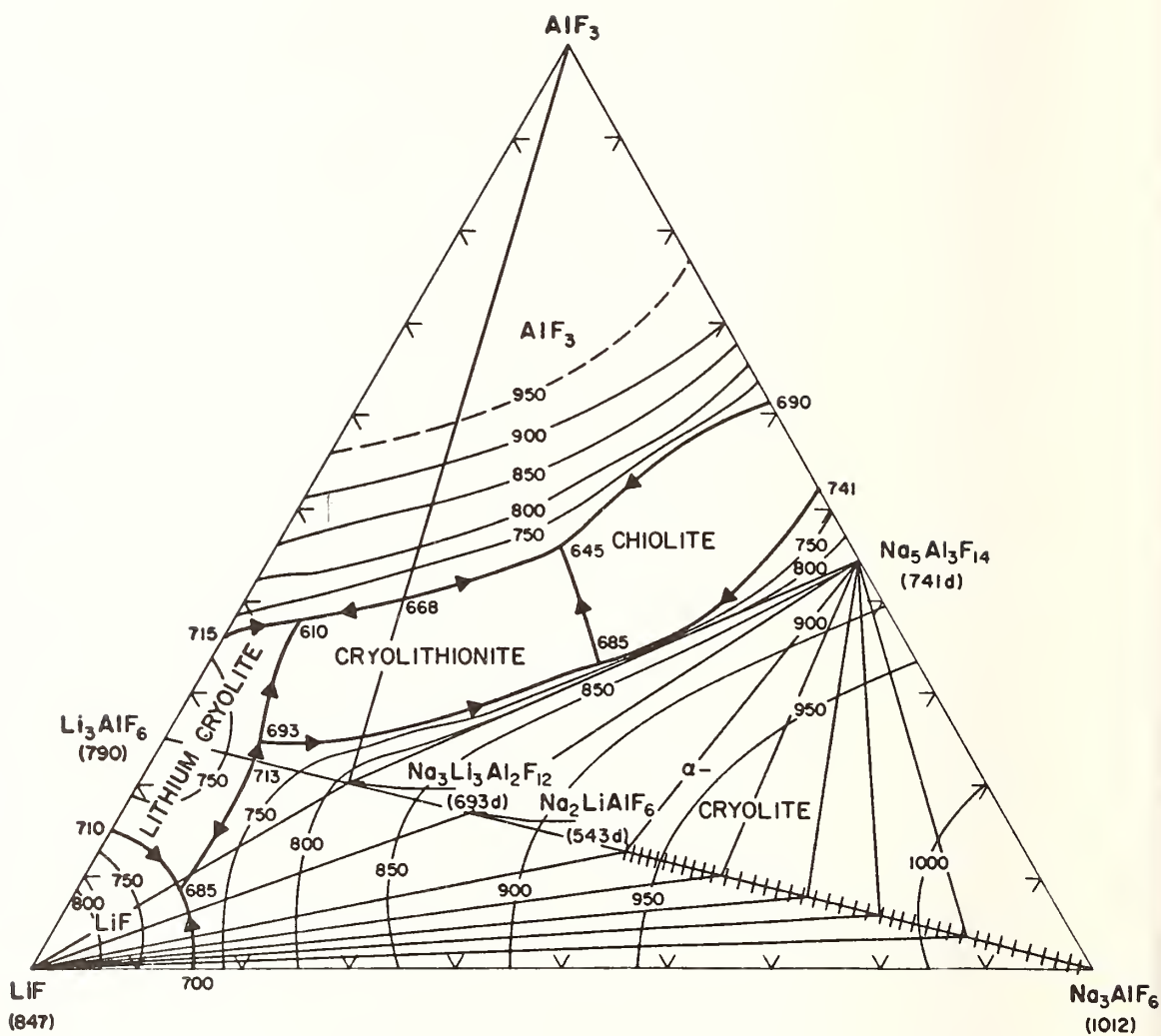


Figure 22. System $\text{LiF}-\text{AlF}_3-\text{Na}_3\text{AlF}_6$ (106).

located the invariant point for the ternary eutectic system (Figure 23) at 665°C and 25 mole % Li_3AlF_6 , 52% LiF and 25% CaF_2 .

D. Four Component Systems

1. System Na_3AlF_6 - AlF_3 - CaF_2 - Al_2O_3

The quaternary system Na_3AlF_6 - AlF_3 - CaF_2 - Al_2O_3 has been investigated several times. The studies were performed prior to the reported existence of any ternary compounds and were concerned only with very limited portions of the liquidus surface of the system.

Abramov⁽⁷⁰⁾ et al. studied the $\text{Na}_5\text{Al}_3\text{F}_{14}$ - CaF_2 - Al_2O_3 cross section of the quaternary system. The liquidus surface of the section contained phase fields for cryolite, Al_2O_3 and CaF_2 . A quaternary peritectic at 34.5 mole % Na_3AlF_6 , 45.9% AlF_3 , 13.9% CaF_2 and 5.7% Al_2O_3 and 685°C in addition to a quaternary eutectic temperature of 665°C were reported.

Fenerty and Hollingshead⁽⁵²⁾ studied the system by noting the change in the Na_3AlF_6 - Al_2O_3 and Na_3AlF_6 - CaF_2 boundary curves as mixed additions of up to 15 wt. % AlF_3 and 20 wt. % CaF_2 were added to the system Na_3AlF_6 - Al_2O_3 . An addition of 10 wt. % AlF_3 moved the ternary eutectic for the system Na_3AlF_6 - CaF_2 - Al_2O_3 from 21 wt. % CaF_2 and 933°C to 13 wt. % CaF_2 and 927°C.

Rolin⁽⁷¹⁾ investigated the portion of the system bounded by 10 wt. % CaF_2 and 20% AlF_3 . On the basis of thermal arrest data, a partial diagram of the cryolite rich end of the quaternary system showing the boundary surface between cryolite and Al_2O_3 was presented (Figure 24).

Foster⁽¹⁰⁵⁾ also presented a few selected liquidus curves in the NaF - AlF_3 - CaF_2 - Al_2O_3 system for compositions with constant NaF/AlF_3 ratios.

Craig and Brown⁽⁵⁶⁾ working with samples encapsulated in sealed platinum tubes (reacted in the solid state and in the presence of liquid) established the eight compatibility tetrahedra for the system CaF_2 - AlF_3 -

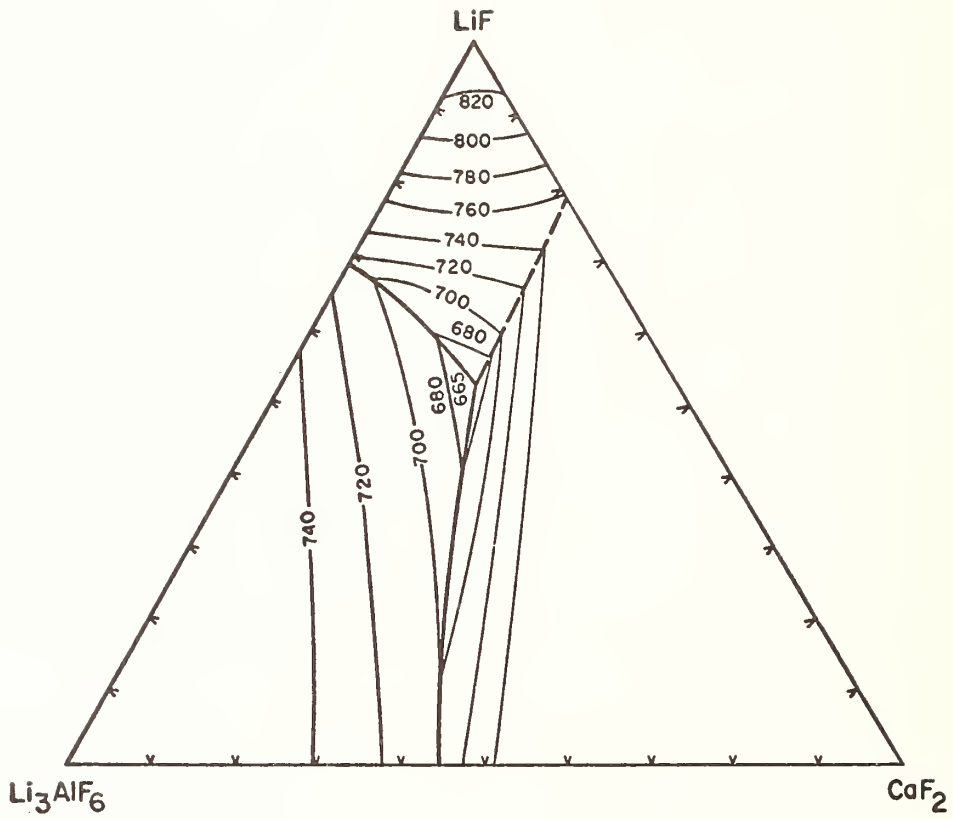


Figure 23. System $\text{Li}_3\text{AlF}_6\text{-LiF-CaF}_2$ ⁽⁹⁹⁾.

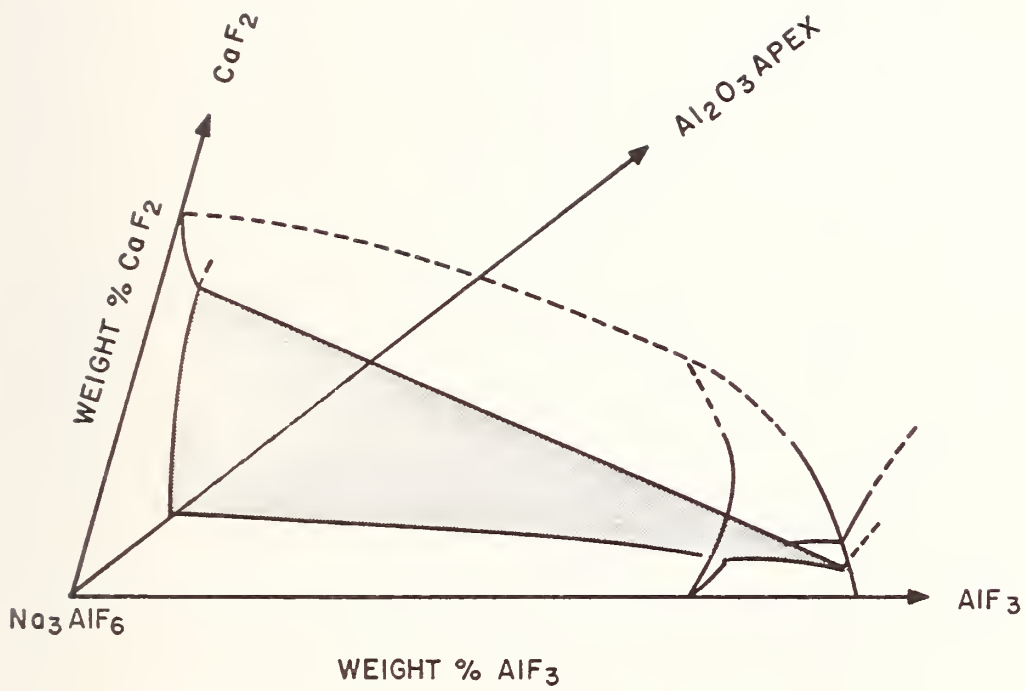


Figure 24. System Na_3AlF_6 - AlF_3 - CaF_2 - Al_2O_3 ⁽⁷¹⁾.

$\text{Na}_3\text{AlF}_6\text{-Al}_2\text{O}_3$ shown in Figure 25. No quaternary compounds were found to exist and in all cases where Al_2O_3 was present it was identified by X-ray diffraction as $\alpha\text{-Al}_2\text{O}_3$.

2. System $\text{Na}_3\text{AlF}_6\text{-AlF}_3\text{-LiF-Al}_2\text{O}_3$

Based on the data thus far presented, it is possible to draw a "not impossible" quaternary diagram for the system. This is shown in Figure 26. As depicted, the system contains seven compatibility tetrahedra, thus giving rise to as many as seven invariant points involving liquid. These invariant points are possibly very important to the Hall electrolyte and should be determined.

3. System $\text{Na}_3\text{AlF}_6\text{-CaF}_2\text{-LiF-Al}_2\text{O}_3$

There are no reported compounds in the $\text{Na}_3\text{AlF}_6\text{-CaF}_2\text{-LiF-Al}_2\text{O}_3$ system; however, there is little information available on the $\text{LiF-Al}_2\text{O}_3$ binary subsystem. If there are no compounds in either this binary or any of the ternary subsystems, it is likely that there is only one compatibility tetrahedron in this system. This would suggest that there exists only one quaternary invariant point involving liquid. The location and temperature of this point should be determined.

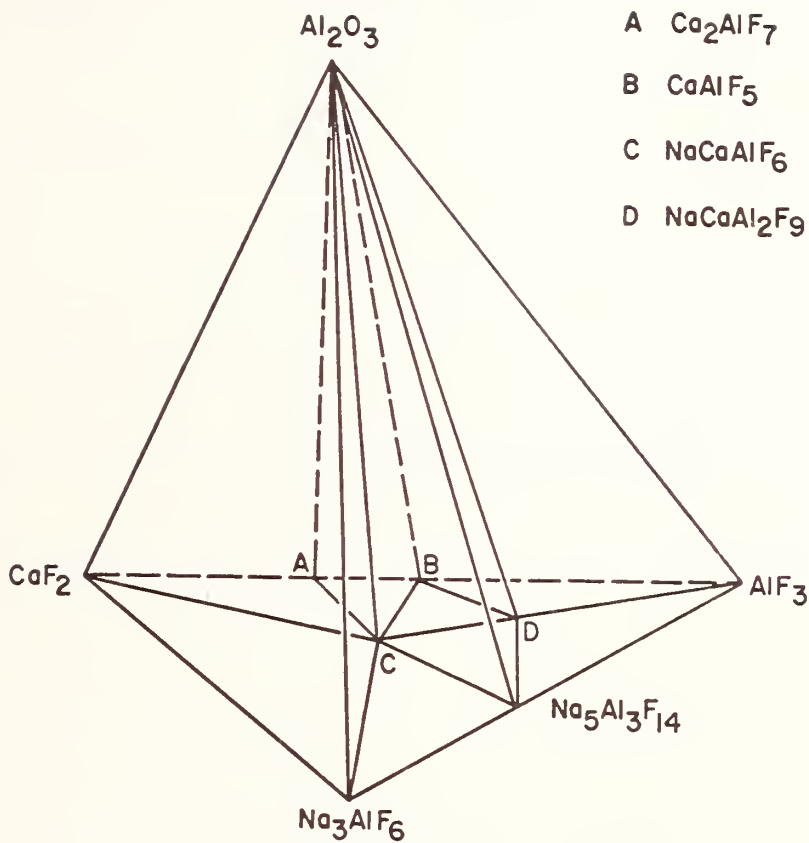


Figure 25. Subsolidus Compatibility Relationships in the system Na_3AlF_6 - AlF_3 - CaF_2 - Al_2O_3 ⁽⁵⁶⁾.

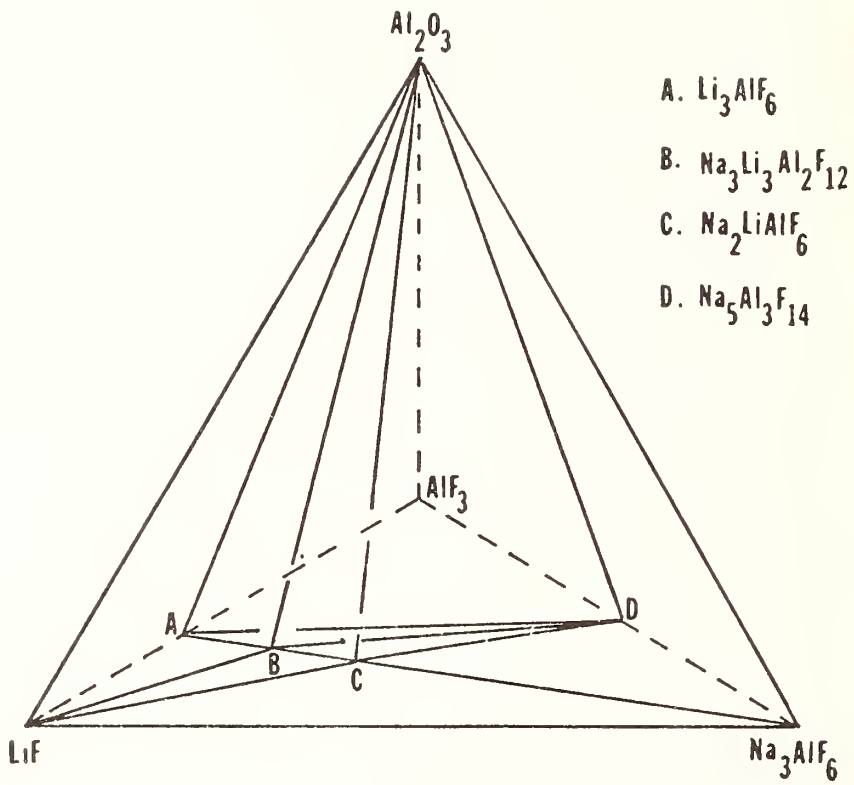


Figure 26. Possible phase diagram for the system $\text{Na}_3\text{AlF}_6\text{-AlF}_3\text{-LiF-Al}_2\text{O}_3$.

REFERENCES

1. Powder Diffraction File, 12-257, Joint Committee on Powder Diffraction Standards, Philadelphia, PA.
2. A. J. Majumdar and R. Roy, "Test of the Applicability of the Clapeyron Relationship to a Few Cases of Solid-Solid Transitions", *J. Inorg. Nucl. Chem.* 27 1961-73 (1965).
3. G. J. Landon and A. R. Ubbelohde, "Melting and Crystal Structure of Cryolite (3NaF , AlF_3)", *Proc. Roy. Soc. (London)* A240 160-72 (1957).
4. C. J. O'Brien and K. K. Kelley, "High Temperature Heat Contents of Cryolite, Anhydrous Aluminum Fluoride and Sodium Fluoride," *J. Am. Chem. Soc.* 79 5616-18 (1957).
5. K. Grjotheim, "Theory of Aluminum Electrolysis", *Kgl. Nor. Vidensk. Selsk. Skr.* 2: (5) 1-90 (1957).
6. W. B. Frank, "Thermodynamic Considerations in the Aluminum-Producing Electrolyte," *J. Phys. Chem.* 65 (11) 2081-87 (1961).
7. P. A. Foster, Jr., "Determination of the Cryolite-Alumina Phase Diagram by Quenching Methods," *J. Am. Cer. Soc.* 43 (2) 66-68 (1960).
8. P. P. Fedotieff and W. P. Iljinsky, "Uber die Schmelzbarkeit des Ternaren Systems: Natriumfluorid, Calciumfluorid, Aluminumfluorid", *Z. Anorg. Chem.* 129 93-107 (1923).
9. M. G. Petit, "Etude Cryoscopique de Solutions de Certains Oxydes Metalliques dans l'Eutectique Cryolithe-Fluorure de Sodium," *Compt. Rend.* 234 1281-83 (1952).
10. N. W. F. Phillips, R. H. Singleton and E. A. Hollingshead, "Liquidus Curves for Aluminum Cell Electrolyte," *J. Electrochem. Soc.* 102 (11) 648-49 (1955).
11. J. L. Holm, "Structural Interpretation of the System Cryolite + Sodium Aluminate," *Trans. Faraday Soc.* 58 (11) 1104-7 (1962).
12. P. A. Foster, Jr., "A Cryolite Melting Point Through Quenching Methods," *J. Phys. Chem.* 61 (7) 1005-6 (1957).
13. P. Pascal, "Die Elektrometallurgie des Aluminums. I. Das Ternare System Tonerde-Fluorit-Kryolith.," *Z. Electrochem.* 19 610-13 (1913).
14. P. A. Foster, Jr., "Melting Point of Cryolite," *J. Am. Cer. Soc.* 51 (2) 107-9 (1968).

15. W. B. Frank and L. M. Foster, "The Constitution of Cryolite and NaF-AlF₃ Melts," J. Phys. Chem. 64 (1) 95-8 (1960).
16. P. A. Foster and W. B. Frank, "The Structure of Cryolite-Alumina Melts," J. Electrochem. Soc. 107 (12) 997-1001 (1960).
17. C. Palache, H. Berman and C. Frondel eds., Dana's System of Mineralogy, John Wiley and Sons, Inc., New York, 1951.
18. F. Hanic, K. Matiasovsky, D. Stempelova and M. Malinovsky, "Über die Kristallstruktur Von AlF₃," Acta Chim. Hung. Tomus 32 309-13 (1962).
19. E. Staritzky and L. B. Asprey, "Aluminum Trifluoride, AlF₃," Anal. Chem. 29 984 (1957).
20. J. L. Holm and J. B. Holm, "Phase Relations and Thermodynamic Properties in the Ternary Reciprocal System LiF-NaF-Na₃AlF₆-Li₃AlF₆," Thermochimica Acta. 6 (4) 375-98 (1973).
21. A. H. Shultz, B. Bieker and J. Krogh-Moe, "Phase Equilibrium in the System BaF₂-AlF₃," Acta Chem. Scand. 26 (7) 2623-30 (1972).
22. D. B. Shinn, D. S. Crockett and H. M. Haendler, "The Thermal Decomposition of Ammonium Hexafluoroferrate (III) and Ammonium Hexafluoroaluminate. A New Crystalline Form of Aluminum Fluoride," Inorg. Chem. 5 (11) 1927-33 (1966).
23. G. Mesrobian, M. Rolin and H. Pham, "Etude Sous Pression des Melanges Fluorure de Sodium-Fluorure d'Aluminum Riches en Fluorure d'Aluminum," Rev. Int. Hautes Temp. Refract. 9 (1) 139-46 (1972).
24. Swanson and Tatge, "Calcium Fluoride, CaF₂," Nat'l. Bur. Std. Circ. 539 Vol. 1, 69-70 (1953).
25. H. Kojima, S. G. Whiteway and C. R. Masson, "Melting Points of Inorganic Fluorides," Can. J. Chem. 46 (18) 2968-71 (1968).
26. E. M. Levin, C. R. Robbins and H. F. McMurdie, eds., Phase Diagrams for Ceramists, American Ceramic Society, Inc., Columbus, Ohio (1964).
27. F. D. Bloss, An Introduction to the Methods of Optical Crystallography, Holt, Rinehart and Winston, New York (1961).
28. Nat. Bur. Stand. U.S. Circ. 539 (9) 3 (1959).
29. P. A. Foster, Jr., "The System Sodium Fluoride-Alumina Investigated by Quenching Methods," J. Am. Cer. Soc. 45 (4) 145-48 (1962).
30. H. C. Stumpf, A. S. Russell, J. W. Newsome and C. M. Tucker, "Thermal Transformations of Aluminas and Alumina Hydrates," Ind. Eng. Chem. 42 (7) 1398-1403 (1950).
31. P. A. Foster, Jr., "The Nature of Alumina in Quenched Cryolite-Alumina Melts," J. Electrochem. Soc. 106 (11) 971-75 (1959).

32. K. Wefers and G. M. Bell, "Oxides and Hydroxides of Aluminum," Tech. Paper No. 19 Aluminum Co. of America, Pittsburgh, PA, p. 37, 1972.
33. Y. I. Chu and A. I. Belyaev, *Izv. Vyssh Ucheb. Zaved., Tsvet. Metal.* p. 59 (1959).
34. J. L. Holm, Lic. Thesis. NTH, Trondheim, 1963; cited from 39.
35. B. Jenssen, Lic. Thesis, NTH, Trondheim, 1969; cited from 39.
36. M. A. Kuvakin, *Zh. Neorg. Khim.* 14 282 (1969).
37. K. Matiasovsky and M. Malinovsky, *Hutn. Listy.* 24, 515 (1969).
38. J. L. Holm, Thesis for a Doctorate Degree. NTH, Trondheim, 1971; cited from 39.
39. I. Kostenska, J. Corba, and M. Malinovsky, "On Solid Solutions in the System $\text{LiF-Na}_3\text{AlF}_6$," *Chem. Zvesti*, 28, 546-552 (1974).
40. R. A. Lewis, Process Metallurgy Division Monthly Report, May, 1948, cited from 41.
41. P. A. Foster, Jr., "The Phase Diagram of the $\text{Na}_3\text{AlF}_6\text{-LiF}$ System," Unpublished Data, Aluminum Company of America, ALCOA Center, Pa. (1968).
42. J. L. Holm, Thermodynamic Properties of Molten Cryolite and Other Fluoride Mixtures, Inst. of Inorganic Chem., The University of Trondheim, NTH Norway, 1971.
43. J. Ravez and P. Hagenmuller, "Les Systemes $\text{CaF}_2\text{-AlF}_3$ et $\text{SrF}_2\text{-AlF}_3$," *Bull. Soc. Chim.* 7 2545-48 (1967).
44. J. Ravez, J. Viollet, R. DePape and P. Hagenmuller, "Les Systemes $\text{MF}_2\text{-FeF}_3$ (M=Ba, Sr, Ca). Les Fluoferrites Alcalino-Terreux," *Bull. Soc. Chim.* 4 1325-31 (1967).
45. J. L. Holm, "Phase Equilibria in the System $\text{CaF}_2\text{-AlF}_3$," *Acta Chem. Scand.* 19 (6) 1512-14 (1965).
46. M. Malinovsky, J. Vrbenska and I. Cakajdova, "Phasediagramm dis Systems $\text{CaF}_2\text{-AlF}_3$," *Chem. Zvesti.* 21 (1967).
47. J. Millet, H. Pham and M. Rolin, "Les Diagrammes de Phase des Systemes Binaires NaCl-AlF_3 et $\text{CaF}_2\text{-AlF}_3$: Extrapolation du Point Triple du Fluorure d'Aluminium," *Rev. Int. Hautes Temp. Refract.* (11) 4, 277-83 (1974).
48. D. Craig and J. Brown, Jr., "Phase Equilibria in the System $\text{CaF}_2\text{-AlF}_3$ " accepted for publication, *J. Am. Cer. Soc.* 1977.

49. H. Grunhager and J. Mergoil, "Decouverte d'Hydrocalamite et Afwillite Associees a l'Ettringite dans les Porcelonites de Boissejour pres Ceyrat (puy-de-Dome), Bull. Soc. Franc. 86 149-57 (1963).
50. H. Evans, D. Appleman, and D. Handwerken, Amer. Crystallographic Assoc. Annual Program Meeting 42-43 (1963).
51. K. Matiasovsky and M. Malinovsky, "Physicochemical Study of Some Species Important in the Production of Aluminum, II. The Phase Diagram of the System Na_3AlF_6 - CaF_2 - NaCl ," Chem. Zvesti. 14 353-64 (1960) Chem. Abst. 54 (20-21) 22100g (1960).
52. A. Fenerty and E. A. Hollingshead, "Liquidus Curves for Aluminum Cell Electrolyte III. Systems Cryolite and Cryolite-Alumina with Aluminum Fluoride and Calcium Fluoride," J. Electrochem. Soc. 107 (12) 993-97 (1960).
53. M. Rolin, "Le Diagramme Binaire Cryolithe-Fluorure de Calcium. La Diagramme Ternaire Cryolithe-Fluorure de Calcium-Alumine," Bull. Soc. Chim. 1120-25 (1961).
54. J. L. Holm, "The Phase Diagram of the System Na_3AlF_6 - CaF_2 , and the Constitution of the Melt in the System," Acta Chem. Scand. 22 (3) 1004-12 (1968).
55. M. Verdan and R. Monnier, "Etude du Systeme Na_3AlF_6 - CaF_2 au Moyen de l'Analyse Thermique Differentielle en Creuset Scelle," Rev. Int. Hautes Temp. Refract. 9 (2) 205-8 (1972).
56. D. Craig and J. Brown, Jr., unpublished results.
57. P. A. Foster, Jr., "Phase Equilibria in the System Na_3AlF_6 - AlF_3 ," J. Am. Cer. Soc. 53 (11) 598-600 (1970).
58. H. Ginsberg and K. Wefers, "Thermochemische Untersuchungen am System NaF - AlF_3 ," Erzmetall 20 (4) 156-61 (1967).
59. M. Rolin, "Sur la Structure Ionique de la Cryolithe pure Fondue II - Determination Experimentale du Diagramme Binaire Cryolithe. AlF_3 ," Bull. Soc. Chim. (4) 671-77 (1960).
60. J. L. Holm, Investigation of Structure and Phase Ratio of Some Systems in Connection with Aluminum Electrolytes, Norwegian Technical Institute, Trondheim, Norway 7-13 (1963).
61. G. A. Roush and M. Miyake, "Equilibrium of the Series Cryolite-Alumina," Trans. Am. Electrochem. Soc. 48 153-57 (1925). Chem. Abst. 19 (8-16) 2455 (1925).
62. M. Rolin, "Le Diagramme Binaire Cryolithe-Alumine. I. Partie Experimentale," Bull. Soc. Chim. (6) 1201-3 (1960).
63. J. J. Duruz and R. Monnier, "Une Methode d'Analyse Thermique Differentielle pour les Substances Volatiles a Point de Fusion Eleve: Application au Systeme Cryolithe-Alumine," Chimia 21 (12) 572-5 (1967).

64. E. W. Dewing, "The Structure of Cryolite-Alumina Melts," J. Electrochem. Soc. 108 (6) 611-12 (1961).
65. G. Gunther, G. Anderson and H. Perlitz, "On the Luminescence of Phosphors of the Aluminum Oxide-Calcium Fluoride Type Activated with Manganese," Arkiv Kemi 1 565-72 (1950).
66. C. Kuo and T. Yen, "Phase Equilibria and Chemical Reactions in the System $\text{CaF}_2\text{-Al}_2\text{O}_3$," Hua Hsueh Hsueh Pao 30 (4) 381-7 (1964). Chem. Abst. 61²(12-13) 15401h (1964).
67. A. K. Cahtterjee and G. I. Zhmoidin, "The Phase Equilibrium Diagram of the System $\text{CaO-Al}_2\text{O}_3\text{-CaF}_2$," J. Mater. Sci. 7 (1) 93-7 (1972).
68. M. Rolin, "Le Diagramme Ternaire Cryolithe-Fluorure d'Aluminium-Alumine." Bull. Soc. Chim. 1112-1120 (1961).
69. M. Rolin and R. Muhlethaler, "Etude du Systeme Cryolithe de Sodium-Cryolithe de Lithium en tant que Solvant de l'Alumine," Bull. Soc. Chim. 2593-99 (1964).
70. G. A. Abramov, A. A. Kestyukov and L. B. Kulakov, "The Structural Diagram of the Quaternary System Cryolite-Aluminum Fluoride-Calcium Fluoride-Alumina," Electromet. Tsvetnykh Metal. No. 188 45-57 (1957). Chem Abst. 53 (13-16) 11975g (1959).
71. M. Rolin, "Le Diagramme Quaternaire Cryolithe-Fluorure d'Aluminium-Fluorure de Calcium-Alumine," Bull. Soc. Chim: 1404-7 (1961).
72. N. Puschin and A. Baskow, "Das Gleichgewicht in binaren Systemen einigen Fluorverbindungen; Z. Anorg. Chem. 81 354 (1913).
73. P. P. Fedotieff and K. Timofeeff, "Schmelzdiagramme der Systeme KF-AlF_3 und LiF-AlF_3 ," Z. Anorg. Chem. 206 266 (1932).
74. E. P. Dergunov, Doklady Akad. Nauk. SSSR 60 (1948) 1185, cited from 42.
75. R. E. Thoma, B. J. Sturm, and E. H. Guinn, U. S. Atom. Energy Comm. ORNL-3594 (1964).
76. M. Malinovsky, I Cakajdova, and K. Matiasovsky, Chem. Zvesti, 21 794 (1967).
77. M. Rolin, H. Latreille, and H. Pham., "Etude de la Dissociation de la Cryolithe de Lithium a la Fustion, Comparaison avec celle de la Cryolithe de Sodium," Bull. Soc. Chim. 2271 (1969).
78. K. Matiasovsky and M. Malinovsky, "Physico-Chemical Properties of Molten LiF-AlF_3 Mixtures," Coll. Czech. Chem. Comm., 36 3746-3751 (1971).

79. G. Garton and B. M. Wanklyn, "Polymorphism in Li_3AlF_6 ," *J. Inorg. Nucl. Chem.*, 27, 2466-2469 (1965).
80. J. L. Holm, "Phase Transitions and Structure of Lithium Cryolite," *Acta Chem. Scand.* 20, 1167-1169 (1966).
81. J. H. Burns, A. C. Tennissen, and G. D. Trunton, "The Crystal Structure of $\alpha\text{-Li}_3\text{AlF}_6$," *Acta. Cryst.*, B24, 225-230 (1968).
82. J. L. Holm and B. Jenssen, "A Note on the Polymorphy and Structure of Li_3AlF_6 ," *Acta Chem. Scand.* 23, 1065-1068 (1969)
83. P. Drossbach, "Zur Elektrometallurgie des Aluminiums," *Z. Elektrochem.*, 42 (2) 65-70 (1936).
84. V. P. Mashovets and V. I. Petrov, "Phase Diagram of the System $\text{Na}_3\text{AlF}_6\text{-Li}_3\text{AlF}_6\text{-Al}_2\text{O}_3$," *Zh. Prikl. Khim.*, 30 (11), 1695-1698 (1957).
85. M. S. Beletskii and Y. G. Saksonov, "Phases in the System $\text{Na}_3\text{AlF}_6\text{-Li}_3\text{AlF}_6$," *Zh. Neorg. Khim. Vol. II*, No. 2, 414-416 (1957).
86. G. Garton and B. M. Wanklyn, "Reinvestigation of the System $\text{Na}_3\text{AlF}_6\text{-Li}_3\text{AlF}_6$," *J. Amer. Cer. Soc.*, 50 (8) 395-399 (1967).
87. J. L. Holm and B. J. Holm, "Phase Investigations in the System $\text{Na}_3\text{AlF}_6\text{-Li}_3\text{AlF}_6$," *Acta Chemica. Scand.*, 24, 2535-2545 (1970).
88. R. Baylor, Jr., D. P. Stinton, and J. J. Brown, "Subsolidus Equilibria in the System $\text{LiF-AlF}_3\text{-Na}_3\text{AlF}_6$," *J. Amer. Ceram. Soc.*, 57, (11) 470-471 (1974).
89. D. P. Stinton and J. J. Brown, "Phase Equilibria in the System $\text{Na}_3\text{AlF}_6\text{-Li}_3\text{AlF}_6$," *J. Amer. Ceram. Soc.*, 58 (5-6) 257 (1975).
90. R. T. Cassidy and J. J. Brown, Jr., Unpublished data, Virginia Polytechnic Institute and State University (1977).
91. O. Ruff and W. Z. Busch, "Elektrolytische Gewinnung von Magnesium usw.," *Z. Anorg. Chem.*, 144, 96 (1925).
92. G. A. Bukhalova and A. G. Bergman, *Dokl. Akad. Nauk. SSSR*, 66, 67 (1949), cited from 101.
93. W. E. Roake, "The Systems $\text{CaF}_2\text{-LiF}$ and $\text{CaF}_2\text{-LiF-MgF}_2$," *J. Electrochem. Soc.*, 104, 661 (1957).
94. G. A. Bukhalova and V. T. Berezhnaya, *Zh. Neorg. Khim.* 2, 1409 (1957), cited from (100).
95. C. J. Barton, L. M. Bratchev, and W. R. Grimes, Phase Diagrams of Nuclear Reactor Materials. (R. E. Thoma, Ed.) Oak Ridge Natl. Lab., ORNL 2548, 29 (1959).

96. G. Bukhalova, K. Sulaymankulov, and A. K. Bostandzhiyan, "The Melting Diagram of the System Consisting of Fluorides of Lithium, Sodium and Calcium," *Zh. Neorg. Khim.*, 5, 1138-1140 (1959).
97. D. L. Deadmore and J. S. Machin, "Phase Relations in the Systems CsF-LiF, CsF-NaF, and CaF₂-LiF," *J. Phys. Chem.*, 64, 825 (1960).
98. V. A. Gladushchenko and M. A. Zakharchenko, *Zh. Neorg. Khim.*, 11 916 (1966), cited from 101.
99. J. Vrbenska and M. Malinovsky, "Phasendiagramm des Dreistoffsystems Li₃AlF₆-LiF-CaF₂," *Chem. Zvesti.* 21 819 (1967).
100. I. Kostenska, J. Vrbenska, and M. Malinovsky, "The equilibrium 'solidus-liquidus' in the system lithium fluoride-calcium fluoride," *Chem. Zvesti.* 28 531-538 (1974).
101. M. Rolin, "Le Diagram Ternaire Cryolithe-Fluorure d'Aluminium-Fluorure de Calcium," *Bull. Soc. Chim.* 1351-54 (1961).
102. H. Pfundt and H. Zimmermann, "The Quasi Binary System NaF-CaAlF₅, An Investigation from the Ternary System NaF-AlF₃CaF₅," *Ertzmetall* 25 (11) 564-72 (1972).
103. E. W. Dewing, "Solid Solubility of CaF₂ in Cryolite," *Tran. of The Metal. Soc. of AIME* 245 (8) (1969).
104. P. A. Foster, Jr., "Phase Diagram of a Portion of the System Na₃AlF₆-AlF₃-Al₂O₃," *J. Am. Cer. Soc.* 58 (7-8) 288-91 (1975).
105. P. A. Foster, Jr., "Liquidus Curves in the Quaternary System NaF-AlF₃-CaF₂-Al₂O₃," *J. Am. Cer. Soc.* 43 (8) 437-38 (1960).
106. D. P. Stinton and J. J. Brown, Jr., "Phase Equilibria in the System LiF-AlF₃-Na₃AlF₆," *J. Am. Ceram. Soc.*, 58, 264 (1976).



Краткие сведения

о содержании третьего, четвертого и пятого томов труда
А.Е.Вол и И.К.Каган "Строение и свойства двойных металлических систем" и методах работы по их составлению.

Во всех томах принят единый принцип расположения материала, а именно, как металлы, так и образуемые ими двойные системы располагаются в алфавитном порядке по их наименованиям на русском языке. При этом для каждой системы, в зависимости от степени ее изученности, приводятся следующие данные:

1. Диаграмма состояния и кристаллическая структура;
2. Физические и механические свойства (термодинамические, механические, электрические, термоэлектрические и магнитные свойства, поверхностное натяжение и вязкость, упругость паров, плотность, теплоемкость, теплопроводность, термическое расширение);
3. Химические свойства (коррозионная стойкость в атмосферных условиях, а также в различных агрессивных средах и в газах, стойкость против окисления при высоких температурах);
4. Список использованной литературы.

Авторы уделяют очень большое внимание вопросу более полного использования, имеющихся в литературе данных по каждой рассматриваемой системе. При написании третьего тома, в который вошли системы золота, индия, иридия, иттербия и иттрия, были использованы данные, опубликованные по 1970-71 гг. включительно. При подготовке материалов для 4-го тома, в который войдут системы кадмия, калия и кальция, используются данные, опубликованные по 1973-74 гг. включительно. Для составления 5-го тома, в который войдут системы кислорода, кобальта и кремния, будут использованы литературные данные, опубликованные по 1975-76 гг. включительно.

В третьем томе (объем ~ 70 печатных листов), выход которого из печати ожидается в ноябре-декабре 1976 г., приводятся данные

по 288 двойным системам, в том числе для 116 систем приведены диаграммы состояния во всей области концентраций и сделан подробный обзор свойств сплавов; для 23 систем приведены диаграммы состояния не во всей области концентраций и менее подробное описание свойств; сведения о растворимости в жидком и твердом состояниях, составе промежуточных фаз с описанием в ряде случаев отдельных свойств, приведены для 149 двойных систем.

При построении диаграмм состояния предпочтение отдавалось данным, полученным при исследовании наиболее чистых сплавов с одновременным применением нескольких современных методов физико-химического анализа. В тех случаях, когда имеющихся в распоряжении авторов данных было недостаточно для однозначного решения, в книгу помещали два варианта одной и той же диаграммы состояния с указанием литературных данных, использованных для построения каждой из них (см. например системы *Au-In*, *Au-Pu*, *In-Mg*, *In-Na*, *In-Tl*, *Ir-Ti*).

Объем использованной в 3-м томе литературы можно иллюстрировать такими примерами: при рассмотрении системы *Au-Cu* использовано 345, системы *In-Sb* - 214, системы *Au-Ag* - 162 литературных источника. Таким образом, только для этих трех систем использовано более 700 литературных источников.

В 4-м томе (объем около 50 печатных листов) рассмотрено 163 системы. В этом томе для 54 систем приведены диаграммы состояния во всей области составов и сделан подробный обзор свойств сплавов. Для остальных 109 систем приведены сведения о взаимной растворимости компонентов системы и (или) составе образуемых ими промежуточных фаз с описанием в ряде случаев свойств сплавов.

Объем 5-го тома предполагается ~ 50 печатных листов с рассмотрением около 140 систем.

В качестве основных материалов для написания перечисленных

выше трудов авторы используют свою обширную картотеку, начало которой было положено одним из них (А.Е.Вол) еще в 1931 г., когда подготавливались к изданию книги "Цинк и его сплавы" (Стандартгиз, 1933 г.), "Никель и его сплавы" (Цветметиздат, 1932 г.) и "Кремнистые бронзы и их промышленное применение" (Объедин. научно-технич. изд-во, 1935 г.). Эта картотека продолжала непрерывно пополняться по новым литературным источникам и в настоящее время включает в себя карточки по литературным данным по 1973-1974 г.г. включительно. Каждая карточка является подробным рефератом с приложением графиков и таблиц оригинального источника по двойным системам и содержит данные, используемые авторами в своих трудах при описании той или иной системы. Карточки составляются только по первоисточникам. Даже в тех случаях, когда имеется заслуживающая доверия компиляция (например книги Хансена, Эллиотта и Шенка по двойным системам), имеющиеся в них ссылки на оригинальные работы, используются как библиографические данные для составления подробной карточки по первоисточникам. Это обусловлено тем, что в упомянутых работах приводятся только диаграммы состояния и нет никаких данных по свойствам сплавов, исследования которых послужили основанием для построения этих диаграмм. В случае невозможности ознакомления с первоисточниками - используются данные компилятивных работ с ссылками как на первоисточник, так и на компилятивную работу.

Выбор статей для составления подробных карточек производится:

1. путем систематического просмотра целого ряда журналов, издаваемых в СССР и в других странах (перечень журналов см. ниже);
2. путем систематического просмотра *Metallurgical Abstracts in Journal Institute of Metals (London)*;
3. путем систематического просмотра реферативных журналов "Металлургия" и "Химия", издаваемых в СССР.

Классификация карточек в картотеке полностью отвечает принятой для издания трудов. Каждому элементу периодической системы Д.И. Менделеева присвоен порядковый номер, соответствующий его расположению по наименованию в русском алфавите, а бинарная система обозначается дробным числом, состоящим из порядковых номеров обоих входящих в нее элементов. По этой классификации, например, азот обозначен цифрой 1, алюминий – цифрой 3, ванадий – цифрой 7, а сплавы систем: азот–алюминий – дробным числом 1/3, алюминий – ванадий – 3/7, азот – ванадий – 1/7 и т.д. Такая нумерация карточек дает возможность быстро рассортировать их и расположить в картотеке в той последовательности, в какой описываются системы.

Перечень систематически просматриваемых журналов:

1. Атомная энергия,
2. Доклады Академии Наук СССР,
3. Журнал неорганической химии,
4. Журнал прикладной химии,
5. Журнал структурной химии,
6. Журнал физической химии,
7. Известия Академии Наук СССР. Неорганические материалы,
8. Известия Академии Наук СССР. Металлы,
9. Известия Высших учебных заведений. Цветная металлургия,
10. Кристаллография,
11. Металловедение и термическая обработка металлов,
12. Украинский химический журнал,
13. Физика металлов и металловедение,
14. Acta Crystallographica,
15. Acta Metallurgica,
16. Comptes rendus Acad. Sci., Paris,
17. Journ. Less-Common Metals,
18. Journ. Institute of Metals,

19. Transactions ASM,
 20. Transactions AIME (Trans. Metallurg. Soc. AIME),
 21. Metallurgical Transactions c 1970,
 22. Zeitschrift für anorganische Chemie,
 23. Zeitschrift für Kristallographie,
 24. Zeitschrift für Metallkunde.
- } 1970r

AM
Revised

Brief Summary

The 3rd, 4th, and 5th volumes of the "Handbook of Binary Metallic Systems" and the Methods of compilation & editing.

*by A. E. Vol & E. K. Kagan
Leningrad, USSR*



An English translation prepared by G. Marinenko, Analytical Chem. Div., NBS

Brief Information on the Content of the Third, Fourth, and Fifth Volumes of the Collection "Structure and Properties of Binary Metallic Systems" by A. E. Vol and I. K. Kagan, As Well As Presentation Of The Methods Of The Work In Compilation Of These Volumes

A. E. Vol and I. K. Kagan
Leningrad, USSR

In all of the volumes a single principle of organizing the material was adhered to; namely, both metals, as well as the binary systems which these metals form, were arranged in alphabetical order in accordance with their chemical symbols in the Russian language. At the same time for each system, depending on the degree to which the system was studied, the following data were cited:

- (1) Phase Diagram and Crystal Structures;
- (2) Physical and Mechanical Properties (Thermodynamic, Mechanical, Electrical, Thermoelectric and Magnetic Properties, Surface Tension and Viscosity, Vapor Pressure, Density, Heat Capacity, Thermoconductivity, and Thermal expansion);
- (3) Mechanical Properties (Corrosion Stability under atmospheric conditions, as well as in various other corrosive media and gasses, Oxidation Stability at elevated temperatures);
- (4) Enumeration of bibliography which was used.

The authors devote extremely great attention to the question of fuller utilization of data which are available in the literature on each of the considered systems. In writing the third volume, which contained systems of Au, In, Ir, Yb, and Y, data were utilized which were published until 1970-1971 inclusively. In preparation of the materials for the fourth volume which included Cd, K, and Ca systems, data were utilized which were published until 1973-1974 inclusively. In compilation of the fifth volume, which contains O, Co, and Si systems, literature data published until 1975-1976 inclusively were utilized.

The third volume (amounting to approximately 70 printed pages), publication of which is expected to be in Nov.-Dec. 1976* the data are cited on 288 binary systems, including phase diagrams over the entire composition range and detailed studies of the properties for 116 systems; for 23 systems phase diagrams are provided, but not over the entire composition range and the descriptions of the properties are less detailed. Information on the solubility in liquid and solid states, composition of the intermediate phases with the description in a number of cases of individual properties are given for 149 binary systems.

In constructing the phase diagrams the preference was given for data which were obtained with the study of the purest alloys with simultaneous use of several modern methods of physico-chemical analysis. In those cases where the data available to the authors were insufficient for a single-valued decision, two variations were included in the book for the same phase diagram indicating the literature data which were utilized for the construction of each of these (see for example the following systems: Au-In, Au-Pu, In-Mg, In-Na, In-Tl, Ir-Ti).

The scope of literature utilized in the third volume can be illustrated with the following example: in considering the Au-Cu system, 345 literature sources were used, for In-Sb system 214 sources were used, while for Au-Ag system, 162 sources were utilized. Thus, for these three systems only, more than 700 literature sources were utilized.

In the fourth volume (approximated 50 printed pages) 163 systems are considered. Phase diagrams are provided over the whole composition range and a detailed review of the properties of 54 alloy systems is made. For the remaining 109 systems, information is given on the mutual solubility of the components of the systems and/or composition of the intermediate phases which are formed by the component metals along with a description of the properties of the alloys in a number of cases.

The fifth volume is expected to be approximately 50 printed pages and to contain approximately 140 systems.

*Translator's note: has been published by "Nauka", Moscow, 1976.

The basic materials which were used for compilation of the above cited work were the extensive card file of the authors, which was initiated by one of the authors (A. E. Vol) back in 1931, when the books "Zinc and Its Alloys" ("Standartgiz" Publishing House, 1933), "Nickel and Its Alloys" ("Tsvetmetizdat" Publishing House, 1932) and "Silicon Bronzes and Their Industrial Applications" ("Ob'Yedin. Nauchno-Tkhnich." Publishing House, 1935) were being prepared for publication. This card file was continuously updated from new literature sources and at present includes literature data up to 1973-1974 inclusively. Each card is a detailed reference with the attached graph and tables of the original source on the binary systems and contains data which are utilized by authors in their work in describing these various systems. The cards are compiled only from the original sources. Only in those cases, when reliable compilations are available (for example, the books by Hansen, Elliott, and Shunk on binary systems), the references contained in those books to the original works were utilized as bibliographic data for the compilation of a detailed card file on primary sources. This results from the fact that in the above works only phase diagrams are given and there are no data on the properties of alloys, the studies of which served as the basis for the construction of these phase diagrams. In a case when it is not possible to become familiar with the primary source, the data of compiled works are utilized with references both to the primary source as well as to the compilation utilized.

Choice of articles for compilation of the detailed card file is performed as follows:

1. By systematic review of the whole series of journals which are published in the USSR and other countries (for a list of journals, see below);
2. By systematic review of the Metallurgical Abstracts in the Journal of Institute of Metals (London);
3. By systematic search of the reference journals ("Referativni Zhurnal") "Metallurgiya" and "Khimiya", published in the USSR.

The classification of cards in the card file corresponds completely to the format used in publishing the work. An ordinal number is given to each of the elements of the periodic system of elements of D. I. Mendeleev, which corresponds to its alphabetical position in a list of chemical symbols in the Russian language, and binary systems are denoted by fractional numbers, which consist of both ordinal numbers of the elements which comprise the system. In accordance with this classification, for example, nitrogen

is designated by 1, Aluminum by 3, Vanadium by 7, and the alloys of the systems: nitrogen-aluminum by 1/3, aluminum-vanadium by 3/7, nitrogen-vanadium by 1/7, etc. Such numbering of cards enables one to quickly sort them and place them into the card file in the sequence which corresponds to the description of the system.

The list of journals which are systematically searched:

1. Atomnaya Energiya (Atomic Energy),
2. Doklady Akademii Nauk SSSR (reports of the Academy of Sciences of the USSR),
3. Zhurnal Neorganicheskoy Khimii (Journal of Inorganic Chemistry),
4. Zhurnal Prikladnoy Khimii (Journal of Applied Chemistry),
5. Zhurnal Strukturnoy Khimii (Journal of Structural Chemistry),
6. Zhurnal Fizicheskoy Khimii (Journal of Physical Chemistry),
7. Izvestiya Akademii Nauk SSR. Neorganicheskiye Materialy (News of the Academy of Sciences of the USSR, Inorganic Materials),
8. Izvestiya Akademii Nauk SSSR. Metally (News of the Academy of Sciences of the USSR, Metals),
9. Izvestiya Vysshikh Uchebnykh Zavedeniy. Tsvetnaya Metallurgiya (News of the Institutions of Higher Learning. Nonferrous Metallurgy),
10. Kristallografiya (Crystallography),
11. Metallovedeniya i Termicheskaya Obrabotka Metallov (Metal Science and the Thermal Treatment of Metals),
12. Ukrainskiy Khimicheskii Zhurnal (Ukrainian Chemical Journal),
13. Fizika Metallov i Metallovedeniya (Physics of Metals and Metal Science),
14. Acta Crystallographica,
15. Acta Metallurgica,
16. Comptes rendus Acad. Sci., Paris,
17. Journ. Less-Common Metals,
18. Journ. Institute of Metals,
19. Transactions ASM,
20. Transactions AIMME (Trans. Metallurg. Soc. AIME),
21. Metallurgical Transactions c1970,
22. Zeitschrift fur anorganische Chemie,
23. Zeitschrift fur Kristallographie,
24. Zeitschrift fur Metallkunde.



The Determination of Phase Diagrams for Liquid
Oxides and Metallurgical Slags by
Hot-Wire Microscopy

by

H. Alan Fine
Department of Metallurgical Engineering
University of Arizona
Tucson, Arizona 85721

Hot-wire microscopy has been used successfully to determine the liquidus surfaces for many oxide systems. The technique, which lends itself to measurements in all temperature ranges, can be used to determine liquidus temperatures for transparent or semi-transparent melts under reducing, neutral or oxidizing conditions.

A review of the development of hot-wire microscopy is presented. The limitations and the experimental idiosyncrasies of the technique are discussed and special equipment necessary for atmosphere control within the hot-wire microscope are described.

INTRODUCTION

The phase diagrams for liquid oxides and slags that occur in metallurgical operations are important tools for developing a better understanding of the phase relations and physical chemistry of the processes. The classical quenching technique used for determination of these phase diagrams was, however, a very long and tedious procedure. Consequently, many important phase diagrams were not known. Within the last twenty-five years, a new technique known as hot-wire or hot-filament microscopy has been developed for direct observation of oxide melts. Using this device, the liquidus surfaces of many phase diagrams have been easily and quickly determined. This article reviews the development of the hot-wire microscope, with special emphasis being placed on its use for determination of the liquidus surfaces of oxide mixtures and metallurgical slags. Modifications to the standard hot-wire microscope which are being used to study blast-furnace slags in atmospheres containing an oxygen partial pressure of 10^{-15} atm. are also described.

HOT-WIRE APPARATUS

The development of micro-furnaces for the direct microscopic observation of melts dates back to 1891⁽¹⁾. However, it was the development of a micro-furnace by Ordway⁽²⁾ in 1952, which could be used to contain, heat and monitor the temperature of a sample, that lead to the hot-wire technique for the determination of the liquidus surfaces of oxides. In Ordway's original apparatus, a small sample was held by capillarity on a Pt/Pt-10% Rh thermocouple. The thermocouple, made from 0.25 mm wires, served as the heating element, i.e. furnace, and the container for the sample. A high frequency current produced by an audio amplifier, which was driven by an audio oscillator, was used to heat the thermocouple and sample. The simultaneous measurement of the thermocouple emf was made by placing a low-pass filter between a second pair of leads connected to the thermocouple and a voltage measuring device, such as a potentiometer.

A modification suggested by Welch⁽³⁾ to the electrical circuit substantially simplified and reduced the cost of Ordway's unit. In Welch's circuit, a high-speed polarized relay which vibrated at the power main frequency (50 or 60 hz.) was used to replace the low-pass filter and to eliminate the need for a high-frequency heating current. The relay simply switched connections within the circuit so that heating of the thermocouple by the main current was done during one half of the power cycle, while temperature measurement was made during the other. To attain higher operating temperatures and to eliminate the need for a cold junction, Welch also suggested that the Pt/Pt-10% Rh thermocouple used by Ordway be replaced by a Pt-5% Rh/Pt-20% Rh thermocouple.

A microscope with a working distance of approximately 25 mm was also commonly used with the unit to facilitate observation of the sample and thermocouple assembly. Modifications to protect the microscope from damage by the hot-wire unit were not necessary because of the small thermal capacity and low power dissipation (usually much less than 50 W) from the sample.

Even though the aim of Ordway's initial work was to develop a furnace for growing single crystals of refractory materials, the usefulness of this apparatus for liquidus determinations was evident. Within a few years of the report of his work, the hot-wire microscope had been successfully used by Welch⁽⁴⁾ and Baldwin⁽⁵⁾ to determine blast furnace slag liquidus temperatures. The work of Welch⁽⁴⁾ proved that the hot-wire method was a viable technique for liquidus measurement, by showing that excellent agreement could be obtained from experiments performed using hot-wire microscopy, the classical quenching technique and thermal analysis. A comparison of results of experiments performed by Welch and Baldwin⁽⁵⁾ showed that excellent agreement on tests performed in different laboratories was also possible.

Further modifications to the hot-wire unit reduced contact wear and stray voltages that were produced in the relay. A simultaneous reduction in the variations in sample temperature resulting from main power drift was also achieved.^(6,7) Slightly different circuit designs allowed the hot-wire unit to be used for thermal analysis⁽⁸⁾ and differential thermal analysis⁽⁹⁾. The use of an Ir-40% Rh/Ir-60% Rh thermocouple increased the working temperature of the unit to 2150°C⁽¹⁰⁾.

EXPERIMENTAL PROCEDURE AND SOURCES OF ERROR

The procedure for liquidus temperature determination consists of a sample preparation step and a temperature measurement step. A discussion of the complete procedure and sources of error follows.

Sample Preparation - The hot-wire technique requires that a small sample, usually around one milligram, of known composition, be held by capillarity on a thermocouple junction. Samples of this size are, however, quite difficult to prepare. Hence, representative samples of a larger master sample of known composition are studied. To insure that representative samples are obtained, most investigators have thoroughly mixed a several-gram sample of the oxide mixture. The sample is then fused, equilibrated for approximately an hour and quenched to prevent segregation during solidification. The master sample is then finely ground and if necessary, fused, etc. again. Hot-wire samples are taken by moistening the thermocouple junction and inserting the junction into the finely powdered master sample. The moisture in the small sample is then driven off by heating the sample above 100°C and holding it at that temperature for several minutes.

Perhaps the most serious error when using the hot-wire technique is associated with obtaining a representative sample of the oxide mixture. Sample homogeneity, however, is easily checked using the hot-wire technique, as a sample that is not well mixed will produce a wide band of experimental results for the same master slag sample.

Temperature Measurement - After drying a sample on the thermocouple, the sample is usually heated until molten and held for several minutes. The sample is then slowly cooled until the first crystal

solidifies within the melt and the temperature is noted. The temperature at which this crystal is in equilibrium with the melt is the liquidus temperature of the sample. It is usually best to determine a rough estimate of this temperature and then refine the value by slowly heating and cooling the sample in the temperature range around the initial estimate.

Another experimental error can arise if formation of the first crystal of solid does not occur at the thermocouple junction. As shown by Cavalier⁽¹¹⁾, temperature differences as large as 30°C can exist within the oxide sample. It is, therefore, necessary that the first crystal which solidifies from the melt be in equilibrium with the melt and at the thermocouple junction.

Several different methods have been used to correct this problem. A second small thermocouple which has been inserted into the melt has been used to measure the liquidus temperature^(11,12). In this procedure, the second thermocouple acts like a heat sink, causing solidification to occur on this thermocouple. However, an error may still be present with this procedure, as the thermocouple wires will tend to carry heat away from its junction, and produce a temperature gradient in the melt. Consequently, care must be taken to measure the liquidus when the first crystal on the secondary thermocouple is stable, i.e. not growing or melting. Perhaps a more satisfactory method for making the first crystal form on the thermocouple junction is to adjust the shape of the thermocouple, i.e. the furnace. In principle, by making the coldest portion of the thermocouple the junction, the first crystallization should be forced to occur at the

junction. In Ordway's⁽²⁾ and Welch's^(3,4) work a V-shaped thermocouple with the junction at the base of the V was used to produce solidification at the junction. Baldwin⁽⁵⁾ used a U-shaped element with a smaller diameter junction at the base of the U to obtain the same results. A thermocouple with three leads, the extra lead to facilitate emf measurement, may also result in first solidification at the junction, because of less power generation due to a larger cross-section at this point⁽¹³⁾. There is probably not a single solution to this problem. The type of junction that should be used is probably dependent on the particular experiments. However, regardless of the type of junction used, extreme care must be taken to assure that the first crystal forms on the junction and is stable, to obtain a correct liquidus measurement.

Even when precautions are taken to obtain a stable crystal, it is still possible to make an incorrect measurement. Some oxide mixtures, and especially those high in SiO_2 , do not crystallize easily upon solidification⁽¹⁴⁾. It is thus possible to "miss" the liquidus temperature. Under these circumstances, it is necessary to solidify and crystallize the oxide mixture. Then, slowly heating the solid and observing the temperature at which the last crystal is in equilibrium with the melt will allow measurement of the liquidus^(15,16). Again, care must be taken to have the last crystal at the thermocouple junction. In order for this to occur, it may be necessary to use a differently shaped thermocouple.

When elements such as FeO and/or MnO are present in the oxide, the liquidus may be missed because the sample becomes opaque. To aid

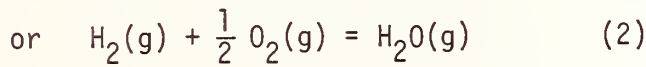
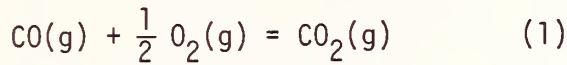
in the observation of solidification within the melt, polarized light or ultra-violet light can be used. However, in general the technique works best for transparent melts and the accuracy decreases as the melt becomes opaque. For transparent melts, overall experimental errors of $\pm 1^\circ\text{C}$ have been obtained in calibration experiments⁽⁵⁾. Errors of $\pm 3^\circ\text{C}$ have been estimated for liquidus temperature measurements^(4,5). Larger errors would be anticipated for melts that were not transparent.

MODIFICATIONS FOR THE CURRENT INVESTIGATION

The vast majority of the previous studies which employed hot-wire microscopy were done on oxide mixtures made of very stable oxides, such as CaO, MgO, SiO₂ and Al₂O₃. For these oxides, almost any atmosphere would be "inert", i.e. would not change the melt composition. Consequently, the studies were done within a small container to minimize temperature variations produced by convection and the container was filled or continuously flushed with air.

In the present work, the effect of the minor constituents of blast furnace slag, such as FeO, MnO, Na₂O and TiO₂, on the liquidus surface of the CaO - SiO₂ - MgO - Al₂O₃ system was to be determined. In this study, the oxygen partial pressure would affect the state of oxidation of the minor constituents. Hence, careful control of the atmosphere at an oxygen partial pressure of 10^{-15} atm. was necessary. A description of the system used to produce a controlled atmosphere for these experiments follows. Several other modifications to the basic hot-wire microscope are also described and the results of several preliminary experiments are given.

Gas System - The standard procedure for fixing the oxygen potential of a gas phase is based upon the reaction



At equilibrium

$$P_{\text{O}_2} = \frac{1}{K_c} \frac{P_{\text{CO}_2}^2}{P_{\text{CO}}} \quad (3)$$

$$\text{or } P_{\text{O}_2} = \frac{1}{K_H} \frac{P_{\text{H}_2\text{O}}^2}{P_{\text{H}_2}} \quad (4)$$

where P_{O_2} , P_{CO_2} , ... are the partial pressures of O_2 , CO_2 , ..., respectively. K_c and K_h are the equilibrium constants for reaction 1 and 2, respectively and are both functions of temperature.

In hot-wire microscopy, a very small sample is contained within an otherwise cold enclosure. It was anticipated that a large temperature gradient would exist in the general region next to the surface of the sample, making it impossible to accurately determine the temperature of the gas in this region. Without an accurate temperature, K_c and K_h cannot be determined. Hence, proper gas mixture cannot be made. Therefore, this standard technique would not work for hot-wire microscopy.

The solution to this problem was to build a gas system that produced an inert gas that contained the specified partial pressure of oxygen. This was accomplished by passing dried nitrogen through a

fluidized-bed reactor that contained a mixture of -200 mesh Fe_3O_4 and Fe_2O_3 , see Fig. 1.

Equilibrium is attained very rapidly in Fluidized beds⁽¹⁷⁾. Consequently, the partial pressure of oxygen in the nitrogen was fixed by the $\text{Fe}_3\text{O}_4/\text{Fe}_2\text{O}_3$ equilibrium and was dependent on bed temperature only. A solid electrolytic cell⁽¹⁸⁾ contained in an auxiliary furnace, see Fig. 2, that could be inserted into the gas system was occasionally used to check oxygen partial pressures. Excellent agreement was obtained between calculated values based upon $\text{Fe}_3\text{O}_4/\text{Fe}_2\text{O}_3$ equilibrium and the electrolytic cell. Further verification of the technique was made by replacing the Pt/Pt-10% Rh thermocouple with a Cu/Constantan thermocouple. Measuring the temperature at which the copper oxidized in the atmosphere, again gave good agreement between the calculated and experimental temperatures.

Thermocouples - The manufacture of a large number of small thermocouples for use in the hot-wire unit can be a very costly and time-consuming process. An inexpensive and easily done technique for making small butt-weld thermocouples which had been developed earlier was therefore used⁽¹⁴⁾.

A large number of thermocouples were made by electron-beam welding the edge of a 0.05 mm sheet of platinum to the edge of a 0.05 mm sheet of platinum-10% rhodium. The sheets were then sheered perpendicular to the welded seam to produce thermocouples that had a uniform cross-section and were 0.05 mm thick, 0.2 mm wide and approximately 25 mm long.

For many slag compositions, it was often necessary to perform heating experiments. A thermocouple bent into a U-shape with a

slightly larger bottom than top works well in both heating and cooling experiments, see Fig. 3. The support stations for the hot-wire unit were made from 0.8 mm platinum and platinum-10% rhodium wires. All other connections to the unit were made from compensating wire. The complete probe is shown in Fig. 4.

Electrical Circuit - An electrical circuit modified from one used by Haupin⁽¹⁹⁾ for measuring thermal conductivities, was used in this study, see Fig. 5. Temperature control to 1°C was attained by using three variacs; one as a coarse adjustment, one as a fine adjustment and one to set the span of the fine adjustment. A Doric DS-100 integrating millivoltmeter was used for emf measurement. This unit together with the low-pass filter in the circuit reduced the ac heating voltage and noise to less than 1 μ V and permitted temperature measurement to 0.1°C.

Calibration of the thermocouples and electronics was done by measuring the melting point of Na₂SO₄. The results of many experiments performed on several different thermocouples were always within $\pm 1^\circ\text{C}$ of the published value⁽²⁰⁾.

Initial Experiments - The effect of small additions of Na₂O on the liquidus surface of the CaO - SiO₂ - MgO - Al₂O₃ system were studied first. The result of one set of experiments are tabulated below and shown in Fig. 6. A measurement of the liquidus temperature of the slag without an addition of Na₂O was not made. However, the value of 1513°C obtained by extrapolation of the line fit by least-square regression analysis. To 0% Na₂O is in excellent agreement with the value of 1510°C determined from the expanded section of the phase diagram determined by Snow⁽²¹⁾.

THE EFFECT OF Na₂O ON THE LIQUIDUS TEMPERATURE OF BLAST-FURNACE SLAGS

Sample Number	Weight percentage					Measured liquidus temp °C
	CaO	MgO	SiO ₂	Al ₂ O ₃	Na ₂ O	
2 ₁	48.66	3.97	36.75	10.16	(0.43)	1502 [±] 1
2 ₂	48.71	3.98	36.78	10.17	(0.35)	1503 [±] 2
2 ₃	48.54	3.96	36.66	10.13	(0.69)	1488 [±] 2
2 ₄	48.77	3.98	36.82	10.18	(0.23)	1504 [±] 2
2 ₅	48.79	3.98	36.84	10.19	(0.17)	1506 [±] 2

Compositions listed in parentheses have been determined by chemical analysis.

CONCLUDING REMARKS

The hot-wire microscope with its maximum operating temperature of 2150°C under reducing, neutral or oxidizing conditions, has been shown to be a useful tool for determination of the liquidus temperatures of oxide mixtures. Because of its simplicity and low cost, the technique should be considered by phase diagram researchers, when dealing with transparent or semi-transparent melts.

ACKNOWLEDGMENTS

The author wishes to thank Janna McIntosh and Sabri Arac for their help in preparing this paper. The American Iron and Steel Institute is also gratefully acknowledged for financial support of the blast furnace slag work.

REFERENCES

1. Joly, J., Proc. Rev. Irish Acad. 2 (1891), 38.
2. Ordway, F., J. Res. Nat. Bur. Stand. 48 (1952), 152.
3. Welch, J. H., J. Sci. Instrum. 31 (1954), 458.
4. Welch, J. H., J. I. S. I. 183 (1956), 275.
5. Baldwin, B. G., J. I. S. I. 186 (1957), 388.
6. Welch, J. H., British Patent Application No. 24573/59, 1959.
7. Welch, J. H., J. Sci. Instrum. 38 (1961), 402.
8. Mercer, R. A. and Miller, R. P., J. Sci. Instrum. 40 (1963), 352.
9. Miller, R. P. and Sommer, G., J. Sci. Instrum. 43 (1966), 293.
10. Gutt, W., J. Sci. Instrum. 41 (1964), 393.
11. Cavalier, G., Cer. Bul. 39 (1960), 142.
12. Derge, G., Trans. AIME 239 (1967), 1480.
13. Causer, R. L., J. Sci. Instrum. 43 (1966), 650.
14. Fine, H. A., Sc. D. Thesis, M.I.T., Cambridge, Mass., 1973.
15. Ohno, A. and Ross, H. U., Can. Met. Quat. 2 (1963), 243.
16. Rennie, M. S. et al., J. S. African Inst. Min. Met. 73 (1972), 1.
17. Frantz, J. F., Chem. Eng. 69 (1962), 89.
18. Kiukkola, K. and Wagner, C., J. Electrochem. Soc. 104 (1957), 379.
19. Haupin, W. E., Cer. Bul. 39 (1960), 139.
20. Handbook of Chemistry and Physics, 48th ed., Chemical Rubber Co., Cleveland, Ohio, 1967, p. 13-226.
21. Snow, R. B., Proc. Blast Furnace, Coke Oven and Raw Mat. Conf., AIME, 1962, p. 21.
22. Arac, S., M. S. Thesis, U. of AZ., Tucson, Arizona, 1976.

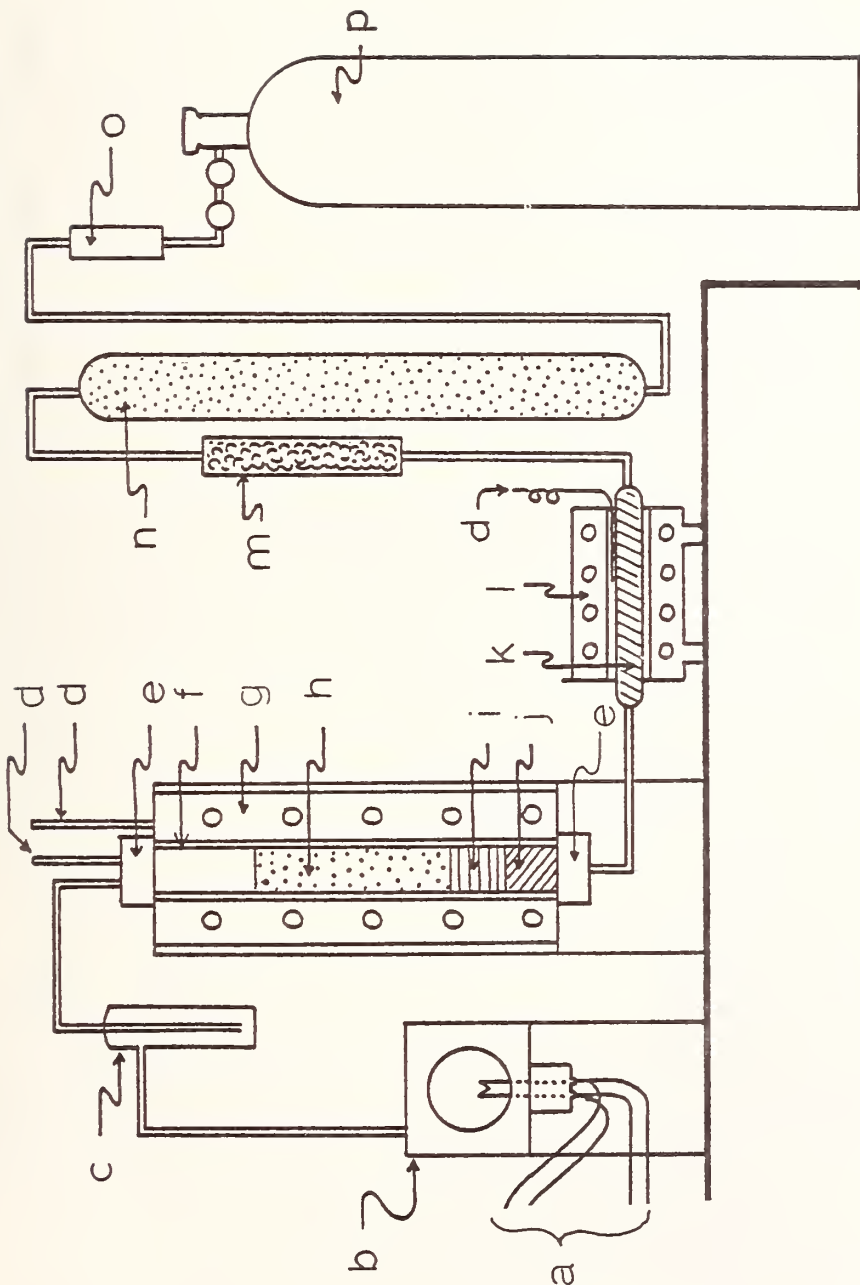


Fig. 1 Gas system; (a) hot-wire thermocouple leads, (b) hot-wire unit and container, (c) dust filter, (d) chromel/alumel thermocouple, (e) brass fitting, (f) quartz tube, (g) tube furnace, (h) Fe_3O_4/Fe_2O_3 fluidized bed, (i) quartz wool, (j) mullite chips, (k) pyrex wool, (l) tube furnace, (m) P_2O_5 , (n) drierite, (o) flow meter, and (p) N_2 supply. All other gas connections were made with pyrex glass. (Modified from Ref. 22).

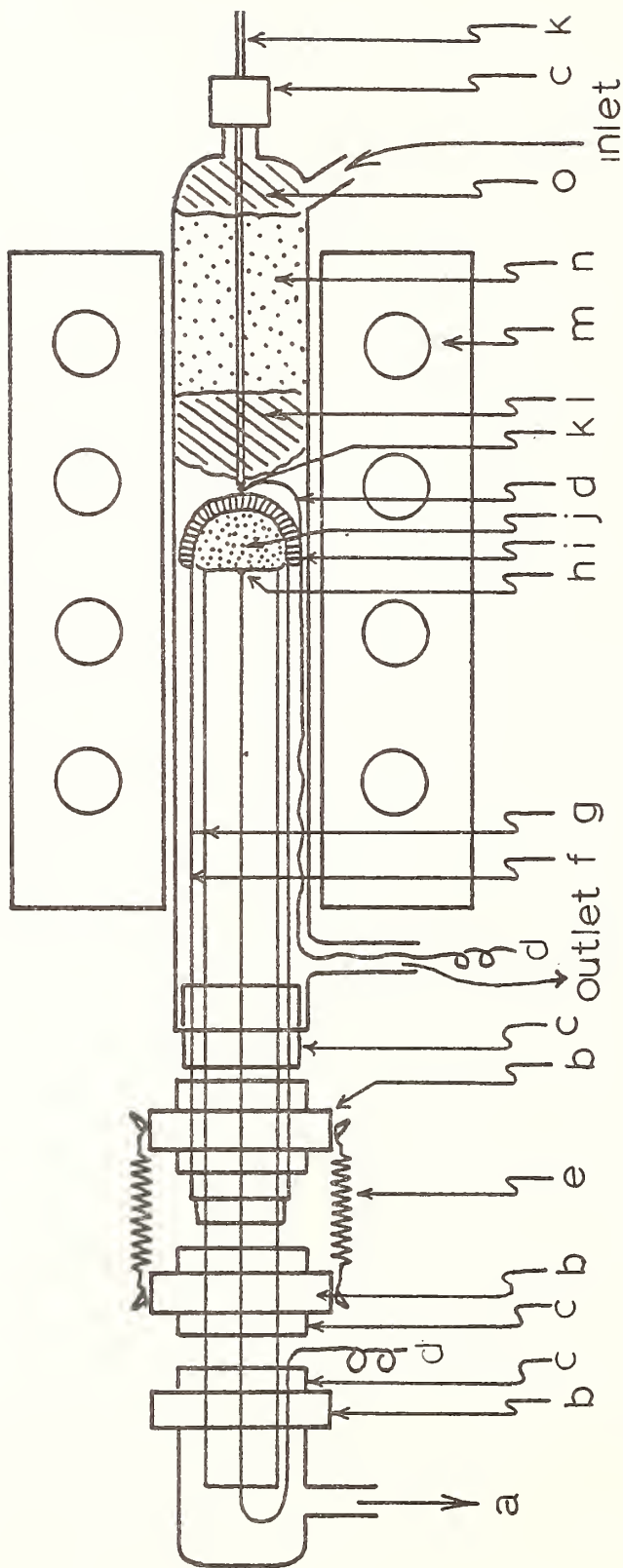


Fig. 2 Oxygen probe; (a) to vacuum pump, (b) metal clamp, (c) rubber seal, (d) Pt wire, (e) springs (f) lime-stabilized Zirconia tube, (g) mullite tube, (h) Pt foil, (i) Pt-gauze, (j) Ni/NiO reference electrode, (k) chromel/alumel thermocouple, (l) quartz wool, (m) tube furnace, (n) silica sand, (o) pyrex wool. (Modified from Ref. 22).

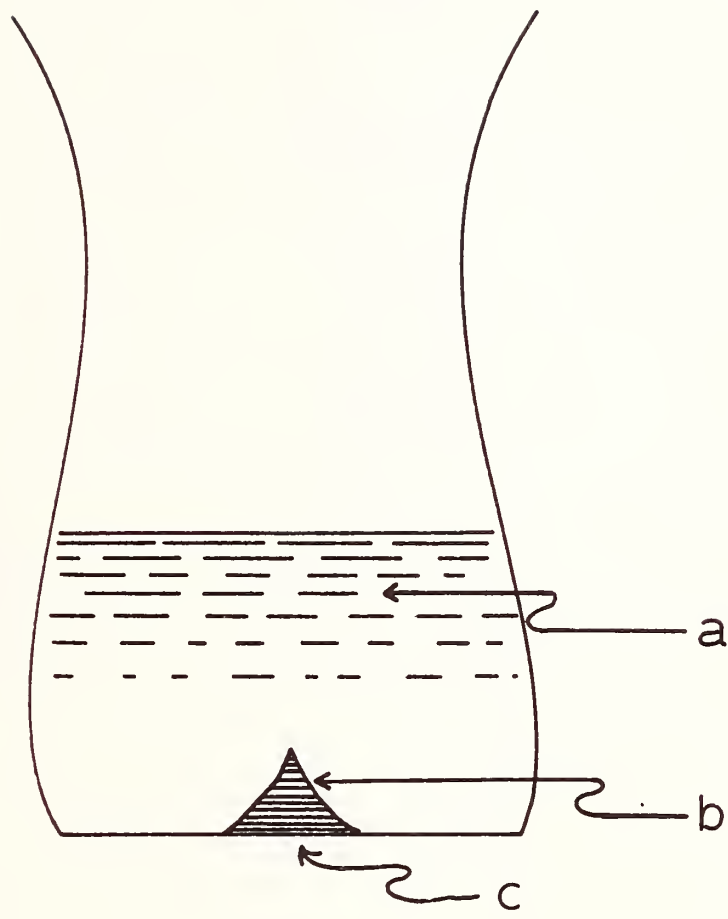


Fig. 3 Schematic representation of hot-wire thermocouple; (a) melt, (b) first crystal, and (c) thermocouple junction (Modified from Ref. 22).

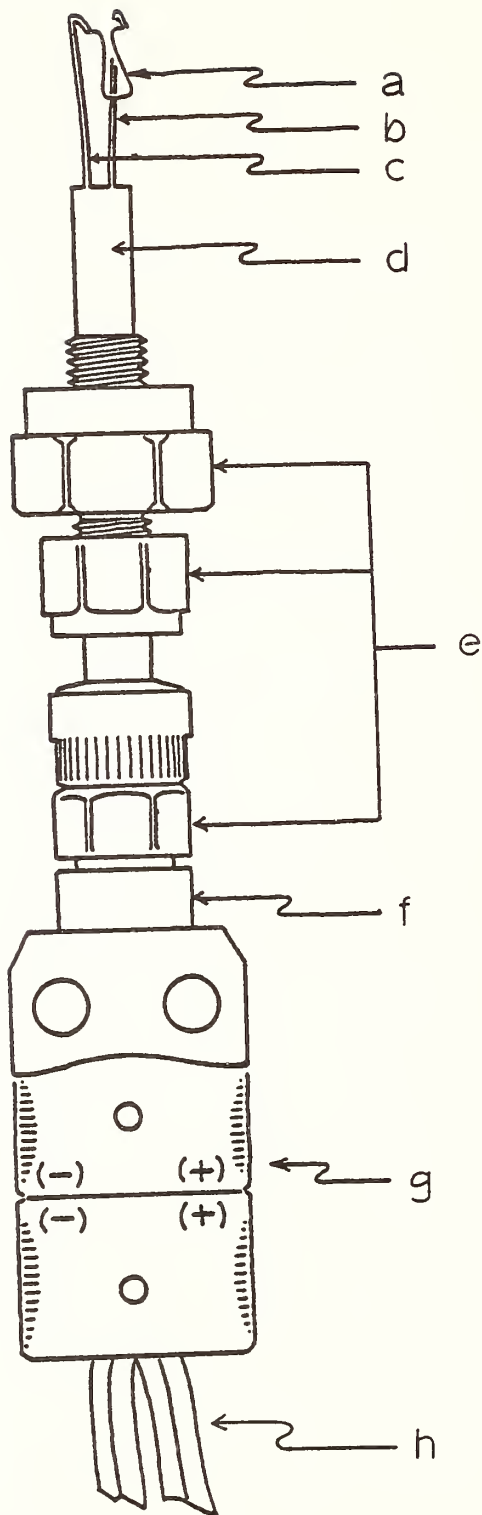


Fig. 4 Complete hot-wire assembly; (a) thermocouple, (b) Pt support and lead, (c) Pt-10% Rh support and lead, (d) Al_2O_3 insulator, (e) Swage lok fittings, (f) tube clamp, (g) Omega Eng. thermocouple connector, and (h) compensating wire for Pt/Pt-10% Rh thermocouples (Modified from Ref. 22).

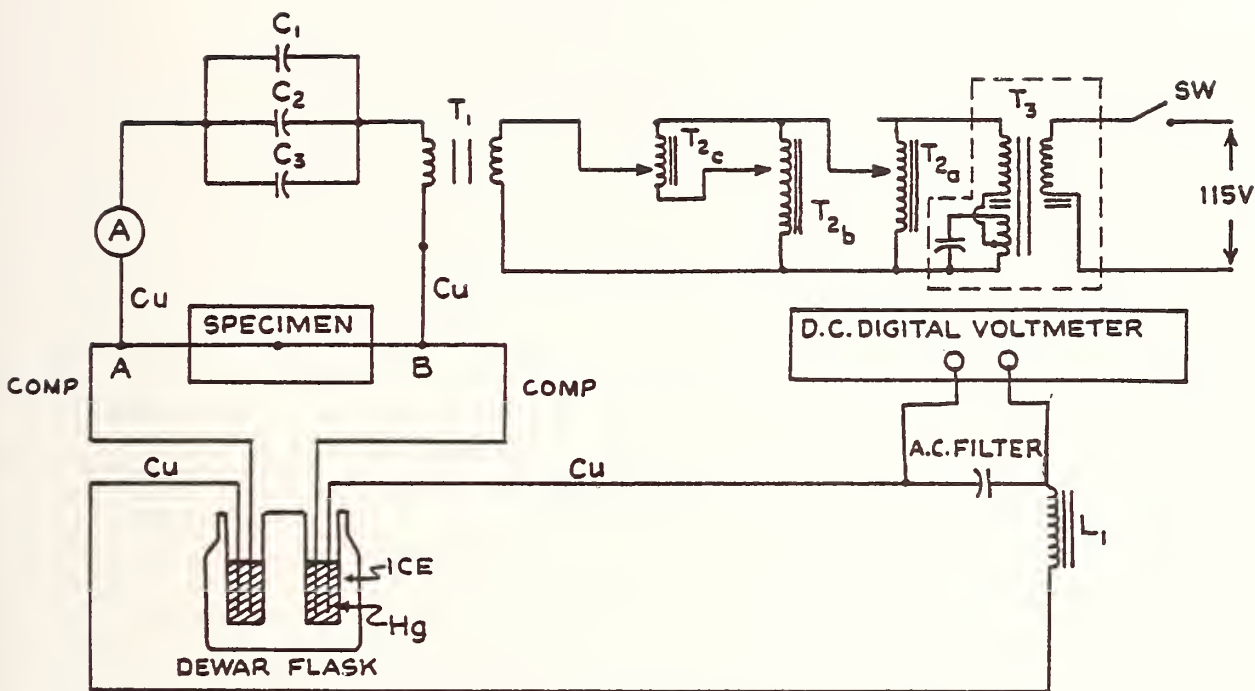


Fig. 5 Schematic diagram for electronic circuit; (C_1, C_2, C_3) 250 μF , 2.5 V ac electronic capacitor, (C_4) 500 μF , 1.5 V dc electronic capacitor, (L_1) 10H, 200 mA, 140 Ω choke, (T_1) 115 to 25 V, 250 VA transformer, (T_2) 115 V, 420 VA variable transformer, (T_2^A) coarse adjustment, (T_2^B) span adjustment, (T_2^C) fine adjustment, (T_3) 115 V, 250 VA voltage regulating transformer, (A) 0-5 A ammeter, (S W) on-off switch, (Cu) copper wire, and (Comp) compensating wire. (Modified from Ref. 19 and 22)

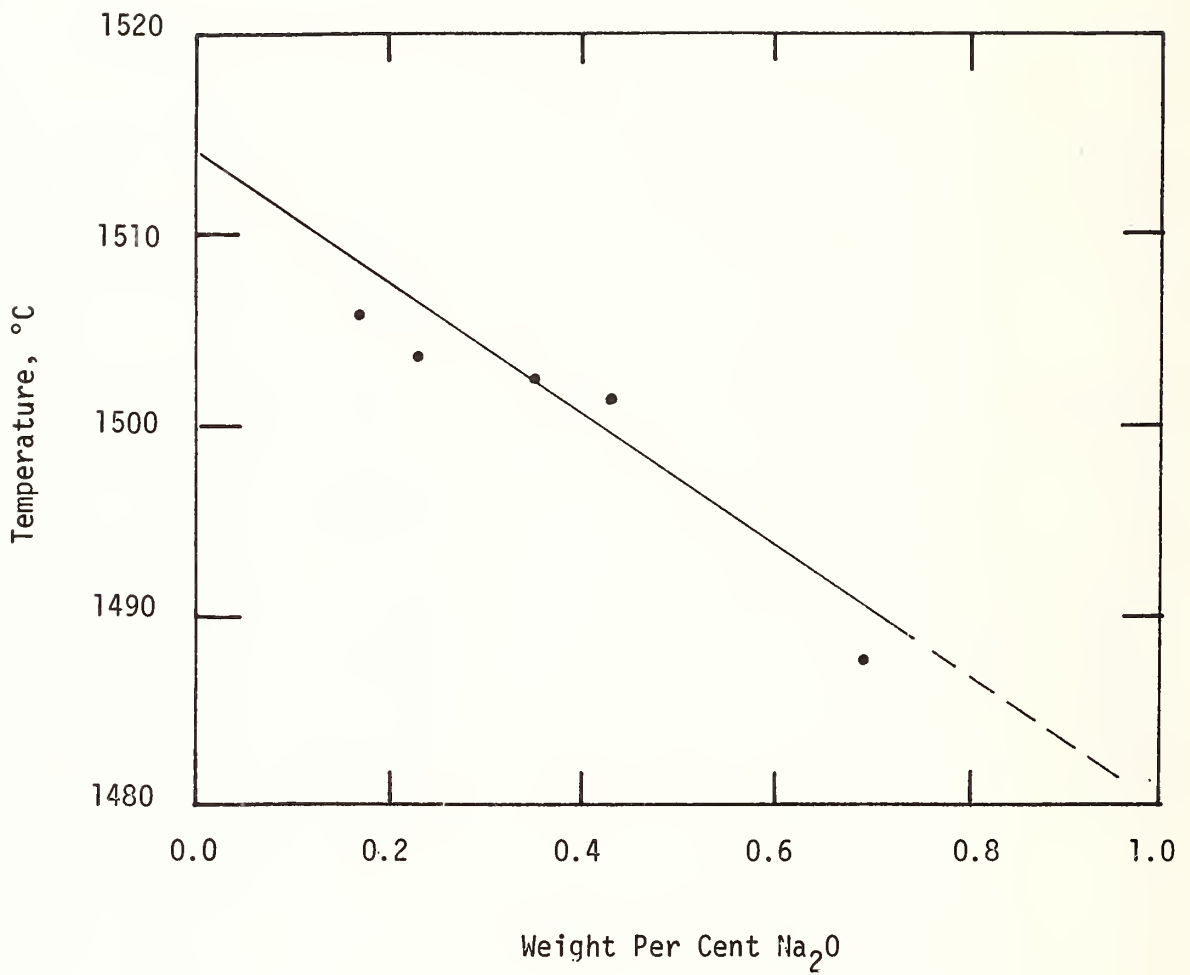


Fig. 6 The effect of Na₂O on the liquidus temperature of an oxide melt having a % CaO + % MgO/% SiO₂ + % Al₂O₃ ratio of 1.12.



EXPERIMENTAL TECHNIQUES IN PHASE DIAGRAM DETERMINATION OF SUPERCONDUCTING COMPOUNDS CONTAINING VOLATILE COMPONENTS AT TEMPERATURES UP TO 2200 °C

by

R. FLÜKIGER and J.-L. JORDA

Département de Physique de la Matière Condensée
24, quai Ernest-Ansermet
1211 - Geneve - 4
Switzerland

I - INTRODUCTION

In addition to their individual metallurgical properties, a great number of binary and ternary intermetallic compounds possess a further important property : they are superconducting. The superconducting transition temperature, T_c , of a compound is strongly related to its electronic structure and phonon spectrum. It is now widely accepted that to a well-defined superconducting bulk compound there corresponds a well-defined value of T_c . Within the homogeneity range of a given crystallographic structure, T_c has been found to vary more or less with the atomic composition. Thus superconductivity can be used as an additional technique in establishing phase diagrams. This means in turn that a precise knowledge of the phase field gives some indication about the maximum value of T_c which can be reached in a given phase.

The technically most promising superconductors known to date, such as the Al5 type compounds or the $R\bar{3}$ type compounds (Chevrel phases), generally form at temperatures well above 1700°C. Almost all of them contain at least one volatile component, e.g. Ga, Al, Sn, ... for the Al5 type compounds or S, Se, Te, Pb, Sn... for the $R\bar{3}$ type compounds. At the formation temperature of these superconducting phases, i.e. in the range of $1700 < T < 2200^\circ\text{C}$, the contamination of the alloys by the crucible material or by impurities in the heating chamber becomes increasingly important. Furthermore, the evaporation of such a compound at these temperatures increases the fluctuations on the DTA base line, which

in addition shows a more or less important curvature, thus rendering the detection of thermal arrests very difficult. The analysis under these conditions presents another inconvenience, namely the short lifetime of the measuring cell which may be affected by the reactivity of the metal vapors either with the thermocouples or with the ceramics. It is thus not surprising that the high temperature phase fields of the majority of these systems are far from being really known.

In this article we will show from some selected cases that the high temperature details of the phase field of a superconducting phase are of importance in attempting to reach the maximum superconducting transition temperature for a given compound. It should be noted that the precise determination of these high temperature details has to be carried out very carefully in order to prevent contamination. The high temperatures involved require specially designed measuring devices, which will be described in detail.

II - EXPERIMENTAL TECHNIQUES

From the above mentioned difficulties encountered in the study of the high temperature part of compounds containing volatile components, it follows that the results obtained using a given experimental device have to be treated with scepticism, unless their accuracy has been confirmed by other experiments under different conditions. Even still, when changing the experimental conditions one has to be careful to eliminate the causes which really influence the measured values.

On the other hand, the extreme concentrations in a phase field, which are often stable at high temperatures only, have to be quenched at sufficiently high rates in order to be retained for a subsequent analysis. Quenching experiments are, however,

dependent on kinetics and thus give only an indirect image of the high temperature behavior. This image does not necessarily correspond to the real situation: it can even represent a non-equilibrium. Thus quenching experiments alone cannot give a definite answer to the question of the equilibrium phase limits at high temperatures. The only way of solving the problem with accuracy is to combine the quenching experiments with the direct high temperature observations.

A. DIRECT METHODS OF OBSERVATION

By direct observation methods we define all techniques which are independent of kinetics, i.e. which reflect the real behavior at high temperatures. The methods used in the present investigation are described in the next section.

A.1. Differential Thermal Analysis (DTA)

The commonly used method for the detection of phase transformations at high temperatures is DTA [1]. A DTA apparatus working up to 2200°C under an inert gas pressure up to 10 atm. is not commercially available : it was thus necessary to develop such a device. Carbon was found to be the heating resistance material having the longest lifetime under the required working conditions. In order to ascertain that the carbon impurities did not affect the phase relations of interest, we have compared the DTA results of all investigated systems with those obtained using a carbon-free device, which will be discussed in Section A.2. Theoretically, the best material for the heating resistance is tungsten. It was excluded because of its brittle nature, which is mainly caused by recrystallization and reaction of the tungsten with small amounts of oxygen present in the furnace atmosphere. The latter is contained in the argon (99.995%) or arises from the water adsorbed at the surface of the ceramics or of the furnace walls.

Our cylindrical carbon resistance, supplied by Sétaram (France), has a total length of 400 mm and an inner diameter of 34 mm. By applying a power of 8 kw, it develops a temperature of 2400°C at the hot zone. The resistance has a complex shape, designed for a homogeneous temperature zone of approximately 40 mm length at 1900°C. The temperature gradient in this zone, parallel to the axis of the cylinder is of the order of 0.5°C/cm. Due to the considerable length of the heating resistance, the sample-holder has a total length of 450 mm. In order to avoid the mechanical problems due to the softening of the central 4-hole BeO tube at high temperatures, it was mounted so that it hung from the top of the furnace. The details of this holder are shown in Fig. 1. The materials used for its construction are BeO and molybdenum, which form a cylindrical box of the approximate size of the homogeneous zone. The samples, contained by small BeO crucibles, are located at the centre of the box in a plane normal to the axis. The junction measuring the temperature was placed at the centre of this plane. The melting points of platinum (1772°C) and rhodium (1966°C) were used as temperature standards. The size of these crucibles was kept as small as possible in order to minimize the temperature variation in the samples, which is estimated to be at less than 0.1°C. The mass of the crucibles is comparable to that of the samples (0.2 - 0.25g). The BeO crucibles were supported by the thermocouple junctions and the samples separated from the latter by a thin BeO wall of 0.4 mm thickness, thus providing a good thermal contact.

For linear variation of the temperature, a proportional feedback temperature programmer was used. It was driven by a supplementary W-3% Re vs. W-25% Re thermocouple placed just below the sample-holder. The DTA signal was measured with a nanovoltmeter and registered with a multi-channel recorder. All parts of the sample-holder can serve for numerous runs, except the thermocouples, which have to be changed after 10 to 20 runs, depending on the substance under investigation and on their thickness (which, in our experiments, varied between 0.25 and 0.5 mm). Apart from the above mentioned non-linear deviations of the base-line, the described DTA apparatus enables very sensitive measurements up to 2200°C or more to be made. As an illustration, we have presented the results of a DTA run on the alloy Nb_{0.74}Ga_{0.26} in Fig. 2. Although this apparatus works satisfactorily under these conditions, the measured thermal arrests may be affected by several parameters such as the carbon and the oxygen content of the furnace atmosphere and the choice of the crucible material. In order to determine if these parameters had some influence on our DTA results, two methods, described in the next sections, appeared to be particularly useful in this respect.

A.2. Simultaneous Stepwise Heating

The obvious advantage of a long-life carbon heating element is counter-balanced by the presence of carbon impurities in the furnace atmosphere. Therefore the DTA results obtained have to be confirmed by measurements effectuated under the same conditions as in the DTA apparatus, but in a carbon free atmosphere. The horizontal lines in the phase diagram, such as eutectic or peritectic temperatures appear to be particularly convenient for the proposed comparison. We have checked these temperatures by using a very simple technique, "simultaneous stepwise heating", which is based

on the fact that the number of liquid phases changes by crossing the eutectic or a portion of the peritectic line. This technique consists of heating pieces of the same master sample at different temperatures above and below the desired eutectic or peritectic temperature. After cooling, they are analyzed visually or microscopically in order to decide if the solidus had been reached during the high temperature exposure. The step between the annealing temperatures being of the order of 5°C , the value of the eutectic or the peritectic temperature can be found with good precision, and can be compared with that obtained by DTA.

When studying the phase diagrams of the binary systems Nb-Ge and Nb-Ga, we found in addition that this technique furnishes precise information on the extreme Ga or Ge solubility in the Al₅ phase if several samples of different, but neighbouring compositions are heated simultaneously. It is thus possible to study at the same time the influence of carbon impurities on the eutectic or peritectic temperature and the extreme composition of a given phase which renders the method as being quite powerful.

Fig. 3 illustrates the high temperature cell which was used for the "simultaneous stepwise heating" experiments. These were carried out in a 30 kW high frequency furnace under the same pressure conditions with the same inert gas as in the DTA apparatus. The samples were contained in BeO crucibles located inside a double walled molybdenum cylinder, which, in turn, was placed in a tantalum susceptor. Because of the cylindrical symmetry, the difference in temperature between the samples is less than 5°C at 1800°C . As for DTA, the temperature was measured with a W-3% Re vs. W-25% Re thermocouple, which was in good thermal contact with one of the BeO crucibles.

A.3. Thermal Analysis on Levitating Samples

At first sight, the possible influence of the crucible material on the DTA results seems to be easily avoidable by using different materials. However, the number of commercially available ceramics which can be used at 1800°C and more is small. In addition, the costs of DTA crucibles of the same shape as in Fig. 1 made from ThO_2 or HfO_2 are prohibitively high. The generalized use of BN at $T > 1800^{\circ}\text{C}$ is problematic because of the hygroscopic behavior of this material. A technique which completely eliminates the problem of contamination by crucibles is electromagnetic levitation, introduced by Fogel et al. (2). We performed the thermal analysis on levitating samples weighing 1-2 g using a 30 kW h.f. generator at a frequency of 300 kc and a watercooled Cu induction coil as shown in Fig. 4.

As in usual thermal analysis, the temperature of the sample is varied by a gradual change of the generator power. The sample temperature was measured with a Leybold two-color pyrometer.

The main problem arising from such temperature measurements lies in the unknown behaviour of the emissivity of our alloys as a function of the observing wavelength of the pyrometer (4500 and 6500 Å). The observed alloys, however, do not necessarily behave like grey bodies, as required for an accurate temperature determination with a two-color pyrometer. In addition, the window absorption has to be corrected, even using a two-color pyrometer, which disagrees with the currently used selling arguments for these instruments. Thus, a reliable determination of the temperature requires a calibration of the pyrometer. This calibration has been carried out by measuring simultaneously the temperature of a sample with a thermocouple and the pyrometer, up to 1900°C. The sample was placed in a BeO crucible which was contained by the "simultaneous stepwise heating" device described above (Fig. 3).

With the variation of the composition on a given binary system, as Nb-Ge or Nb-Ga, the emissivity is expected to undergo a variation. Nevertheless, we have found that a horizontal line (the eutectic), as it occurs in the systems Nb-Ga and Nb-Ge can be reproduced as a horizontal line by the pyrometer method. This indicates that for these systems the variation of the emissivity as a function of the Ga or the Ge concentration, at least for the mentioned composition range, can be neglected. This is a very encouraging argument for the proposed technique, which, in addition to the elimination of the crucible problem, presents another advantage: rapidity. In fact, since the sample is the only part heated, the furnace is ready to be opened a few minutes after the measurements. We are currently trying to improve this thermal analysis method, the precision in the absolute temperature being better than 15°C at 1800°C. A more detailed work is in press (13).

B. INDIRECT METHODS OF OBSERVATION

In order to retain a high temperature phase or a composition of this phase which is stable at high temperatures only, more or less severe quenching is necessary. The quenching rate is considered to be sufficient if it is higher than the rates of phase transformations or segregation occurring during the cooling process. However, from the analysis of a quenched sample alone it cannot be affirmed with certainty if it really reflects the equilibrium high temperature relationships: it may represent a non-equilibrium situation due to an insufficient cooling rate. The latter possibility has to be taken into account, particularly if solid samples have to be quenched. Liquid samples of the same material can be quenched at much higher rates.

B.1. Splat Cooling on Liquid Samples

This method was first used by Duwez et al. (4) and has since been modified by many authors. We used a combination of magnetic levitation and two watercooled Cu pistons, an illustration of which is shown in Fig. 4. By suddenly switching off the h.f. power, the levitating, molten sample falls through the levitation coil and is squeezed by the polished front of the Cu pistons, which are accelerated against each other by two strong electromagnets. The magnets are activated by the h.f. power switch with an appropriate time delay which takes into account the falling time of the sample. The thickness of the splat-cooled sample varies between 50 and 100 μ , the initial quenching speed being estimated at $\sim 10^6$ °C.

B.2. Argon Jet Quenching on Solid Samples

A solid sample can be quenched by falling into a liquid metal

(Ga or Ga-Sn) or an oil bath. However, this method has a disadvantage: as the hot sample enters into the bath, the liquid in contact with its surface evaporates, forming an insulating layer which reduces the heat exchange and thus the cooling speed. We have used another method, the argon jet quenching, which allows higher cooling rates to be reached, provided the sample is small enough. On samples having a mass of 0.3 g, we have measured initial quenching rates of the order of 10^4 °C, i.e. 100 times less than for the splat cooled samples.

Our argon jet apparatus (Fig. 5) was mounted in an h.f. furnace, which has the advantage that the total mass of the heated assembly is small, which is a stringent condition for a rapid quench. The argon gas is introduced through a thin-walled tantalum tube into the high temperature cell. This cell consists of a double-walled molybdenum cylinder made from rolled Mo sheets of 0.1 mm thickness. It is designed in such a manner that the top and the bottom of the cylinder can be blown away by the argon jet, leaving the thermocouple in place. The sample hangs on a tantalum wire fixed inside the tantalum tube and is located at the centre of the cell, just above the W-3% Re vs. W-25% Re thermocouple.

C. SUPERCONDUCTIVITY AS A SUPPLEMENTARY ANALYSIS METHOD.

The analysis of the samples studied has been carried out by classical methods, such as metallography, microhardness, X-ray diffraction combined with chemical and electron microprobe analyses. For a more detailed description of these current analytical methods, we refer to the articles which deal with the Nb₃Ga(5) and Nb-Ge phase diagrams. In this section we discuss the role of the superconductivity and, more precisely, the superconducting transition temperature, T_C , as an additional analytical method in the determination of the phase limits of a given phase.

The value of T_c characterizes a bulk superconducting compound as well as for example the lattice constant: there is a reproducible relation between the variation in composition within the homogeneity range of a superconducting phase and the variation of T_c . For hexagonal phases this may be illustrated by Fig. 6. This figure shows only a small part of the known data, the other systems having been omitted for clarity. Since the crystal structures of the compounds represented in Fig. 6 are disordered (A3 type structures), the attainment of T_{cmax} (shown by arrows in the lower figure) depends only on the quenching speed, which has to be fast enough to retain the extreme concentration limit of the superconducting phase after high temperature treatments at the appropriate temperature. This compositional effect also works for ordered phases such as the A15 type compounds. However, for the latter compounds, the situation is somewhat complicated by the fact that rapid quenching introduces a partial disordering, thus lowering T_c (see Section III).

C.1. Analysis of the Superconducting Data

The superconducting transition temperature can be determined either by induction methods or by measuring the resistivity of a sample by the four points method. As several measuring devices have been reported in the literature (6), we limit our discussion to the practical problems related to the analysis of the measured T_c values.

Screening Effects

The vast majority of erroneous results on measurements of the superconducting transition temperature of a given bulk sample belonging to a given structure are due to screening effects. These effects are connected with the presence of additional phases having a higher value of T_c than that of the phase

under study. The presence of these additional phases may be due to several causes:

- a) the microstructure of the sample shows that the phase of interest is enclosed in a matrix of another phase,
- b) an additional phase is formed at the surface due to contamination during the heat treatment in quartz tubes,
- c) one of the components of the alloy evaporates during the heat treatment, creating at the surface a layer of the same phase, but at different concentration,
- d) the layer formed in c) is of another phase type.

The screening effects are caused by different mechanisms, depending on the measuring technique applied. When measuring the electrical resistance, the superconducting layer at the surface short-circuits the current passing through the sample, thus masking all transitions at lower T_C . On the other hand, the screening effects encountered on inductive measurements are due to the expulsion of the magnetic field at the surface of the superconducting sample (Meissner effect). The surface layer will thus act as a shield which prevents the weak applied magnetic field penetrating the sample,

A layer thickness of several μ is sufficient for a total screening of the lower superconducting transitions. After grinding, the screening effects are thus eliminated for the cases b), c) and d), while they persist for the case a), as to be expected from the microstructure. For this case, the lower superconducting transitions appear only after the crushing of the samples down to particles of the order of the grain size. From these remarks it can be said that in order to determine the value of T_C which really corresponds to the measured bulk sample, it is generally useful to grind the sample at the surface and then to crush it down to 10μ particle size.

III - RESULTS

The binary compounds having the highest known value of T_c are Nb_3Ge ($23.2^\circ K$ {7}) and Nb_3Ga ($20.7^\circ K$ {8}). Both systems contain a component which can be said to be volatile at the formation temperature of the $A15$ phase in these systems, i.e. higher than $1800^\circ C$. This is illustrated in Fig. 2 which shows for the alloy $Nb_{.74}Ga_{.26}$ an increased evaporation at the liquidus temperature. In addition, we found in our investigations that these compounds react with most crucible materials and thus particular attention has been paid to this problem. The techniques described in this article appear to be the most convenient for studying the high temperature behavior of these systems.

A. The system Nb-Ga

The phase diagram of the binary system Nb-Ga has been studied by several authors, who have centered their attention on the superconducting $A15$ phase. Some recent works have been published by Webb et al. {7}, Oden et al. {9}, Feschotte et al. {10} and Ashby et al. {11}. A very careful investigation of the high temperature part which was recently undertaken in our laboratories using the techniques described above is currently in press {5}. A comparison of the $A15$ phase fields reported by the different authors, shows that there is general agreement concerning the peritectic formation of this phase which was found to occur between $1850^\circ C$ {11} and $1900^\circ C$ {9}, {10}. The $A15$ phase limits, however, vary considerably from one author to another : they have been reproduced in Fig. 7 for comparison. It is seen that the Ga-rich limit and particularly its variation with temperature, is controversial. All the phase limits in Fig. 7 having been obtained by means of the electron microprobe, this illustrates the drastic variation between

different investigations which can be attributed to the use of different standard materials and different correction programmes. In one case {11}, the oxygen content of the samples may cause a shift in composition. We have checked our microprobe results {5} by comparing them with the maximum weight loss observed after arc-melting under an argon pressure of several atmospheres. From this comparison it follows that the maximum error of our microprobe results is around ± 1 at.%. Another important point is the shift of the Ga-rich Al₅ phase limit with temperature : its maximum value was determined to 2 at.% by Feschotte et al. {10} and Ashby et al. {11}, while Jorda et al. {5} reported 4.2 at.%. This discrepancy is essentially due to the different cooling rates after high temperatures annealings : it was found that initial quenching rates of more than 10^3 °C/sec, obtained by spraying with an argon jet, are necessary to prevent the segregation which occurs on cooling. Webb et al. {8} obtained similar cooling rates by dropping the samples in a Ga-Sn bath, while the same method, used by Ashby et al. {11} who replaced the Ga-Sn bath by water, was apparently not successful. This is shown by an analysis of the lattice constants (Fig. 8) : the values obtained for the water-quenched samples {11} are considerably higher than those obtained by dropping in a metal bath {7} or by argon jet quenching {5}, thus suggesting Ga contents markedly lower than 25 at.%. It therefore appears that the segregation into the Al₅ + Nb₅Ga₃ phases, which could not be avoided, is responsible for the apparently temperature independent Ga-rich phase limit.

If such a curved phase limit really corresponds to the equilibrium, it must be reversible. Jorda et al. {5} confirmed this reversibility on the basis of micrographic observations, lattice constant measurements and microprobe analysis. However the best method for demonstrating this reversible behaviour is seen from superconductivity measurements, as was recently found {12}. From the results shown in Fig. 9 it is seen that the superconducting temperature T_c increases strongly

with the temperature at which the samples were treated before argon jet quenching. This increase of T_c is correlated with the variation of the Ga solubility in the Al5 phase, which occurs after quenching from different temperatures. The highest value of T_c (18°K) corresponding to the stoichiometric composition could be obtained after quenching from 1740°C, the eutectic temperature.

Subsequent annealings at temperatures low enough so that segregation does not occur (<700°C) cause an increase of the long-range order (LRO) parameter {13}, {14} and thus a further increase of T_c to its maximum value, 20.7°K {8}, {12}.

This example shows a concrete application of the superconductivity as a supplementary argument in determining the precise limits of a given phase, which is of course connected with the problem of determining the maximum possible value of T_c in a compound. For Nb₃Ga, the "simultaneous stepwise heating", together with the electron microprobe and DTA measurements suggest that the stoichiometric composition has been reached within less than 1 at.%. A spectacular further increase of T_c above 20.7°K is thus not to be expected.

B. THE NIOBIUM-GERMANIUM SYSTEM

By means of splat cooling experiments, Matthias et al. {15} suggested that the Ge-rich limit of the Al5 phase in the system Nb-Ge had a curved shape, as in the system Nb-Ga : the Ge solubility of the Al5 phase increases with temperature, tending towards the stoichiometric composition. This fact was partly confirmed by Pan et al. {16}, who have investigated the complete phase diagram of the system Nb-Ge. In Fig. 10 where we have reproduced the Nb-rich part of their diagram {16}, it is seen that the Ge-rich limit of the Al5 phase varies from 18 at.% Ge at 1000°C to approximately 20 at. % Ge at the eutectic temperature. On the same figure we have superposed the shape of the Al5

phase field as reported by Müller {17} who found nearly temperature independent phase limits.

The question which arises is whether the quench-induced extension of the A15 phase found by Matthias et al. (15) really corresponds to a high temperature equilibrium situation. The T_c value for Nb_3Ge as found from the quenching experiment was $17^\circ K$, while a value of $23^\circ K$ has been reported by Gavalier et al. (18), which they obtained from sputtered samples. It is therefore seen from the lower values of T_c , which are parallel to an increase of the lattice constant, that even splat-cooling experiments do not allow the retention of the stoichiometric composition Nb_3Ge for which T_c is maximum.

It is of fundamental interest to know if the values of T_c above $20^\circ K$ really correspond to the binary Nb-Ge compound or if some impurities, introduced during the sputtering process have an effect on its superconducting transition temperature. We thus decided to reinvestigate the high temperature part of the Nb-Ge system. However, the experimental difficulties encountered studying this system are even greater than those for Nb-Ga. The main reason is the extreme reactivity of this material with most refractory ceramics such as Al_2O_3 , ZrO_2 , BeO and ThO_2 , particularly at temperatures above $1870^\circ C$. The only exception is BN which allowed at least one DTA run up to $1950^\circ C$ before it also reacted {19}. In all these cases, reaction means that the peritectic temperature was in some cases considerably lowered by the presence of the ceramics, particularly by ZrO_2 . It is interesting to note that this lowering effect was observed only on concentrations less than 20 at.% Ge. Thus the only valid measurements for the peritectic temperature have been obtained by using the "simultaneous stepwise heating", using tungsten as crucibles. However, even the tungsten vapor has been found to react at the surface of the samples, thus

lowering their melting points. By reducing the high temperature exposure time, it was possible to limit this effect to the surface. On the other hand, the eutectic temperature, which is only 35°C lower, was measured on samples containing 23 to 30 at.% Ge without difficulty.

Because of the contamination problems already mentioned, the only possible way of obtaining meaningful results seems to be thermal analysis on levitating samples. As described in the preceding section, the actual precision of this technique is not better than $\pm 15^\circ\text{C}$ at 1800°C , but we estimate that our results shown in Fig. 11 are representative.

The thermal analysis on levitating samples is particularly useful in determining the solidus lines of a phase diagram. It is thought that it can be used for the liquidus lines, too. In the case of Nb-Ge however, the evaporation makes the precise determination of the temperature very difficult and additional corrections have to be used. The extent of these corrections is, as yet, unknown, and has to be found by other measurements. This is currently being done in our laboratories.

From Fig. 11 it can be seen that the peritectic and the eutectic temperatures are very close to each other: $1900 \pm 15^\circ\text{C}$ and $1865 \pm 10^\circ\text{C}$, respectively. The formation temperature of the Nb_5Ge_3 phase was found to be $2100 \pm 20^\circ\text{C}$ at 36 ± 1 at.% Ge, which is just between the values 2150°C and 2065°C , reported by Pan et al. (16) and Müller (17) respectively. The eutectic composition as determined micrographically was found at 26 ± 1 at.% Ge which is comparable to the values given in Ref. 16 and 17, which are 27 and 22 at.% Ge respectively.

The most important value, the maximum Ge solubility of the A15 phase, could not be determined with the desired precision but we estimated it at 22 ± 1 at.% Ge. Further measurements are

in progress to improve the accuracy of this value. Nevertheless, it can be stated without any doubt that the stoichiometric composition is not included in the equilibrium phase field of the A15 phase.

It is thus not surprising that quenching experiments did not produce transition temperatures above 17 or 18°K: this value corresponds to the high temperature phase limit of approximately 22 at.% Ge. This means that the further increase of T_c up to 23°K (18) can be attributed to compositional effects. If we take in account that

a) the superconducting transition temperature of ordered alloys depends only on the composition and the LRO parameter (12), and b) the variation of 1 at.% in composition causes the same change of 2.5°K for the systems Nb_3Al , Nb_3Ga and Nb_3Sn (12), it appears that a further spectacular increase of T_c for Nb_3Ge is not to be expected.

IV. CONCLUSION

It is a fact that a great majority of high T_c superconductors contain elements which are volatile at their formation temperatures. At these temperatures they are characterized by a strong reactivity with the crucible material which makes the correct determination of the high temperature relationships quite difficult. We have discussed in this paper several methods which seem particularly useful to overcome this problem. We emphasize that a high temperature result on the investigated compounds cannot be accepted as accurate without further confirmation by at least another, independent measurement. This is a consequence of the considerable amount of perturbing factors, such as the contamination by the crucible material,

the oxygen content of the furnace atmosphere, the reaction of the metal vapors with the thermocouples and other materials.

The present work was originally undertaken to study the possibilities of increasing the superconducting transition temperature by extending the phase fields of selected compounds. From our investigations it emerged that superconductivity represents a useful supplementary analytical method for a precise determination of the phase fields. At the first sight, it may seem surprising that low temperature properties can be used for understanding high temperature relationships. The reason becomes apparent, however, if one takes into account the fact that this property (present in a large number of materials) is a function of the atomic composition for a given compound, as for example the lattice constant. This illustrates the role of physical properties as a supplementary means for precise phase diagram determinations.

REFERENCES

- {1} W.Wm. Wendtlandt, "Thermal Analysis Methods",
Ed. P.J. Elving and I.M. Kolthoff, John Wiley & Sons, 1964
- {2} A.A. Fogel, T.A. Sidorova, V.V. Smirnov, Z.A. Guts and
I.V. Korkin, Russ. Met., 2, 89 (1968)
- {3} J.L. Jorda and R. Flükiger, to be published in J.
Appl. Phys.
- {4} P. Duwez, "Progress in Solid State Chemistry", Pergamon
Press, New York, Vol. 3, p. 377 (1966)
- {5} J.L. Jorda, R. Flükiger and J. Muller, to be published
in J. Less-Common Metals
- {6} A.L. Schavlov and G.E. Devlin, Phys. Rev. 113, 120 (1959)
- {7} L.R. Testardi, J.H. Wernick and W.A. Royer, Sol. State
Comm. 15, 1 (1974)
- {8} G.W. Webb, L.J. Vieland, R.E. Miller and A. Wicklund
Sol. State Comm., 9, 1769 (1971)
- {9} L.L. Oden and R.E. Siemens, J. Less-Common Met.,
14, 33 (1968)
- {10} P. Feschotte and F.L. Spitz, J. Less-Common Met.,
37, 233 (1974)
- {11} D.A. Ashby and R.D. Rawlings, J. Less-Common Met.,
50, 111 (1976)

- {12} R. Flükiger and J.L. Jorda, accepted by Sol. State Comm.
- {13} E.C. van Reuth, R.M. Waterstrat, R.D. Blaugher, R.A. Hein and J.E. Cox, Proc. LT10, Moscow, Vol. 1b, Viniti, p. 137 (1967)
- {14} R. Flükiger, J.L. Staudenmann and P. Fischer, J. Less-Common Met., 50, 253 (1976)
- {15} B.T. Matthias, T.H. Geballe, R.H. Willens, E. Corenzwit and G.W. Hull, Phys. Rev., 139, A1501 (1965)
- {16} V.M. Pan, V.I. Latyscheva and E.A. Shishkin, Phys. Chem. and Metal Phys. of Superconductors, Izd. Nauka, Moscow, p. 157 (1967)
- {17} A. Müller, Z. Naturforschung, 25a, 1659 (1970)
- {18} J.R. Gavaler, Appl. Phys. Lett., 23, 480 (1973)
- {19} BN has to be treated at 1900°C under 1 atm. argon pressure before it can be used as crucible at $T > 1800^{\circ}\text{C}$.

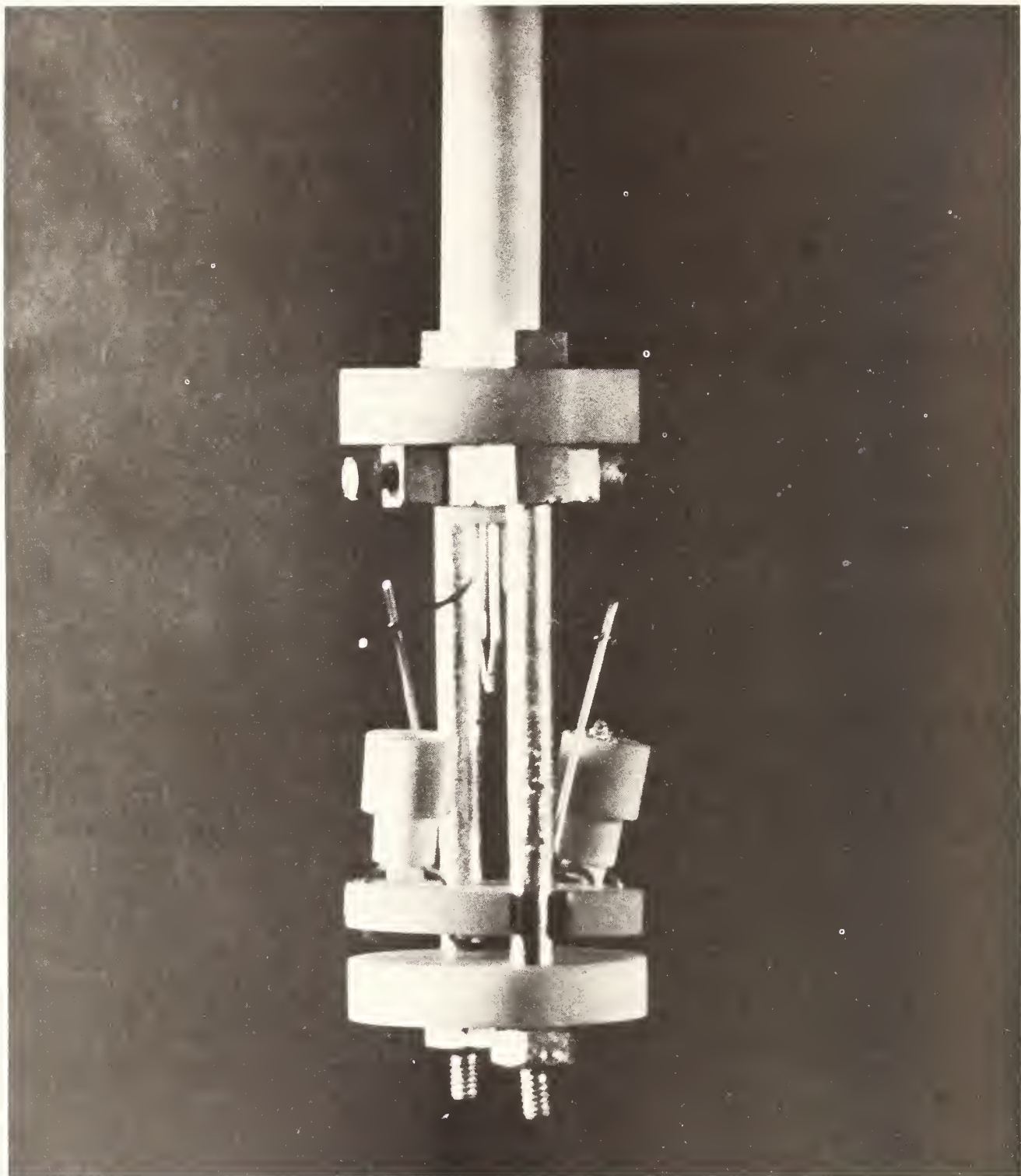


FIGURE 1. The DTA sample-holder used up to 2200°C. It is entirely constructed on BeO and Mo. As thermocouple material, W-3% Re vs. W-25% Re wires of 0.25 or 0.5 mm diameter were used. The BeO crucibles are directly supported by the thermocouple junctions.

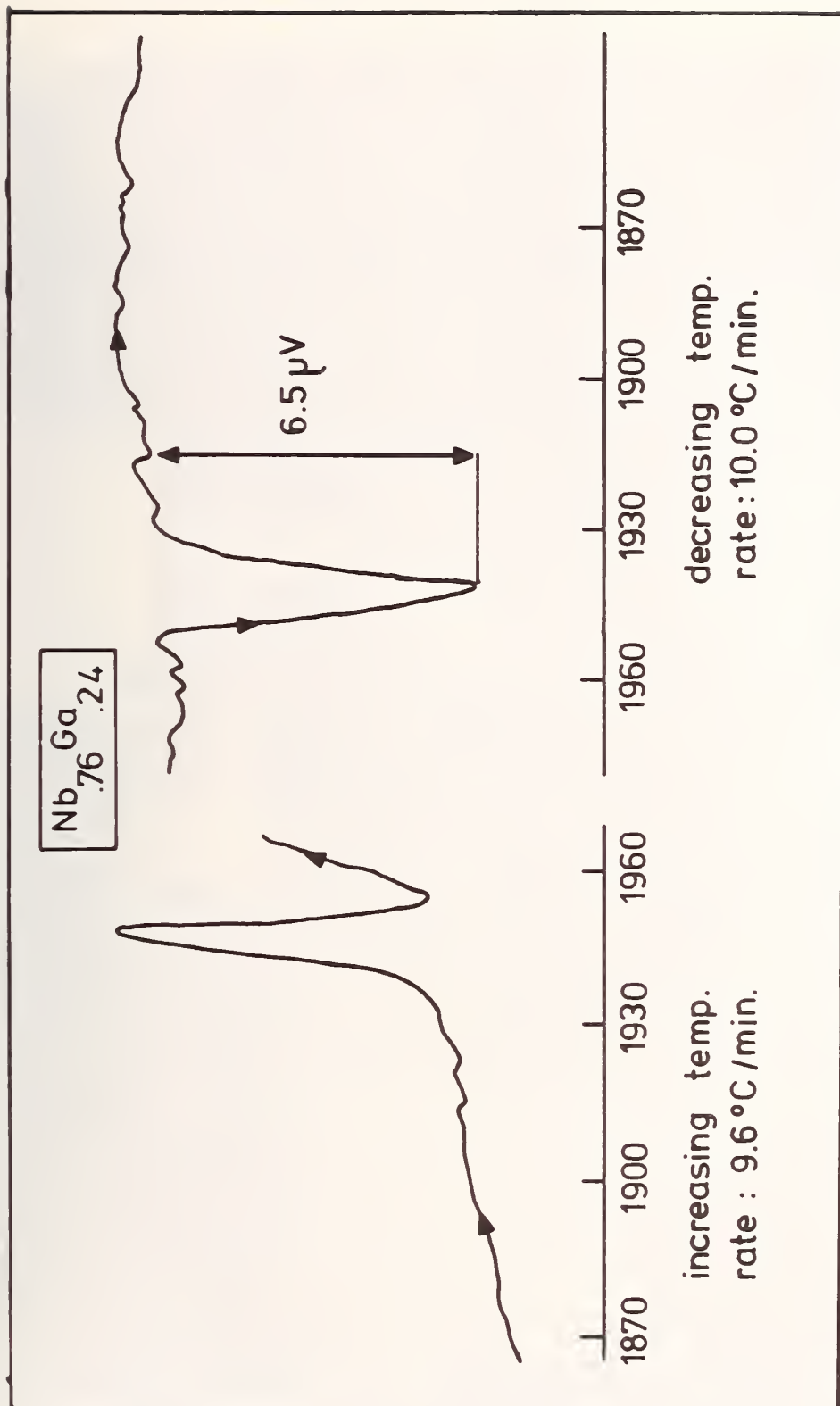


FIGURE 2. A high temperature DTA run of the alloy $\text{Nb}_{.76}\text{Ga}_{.24}$. The observed thermal arrest corresponds to the liquidus temperature. Note the strong curvature of the base line on increasing temperature, showing beginning evaporation.

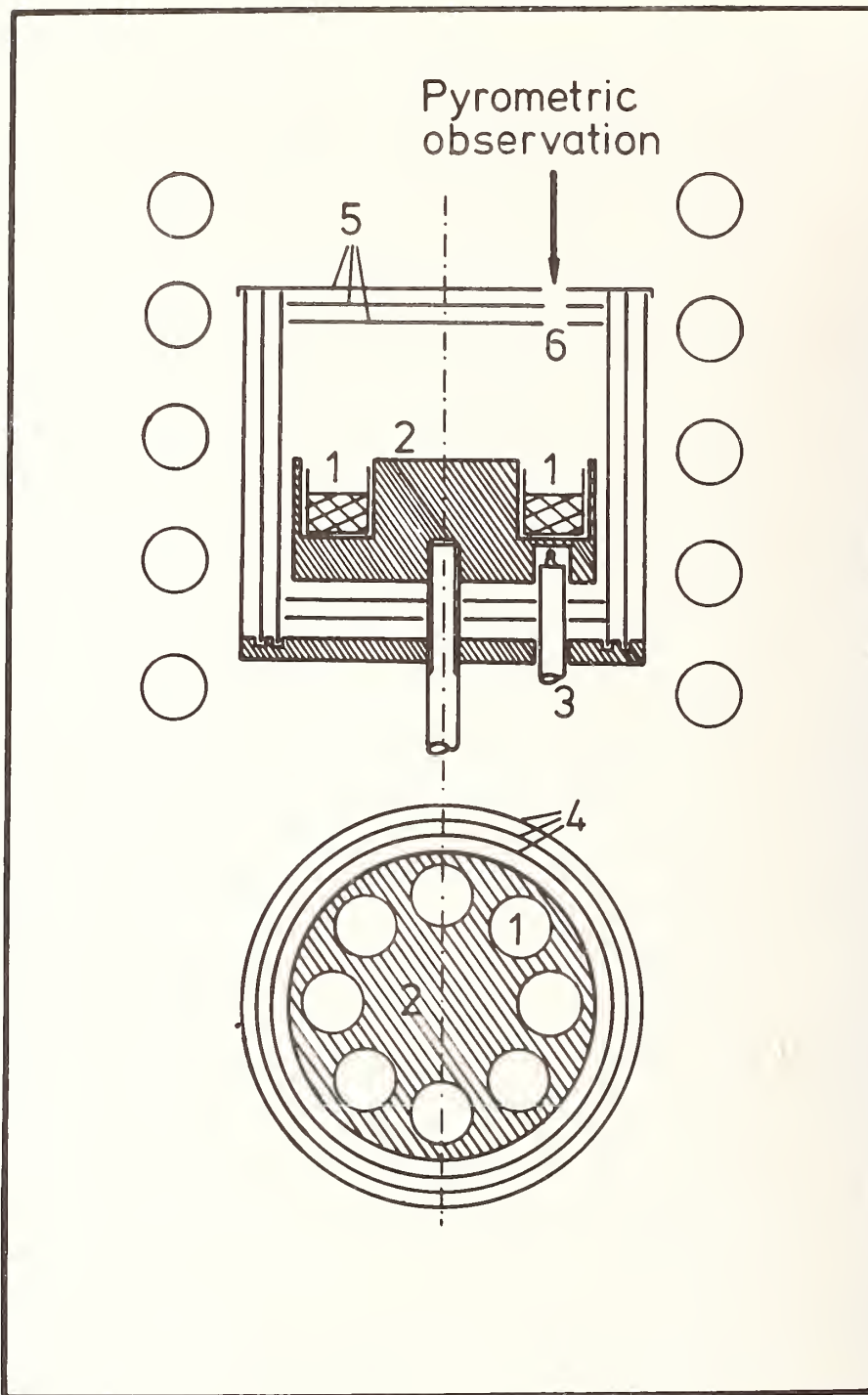


FIGURE 3. The high temperature cell for the "simultaneous stepwise heating", mounted in a HF coil. The sample temperature is measured both by thermocouples and a two-color pyrometer, allowing a "calibration" of the latter for measurements at higher temperatures. 1 : samples, 2 : Molybdenum block, 3 : Thermocouple, 4,5 : Molybdenum shields, 6 : hole for pyrometric observation.

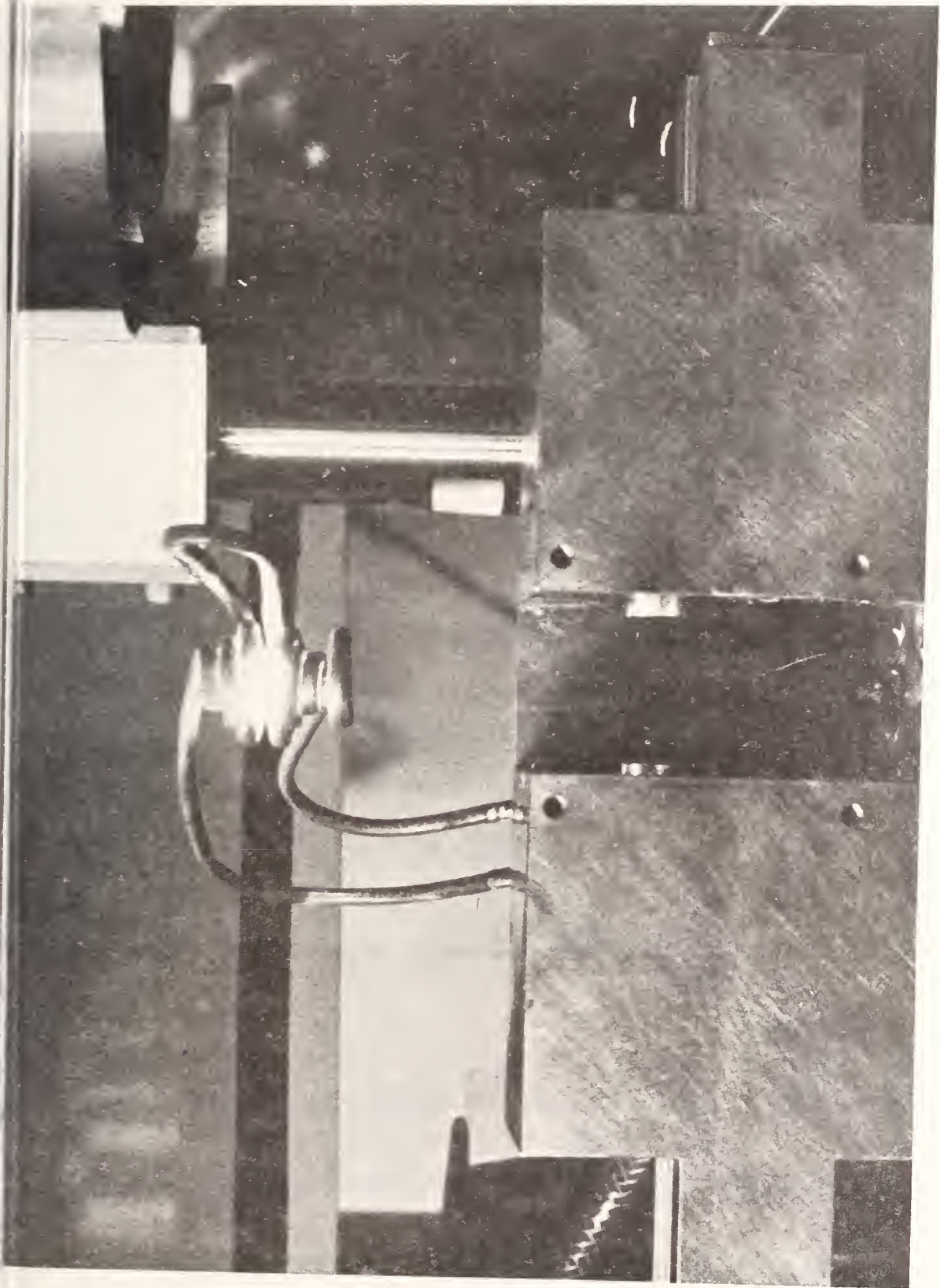


FIGURE 4. Splat cooling device, consisting in a levitation coil and two copper pistons which are accelerated against each other.

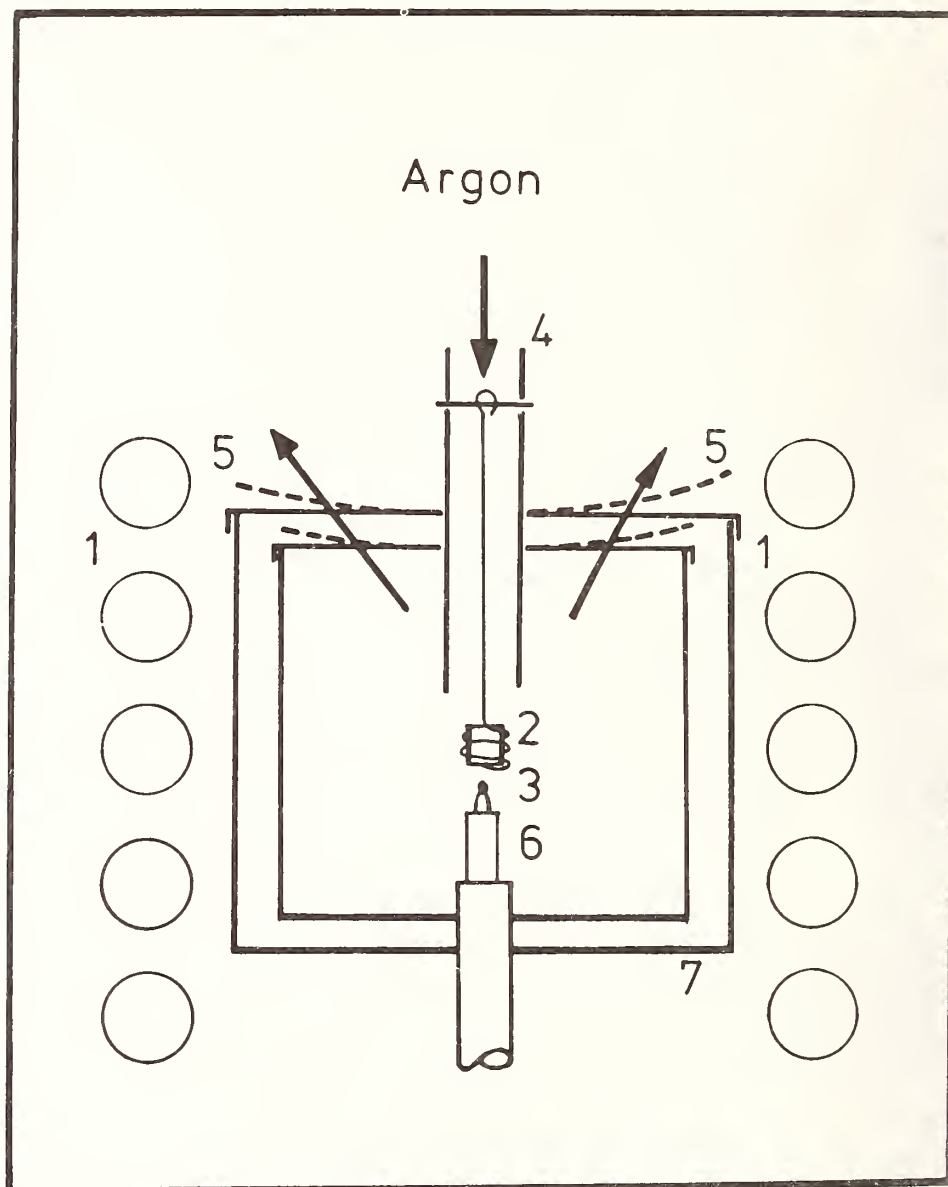


FIGURE 5. The argon jet quenching device. 1 : HF coil, 2 : sample, hanging on a tantalum wire, 3 : Thermocouple, 4 : Tantalum tube, 5 : Molybdenum lid, is blown away by the argon jet, 6 : 2 hole BeO tube for the thermocouple wires.

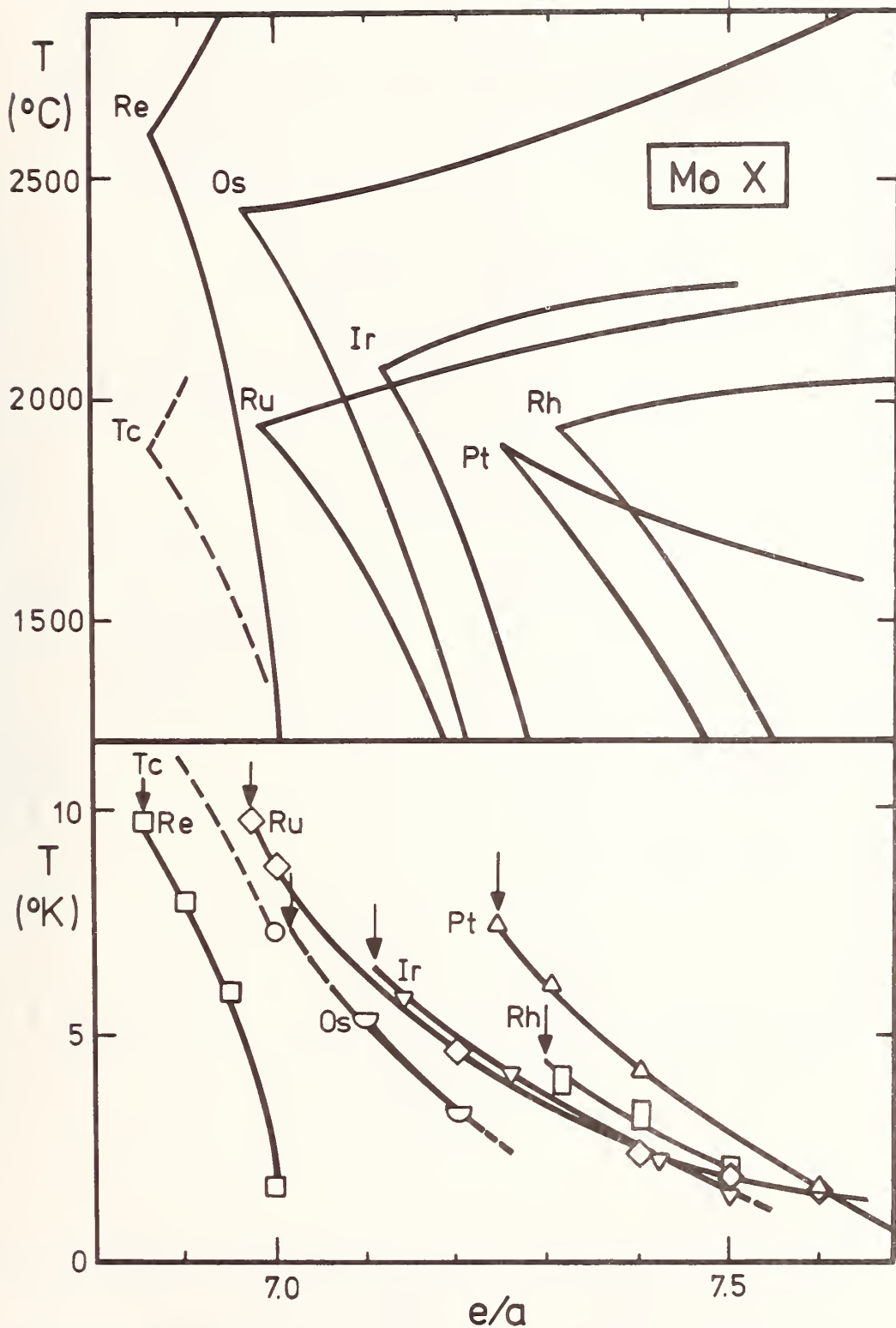


FIGURE 6. The dependence of T_c on the number of electrons per atom for several hexagonal Mo-X compounds. The arrows denote the highest value of T_c in a given system, corresponding to the extreme solubility limit of the hexagonal phase at high temperature, as it follows from the upper picture.

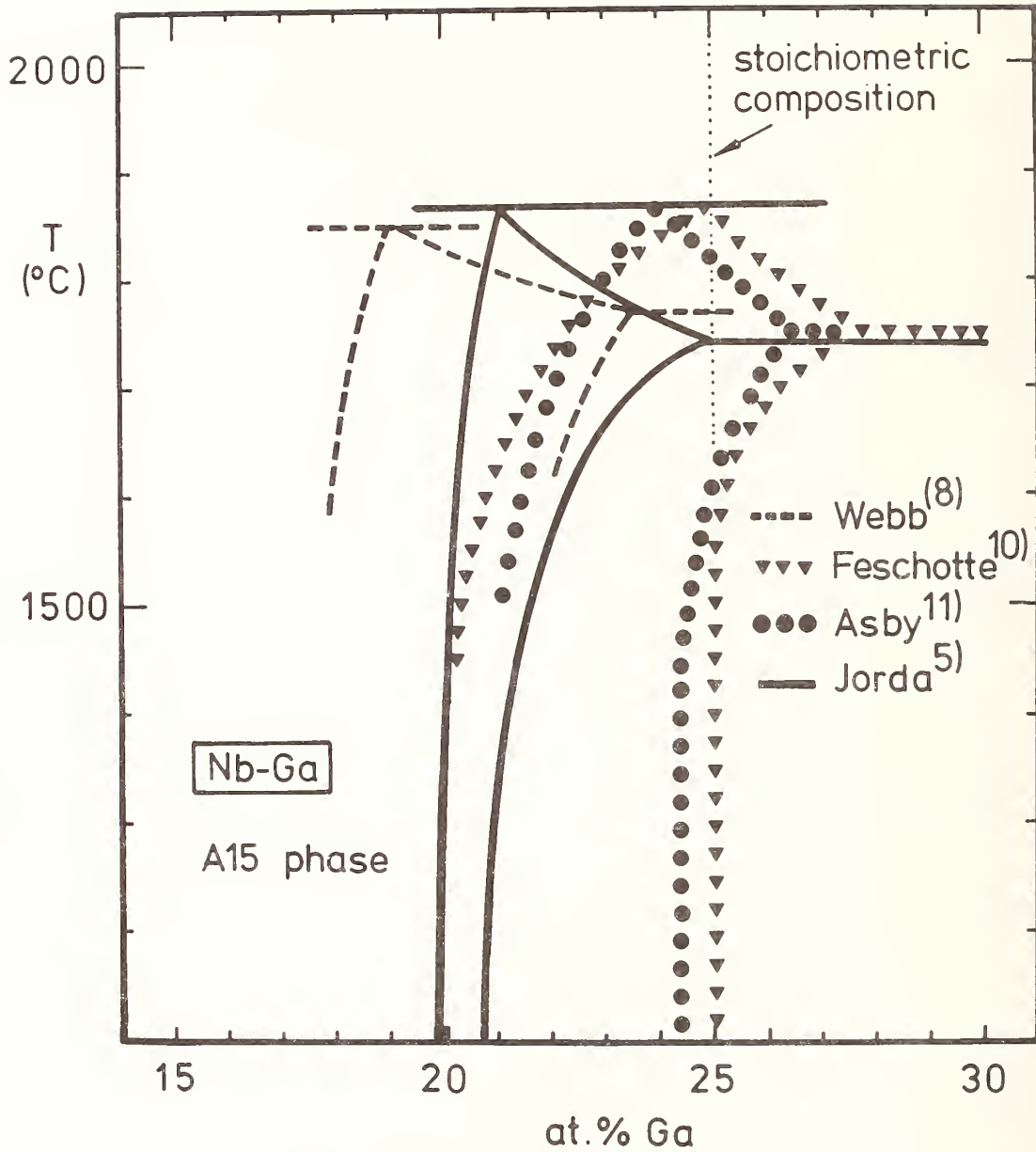


FIGURE 7. The A15 phase field in the Nb-Ga system as reported by different authors. The strong dependence of the Ga-rich limit on the temperature observed by Jorda et al. {5} was obtained using argon jet quenching at different temperatures between 1100 and 1740°C.

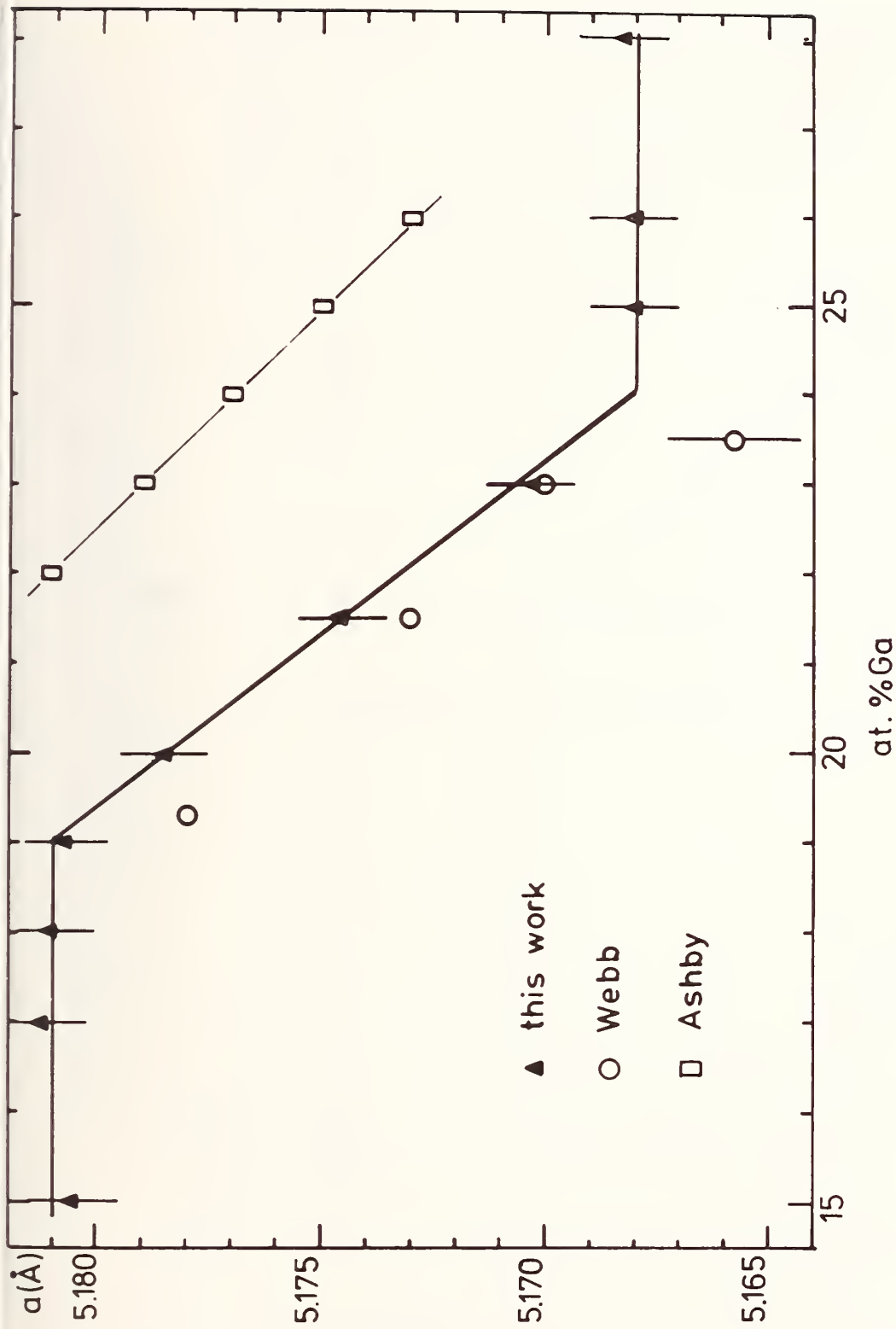


FIGURE 8. The variation of the lattice constant for the Al₅ phase of the Nb-Ga system. The values of Ashby et al. {11} can be brought to cover with those of Webb et al. {8} and Jorda et al. {5} by a shift of 3 at.% Ga.

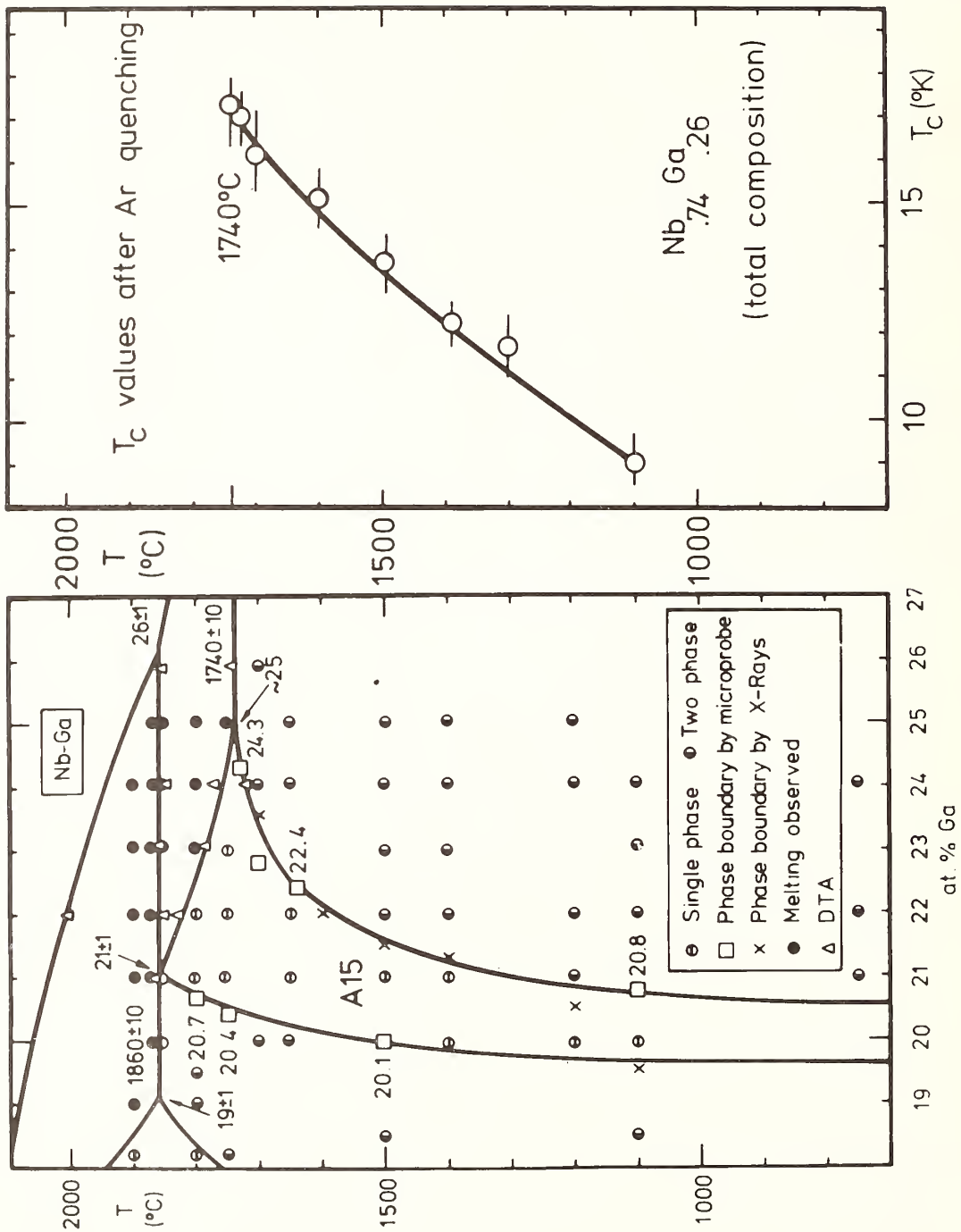


FIGURE 9. The variation of T_c for the compound $Nb_{.74}Ga_{.26}$ after quenching from different temperatures by a jet of cold argon. In the range $1100 < T < 1740^\circ C$, it corresponds to the curvature of the Ga-rich limit of the A15 phase Nb_3Ga (12).

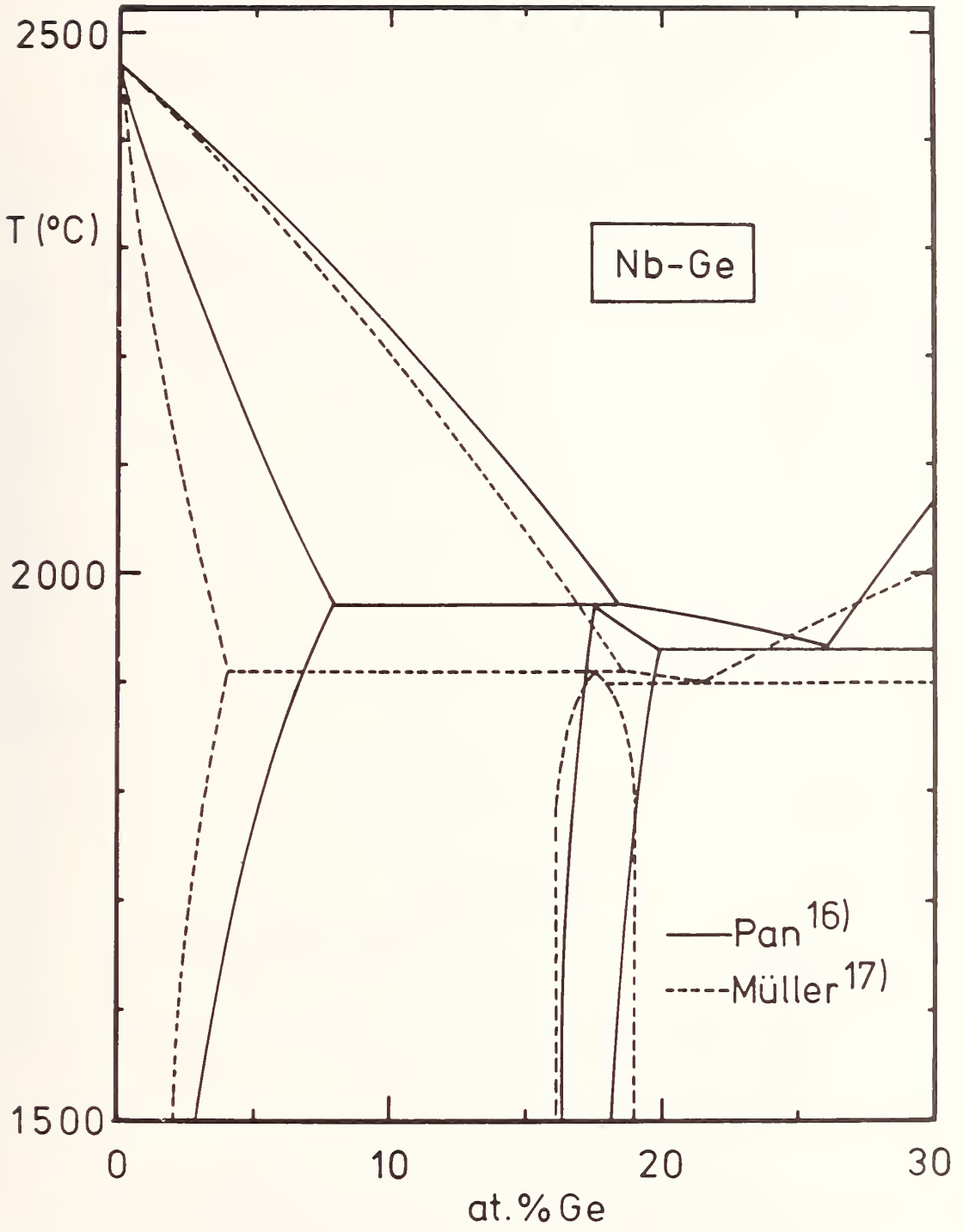


FIGURE 10. The high temperature part of the Nb-Ge system as reported by Pan et al. {16} and Müller {17}.

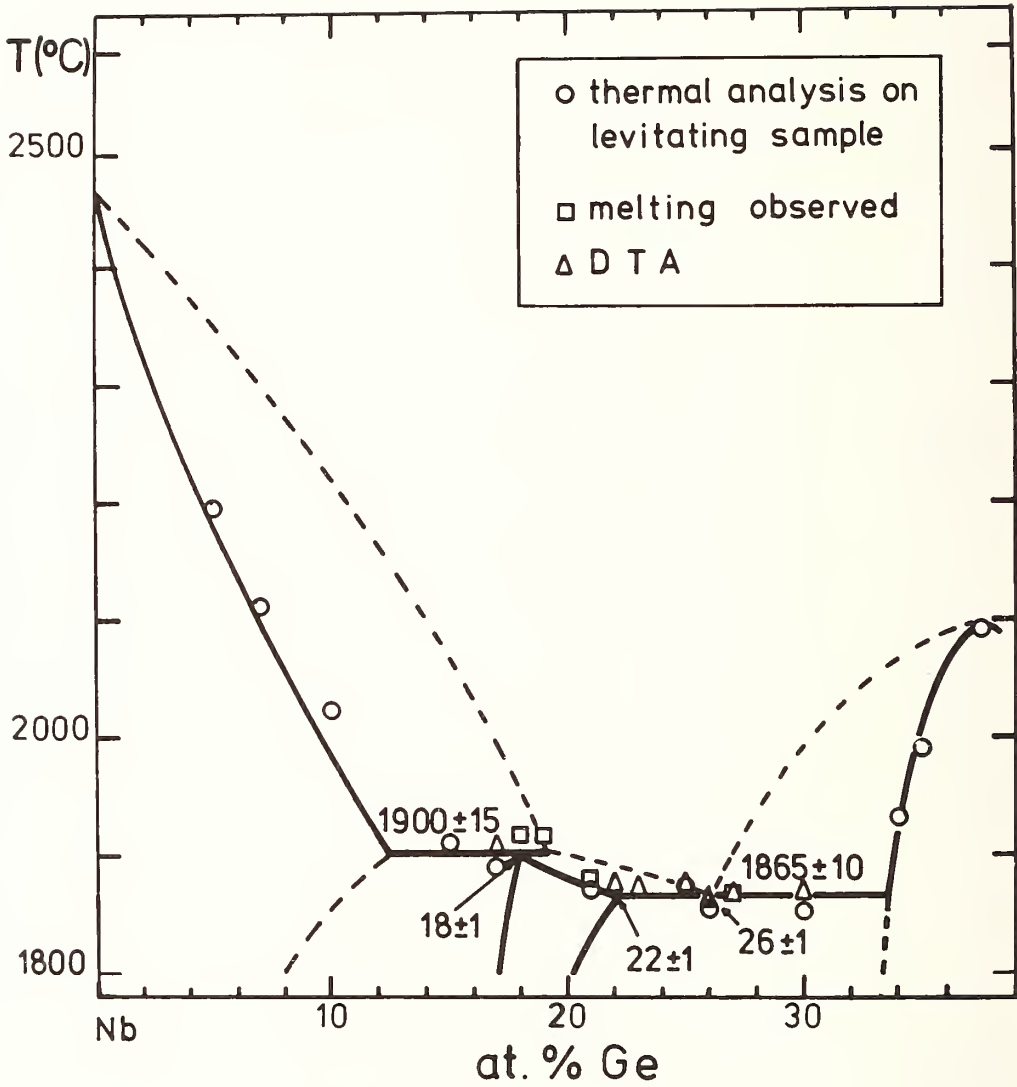


FIGURE 11. The high temperature part of the Nb-Ge phase diagram as obtained by thermal analysis on levitating samples, combined with DTA and "simultaneous stepwise heating".



APPLICATION OF EXPERIMENTAL TECHNIQUES AND THE CRITICAL DETERMINATION OF PHASE EQUILIBRIA IN OXIDE SYSTEMS

F.P. GLASSER

Department of Chemistry, University of Aberdeen,
Old Aberdeen, AB9 2UE, Scotland.

ABSTRACT

Experimental determination of phase equilibria in oxide systems has been greatly assisted by improvements in technique. For example, the focussing X-ray camera is superior to the diffractometer in its ability routinely to detect small quantities of a second phase and its more general use is advocated. It is almost always necessary to use another method of phase identification in conjunction with X-rays: optical microscopy, if possible. Selected applications of single-crystal data to the determination of phase composition is illustrated and the use of continuous high-temperature X-ray diffraction as a complimentary technique to DTA is described. It is concluded that despite the existence of critical compilations of data on oxide systems, the need exists for more experimental work to be done before our existing store of data can be considered reliable.

1. INTRODUCTION

During the past decade, the writer has increasingly been concerned at the general lack of critically-determined phase equilibrium data on oxide systems. Two principal areas of concern exist: firstly, the low reliability of data on systems which have supposedly been critically studied in the past, and secondly, the general attitude that it will be extremely difficult to extend studies on 'simple' systems to yet more complex systems by experiment. For example, the attitude is prevalent that quaternary oxide systems are, in general, too complex to study within the time scale usually available to the experimenter. Of course, if reliable data are not available on the limiting unary, binary or ternary portions of a complex system, it is not surprising that experimenters are unable to produce data on hitherto-unexplored systems quickly.

Critical compilations, such as the 1975 edition of "Phase Diagrams for Ceramists", are of only limited value in producing correct phase diagrams. While the compiler

can point out or correct obvious errors or inconsistencies - for example, violations of the phase rule - thereby at least producing consistent diagrams, these will not necessarily be correct. Errors such as the omission of compounds, undetected polymorphic transitions, etc., will almost inevitably not be detected by the compiler, without recourse to experiment. Errors in the literature thereby tend to become perpetuated in compilations and data banks.

Our experimental activities have largely been confined to systems containing oxides which are abundant in the crust of the earth. Most of these contain Al_2O_3 or SiO_2 or both : a list of systems studied in the writers' laboratory is given in the Appendix. This choice of systems is deliberate, for we believe that critically-determined data on these are most needed by technology, yet because they lack glamour are unlikely to be the subject of special funding. It follows that trained personnel have not always been available to work on our program and it has usually been necessary to work through students, giving each the necessary formal training both in theory and method. However, a judicious blend of modern equipment and procedures, combined with an enthusiastic and able team, enable complex oxide systems to be determined experimentally with an accuracy and rapidity which was not until recently possible. We remain optimistic about prospects for experimental studies of phase equilibria in oxide systems.

This paper does not seek to give a comprehensive account of the techniques of phase diagram determination : several Chapters in the series edited by Alper* fill this need. I concentrate on describing several useful techniques which have not been adequately described elsewhere.

* "Phase Diagrams - Materials Science and Technology"
Ed., A.M. Alper, 3 Vol. Academic Press, New York.

X-ray powder diffraction was first applied to phase equilibrium studies within a few years of the discovery of X-ray diffraction. Since that time, many improvements have been made in the ease of recording the pattern; for example, the combination of electronic measurement and automatic recording of the diffraction pattern which makes the diffractometer possible. Although the latter is certainly more convenient and more rapid than the powder camera, its response is basically no more sensitive than that of the conventional Debye-Scherrer camera. Most experimental studies of phase equilibrium have tended routinely to rely on the diffractometer for phase identifications but few investigators would regard it as a sufficiently sensitive method for the location of a second phase to rely on it accurately to locate phase boundaries. Significant advances in the technique have, however, occurred. An example is the development of the focussing X-ray powder camera. In focussing cameras, an intense beam of X-radiation is produced which is not only strictly monochromatized but which is also focussed. This is achieved by using a strong Bragg reflection, for example $10\bar{1}1$ of quartz, and simultaneously bending the crystal by applying mechanical pressure to achieve a focussing effect. Photographs may be obtained in the transmission mode using the Guinier geometry. Typically, a modern focussing camera gives exposures in 15 - 30 min. and requires 1.0 - 20 mg of sample. The time taken is comparable with that required to record a diffractometer trace, although it is of course necessary to process a strip of film. Nevertheless, the combination of the human eye and photographic film gives a better signal-to-noise ratio than can be obtained by diffractometry. Admittedly, the 'smear' method of preparation - often used in diffractometry - is not the best method of sample preparation, but it is quicker and often the quantity of sample available is only sufficient for a 'smear'. Moreover, while the X-ray system itself

may be at or near optimum performance, other variables - especially specimen preparation - may detract from obtaining the optimum results. In the course of studying a moderately complex system, it might be necessary to X-ray several hundred specimens: it is rarely possible to optimize all the variables affecting the quality of the diffraction pattern for each individual specimen. Therefore X-ray records obtained either from films or diffractometer traces, and which provide evidence of the phase distribution, are likely to be obtained under average rather than optimum conditions of system performance. These factors combine to give the focussing camera a marked advantage over the diffractometer.

A practical illustration of the relative ability to resolve mixtures of phases using optical and X-ray powder diffraction techniques will now be given. It is based upon data obtained in the course of a critical re-examination of the $\text{MgO-Al}_2\text{O}_3\text{-SiO}_2$ system. In the Al_2O_3 -rich corner of this system, two binary phases are encountered - mullite, $\text{Al}_6\text{Si}_2\text{O}_{13}$ and spinel, MgAl_2O_4 - as well as two ternary phases: cordierite, $\text{Mg}_2\text{Al}_4\text{Si}_5\text{O}_{18}$, and sapphirine, $\text{Mg}_4\text{Al}_{10}\text{Si}_2\text{O}_{23}$. These formulae are approximate but suffice for present purposes. Let us examine the problems involved. All the phases have distinctive powder patterns except for those of sapphirine and spinel, which are similar. Good structural reasons exist for the similarity between the powder X-ray patterns of the two phases. Sapphirine contains cubic close packed oxygens in an arrangement which is almost identical to that of spinel: moreover, many of the cations in sapphirine occupy positions spatially similar to those which they would have in a spinel. One consequence of this similarity is that the sapphirine powder pattern resembles that of spinel in the positions and intensity of its more intense reflections, although the greater structural complexity of sapphirine creates another, and characteristically weaker, set of powder lines which are absent in spinel. The main powder reflections of both

phases overlap, and in mixtures of the two phases they tend to be superimposed except at low d-spacings. Therefore, positive confirmation of the presence of sapphirine in mixtures with spinel depends crucially upon the ability to locate the weaker set of reflections which are characteristic of the latter phase, whereas the identification of spinel in the presence of sapphirine depends upon resolving closely-spaced reflections : in particular the (440) reflection of spinel from the adjacent reflections due to sapphirine. The resolution of mixtures of the two phases is therefore handicapped to some extent by similarities in the powder X-ray patterns of spinel and sapphirine. Such similarities are not isolated occurrences. Several phases in a system may frequently share the same basic substructure; failure to recognize that this may occur frequently leads to mistaken judgments concerning the number of phases which exist, as is shown in this instance by the length of time which it took for sapphirine to be recognized as a phase which was chemically and structurally distinct from spinel.

3. X-RAY AND OPTICAL METHODS COMPARED

An exact comparison between optical and X-ray methods is rendered difficult because much depends upon the skill of the microscopist. Table 1 contrasts both of these methods. The comparison is based on samples which have been heated to within $\sim 20^{\circ}\text{C}$ of the solidus. This results in comparatively large crystals (2 - 5 μ) developing in heat treatments of 24 - 48 h duration, so that the optical character of the crystals may readily be determined. In these, sapphirine may readily be distinguished from spinel on account of the weak birefringence of the former and from cordierite by the lower mean refractive index of the latter. Mullite is readily recognized even in traces on account of its needle-like or elongated lath-shaped crystals.

TABLE 1

Sensitivity of X-ray and Optical Methods Used to Determine the Presence of a Second Phase Occurring with Sapphirine Compared.

<u>Nature of Second Phase</u>		<u>Minimum Quantity Required For Reliable Identification</u>	
<u>NAME</u>	<u>FORMULA</u>	<u>X-RAY</u>	<u>OPTICAL</u>
SPINEL	$MgAl_2O_3$	1%	1%
CORDIERITE	$Mg_2Al_4Si_5O_{18}$	0.5%	Difficult
MULLITE	$Al_6Si_2O_{13}$	2.0%	1.0%
CORUNDUM	Al_2O_3	2.0%	Difficult

The X-ray data shown in this table were obtained from trials made using weighed mixtures of phases and the detection limits cited were obtained using focussing cameras and 'routine' exposure conditions, as described previously. Similar trials using 'smear' mounts and a modern diffractometer, show that a gain in sensitivity of 4 to 5 times is achieved with the focussing camera. The comparison appears very favourable to optical methods: however, as the sintering temperature is decreased, the mean size of the crystals also decreases and the sensitivity of phase detection by optical methods decreases rapidly. X-ray methods are much less susceptible to variations in sensitivity arising from changes in particle size until line-broadening eventually occurs. Therefore, X-ray methods are especially useful in determining the phases present in experiments made below the solidus. On the other hand, as temperatures approach and eventually exceed the solidus, the appearance of liquid - even in traces - is readily revealed by optical examination. Even if the liquid cannot at first directly be perceived, the microstructure usually undergoes an abrupt change when the solidus temperature is exceeded. Therefore, optical and X-ray examination are complementary rather than competitive techniques. It is to be regretted that it is becoming increasingly difficult for those entering the field to obtain

the good training in microscopy which scientists of previous generations took for granted.

4. X-RAY DIFFRACTION COMBINED WITH OTHER TECHNIQUES

a. Determination of phase composition. Many systems which supposedly have been thoroughly studied are found when re-examined to show hitherto undetected phases. For example, the $\text{Na}_2\text{O}-\text{SiO}_2$ system was studied by Kracek (Phase Diagrams for Ceramists: Fig. 192) who found a simple eutectic between $\alpha\text{-Na}_2\text{Si}_2\text{O}_5$ and SiO_2 (quartz). However, a re-examination of this system disclosed that compositions between 70 - 75 mol % SiO_2 gave a powder X-ray pattern which was not that of mixtures of any known polymorphs of SiO_2 and $\text{Na}_2\text{Si}_2\text{O}_5$. Investigation showed that a hitherto unidentified phase occurred. Persistent but incompletely - confirmed reports in the literature of a "sodium trisilicate" led us first to suspect that this phase was the elusive $\text{Na}_2\text{Si}_3\text{O}_7$. The composition of the newly-discovered phase was determined unequivocally as follows. Although it melted incongruently, one temperature-composition region of the phase diagram was found in which small laths 20 - 30 μ in length could be grown in contact with liquid. Single laths were isolated on the stage of a petrographic microscope. These were not completely free from adhering glass, but the latter does not interfere with a determination of the symmetry of the crystal. Single crystal X-ray photographs were obtained: these were consistent with monoclinic symmetry, although the crystals were geometrically orthorhombic. Systematic absences indicated the space group $\text{P}2_1/c$: $a = 4.90 \text{ \AA}$, $b = 23.4$
 $c = 15.4 \text{ \AA}$, $\beta = 90.0^\circ$. The unit cell volume was 1768 \AA^3 . Meantime, sintering of compositions close to the trisilicate ratio at subsolidus temperatures disclosed that at both 74 and 75% SiO_2 quartz remained in excess, while at 72 and 73% SiO_2 , an apparently single phase preparation resulted. However, at 71% SiO_2 , $\text{Na}_2\text{Si}_2\text{O}_5$ was definitely present. Therefore, the phase appeared not to be the trisilicate. The density of the apparently homogeneous sinters obtained at the 72 and 73% compositions were both $2.495 \pm 0.002 \text{ g/cc}$. We note

also that the unit cell contents must obey the restriction that they must fill the unit cell volume to give the observed density. Moreover, this space-group symmetry places an additional restriction on the possible unit cell contents; namely, that barring a statistical distribution of atoms, the content must have an even number of each species - Na, Si and O. With this in mind, we can construct a plot, shown in Fig. 1, of the unit cell contents of some hypothetical sodium silicates having $V = 1768 \text{ \AA}^3$ and a density of 2.50 g/cc : two other parallel lines are shown to allow for errors in the density determination of $\pm 0.05 \text{ g/cc}$. Bearing in

mind the symmetry-imposed restriction, possible fits within this regions occur at the ratios of $\text{Na}_2\text{O}:\text{SiO}_2$ equal to 14:30, 12:32 and 10:34. These ratios correspond respectively to ≈ 68 , 72.7 and $\approx 77 \text{ mol \%}$ SiO_2 . However, from observing the phase purity of the sintered preparations we can readily exclude the 14:30 ratio as this composition was observed to yield much $\text{Na}_2\text{Si}_2\text{O}_5$, while the 10:34 ratio yielded much unreacted SiO_2 . This

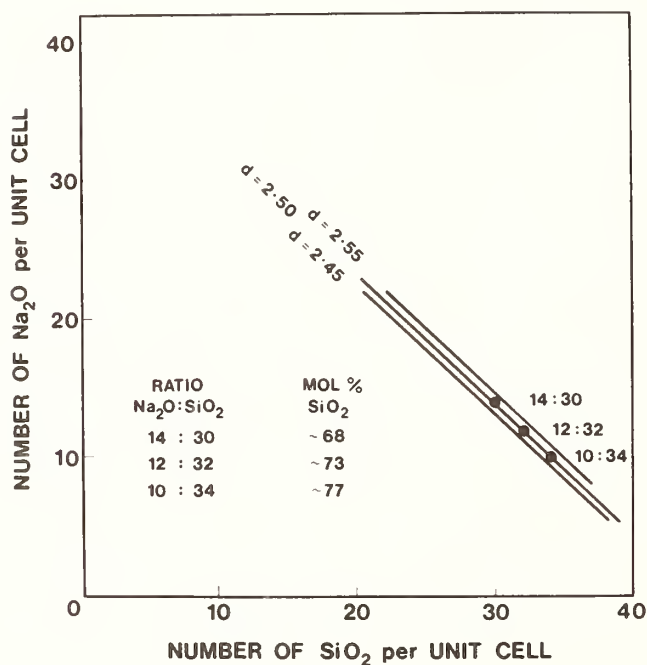


FIG. 1. Applications of Crystal Data to Sodium Silicates.

leaves only the 12:32 ratio, which must therefore be the only empirical formula which is consistent with all the data. Hence the phase is unequivocally shown to be $3\text{Na}_2\text{O} \cdot 0.8\text{SiO}_2$, or $\text{Na}_6\text{Si}_8\text{O}_{19}$. It is important to note that other ratios close to 3:8 could not be excluded except by using the additional constraints imposed by crystallographic symmetry.

It is noteworthy that, although $\text{Na}_2\text{Si}_3\text{O}_7$ is not a thermodynamically stable phase at any temperature, it is readily prepared by devitrifying glasses (ref. 11, appendix) the same procedures were again applied to prove that the formula of this metastable phase was $\text{Na}_2\text{Si}_3\text{O}_7$.

A useful additional check on the validity of this type of calculation is to apply the Lorentz-Lorenz relation, which states

$$R = \frac{n^2 - 1}{n^2 + 2} \times \frac{M}{d}$$

where R is the atomic refractivity, n the mean refractive index, M the formula weight and d the density. We take the value of R for Si from the low-density phases of SiO_2 , in which $R_{\text{Si}} \simeq 0.0$ and those of Na and O from sodium silicates, in which $R_{\text{Na}} \simeq 1.6$ and $R_{\text{O}} \simeq 3.7$. For example, knowing that the mean refractive index of $\text{Na}_3\text{Si}_8\text{O}_{19}$ is 1.503 (its birefringence is low) we can calculate its density. The value thus obtained, 2.47 ± 0.03 g/cc, agrees well with the observed density.

The principle has been explained with reference to an example from a two-component system but it is even more useful when applied in systems of greater chemical complexity: thus when a ternary compound stable to its incongruent melting point was encountered in the $\text{Na}_2\text{O}-\text{CaO}-\text{SiO}_2$ system, classical phase equilibrium methods were again combined with crystallographic data (symmetry, unit cell size and density) to show that the phase was $\text{Na}_2\text{CaSi}_5\text{O}_{12}$ (ref. 12, appendix). In the $\text{Na}_2\text{O}-\text{BaO}-\text{SiO}_2$ system (ref. 18 - 20 appendix) this combination of techniques was again sufficient to determine that the composition of a ternary phase was $\text{Na}_2\text{Ba}_4\text{Si}_{10}\text{O}_{25}$, despite the rather large unit cell size arising from the long \underline{a} axis ($\underline{a} = 39.35 \text{ \AA}$) and the low symmetry of this phase (ref. 18, appendix).

It is almost always practicable to obtain single crystals sufficient for crystallographic measurements. With care and practise, crystals which are only 10 - 20 μ in maximum dimension will usually suffice. During the course of phase

equilibrium studies, one would expect to encounter a particular phase in the course of making many experiments in which time, temperature and bulk composition were important variables. Observing the relative size of the crystals would generally suffice to indicate conditions most favourable for crystal growth, should it be required specially to grow crystals. If, however, it proves impossible to obtain crystals of sufficient size for X-ray diffraction, electron diffraction may instead be used to obtain the necessary crystallographic data.

The crystallographic information required to implement the procedures described above do not require that a full structure determination be made. There are, however, some instances in which full structure determination is required. Thus, a structure determination has been helpful, for example, in understanding the cation distribution in sapphire.* But it is by no means certain that all sapphire must have the composition -close to the molar ratio $7\text{MgO} \cdot 9\text{Al}_2\text{O}_3 \cdot 3\text{SiO}_2$ - of the crystal which was studied. Therefore, even the best crystal structure determinations will not necessarily suffice to determine the limits of homogeneous single-phase formation, although refinements based on site occupancy factors may correctly show the composition of an individual crystal. Moreover, an accurate crystal structure determination may not be possible if the crystals suffer from twinning and polytypism or both. Examples of the latter occur in the system $\text{Na}_2\text{O}-\text{BaO}-\text{SiO}_2$ (refs. 19, 20, Appendix) in which two phases, designated X and Y were encountered. Not only did the crystals prove to be difficult subjects for growth at liquidus temperatures, but crystals of both phases had extremely large and complex unit cells. We therefore had to be content with the best estimate of the compound compositions, taking into account the results of subsolidus equilibration. Tentatively, X was ascribed the formula $\text{Na}_2\text{Ba}_{18}\text{Si}_{28}\text{O}_{75}$ and Y, $\text{Na}_2\text{Ba}_{45}\text{Si}_{73}\text{O}_{192}$.

* Moore, P.B. Amer. Miner., 54, 31 (1969).

If it is possible to obtain chemical data on the composition of a phase by some direct technique, e.g., from microprobe analyses, this information should of course be utilized to the fullest. During our studies of silicate systems containing alkali ions, we have frequently made microprobe analyses in order to determine the alkali and SiO_2 contents of crystalline phases. In general, the quantitative worth of the results has been disappointing. When the phases being analyzed contained a preponderance of low atomic-weight elements, the volume which is sampled by the electron beams for analytical purposes may be approximately equivalent to a sphere of 100 - 200 μ diameter, even though the focal spot of the beam may be much smaller, typically 1 - 2 μ . In my experience, it is impracticable routinely to grow crystals of sufficient size to obtain reliable probe analyses for Na, Mg, etc. The advent of new types of electron-optic instruments with analytical capabilities, e.g., STEM, CORA, etc., give real hope that it will be possible to obtain 'spot' analyses which are able to more accurately determine the phase composition especially of micron-size crystals that are apt to occur in sintered mixtures.

b. Continuous High-Temperature X-ray Diffraction:
a complementary tool to DTA. On a focussing camera all X-ray reflections within the range of the instrument are recorded simultaneously. This is unlike the diffractometer which 'scans' the pattern, thereby making it almost essential that in a high temperature diffractometer, all other variables (temperature, pressure) should remain at least approximately constant during each individual scan. The different mode of operation of the focussing camera has lead to an ingenuous commercially-available design for a high-temperature instrument in which a sheet of photographic film is translated past a set of narrow (2 - 4 mm wide) slits, thereby exposing only a small strip at any instant. Starting from the origin, distance along the strip is proportional to θ (or 2θ), as in a normal photograph. However, the film translation motion is linked to a temperature programmer, so that the direction

on the film normal to the θ axis becomes an axis of changing temperature. The X-ray reflections in this direction are recorded continuously as a function of temperature. Typical heating and cooling rates using in the camera are $1^{\circ} - 2^{\circ}\text{C min}^{-1}$, or about an order of magnitude lower than those usually employed in DTA. The two techniques are, in general, complimentary and it is frequently helpful to have both. Usually, the same interpretation can be reconciled with both sets of data. There are, however, instances in which apparently different interpretations of the same events are required. In this connection, it is relevant to recount an actual example concerning the polymorphism of $\text{Na}_2\text{Si}_2\text{O}_5$. Fig. 2 shows schematically the most probable free-energy-temperature relations at 1 atm. The α phase and its variants are stable between 710° and the melting point (874°) but readily persist to lower temperatures. Samples of $\alpha \text{Na}_2\text{Si}_2\text{O}_5$ can readily be heated and cooled on the DTA without converting to the more stable β phase. The α phase is thermally active: it undergoes two rapidly-reversible inversions one at 680° the other at 707°C .

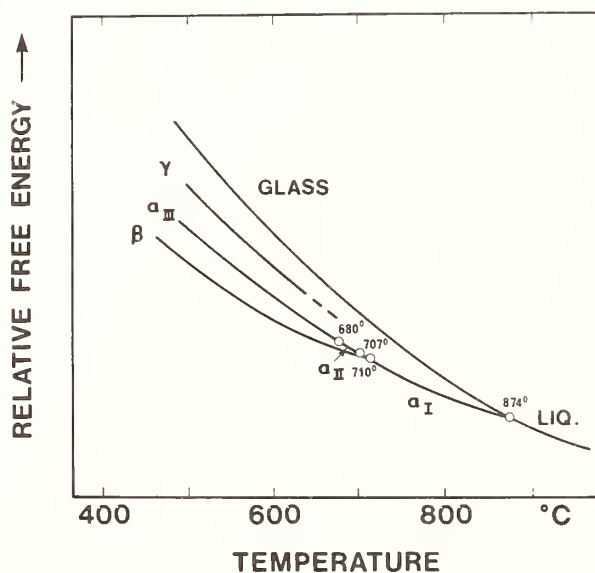


FIG. 2 Schematic free energy vs temperature diagram for $\text{Na}_2\text{Si}_2\text{O}_5$ at 1 atm. pressure.

However, when examined by continuous X-ray diffraction, only one change in the powder X-ray pattern - at 707° - is recorded. This apparently contradictory state of affairs is explained as follows: the low, or α_{III} , phase is orthorhombic. At 680° , it converts to the monoclinic, geometrically orthorhombic α_{II} phase having an orthorhombic pseudo-cell with cell dimensions identical to those of the α_{III} phase and, presumably because the atomic coordinates also change little, a powder pattern which is essentially identical to that of the α_{III} phase. At the 707° phase change the monoclinicity increases, resulting in a splitting of reflections which were previously coincident in the α_{II} and α_{III} phases.

However, α_I also has a much smaller b axis periodicity relative to the α_I and α_{II} phases. Therefore, above 707° some reflections which were present both in α_I and α_{II} phases also disappear. Without this interplay of techniques, it would not be possible to explain in such detail the nature of the phase transitions and to realize that each technique senses only a part of the picture. It would, however, be unwise to conclude that DTA is generally more sensitive than powder X-ray as a way of detecting phase transitions. By DTA, the γ family appears to have three rapid inversions, suggesting its subdivision into γ_I , γ_{II} , γ_{III} and γ_{IV} phases. However, the high-temperature X-ray suggests that the true picture is more complex, and the presumption is that the DTA fails to record those phase transformations for which ΔH is fortuitously equal to or very close to zero.

5. ROLE OF EXPERIMENTAL TECHNIQUES IN THE CRITICAL DETERMINATION AND EVALUATION OF PHASE RELATIONS.

Within the next decade, much effort will certainly be devoted to predicting phase relations in oxide systems. This is a welcome development especially to the technologist who almost always needs to 'stretch' the available data to predict the behaviour of chemically complex systems. At first sight, the development of predictive methods might appear to end or at least greatly to reduce the need to have recourse to experiment in order to determine phase relations. This is unlikely to be the case for a number of reasons. Firstly, there are many systems on which the necessary data either do not exist or are too fragmentary to be adequate. These system must, in the first instance, be studied experimentally. Secondly, there exists a less obvious region in which we appear to have much data for a particular system. Yet, upon intensive critical study, these data are shown to be incorrect. We have given several examples, but offer one more. The system $\text{CaO-MgO-Al}_2\text{O}_3\text{-SiO}_2$ is one of the great importance to petrologists and one which has apparently been thoroughly studied and a critical compilation made*. Together, these show that the

*Osborn, E.F., Gee, K.H., Muan, A, Roeder, P.L. and Ulmer, G.C. Bull. Earth, Min. Sci. Expt. Station, Penn. State Univ., 85 pp 80 (1969).

system does not have any quaternary compounds: i.e., it has no phases which require essential quantities of all four oxides in order to have a range of thermodynamic stability. However, Parker* has reported the existence of a quaternary compound (Q) to which he assigned the formula $6\text{CaO} \cdot 4\text{MgO} \cdot \text{Al}_2\text{O}_3 \cdot \text{SiO}_2$. Compilations made subsequently have omitted this compound: the compilers were probably influenced by the fact that sintered oxide preparations made at that composition do not yield Q. However, a re-examination of this system (ref. 25, Appendix) has shown that the Q can readily be prepared by sintering, and that judged by all criteria usually used to decide if a phase is stable, it should be admitted to the phase equilibrium diagram. The difficulty in preparing Q arose because the composition given by Parker was wrong. It was therefore necessary to resort to experiment and ultimately to show that a single-phase sinter could be obtained at the composition (in wt %) 42.2 CaO, 45.4 Al_2O_3 , 4.1 MgO and 8.2 SiO_2 . The existence of Q and R phases (the system in fact contains two quaternary phases, the second having been designated R) considerably alter phase relations in the MgO-rich portions of the quaternary system. The important point to be made here is that no amount of compilation activity divorced from experiment is likely to provide validated data on complex oxide systems. It is important, therefore, that the application of predictive methods should not be handicapped by the lack of these data.

Finally, phase equilibrium determinations frequently encounter persistent non-equilibrium states. While the existence of some of these states might be predicted, others may not. In any event, our knowledge of the kinetics of solid-state reactions is generally insufficient to enable us to predict how persistent a given metastable state would be or what specific conditions would favour development of a particular metastable state. This is another advantage of having experimental data, which readily reveals the existence of persistent metastable phases.

* Parker, T.W. Proc. Intl. Symp. Chem. Cement (London, 1952) 485.

S U M M A R Y

During the past decade, no revolutions have occurred in the experimental methods used to study phase relations in oxide systems. Nevertheless, steady progress has been made and it is now possible to study complex oxide systems more rapidly yet with greater precision than in the past. The writer's experience has been that even supposedly well-known systems require major modifications to 'accepted' phase diagrams. It is considered especially important if predictive studies are to be given a fair start that a store of validated data on oxide systems must be available upon which to base calculations: at present, it is felt that this store is not adequate. Hence the need for continuing experimental studies on oxide systems with an emphasis on those of fundamental importance to technology.

A P P E N D I X

SUMMARY OF PHASE EQUILIBRIA STUDIES IN SILICATE AND ALUMINATE SYSTEMS UNDERTAKEN AT THE UNIVERSITY OF ABERDEEN

<u>System</u>	<u>Ref.</u>	<u>System</u>	<u>Ref.</u>
$\text{Li}_2\text{O}-\text{SiO}_2$	1,2,3	$\text{MgO}-\text{Al}_2\text{O}_3-\text{TiO}$	22
$\text{Li}_2\text{O}-\text{BaO}-\text{SiO}_2$	4	$\text{MgO}-\text{Al}_2\text{O}_3-\text{SiO}_2$	23
$\text{Li}_2\text{O}-\text{ZnO}-\text{SiO}_2$	5,6		
$\text{Li}_2\text{O}-\text{MgO}-\text{ZnO}-\text{SiO}_2$	7,8	$\text{CaO}-\text{SrO}-\text{BaO}-\text{SiO}_2$	24
$\text{Li}_2\text{O}-\text{Pd}-\text{O}$	9	$\text{CaO}-\text{MgO}-\text{Al}_2\text{O}_3-\text{SiO}_2$	25
$\text{Na}_2\text{O}-\text{SiO}_2$	10,11	$\text{CaO}-\text{Al}_2\text{O}_3-\text{Fe}_2\text{O}_3$	26,27
$\text{Na}_2\text{O}-\text{CaO}-\text{SiO}_2$	12,13,14	$\text{CaO}-\text{Al}_2\text{O}_3-\text{FeO}-\text{Fe}_2\text{O}_3$	28,29
$\text{Na}_2\text{O}-\text{CaO}-\text{MgO}-\text{SiO}_2$	15	$\text{CaO}-\text{Al}_2\text{O}_3-\text{Fe}_2\text{O}_3-\text{SiO}_2$	30,31
$\text{Na}_2\text{O}-\text{CaO}-\text{Al}_2\text{O}_3-\text{SiO}_2$	16		
$\text{Na}_2\text{O}-\text{CaO}-\text{SrO}-\text{SiO}_2$	17	$\text{PbO}-\text{SiO}_2$	32
$\text{Na}_2\text{O}-\text{BaO}-\text{SiO}_2$	18,19,20		

$\text{K}_2\text{O}-\text{BaO}-\text{SiO}_2$

References

1. Phys. Chem. Glasses 8, [6] 224 - 32 (1967).
2. Mater. Res. Bull. 5, 837 - 43 (1970)
3. Advances in Nucleation and Crystallization in Glasses
Amer. Ceram. Soc. Spec. Pub. 5 (1972) (pp. 151 - 65).
4. Trans. and Jour. Brit. Ceram. Soc. 73, 207 - 11 (1974).
5. Jour. Mater. Sci. 5, 557 - 65 (1970).
6. " " " 5, 676 - 88 (1970).
7. " " " 6, 1100 - 10 (1971).
8. " " " 7, 895 - 908 (1972).
9. Jour. Solid State Chem. 6, 329 - 34 (1973).
10. Science 148, No. 3677, 1589 - 91 (1965).
11. Phys. Chem. Glasses, 7 [4], 127 - 38 (1966).
12. Jour. Amer. Ceram. Soc. 53 [7], 423 (1970).
13. Phys. Chem. Glasses, 12, 50 - 7 (1971).
14. " " " 15, 6 - 11 (1974).
15. " " " 13, 27 - 42 (1972).
16. " " " 17, 45 - 53 (1976).
17. Trans. & Jour. Brit. Ceram. Soc. 73, 199 - 206 (1974).
18. Phys. Chem. Glasses, 13, 125 - 30 (1972).
19. Trans. & Jour. Brit. Ceram. Soc., 72 [7], 299 - 305 (1973).
20. J. Amer. Ceram. Soc. 57, 201 - 4 (1974).
21. " " " 58, 233 - 6 (1976).
22. Trans. & Jour. Brit. Ceram. Soc. 72 [5], 215 - 20 (1973).
23. Jour. Mater. Sci. 11 [8] 1459 - (1976).
24. Zeit. Krist. 141, 437 - 50 (1975).
25. Trans. & Jour. Brit. Ceram. Soc. 4 [4], 113 - 9 (1975).
26. "Science of Ceramics" Vol. 3, Academic Press London (1967)
pp. 191 - 214.
27. Trans. & Jour. Brit. Ceram. Soc. 66 [7], 293 - 306 (1967).
28. " " " " " 70 [6], 227 - 34 (1971).
29. " " " " " 72 [5], 221 - 28 (1973).
30. " " " " " 74 [7], 253 - 6 (1975).
32. " " " " " 75 [5], 95 - 103 (1976).
32. Jour. Amer. Ceram. Soc. 57 [9], 378 - 82 (1974).



PROTECTIVE COATINGS FOR SUPERALLOYS AND THE USE OF PHASE DIAGRAMS

M. R. Jackson and J. R. Rairden
General Electric Company
Corporate Research & Development
Schenectady, New York

Abstract

Compositional modifications to increase the strength of superalloys have produced parallel decreases in environmental resistance, both for oxidation limited jet engine applications and hot corrosion limited gas turbine applications. Simple aluminide coatings have been formed by pack aluminization, but with greater demands on oxidation resistance, $M\text{CrAl}(Y)$ coatings have come into use (M is Ni, Co and/or Fe), and duplex coatings have been formed by aluminizing the $M\text{CrAl}(Y)$ coatings. Other elements are also of interest as additions to coatings, either homogeneously distributed throughout the coating or localized as an inner or outer layer of the coating.

Phase equilibria in ternary and higher order systems can be extremely useful in correlating coating/substrate compositions, microstructures and behavior. For example, the time-temperature changes in formation and degradation of coatings on superalloy surfaces can be understood in terms of multi-element diffusion between the elements added and the elements in the substrate by mapping the diffusion paths through the appropriate phase diagrams. This understanding can be useful in developing improved coating compositions.

Specific examples of the application of phase diagrams to the understanding of coating formation and degradation are presented: aluminization of superalloys, duplex aluminized coatings, and aluminization of platinide coatings on superalloys. Systems where only limited diagrams exist are also discussed.

INTRODUCTION

Coatings are used in many metallurgical applications to create composite systems whose properties are optimized with (a) a surface layer for stabilized interfacing with the environment, and (b) a substrate for economically meeting the mechanical requirements. Common examples are galvanized steel to resist rusting, and carburized steel to resist wear. In both these systems, coating formation is at high temperature, but service is at relatively low temperature. Coating formation involves diffusive interactions with the substrate, but coating degradation in service involves predominantly the interaction with the environment.

In contrast, coatings for hot gas components must resist high temperature oxidation and corrosion in the severe environment of gas turbines and jet engines.¹ The Ni-base superalloy substrates are protected with coatings that form dense, adherent oxide scales. For these coatings, degradation in high temperature service (as well as coating formation) involves interdiffusion between the coating and substrate.² For many applications, compositions for resistance to oxidation and/or hot corrosion have been identified. Successful coatings form and retain a desired surface structure for times approaching several years at 1000°C.

An understanding of the phase distribution established between coating and substrate, and how that distribution changes in service as the system tries to move toward equilibrium, can be achieved in terms of the relevant phase diagrams. When the diagrams are available, the diffusion path taken by the coating/substrate system can be considered directly. When the diagrams are unavailable, a study of the diffusion path taken can be used to gain phase diagram information. To advance current coating technology, a detailed definition of relevant phase diagrams over a range of temperatures is needed. This information can be used to devise coatings which maintain the desired surface structure by following diffusion paths through the phase diagram chosen to minimize the rate of approach to equilibrium.

The Ni-base superalloys contain on the order of 10-25% Cr, 0-10% Co and 2-10% Al, by atom percentages, as well as lesser amounts of other elements for further strengthening.³ The major phases present are the fcc Ni solid solution (γ) and an ordered precipitate phase based on Ni₃Al (γ'). Some elements, such as Ti or Ta, are added to strengthen the γ'

phase, while others, such as Mo or W, are added to strengthen the γ matrix. Further additions are made to form carbides or borides, generally in amounts of less than 2 v/o of either phase.

A typical superalloy composition specification may include 9-14 different elements. These complex alloys might appear to prohibit any use of phase diagrams to understand their behavior. However, some simplifying assumptions can be made, similar to these made in "phacomp" stability calculations.³ Since the borides and carbides represent a small volume fraction of the system, they generally have a small influence on phase equilibrium of the superalloy, although they are not inert. The elements involved in these phases can be subtracted from the bulk chemistry proportionately to their presence in these phases. Furthermore, elements which influence the phase equilibrium in a manner similar to Cr can be treated as additional Cr atoms.⁴ This includes Mo, W and V. The elements Ta, Ti and Nb influence the phase equilibrium in a manner similar to Al, and can be treated as additional Al atoms.⁴ These simplifications reduce the complex chemistry of most superalloys to Ni, Co, Cr and Al. For most alloys, Co can be equated to Ni, and the alloys can be treated as ternary systems of Ni, Cr and Al.

Rules governing the description of diffusion paths in multicomponent systems have been discussed in the literature.⁵⁻⁷ It should be noted that for diffusion paths plotted on phase diagrams, dashed lines do not represent distance in the actual diffusion couple, but represent an interface. In a true ternary system, a three-phase field will have no width in a diffusion couple because of the constant chemical potentials within that field.⁶ In the ternary approximations of 10-12 element systems, we have not observed three-phase fields in diffusion couples.⁴ However, for practical systems such as silicided superalloys, we have observed three-phase structures developing in the diffusion couples.⁸

We will illustrate the use of existing diagrams for protective coatings on superalloys by examples of aluminization, and then go on to generation of phase diagram information by the use of diffusion path studies where details are unavailable. Finally, further systems of interest for which incomplete information exists will be discussed.

ALUMINIZATION

Compositional modifications to increase the strength of the superalloys have usually involved reductions in Cr content. The greater strengths permit the use of the superalloys at higher temperatures. For both oxidation limited jet engine applications and hot corrosion limited gas turbine applications, lower Cr and higher temperatures have necessitated the use of coatings.¹ Initially, simple diffusion aluminide coatings were formed by pack aluminization.⁹ The part to be coated is placed in a pack consisting of Al_2O_3 powder mixed with a small percentage of aluminum or aluminum-bearing powder. Generally, the pack is "activated" by inclusion in the pack of a halide such as NH_4F . The pack is heated to a high temperature (850-1150°C) for a period of several hours, during which time Al is transported to and deposited on the substrate surface. The generally accepted view is that the deposition is an approximately steady-state process,¹⁰ although we have recent experimental evidence which indicates that Al transfer is largely completed by the time the pack reaches the aluminizing temperature, and that the time at temperature is predominantly a diffusion heat treatment.⁴ In any event, the coating/substrate microstructure can be observed and the structures formed can be plotted in the ternary phase diagram. The binary Ni-Al diagram¹¹ has been used successfully to describe aluminization of Ni,^{12,13} but aluminization of more complex alloys requires higher order diagrams.

The observed microstructure formed in aluminizing a complex Ni-base superalloy, IN-738, is illustrated in Figure 1. Phase identification for this type of microstructure involves metallographic examination, electron microprobe analysis of the phase chemistries, and x-ray diffraction to verify chemistries on the basis of crystal structures known from each of the binary systems involved.⁴ The diffusion path through the ternary diagram is shown in the schematic diagram of Figure 1. The diagram is based on information in the literature, but is hypothetical for Al-rich compositions beyond the $\beta+\alpha$ field.^{11,14-16} The $\delta+\alpha$ (Ni_2Al_3 + Cr solid solution) field is observed experimentally in aluminized structures, while the higher Al fields are assumed. In the Ni-Cr-Al diagram, the $\gamma'+\alpha$ field is prevented by a $\gamma+\beta$ field at temperatures greater than $\sim 1000^\circ\text{C}$. However, for the superalloys, the additions of Ta, Ti and Nb raise the temperature of the $\gamma'+\alpha$ / $\gamma+\beta$ transition.¹⁷ For the alloys IN-738, IN-100,

and René 80, for example, the $\gamma'+\alpha$ field is observed at 1060°C, but not at 1160°C.⁴ One further point to be made about the diagram involves the presence of α . For alloys high in Mo and/or W, a topologically close-packed phase (σ) intervenes between γ and α .¹⁸ Therefore, depending on the substrate composition and the coating/substrate interaction, $\gamma'+\sigma$ may be observed rather than $\gamma'+\alpha$.

The path shown in Figure 1 is for the coating formed by aluminizing IN-738.⁴ The initial couple can be considered as between IN-738 and Al. Typically, aluminization of a turbine blade involves the deposition of ~ 6 mg/cm² of Al which is equivalent to the deposition of an $\sim 25\mu\text{m}$ thick layer on the substrate. Therefore, the IN-738 acts as an infinite sink for a finite amount of Al. For IN-738 (11.8 a/o Al, 19.5 a/o Cr in the ternary approximation), the final equilibrium for a coated .25cm thick substrate would be 12.7 a/o Al, 19.3 a/o Cr, still well within the $\gamma+\gamma'$ field for the substrate. Since this composition would be only marginally more resistant to the environment than the base composition of IN-738, it is desirable to minimize the rate of equilibration of the coating with the substrate and to retain the high-Al β and δ phases for long service life. During coating formation, the outermost part of the coating corresponds in the phase diagram to the first completely solid phase field intersected by a line joining the terminals of the couple, IN-738 and Al. The remainder of the path is governed by the relative diffusivities of Ni, Cr and Al. Presumably, Cr is the slowest in diffusion in the phases formed in the coating,¹⁹ so the path swings away from the Cr corner of the diagram initially, and then swings back toward the Cr corner, crossing the line joining the terminals of the couple in order to maintain the Cr mass balance.

In service, the coating degrades by two mechanisms.⁹ (1) The interaction with the environment causes the preferential oxidation of Al and Cr. These elements are lost when the oxide scale spalls and additional Al and Cr from the coating are required to form a new oxide layer. (2) The interaction with the substrate causes a loss of Al from the coating to the substrate by inward diffusion and a gain of Ni in the coating by outward diffusion. In the microstructure, the β phase is seen to grow at the expense of δ as Al is lost at the surface. The disappearance of the

δ phase in service generally occurs rapidly. The IN-738 terminal of the couple does not change location, but the Al-rich terminal migrates toward the IN-738 terminal, as shown in Figure 1c. In a closed system, the diffusion path would have to cross the line joining Al and IN-738 so that mass balance would be maintained. Although spallation of oxidized material eases that restriction, the general observation is that the path does cross that line throughout the useful service life of the coating.

OVERLAYER AND DUPLEX COATINGS

The most advanced higher temperature capability Ni-base superalloys have quite low Cr contents. For many of these materials, operation at the extreme of their capability requires more environmental resistance than can be provided by a simple diffusion aluminide coating. Coatings known as MCrAlY's (the M being the major element, Ni, Co and/or Fe) have been devised which contain enough Cr and Al to be extremely resistant to high temperature aggressive environments.¹ The amount of Y present in the actual coating is generally small, on the order of 0.05 a/o, and is localized primarily at grain boundaries in the coating. For phase equilibrium purposes, we can ignore Y, although its presence is very important. As a protective Al, Cr oxide scale forms at the surface of the coating, Y_2O_3 forms at the boundaries and is interconnected with the surface oxide.²⁰ The interconnection serves to promote adherence of the surface scale to the coating. Because of differences in expansion coefficient between coating and oxide, temperature cycling can cause stresses which act to spall the protective oxide and degrade the coating by allowing new scale formation. The presence of Y tends to prolong the adherence of the protective surface scale.

The MCrAlY overlay coatings can be deposited by several methods. Physical vapor deposition is accomplished by heating a source of the desired composition with an intense electron beam to produce melting and vaporization.²¹ Another commonly used technique involves thermal spraying where the coating is deposited by passing powder of the desired composition through a plasma torch impinging on the substrate or by passing the coating as a wire source through a high temperature flame.²²

As noted earlier, the Ni-Cr-Al ternary diagram exhibits the transition $\gamma+\beta \leftrightarrow \gamma'+\alpha$, with $\gamma+\beta$ present above 1000°C, and $\gamma'+\alpha$ present below 1000°C (Figure 2). In the superalloys, γ' is stabilized by additions of elements such as Ta, Ti and Nb, so that the transition occurs at somewhat higher temperatures. This leads to some complications for understanding microstructures for NiCrAlY coatings on Ni-base superalloys after service in the range of 1000-1100°C. For example, consider a coating whose composition is located in the $\gamma'+\alpha$ field at low temperatures and the $\gamma+\beta$ field at high temperatures. Above 1000°C, the bulk of the coating will be in the $\gamma+\beta$ field. However, at the coating/substrate interface, sufficient interdiffusion may occur in service so that γ' stabilizing elements reach levels in the coating sufficient to raise the transition temperature above the service temperature and form $\gamma'+\alpha$. This can occur for compositions outside the narrow range already described. For example, compositions in the $\gamma+\gamma'+\alpha$ field at low temperature may fall in $\gamma+\gamma'+\beta$, $\gamma+\beta$ or $\gamma+\beta+\alpha$ at high temperatures, and interdiffusion can lead to differences in the ternary section which describes the structure in the different parts of the coating. For example, a coating of Ni-20a/o Cr-20a/o Al with 0.05 a/o Y on IN-738 at 1060°C is $\gamma+\beta$ for the bulk of the coating, but produces $\gamma'+\alpha$ at the coating/substrate interface.⁴ As Al and Cr diffuse from the coating into the substrate, σ precipitates within the substrate.

Coatings of the CoCrAlY type are very similar to the NiCrAlY coatings, but there are differences. The γ phase of the coating transforms to the hexagonal close-packed ϵ phase at temperatures below about 800°C.¹¹ However, for use temperatures where interdiffusion is rapid, the CoCrAlY coatings consist principally of the γ fcc phase. There is a pronounced influence of Co on the NiAlCr phase equilibrium.¹⁷ The γ' phase is destabilized, and with sufficient amounts of Co, the $\gamma+\beta$ field is stable to room temperature and $\gamma'+\alpha$ does not form.

Interdiffusion between Ni-base substrates and CoCrAlY overlayers can be plotted in the quaternary diagrams, (Figure 2). The paths can change considerably with coating composition, and frequently traverse the interior of the quaternary section. At present, there is no convenient way to represent the paths visually, and we will not attempt to do so here. For

the bulk of the interaction, however, the paths will be quite close to the ternary faces of the quaternary sections. For example, a thick CoCrAlY coating will not have high Ni concentrations until very far into its useful life. The interdiffusion path for the outer region of the coating will lie very close to the CoCrAl surface of the quaternary, and for the major portion of the coating life, Ni that diffuses to the outer region of the coating can be treated as additional Co atoms and the path can be plotted in ternary space. Similarly for the substrate/coating interaction in the substrate, insufficient Co will be present to move the diffusion path significantly far from the NiCrAl ternary surface. The remainder of the coating will have a diffusion path which traverses the quaternary section too far from a ternary surface to be represented visually in two dimensions. It should also be noted in Figure 2 that Co tends to stabilize the σ phase in the simple quaternary alloys.²³ For the Ni-base superalloys, where σ is nearly stable, diffusion of Co into the substrate may alter the appropriate diagram to include the σ phase.

Coatings of the FeCrAlY type present equally difficult problems of visualization. The major phase of the coating is bcc and for many FeCrAlY compositions that is the only phase.²⁴ For these coatings the diffusion couple is α versus $\gamma+\gamma'$. Since Fe tends to stabilize a $\gamma+\beta$ field in favor of a $\gamma'+\alpha$ field when added to the Ni-Cr-Al systems,^{17,25} diffusion paths again can be quite complex and are strongly dependent on the coating composition. Stabilization of σ by additions of Fe occurs at lower temperatures, although not for the temperature of the section shown in Figure 2.

The overlayer coatings can be described in terms of diffusion paths just as was the case for aluminization of superalloys. However, little detailed information is available regarding the interior of the Ni-Cr-Al-Fe and Ni-Cr-Al-Co quaternary sections at any temperature. The diagrams of Figure 2 contain many field boundary locations that are completely hypothetical. In fact, the Co-Cr-Al system is not well characterized, even though the CoCrAlY coatings are in use for their exceptional resistance to hot corrosion. Much work could be done to improve our understanding of the quaternary systems which could lead to optimum environmental coatings.

Duplex aluminizing of MCrAlY coatings on Ni-base substrates is a simpler case for coating formation. The situation for aluminization of NiCrAlY, CoCrAlY and FeCrAlY coatings can be treated as ternary diffusion problems, without difficulties that arise in the more complex superalloys. Since γ' stabilizing elements are not present, the ternary diagram for Ni-Cr-Al is accurate and the temperature for the $\gamma+\beta\rightleftharpoons\gamma'+\alpha$ transition is better defined. However, consideration of coating degradation by reaction with the environment and interdiffusion with the Ni-base substrate still requires more detailed evaluation of the appropriate quaternary systems.

PLATINUM ALUMINIDE COATINGS

Another coating system is extremely resistant to hot corrosion environments.²⁶⁻²⁸ A 10-20 μm layer of Pt is deposited on the Ni-base substrate and the structure is pack aluminized. Many different coating microstructures can be formed, depending on the relative amounts of Pt and Al present in the coating.²⁹ Coating degradation involves interdiffusion of the coating and substrate at temperatures of 875-1000°C.

The phases present in the Al-Pt diagram have not been completely characterized.^{30,31} However, a recent study appears to give the best definition of the system.³² Our studies of the aluminization of pure Pt²⁹ are consistent with the diagrams of Chatterji, et al.³² In aluminizing for very short times, the phases that develop are PtAl₃, PtAl₂, Pt₂Al₃ and PtAl. After 1/2 hour of treatment, the PtAl₃ and PtAl₂ phases are eliminated by rapid interdiffusion. The major phase is Pt₂Al₃, but small amounts of Pt₂Al and Pt₃Al also are observed.

Since the Pt-Al diagram has not been characterized fully, it is difficult to consider platinum aluminide coatings on Ni-base superalloys in terms of the Ni-Cr-Al-Pt phase diagram. We have performed microstructural and microchemical analyses of coated IN-738, and as a result we now have a limited picture of the phase diagram.²⁹ The IN-738 substrate was coated with Pt so that a non-uniform thickness was deposited on the circular cross-section. The Pt layer varied in thickness from zero to 25 μm . After aluminization, a single microsection contained a large spectrum of Pt/Al ratios. Several paths are plotted in Figure 3 to show some of the possible coating/substrate systems. The Al-Cr-Pt diagram is not critical to the explanation, and too little data are available

to permit speculation on the appearance of the ternary isothermal section. Paths through the interior of the quaternary cannot be mapped on the unfolded diagram. However, most paths observed traversed the pyramid along ternary faces or just below the faces.

The path marked 1 is for the case of a Pt coating that is thick relative to diffusion distances. The initial part of the path is that seen for aluminization of bulk Pt, and the remainder is for diffusion that occurs between bulk Pt and IN-738. Path 2 is for 1060°C aluminization of the ~25 μ m thick-Pt coated IN-738 just as the pack reaches temperature. The path departs from that of bulk Pt below the PtAl layer and enters the two-phase PtAl + β NiAl phase field, but it quickly crosses to Pt-rich γ and finally to $\gamma+\gamma'$ substrate. The diagram is drawn so that a PtAl + γ field exists. It is possible, however, that this field does not exist but is blocked by Pt₂Al + β and Pt₃Al + β fields. These fields may not be observed because of kinetics of formation of Pt₂Al and Pt₃Al.

Path 3 is based on observations of the 3-hour aluminization of the thick-Pt coated IN-738. Diffusion of Al inward has eliminated the outer PtAl₂ region, and γ has been replaced with β (Ni, Pt)Al. Microanalysis indicates the β phase contains about 12.5 a/o Pt, with Pt apparently substituting for up to one-fourth of the Ni. For path 3, a three-dimensional depiction of its position is really more accurate. The path is shown as far as β in the Ni-Al-Pt ternary, and beginning again at β in the Ni-Al-Cr ternary. The path leaves β to form the $\beta+\alpha$ Cr finger zone, and then goes to the $\gamma+\gamma'$ substrate. The dashed lines indicate that $\beta+\alpha$ and $\gamma+\gamma'$ have a planar interface. The $\gamma'+\alpha$ phase field, as would be expected for the Ni-Al-Cr ternary isotherm, is not observed. The $\beta+\alpha$ phase field has between 5 and 8 a/o Pt which may put the actual path far enough into the quaternary isotherm that a ternary description is no longer valid. As Pt is added to a composition initially in the $\gamma'+\alpha$ field, the composition may move into a $\gamma+\gamma'+\alpha$ field, and then to a $\gamma+\beta+\alpha$ field. Path 3 may pass from $\beta+\alpha$ to $\gamma+\gamma'$ at the interface describing passage through the $\gamma+\beta+\alpha$ field.

Path 4 describes the aluminization of thin-Pt coated IN-738 just as the pack reaches temperature. The path begins along the Pt-Al binary but quickly moves into the Ni-Pt-Al ternary isotherm. The Pt content reaches zero in the β phase, so path 4 is expected to be entirely in the Ni-Cr-Al ternary isotherm from that point on. As is seen for the aluminization of bare IN-738, the path exhibits two finger zones: $\beta+\alpha$ and $\gamma'+\alpha$. Path 5 for the 3-hour condition, thin-Pt coated IN-738, begins well into the ternary Ni-Pt-Al. Again, Pt drops to zero in β , and the remainder of the path duplicates path 4. Path 6 is the path for 0 Pt; i.e., for aluminization of bare IN-738. For very thin Pt coatings on IN-738, the microstructure would be expected to follow path 6.

A pattern emerges from the observed microstructures: for Pt coatings that are thick relative to diffusion distances for a given time-temperature treatment, the system behaves as two unconnected couples, IN-738/Pt and Pt/Al. As the Pt layer becomes thinner relative to diffusion distances, the two couples begin to interact through the common Pt terminus. With increasing time at temperature, the diffusion paths tend to move in the direction of less Al and less Pt at the surface, as expected. Commercial Pt-Al coatings are frequently heat treated at lower temperatures and longer times, but they probably go into service with a coating described by path 3 or 5. If Al is consumed in service by oxidation or by more rapid inward diffusion than that for Pt diffusion into the substrate, the outer surface composition may again move toward the Pt corner of the quaternary isotherm.

The platinum aluminide coating system for Ni-base superalloys is an example of the generation of phase diagram information from coating formation studies. However, a detailed characterization would be helpful in developing optimum coatings. As noted, path 3 may be that followed by coatings going into service, yet much of this path traverses the interior of the pyramidal section where we have little information.

OTHER COATING SYSTEMS

The Ni-base superalloys can also be protected using coatings which contain other elements. Additions of Si to NiCrAlY coatings have resulted in improved oxidation resistance.^{8,33} Depending on the amount of Si present, phases in addition to those in the Ni-Cr-Al ternary system may or may not be present. Additions of Hf have been shown to have a dramatic influence on the oxidation resistance of other NiCrAl coatings.³⁴ Phase diagram analyses for the coating formation and service temperatures are not well characterized for either of these additions. It seems likely that as coating development proceeds, other elements will become important ingredients in high temperature coatings. These other additions, such as Ta, Ti or W, may be present in amounts sufficient to alter the phase equilibrium as described in the simple Ni-Cr-Al diagram.

SUMMARY

We have attempted to show how the appropriate phase diagrams can be used to characterize the coating formation and degradation processes in simple aluminide coatings and in overlayer MCrAlY and duplex coatings for high temperature Ni-base superalloys. Even for these systems, the available phase diagram information is inadequate in many cases to be useful in coating design to retain the desired phases for extended service life. In more complex systems, such as platinum aluminide coatings, the study of coating microstructure and microchemistry has allowed the development of a qualitative description of the Ni-Cr-Al-Pt phase diagram. However, much more detailed information would be needed to be more useful in coating design. The area of environmentally resistant high temperature coatings would be benefited by a better definition of the appropriate ternary, quaternary and possibly quinary systems.

REFERENCES

1. S. J. Grisaffe, in The Superalloys, ed. C. T. Sims and W. C. Hagel, John Wiley, New York, p. 341, 1972.
2. G. W. Goward, D. H. Boone and C. S. Giggins, ASM Trans., Quart., 60, 228 (1967).
3. R. F. Decker and C. T. Sims, in The Superalloys, ed. C. T. Sims and W. C. Hagel, John Wiley, New York, p. 33, 1972.
4. J. R. Rairden and M. R. Jackson, "The Aluminization of Nickel-Base Superalloys," submitted to Met. Trans.
5. J. B. Clark and F. N. Rhines, Trans., ASM, 51, p. 199 (1959).
6. J. S. Kirkaldy and L. C. Brown, Canadian Met. Quart., 2, p. 89 (1963).
7. J. Kirkaldy, Can. J. Phys., 36, p. 907, 1958.
8. J. R. Rairden and M. R. Jackson, General Electric Co., Schenectady, N.Y., unpublished research, 1976.
9. G. W. Goward and D. H. Boone, Oxidation of Metals, 3, 475 (1971).
10. R. L. Wachtell, Science and Technology of Surface Coating, Edited by B. N. Chapman and J. C. Anderson, Academic Press (1974).
11. M. Hansen and K. Anderko, Constitution of Binary Alloys, McGraw-Hill Book Co., Inc., New York (1958).
12. M. M. P. Janssen and G. D. Rieck, Trans., TMS-AIME, 239, 1372 (1967).
13. A. J. Hickl and R. W. Heckel, Met. Trans., 6A, 431, 1975.
14. A. Taylor and R. W. Floyd, J. Inst. of Metals 81, p. 451 (1952-53).
15. A. Taylor, Trans. AIME, 206, p. 1356 (1956).
16. I. I. Kornilov and R. S. Mints, Russ. J. Inorg. Chem., 3 p. 214, 1958.
17. M. R. Jackson and J. L. Walter, in Superalloys: Metallurgy and Manufacture, ed. B. H. Kear, D. R. Muzyka, J. K. Tien and S. T. Wlodek, Claitor's Publishing, Baton Rouge, p. 341, 1976.
18. Appendix A, Phase Diagrams, The Superalloys, ed., C. T. Sims and W. C. Hagel, John Wiley, New York, p. 577, 1972.

19. R. T. DeHoff, K. J. Anusavice and C. C. Wan, *Met. Trans.*, 5, p. 113, 1974.
20. E. J. Felton, *J. Electrochem. Soc.*, 108, p. 490, 1961.
21. Vapor Deposition, ed. C. F. Powell, J. H. Oxley and J. M. Blocher, Jr., John Wiley, New York, 1966.
22. H. S. Ingham and A. P. Shepard, Metco Flame Spray Handbook, Vol. III., Plasma Flame Process, Metco, Inc. Westbury, New York, 1965.
23. K. R. Gupta, N. S. Rajan and P. A. Beck, *Trans., AIME.*, 218, p. 617, 1960.
24. Metals Handbook, 8th ed., 8, American Society for Metals, Metals Park, Ohio, 1973.
25. M. R. Jackson, in Conference on In Situ Composites-II, ed. M. R. Jackson, J. L. Walter, F. D. Lemkey and R. W. Hertzberg, Xerox-Individualized Publishing, Lexington, Mass., p. 67, 1976.
26. G. Lehnert and H. W. Meinhardt, *D.E.W., Tech. Ber.*, 11, p. 236, 1971.
27. G. Lehnert and H. W. Meinhardt, *Electrodep. Surface Treat.*, 1, p. 189, 1972-1973.
28. G. Lehnert and H. W. Meinhardt, *Electrodep. Surface Treat.*, 1, p. 71, 1972-1973.
29. M. R. Jackson and J. R. Rairden, "The Aluminization of Platinum and Platinum-Coated IN-738," accepted for publication, *Met. Trans.*
30. F. A. Shunk, Constitution of Binary Alloys, 2nd Supplement, McGraw Hill, 1969.
31. R. Huch and W. Klemm, *Z. Anorg. Chemie*, Band 329, p. 123, 1964.
32. D. Chatterji, R. C. DeVries and J. F. Fleischer, *J. Less-Common Metals* 42, p. 187, 1975.
33. G. J. Santoro, D. L. Deadmore and C. E. Lowell, NASA TN D-6414, NASA, Lewis Research Center, Cleveland, Ohio, 44135, 1971.
34. D. R. Chang, "The Oxidation Behavior of Aluminide Coatings on René 120 and René 125", Abstract #108, Abstract Book for 1975 Materials Science Symposium, American Society for Metals, Metals Park, Ohio, p. 30, 1975.

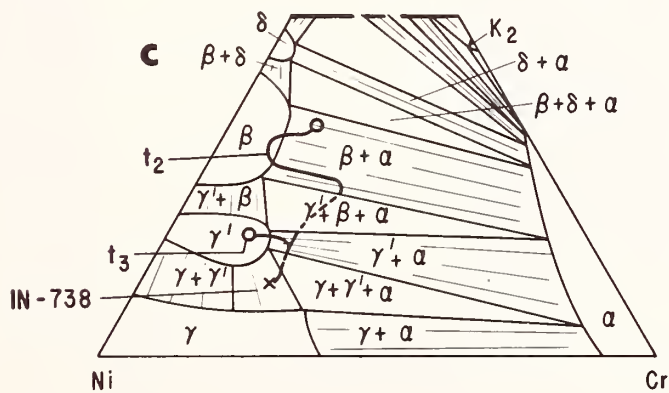
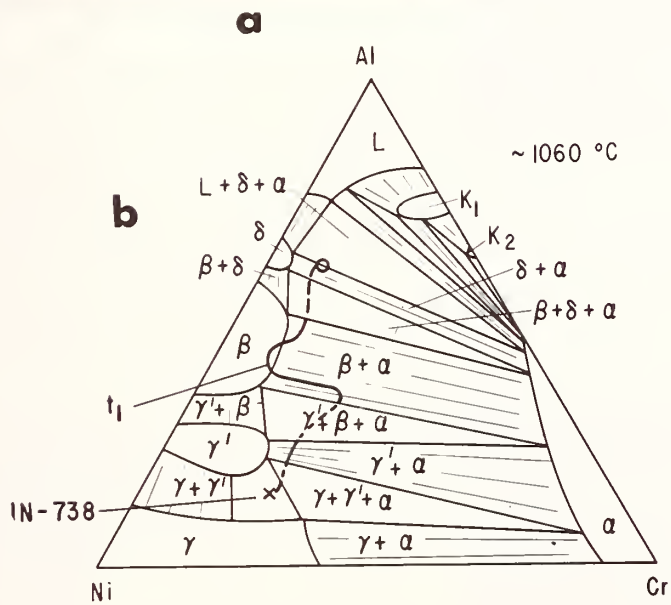
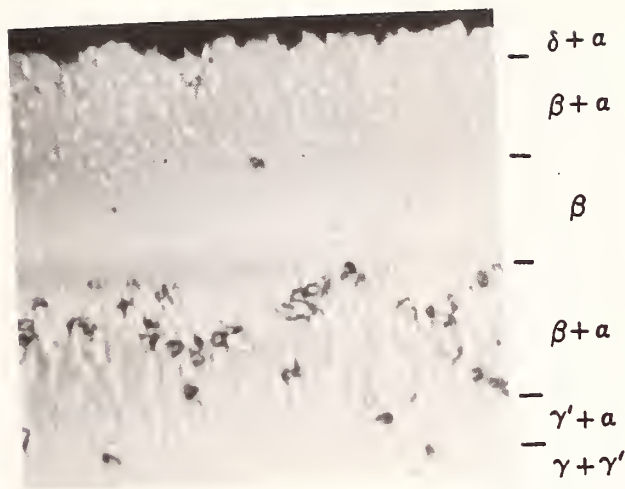


Fig. 1: (a) The microstructure formed on aluminizing IN-738 and the phase diagram Ni-Cr-Al with diffusion paths describing (b) coating formation and (c) degradation.

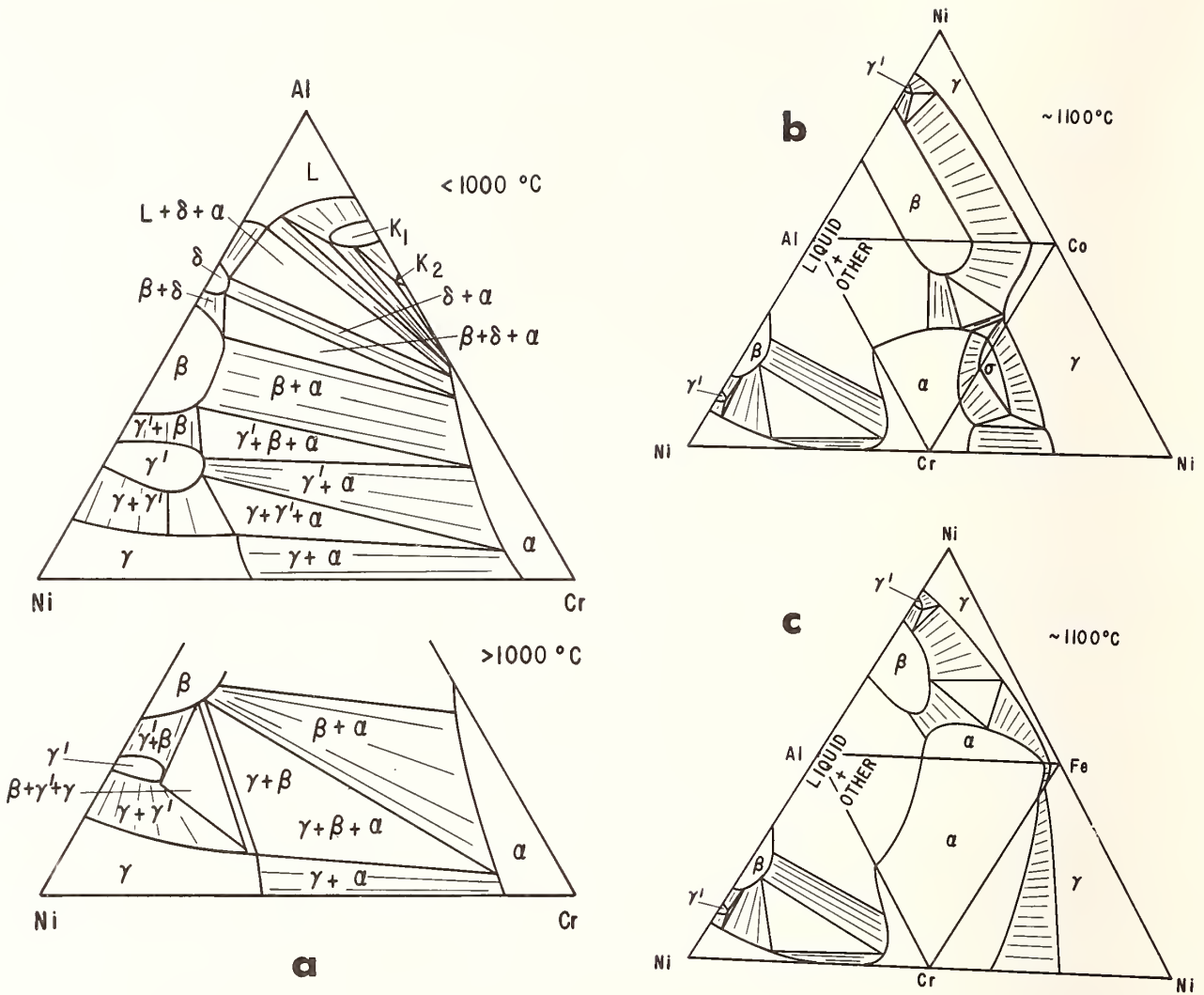


Fig. 2: Phase diagrams for coatings on superalloys; (a) Ni-Cr-Al, (b) Ni-Cr-Al-Co, (c) Ni-Cr-Al-Fe.



APPLICATION OF THE SCANNING ELECTRON MICROSCOPE TO THE STUDY OF HIGH TEMPERATURE OXIDE PHASE EQUILIBRIA

L. P. Cook and D. B. Minor

National Bureau of Standards
Institute for Materials Research
Washington, D. C. 20234

INTRODUCTION

Instrumentation

An early scanning electron microscope (1) was built several years before invention of the electron microprobe x-ray analyzer by Castaing (2), yet the latter was the first type of analytical electron beam instrument available commercially in a fully developed form. In the last ten years, electron microbeam instrumentation has evolved rapidly and the distinction between microprobes and SEM's has in many respects vanished. It is convenient to differentiate modern electron microprobes by the presence of wavelength dispersive spectrometers and high precision stages. High resolution SEM's usually employ energy dispersive x-ray analysis (EDX) systems, more convenient for the rapid accumulation of spectral information. Since the work of Fitzgerald *et al.* (3), EDX resolution and associated software have developed to the point where quantitative analyses are possible if proper operating conditions and data reduction methods are employed (4).

Reviews of basic microprobe and SEM instrumentation are given by Fitzgerald (5), Wells (6) and others. EDX instrumentation and operation are discussed by Lifshin *et al.* (7) and Gedcke (8).

Application

Microchemical characterization aids significantly in the determination of phase diagrams (9). Examples of electron microprobe application to the study of oxide phase equilibria are numerous (see for example, 10). However as Keil (11) notes, use of classical microprobe methods in the study of fine grained experimental products has been limited by the relatively poor spatial resolution of x-ray information (1.0 to 0.1 μm).

One of the first SEM uses in the study of ceramic systems is the work of Thornley and Cartz (12); subsequent SEM studies of ceramic materials have been published at an increasing rate (13). Although reviews have been written on SEM application to ceramic studies (see for example, 14), SEM potential in phase equilibrium investigations has not been emphasized. We will demonstrate in this paper how the SEM/EDX combination is a particularly powerful tool in the study of oxide phase equilibria, where otherwise unobtainable information can be gathered for reactants. Examples given below are primarily from experiments made using the quenching technique, but SEM/EDX has application to the results of other methods used in the determination of oxide phase diagrams such as DTA, TGA, and the various hydrothermal, effusion, diffusion and electrochemical techniques.

EXAMINATION OF EXPERIMENTAL PRODUCTS

Subsolidus Studies

While much of the characterization of reactions in the solid state must be done by x-ray diffractometry, SEM studies of polished surfaces can sometimes detect small amounts of a second phase not present in large enough quantities to give an easily detectable x-ray powder diffraction pattern. Moreover SEM examination in such cases can give an indication of textural relationships. Figure 1 shows an iron $K\alpha$ x-ray map of Fe_2O_3 exsolution laths in a (Mg, Al, Fe)-spinel matrix. These laths are at the limit of x-ray spatial resolution and x-ray maps must be supplemented with the SEM image (Figure 2) for proper interpretation. It should be noted that surface preparation was of utmost importance in this example. The difference in atomic number is the main contrast mechanism when examining smooth polished surfaces such as this and because backscattered electrons are involved, resolution is correspondingly less, of the order of 30 nm (15) as opposed to 7 nm or better for high resolution secondary electron images.

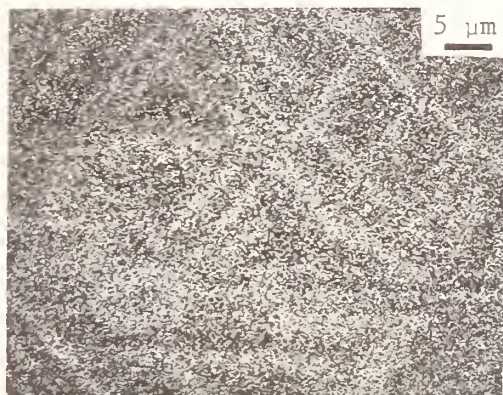


Figure 1. Fe $K\alpha$ x-ray map of polished surface showing exsolution of Fe_2O_3 in (Mg,Al,Fe)-spinel (see Figure 2).

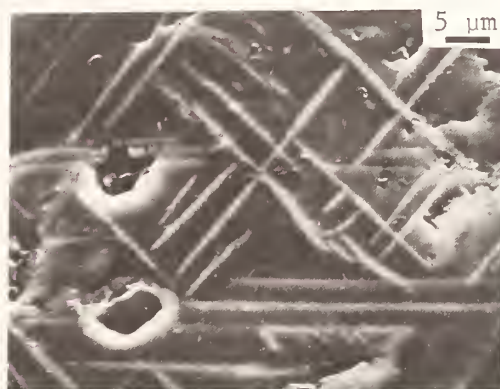


Figure 2. Secondary electron image of area corresponding to Figure 1. 20 kV, 45° tilt.

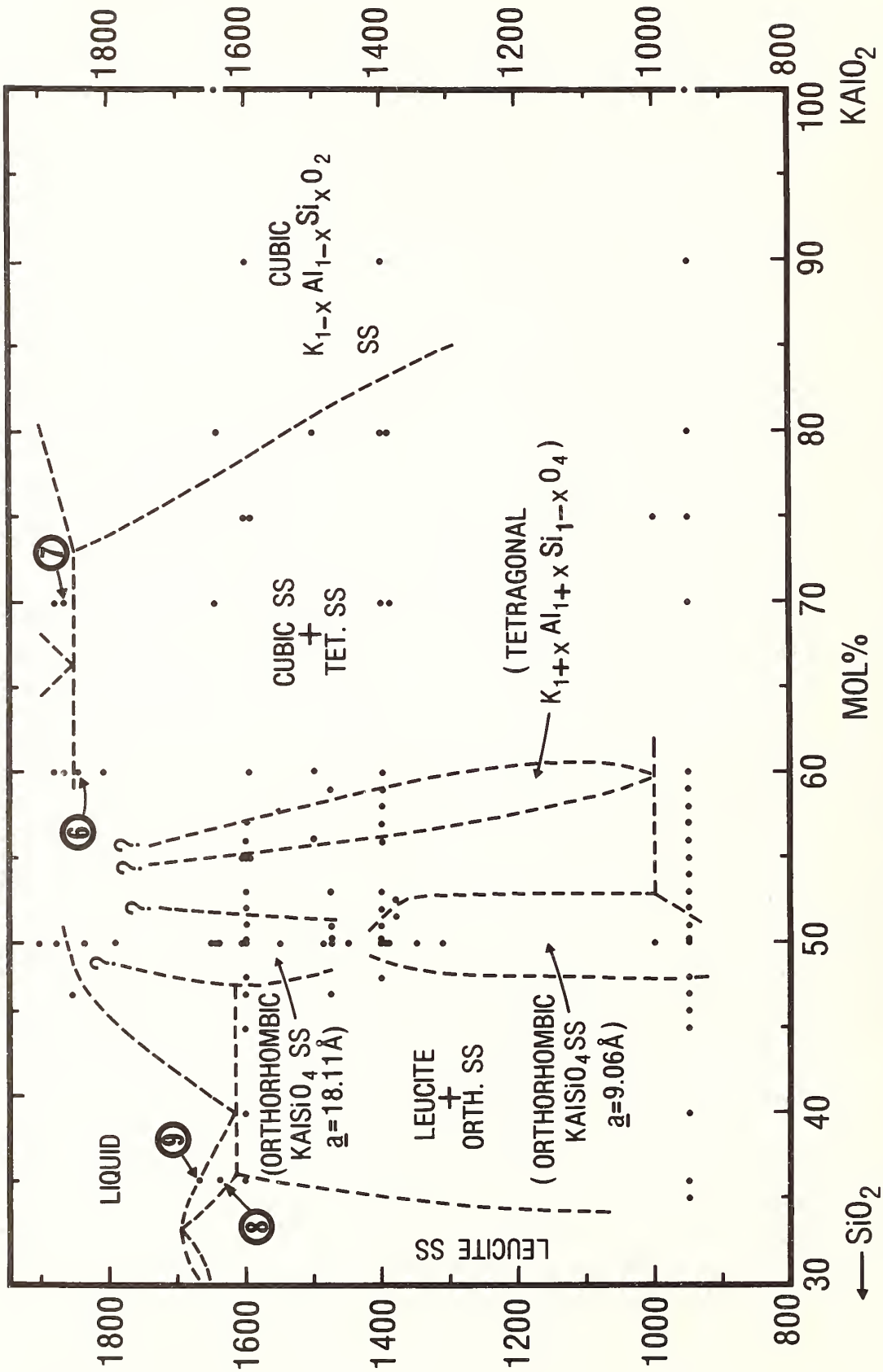


Figure 3. Hypothetical phase diagram of the $KAlO_2$ - SiO_2 system, showing some of the experiments examined with the SEM. Numbers refer to Figures in which micrographs of experimental products are shown.

In some cases, especially where solid-liquid and solid-gas equilibria are involved high resolution secondary electron images allow one to determine the type of solid phase present, and the reaction which is occurring, on the basis of crystal morphology (16, 17). If morphologies are distinctive this can be done in situ for sparse crystals which could not be investigated by other means.

We have made particular use of SEM/EDX methods to correlate the results of flux syntheses with quench experiments in the system $\text{KAlO}_2\text{-SiO}_2$ (Figure 3). Flux-grown single crystals were used for x-ray diffraction precession analyses to establish the unit cell and space group of the solids appearing on the phase diagram, then mounted on a carbon planchet using the technique described by Brown and Teetsov (18). Semi-quantitative analyses were performed for single crystals of orthorhombic and tetragonal (Figure 4) phases, by normalizing and comparing intensities with those from standard glasses (a typical EDX spectrum is shown in Figure 5). During analysis the electron beam was rapidly rastered over an area $100\ \mu\text{m} \times 100\ \mu\text{m}$ to prevent specimen charging and compositional changes. The SEM goniometer stage was of particular use in selecting an uncontaminated flat face on the crystal and orienting it as precisely as possible for analysis. For both tetragonal and orthorhombic phases, semi-quantitative analyses of single crystals (excluding fluorine) allowed us to state that: 1) single crystals plot on or near the join $\text{KAlO}_2\text{-SiO}_2$; 2) they plot close to or within the phase regions outlined by quench experiments.



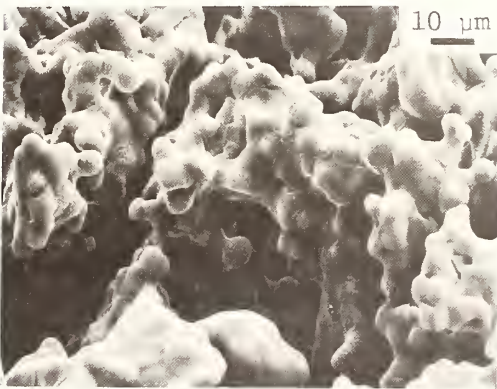
Figure 4. Single crystal of flux-grown tetragonal $\text{K}_{1+x}\text{Al}_{1+x}\text{Si}_{1-x}\text{O}_4$. Note flat faces suitable for semi-quantitative analysis. 20 kV, 0° tilt.



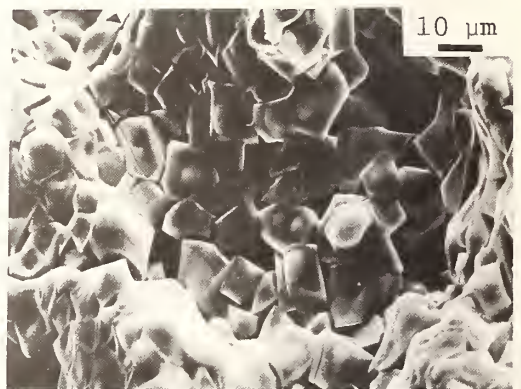
Figure 5. A typical EDX spectrum of material in Figure 4.

Solidus Studies

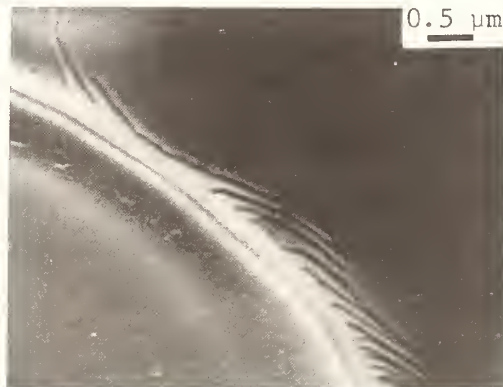
For many high temperature applications equilibria may be very complicated and yet a detailed phase diagram is needed. Such systems may have steeply dipping liquidii and closely spaced compounds. A major problem then comes in interpreting the character of quench experiments: does sintering result from grain boundary growth and annealing, or does it result from small amounts of quenched equilibrium melt, recrystallized equilibrium melt, or some combination thereof? This problem has been approached with the SEM in our preliminary work on the system $KAlO_2-SiO_2$. The overall appearance of both specimens shown in Figures 6 and 7 suggested melting when results were examined with the binocular microscope. Light optical examination of immersion mounts also proved inconclusive, and so both were subjected to SEM examination at high magnification. In the $(KAlO_2)_{60}(SiO_2)_{40}$ specimen (Figure 6) the melting was apparently a transitory phenomenon, perhaps spurred by the presence of a non-equilibrium solid assemblage or by the requirement to minimize surface free energy. Grain boundaries appear sharp and equant throughout the sample (Figure 6-c), and no areas suggestive of melt segregation can be found. The recrystallization was more intense in some areas of the sample (Figure 6-b) than others (Figure 6-a), suggesting limited migration of a metastable melt during recrystallization.



6a) Weakly sintered area.



6b) Highly sintered area.



6c) High magnification micrograph of grain boundary in (a). Note sharpness compared to Figure 7-c.

Figure 6. Solidus studies - experiment below solidus. $K_{60}S_{40}$, 1850°C. Micrographs taken at 20 kV, 45° tilt.

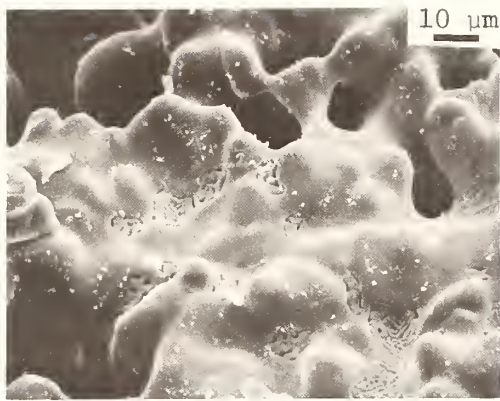
By contrast, the $(\text{KAlO}_2)_{70}(\text{SiO}_2)_{30}$ sample (Figure 7) contains fine grained low-lying areas between larger grains (Figure 7-a) suggestive of recrystallized equilibrium melt (Figure 7-b). The grain boundary in Figure 7-c shows what appears to be an intergranular phase. Owing to the difficulty of temperature control with the induction furnace used, this run was of short duration at maximum temperature attained and any melt formed may not have had time to segregate completely into larger volumes. Alternatively, since the grain boundaries in Figure 7-c were close to the area of melt in Figure 7-b, we may be looking at the effect of capillary action.

The $\text{K}_{60}\text{S}_{40}$ example above is similar in some respects to the recrystallization of MgAl_2O_4 observed by Daw and Nicholson (19). Froschauer and Fulrath (20) have observed formation of a liquid phase at grain boundaries during sintering of particles on a high temperature stage in the SEM.

Liquidus Studies

In many instances there are advantages in looking at the undisturbed quench specimens, as removed from the capsule. Figures 8-a, b are micrographs of the surface of a sample of $(\text{KAlO}_2)_{36}(\text{SiO}_2)_{64}$ heated at 1641°C . Dendritic outlines protruding into areas of low relief suggest non-equilibrium crystallization from the melt during quench. Also present on the surface of the specimen are coarser crystals having well developed sharp boundaries and roughly equant shapes, interpreted as formed under equilibrium conditions. In contrast, the surface of a sample of $(\text{KAlO}_2)_{36}(\text{SiO}_2)_{64}$ heated at 1658°C , that was completely melted, is largely featureless (not shown).

As shown in Figures 8-c, d the manner in which glass fractures allows the detection of crystalline phases on fracture surfaces with the SEM. For the KAlO_2 - SiO_2 experiments mentioned above, conclusions drawn from outer surfaces and fracture surfaces are similar. Coarser grains, presumably formed at equilibrium are conspicuous because of the regular, structurally controlled features visible on fracture surfaces (Figure 8-c). The fine-grained quench structures are less apparent, but nonetheless distinguishable (Figure 8-d). The completely melted sample (Figure 9) shows only a smooth conchoidal fracture surface.



7a) Micrograph showing rounded grains separated by voids and areas with fine structure.

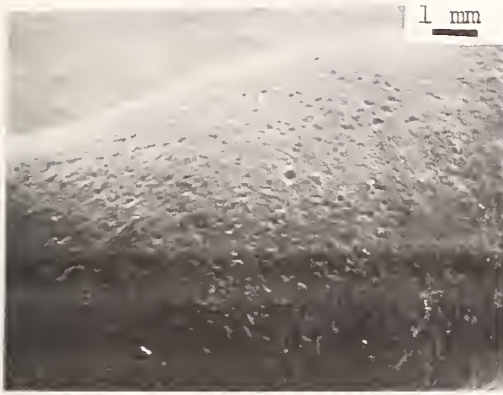


7b) Detail of (a). Dendritic texture is interpreted as re-crystallized melt.



7c) High magnification micrograph of area in upper left of (b). Note what is interpreted as film of quenched melt along grain boundaries.

Figure 7. Solidus studies - experiment above solidus. $K_{70}S_{30}$, 1880°C. Micrographs taken at 20 kV, 45° tilt.



8a) Low magnification micrograph of outer surface of experiment.



8b) High magnification detail of (a). Dendritic texture suggests growth from melt upon quench. Grains at top and right may represent solids in equilibrium with melt.



8c) Fracture surface. Relatively large crystal (corrugated surface) in glass, interpreted as formed at equilibrium.



8d) Fracture surface. Fine grained aggregate of crystallites in glass, interpreted as forming on the quench.

Figure 8. Liquidus studies - experiment below the liquidus. $K_{36}S_{64}$, 1641°C. Micrographs taken at 20 kV, 45° tilt.



Figure 9. Liquidus studies - experiment above liquidus. $K_{36}S_{64}$, 1658°C. Fracture surface, no evidence of crystalline phases in glass. 20 kV, 45° tilt.

CONCLUSIONS

The scanning electron microscope can be applied to the study of high temperature oxide phase equilibria for examination of experimental results. Many of the functions of conventional light microscopy in the analysis of phase equilibria products can be performed, at higher magnification, and without disrupting the specimen. Correlation between single crystal syntheses and quench experiments is facilitated. Precise determination of solidus boundaries in complex systems using the quenching technique is made more feasible. Perhaps the most important advantage of the SEM/EDX technique is the presentation of textural relations between phases which are not as conveniently studied at high magnification with the immersion method of light microscopy. This advantage arises not only because of the superior resolution of the SEM, but also because of its much greater depth of focus.

ACKNOWLEDGEMENTS

The authors wish to thank Dr. R. S. Roth for stimulating discussion which has led to preparation of this paper. Dr. T. Negas kindly supplied the micrographs in Figures 1 and 2. J. Waring and C. Harding performed the high temperature experiments. E. Farabaugh and Dr. D. Newbury improved the manuscript through their critical reviews.

REFERENCES

1. V. K. Zworykin, J. Hillier, and R. L. Snyder, *ASTM Bull.* 117, 15 (1942)
2. R. Castaing, Ph.D. Thesis, Univ. of Paris, 1951.
3. R. Fitzgerald, K. Keil and K.F.J. Heinrich, *Science* 159, 528 (1968).

4. C. E. Fiori, R. L. Myklebust and K.F.J. Heinrich, *Microbeam Anal. Soc.*, Proc. 11th Ann. Conf. Miami Beach, 1976, Paper 12.
5. R. Fitzgerald, in "Microprobe Analysis", C. A. Andersen, Ed., Wiley-Interscience, New York, 1973, pp 1-51.
6. O. C. Wells, "Scanning Electron Microscopy," McGraw-Hill, New York, 1974, 421 p.
7. E. Lifshin, M. F. Ciccarelli, and R. B. Bolon, in "Practical Scanning Electron Microscopy", J. I. Goldstein and H. Yakowitz, Eds., Plenum Press, New York, 1975, pp. 263-297.
8. D. A. Gedcke, in "Quantitative Scanning Electron Microscopy," D. B. Holt, M. D. Muir, P. R. Grant and I. M. Boswara, Eds., Academic Press, New York, 1974, pp. 403-450.
9. A. D. Romig, Jr., and J. I. Goldstein, Workshop on Applications of Phase Diagrams in Metallurgy and Ceramics. National Bur. Standards, Gaithersburg, MD, January 1977, Paper MPSII-7.
10. K. L. Keester and W. B. White, *J. Amer. Ceram. Soc.* 53, 39 (1970).
11. K. Keil, in "Microprobe Analysis", C. A. Andersen, Ed., Wiley-Interscience, New York, 1973, pp. 189-239.
12. R. R. M. Thornley and L. Cartz, *J. Amer. Ceram. Soc.* 45, 425 (1962).
13. V. E. Johnson, in "Scanning Electron Microscopy/1974", O. Johari and I. Corvin, Eds., IIT Research Inst., Chicago, 1974, pp. 763-812.
14. E. W. White and R. Roy, in "Scanning Electron Microscopy/1968", O. Johari, Ed., IIT Research Inst., Chicago, 1968, pp. 89-94.
15. O. C. Wells, in "Scanning Electron Microscopy/1974", O. Johari and I. Corvin, Eds., IIT Research Inst., Chicago, 1974, pp. 361-368.
16. S. T. Liu, G. H. Nancollas and E. A. Gasiecki, *J. Crystal Growth* 33, 11 (1976).
17. S. Chatterji and J. W. Jeffrey, *Nature* 209, 1233 (1966).
18. J. A. Brown and A. Teetsov, in "Scanning Electron Microscopy/1976", O. Johari, Ed., IIT Research Inst., Chicago, pp. 385-392.
19. J. D. Daw and P. S. Nicholson, *J. Amer. Ceram. Soc.* 58, 109 (1975).
20. L. Froschauer and K. M. Fulrath, *J. Mater. Sci.* 10, 2146 (1975).



Hyperfine Techniques and the Determination of Phase Diagrams

R. C. Reno*

Department of Physics

University of Maryland, Baltimore County

Baltimore, MD 21228

and

L. J. Swartzendruber, G. C. Carter and L. H. Bennett

Institute for Materials Research

National Bureau of Standards

Washington, DC 20234

I. Introduction

Within any material there exist internal electric and magnetic fields which are produced by the positively charged atomic nuclei and the negatively charged core and valence electrons. The fields depend upon the arrangement of these constituents (e.g., spatial ordering of the ion cores) as well as interactions between the constituents (e.g., chemical bonding and electron exchange effects). Of particular interest are the internal fields present at the positions of the atomic nuclei. These "hyperfine" fields interact with the nuclei and shift the discrete energy levels, allowing nuclear transitions which can be observed by a number of techniques¹.

This review will discuss three well-established techniques for measuring the nuclear hyperfine interaction - nuclear magnetic resonance (NMR)^{2,3}, the Mössbauer effect (ME)² and the perturbed angular correlation of gamma rays (PAC)⁴. It will discuss how the hyperfine interaction is influenced by the chemical, magnetic, and structural properties of the material involved and will illustrate how each of the above techniques can be used to provide information useful in constructing phase diagrams.

II. Description of the Techniques

All three of the above hyperfine techniques detect a change in the nuclear energy levels of the atom in the material studied by observing transitions between levels.

The ⁵⁷Fe nucleus can best illustrate the similarities and differences in the three techniques. In addition to the ground state, ⁵⁷Fe has two excited nuclear energy levels as shown in Fig. 1. The ground state

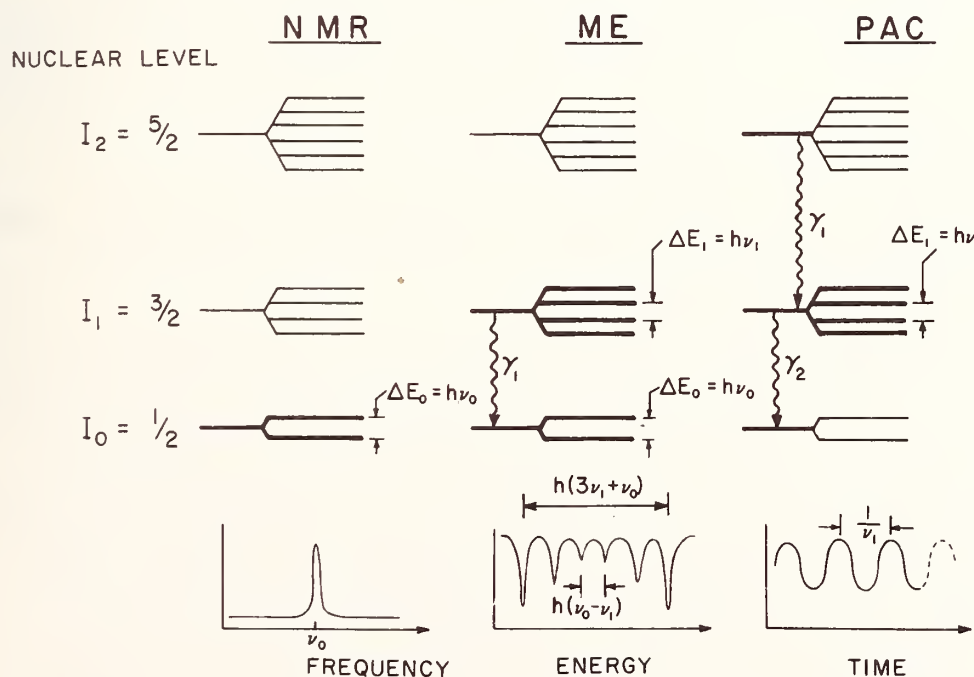


Fig. 1. An example of the energy levels and transitions used in nuclear magnetic resonance (NMR), Mossbauer effect (ME), and perturbed angular correlation experiments. The nuclear spins and energy levels shown are those appropriate for an ⁵⁷Fe nucleus in the presence of a magnetic field. The types of resonances observed for each method are also illustrated.

nucleus has a spin of $1/2$ while the first and second excited states have spins $3/2$ and $5/2$, respectively. When ^{57}Fe nuclei interact with a hyperfine field, these levels will be split into discrete sublevels, the number and spacing of which depend on the type and strength of the field. If, for example, a static magnetic field, H , acts on the nucleus, the levels will be split in accordance with the well known Zeeman effect, as shown in the figure. The degree of splitting of the ground state will differ from that of the excited states since each state has a different magnetic moment, μ . It will be sufficient to consider only the ground state splitting ($\Delta E_0 = \mu_0 H$) and the first excited state splitting ($\Delta E_1 = \mu_1 H$).

In a nuclear magnetic resonance experiment, the nuclei of interest are those in the ground state (the lowest energy configuration), where $\Delta E_0 = \mu_0 H$ is small compared to the energy difference between ground and first excited state. The presence of electromagnetic radiation will promote transitions between the two sublevels of the ground state. A resonant absorption of energy is observed when the frequency, ν_0 , satisfies the condition $h\nu_0 = \mu_0 H$ where h is Planck's constant, and ν_0 is on the order of radio frequencies.

In the Mössbauer effect, one observes transitions between the first excited state and the ground state. The magnetic hyperfine field will cause Zeeman splittings in both of these states and therefore eight (4×2) transitions could occur between the excited state and the ground state. Of these eight, only six are allowed by quantum mechanical selection rules and they are observed by measuring the six energies necessary to

excite nuclei from their ground state to the first excited state. The excitation energies are measured by doppler shifting the exciting radiation (14 keV gamma rays) until a recoilless absorption occurs and a resonant dip appears in gamma ray transmission through the sample. The positions of the six resonant energies depend upon ΔE_0 and ΔE_1 , both of which depend upon the magnetic field strength.

In perturbed angular correlation experiments, the nucleus is prepared in the second excited state and is then allowed to decay spontaneously to the ground state by the two step process, $I_2 \xrightarrow{\gamma_1} I_1 \xrightarrow{\gamma_2} I_0$. This involves the emission of two gamma rays γ_1 , and γ_2 in time coincidence, the delay between emissions being on the order of 10^{-7} sec. The presence of a hyperfine field H at the nucleus during this time interval will cause the coincidence rate to vary sinusoidally in time with a period T equal to $1/\nu_1$. This is the Larmor period - the time necessary for the nuclear spin to precess once about the field direction - and depends upon the field strength since $1/\nu_1 = h/\mu_1 H$.

Thus, all three techniques sense the splitting in one or more nuclear levels produced by interaction with the hyperfine field. While the above discussion used a *magnetic* field for illustrative purposes, the same type of effects will be observed for the interactions between the nuclear quadrupole moment and *electric field gradients*. Magnetic fields may be either externally applied, or internally generated by the presence of permanent or induced magnetic moments. Electric field gradients of sufficient magnitude to give observable effects cannot be externally applied, and are present only when the nucleus is in a non-cubic environment.

Although the information obtained by all three techniques is similar, the mode of detection varies considerably and each technique has limitations

as well as advantages. Table I summarizes the salient differences between NMR, ME, and PAC.

III. Applications

The hyperfine field at an atom in a material depends on the crystal structure in the region of the atom and on the electronic structure of the atom and its neighbors. Common types of hyperfine interactions include electric field gradients due to non-cubic crystal symmetry, isomer and Knight shifts due to electron density changes and magnetic fields due to cooperative electron spin effects (magnetism). The hyperfine field often changes measurably when the material changes phase. This property can provide a signature by which to identify each phase. Furthermore, two-phase mixtures can be analyzed with the three presently described hyperfine techniques, using a lever rule which becomes enhanced due to the preferential concentration of the field-sensing atoms in one phase. This "enhanced" lever rule⁵ can be expressed for an A-B alloy with an α and β phase, as

$$R = \frac{C_{\alpha} f_{\alpha}}{C_{\beta} f_{\beta}}$$

where R is the ratio of the intensity of the NMR, ME, or PAC signal from the B atoms in the α phase to the intensity from those in the β phase, C_{α} and C_{β} are the concentration of B atoms in the α and β phase, respectively, and f_{α} and f_{β} are the fractions of α phase and β phases present, as given by the ordinary lever rule. When close to the α -phase boundary, the "enhancement" of the signal from the minority β phase arises from the high concentration of B atoms in the β phase. An example of the signals obtained from the pseudo-binary system $\text{AuAl}_2\text{-AuIn}_2$ is shown in Fig. 2.

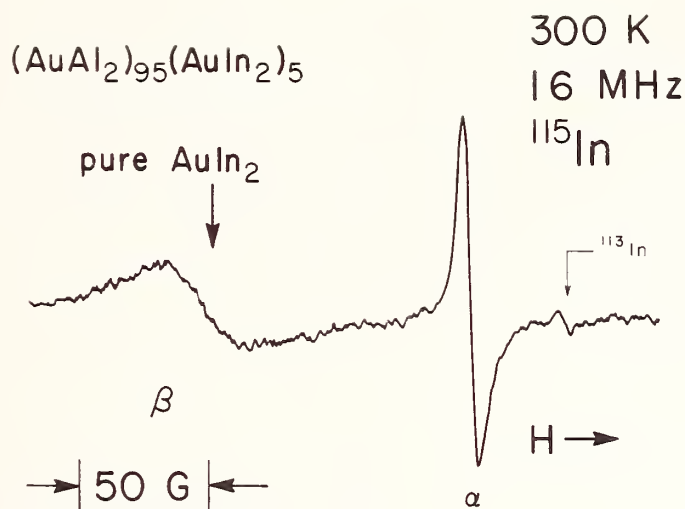


Fig. 2. ^{115}In NMR spectrum for the alloy $(\text{AuAl}_2)_{95}(\text{AuIn}_2)_5$, showing a separate resonance for the indium nuclei in each of the two phases. The separation of the two resonances is due to the NMR metallic shift (known as the Knight Shift) caused by different hyperfine fields at the In sites in the two different phases. From this resonance, the solubility of AuIn_2 in AuAl_2 (at the homogenization temperature of 500°C) can be obtained very accurately (from ref. 5).

NMR contributions to phase determinations include measurements of: the solubility of AuAl_2 in AuIn_2 ⁶; liquid-solid phase equilibria in Cu-Te alloys⁷; phase changes in La, Nb and Ta hydrides⁸; phase identification in Na-Tl alloys⁹; and Hg concentration in Cd-Hg alloys¹⁰. The NMR measurements on Cu-Te alloys⁷ are extremely useful since one phase is liquid and some alternative techniques, such as x-ray diffraction, cannot be utilized. The measurements on Na-Tl⁹ provided evidence that an ordered compound NaTl_2 exists with the same crystal structure as NaTl - a fact hard to obtain from x-ray analysis alone since Na has a much smaller scattering factor than Tl and both lattices have the same arrangements of Tl atoms.

Mössbauer measurements of multi-phase systems include: detection of microprecipitates in Fe-Cu-Ni alloys¹¹, the observation of a metastable (θ) phase in Fe-Ti¹², a study of phase boundaries in TiFe-H¹³, an examination of phase changes during the sintering of β -Fe₅Ge₃¹⁴; and studies of surface-induced changes in supported Pt and Pd particles as small as 3nm¹⁵. Some spectra of TiFe-H are shown in Fig. 3. The Mössbauer

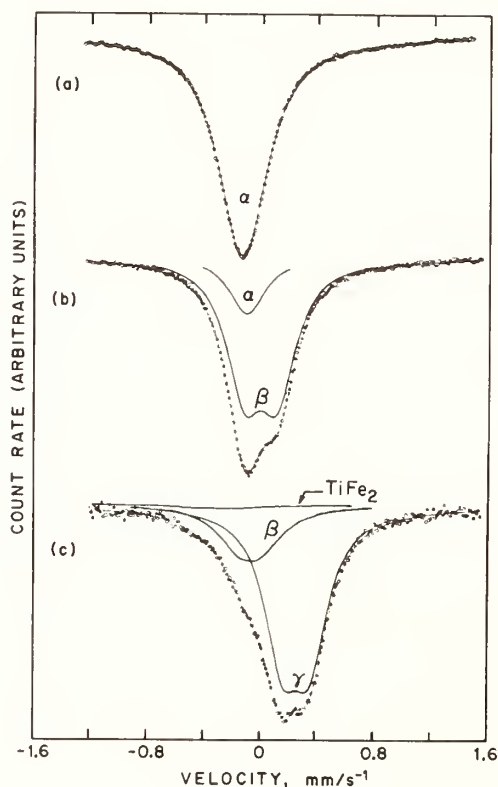


Fig. 3. Room temperature Mössbauer absorption spectra for TiFeH_x. The line through the data points is a least-squares fit which is the sum of the contributions from the individual phases. (a) x = 0.1, 100% α phase. (b) x = 0.9, 19% α phase and 81% β phase. (c) x = 1.7, which consists of 23% β phase, 75% γ phase, and 2% of spurious TiFe₂. (After Ref. 13).

measurements on Fe-Cu-Ni alloys¹¹ indicated the maximum solubility of Fe in a Cu-Ni alloy and showed that excess Fe formed precipitates too small to be observed by conventional techniques. The presence of these precipitates could be correlated with increased corrosion of the alloy in saline environments. The measurements on Fe-Ge¹⁴ illustrate the kinetics involved in the transformation of Fe and Ge to β -Fe₅Ge₃. During the sintering

process the following phases were observed: Fe, γ -FeGe, ϵ -Fe₃Ge, η -Fe_{1.4}Ge and β -Fe₅Ge₃. The η phase has not been observed unambiguously by x-ray diffraction but clearly shows up in Mössbauer spectroscopy.

Perturbed angular correlation measurements of multi-phase systems are less numerous than those done by NMR and Mossbauer effect, primarily because the sample under study must be made radioactive. Studies do exist, however, on Ni-Hf alloys¹⁶, Zr-Hf hydrides¹⁷, and In-Bi liquid alloys¹⁸. The data on In-Bi liquid alloys seem to indicate that some ordering takes place in the liquid phase since liquids around the composition In₂Bi show hyperfine interactions characteristics of an ordered array of atoms. NMR studies have also given qualitative evidence for the existence of In₂Bi groupings in liquid In-Bi alloys¹⁹.

In addition to hyperfine studies which detect two or more phases simultaneously, there exist a wide range of NMR, Mössbauer and PAC measurements that are concerned with single phase materials that undergo first or second order phase transitions. Numerous hyperfine measurements have been done, for example, on the transition from ferromagnetic (or anti-ferromagnetic) to paramagnetic behavior in pure, single phase materials²⁰⁻²². Hyperfine techniques have also been used to study structural phase transitions^{23,24} and ferroelectric transitions²⁵⁻²⁷.

References

*Also a consultant, Alloy Physics Section, Institute for Materials Research, National Bureau of Standards.

1. e.g. Hyperfine Interactions, ed. by A. J. Freeman and R. B. Frankel, (Academic Press, New York, 1967).
2. I. D. Weisman, L. J. Swartzendruber, and L. H. Bennett, Nuclear Resonances in Metals: Nuclear Magnetic Resonance and Mossbauer Effect, chapter VI-2, in Techniques of Metals Research, ed. by R. F. Bunshah (John Wiley & Sons, 1973).
3. G. C. Carter, D. J. Kahan and L. H. Bennett, Metallic Shifts in NMR, *Progress in Materials Science* 20, 1 (1976).
4. M. Frauenfelder and R. M. Steffen, in Alpha-, Beta- and Gamma-Ray Spectroscopy, Vol. 2, ed. by K. Seigbahn (North Holland Pub. Co., Amsterdam, 1966). p. 997.
5. L. H. Bennett and G. C. Carter, *Metallurgical Transactions* 2, 3079 (1971).
6. G. C. Carter, I. D. Weisman, L. H. Bennett and R. E. Watson, *Phys. Rev. B* 5, 3621 (1972).
7. W. W. Warren, Charge Transfer/Electronic Structure of Alloys, ed. by L. H. Bennett and R. H. Willens (Metallurgical Society of America, New York, 1974) p. 223.
8. D. Zamir and R. M. Cotts, *Phys. Rev.* 134, A666 (1964); D. S. Schreiber and R. M. Cotts, *Phys. Rev.* 131, 1118 (1963); B. Pedersen, T. Krogdahl and O. E. Stokkeland, *J. Chem. Phys.* 42, 72 (1965).
9. L. H. Bennett, *Acta. Met.* 14, 997 (1966).

10. V. V. Zhukov, I. D. Weisman and L. H. Bennett, *J. of Research* 77A, 713 (1973).
11. L. H. Bennett and L. J. Swartzendruber, *Acta. Met.* 18, 485 (1970).
12. M. M. Stupel, M. Ron and B. Z. Weiss, *Journal de Physique, Colloque C6*, 35, 483 (1974).
13. L. J. Swartzendruber, L. H. Bennett and R. E. Watson, *J. Phys. F: Metal Phys.* 6, L331 (1976).
14. D. Eliezer, S. Nadiv and M. Ron, *Journal de Physique, Colloque C6*, 35, 477 (1974).
15. C. H. Bartholomew and M. Boudart, *J. Catalysis* 29, 278 (1973); R. L. Garten and D. F. Ollis, *J. Catalysis* 35, 232 (1974).
16. E. Gerdau, H. Winkler, W. Gebert, B. Giese and J. Braunsfurth, *Hyperfine Int.* 1, 459 (1976).
17. R. L. Rasera, University of Maryland, Baltimore County, private communication.
18. S. Tamaki, Y. Tsuchiya, A. Furusawa and H. Okazaki, *J. Phys. F: Metal Phys.* 6, 2009 (1976).
19. G. A. Styles, *Adv. Phys.* 16, 275 (1967).
20. NMR studies of magnetic phase transitions include:
P. Heller, *Phys. Rev.* 146, 403 (1966); E. Sawatsky and M. Bloom, *Canad. J. Phys.* 42, 647 (1964); S. D. Senturia and G. B. Benedek, *Phys. Rev. Letters* 17, 475 (1966); A. M. Gottlieb and P. Heller, *Phys. Rev.* B3, 3615 (1971); P. J. Segranean, W. G. Clark, Y. Chabre, and G. C. Carter, *J. Phys. F: Metal Phys.* 6, 453 (1976).

21. Mossbauer studies of magnetic phase transitions include:
G. K. Wertheim, H. J. Guggenheim and D. N. E. Buchanan, Phys. Rev. 169, 465 (1968); H. C. Bensi, R. C. Reno, C. Hohenemser, R. Lyons and C. Abeledo, Phys. Rev. B6, 4266 (1972); R. S. Preston, J. Appl. Phys. 39, 1231 (1968); D. G. Howard, B. D. Dunlap and J. G. Dash, Phys. Rev. Letters 15, 628 (1965); M. A. Kobeissi and C. Hohenemser, AIP Conf. Proc. 29, 497 (1976).
22. PAC Studies of magnetic phase transitions include:
R. C. Reno and C. Hohenemser, Phys. Rev. Letters 25, 1007 (1970);
R. M. Suter and C. Hohenemser, AIP Conf. Proc. 29, 493 (1976);
J. L. Oddou, J. Berthier and P. Peretto, Phys. Letters 45A, 445 (1973).
23. D. N. Pipkorn, C. K. Edge, P. Debrunner, G. dePasquali, H. G. Drickamer and H. Frauenfelder, Phys. Rev. 135, A 1604, (1964).
24. T. A. Kovats and J. C. Walker, Phys. Rev. 181, 610 (1969).
25. PAC papers include:
H. V. Einsiedel and S. S. Rosenblum, Phys. Stat. Sol. (b) 65, K5 (1974); S. P. Solov'ev, V. V. Zakurkin, Z. I. Shapiro, V. A. Klyucharev, V. I. Bozhko and A. P. Gaidamaka, Ferroelectrics (GB) 8, 543 (1974).
26. Mossbauer papers include:
G. D. Sultanov, F. A. Miriskli and I. H. Ismailzade, Ferroelectrics (GB) 8, 539 (1974); E. A. Samuel and V. S. Sundaram, Phys. Letters 47A, 421 (1974).
27. NMR papers include:
J. Y. Nicholson and J. F. Soest, J. Chem. Phys. 60, 715 (1974);
D. Slotfeldt-Ellingsen and B. Pedersen, Phys. Stat. Sol. (a) 24 191 (1974).

Table I: Comparison of Hyperfine Techniques

Property:	NMR	ME	PAC
Sensitive Chemical species	Most elements in the periodic table are suitable for NMR	Fe, Sn, Sb are routine; Ge, Zn, Dy, Au and several others can be done under specialized conditions	Hf, Cd, Sc, In, Re, Rh, Ru, Fe, Pd, Tc and Cs are routine; Dy, Yb, Lu, F, Hg, Pb, Te and others can be done under specialized conditions
Source and Detecting apparatus	RF generation & detection, signal averaging, recorder, static magnetic field	Gamma ray source, non-radioactive absorber, gamma ray counting	Radioactive sample, $\gamma\gamma$ coincidence spectroscopy
Sample	Stable elements	Stable elements (absorber expt.) or radioactive tracers (source expt.)	Radioactive tracers
Number of sensitive nuclei needed	$\sim 10^{21}$	$\sim 10^{15}$ (source expt.) $\sim 10^{20}$ (absorber expt.)	$\sim 10^{12}$
Physical form of sample	solids, liquids	solids only	solids, liquids



Experimental Determination of Phase Diagrams with the Electron Microprobe and Scanning Transmission Electron Microscope

A. D. Romig, Jr. and J. I. Goldstein
Department of Metallurgy and Materials Science
Lehigh University, Bethlehem, PA 18015

ABSTRACT

Within the past dozen years the electron microprobe (EMP) has proven itself a valuable tool in the determination of phase diagrams (solid phase regions). A literature survey indicates that over thirty (30) metallic systems have been determined with this instrument.

An important advantage of this technique is that one can determine equilibrium tie lines even when the bulk phases themselves are not in equilibrium. This advantage is best realized when one is considering a system where diffusion rates are so slow that the bulk equilibrium condition cannot be reached in a reasonable time period, or where the phase diagram contains a metastable phase that will decompose if heat treatments long enough to produce homogeneous phases are used.

Several factors affect the accuracy of the EMP measurements:

(1) spatial resolution; (2) X-ray absorption; and (3) X-ray fluorescence. Even under optimum conditions it is not possible to generate X-rays from a volume with a diameter less than $1\ \mu\text{m}$ and interface compositions must be determined by extrapolation to the interface position. This is a reasonable procedure, unless the concentration gradient is too steep. The use of the EMP technique is illustrated by its application to the Fe-Ni-Co and Fe-Ni-C systems.

The newly developed scanning transmission electron microscope (STEM) will allow X-ray excitation from regions less than $0.10\ \mu\text{m}$ in diameter. The technique requires thin foils which are transparent to the incident electron beam (typically 80/100 kV). The use of thin foils and high excitation voltages usually eliminates the fluorescence and absorption problems present in microprobe analysis, thus permitting the application of a relatively simple matrix correction technique. The STEM methods have now been developed to the point where phase diagram determination is possible. Measurements of the Fe-Ni-Co system using this technique are presented and agreement with the accepted diagram is demonstrated.

Introduction

The experimental determination of solubility limits and tie lines in the solid regions of multicomponent phase diagrams is difficult. The phases which are present are often small, and sometimes the bulk specimen is not even equilibrated. In addition the necessary heat treatment cycles are usually lengthy and a large number of specimens are usually required. Many experimental techniques have been employed including X-ray diffraction, metallography and differential thermal analysis. All of these techniques require well equilibrated samples for analysis. The electron microprobe (EMP) has been used since the mid-1960's to determine the composition of the equilibrated phases directly. One specific advantage of the EMP technique is the spatial resolution which approaches 1 μm . This technique enables one to obtain tie line compositions directly, even in alloys with three or more components. Composition-distance profiles can be used in special cases even when bulk equilibration has not been attained.

The purpose of this paper is to describe the use of the EMP in the determination of multicomponent phase diagrams. Heat treatment cycles, EMP spatial resolution, and the accuracy of tie line measurements will be discussed. Examples of the use of the EMP in determining isothermal sections of ternary phase diagrams will also be discussed. In addition a description of the newly developed scanning transmission electron microscopy (STEM) technique for phase diagram analysis will be given.

Sample Analysis Techniques

Two techniques have been developed to obtain suitable samples for EMP analysis: 1) diffusion couple and 2) heat treatment.¹ The diffusion

couple technique requires the bonding of two pieces of single phase material (a pure metal or alloy) and the subsequent annealing at a desired temperature.² The resulting concentration gradient is then measured. The composition gradient will vary continuously through solid solutions and exhibit a sharp discontinuity at the boundary of a two phase region. As long as the two phases at the interface are in local equilibrium,² the compositions at the interface correspond to an equilibrium tie line. The diffusion couple technique is applicable to binary, ternary, and higher order systems. The basic requirement is that the interface compositions be resolved with the EMP. The concentration gradients which result must not be too steep or accurate extrapolation to the two phase interface cannot be accomplished.

The second technique involves the heat treatment of an alloy within a 2 or 3 phase field at a desired temperature. The sample is usually one phase and compositionally homogeneous before heat treatment. A second or third phase is obtained by a specified heat treatment cycle.

After heat treatment, the composition of the resulting phases is measured with the EMP. In some cases the bulk alloy may not be equilibrated. Even so appropriate tie line measurements can be obtained if local equilibrium is maintained at phase interfaces² and if composition gradients in the various phases measured with the EMP are small. The heat treatment technique has been applied to a large number of alloy systems and is used more often than the diffusion couple technique.

For ternary two phase alloys the measured tie line need not go through the bulk alloy composition unless the sample is completely equilibrated after heat treatment. This effect is illustrated in Figure 1 where the 650°C isothermal section of the iron rich portion of the FeNiCo phase diagram³ is given. The measured $\alpha + \gamma$ tie lines do

not pass through the bulk composition of the alloys but are displaced to higher Co contents. The requirements of interface mass conservation and local equilibrium in ternary systems permit phase growth to occur by continuous adjustment in the tie line selected and in the rate of growth of the precipitate.⁴ Note that in the low Co alloy #9, equilibrium has been achieved in the heat treatment time allotted.

Specimen Preparation

Usually sample preparation involves melting an alloy of appropriate composition from either pure elements or master alloys of known composition. Induction melting, arc melting, resistance furnace melting, and other methods may be used depending on the specific alloy or oxide system. After melting, the sample should be homogenized to insure uniform composition throughout the sample. The time and temperature required for homogenization will again depend on the alloy or oxide system. Homogenization can be established by mounting-polishing selected samples and by using standard EMP analysis techniques.⁵ In some cases the as-cast alloy is used directly for the heat treatment cycle without prior homogenization. This procedure is not recommended in that the EMP data obtained from the sample will vary from place to place across the alloy.

Diffusion couples can be produced by standard techniques. Usually the interfaces between the two single phase samples are polished and are clamped together by an appropriate device until bonding is achieved. The clamp is often removed before the final diffusion treatment.

The number of heat treatment samples necessary for a phase diagram study can be minimized by use of the EMP technique. The same samples may be used to determine several isotherms. In addition for ternary systems

only one sample is necessary to determine the outline of an entire 3 phase field. A few strategically located alloys may in fact serve to determine an entire isothermal section.

Several heat treatment cycles are available for a given sample.

These heat treatment cycles are:

- (A) Annealing cycle. The sample (usually one phase) is rapidly cooled from a high temperature directly to the temperature of interest (usually in a two or three phase field) and held at that temperature until sufficient phase growth occurs. This type of cycle is used to avoid unwanted phases from forming during heat treatment and to promote nucleation.
- (B) Quench and anneal cycle. The sample (usually one phase) is quenched from a high temperature to a low temperature and is reheated to the temperature of interest (usually in a two or three phase field). The sample is held at that temperature until sufficient phase growth occurs. This type of cycle is often used to promote nucleation of the phases of interest. In some alloy systems a martensitic structure is formed during the quench.
- (C) Controlled cooling cycle. In this scheme the sample (usually one phase) is cooled from a high temperature to the temperature of interest (usually in a two or three phase field) by some continuous and/or step cooling sequence. The sample is maintained at this temperature for a specified time period. This type of cycle controls the amount of nucleation of a second phase during cooling and increases the amount of growth of the phases which form.

In all of these heat treatment cycles the sample is quenched immediately after removal from the final isothermal treatment.

Cycles (B) and (C) were used in the determination of the $\alpha + \gamma$ tie lines of the FeNiCo system.³ The quench and anneal technique (B) (heated up cycle--Fig. 1) yields fine platelets of γ which have precipitated from a martensitic α_2 structure and whose compositions can be measured directly with the EMP. The controlled cooling cycle (C) (cooled down cycle--Fig. 1) yields α grain boundary allotriomorphs in a γ matrix. The α phase composition can be measured directly. However a steep Ni concentration spike was measured in γ making a measurement of the γ tie line composition impossible using cycle C.

The controlled cooling cycle (C) may be required when one is attempting to determine phase equilibria with a metastable phase. For example, when attempting to determine the composition and temperature range over which $(\text{Fe,Ni})_3\text{C}$, cohenite, can exist in the Fe-Ni-C system it was discovered that the carbide cannot be grown by either cycles (A) or (B). The cohenite is metastable with respect to metal plus graphite and the conventional heat treatment cycles, (A) and (B), produced the stable assemblage. However, cohenite precipitates, up to 5 microns in size, which are sufficiently large for EMP analysis, have been grown with the controlled cooling cycle technique.

Electron Microprobe Analysis

After the heat treatment cycle the sample is mounted and polished with standard metallographic techniques. Etching, surface marking, and repolishing may be necessary if the microstructure cannot be seen in the as-polished condition. The sample is then coated with a thin conducting layer to prevent charging during EMP analysis.

To obtain the most meaningful results from the probe analysis the operating conditions must be optimized. Operating potential, sample current, and counting time are perhaps the most critical parameters. The optimization of these parameters have been discussed in detail⁵ and will only be described briefly in this paper.

A ratio of operating voltage to excitation potential for the measured characteristic X-ray lines of approximately 2 to 3 is desirable in order to maximize peak to background ratios and minimize the X-ray source size-resolution. Hence, if the characteristic X-rays being detected vary greatly in excitation potential, a multiple analysis at more than one operating potential may be necessary. The sample current is chosen so that X-ray counts are maximized for a statistically meaningful analysis without greatly increasing the electron beam size. Count times must be sufficiently long to allow the collection of enough X-ray counts for statistically meaningful results. The total number of counts accumulated is the critical variable in determining the detectability limit and sensitivity for each element in the analysis. The X-rays generated may be detected by either wavelength dispersive or energy dispersive spectrometers. Both systems have specific advantages and the choice will depend on the alloy system. For example, in systems containing light elements and/or overlapping spectra the wavelength dispersive spectrometer would most likely be selected. In many modern EMP systems both types of spectrometers can be used simultaneously.

Accuracy of Phase Diagram Determination

The accuracy of phase boundary measurement with the EMP is limited by three main factors: X-ray spatial resolution, X-ray absorption and

X-ray fluorescence. These factors are discussed in turn in the following paragraphs.

The X-ray source size or X-ray spatial resolution in which primary X-rays are produced is much larger than the size of the electron beam. The X-ray source size is defined by the amount of elastic scattering which occurs in a solid sample and is almost always $1\ \mu\text{m}$ or larger in diameter even under optimum conditions.⁵ Therefore the direct measurement of the phase boundary composition is impossible within a distance equivalent to the X-ray source size of the analyzed phase. Typically then, the interface composition is determined by extrapolation to the interface position. The extrapolation procedure can only be used if the concentration gradient is small. Deconvolution techniques have been developed to account for "smeared" interface gradients. These techniques are not very useful when compositional accuracy of the type necessary for phase diagram measurements is desired. In most cases, the necessity for extrapolation is the most serious limitation of the EMP technique.

The X-ray absorption effect occurs when X-rays produced at one point within the specimen travel through material of different composition, and perhaps different mass absorption coefficients on their way to the spectrometer. To avoid such an absorption effect, it is necessary to orient the interface perpendicular to the surface of the specimen and the interface parallel to the X-ray path to the spectrometers.

The X-ray fluorescence effect occurs when characteristic lines of a given element are excited by the continuum and the characteristic spectrum of other lines at a distance away from the electron beam ($\geq 5\ \mu\text{m}$). In this case additional X-ray excitation may occur on one side of the two phase interface even though the electron beam and the analysis point is on the

other side of the interface. In such a situation, it is best to determine how large the effect is by using undiffused couples and to correct the data accordingly.

In addition the measured X-ray counts from the EMP must be converted to composition (weight percent). The most common method used in solid materials applications is the (ZAF) matrix correction technique. The X-ray counts from the point of beam impingement are ratioed against the counts obtained from a homogeneous standard of known composition. Weight percents are obtained from these ratios after correcting for effects of atomic number, absorption, and fluorescence.

Application of the EMP to the Determination of the Fe-Ni-C Phase Diagram

In the Fe-Ni-C system equilibrium occurs between the f.c.c. (γ) phase, b.c.c. (α) phase, and the metastable line compound $(\text{Fe,Ni})_3\text{C}$. Figure 2 shows the metallography of an Fe-3.75 wt% Ni-1.0 wt% C alloy obtained by continuous cooling from 1000°C at 25°C/hour to 730°C with an isothermal 24 hour hold at that temperature. The matrix of the alloy is now martensite, produced at the end of the heat treatment when γ was quenched from 730°C to room temperature. The grain boundary precipitate is $(\text{Fe,Ni})_3\text{C}$. Microprobe traverses were made across the carbides. One such traverse is shown in Figure 3. The interface compositions are indicated on the figure and the corresponding tie line is plotted on the 730°C isotherm, Figure 4. Several other measured tie lines are shown in this Figure. It should be noted that the tie lines in the $\gamma + \text{Fe}_3\text{C}$ phase field do not go through the bulk alloy compositions.

Summary - EMP Technique

The method of phase diagram determination with the EMP is well developed and has been used to determine phase diagrams in over 30 systems. Table 1 lists several systems where the EMP has been used to determine at least part of the phase diagram.

The utility of the technique has been fully described in this work, yet it is not without its shortcomings. One area where improvement is possible is in spatial resolution. Errors attributable to extrapolated interface compositions could be minimized and steeper gradients could be measured if a small excitation volume could be obtained.

Application of STEM Techniques to Phase Diagram Determination

In the last few years the scanning transmission electron microscope has been developed. It is now possible to focus the primary electron beam of this instrument to $\leq 100\overset{\circ}{\text{A}}$ spot size on the specimen. Similar to the EMP, the excited characteristic X-rays can be measured in a suitable detector and used for localized chemical analysis. The major advantage of this technique is that, by using electron microscope thin films and operating voltages of 80 to 200 kV, little electron scattering occurs in the sample. The X-ray source size obtained is $< 0.1 \mu\text{m}$, a factor of 10 better than the EMP. With sufficiently thin samples, the X-ray source size may be $< 0.01 \mu\text{m}$. In addition, the use of thin films at high electron beam excitation voltages eliminates, in most cases, the need to correct for absorption and fluorescence effects in the conversion of X-ray data to composition.

As an example of the use of the STEM technique for phase diagram determination the Fe-Ni-Co system will be considered. The phase diagram has recently been redetermined by microprobe analysis at several temperatures.³ The 650°C isotherm is given in Figure 1. The alloy samples used for this isotherm were heat treated for times of up to 6 months and analyzed with the EMP techniques previously described. The 6 month treatment time was necessary to produce γ plates $\geq 5 \mu\text{m}$ in width for EMP analysis. To evaluate the applicability of the STEM to phase diagram determination an Fe-8.96 wt% Ni-7.92 wt% Co alloy was prepared using a quench and anneal cycle (B). The alloy sample was heat treated at 650°C for only 2 weeks and the γ plates produced were 0.3-0.5 μm in width. A thin foil transmission microscope sample was prepared from the specimen by ion etching.

Figure 5 shows a scanning transmission image of the γ plates and α matrix prior to data acquisition. A Philips 300 STEM instrument was used with an operating potential of 80 kV and with the specimen tilted at 36°. Data was taken across the γ platelets and the α matrix with an electron beam $\sim 320\text{\AA}$ in diameter. The position of the beam during analysis are visible due to sample contamination as shown in Figure 6.

X-ray data was collected on a solid state X-ray detector with a counting time of 60 sec. per point. The $\text{Fe}_{K\alpha}$ and $\text{Ni}_{K\alpha}$ integrated peak intensities were measured and the continuum background was subtracted. A plot of $I_{\text{Ni}}/I_{\text{Fe}}$ vs. distance was constructed and is shown in Figure 7. The circles represent data points as measured on the STEM. The 2σ error bars were calculated from the accumulated X-ray counts on the specimen. The bulk alloy $I_{\text{Ni}}/I_{\text{Fe}}$ value was determined by scanning the electron beam over the entire area of Figure 5.

The diameter of the X-ray generation region is indicated on Figure 7 by R(x). For the EMP R(x) is a nominal 1 μm and represents the diameter of the X-ray excitation volume. For the STEM, R(x) represents the 320 \AA beam diameter plus an estimate of the amount of beam spreading in the specimen, about 200 \AA for a 1000 \AA iron thin foil.⁶

Cliff and Lorimer⁷ have outlined a simple technique to carry out the quantitative analysis of thin foils with the STEM analytical electron microscope. For very thin foils where X-ray absorption and fluorescence can be neglected, the following expression may be used:

$$\frac{I_A}{I_B} = (k_{AB})^{-1} \frac{C_A}{C_B} \quad (1)$$

where I_A and I_B are the measured characteristic X-ray intensities, and C_A , C_B are the weight fractions of two elements A and B in the thin film. The constant k_{AB} varies with operating voltage but is independent of sample thickness and composition if the two intensities are measured simultaneously. This method has been often referred to as the standardless method in that pure bulk standards are not needed for the analysis.

These k_{AB} values can either be measured or calculated. The value of k_{NiFe} used in this experiment was calculated using the expressions developed by Goldstein et al.⁶ A value of $k_{\text{NiFe}} = 1.081$ for 80 kV operating potential was calculated using the method of Goldstein et al.⁶ which corrects for the absorption of the Be window in the detector and the relativistic nature of the electron beam.

STEM - Discussion

Using Equation 1 and the calculated k_{NiFe} value one can calculate the expected $I_{\text{Ni}}/I_{\text{Fe}}$ ratios for the α and γ phase compositions using measured C_{Ni} , C_{Fe} values obtained from a tie line drawn through the bulk

composition of the Fe-8.96 wt% Ni-7.92 wt% Co alloy at a temperature of 650°C (Figure 1). The solid lines of $I_{\text{Ni}}/I_{\text{Fe}}$ plotted on Figure 7 for the α and γ phases were determined by this procedure. The bulk alloy intensity ratio was calculated similarly. It is apparent that excellent agreement has been obtained between measurements of tie line compositions by EMP and STEM techniques.

It is clear from this example that phase diagram determination by STEM techniques has a promising future. The increased spatial resolution will allow analyses of phases 0.5 μm in size and possibly smaller. Growth times for precipitates will also be greatly reduced by this technique. A major advantage will be the extension of phase diagram analysis to lower temperatures than have been possible to date. Problems of contamination, X-ray absorption, and thin film preparation in STEM analysis have yet to be completely solved, however.

Acknowledgements

The authors wish to thank D. Richards for the preparation of the STEM sample and R. Korastinsky for assistance with the STEM analysis work. We thank D. Williams and S. Widge for helpful discussions and suggestions. This work was supported by NASA Grant NGR 39-007-056.

REFERENCES

1. Goldstein, J. I. and Ogilvie, R. E. in X-ray Optics and Microanalysis, ed. by R. Castaing, P. Deschamps and J. Philibert, Hermann, Paris (1966), pp. 594.
2. Ogilvie, R. E., Sc.D. Thesis, MIT, (1955).
3. Widge, S. and Goldstein, J. I., Met. Trans. A, to be published (1977).
4. Randich, E. and Goldstein, J. I., Met. Trans. 6A, 1553 (1975).
5. Goldstein, J. I. and Yakowitz, H., eds. Practical Scanning Electron Microscopy, Plenum, New York (1975).
6. Goldstein, J. I., Costley, J. L., Lorimer, G. W. and Reed, S. J. B. in SEM/1977, ed. by O. Johari, to be published (1977).
7. Cliff, G. and Lorimer, G. W., Proc. Fifth Euro. Conf. on EM, Institute of Physics, London, 1972, pp. 140-141.
8. Rexer, J., Z. Metallkde, v. 62, (1971), pp. 844-848.
9. Kirchner, G., Nishizawa, T. and Uhrenius, B., Met. Trans., v. 4, (1973), pp. 167-174.
10. Waterstrat, R. M., Met. Trans., v. 4, (1973), pp. 1585-1592.
11. Kirchner, G., Harvig, H. and Uhrenius, B., Met. Trans., v. 4, (1973), pp. 1059-1067.
12. Goldstein, J. I. and Ogilvie, R. E., Trans. TMS-AIME, v. 233, (1965), pp. 2083-2087.
13. Hofmann, H., Löhberg, K. and Rerf, W., Arch. Eisenhüttenwes, v. 41, (1970), pp. 975-982.
14. Wald, F. and Sturmont, R. W., Trans. TMS-AIME, v. 242, (1968), pp. 72-74.
15. Heijwegen, C. and Rieck, G., Z. Metallkde, v. 64, (1973), pp. 450-453.
16. Meussner, R. and Goode, R., Trans. TMS-AIME, v. 233, (1965), pp. 661-671.
17. Waterstrat, R., Met. Trans., v. 4, (1973), pp. 455-466.
18. Maxwell, I. and Hellowell, A., Met. Trans., v. 3, (1972), pp. 1487-1493.
19. Urednicek, M. and Kirkaldy, J., Z. Metallkde, v. 64, (1973), pp. 419-427.
20. Cisse, J. and Davies, R., Met. Trans., v. 1, (1970), pp. 2003-2006.
21. Rosenbach, K. and Schmitz, J., Arch. Eisenhüttenwes, v. 45, (1974), pp. 843-847.

22. Karnowsky, M. and Yost, F., Met. Trans. A, v. 7A, (1976), pp. 1149-1156.
23. Carmio, S. and Meijering, J., Z. Metallkde, v. 3, (1973), pp. 170-175.
24. Benz, R., Elliott, J. and Chipman, J., Met. Trans., v. 4, (1973), pp. 1975-1986.
25. Sharma, R. and Kirkaldy, J., Can. Met. Quat., v. 12, (1973), pp. 391-401.
26. Reinbach, R. and Baer, H., Z. Metallkde, v. 5, (1969), pp. 453-456.
27. Schultz, J. and Merrick, H., Met. Trans., v. 3, (1972), pp. 2479-2483.
28. Massalski, T. and Perepezko, J., Z. Metallkde, v. 3, (1973), pp. 176-181.
29. Budurov, S., Krassimir, R., Kovatchev, P., Toncheva, S. and Komenova, Z., Z. Metallkde, v. 65, (1974), pp. 683-685.
30. Doan, A. and Goldstein, J. I., Met. Trans., v. 1, (1970), pp. 1759-1767.
31. Chiang, P.-W. and Gluck, J. V., Trans. TMS-AIME, v. 242, (1968), pp. 2229-2236.
32. Brunch, A. and Steeb, S., Z. Metallkde, (1974), pp. 714-720.
33. Wald, F., Bates, H. and Weinstein, M., Trans. TMS-AIME, v. 242, (1968), pp. 760-761.

Table I

Summary of Phase Diagrams

Tabulation of systems where the EMP has been used in the determination of solid solubility limits, tie-lines, tie-triangles, and phase identification.

System	Temperature Range (°K)	Technique*	Measured Parameter (Phase Relationship)
Al-Mo ⁸	1673-1873	D.C.	solubility limits: Al ₃ Mo ₃ - Al ₆₃ Mo ₃₇ AlMo - AlMo ₃ - Mo
Cr-Fe ⁹	1123-1373	HTB	tie-lines: $\alpha + \gamma$
Cr-Pt ¹⁰	970-2133	HTB	tie-lines: $\gamma + \beta$, $\beta + \alpha$, $\gamma' + \beta$
Fe-Mo ¹¹	1073-1773	HTB	tie-lines: $\alpha + \gamma$
Fe-Ni ¹²	773-1073	HTB, D.C.	tie-lines: $\alpha + \gamma$
Fe-P ¹³	1133-1273	D.C.	solubility limits: $\alpha - \text{Fe}_3\text{P}$
Fe-PbTe ¹⁴	1073-1195	HTB	solubility limits: Fe-PbTe
Fe-W ¹¹	1173-1813	HTB, D.C.	tie-lines: $\alpha + \lambda$, $\lambda + \mu$, $\alpha + \mu$, $\mu + \text{'W'}$
Mo-Ni ¹⁵	1073-1568	D.C.	tie-lines: (Mo) + ζ , (Ni) + ζ , $\zeta + \gamma$ ($\zeta - \text{MoNi}$, $\gamma - \text{MoNi}_3$, $\beta - \text{MoNi}_4$)
Nb-Zn ¹⁶	1293-1393	HTB	compound identification: NbZn ₃ , NbZn ₂ , NbZn _{1.5} , NbZn
Pt-V ¹⁷	1173-1973	HTB	tie-lines: $\zeta + \beta$, $\alpha + \beta$, $\gamma + \beta$ ($\beta - \text{V}_3\text{Pt}$, $\zeta - \text{VPt}$)
Al-B-Ti ¹⁸	923	HTB	compound identification: Al ₃ Ti, AlB ₂ , TiB ₂
Al-Fe-Zn ¹⁹	723	solid-liquid equilibration	phase and compound identification: FeAl, FeAl ₂ , Fe ₂ Al ₅ , δ_1 , ζ , two ternary phases solubility limits: compounds-terminal phase
Al-Nb-Ni ²⁰ (Ni ₃ Al-Ni ₃ Nb-Ni)	1073-1473	HTA, D.C.	solubility limits: $\gamma' - \text{Nb}$ tie-lines: $\gamma + \gamma'$
Al ₂ O ₃ -Cr ₂ O ₃ -FeO ²¹	1923-2073	HTB	solubility limits: FeO · Cr ₂ O ₃ - FeO · Al ₂ O ₃ quasi-binary
Au-In-Pb ²²	432-706	HTB	phase identification: AuIn, AuIn ₂

Table I (continued)

System	Temperature Range (°K)	Technique*	Measured Parameter (Phase Relationship)
Au-Ni-Pt ²³	1085-1533	HTB	tie-lines: solid 1 - solid 2 miscibility gap
C-Fe-Mn ²⁴	1163-1373	HTB	tie-lines: $\gamma + M_3C$ phase identification: M_3C , $M_{15}C_4$, $M_{23}C_6$, ϵ
C-Fe-Ni ²⁵	773-1003	HTB, HTC	tie-lines: $\alpha + \gamma$, $\gamma + (Fe, Ni)_3C$, $\alpha + (Fe, Ni)_3C$
C-Fe-P ¹³	873-1173	D.C.	solubility limits: $\alpha - (Fe, Ni)_3P$
Co-Be-Cu ²⁶	673-1373	HTB	solubility limits: $\alpha - \beta$, $\alpha - \gamma_2$, $\alpha - \gamma_1$
Co-Fe-Ni ³	926-1073	HTB, HTC	tie-lines: $\alpha + \gamma$
Cr-Fe-Ni (Al, Nb, Si, Ti) ²⁷	1089-1533	HTB	solubility limits: $\alpha' - \gamma$ tie-lines: $\alpha' + \gamma$
Cu-Al-Ag ²⁸	848-898	HTB	solubility limits: terminal regions ($\alpha_1 - (Ag)$, $\alpha_2 (Cu)$)
Fe-Mn-Zn ²⁹	893-1273	HTB	tie-lines: $\alpha + \gamma$
Fe-Mo-W ¹¹	1373-1578	HTB	tie-lines: $\alpha + \gamma$, $\alpha + \mu$, $\alpha + R$
Fe-Ni-P ³⁰	823-1373	HTB, HTC	tie-lines: $\alpha + (Fe, Ni)_3P$, $\gamma + (Fe, Ni)_3P$, $\alpha + \gamma$, $\alpha + liquid$, $\gamma + liquid$
Sb-Te-Tl ³¹	483-518	HTB	phase identification: $\alpha (Tl_2, Te_3)$, $\delta (Sb_2Te_3)$, $\epsilon (SbTlTe_2)$, $\theta (Te)$
Ti-V-Zr ³²	1073	HTA	tie-lines: $\alpha + \gamma$, $\beta + \gamma$, $\delta + \beta$, $\gamma + \delta$
C-Cr-Ni-Si ³³	1173	HTB	phase identification: Cr_3C_2 solubility limit: $\gamma - Cr_3C_2$

- * Codes: D.C. - diffusion couple
HTA - heat treatment A - quench from high temperature to temperature of interest (annealing cycle)
HTB - heat treatment B - quench from high temperature to low temperature, then reheat at temperature of interest (quench and anneal cycle)
HTC - heat treatment C - controlled cooling from high temperature to temperature of interest (controlled cooling cycle)

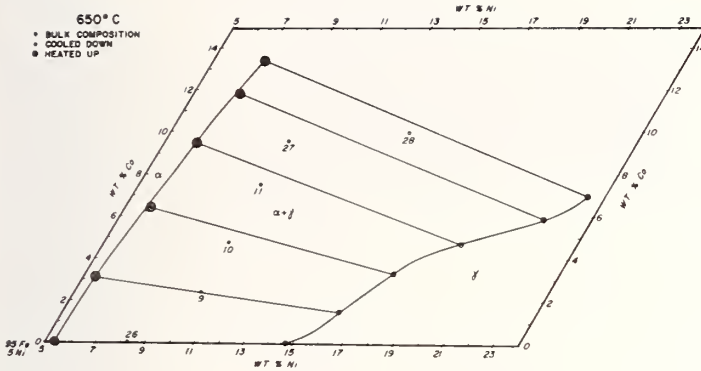


Figure 1

Isothermal section of Fe-Ni-Co ternary diagram at 650°C.³ Origin is at 95Fe-5Ni, and heat treatments are as indicated in the text.

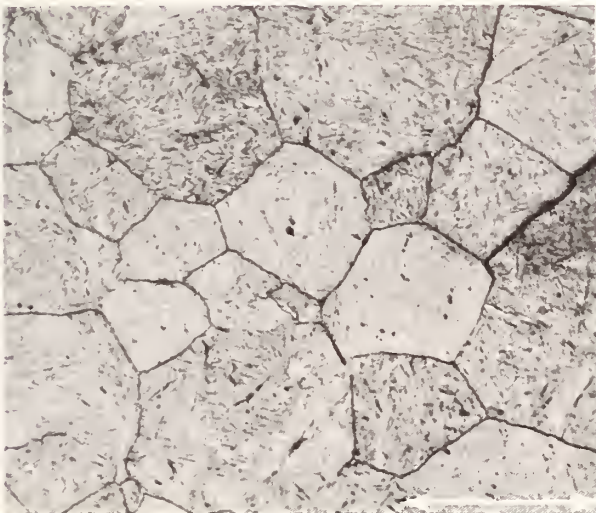


Figure 2

Microstructure of an Fe-3.75 wt% Ni-1.0 wt% C alloy. Austenitized at 1000°C and then cooled to 730°C at 25°C/hour and isothermally treated for 24 hours. Matrix is martensite and grain boundary precipitate is $(Fe,Ni)_3C$. 2% Nital Etch. Scale Bar \approx 200 μ m.

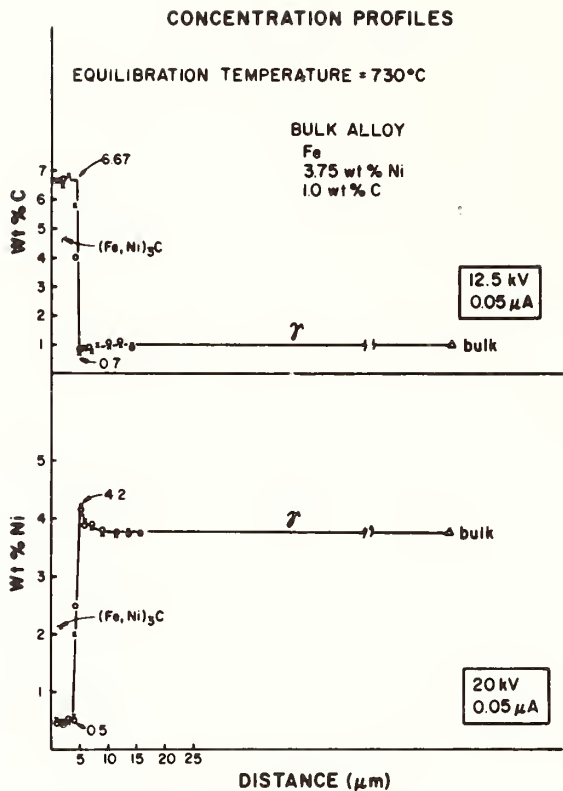


Figure 3
Microprobe traces taken in an Fe-3.75 Ni-1.0 C alloy. x and o represent data points from two separate traces.

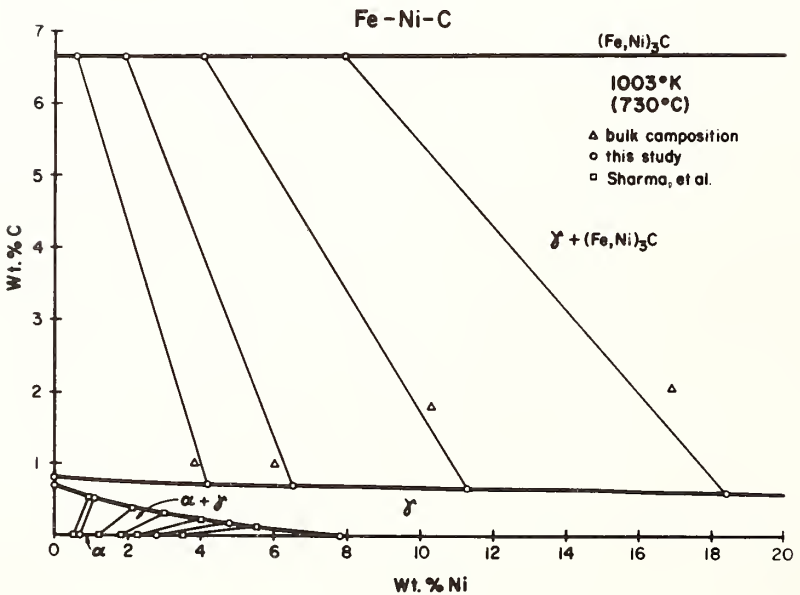


Figure 4
Fe-Ni-C 730°C isotherm.



Figure 5

Fe-8.96 wt% Ni-7.92 wt% Co alloy treated at 650°C using the quench and anneal cycle. STEM image of the thin foil prior to composition analysis. Scale Bar = 1 μm .

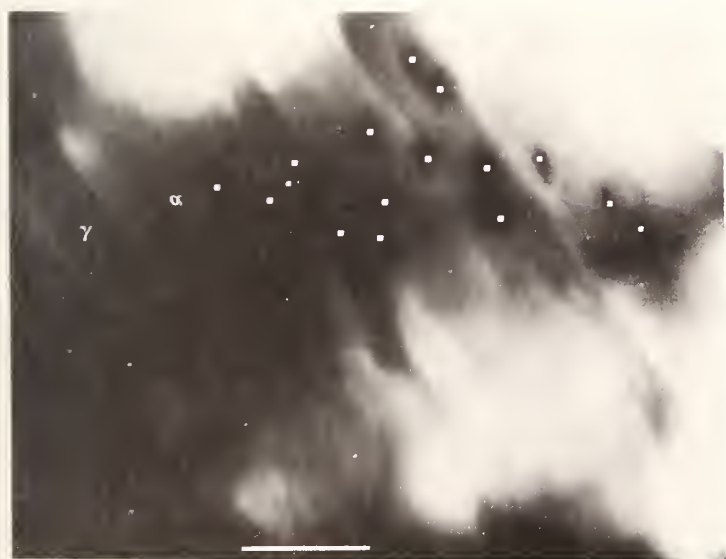


Figure 6

Fe-8.96 wt% Ni-7.92 wt% Co alloy treated at 650°C using the quench and anneal cycle. STEM image of the thin foil after composition analysis. Scale Bar = 1 μm . The analysis points can be observed by the contamination spots left on the foil. The white dots are placed on the photograph to more clearly indicate the analysis points.

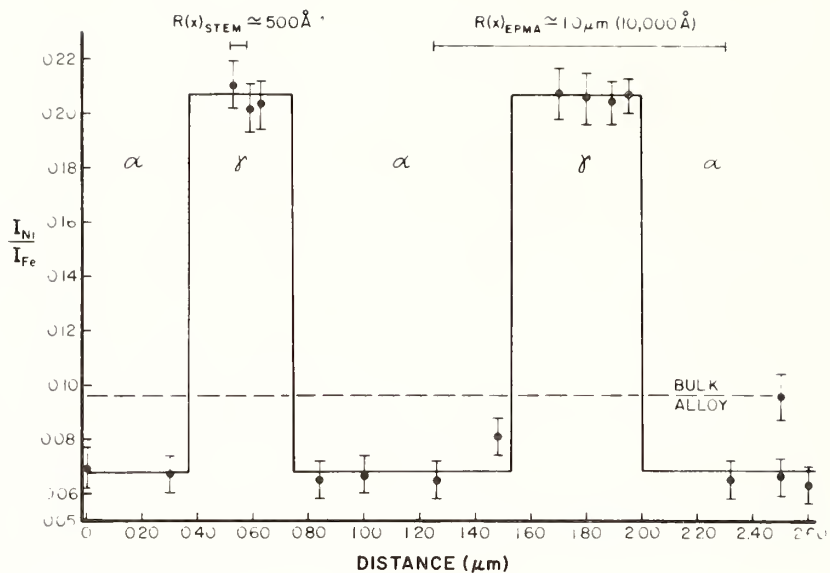


Figure 7

STEM trace across the α and γ phases formed in a Co alloy annealed at 650°C for 2 weeks. Solid circles are data points and 2 σ error bars are shown. The solid lines are calculated from the known Fe-Ni-Co phase diagram and the dashed line is calculated from the bulk alloy composition. The spatial resolution of the STEM and typical resolution of the EMP are also shown.



THE INTERNATIONAL NICKEL COMPANY, INC.
PAUL D. MERICA RESEARCH LABORATORY
STERLING FOREST
SUFFERN, NY 10901

INTERRELATIONS BETWEEN PHASE DIAGRAMS AND
HYDRIDING PROPERTIES FOR ALLOYS BASED ON
THE INTERMETALLIC COMPOUND FeTi

by

G.D. Sandrock*, J.J. Reilly** and J.R. Johnson**

ABSTRACT

Hydriding alloys based on the intermetallic compound FeTi have potential for the safe and convenient storage of hydrogen, both for mobile and stationary applications. In spite of its simple formula, the hydriding behavior of FeTi is quite complex and a strong function of alloy microstructure. The alloy microstructure, in turn, depends on composition, not only deviations from stoichiometry but also various impurities. In this paper we discuss some of the interrelations among composition, microstructure, and hydriding behavior that can be related to phase diagram information. In particular, we discuss the Fe-Ti, Fe-Ti-O, and Fe-Ti-Mn phase diagrams and their relationships to hydriding properties. The use of hydriding data to infer metal-hydrogen phase diagrams is also briefly discussed.

*The author is with The International Nickel Company, Inc., Paul D. Merica Research Laboratory, Sterling Forest, Suffern, NY

**The authors are with Brookhaven National Laboratory, Department of Applied Science, Upton, NY

INTRODUCTION - FeTi FOR HYDROGEN STORAGE

In the past few years considerable interest has developed in using rechargeable metal hydrides for hydrogen storage, both for stationary and vehicular applications(1-4). Of particular interest has been the hydrogen storage properties of the intermetallic compound FeTi(5). In spite of its simple formula, however, the hydriding behavior of FeTi is complex and a strong function of alloy microstructure(6,7). Alloy microstructure, in turn, is influenced by deviations from stoichiometry and various impurities. As with other engineering alloys, phase diagram information can be very useful in interpreting the microstructures of FeTi and relating these microstructures to hydriding data. In this paper we present a few specific examples of these interrelations.

Before discussing specific examples of the use of phase diagrams to interpret hydriding data, however, a brief introduction to ideal (high purity) FeTi hydriding behavior should be given. At ambient temperatures and a few atmospheres pressure, FeTi reacts with hydrogen to form a monohydride and a dihydride according to the approximate reactions:



The hydriding reaction is similar to corrosion reactions such as oxidation as shown metallographically in Figure 1.

There is a positive volume change during the hydriding reaction so that the brittle FeTi cracks as a result of stresses generated during first hydriding (activation). After activation each particle is highly cracked on a fine scale (Figure 2) and thus provides a relatively large surface area for the occurrence of subsequent hydriding and dehydriding reactions. Because the reactions are easily reversible, FeTi can be effectively charged and discharged, thus serving as a solid "sponge" for the storage of hydrogen. Examples of charging and discharging curves are shown in Figure 3. Once the alloy is fully activated (finely cracked) kinetics are very rapid and are for practical purposes determined by the rate the heat of reaction can be removed from the bed during hydriding or added to the bed during dehydriding.

PHASE DIAGRAM - HYDRIDING INTERRELATIONS

The curves shown in Figure 3 were obtained with carefully prepared, high purity, nearly stoichiometric FeTi. Practical production of engineering quantities of FeTi for hydrogen storage will result in alloys that are less than perfect from stoichiometry and purity points of view. Phase diagrams can be very useful in understanding these deviations from ideality and can provide useful production targets. In this section we present a few examples of the use of phase diagrams in the interpretation of FeTi hydrogen storage behavior. In particular we will consider the Fe-Ti,

Fe-Ti-O and Fe-Ti-Mn phase diagrams, although others have been consulted in our studies of FeTi(7). The hydriding properties we will concentrate on most will be hydrogen storage capacity, although others such as activation and decrepitation (particle size breakdown with cycling) have been considered(6,7).

Fe-Ti BINARY SYSTEM

An understanding of the metallurgy of FeTi should begin with the Fe-Ti binary phase diagram, reproduced in Figure 4. Hydrogen desorption curves for selected binary alloys are shown in Figure 5. The phase of interest for hydrogen storage purposes is the FeTi phase which exists over a narrow ($\sim 2.5\%$) composition range near the center of the phase diagram. For maximum hydrogen storage capacity it is important that the alloy composition be within the single phase FeTi field. If the prepared composition is only slightly deficient in Ti ($< \sim 49.5$ at. % Ti) the two-phase FeTi + Fe₂Ti field is entered. The presence of Fe₂Ti in the microstructure is undesirable because it apparently does not hydride. Thus the overall storage capacity is reduced by the presence of the inert Fe₂Ti phase. From the phase diagram, it is evident from the lever rule that only moderate decreases in Ti content below 49.5 at. % can result in substantial amounts of Fe₂Ti. For example, an alloy of ~ 41 at. % Ti would contain $\sim 50\%$ Fe₂Ti. The drastic reduction in hydrogen storage capacity accompanying such a decrease in Ti content is shown in Figure 5.

On the other hand, if the Ti content of the prepared alloy is in excess of ~ 52 at. %, the two-phase FeTi + Ti solid solution (α -or β -Ti) field is entered. The Ti solid solution phase hydrides readily, tending to form essentially TiH_2 . Unfortunately, however, this hydride is not readily reversible (i.e., it is much too stable) and is thus not useful for reversible hydrogen storage purposes at near ambient temperatures. Thus, as graphically confirmed by the right curve in Figure 5, alloys with substantial excess free Ti should also be avoided for maximum reversible storage capacity. From the geometry of the phase diagram (Figure 4) a given error is somewhat less deleterious if it is on the Ti-rich side rather than the Ti-lean side of 50-50 at. % Fe-Ti. This, coupled with the fact the equiatomic alloy solidifies through a peritectic reaction (i.e., as shown in Figure 4, the first few crystals to form in the cooling melt are Fe_2Ti), makes it desirable in practice to aim for slightly Ti-rich alloys (say 50.5-51 at. % Ti).

Depending on the hydriding properties desired, there may be advantages to use alloys slightly richer than 51 at. % Ti. As shown in Figure 5, excess Ti (say ~ 53 at. %) lowers the overall dissociation pressure and makes the plateau much more inclined. The reason for this is not completely clear, but appears to involve non-equilibrium segregation effects during solidification (i.e., effects not directly relatable to the equilibrium phase diagram).

In addition we have qualitatively found that the presence of some free Ti solid solution in the microstructure aids activation by providing preferred paths for initial hydride penetration. Fe₂Ti probably also aids activation. In fact, most second phases seem to assist the activation process.

Fe-Ti-O TERNARY SYSTEM

Of the common trace element impurities in FeTi, oxygen is the most influential on the hydriding properties. Like most other high-Ti alloys, liquid FeTi has a very high affinity and solubility for oxygen. Of importance to the hydriding behavior is the microstructural role oxygen plays in the solidified alloy.

After studying this problem in some detail, we conclude the role of oxygen can be explained well by the Fe-Ti-O ternary phase diagram of Rostoker(9), shown in Figure 6. Rostoker's diagram indicates that the introduction of oxygen results in the formation of a ternary "T-phase" (Ti₄Fe₂O-Ti₃Fe₃O). In fact, we metallographically find that the amount of a second phase increases directly with increasing oxygen content. This is shown in Figure 7. Microprobe analysis of the second phase particles conform reasonably well with the homogeneity range of the T-phase. Our data points cluster around the approximate stoichiometry Fe₇Ti₁₀O₃ (Figure 6). This phase is crystallographically equivalent to that reported originally by Rostoker(9) and again recently by Pick and Wenzl(10) in O-contaminated FeTi. The only

difference we note between our observations and Rostoker's phase diagram (Figure 6) is that we see eutectic $\text{Fe}_7\text{Ti}_{10}\text{O}_3$ particles in as-cast microstructures with O-contents as low as 0.01 wt. % (Figure 7a), whereas Rostoker suggests a solubility (at 1000°C) of 1-2 at. % (0.3-0.6 wt. %) oxygen in the FeTi phase.

The problem with $\text{Fe}_7\text{Ti}_{10}\text{O}_3$ is that it does not hydride, at least at the temperatures and pressures routinely used for FeTi. This, coupled with the fact that each O-atom ties up about $17/3 = 5.67$ metal atoms, results in a substantial loss in hydrogen storage capacity. This is shown graphically in Figure 8, which presents a series of desorption isotherms for FeTi samples with different O-contents. The measured loss in capacity corresponds closely with that which would be predicted by the Fe-Ti-O phase diagram; i.e., calculated assuming all the oxygen goes to form an inert $\text{Fe}_7\text{Ti}_{10}\text{O}_3$ phase.

The presence of $\text{Fe}_7\text{Ti}_{10}\text{O}_3$ affects other hydriding properties such as activation and decrepitation(6,7). As with other second phases, the $\text{Fe}_7\text{Ti}_{10}\text{O}_3$ particles accelerate activation by serving as sites for preferred hydride penetration and nucleation. In a related way, decrepitation (particle size breakdown) is also accelerated by the presence of the ternary O-rich phase. In summary, it is desirable to heed the overall lesson of the Fe-Ti-O phase diagram in the production of FeTi and set as a target the minimum O-contamination practical so as to minimize the amount of $\text{Fe}_7\text{Ti}_{10}\text{O}_3$ in the microstructure.

Fe-Mn-Ti TERNARY SYSTEM

A number of transition metal elements (e.g., Mn, Cr, V, Co or Ni) can be at least partially substituted into the FeTi lattice(11). Which element (Fe or Ti) the ternary addition substitutes for, as well as the rough limits of substitution can often be qualitatively inferred from existing binary or ternary phase diagram information(7). However, an equilibrium phase diagram can be slightly misleading in attempting to interpret the hydriding behavior of non-equilibrium microstructures that often result from solidification at conventional rates.

An example of this can be seen with the Fe-Mn-Ti ternary system. A portion of the ternary phase diagram is shown in Figure 9. The dotted lines indicate the limits of 1000°C homogeneity reported for the Ti(Fe,Mn) phase by Murakami and Enjyo(12). They indicate that the FeTi phase has a substantial solubility for Mn and in fact the homogeneity range for the phase is actually widened by the substitution of Mn. We find that this diagram, determined by annealing samples at 1000°C, is not representative of as-cast structures. Shown on Figure 9 are a number of ternary alloys prepared and metallographically examined during our study. In no case was a strictly single phase Ti(Fe,Mn) microstructure found, but invariably some (Fe,Mn)₂Ti and Ti solid solution was found within the single phase region of the reported phase diagram. This, of course, does not contradict the work of Murakami and Enjyo, but merely

repeats the well established fact that "equilibrium" phase diagrams can be misleading under non-equilibrium solidification conditions.

The implications of this particular example on the hydriding behavior of Fe-Mn-Ti alloys are as follows. By substituting Mn directly for Fe (i.e., along the $TiFe_{1-x}Mn_x$ line in Figure 9) the two-phase $Ti(Fe,Mn) + (Fe,Mn)_2Ti$ is quickly entered in as-cast alloys. Assuming one does not wish to go to the expense of extensively annealing to establish the equilibrium single phase, the result is some loss in H-storage capacity because the $(Fe,Mn)_2Ti$ phase does not hydride. An example of this is shown by the $TiFe_{0.7}Mn_{0.3}$ desorption curve in Figure 10. For maximum storage capacity it is desirable to maximize the amount of the $Ti(Fe,Mn)$ phase. As shown by the as-cast results of Figure 9, this can be done by melting slightly Ti-rich [i.e., at an atomic ratio $(Fe+Mn)/Ti$ slightly less than 1]. The improved storage capacity of such an alloy, $TiFe_{0.7}Mn_{0.2}$, is shown in Figure 10.

There are other aspects of the curves in Figure 10 that are not explained by phase diagrams. The general lowering of the hydride pressures by substitution of Mn into the FeTi structure is a consequence of subtle bonding effects not directly reflected in the phase diagram(6). Similarly the sloping plateaus that result in the Mn-containing alloys are a result of non-equilibrium segregations of Mn that occur within the $Ti(Fe,Mn)$ phase itself during solidification.

Although phase diagrams do not answer all the questions regarding the complex hydriding behavior of FeTi and its related alloys, they are very important to establishing the basic metallurgical understanding of this system which must accompany engineering use for hydrogen storage.

USE OF HYDRIDING DATA TO INFER METAL-HYDROGEN PHASE DIAGRAMS

Thus far we have discussed the use of metal-metal phase diagrams to rationalize observed hydriding data. The situation may be somewhat reversed, whereby hydriding data as a function of temperature may be used to infer the M-H phase diagram. As an example we will briefly show the application of this to the FeTi-H phase diagram(5).

A series of hydrogen desorption isotherms for high purity FeTi (49.6 at% Fe) is shown in Figure 11. Each curve has essentially five regions. Starting from the left of the plot they are: (a) an almost vertical portion, which represents the solubility limit of H in FeTi; (b) a horizontal plateau, which represents a two-phase mixture of hydrogen saturated FeTi and the monohydride (\sim FeTiH); (c) a rising portion which represents some increased solubility of H in the monohydride; (d) another plateau, representing the two-phase monohydride + dihydride field; and (e) another steeply rising portion, representing a slight further increase in the solubility of H in the dihydride phase. By plotting the approximate points separating these five regions in Figure 11, the FeTi-H phase diagram of Figure 12 was created. Such

a construction only helps to infer a phase diagram and must, of course, be supported by independent x-ray diffraction data. A limited amount of room temperature XRD confirming data is shown in Figure 12.

The gradual elimination of the upper plateau at higher temperatures has been tentatively interpreted as a closing off of the two-phase $\beta + \gamma$ field at a consolute temperature of about 60°C, although the exact temperature is rather difficult to determine from the hydriding data (Figure 11). Above this temperature it is assumed the monohydride can continuously change to the dihydride by hydrogen absorption in a manner similar to the formation of the V, Nb, Ta and Pd hydrides at high temperatures(13). It should be noted, however, that this has not yet been confirmed for the FeTi case by x-ray diffraction.

CONCLUSION

The optimum use of hydriding alloys for hydrogen storage requires an intimate knowledge of the metallurgy of the alloys involved. We have shown for FeTi, and related hydrogen storage alloys, the application of metallurgical phase diagram information can greatly aid the interpretation of hydriding data. In a related manner, hydriding data can be used in the construction of metal-hydrogen phase diagrams

and, as an example, the FeTi-H phase diagram was derived. The generalities derived from work such as this on FeTi should be applicable to other rechargeable hydride systems.

REFERENCES

1. K.C. Hoffman, J.J. Reilly, F.J. Salzano, C.H. Waide, R.H. Wiswall and W.E. Winsche, "Metal Hydride Storage for Mobile and Stationary Applications", *Hydrogen Energy*, 1, 133 (1976).
2. D.L. Henriksen, D.B. Mackay and V.R. Anderson, "Prototype Hydrogen Automobile Using a Metal Hydride", Proc. 1st World Hydrogen Energy Conf., III, 7C-1, Miami Beach, 1976.
3. R.E. Billings, "A Hydrogen-Powered Mass Transit System", Proc. 1st World Hydrogen Energy Conf., III, 7C-27, Miami Beach, 1976.
4. A. Buchner and H. Saüfferer, "The Short and Medium Term Development and Practical Application of Hydrogen-Powered Vehicles", 2nd Symposium on Low Pollution Power Systems Development, Duesseldorf, 1975.
5. J.J. Reilly and R.H. Wiswall, Jr., "Formation and Properties of Iron Titanium Hydride", *Inorganic Chem.*, 13, 218 (1974).
6. G.D. Sandroock, J.J. Reilly and J.R. Johnson, "Metallurgical Considerations in the Production and Use of FeTi Alloys for Hydrogen Storage", Proc. 11th Intersociety Energy Conversion Engineering Conference, I, 965 (1976).
7. G.D. Sandroock, "The Interrelations Among Composition, Microstructure and Hydriding Behavior for Alloys Based on the Intermetallic Compound FeTi", Final Report, Contract BNL-352410S, June 30, 1976.

8. T. Lyman, Editor, Metals Handbook, Vol. 8, American Society for Metals, Metals Park, OH, 1973, p. 307.
9. W. Rostoker, "Selected Isothermal Sections in the Titanium-Rich Corners of the Systems Ti-Fe-O, Ti-Cr-O, and Ti-Ni-O", Trans. AIME, 203, 113 (1955).
10. M.A. Pick and H. Wenzl, "Physical Metallurgy of Fe-Ti-Hydride and Its Behavior in a Hydrogen Storage Container", Proc. 1st World Hydrogen Energy Conf., II, 8B-27, Miami Beach, 1976.
11. J.J. Reilly and J.R. Johnson, "Titanium Alloy Hydrides; Their Properties and Applications", Proc. 1st World Hydrogen Energy Conf., II, 8B-3, Miami Beach, 1976.
12. Y. Murakami and T. Enjyo, "Investigation of Ti-Rich Ti-Fe-Mn Alloy System on the Solid Equilibrium Relation in the Ti-Fe-Mn System", Nippon Kinzoku Gakkaishi, 22, 328 (1958).
13. G.G. Libowitz, The Solid State Chemistry of Binary Metal Hydrides, Benjamin Press, New York (1965), pp. 34-37.



FIGURE 1

PARTIALLY HYDRIDED PARTICLE OF FeTi
200X



FIGURE 2

FULLY ACTIVATED PARTICLE OF FeTi (IN
DEHYDRIDED CONDITION)
200X

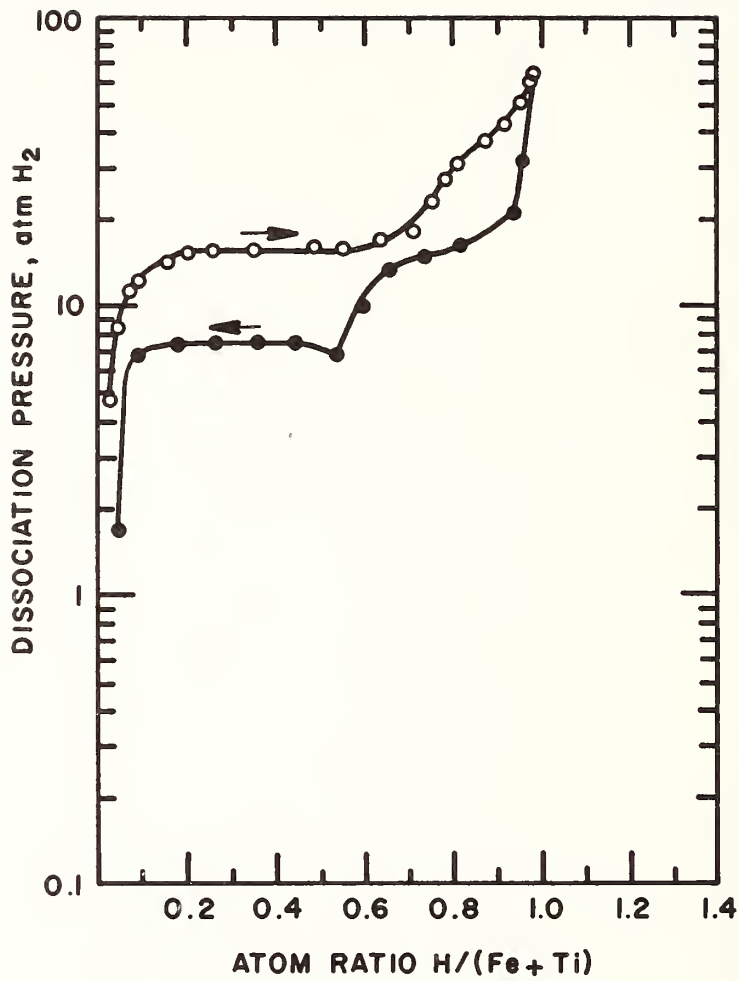


FIGURE 3 - FeTi-H CHARGING AND DISCHARGING CURVES AT 40°C.

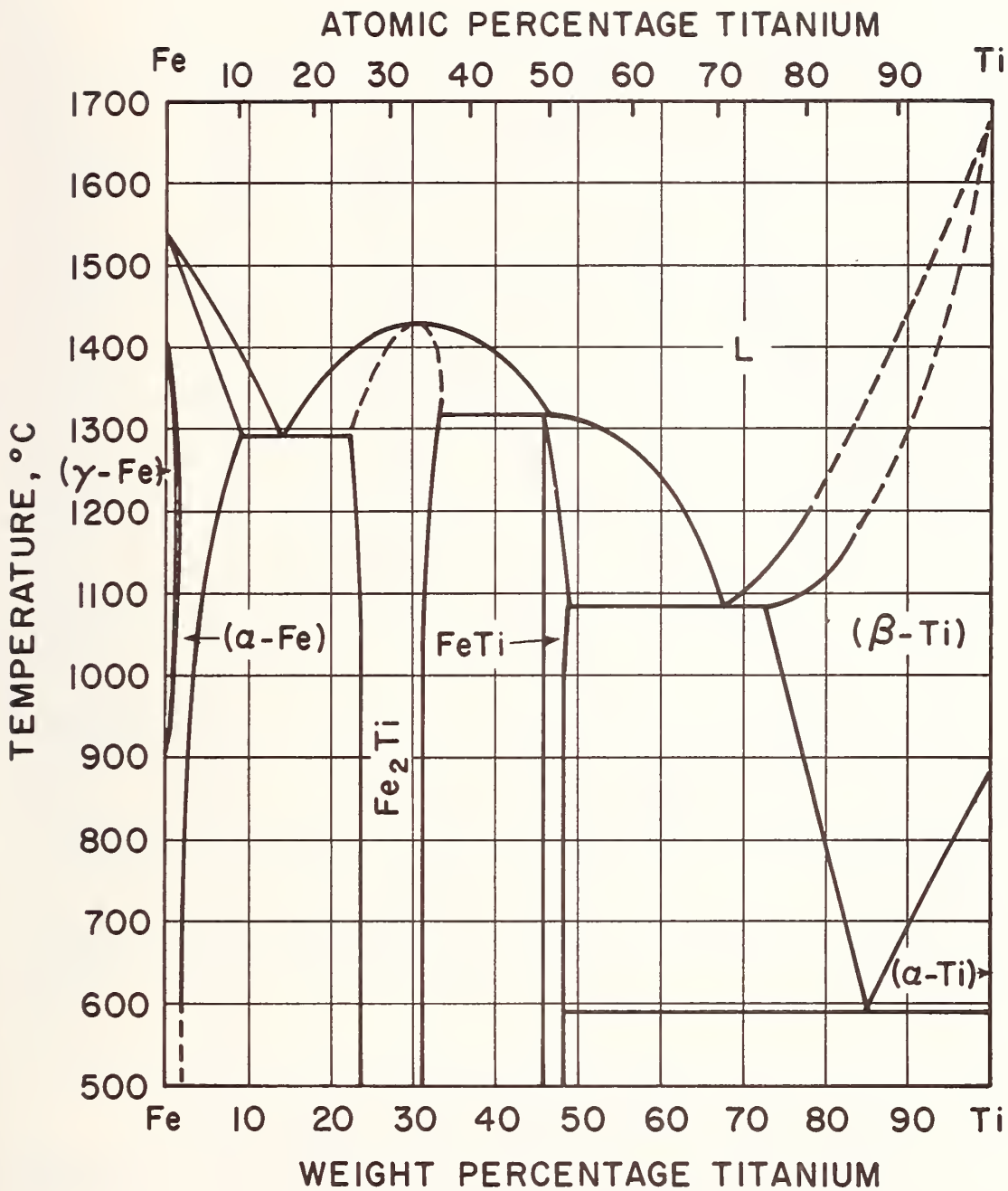


FIGURE 4 - Fe-Ti PHASE DIAGRAM. (AFTER REF. 8)

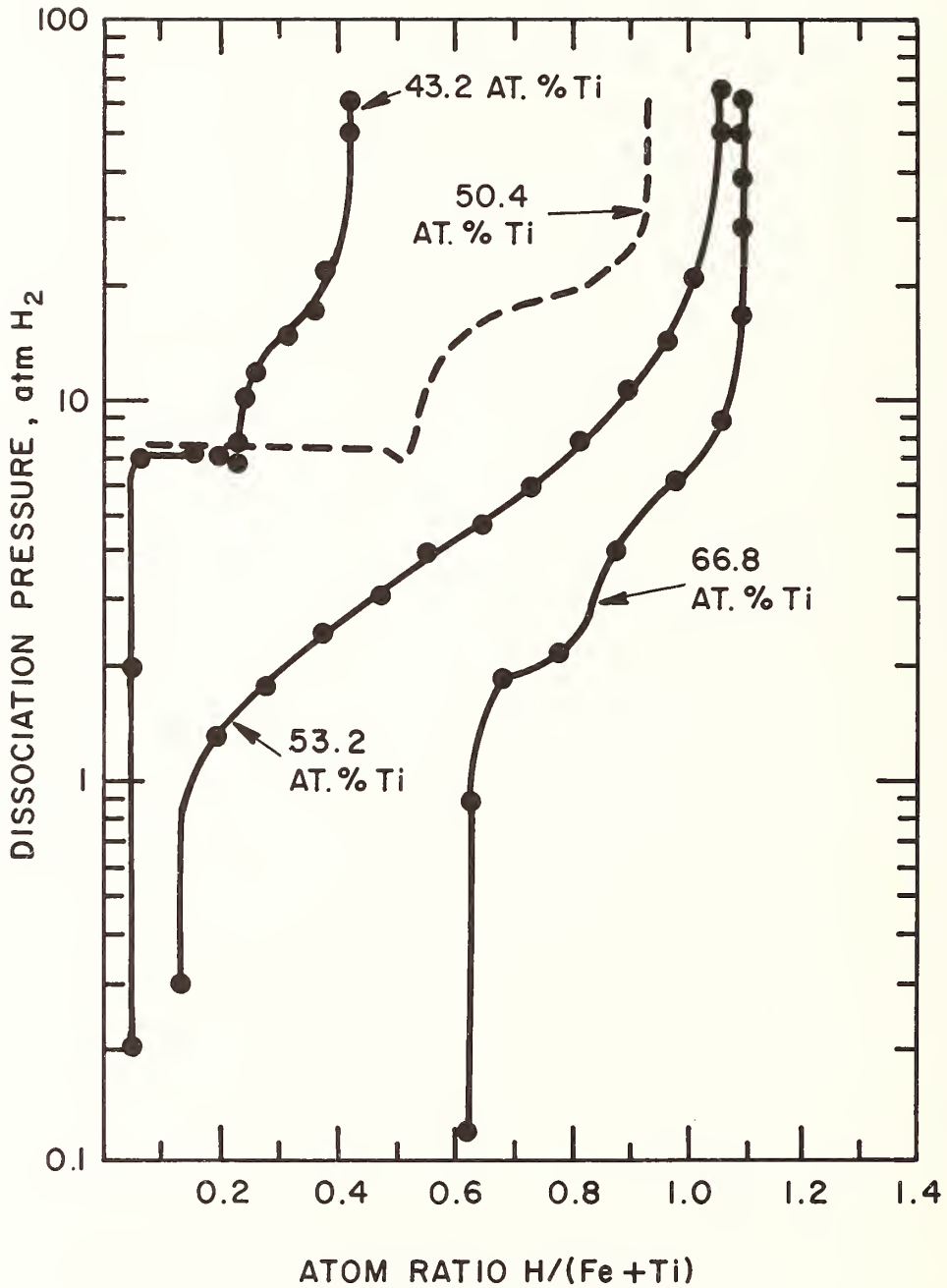


FIGURE 5 - EFFECT OF Ti CONTENT ON 40°C DESORPTION ISOTHERM OF Fe-Ti ALLOYS.

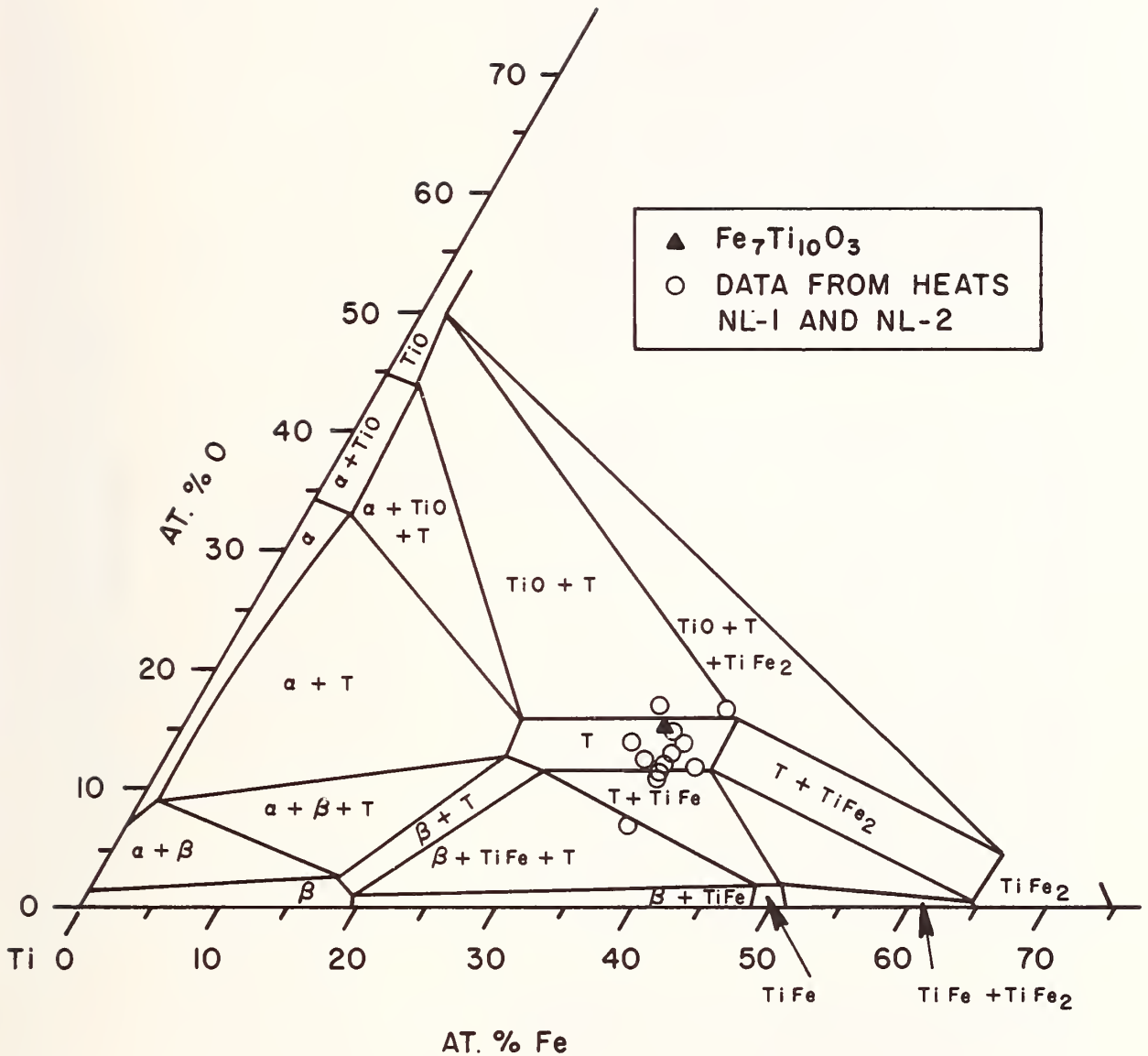


FIGURE 6 - MICROPROBE DATA FOR O-RICH SECOND PHASE PARTICLES FOUND IN MICROSTRUCTURE OF O-CONTAINING FeTi HEATS COMPARED TO THE Ti-Fe-O TERNARY PHASE DIAGRAM OF ROSTOKER (REF. 9). HEATS STUDIED CORRESPOND TO FIG. 7b AND c.



(a) 0.010% O



(b) 0.062% O



(c) 0.30% O

FIGURE 7

EFFECT OF OXYGEN CONTENT (IN WT. %) ON THE MICROSTRUCTURE OF FeTi
250X

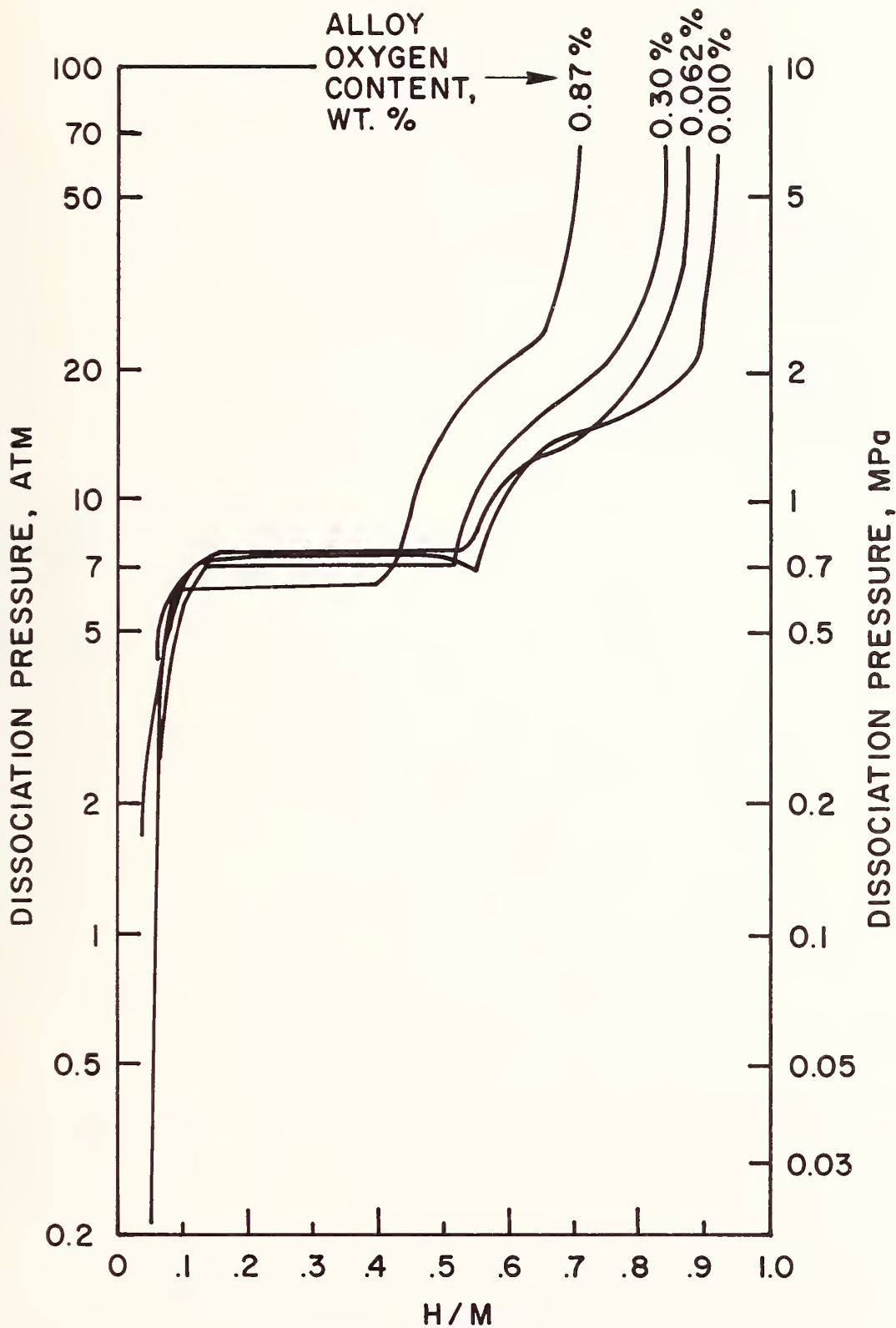


FIGURE 8 - EFFECT OF ALLOY OXYGEN CONTENT ON THE 40°C HYDROGEN DESORPTION ISOTHERM OF FeTi.

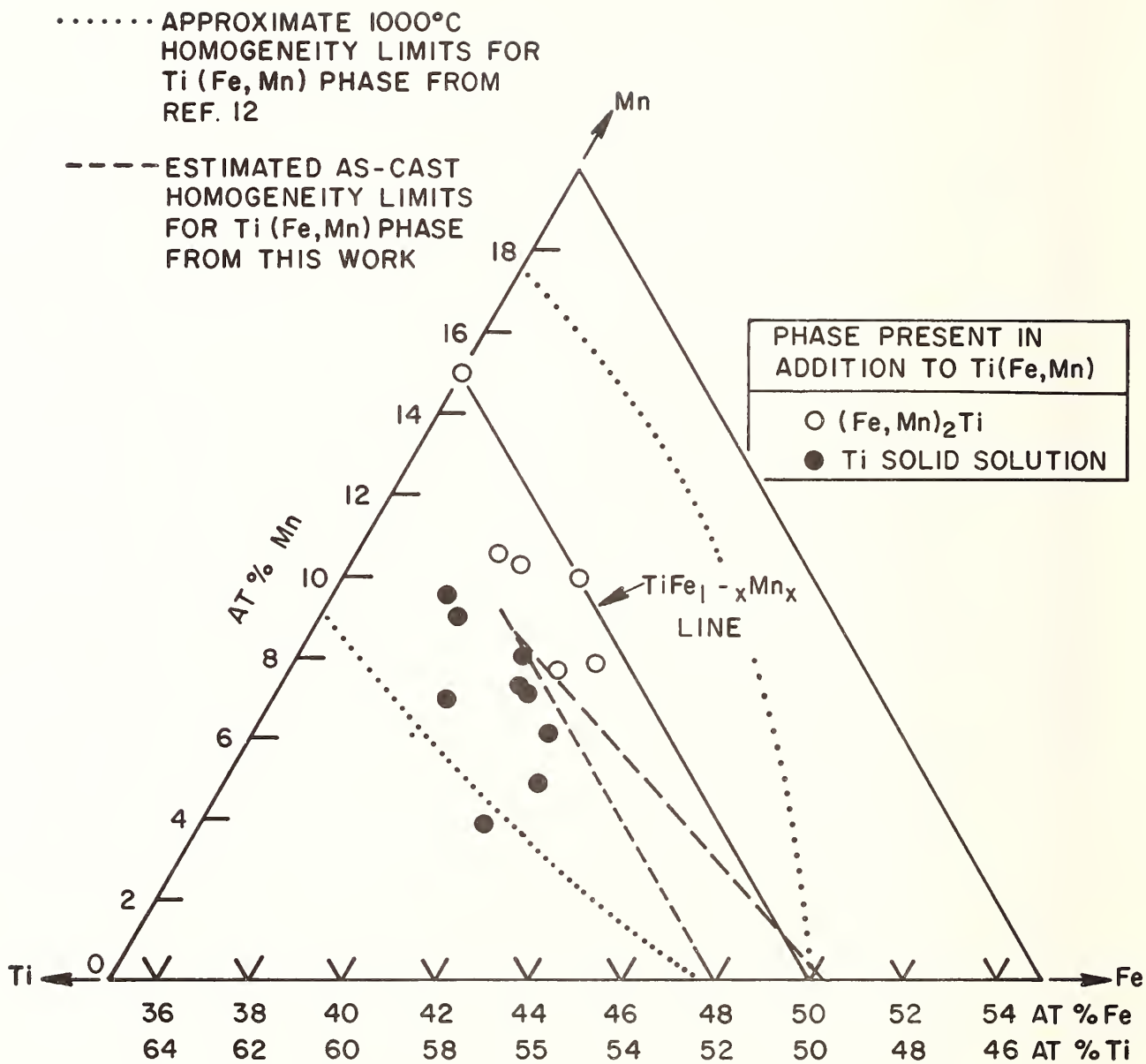


FIGURE 9 - Ti-Fe-Mn ALLOYS STUDIED IN AS-CAST
CONDITION COMPARED TO THE 1000°C
TERNARY PHASE DIAGRAM OF REF. 12.

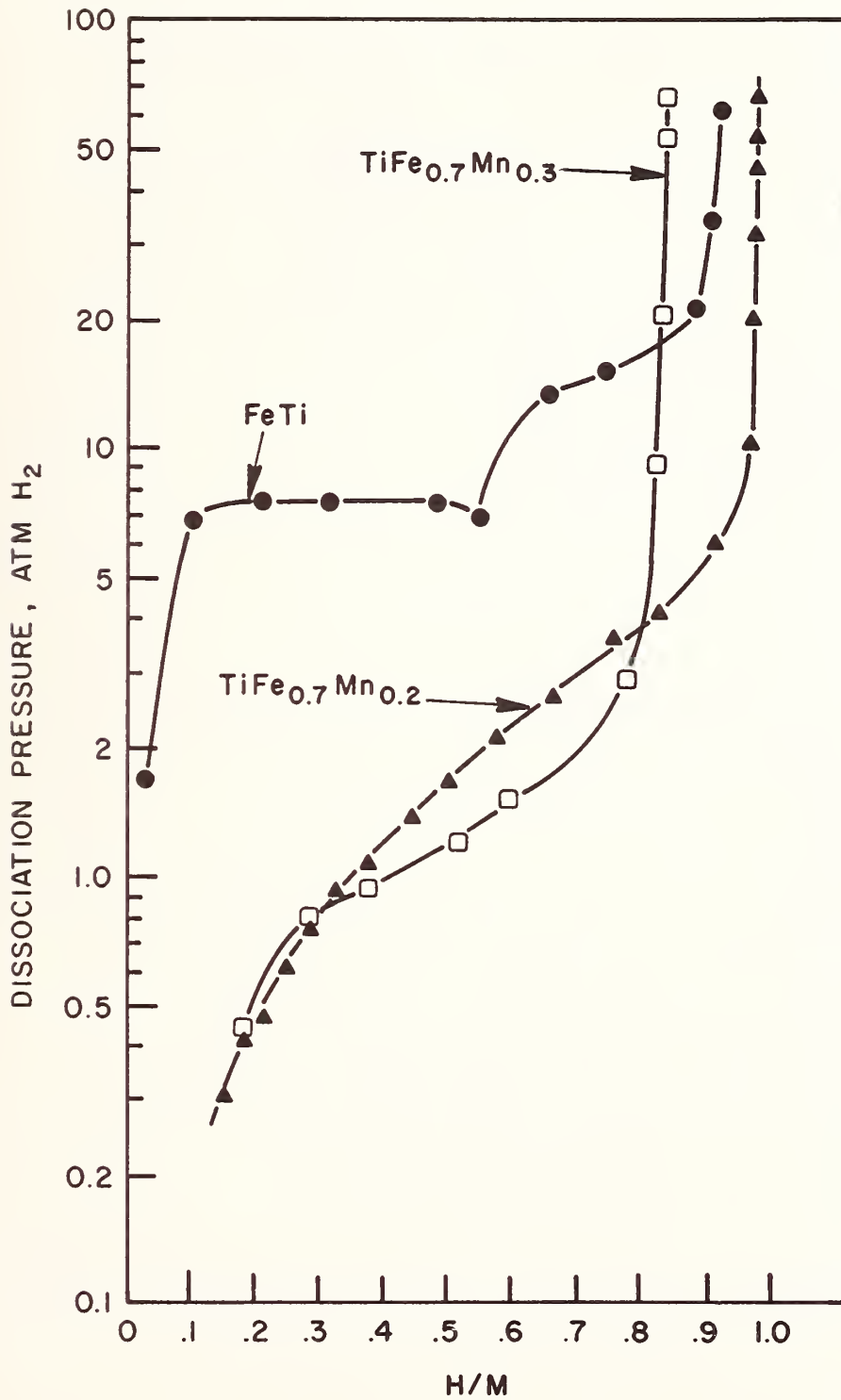


FIGURE 10 - EFFECT OF Mn SUBSTITUTION ON THE 40°C DESORPTION ISOTHERM OF FeTi.

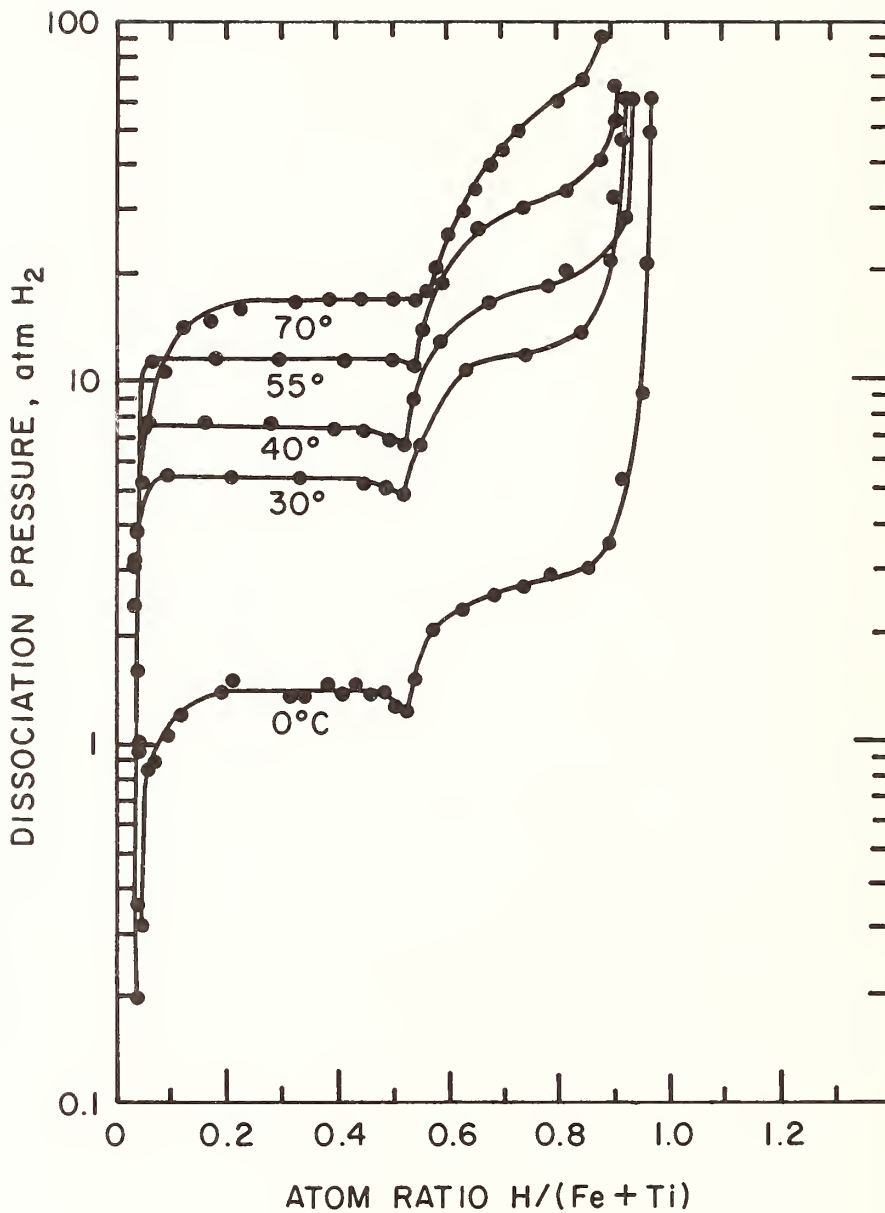


FIGURE II - PRESSURE-COMPOSITION ISOTHERMS FOR THE FeTi-H SYSTEM.

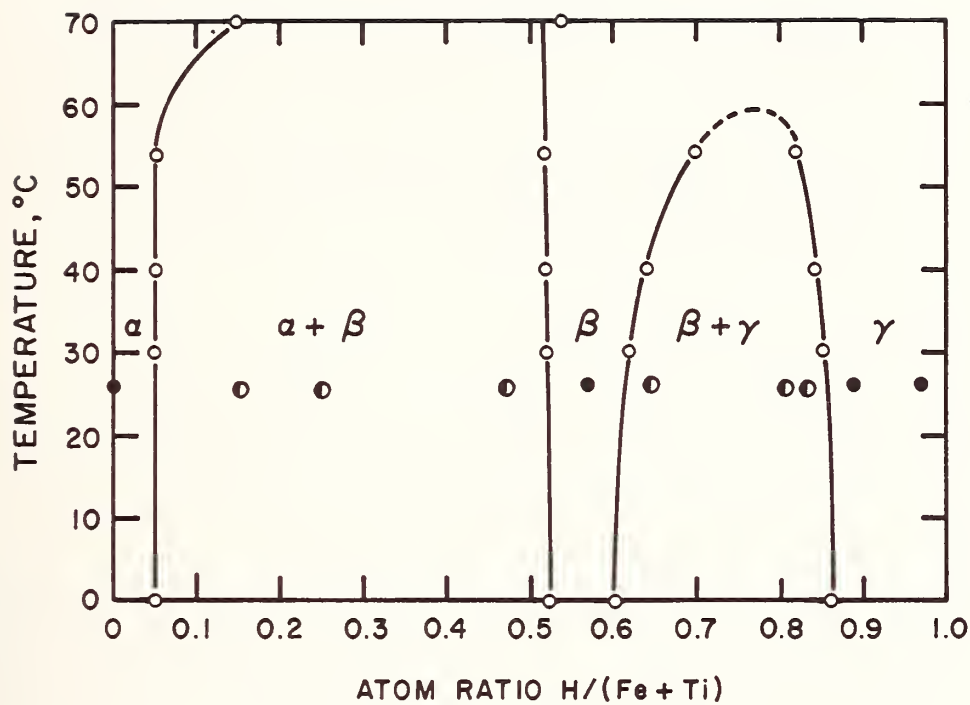


FIGURE 12 - PHASE DIAGRAM OF THE FeTi-H SYSTEM AS DERIVED FROM PRESSURE - COMPOSITION DATA. X-RAY DIFFRACTION PATTERNS TAKEN AT COMPOSITIONS INDICATED: ●, ONE SOLID PHASE, ○, TWO SOLID PHASES. $\alpha = \text{FeTi}$, $\beta \approx \text{FeTiH}$, $\gamma \approx \text{FeTiH}_2$.



Phase Equilibria in the System $\text{MgO-RC}\ell$ ($\text{R}=\text{Li, Na and K}$)
Solution under Hydrothermal Conditions by Means of a
Capsule Bursting Method

Shigeyuki Sōmiya, Kazuo Nakamura, Shin-ichi Hirano and
Shinroku Saito

Research Laboratory of Engineering Materials
Tokyo Institute of Technology
Ookayama, Meguroku, Tokyo, 152, Japan

Introduction

Brucite $\text{Mg}(\text{OH})_2$, is one of the raw materials to produce basic bricks. Brucite is obtained from sea water by precipitation or as natural rock which occurs in hydrothermal veins. The researches on the phase equilibrium in the system $\text{MgO-Mg}(\text{OH})_2$ in pure water have been carried out by many researchers by means of various methods including the thermodynamic calculation. The phase equilibrium curves obtained, however, dispersed in wide temperature range because of the difficulty of quench of periclase, MgO .

It is well known that the hydrothermal solutions often contain alkali chlorides. But the literature that can be found on the phase equilibria in the system $\text{MgO-Mg}(\text{OH})_2$ in alkali chloride solution, was scarce.

The purpose of the present work is to clear up the effect of the kind of the alkali chloride such as LiCl , NaCl and KCl on the phase equilibrium curve of the system $\text{MgO-Mg}(\text{OH})_2$ up to $1,500 \text{ kg/cm}^2$ by means of a capsule bursting method.

Experimental

In this investigation test-tube-type hydrothermal vessels were employed and water was used as a pressure medium. Pressure was measured with a 12 inch Heise Bourdon tube pressure gauge. Temperature was measured with a platinel thermocouple calibrated against the melting points of gold ($1,064.4^\circ\text{C}$) and zinc (419.5°C). Temperature

was controlled with an automatic electronic controller combined with a SCR system (Ohkura Electric Co. Ltd., Tokyo, Japan) within $\pm 3^{\circ}\text{C}$. The accuracy of pressure during a run was $\pm 30 \text{ kg/cm}^2$.

The starting material of MgO was prepared by calcination at 600°C in Pt crucible for 24 hrs from magnesium nitrate, which had been obtained by the reaction of reagent grade nitric acid (Wako Pure Chemical Industry, Osaka, Japan) and magnesium metal (99.94% Furukawa Magnesium, Tokyo Japan). Five molar percent solutions were prepared from reagent grade alkali chloride (Wako Pure Chemical Industry) and redistilled water.

A gold capsule, 3.0 mm in OD, 2.7 mm in ID and 35 mm in length, including the desired quantity of MgO powder and 5 mol% RCl solution was sealed by an electric arc. The quantity of H_2O in the capsule was from 0.6 to 0.8 in molar ratio necessary to convert MgO into $\text{Mg}(\text{OH})_2$.

The process of hydrothermal treatment are the same as in the study of the system $\text{MgO-Mg}(\text{OH})_2$ in pure water⁽¹⁾; that is, pressure was initially applied to the desired value and then the temperature was increased to the desired value at the constant pressure. Samples were subjected to the constant temperature and pressure for a given duration. After the run pressure was released quickly to the atmospheric pressure and subsequently the vessel was quenched in cold water. This process is called "Capsule Bursting Method".

If the set point of temperature and pressure was on the higher temperature side of the equilibrium curve, the capsule would be burst by unreacted solution. In contrast, if it was on the lower temperature side, water inside the capsule was completely consumed up to form $\text{Mg}(\text{OH})_2$. Therefore the capsule would not be burst but squeezed. After the run, the sample taken out of the capsule was examined by the Xray powder diffraction method using copper K_{α} radiation. The result was accepted when the results of Xray powder diffraction coincided with those of the capsule bursting method of two set of the capsules in one vessel.

Results and Discussion

The outside feature of the capsule showed the stable phase which existed in the capsule at each temperature and pressure in the system containing alkali chloride solution as in the system with pure water.

The phase equilibrium curves in LiCl solution, NaCl solution and KCl solution obtained are shown in Figs. 1, 2 and 3, respectively. Fig. 4 shows these curves including one in the system of MgO- pure H₂O which was studied by authors with the same method.¹⁾ The equilibrium temperatures of each system at 500, 1,000 and 1,500 kg/cm² are shown in table 1. For example, equilibrium temperatures at 1,000 kg/cm² are 517°C in 5 mol% LiCl solution, 559°C in 5 mol% NaCl solution and 537°C in 5 mol% KCl solution. On the other hand it is 595°C in pure water.

All the equilibrium curves in RCl solution are in lower temperature side than that in pure water except for the region below about 200 kg/cm² in NaCl solution. The three equilibrium curves in RCl solution are nearly parallel and steeper than that in pure water. The effect of LiCl on lowering the equilibrium temperature is the greatest among the three kinds of solutions. The order of the effect, however, does not obey the order in the periodic table. It is known that such the effect is raised by the decrease of the fugacity of water due to the interaction of solute with water.²⁾

From these results, the capsule bursting method is recognized as one of the acceptable methods for the study of phase equilibria under hydrothermal conditions whenever the reaction rate of hydration is rapid.

Reference

- 1) S. Hirano, K. Nakamura and S. Sōmiya
Am. J. Sci, submitted
- 2) H. L. Barnes and W. G. Ernst, Am. J. Sci, 261 129 (1963)

Table 1. Phase equilibrium temperatures of the system $\text{Mg}(\text{OH})_2\text{-MgO}$ in pure water, 5 mol% LiCl solution, 5 mol% NaCl solution at 500, 1,000 and 1,500 kg/cm^2 .

	Pressure (kg/cm^2)		
	500	1,000	1,500
System of $\text{Mg}(\text{OH})_2\text{-MgO}$			
pure water ¹⁾	567	595	614
5 mol% LiCl solution	505	517	524
5 mol% NaCl solution	553	559	562
5 mol% KCl solution	530	537	544

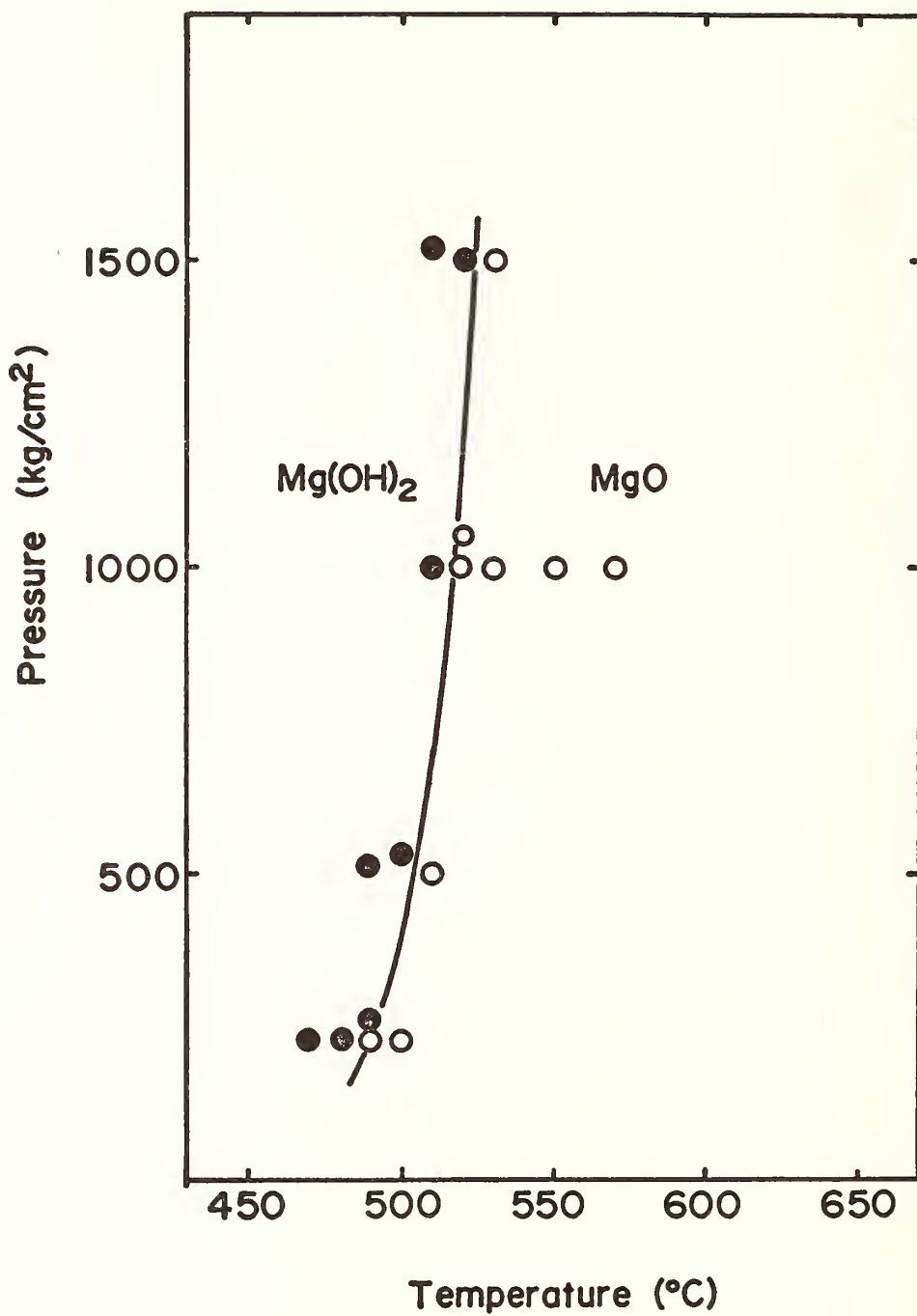


Fig.1 P-T diagram of the system MgO-Mg(OH)₂ in 5 mol% LiCl solution.

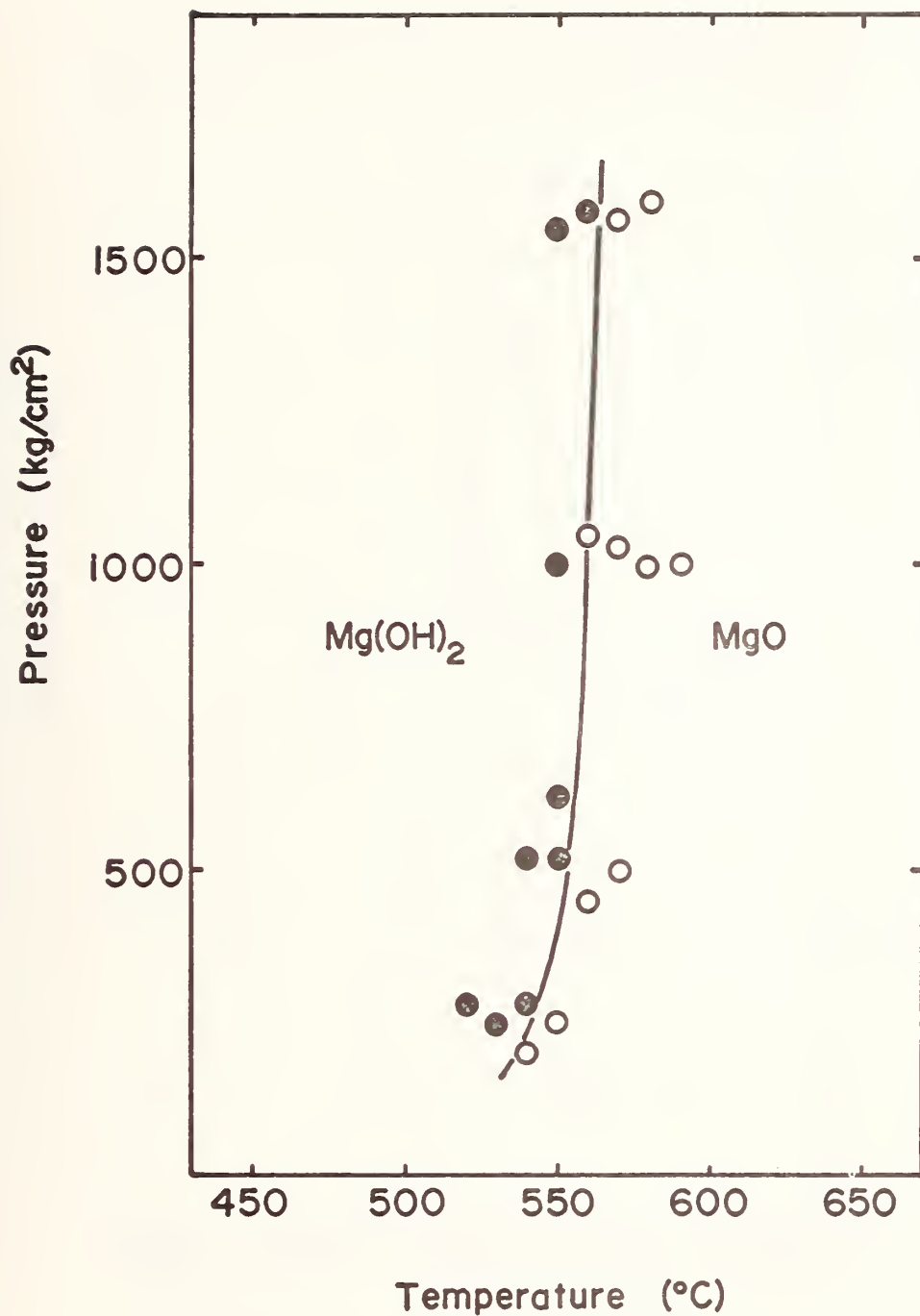


Fig.2 P-T diagram of the system MgO-Mg(OH)₂ in 5 mol% NaCl solution.

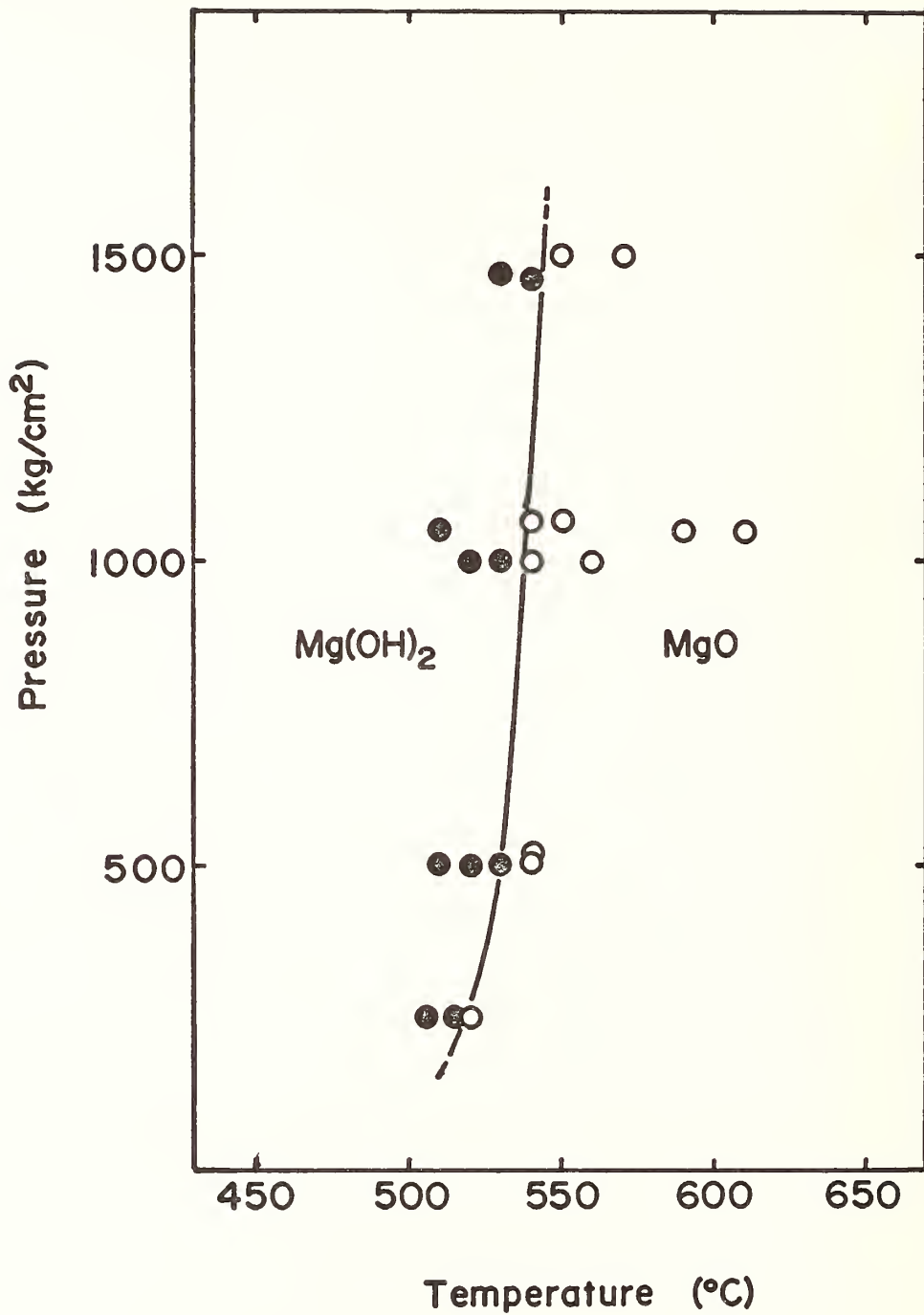


Fig.3 P-T diagram of the system MgO-Mg(OH)₂ in 5 mol% KCl solution.

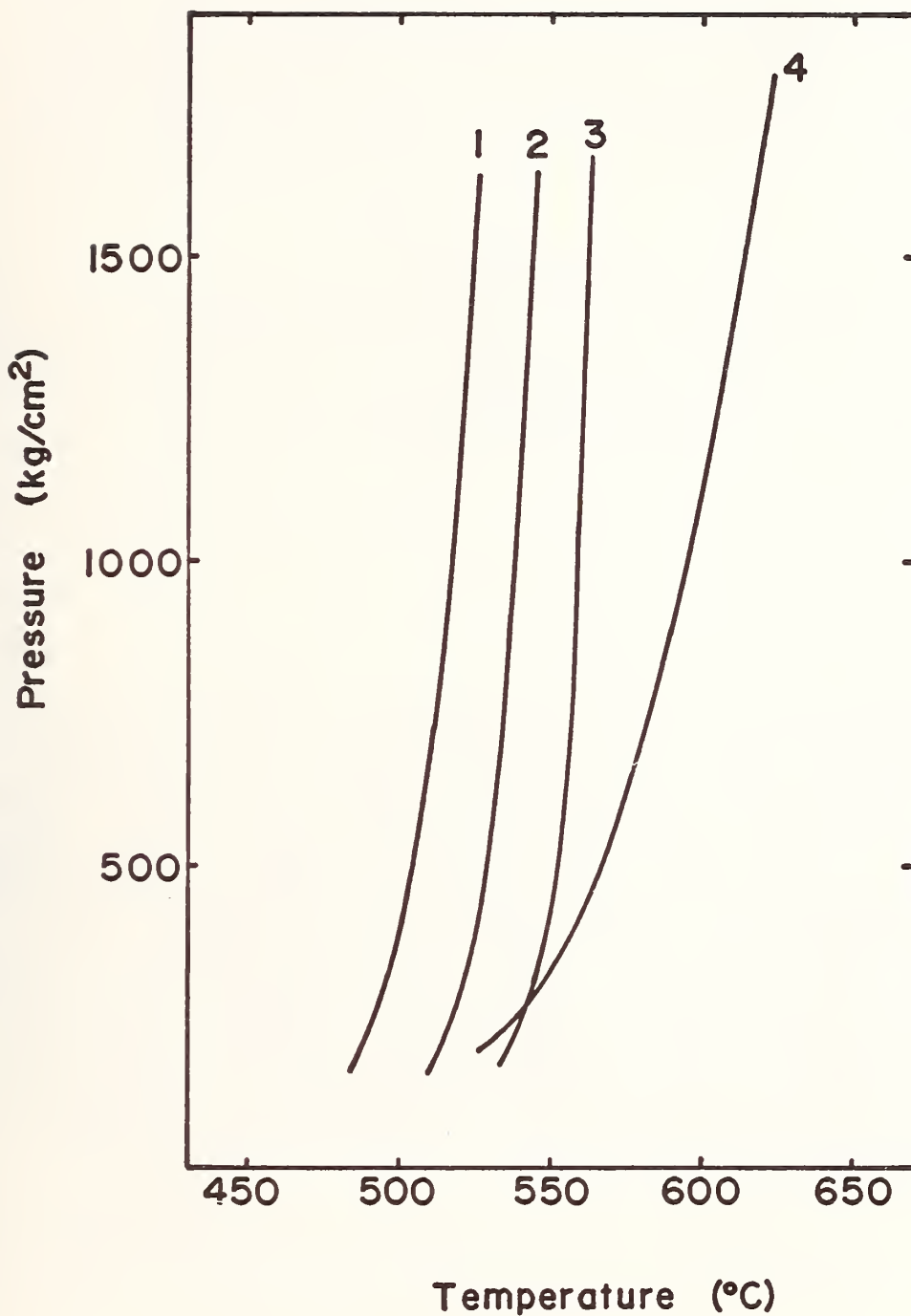


Fig.4 P-T diagram of the system MgO-Mg(OH)₂ in 5 mol% LiCl soln.(1), 5 mol% KCl soln. (2), 5 mol% NaCl soln.(3) and pure water (4).



HIGH-ENERGY ION BEAMS IN PHASE DIAGRAM DETERMINATION*

J. E. Smugeresky
Metallurgy & Electroplating Division 8312

S. M. Myers
Ion-Solid Interactions Division 5111
Sandia Laboratories

ABSTRACT

Phase boundaries can now be investigated by a new approach which uses high-energy ion beams. The technique makes use of ion implantation and ion backscattering analysis combined with diffusion annealing treatments. Ion implantation of solute elements into the matrix is used to create a super-saturated solid solution in the first $\cong 0.1 \mu\text{m}$ of the sample. During isothermal annealing the composition-versus-depth profile is monitored nondestructively via 2 MeV He backscattering. These profiles and the appropriate boundary conditions for the diffusion equation can be used to obtain the phase boundaries. The advantages of this technique are threefold: (1) solubility measurements can be made at lower temperatures than by other techniques; (2) the composition can be accurately tailored in complex systems; and (3) very low solubilities can be monitored. This technique has been applied to both binary and ternary systems, and solubilities as low as 70 appm and at temperatures lower by almost 300K have been measured.

*This work was supported by the United States Energy Research and Development Administration. Contract Number AT-(29-1)-789.

HIGH-ENERGY ION BEAMS IN PHASE DIAGRAM DETERMINATION

Introduction

The various methods used in phase diagram determination include classical quenching techniques, thermal analysis, electrical conductivity measurements, metallographic methods, thermal gravimetric analysis, dilatometric analysis, X-ray diffraction techniques, and electromotive force measurements in galvanic cells.^{1,2} The most widely used method involves thermal analysis or differential thermal analysis. However, in cases where temperatures are low, phase transformations tend to be sluggish and the temperature of transformation becomes difficult to assess. In addition, there are cases in which the solid solubility is quite low and thus the accurate determination of phase boundaries becomes quite difficult. It is these situations that led the authors to develop a new technique which uses high-energy ion beams to determine these boundaries more easily and accurately.

In this paper, we will first describe in general terms the technique used to measure solid solubilities, then give the analytical details of the technique, and finally discuss specific examples of its application thus far in both binary and ternary systems.

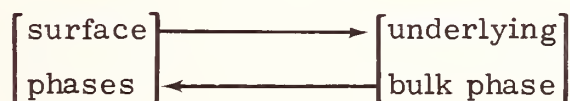
General Description of Method

It is helpful to first consider the sample schematically (Figure 1) by dividing it into three regions: A, the near-surface region; B, the underlying bulk region; and C, the unaffected bulk region equivalent to the starting condition of the sample. Initially, all regions are identical. Then solute ions are accelerated toward the surface with sufficient energy to penetrate the sample and occupy region A. Although the width of this implanted region and the amount of solute contained within it can vary, this region is typically $0.1 \mu\text{m}$ (100 nm) wide and the distribution of solute generally approximates a Gaussian peak. The peak concentrations in region A are typically greater than the solubility, the amount being dependent on the particular systems studied. However, no precipitation of second phases occurs, because the implantation is done at room temperature where the atom mobilities are essentially nil. In effect, the implanted region consists of a supersaturated solid solution.

The implanted concentration can easily be tailored to concentrations much less than 100 percent solutes as is the case in most simple diffusion couples. This is an important benefit most useful when more complex situations are under study, as in the ternary systems described below.

After implantation, an ion backscattering profile is taken to establish the starting conditions. This is done by analyzing the helium backscattering spectrum. From this spectrum, both the identity and the depth distribution of solute or impurity elements can be determined. At this point regions B and C are identical and represent the original condition of the sample.

Next, a diffusion anneal at a temperature of interest is given to the sample. During the anneal, the atoms become mobile enough for precipitation of a second phase, or phases, to occur in region A, the implanted region. At the same time, the excess solute atoms diffuse from the implanted layer into the underlying bulk of the sample (region B). However, precipitation in the implanted region occurs much faster than the diffusion of excess solute into the underlying bulk, so that almost all of an anneal sequence consists of a flow of solute between two well-defined phases at the interface of regions A and B. The situation is not much different from that of a diffusion couple in which a condition of thermodynamic equilibrium exists between these regions, i. e.,



Consequently, the composition of the various phases remains constant during annealing, provided there is an excess of solute atoms in the implanted region. The change that takes place during annealing is in the relative amounts of each phase.

Following the anneal, a second backscattering spectrum is obtained to provide a composition-versus-depth profile. A mathematical analysis of the annealing kinetics allows both the solid solubility and the diffusivity of the solute to be determined. This analysis consists of the application of Fick's law with the appropriate boundary condition.

The measurement of solid solubilities at lower temperatures than by other techniques is possible because of the microscopic scale of the experiment. The implanted layer is typically 0.1 μm thick, so that diffusion

distances need not be very large. Consequently, shorter annealing times are sufficient to get the data at low temperatures. Ion backscattering analyses are ideally suited for microscale situations because of the capability of probing to small depths at high resolution. For helium ions, the maximum depth that can be probed is $2 \mu\text{m}$ while the resolution is of the order of $0.01 \mu\text{m}$. This is a nondestructive technique that can follow the changes in concentration with time. The high resolution and the straightforward quantitative calibration in both depth and concentration are its best assets. Even in cases which require more time, the time necessary for the anneal can be shortened by a factor of typically one to two orders of magnitude by using a modified implant sequence to enhance the diffusion of the solute of interest. By implanting either a lighter element or the solvent element somewhat deeper than the solute implant, a region in which the diffusion rate is greatly enhanced is created between regions A and B as seen in Figure 1. While this modification may not work in all cases, it does allow measurements of solubility to be made at temperatures even lower than those of the unmodified procedure. Now that a general description of the method has been given, some details of the analysis will be described.

Ion Backscattering Analysis

The backbone of this technique is the ion backscattering spectrum. This spectrum is a plot of yield Y , in counts per keV, versus the energy E , in MeV of the backscattered ions. The energy of the backscattered helium ions is dependent upon the atomic mass m of the elements present in the target and the incident ion energy before backscattering. Hence, the fraction of incident ion

energy that is retained by the backscattered ions increases with the atomic mass, as shown in Figure 2. The yield is related to the amount of that element present, as well as to its atomic number Z . The depth at which the element is located also affects the energy of the backscattered ions. Continuous energy losses occur as a result of electronic excitations as the ion traverses the lattice before and after backscattering. Consequently, if all of a particular element were present at the surface, a spike in the yield would occur at the energy corresponding to the fraction of retained energy for that element. For example, a 2 MeV helium ion would retain 0.753 of its incident energy if iron were present and a spike in yield would appear at an energy equal to 1.506 MeV. Several elements and the corresponding fractions of retained energy are indicated on the right margin of Figure 2. If one or more of these impurities is distributed within the sample, the corresponding spike becomes a concentration profile indicating just how the impurity is distributed with depth into the sample. This can best be seen by considering Figure 3, a schematic ion back-scattering spectrum for a sample having three impurities present where $m_A > m_B > m_C$. In this example, element A is confined to an infinitely thin layer on the surface; element B is present in the first y μm of surface at a constant concentration, while element C has a Gaussian concentration distribution with a peak located a distance p from the surface.

The concentration at a given depth x is obtained by analytically transforming the yield-versus-energy (Y vs E) spectrum into a concentration-versus-distance (C vs x) profile for each element k present. Thus

$$Y_k = Y(E) \quad \text{for} \quad E \leq E_k \quad (1)$$

is transformed into

$$C_k = C_k(x) \quad (2)$$

where E_k corresponds to the energy retained by element k . Such a transformation is schematically shown in Figure 4 for a profile of an as-implanted element k . Consequently, one can study the change in profile during annealing by comparing the transformed spectra. The exact analytical expression for the concentration profile is found in the work of Chu, et al.;³ its evaluation in the general case is complex and requires numerical methods described by Brice.⁴ Calculations include electronic stopping rates for pure elements; these are taken from experimental results in the literature.⁵

Solubility Determination

Following a diffusion anneal, the concentration profiles are analyzed and both the solid solubility and the diffusion coefficient D can be determined. During the anneal, a discontinuity in the concentration profile exists at the interface of the implanted layer and the underlying bulk, i. e., the boundary between regions A and B as shown in Figure 5. When this discontinuity remains constant with annealing time at a given concentration C_0 , it indicates that a condition of local thermodynamic equilibrium exists at the interface between regions A and B. This concentration value C_0 is the solubility of the implanted element, and the profile in region B is described by solving the diffusion equation

$$\frac{\partial C(x, t)}{\partial t} = D \frac{\partial^2 C(x, t)}{\partial x^2} \quad (3)$$

where D , the diffusion coefficient, is assumed constant. The initial condition is

$$C(x > 0, t = 0) = 0 \quad (4)$$

and the boundary condition is

$$C(x = 0, t) = C_0 \quad (5)$$

where x is measured from the intersection of the peak and a diffused tail (i. e., boundary of regions A and B in Figure 5). The solution is readily obtained⁶ as

$$C(x, t) = C_0 \operatorname{erfc} \left(\frac{x}{2\sqrt{Dt}} \right) \quad (6)$$

When the actual data are compared with a family of plots for different values of D , the curve with the best fit gives the diffusion coefficient. Since the emphasis here is on phase boundaries, details for diffusivity studies are not described, but they can be found in References 7, 8, and 9.

Enhanced Diffusion

As the temperature of the diffusion anneal becomes lower, the time required for sufficient diffusion to occur becomes longer. Even though the ion beam technique is on a microscopic scale and thus requires only small diffusion distances, the lower temperature diffusion anneals can still become prohibitively long. In these cases, diffusion can be enhanced by implanting a second element in addition to the solute and deeper than the solute. In effect, this introduces an intermediate region between regions A and B in Figure 1, which we will call region A'. The as-implanted profile of the solute of interest

is essentially unaffected by this procedure. However, after the anneal, the shape of the diffused tail is qualitatively different, in that it exhibits a plateau in region A'. The concentration profile in region A is essentially the same as for the normal implant procedure, while in region B much less solute diffuses because of the low temperature and short anneal time. The implantation of the second element, which can be an inert element such as neon or the solvent itself, produces lattice damage in the sample just beyond the implanted solute. This allows the solute to diffuse more rapidly than before so that the concentration builds up to the solubility limit more rapidly in the damaged lattice. Consequently, the plateau concentration corresponds to the solubility. However, the equilibrium diffusion coefficient cannot be determined by this procedure. In addition, the applicability of enhanced diffusion may not be as general as the normal implantation procedure described above. It has been applied to several systems but has not been successful in all cases. Now that the techniques have been discussed generally, a deeper insight can be gained from the specific examples described below.

Applications

(a) Binary Cases The first systems investigated by the authors used beryllium as the solvent. This metal perhaps represents the most ideal case, since it has so low a Z that any impurity or solute element of interest has a higher Z . Consequently, the backscattered energy of the host material

is lowest and this allows easy resolution on the backscattered spectrum of any solute of interest. The implanted solute species were copper, iron, and aluminum.^{7, 8} The as-implanted backscattered spectrum for the beryllium-copper binary system is shown in Figure 6. In these experiments, the usual configuration for ion backscattering measurements with 2 MeV helium was used.³

A magnetically analyzed helium beam from a Van de Graff accelerator was collimated to a 1 mm square and allowed to strike the sample normal to its surface. A silicon surface-barrier detector of 25 mm² surface area and 13 keV FWHM (full width at half maximum) resolution faced the sample at a distance of 180 mm at an angle of 170 degrees from the incident beam. The backscattered ions produced a current pulse with an amplitude proportional to energy and a spectrum of these energies was accumulated by a multichannel analyzer. The beam current was $\cong 40$ nA and an accumulated charge of the order of 20 μ C (i. e., $\sim 10^{16}$ He/cm²) per spectrum was used. Effects of the helium analysis beam on the experimental results were checked by sampling a virgin spot periodically, but no significant differences were ever found. An additional measure when the solubilities were low involved use of a second set of collimation slits to reduce halo effects⁷ about the incident beam.

The transformed data are shown in Figure 7 for both the as-implanted and after-annealing conditions. Actual values of solubility of copper in beryllium were measured at 593K, 673K, 773K and 1023K.^{8, 9} A plot of the solubility versus T^{-1} (Figure 8) resulted in the following relation for the solubility:

$$C_0(\text{Cu}) = (12.6 \text{ atomic percent}) \exp\left(\frac{-842\text{K}}{T}\right) \quad (7)$$

Included in the plot are values from other workers,^{10, 11} showing the excellent agreement between data obtained using high-energy ion beams and data obtained by other techniques.

In the Be-Fe system, the solubility of iron is very low and is complicated by the role played by aluminum in commercial purity beryllium.¹² Previous workers^{10, 13, 14} had measured the solid solubility, but only at temperatures above 973K. By using this high-energy ion beams technique, the present authors⁷ made measurements at temperatures as low as 773K. A plot of the solubilities, which are less than 0.2 at.%, versus T^{-1} (Figure 9) resulted in the relation:

$$C_0(\text{Fe}) = (14.0 \text{ at. } \%) \exp\left(\frac{-5246\text{K}}{T}\right) \quad (8)$$

A comparison with data gathered at higher temperatures^{10, 13} showed excellent agreement.

The validity of the application of the diffusion equation and assumed boundary condition was subjected to two additional checks: (1) the amplitude of the diffused tail at the discontinuity should be independent of both anneal time and the amount of implanted iron at a given temperature and (2) the amount of iron per unit area L which has diffused from the implanted region should vary with the isothermal anneal time t as⁷

$$L(t) = C_0 \left(\frac{4Dt}{\pi}\right)^{1/2} \quad (9)$$

Both of these criteria were satisfied with the relationship between L and t shown in Figure 10.

In the case of aluminum, the solubility was below the limits of detectability of the apparatus. The upper bound was established as 70 appm at both 873 and 1073K.

The enhanced diffusion technique has been used in the Be-Cu system to determine the solubility at 593K. The second implanted species was neon, which was immobile during the anneal. The concentration profiles for Cu and Ne after the anneal are shown in Figure 11. Here it is seen that the plateau in the copper profile overlaps the neon-implanted region. This technique resulted in an anneal time of only 175 hours instead of the six months required for normal diffusion rates. Thus the time required to do the experiment was dramatically reduced.

As a consistency check, the enhanced diffusion technique was also used for 673K. The solubilities measured were 3.62 at. % for the normal diffusion case and 3.50 at. % for the enhanced diffusion case, both well within the experimental error.

(b) Ternary Cases The ternary systems investigated were Be-Fe-Al, Be-Cu-Al, Be-Cu-Si.^{7,8} The primary concern here was the effect of the third element on the solubility of the primary solute: in essence, the effects of aluminum and/or silicon on the solubility of iron and copper in beryllium.

The ternary solute effect was strongest for the Be-Fe-Al system, in which the presence of aluminum reduced the solubility of iron below the limits of detectability by this technique, i. e., less than 100 appm for temperatures less than 1123K. This represents an order of magnitude decrease.

In the case of Be-Cu-Al,⁸ the effect was well within the experimental error. At 773K the solubility of Cu is 4.25 atomic percent, while in the presence of aluminum, a value of 4.15 atomic percent was measured.

Silicon, however, made a measurable difference. At 673K the measured solubility of copper was 3.6 atomic percent in the binary case but dropped to 2.82 atomic percent in the presence of silicon.

In each of the ternary cases noted here, the implantation concentration was sufficient to ensure the establishment of equilibrium at the interface between regions A and B of the sample. The situation is entirely analogous to the binary if the implant concentration is high enough and the overall composition of regions A and B in Figure 1 is in a three-phase region of the phase diagram. Thus the implanted concentration must not only exceed the solubility on the binary leg of a ternary diagram, but also ensure establishment of a three-phase equilibrium locally. With reference to Figure 12, this amounts to being at points Y or Z instead of X. In these situations, the diffusion equation solutions used for the binary case are still valid. However, if the sample is at composition X in Figure 12, more complex analytical solutions are required. As yet, these have not been developed.

As a check on the establishment of equilibrium consistent with points Y and Z in three-phase equilibrium, samples were examined by transmission electron microscopy.¹⁵ The presence of these phases was established by diffraction analysis. Similar confirmation has also been obtained for binary systems.¹⁵

In the ternary cases, the requirement of obtaining specific concentrations to ensure the attainment of equilibrium for three phases at various regions of the phase diagram is easily satisfied by ion implantation. The local concentration corresponding to the peak of the Gaussian distribution can easily be modified and does not have to be 100 percent as is the case in vapor-deposited layers in diffusion couple studies. In the examples described above, peak concentrations were of the order of 20 atomic percent at a depth of approximately $0.04 \mu\text{m}$ with a full width at half amplitude of $0.04 \mu\text{m}$; this is in excellent agreement with values calculated from the ion range theory of Brice.¹⁶ This ability to tailor the composition locally greatly facilitates studies in complex situations.

Summary

We have described here a new technique for determining phase equilibria in condensed systems. It consists of ion implantation of solute species in the first $\approx 0.1 \mu\text{m}$ of the sample at concentrations less than 100 percent, combined with ion backscattering analysis of samples subjected to diffusion anneals.

By an analytical transformation of the ion backscattering spectrum, the concentration profile of the solute species is obtained. An analysis of this profile, along with the application of the diffusion equation, allows determination of the solid solubility, but can also be used to obtain the diffusion coefficient of the solute. This technique can be applied to both binary and ternary systems for solid solubility measurements. The main

advantages are (1) solubility measurements at lower temperatures than by other techniques (examples were given for almost 300K lower); (2) the ability to tailor the implanted composition accurately at values considerably less than 100 percent to suit the needs of complex situations; and (3) the ability to measure very low solubilities. The technique is best applied to situations in which the solute elements have a higher atomic number than the solvent. So far, this technique has been applied to both binary and ternary systems where beryllium was the solvent, with the solubilities of iron and copper being measured at temperatures almost 300K lower than had been previously reported.

REFERENCES

1. A. Reisman, Phase Equilibria, Academic Press, 1970.
2. J. B. Macchesney and P. E. Rosenberg, Phase Diagrams, Vol. 1, ed. by A. M. Alper, Academic Press, 1970, p. 114.
3. See W. K. Chu, J. W. Mayer, M. A. Nicolet, T. M. Bach, G. Ansel, and F. Eisen, Thin Solid Films, 17 (1973) 1, for a review of ion beam analysis.
4. D. K. Brice, Thin Solid Films, 19 (1973), p. 121.
5. See, for example, J. F. Ziegler and W. K. Chu, Atomic Data and Nuclear Data Tables, 13 (1974), p. 463.
6. P. G. Shewmon, Diffusion in Solids, McGraw Hill, 1963.
7. S. M. Myers and J. E. Smugeresky, Met. Trans. 7A (1976), p. 795.
8. S. M. Myers and J. E. Smugeresky, to be published in Met. Trans. A.
9. S. M. Myers, S. T. Picraux, and T. S. Prevender, Phys. Rev. B 9 (1974), p. 3953.
10. M. L. Hammond, A. T. Davinroy and M. I. Jacobson, Beryllium-Rich End of Five Binary Systems, Air Force Materials Laboratory Report, AFML-TR-65-233, 1965.
11. A. R. Kaufmann, P. Gordon, and D. W. Lillie, Trans. ASM, 42 (1950), p. 785.

12. S. H. Gelles, Impurity Effects in Beryllium, Metals and Ceramics Information Center, Report MCIC 72-06, 1972, Columbus, OH.
13. G. Donze, R. LeHazif, F. Maurice, D. Dutilloy, and Y. Adda, Compt. Rendu., 254 (1962), p. 2328.
14. S. H. Gelles, J. J. Pickett, E. D. Levine, and W. B. Nowak, in "The Metallurgy of Beryllium," Inst. of Metals Monograph, London (1963), p. 588.
15. J. E. Smugeresky, G. J. Thomas, and S. M. Myers, unpublished research 1976.
16. D. K. Brice, Radiation Effects, 11 (1971), p. 227.

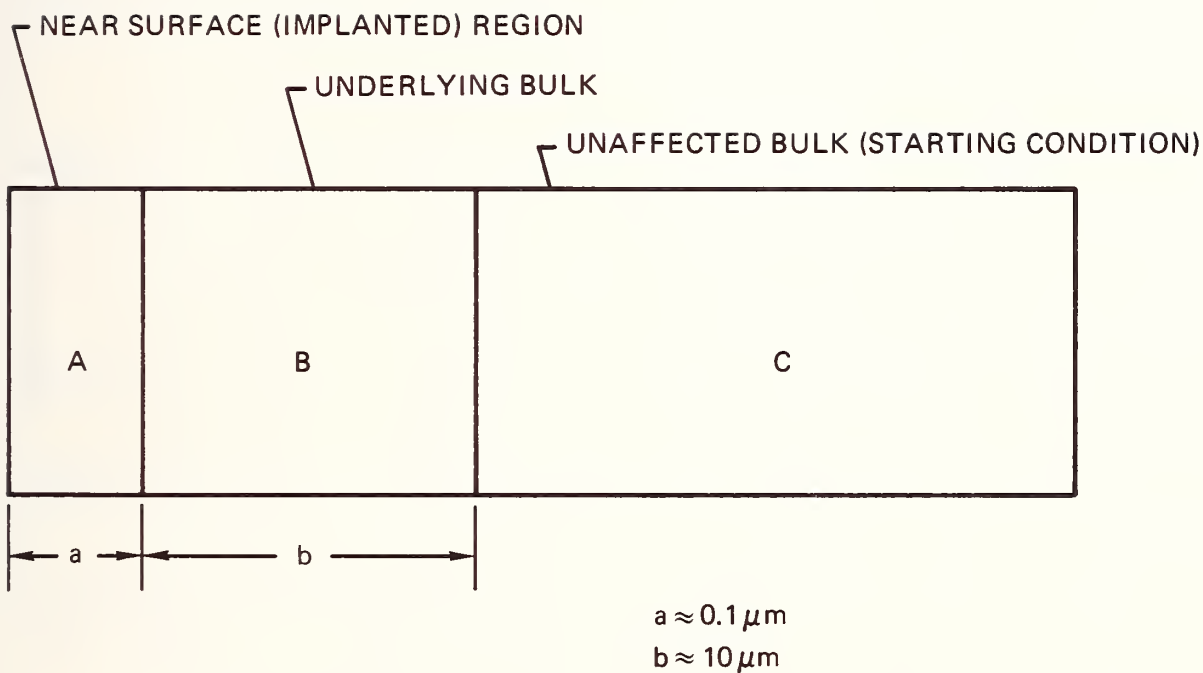


Figure 1. Schematic of sample showing implanted region (A), underlying bulk (B), and unaffected bulk (C). Diffusion of solute from region A occurs in region B during annealing.

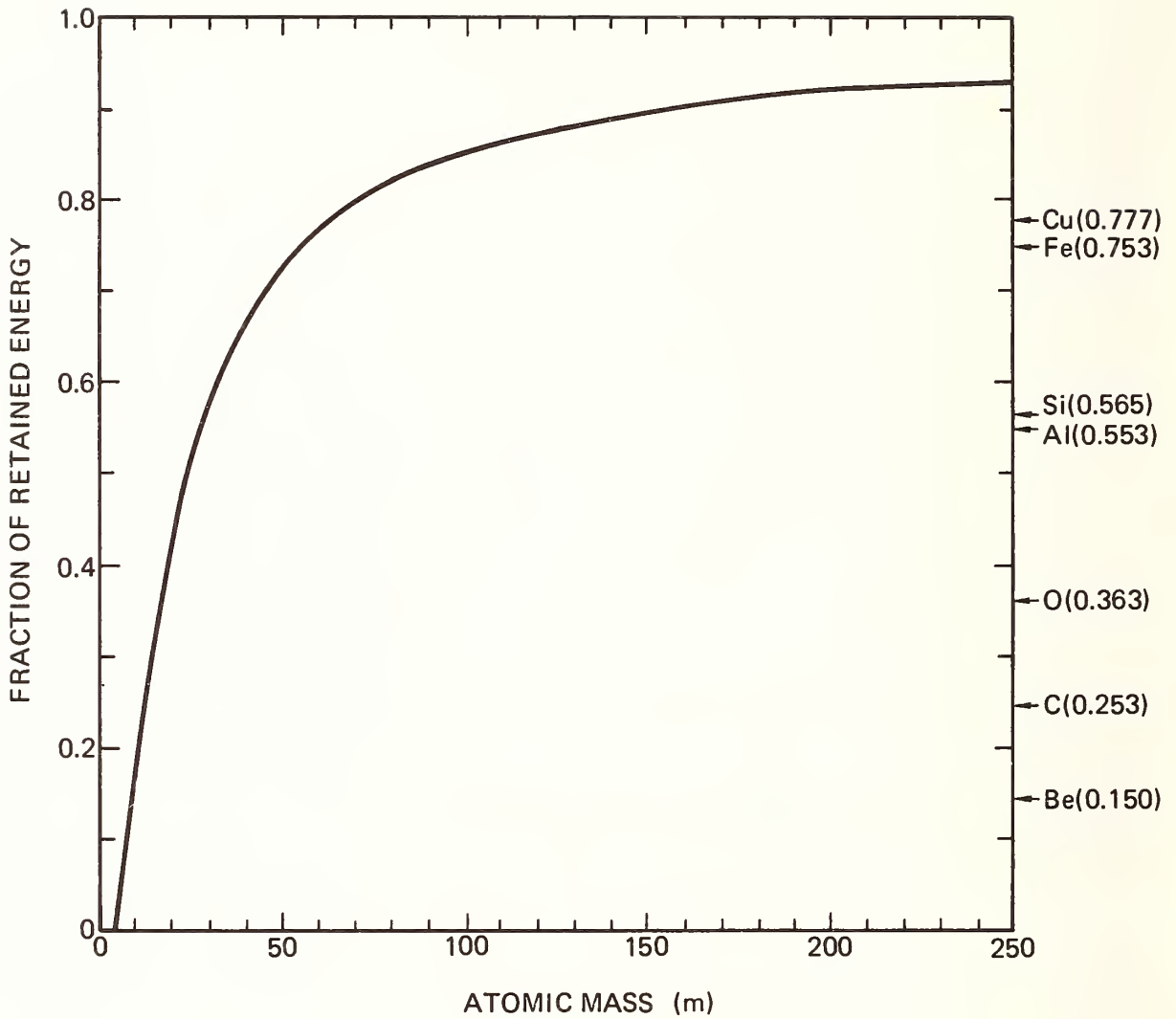


Figure 2. Relation between energy of backscattered ions and atomic mass of scattering species for backscattered angle of 170° . Values for several elements are listed at right.

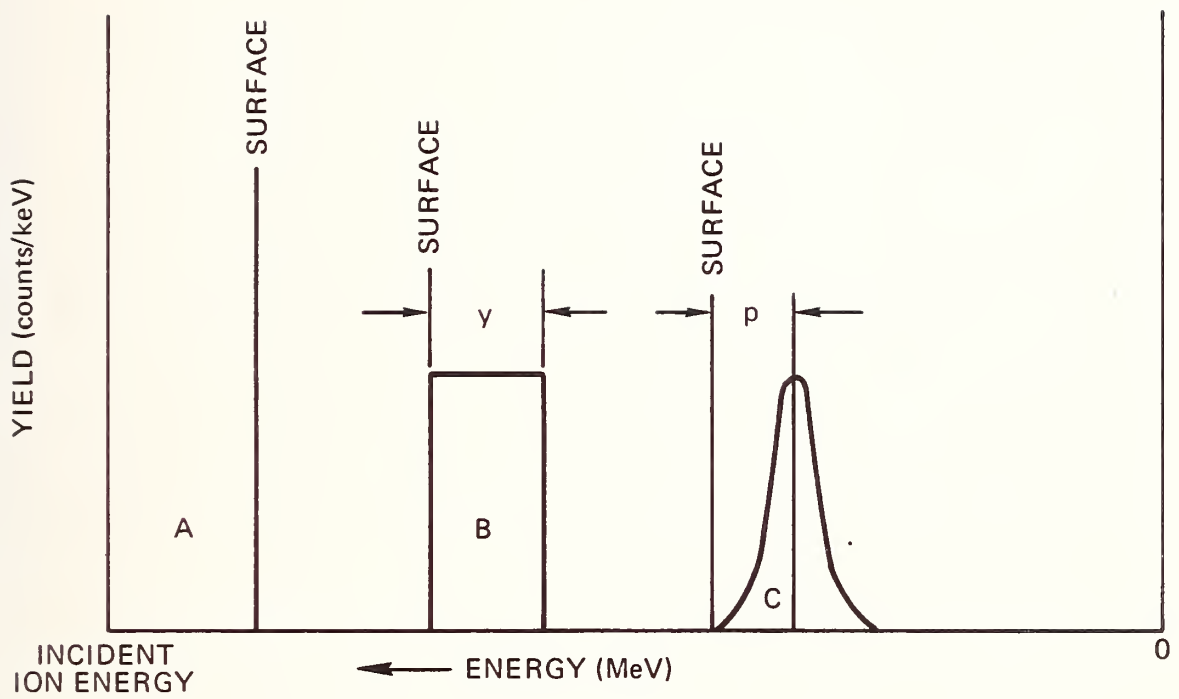


Figure 3. Schematic ion backscattering spectrum of sample containing three impurities: A, B, and C where $m_A > m_B > m_C$. In each case the impurity distribution is located near the surface.

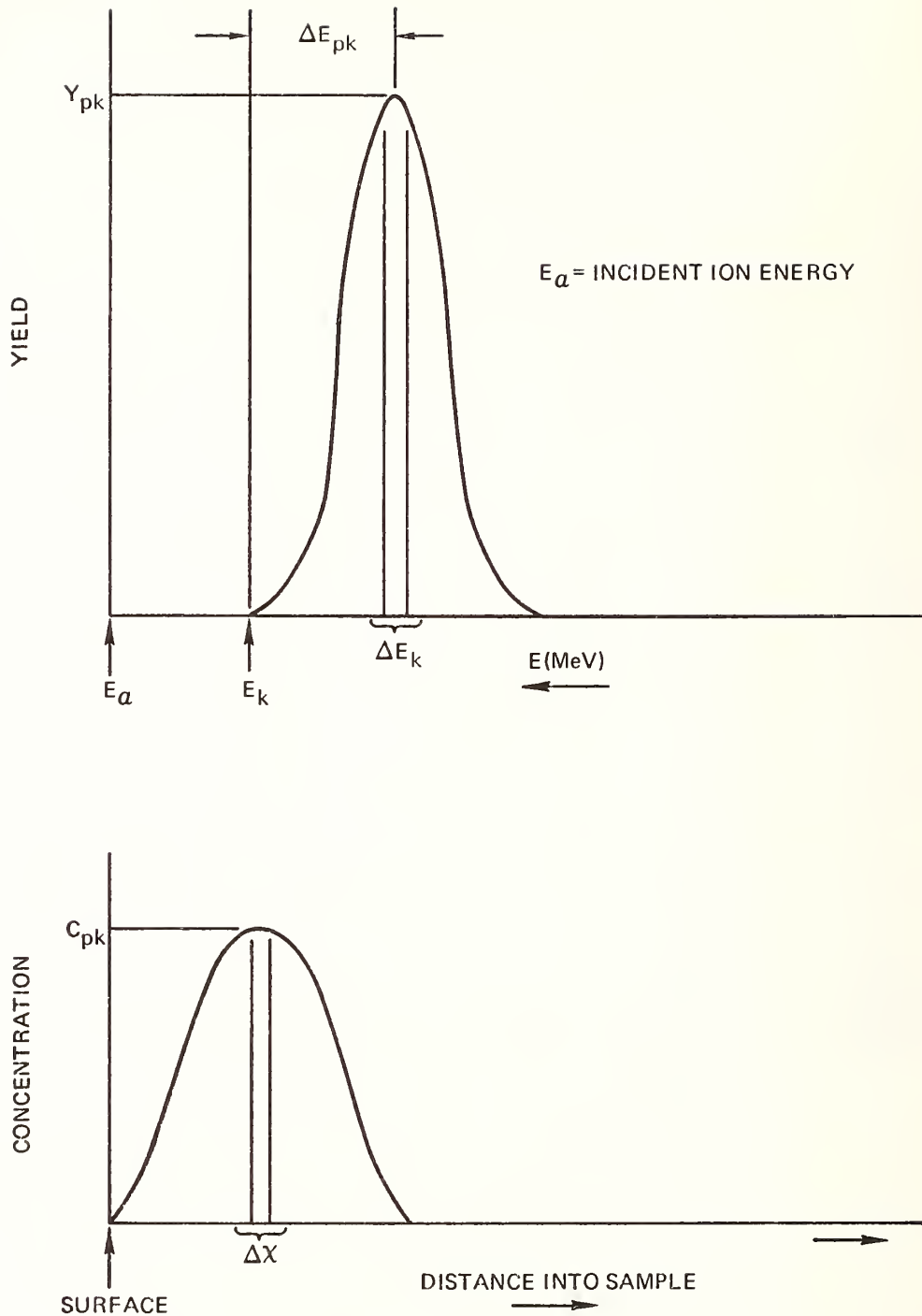


Figure 4. Schematic of ion backscattering spectrum of implanted region showing its transformation to a concentration profile. Note that E_k corresponds to element k present at the surface of the sample.

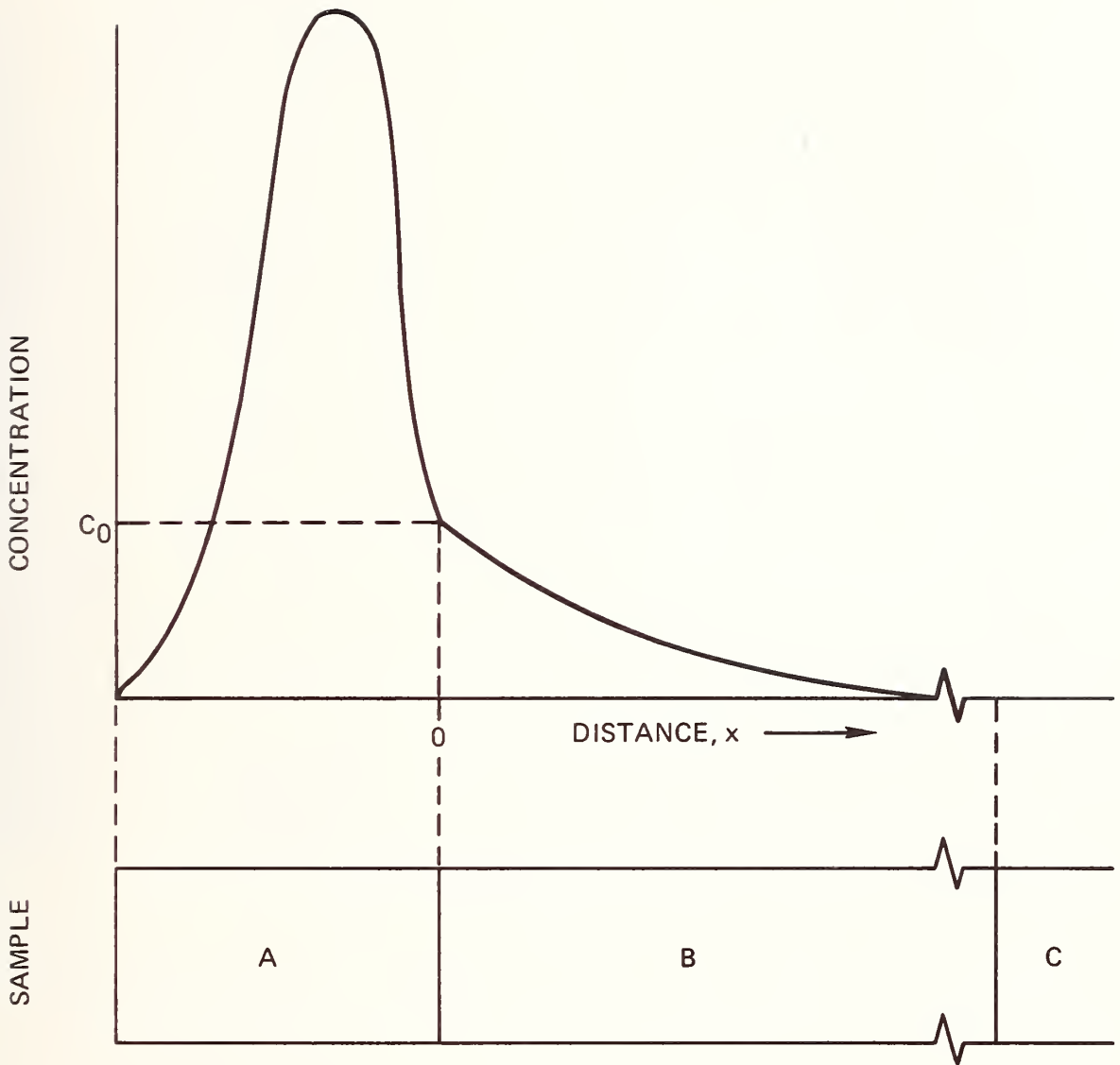


Figure 5. Schematic of diffused tail region showing discontinuity at C_0 and the concentration profile for the regions of interest in the sample.

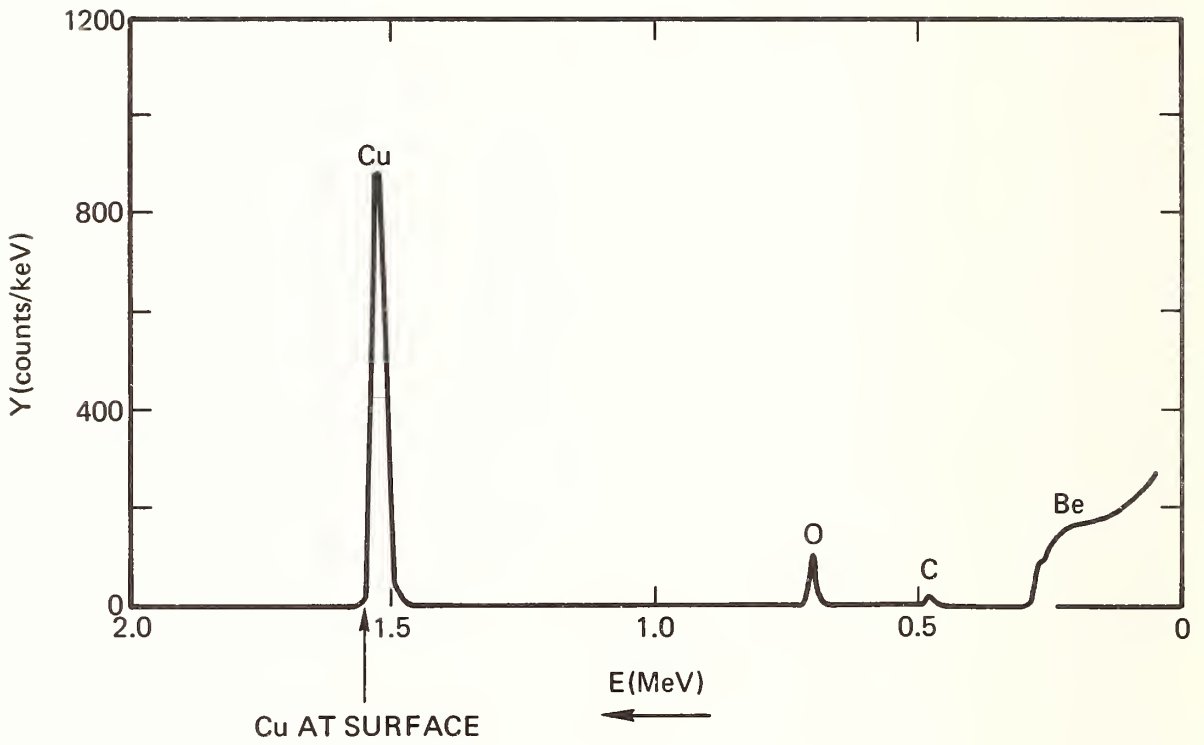


Figure 6. Actual ion backscattering spectrum of yield versus energy of backscattered ions for 2 MeV incident ions. Note that energy increases to the left.

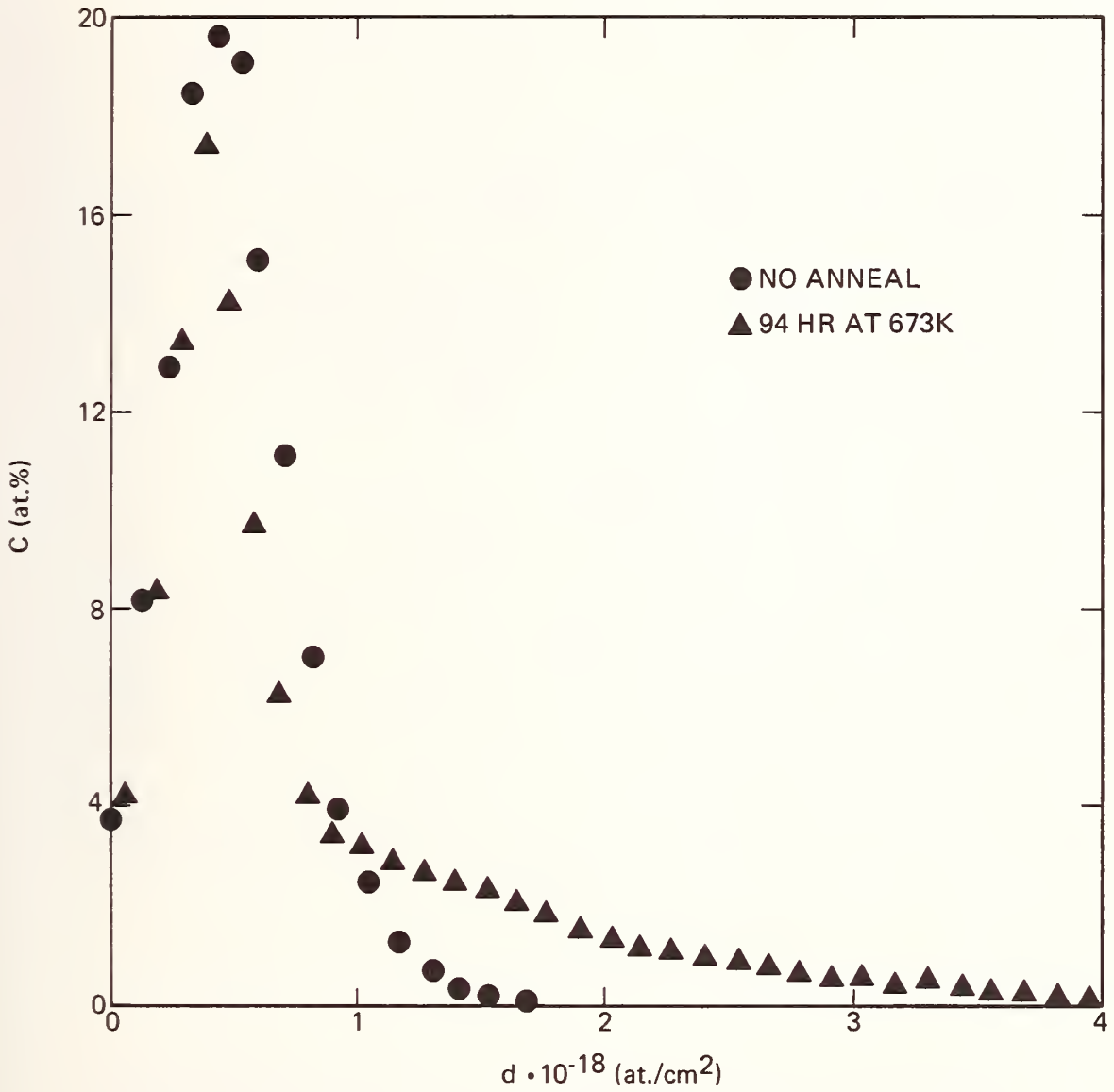


Figure 7. Concentration profile of copper implanted into beryllium before and after anneal, showing discontinuity in actual data.

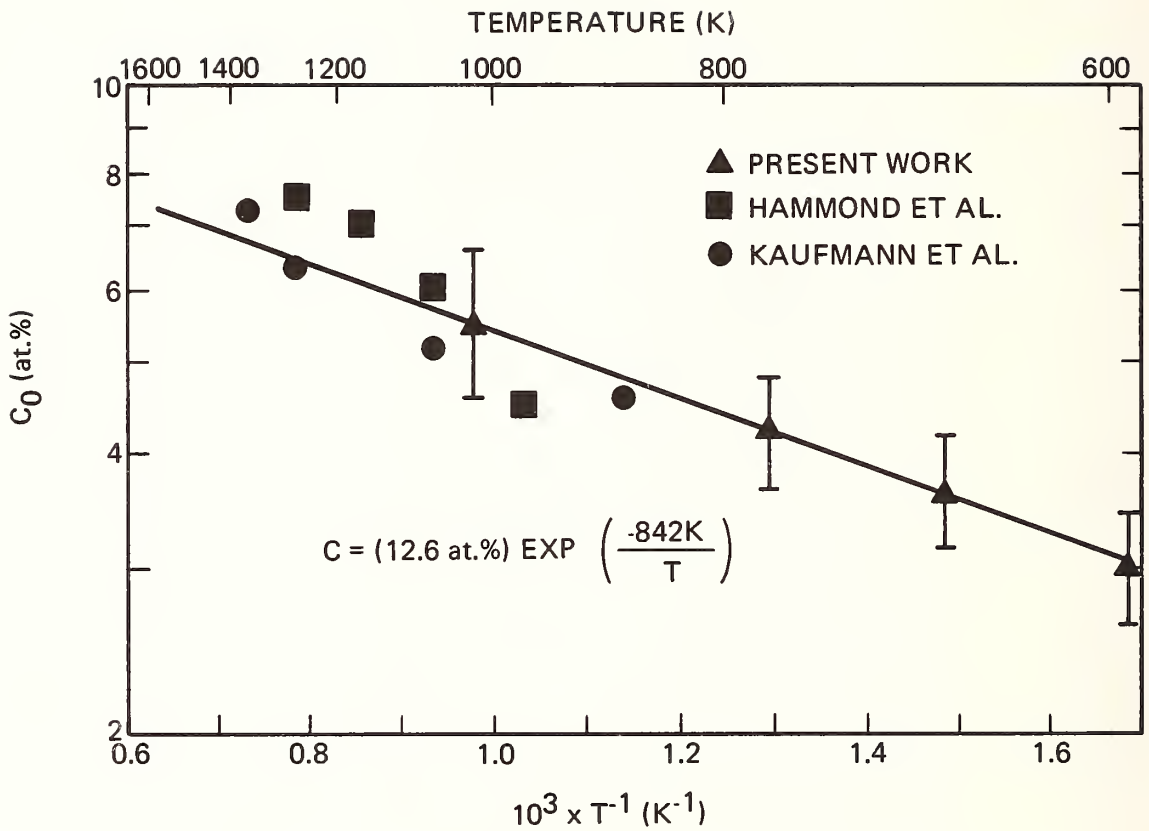


Figure 8. Solubility of copper in beryllium as a function of temperature on a log solubility versus T^{-1} plot. Plot shows data, while analytical expansion represents best fit.

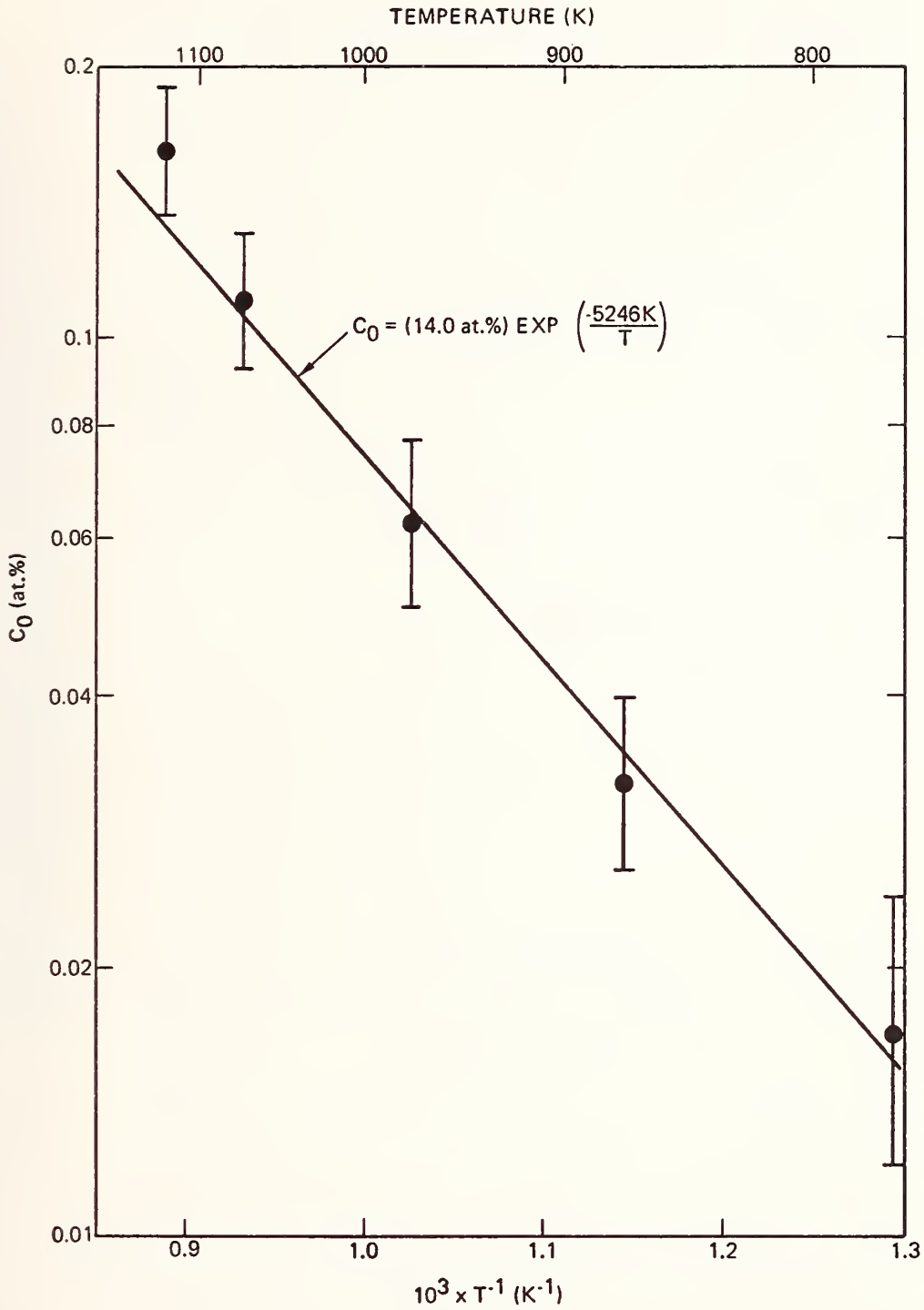


Figure 9. Solubility of iron in beryllium as function of temperature. Plot shows data, while analytical expression was obtained from best fit.

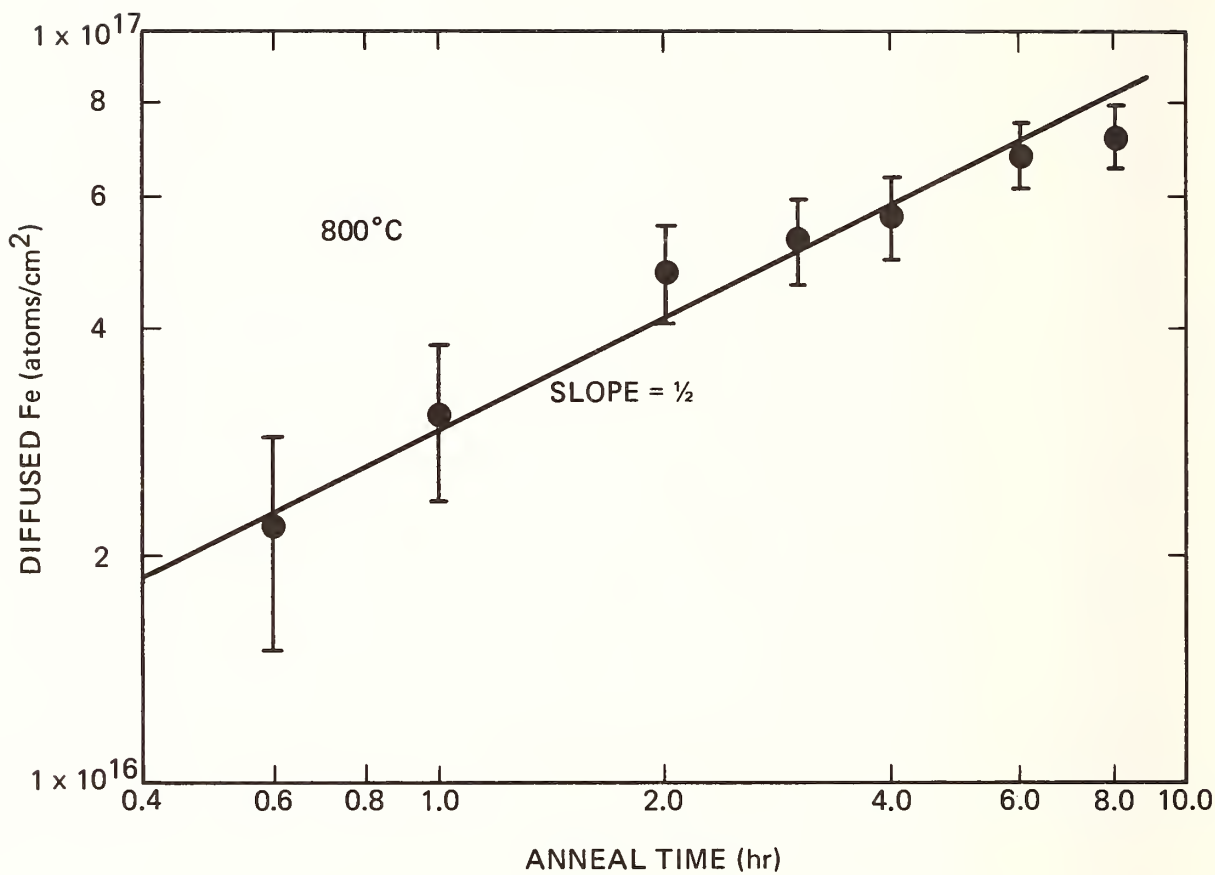


Figure 10. Time dependence of the amount of iron diffused into sample from implanted region during anneal at 800°C. Slope of 1/2, predicted from analysis, supports validity of assumptions.

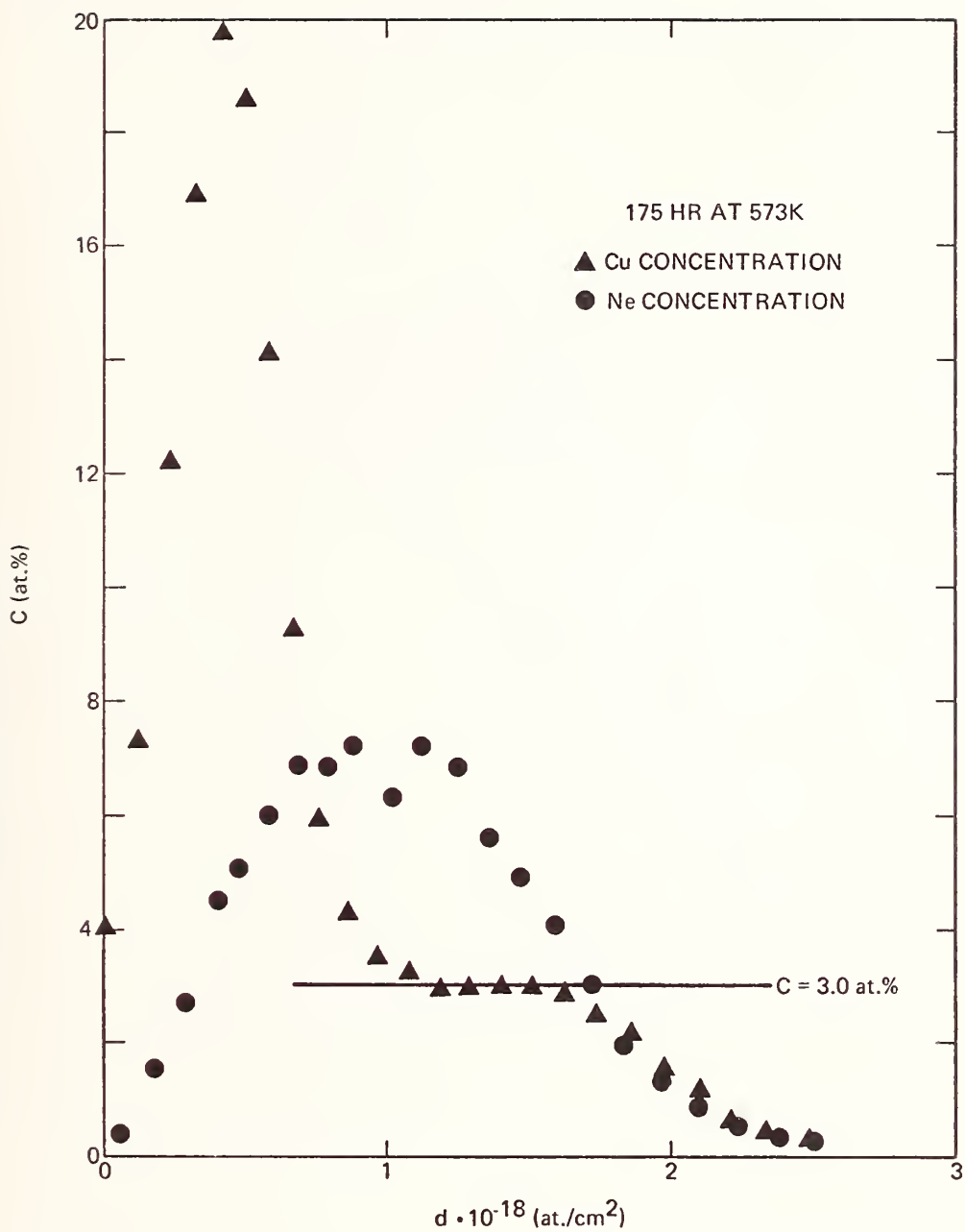


Figure 11. Concentration profile after annealing for enhanced diffusion experiment. Note overlays of plateau region of copper concentration and neon profile as implanted.

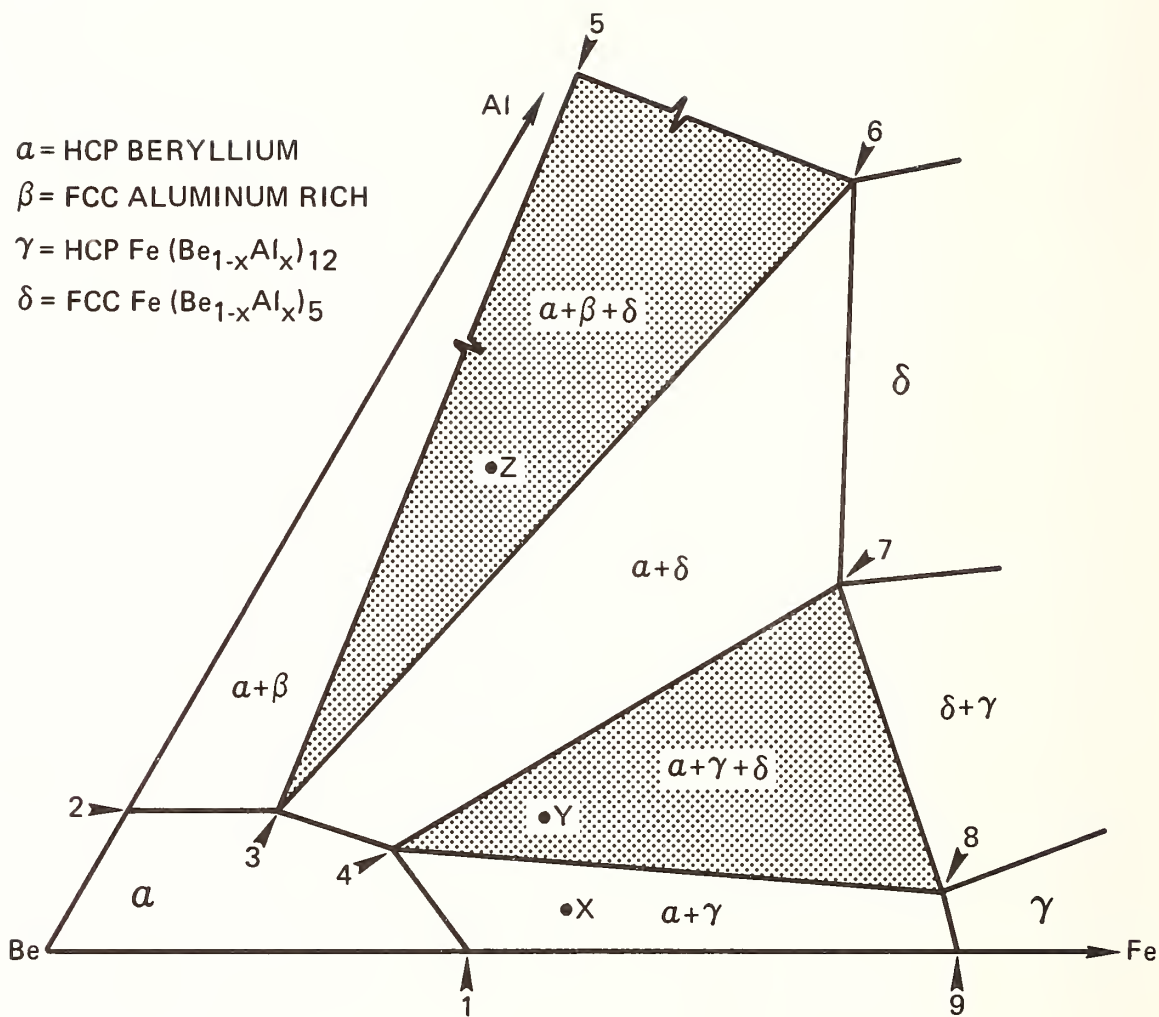


Figure 12. Schematic ternary phase diagram for Be-Fe-Al system showing relationship between two-phase and three-phase regions. Sample concentration during anneals must be in three-phase region, e.g., at points Y and Z, but not at X.



PHASE EQUILIBRIUM DIAGRAMS IN TERMS OF
ELECTRONIC STRUCTURE

Frederick E. Wang

Materials Division
Naval Surface Weapons Center
White Oak, Silver Spring, Md. 20910

In a continuing effort^{1,2} to understand the nature of superconductivity in the A_3B (A15-type) compounds, I have observed³ not too long ago some interesting correlations between the superconducting characteristics and the phase equilibrium diagrams of these compounds. These correlations were interpreted in terms of a proposed "A-chain integrity"⁴ in the superconductivity of the A15 compounds and subsequently related to the electronic structure of the compounds.

The correlations thus observed are aesthetically satisfying on two accounts:

1) The importance of "A-chain integrity" in the superconducting characteristics of these compounds is supported by a number of experiments and observations, e.g., the isotopic substitution of A or B elements,⁵ Matthias' rule is followed only when the e/a ratio is reached by B element substitution (A element substitution invariably degrades T_C),⁶ and more recently direct evidence of T_C degradation due to "A-chain" disruption through thermal neutron bombardment.⁷

2) Since a phase equilibrium diagram is a manifestation of all the thermodynamic properties, it must contain information concerning electronic arrangements as well as atomic arrangements. The manifestation of electronic arrangements, while subtle in phase diagrams, can therefore be related with a phenomenon that is supersensitive to their electronic property, i.e., superconductivity.

However, experimentally the correlations are not obeyed rigorously (as was indicated in the original paper,³ e.g., V_3Si , Mo_3Os

systems). It was pointed out that these deviations from the correlations may be attributable to the following possibilities: a) the phase diagrams reported may be in error, b) the T_C 's reported may be inaccurate (or the T_C 's may be measured correctly but the material under investigation may contain fractional impurities leading to an erroneous T_C). Therefore, the final acceptance or abandonment (or modification) of the correlation requires more (in number) and better (accurate) phase diagrams and T_C data for the Al5 compounds.

A significant number of new or revised phase diagrams have appeared in the literature since the original paper³: the Cr-Ir,⁸ V-Au,⁹ V-Ga,¹⁰ V-Rh¹¹, V-Si¹², V-Pt¹³, Nb-Au¹⁴, Nb-Ga¹⁵, Nb-Os¹⁶, and Nb-Pt¹⁴ systems. While the majority of these systems conform to the correlations, there are a few systems that appear to directly contradict the correlation. For example, V_3Rh and Nb_3Os are both peritectically formed and have SSR (solid solubility range) of 12 and 4 at/o respectively, and yet, V_3Rh is not superconducting (even at $0.015^\circ K$)¹⁷ while Nb_3Os has a T_C of only $0.94^\circ K$ ¹⁷. A close inspection of these phase diagrams, however, indicates that the SSR for both systems are lopsided on the B-rich side (no solubility range at all on the A-rich side). This implies that the "A-chain integrity" in these two systems are practically non-existent (or extremely weak) and consequently are not superconducting (or have very poor superconducting characteristics). These two systems, therefore, not only do not contradict the correlation (based on the "A-chain integrity" concept) but in fact lend further support to it. To be sure, some modification in the stated correlation is required. More detailed explanation including all other newly characterized systems and modification of the correlation will be published elsewhere¹⁸. However, it is reasonable to conclude at this point that the correlation appears sound and should not be abandoned.

In view of these facts, further investigations into new and/or reinvestigations of the phase diagrams that contain Al5 compounds are urgently needed. These phase diagram investigations should include (or pay special attention to) a) an accurate determination

of the SSR of each Al₅ compound and b) an unequivocal characterization of the nature of its formation (congruent vs. incongruent).

Acknowledgement

I wish to thank Dr. R.M. Waterstrat of the National Bureau of Standards for pointing out a number of new systems in the literature to me.

References

1. F.E.Wang, J.Sol.Stat.Chem. 6, 365(1973).
2. F.E.Wang, and J.R.Holden, Sol.Stat.Comm. 17, 225(1975).
3. F.E.Wang, J.Phys.Chem.Sol. 35, 273(1974).
4. M.Weger, Rev.Mod.Phys. 36, 175(1965).
5. G.E.Devlin, and E.Corenzwit, Phys.Rev. 120, 1964(1960);
B.T.Matthias, T.H.Geballe, E.Corenzwit, and G.W.Hull, Phys.Rev. 129, 1025(1963).
6. B.T.Matthias, T.H.Geballe, and V.B.Compton, Rev.Mod.Phys. 35,
1(1963); B.T.Matthias, T.H.Geballe, L.D.Longinotti, E.Corenzwit
G.W.Hull, R.H.Willens, and R.H.Maita, Science 156, 645(1967).
7. A.R.Sweedler and D.G.Schweitzer, Phys.Rev.Lett. 33, 168(1974).
8. R.M.Waterstrat, and R.C.Manuszewski, J.Less Comm.Met. 32,
79(1973).
9. R.Flukiger, C.Susz, F.Heiniger, and J.Muller, J.Less Comm.Met.
40, 103(1975).
10. J.H.N.vanVucht, H.A.C.M.Bruning, H.C.Donkersloot, and A.H.Gomes
de Mesquita, Phil.Res.Rept. 20, 407(1965).
11. R.M.Waterstrat, and R.C.Manuszewski, J.Less Comm.Met.(in press)
12. H.A.C.M.Bruning, Phil.Res.Rept. 22, 349(1967).
13. R.M.Waterstrat, Trans.AIME 4, 455(1973).
14. J.Muller, R.Flukiger, A.Junod, F.Heiniger, and C.Susz, Proc.
13th International Conference in Low Temperature Physics.
15. D.A.Ashby and R.D.Rawlings, J.Less Comm.Met. 50, 111(1976).
16. R.M.Waterstrat, and R.C.Manuszewski, J.Less Comm.Met. 51, 55
(1977).
17. B.W.Roberts, "Survey of Superconductive Materials and Critical
Evaluation of Selected Properties," J.Phys.Chem. Ref.Data, 5,
No.3(1976).
18. F.E.Wang. To be published.

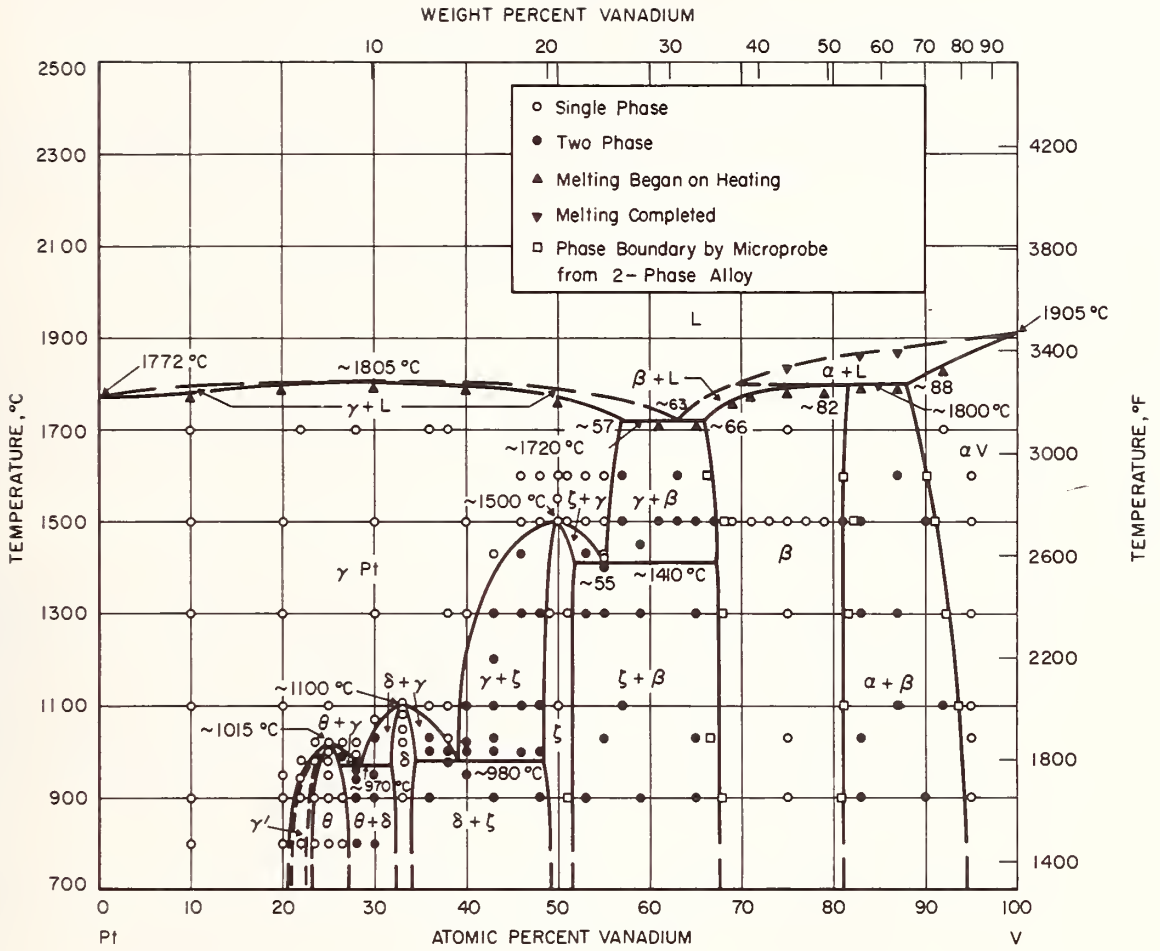


Fig. 1. The Vanadium-Platinum Constitution Diagram.



An English translation may be obtained by contacting the author.

APPORT DE L'ÉTUDE DES SÉGRÉGATIONS DANS LES SOLUTIONS SOLIDES

À LA DÉTERMINATION DE DIAGRAMMES DE SOLIDIFICATION.

APPLICATION À L'ÉTUDE DES SYSTÈMES $Sc_2O_3 - Ho_2O_3$ ET $Sc_2O_3 - Dy_2O_3$

J. M. Badie
Lab. Ultra-Refractaires, Odeillo
66120 Font-Romeu, France

I. INTRODUCTION.

La solidification contrôlée (1) offre des possibilités très intéressantes pour la détermination de courbes ou de surfaces liquidus et solidus de systèmes à deux ou plusieurs constituants. Ces possibilités ne sont que très rarement exploitées.

Nous nous sommes plus particulièrement attachés à l'étude des ségrégation, dans les solutions solides. L'apparition de tels phénomènes implique nécessairement une diffusion faible dans le solide au cours de la solidification. La nature des observations que l'on peut faire par analyse à température ambiante de ces phénomènes est donc étroitement liée à celle du diagramme de solidification et de phases à haute température.

Les résultats de cette étude sont comparés à ceux dus notamment à l'utilisation de méthodes expérimentales permettant un examen "in situ" à haute température telles que la diffraction des rayons X à haute température (2) et l'analyse thermique directe à l'aide d'un four solaire (3).

2. PREPARATION DES ECHANTILLONS.

Les mélanges intimes d'oxydes (pureté 3 N), de 500 mg à 1 gramme, sont fondus au four solaire sur un support réfrigéré. Le globule ($\varnothing \approx 5\text{mm}$), entièrement liquide, est déplacé, dans le gradient de température vertical du four solaire, en s'éloignant du miroir concentrateur. La solidification progresse depuis la base de l'échantillon au contact du support réfrigéré jusqu'à sa partie supérieure où elle se termine. Ces solidifications progressives dirigées ont été effectuées avec deux vitesses de déplacement de l'interface liquide-solide. Ces deux vitesses sont respectivement de $5 \cdot 10^{-3}$ mm/s et 10 mm/s. Dès la fin de solidification, le globule est retiré du foyer ; il se refroidit alors rapidement ($5 \cdot 10^{+2} \text{ } ^\circ\text{C}/\text{s}$) au contact du support et de l'atmosphère ambiante.

3. METHODES EXPERIMENTALES D'ANALYSE.

a) Diffraction des rayons X à température ambiante.

Chaque globule est broyé en totalité. La poudre obtenue, d'une granulométrie de l'ordre de quelques microns, est analysée (Cu K_α et Fe K_α) à l'aide d'un dispositif classique : goniomètre vertical Philips et système d'enregistrement des intensités diffractées par compteur proportionnel. Les enregistrements sont effectués à la vitesse de 1° en 2θ à la minute.

La diffraction par un solide homogène dont la taille des grains est supérieure à quelques milliers d'angstrons conduit à des raies enregistrées dont la largeur à mi-hauteur ne dépend en première approximation que des conditions expérimentales d'analyse (4). Elle est en moyenne de l'ordre de $0,25^\circ$ en 2θ pour nos conditions d'analyse.

L'existence de ségrégations dans les solutions solides peut être mise en évidence par l'élargissement, dissymétrique, des raies caractéristiques de la structure de la solution. Chaque raie est l'enveloppe d'une série de pics élémentaires diffractés par les divers domaines, homogènes en composition, constituant le mélange solide. Les pentes de cette enveloppe définissent deux pics élémentaires dont les positions peuvent être déterminées en tenant compte de leur largeur moyenne à mi-hauteur, ainsi que le montre la figure 1. Ce traitement des raies permet de calculer une valeur approchée des paramètres des solutions extrêmes présentes dans le mélange.

Les courbes représentatives du paramètre de maille, des solutions cubiques à base de Sc_2O_3 , en fonction de la concentration ne présente pas d'écarts notables à la loi de Vegard. Cette relation nous a permis d'atteindre la composition des solutions solides par mesure du paramètre de maille. Nous avons ainsi pu suivre dans de très bonnes conditions l'évolution de la composition des solutions extrêmes en fonction de la composition globale du solide et des conditions variables de la solidification. La sensibilité de la méthode est, en effet, très grande du fait de l'important écart paramétrique qui existe entre Sc_2O_3 , $a = 9,848 \text{ \AA}$ et Ho_2O_3 , $a = 10,606 \text{ \AA}$ ou Dy_2O_3 , $a = 10,665 \text{ \AA}$. La détermination des paramètres qui est faite à 5.10^{-3} \AA près permet de déceler des variations de composition de l'ordre de 1 mol %.

b) Analyse chimique ponctuelle.

Les globules sont sectionnés par leur milieu, parallèlement à la direction de progression du front de solidification. Les analyses des deux éléments métalliques sont effectuées, à l'aide d'une microsonde de Castaing, sur cette section suivant des axes parallèles à la direction de déplacement du globule au cours du refroidissement. La vitesse de déplacement de l'échantillon pendant les analyses est de 17,4 microns par minute. Les compositions sont déterminées avec une précision de l'ordre de 0,5 à 1 mol %. Les références utilisées sont les oxydes de base fondus.

Un résultat d'analyse présenté sur la figure 2 permet de juger de la résolution spatiale de l'appareillage utilisé.

4. RESULTATS DES ANALYSES ET INTERPRETATION.

a) Système Sc_2O_3 - Ho_2O_3 .

Les figures 2 et 3 mettent bien en évidence la présence de ségrégations et les variations du profils des raies de diffraction enregistrées en fonction des conditions de préparation des échantillons.

Seules les interférences caractéristiques de la forme cubique de Sc_2O_3 sont observables dans tous les diffractogrammes, ce qui indique que ce système présente une miscibilité complète dans le solide, tout au moins à haute température.

L'évolution des paramètres extrêmes a_1 et a_2 (fig. 4), en fonction de la composition globale du solide, montre que l'amplitude des ségrégations est maximum vers 75 mol % Sc_2O_3 nulle à 45 mol % Sc_2O_3 . Des élargissements trop faibles des raies, pour les échantillons plus riches en Ho_2O_3 , ne permettent pas un calcul des deux paramètres extrêmes. En fonction, des conditions de solidification, on peut observer une variation notable du paramètre a_2 qui est celui de la solution la moins riche en Sc_2O_3 dans le mélange ($a_2 > a_1$) alors que a_1 reste sensiblement constant.

On peut déduire de ces observations :

- que le diagramme de solidification (à deux fuseaux) présente un point invariant à 45 mol % Sc_2O_3 - 55 mol % Ho_2O_3 ,
- que ce point invariant est un minimum de solidification ; dans l'hypothèse d'un maximum, nous aurions dû observer une variation du paramètre a_1 jusqu'à une valeur égale à celle de Sc_2O_3 à la limite.

- que la diffusion dans le solide est effectivement négligeable dans nos conditions expérimentales ; la détermination de la composition N_1 de la solution extrême de paramètre a_1 permet une première approche satisfaisante de la largeur du fuseau de solidification dans cette partie du diagramme, ainsi que le montrent les résultats rassemblés au tableau 1.

Les résultats que nous avons obtenus, par diffraction des rayons X à haute température, analyse thermique et calcul des courbes d'équilibre C - L (modèle des solutions régulières) et, qui sont rassemblés à la figure 5 permettent de juger de l'intérêt de ce type d'étude. Le diagramme de phases complet, compatible avec le polymorphisme de Ho_2O_3 , qui est proposé est représenté figure 6.

b) Système Sc_2O_3 - Dy_2O_3 .

Seules les solutions cubiques à base de Sc_2O_3 nous ont permis, compte tenu de nos conditions de préparation des échantillons, d'observer des phénomènes de ségrégation nets.

La diffraction par des échantillons contenant moins de 15 mol % Dy_2O_3 ne donne que les interférences caractéristiques de la forme cubique C. A ces dernières s'ajoutent celles du composé DyScO_3 , de structure pérovskite P, à déformation orthorhombique, pour des teneurs plus fortes en Dy_2O_3 (fig. 7).

La présence de deux variétés cristallines dans la plupart des mélanges et l'évolution des paramètres a_1 et a_2 (fig. 8) des solutions extrêmes montrent :

- que la miscibilité est limitée par la formation d'un mélange eutectique. La composition de l'eutectique est de 40 mol % Dy_2O_3 - 60 mol % Sc_2O_3 . C'est la composition de l'échantillon pour lequel l'amplitude des ségrégations s'annule ($a_1 = a_2$). Une analyse par microsonde conduit à une teneur de 41 ± 1 mol % Dy_2O_3 dans l'eutectique,

- que la dissolution limite de Dy_2O_3 dans Sc_2O_3 à la température eutectique est voisine de 22 mol % Dy_2O_3 ($a_0 = a_2$). a_0 est le paramètre de la solution homogène obtenu par trempe à partir d'un équilibre réalisé à haute température. La courbe représentative de a_0 en fonction de la composition obéit à la loi de Végard,

- que nous sommes en présence d'un "faux eutectique" (5) entre 15 et 22 mol % Dy_2O_3 . Ces mélanges ont en effet, une composition globale extérieure à la lacune de miscibilité ($a_2 < a_0 < a_1$) (fig. 8 et 9) ; leur température de fin de solidification a été abaissée, du fait des ségréga-

tions, jusqu'à la température eutectique. Une certaine quantité d'eutectique, mis en évidence par les interférences de la phase P, a pu ainsi être formée en fin de solidification contrairement à ce que pouvait laisser prévoir un tel diagramme.

La mesure du paramètre a_1 permet là aussi, de remonter à une valeur approchée de la composition du premier solide déposé à l'équilibre à partir d'un mélange liquide de composition globale connue (fig. 9).

Les figures 9 et 10 montrent respectivement les résultats expérimentaux obtenus au cours de l'étude complète du diagramme et la proposition qui en est faite, compatible avec le polymorphisme de Dy_2O_3 .

5. CONCLUSION.

Nous avons obtenu, par interprétation de l'évolution des ségrégations dans les solutions solides en fonction de la composition et des conditions de la solidification des informations en bon accord avec les résultats expérimentaux des analyses "in situ" à haute température. L'étude à température ambiante des échantillons préparés par solidification contrôlée solidification "normale" dans notre cas ou fusion de zone, présente donc un grand intérêt pour la détermination de diagrammes de solidification. Nous pensons en particulier aux systèmes pour lesquels des études directes "in situ" à haute température sont rendues très difficiles sinon impossible en raison de problèmes liés, à la réactivité de leurs constituants avec les supports ou contenants ou plus simplement aux quantités de produits réclamées par ces analyses.

BIBLIOGRAPHIE

1. W.G. PFANN, Zone Melting (1966) (Wiley)
2. J.M. BADIE, M. FAURE, J.P. TRAVERSE, 3è colloque International sur les méthodes analytiques par rayonnement X, Nice 16 Septembre 1974
3. M. FOEX, Rev.Int.Htes Temp. et Réfract. 3.309 (1966)
4. A. GUINIER, Théorie et Technique de la radiocristallographie (1964) (Dunod)
5. P. GORDON, Principles of Phases Diagrams in Materials Systems (1968) (Mc Graw Hill).

No	N ₁ cal		N ₁ obs		N ₂ obs	
	x _{«A»}		RX x _{«A»}	M x _{«A»}	RX x _{«A»}	M x _{«A»}
0,9 Sc ₂ O ₃ — 0,1 Ho ₂ O ₃	0,98		0,95	0,96	0,65	0,50
0,8 Sc ₂ O ₃ — 0,2 Ho ₂ O ₃	0,96		0,90	0,93	0,52	0,44
0,7 Sc ₂ O ₃ — 0,3 Ho ₂ O ₃	0,91		0,83	0,87	0,52	0,44
0,6 Sc ₂ O ₃ — 0,4 Ho ₂ O ₃	0,83		0,70	—	0,52	—

Tableau I: Concentration x_{«A»} en Sc₂O₃ dans les solides de composition extrême N₁ et N₂ déterminée expérimentalement par RX et microsonde (M) sur des produits fondus de composition globale No. Les valeurs les plus riches en Sc₂O₃ sont comparées a celles, calculées, du premier solide déposé a partir du liquide No.

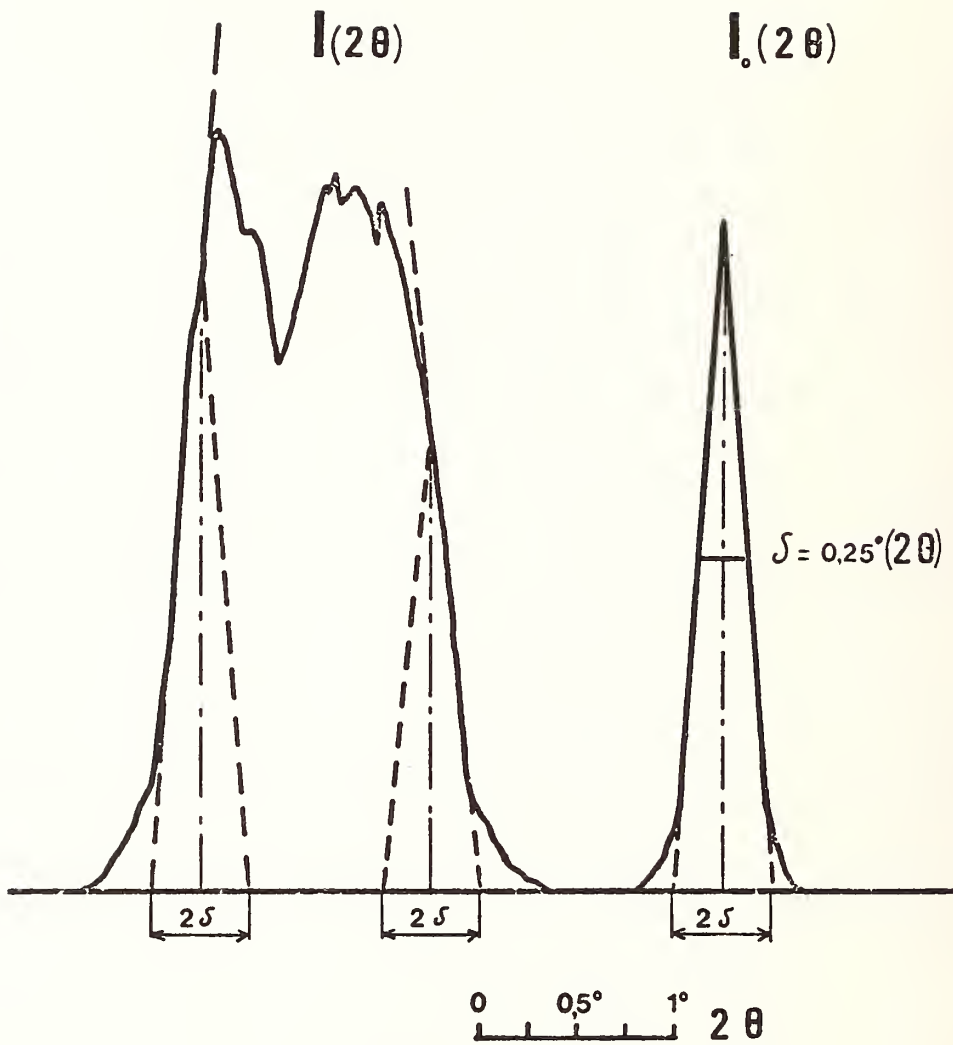


Fig. 1 - Schema de la détermination des composantes extrêmes d'une "raie" de diffraction enregistrée. La raie $I(2\theta)$ est l'enveloppe d'une série de raies élémentaires de profil $I_0(2\theta)$.

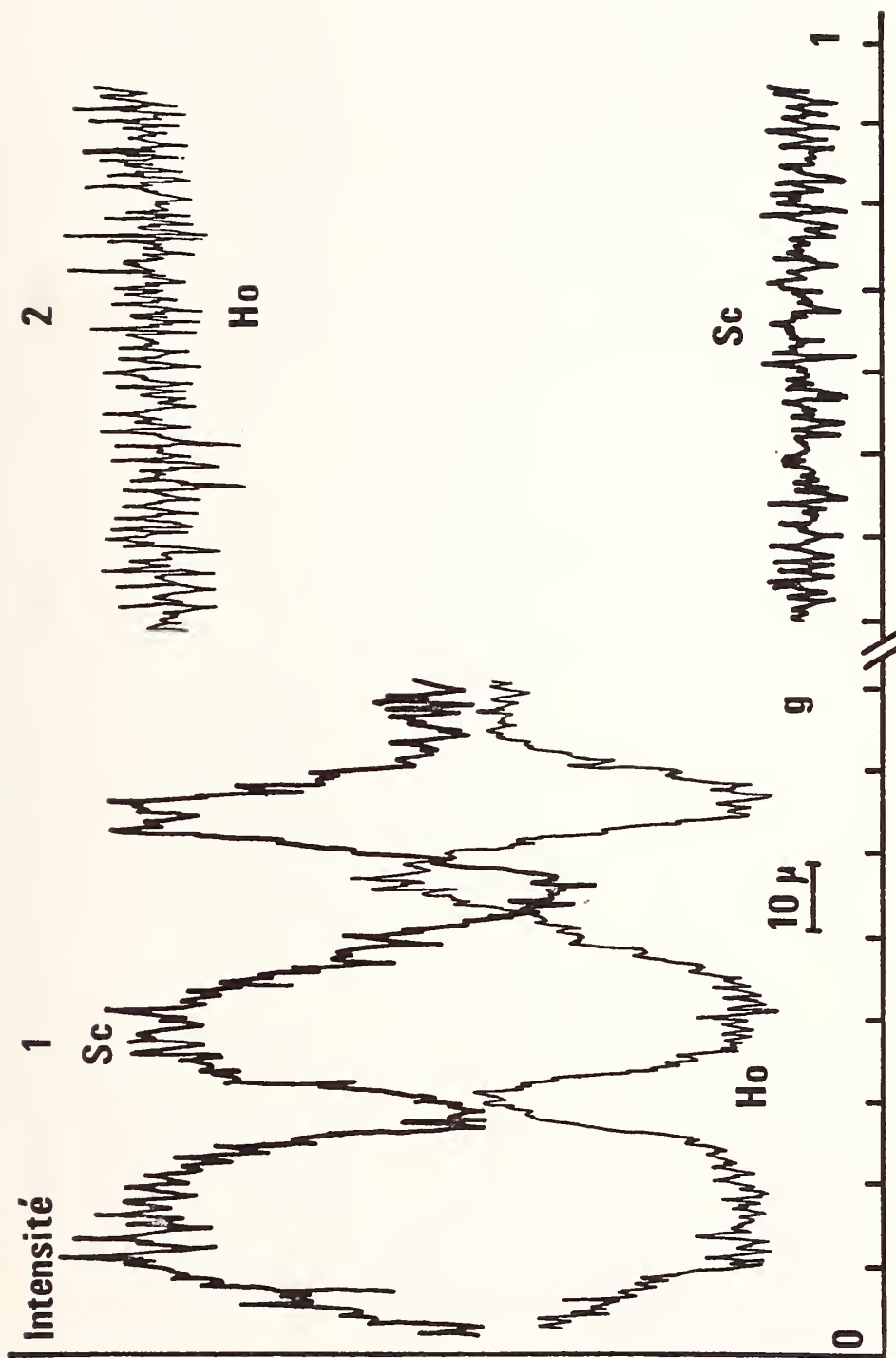


Fig. 2. - Profils des concentrations en Ho et Sc enregistrés par analyse à la microsonde pour un échantillon contenant 80 mole % Sc_2O_3 et préparé par solidification progressive unidirectionnelle.

1. Dans les premières fractions "g" de solide déposé, $0 < g < 0,05$ ($\sim 100 \mu$)
2. Dans les dernières fractions "g" de solide déposé, $0,95 < g < 1$ ($\sim 100 \mu$)

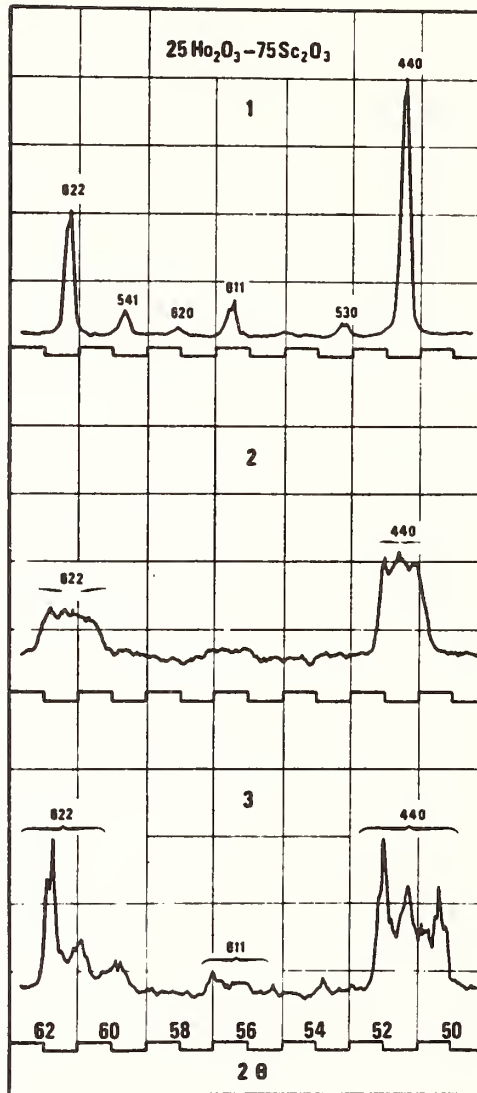


Fig. 3 - Evolution de la largeur des raies de diffraction enregistrées pour un échantillon de composition 25 mole % Ho_2O_3 - 75 mole % Sc_2O_3 en fonction des conditions de traitement thermique.

1. Trempe de la solution solide à l'équilibre aux environs de 2100°C
- 2 et 3. Trempe après solidification unidirectionnelle progressive, vitesse de déplacement de l'interface solide liquide 10 mm/s et 0,005 mm/s respectivement.

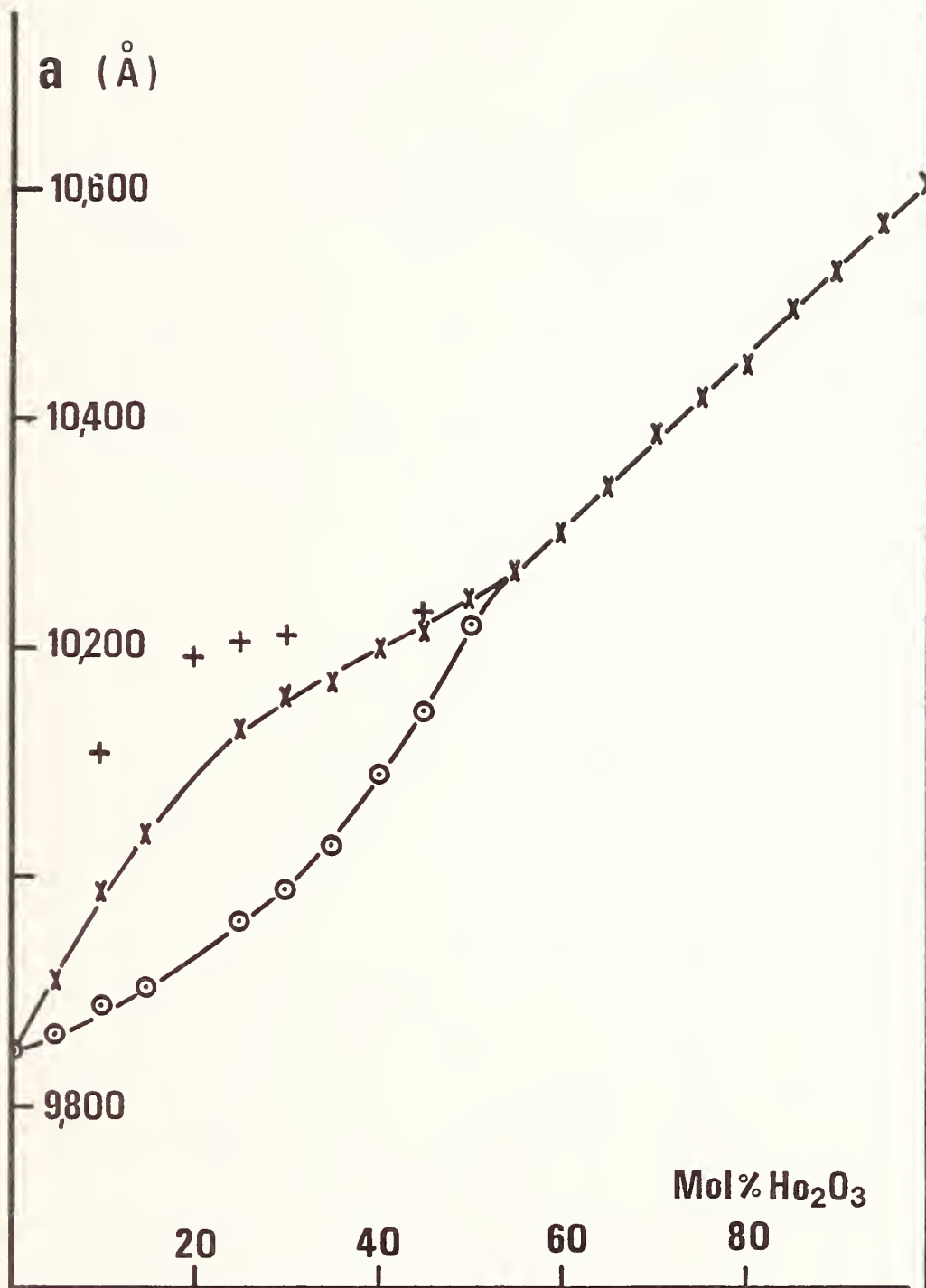


Fig. 4 - Evolution des paramètres a_1 et a_2 des solutions solides cubiques extrêmes dans les produits fondus en fonction de la composition globale des mélanges pour le système $Sc_2O_3-Ho_2O_3$. Vitesses de déplacement de l'interface solide liquide : $v = 10$ mm/s (x, o) et $v = 0,005$ mm/s (+, o).

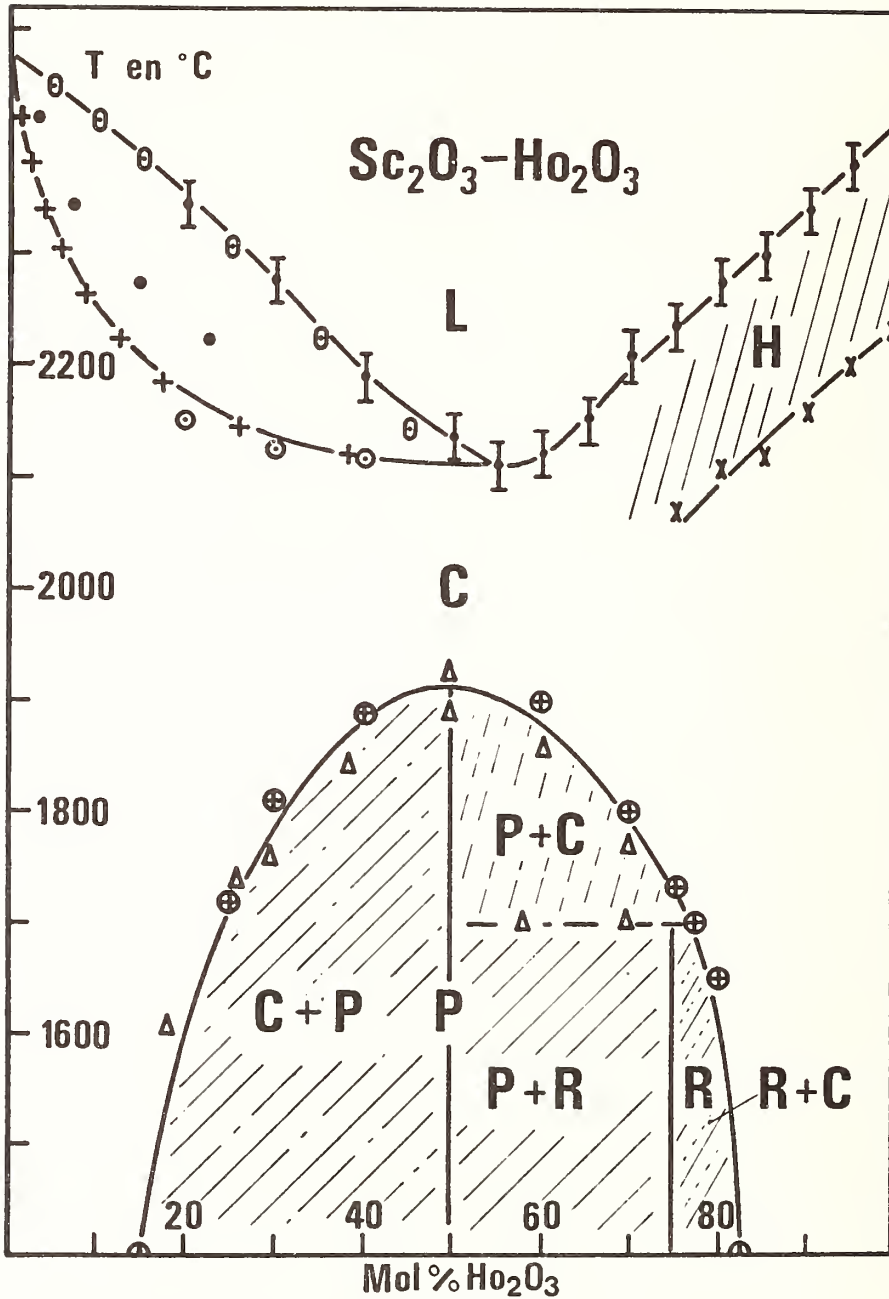


Fig. 5 - Domaines d'existence des différentes phases observées. Résultats expérimentaux et calculés :

- ⊙, ⊖, analyse thermique - Δ diffraction X à haute température
- ⊗, analyse thermique et diffraction X à haute température
- ⊙, diffraction X sur produits trempés
- ⊕, ⊖, liquidus et solidus calculés
- , solidus déduit de l'étude des ségrégations.

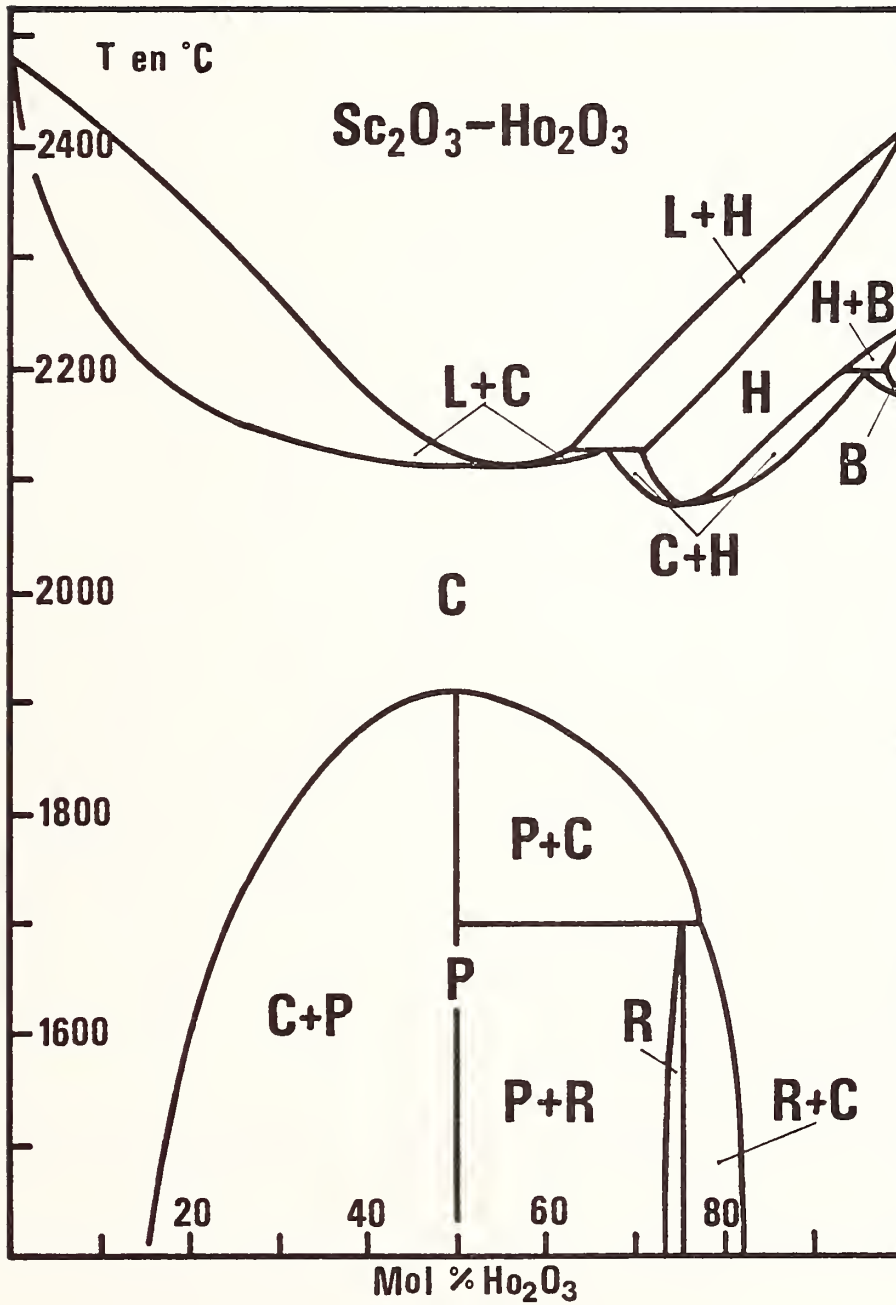


Fig. 6 - Diagramme de phases proposé compatible avec le polymorphisme de Ho_2O_3 .

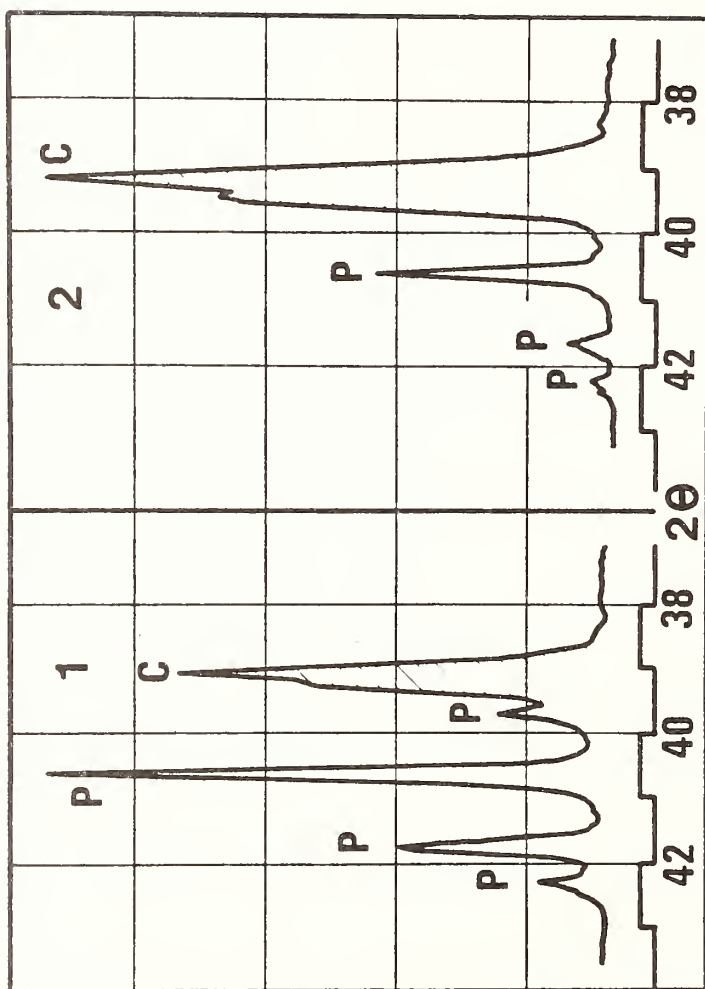


Fig. 7 - Manifestation des phénomènes de ségrégations dans le cas d'un système à miscibilité partielle dans le solide. Produits fondus analysés à T ambiante.

1. Diagramme de poudre d'un échantillon de produit fondu contenant 30 mole % Dy_2O_3 .
2. Diagramme de poudre d'un échantillon de produit fondu contenant 20 mole % Dy_2O_3 .

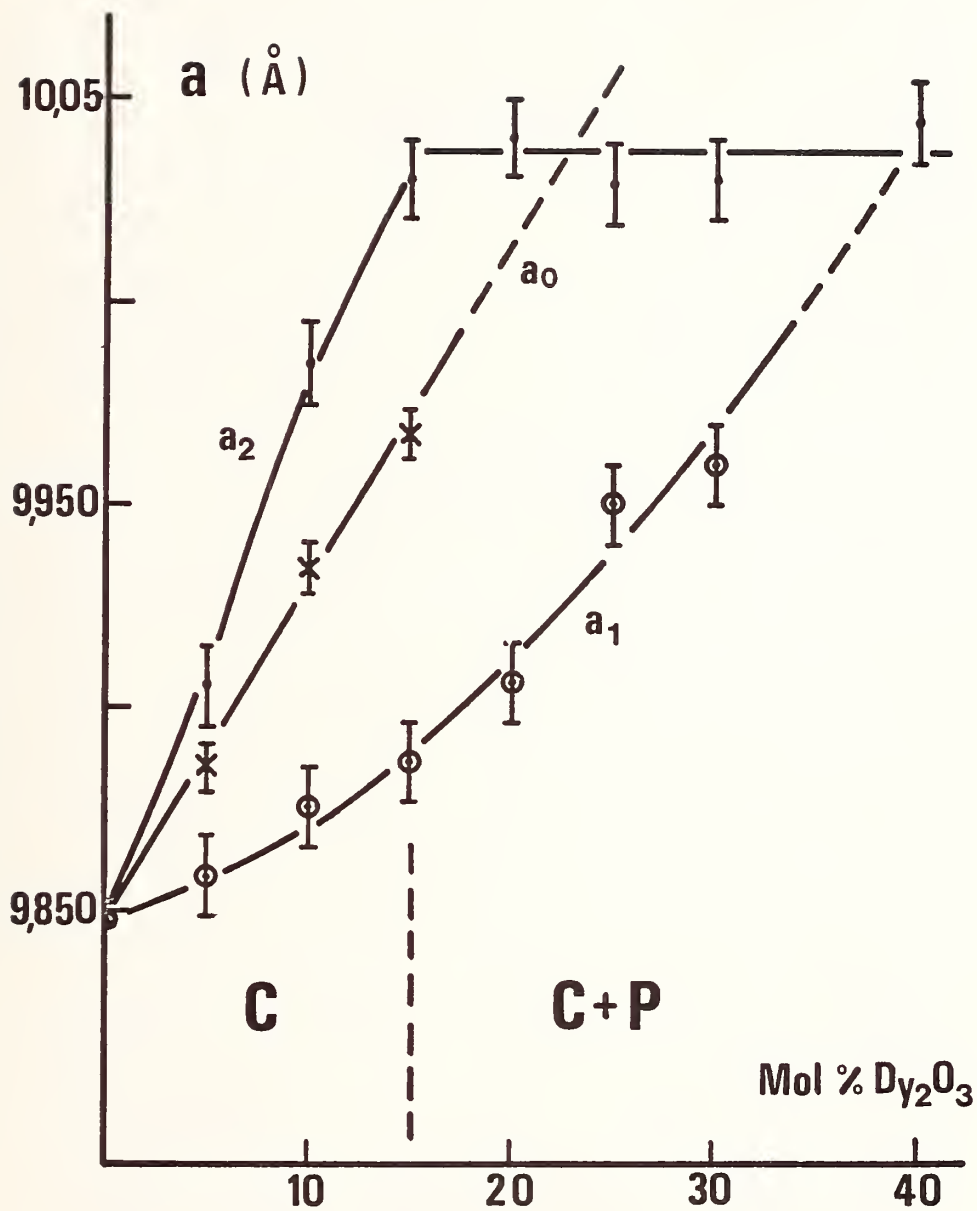


Fig. 8 - Evolution des paramètres a_1 et a_2 des solutions solides cubiques extrêmes présentes dans les produits fondus trempée en fonction de leur composition globale. Ces valeurs sont comparées à celles du paramètre a_0 de la solution homogène obtenue par trempe du solide à l'équilibre à haute température.

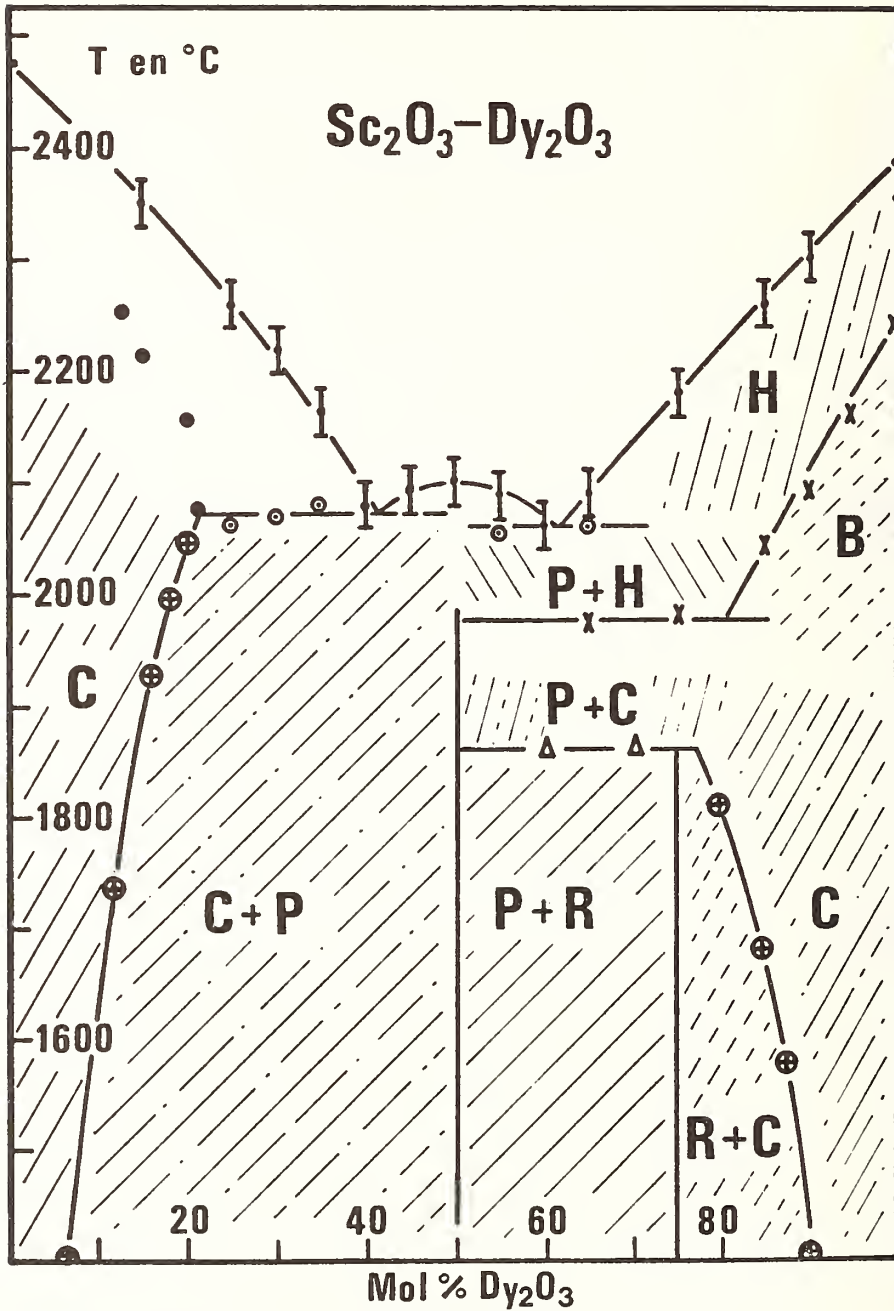


Fig. 9 Domaines d'existence des différentes phases observées (hachures).

Résultats expérimentaux :

- I, ⊕, analyse thermique - Δ diffraction X à haute température,
- X, analyse thermique et diffraction X à haute température
- ⊙, diffraction X sur produits trempés
- , solidus déduit de l'étude des ségrégations.

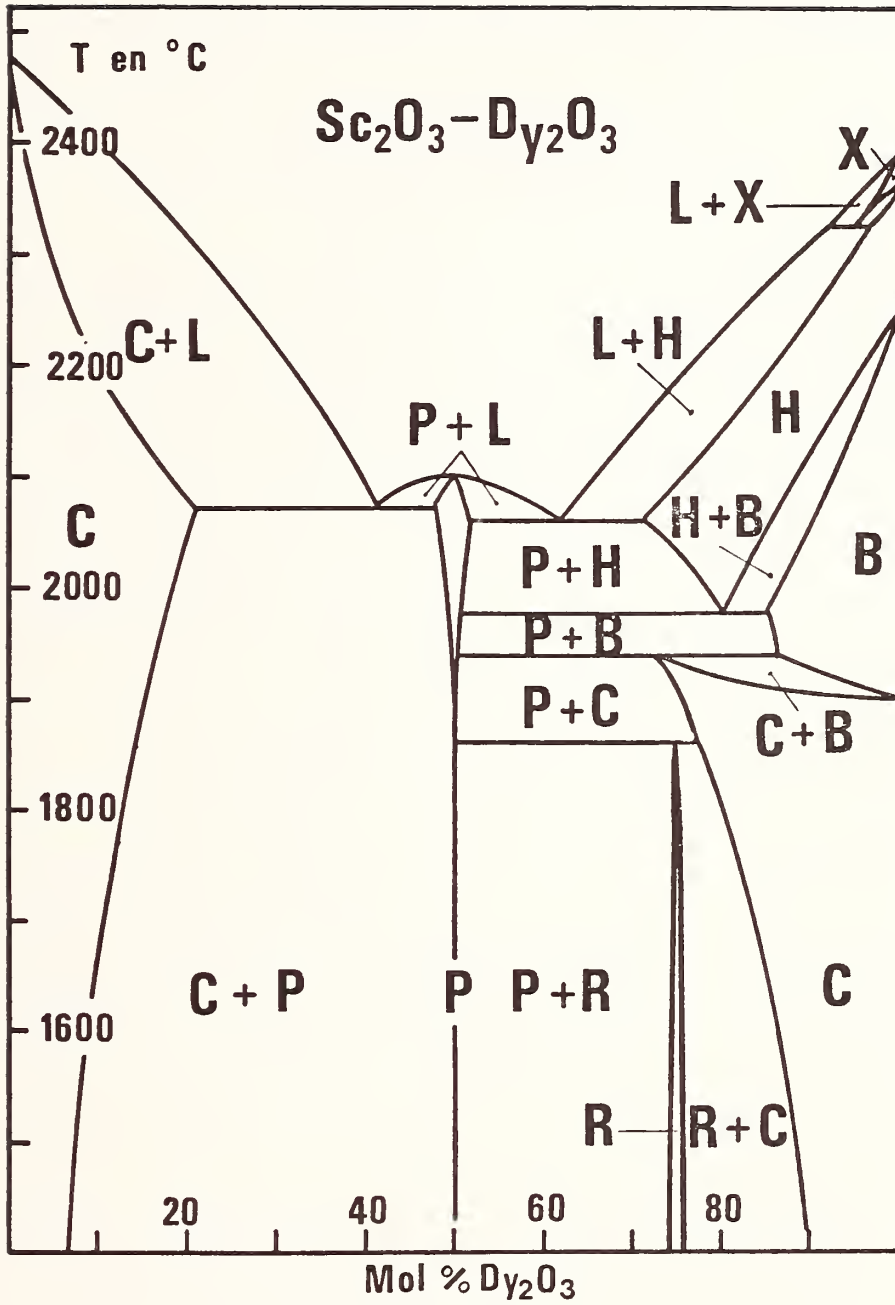


Fig. 10 - Diagramme de phases proposé compatible avec le polymorphisme de Dy_2O_3 .



STUDIES OF THE Fe-C-B PHASE DIAGRAM BY AUTORADIOGRAPHY

Thomas B. Cameron and John E. Morral
Department of Metallurgy and
Institute of Materials Science, U-136
University of Connecticut
Storrs, CT 06268

The iron rich corner of the Fe-C-B phase diagram is being investigated in the first step of a study probing the mechanism behind boron hardenability in steel. The major problems encountered in this type of study are first, obtaining accurate measurements of soluble boron concentrations, on the order of 30 ppm or less; and second, maintaining high purity samples since boron will react with other elements, notably nitrogen, in the ppm range. For these reasons a novel approach is being used in the phase diagram study. Boron concentrations are being measured by neutron autoradiography along the carbon gradient of a carburized Fe-B alloy. The autoradiography technique allows measuring boron concentrations of 5 ± 1 ppm and the use of somewhat massive samples prevents contamination during processing. Isothermal sections of the austenite - borocarbide solvus are obtainable by this technique.



USER NEEDS FOR PHASE DIAGRAMS

by

Dr. Paul J. Fopiano
Army Materials & Mechanics Research Center
Watertown, Massachusetts 02172

In multicomponent systems where two or more phases have important effects on the properties of the alloy, it is rare that the phase compositions are known. Sometimes these compositions can be ignored with impunity but other times this is not the case. In the latter category, the determination of a single tie line only may be required or, because of the prevalence of several alloys using the same alloying elements, a more thorough investigation of phase compositions is justified. In few of these cases, however, is the construction of a phase diagram carried out and widely disseminated. As a result, much otherwise useful data is lost before it can become a useful part of a databank. Examples of one of each type of application are included to indicate the normal limits to which we go to satisfy a specific need. It might be added that without the advent of the probe microanalyzer, little of this work would have been carried out.

TYPICAL EXAMPLES OF PHASE COMPOSITION

Determinations in Commercial Alloys

Titanium-Aluminum-Vanadium Alloys

In the investigation of the phase transformations which occur during the heat treatment of commercial titanium alloys, the presence of two or more phases complicates the interpretation of the mechanical and physical property data. The major strengthening mechanisms can often be related to the compositions of the alpha and beta phases in equilibrium at the solution temperature. Many titanium alloys of commercial interest employ aluminum and vanadium as major alloying elements.

Several standards were made up with various amounts of aluminum and vanadium. The nominal compositions are given in Table 1. Chemical analyses of these alloys were also determined. A probe analysis of these standards yield for our experimental conditions the calibration curve in Figure 1. The least square slope of these lines is given analytically as:

$$w/o V = \frac{I_V - 629}{486}$$

$$w/o Al = \frac{I_{Al} + 27}{1048}$$

where w/oV, w/oAl = weight percent vanadium and aluminum.

Table 1. NOMINAL COMPOSITIONS OF STANDARD ALLOYS IN WEIGHT PERCENT

Specimen	Al	V
76	2	2
77	2	4
78	2	8
81	4	2
82	4	4
83	4	8
84	8	2
85	8	4
86	8	8
43	12	0
44	0	12

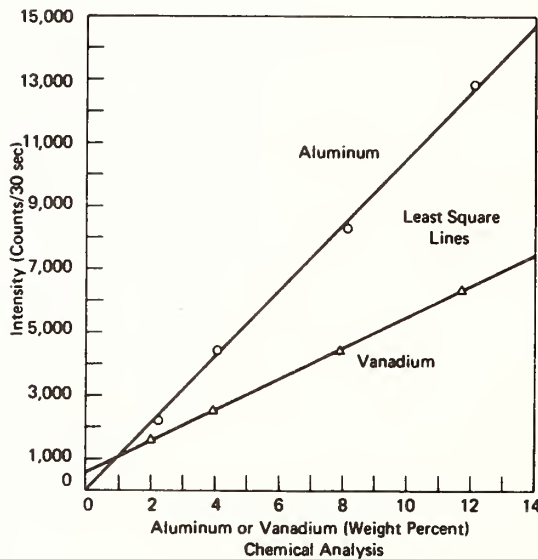


FIGURE 1. Mean Number of Counts (per 30 sec.) Versus Chemical Analysis of Aluminum and Vanadium Standards

$$I_V = \text{counts (vanadium)}/30 \text{ seconds}$$

$$I_{Al} = \text{counts (aluminum)}/30 \text{ seconds}$$

Utilization of this data for the most popular commercial alloy of titanium, Ti-6Al-4V is illustrated in the following discussion. Five solution-treated conditions (all in the alpha beta field) were investigated (Figure 2); i.e.,

Table 2. NUMBER OF COUNTS (per 30 sec) AND CORRESPONDING COEFFICIENT OF VARIATION FOR THE ALPHA AND BETA PHASES FOR SEVERAL SOLUTION TREATMENT CONDITIONS

Sample Designation (and Solution Temp)	Phase (α or β)	Counts/30 Seconds (Coeff. of Variation)	
		A1	V
P-1 (1750 F)	α	7301 (2.5)	1307 (2.9)
	β	6052 (2.6)	2519 (4.3)
P-2 (1700 F)	α	7849 (1.5)	1475 (2.0)
	β	6150 (1.1)	3040 (2.3)
P-3 (1650 F)	α	7078 (4.2)	1593 (2.2)
	β	5779 (1.6)	3686 (3.7)
P-4 (1600 F)	α	7664 (1.4)	1709 (2.5)
	β	5570 (2.2)	4062 (2.3)
P-5 (1550 F)	α	7398 (1.3)	1747 (4.7)
	β	4723 (2.8)	4551 (3.7)

1750, 1700, 1650, 1600, 1550 F with designations P-1 through P-5 respectively. In order to get large enough fields to examine with the probe microanalyzer, it was necessary to heat all specimens to 1850 F for one hour furnace cool to the solution temperature (Figure 3 - 1550 F) and hold for the times indicated in Figure 2.

Probe analysis data of both the alpha and beta phases are presented in Table 2. The measured compositions of the alpha and beta phases are shown in Table 3 (P-1 through P-5). Estimated compositions from published literature is also shown in Table 3 for specimens solution treated at 1562, 1652, and 1742 F. An approximate retrofit of our data to published work on the Ti-6Al-4V alloy is shown in Figure 4. The published work was done before the probe was generally available and was typical of a type of publication then popular. In no sense, however, could it be considered a complete phase diagram even for the titanium-rich corner.

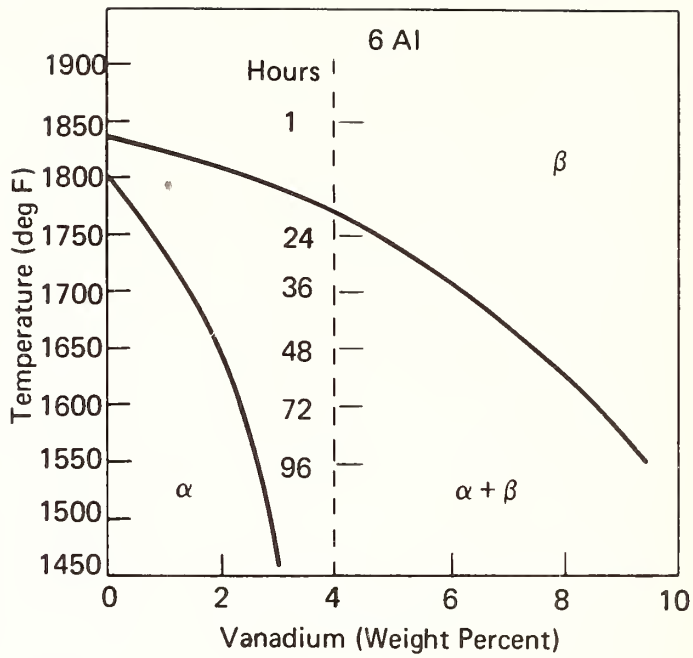


FIGURE 2. Schematic Representation of the 6Al Section of Titanium Corner of Ti-Al-V Ternary

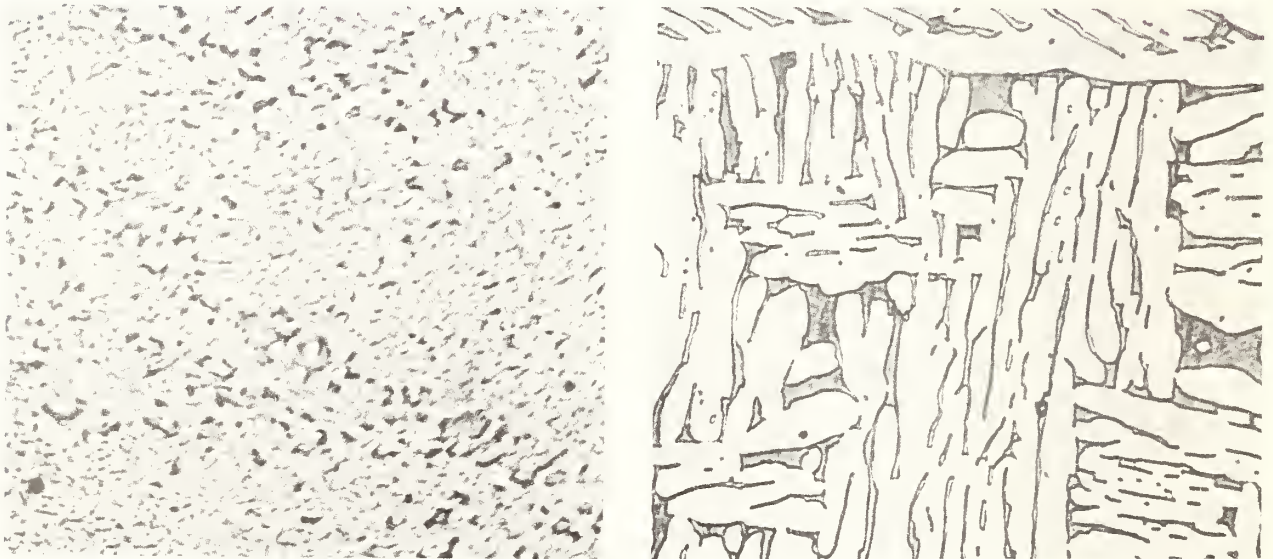


FIGURE 3. Solution-treated Ti-6Al-4V Alloy. Mag. 500X

Table 3. EFFECT OF SOLUTION TEMPERATURE ON THE COMPOSITIONS OF THE ALPHA AND BETA PHASES IN Ti-6Al-4V

Solution Treatment Temperature (deg F)	Weight Percent				Vol % β
	Alpha		Beta		
	Al	V	Al	V	
1550 (P-5)	7.08	2.30	4.53	8.07	25
1562	8	2-1/2	2	8	
1600 (P-4)	7.34	2.22	5.34	7.06	
1650 (P-3)	6.78	1.98	5.54	6.26	38
1652	9	2-1/2	2	6-1/2	
1700 (P-2)	7.52	1.74	5.89	4.96	
1750 (P-1)	6.99	1.40	5.80	3.89	64
1742	10	2	4	5	

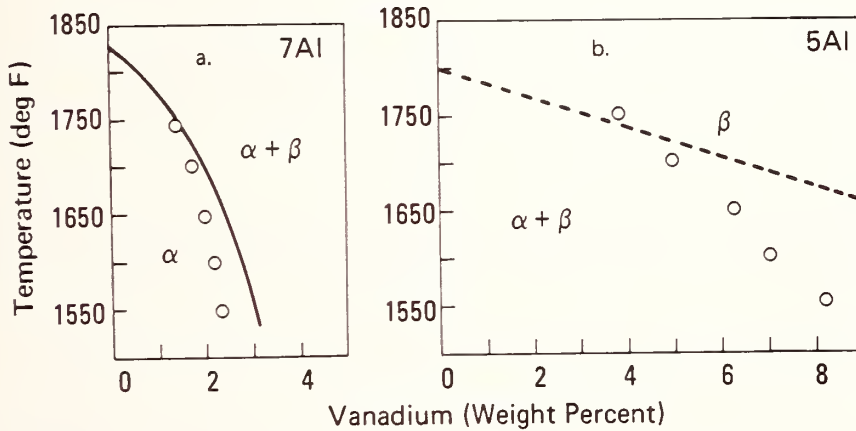


FIGURE 4. Correlation of Probe Data with Published Isothermal Sections (Ref. 5)

43XX Steel

Even though the 43XX steels have been utilized for many years, no phase diagram was available in the literature when the investigation on "Partially Austenitized 43XX Steel" was initiated. A "pseudo" iron-carbon phase diagram was then determined by microstructural analysis. A copy of this "pseudo"

iron-carbon phase diagram for 4300 steels is shown in Figure 5. This is an example where even a very rudimentary phase diagram data was helpful and necessary to develop an optimum compositional and temperature requirements for a new application of a very old alloy.

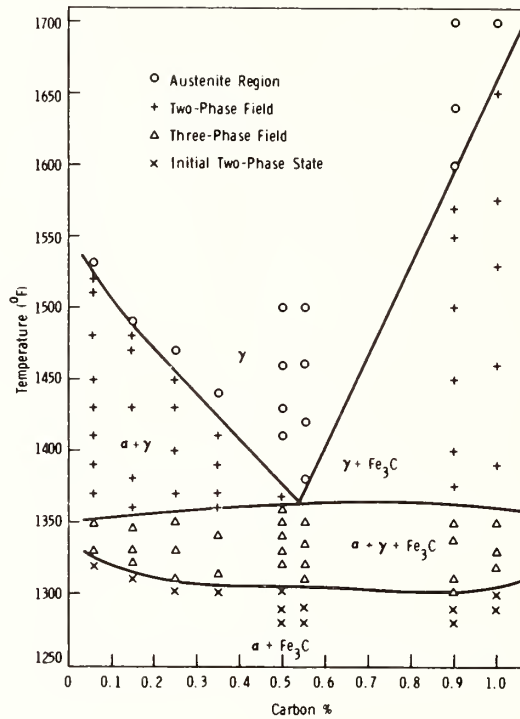


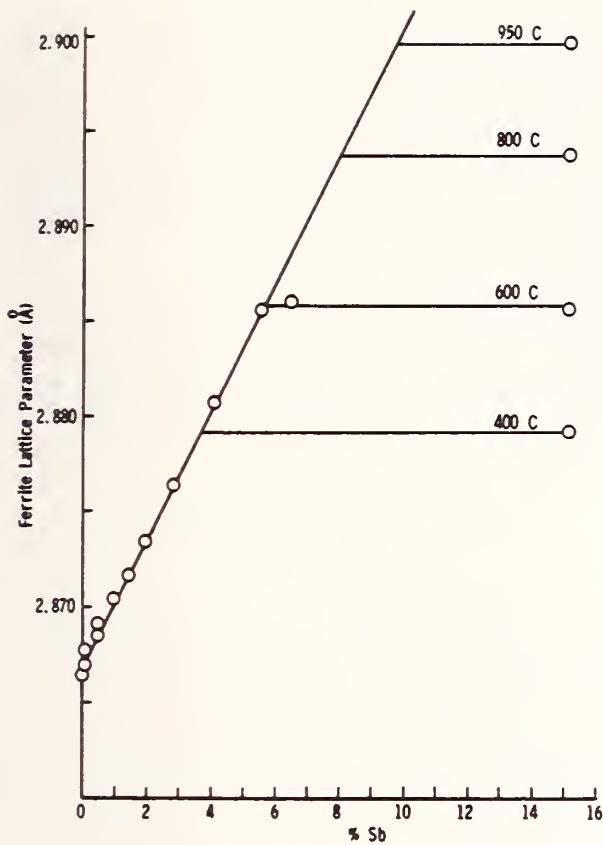
FIGURE 5. Constitution Diagram for 43XX Steels

Partitioning of Impurity Elements in Iron-Carbon Alloys

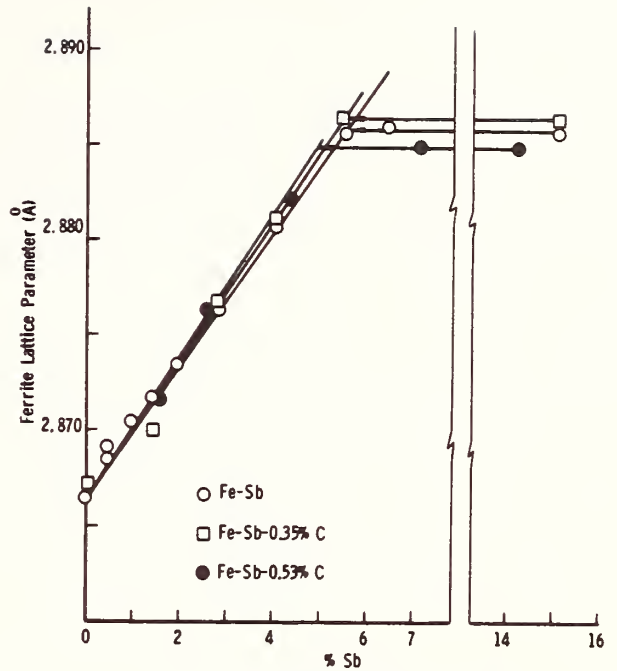
The addition of even small amounts of certain impurity elements to iron-carbon alloys can result in a severe loss in ductility when tempered at 500 C. The partitioning of these elements between the ferrite and the carbide phases was felt critical to better understanding of the problem. Electron probe microanalysis, carbide extraction, and x-ray diffraction techniques were employed to this end. Figure 6 shows some of the data and Figure 7 shows the iron-rich end of the binary phase diagram for one of the impurity elements, antimony. Again, the phase diagram was gemain to the better understanding of the problem.

Heat Treatment of a Modified Tool Steel

In the heat treatment of a modified tool steel where the carbon level is lowered considerably, a much higher hardening temperature than normal was required to eliminate the low temperature ferrite phase which was considered



a. Fe-Sb binary alloys.



b. Fe-Sb and Fe-Sb-C alloys.

FIGURE 6. Ferrite Lattice Parameter as a Function of Antimony Concentration Alloys were Annealed at 600 C Unless Otherwise Indicated

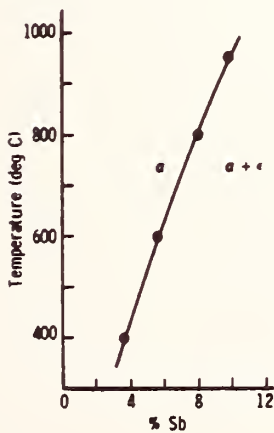


FIGURE 7. The Iron-Rich End of the Iron-Antimony Binary Phase Diagram Based Upon Present Results, Showing the α -Solvus

undesirable for the application. It turned out, however, that the ferrite could be reduced only to an irreducible limit before the hardening temperature became so high as to create a distortion problem. A qualitative probe analysis indicated no significant alloy transfer to the ferrite for normal hardening times and the relatively low amount of delta ferrite could be ignored. This is a very simple example but, in general, phase amounts and compositions would be invaluable in the investigation of the general class of tool steels.

The above examples are typical of the needs of the metallurgist in his investigations of alloys for the important information contained in phase diagrams. Any help that the metallurgist can get in this area whether it be a data bank of available (readily retrievable) information or approximate computational diagrams (generally for multicomponent systems) would be welcome.



Phase Diagram of a Specimen at High Temperatures
under external tensile or Shear Stress or both.

By

K.M. Khanna
Head, Materials Science Deptt.,
National Institute of Foundry
and Forge Technology,
Hatia, Ranchi-834003, India.

Abstract:

Phase Diagrams are graphs that give relationships between various phases in a system as a function of temperature, pressure and composition. To my mind, phase changes at high temperatures under tensile or shear stress or both have not been studied so far. Similarly the corresponding phase diagrams have also not been studied. It will be interesting to plot the phase diagram of a specimen under external tensile or shear stress or both, keeping pressure constant and varying the temperature. Having done so we can have a better insight into the control of micro-structure. We can have an idea of the life time of a specimen that works at high temperatures under external tensile and shear stress. Experimental studies can be made by providing a tensometer type attachment to the dilatometer.

Basic Theory and Discussion:

Let a specimen be under external stress and the temperature gradient. As a consequence of the thermal agitation, the charge density of the electrons at any point and at any instant of time is reduced by an amount which depends only on the temperature under constant external stress. Let the decrease in the charge density be represented by a (T) . Thus the charge density at any point x can be written as,

$$\rho(x) = \frac{ze}{L} \sum_{n=1}^N \sin^2 \frac{n\pi x}{L} - a(T) \quad (1)$$

where L is the side of the box in which the electrons are enclosed and e is the charge on the electron. Eq.(1) can be written as,

$$\begin{aligned} \rho(x) &= e \left[\frac{N}{L} - \frac{\sin 2\pi N x / L}{2\pi x} \right] - a(T) \\ &= \rho_0 - \rho_0 \frac{\sin 2\pi N x / L}{2\pi N x / L} - a(T) \end{aligned} \quad (2)$$

where

$$\rho_0 = \frac{eN}{L} \quad (3)$$

or

$$\frac{\rho(x) - \rho_0}{\rho_0} = \rho = - \frac{\sin 2\pi N x / L}{2\pi N x / L} - \frac{a(T)}{\rho_0} \quad (4)$$

The quantity L will be a function of the external stress F and the temperature T , such that,

$$L = L(F, T) = L_0 + \alpha_F F + \alpha_T T \quad (5)$$

We can write,

$$d\rho = \frac{\partial \rho}{\partial F} dF + \frac{\partial \rho}{\partial T} dT \quad (6)$$

where,

$$\frac{\partial \rho}{\partial F} = \frac{\rho_F}{L} \cos \frac{2\pi N x}{L} - \frac{\rho_F}{2\pi N x} \sin \frac{2\pi N x}{L}$$
$$\frac{\partial \rho}{\partial T} = \frac{\rho_T}{L} \cos \frac{2\pi N x}{L} - \frac{\rho_T}{2\pi N x} \sin \frac{2\pi N x}{L}$$

Eq. (6), therefore, shows that in plotting phase diagrams of specimens under external stress and temperature, the density variations of electrons in the specimen must be taken into account. This concept will add new element of information to the existing knowledge on phase diagrams.



PHASE DIAGRAM OF A METAL - GAS SYSTEM

By

*

V.K. SINHA, B.Sc. Engg.(Met.), Ph.D.

A B S T R A C T

A simple technique for determining various phase relations in metal - gas systems is discussed. The difficulties associated with interpretation of conventional phase diagrams of metal - gas systems are highlighted and a modified format in this context is suggested. The method of computing various thermodynamic quantities from the modified phase diagram is demonstrated. Some of the results obtained for the Zr - H₂ and Zr - Nb - H₂ systems are also included for illustration.

* The author is with Department of Materials Science, National Institute of Foundry and Forge Technology, Hatia, Ranchi-834003, Bihar State, India.

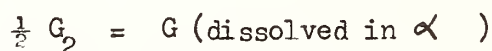
Introduction:

The phase diagram is an indispensable means for representing physico - chemical state of a system in terms of the state variables, pressure (P), composition (C), and temperature (T). For metallic or other systems the phase diagram is conventionally represented⁽¹⁻³⁾ in the form of T - C diagrams at fixed pressure of 1 atm. which suits most of the practical purposes unless otherwise pressure variations are too large. A similar representation for the phase diagram of a metal - gas system is, however , inadequate because of the pronounced effect of gas partial pressure in fixing the physico - chemical state. In the past,⁽¹⁻³⁾ the phase diagrams of metal - gas systems have also been compiled as T - C diagrams which lack information and are difficult to interpret. The author, therefore, recommends that in the latter cases the T - C diagrams must be supplemented either with the isothermal P - C diagrams or the constant composition P - T isochores or both. The P - C - T data contained therein will then provide not only a better understanding of the existence of equilibrium phases in terms of the state variables but also an easy means for computing the various thermodynamic functions.

The purpose of the present paper is to demonstrate a better format of representing the phase diagram of a metal - gas system, with particular reference to the binary Zr - H₂ system. The method of determining various thermodynamic quantities from the modified phase diagram is also discussed.

Discussion:

When a metal (M) at a given temperature is placed in contact with a gas (G), the latter is taken up until its concentration in the metal reaches a particular value. This concentration depends only on the pressure of the gas at that temperature. The phase relations in a metal - gas system can therefore be most conveniently determined with the help of standard thermodynamic relations using the measured pressure of the gas in equilibrium with the metal as a function of temperature and composition. In a binary metal - gas system schematically shown in Fig. 1(a) the dissolution reaction of gas in the α -phase, for example, may be represented as,^(4,5)



At equilibrium, $\frac{1}{2} F_{G_2} = \bar{F}_G(\alpha)$, where F_{G_2} is molar free energy of the gas and $\bar{F}_G(\alpha)$ is the partial gram - atomic free energy of gas in the α -phase. Assuming the gas to behave ideally, $F_{G_2} = F_{G_2}^{\circ} + RT \ln P_{G_2}$ and hence its partial gram - atomic free energy of mixing in the α -phase is,

$$\left(\bar{F}_G - \frac{1}{2} F_{G_2}^{\circ} \right) = \frac{1}{2} RT \ln P_{G_2} \quad (1)$$

The partial gram - atomic enthalpy of mixing of gas, $(\bar{H}_G - \frac{1}{2} H_{G_2}^{\circ})$ in the α -phase of composition $M_x G_y$ is obtained from the van't Hoff equation,

$$\left[\frac{\partial \ln P_{G_2}}{\partial (1/T)} \right]_{M_x G_y} = \frac{2(\bar{H}_G - \frac{1}{2} H_{G_2}^{\circ})}{R} \quad (2)$$

In equations (1) and (2) P_{G_2} is the gas partial pressure, $F_{G_2}^0$ is the free energy in the standard state, y/x is the atomic ratio of gas to metal, T is the temperature in degrees Kelvin and R is the gas constant. The mean partial molar entropy of mixing of gas, $(\bar{S}_G - \frac{1}{2} S_{G_2}^0)$ may be computed from the free energy and enthalpy values. The partial molar quantities of mixing of the metal component and the integral thermodynamic quantities may be obtained from the numerical integration of the Gibb's - Duhem equation. If variables other than P , C , and T are excluded the heterogeneous equilibria can be described by the Gibb's Phase Rule, $\Psi + \Phi = n+2$, where n is the number of components, Φ is the number of phases, and Ψ is the degrees of freedom or independently adjustable variables. Since the metal - gas alloys cannot exist except in equilibrium with the gas phase the equation reduces to $\Psi + \Phi = n+1$. In binary systems, the phase Rule predicts two degrees of freedom in single phase regions and therefore pressure depends both on temperature and composition. In the two - phase regions, there is only one degree of freedom and total composition can vary without affecting the pressure - temperature curve. The thermodynamic properties and Phase Rule lead to determination of various phase fields with the help of the following two methods;

Method I : $P - C$ isotherms ;

Pressure - composition measurements may be carried out experimentally at different temperatures. The points of intersection of steeply sloping isotherms with the plateaus determine the composition

limits of one - phase and two - phase fields. This is illustrated in Fig. 1 (b) at typical temperatures T_1 , T_2 , T_3 and T_4 . The composition limits derived from Fig. 1 (b) are marked in the T - C diagram [Fig. 1 (a)] .

Method II: P - T isochores;

In the van't Hoff plot of $\ln P_G$ against $1/T$ at constant gas concentrations, the one - phase and two - phase regions would be represented by areas and lines respectively. The shape of the line in the two - phase region is determined by the distribution of gas between the two co-existing phases, which is a function of gas solubility and relative amounts of the two phases. If these factors vary with temperature, the line would in general be non-linear⁽⁶⁾. Also, the partial gram - atomic enthalpy of mixing of gas obtained from the slope of the plot would be different for different phases. The P - T isochores for a large number of alloys of varying gas content is schematically shown in Fig. 1 (c) and the various phase fields are also labeled therein. The two - phase regions are ascertained by a non-linear $(\alpha+\beta)$ curve and two straight lines denoting the $(\beta+\delta)$ and $(\alpha+\delta)$ fields. It is observed that the P - T curves representing the $(\alpha+\beta)$, $(\beta+\delta)$ and $(\alpha+\delta)$ fields intersect at a triple point, T_e , which defines the $\beta \rightleftharpoons \alpha + \delta$ eutectoid horizontal of the T - C diagram [Fig. 1 (a)]. For an alloy $M_x G_y$, the line AB in Fig. 1 (c)

represents the $(\alpha + \delta)$ two - phase region. The intersection of the lines CB and AB at B represents the temperature T_1 at which the equilibrium $\alpha - (\alpha + \delta)$ exists. Similarly the intersection point C represents the temperature T_2 for the $\alpha - (\alpha + \beta)$ equilibrium and that of point D represents the temperature T_3 for the $(\alpha + \beta) - \beta$ equilibrium in the T - C diagram [Fig. 1 (a)]. Some of the experimental results of the present author⁽⁷⁻¹⁰⁾ on the Zr - H₂ and Zr - Nb - H₂ systems are shown in Figs. 2 - 5.

The above mentioned technique along with other conventional methods like dilatometric, X-ray diffraction, electrical resistivity, metallographic, tensimetric, thermal gradient, heat capacity measurement etc. have been used by numerous investigators to determine phase relations in various metal - gas systems. For the Zr - H₂ system, the widely accepted T - C diagram⁽¹¹⁾ with modifications^(12, 13) is shown in Fig. 6. The diagram gives instantaneous information about state of the system as a function of temperature and composition, however, without any idea of the hydrogen partial pressure which maintains the equilibrium. Consequently, for full details, the original published work of different investigators are to be referred which is cumbersome and as such the objectives of having separate compilation of phase diagrams are considerably diluted. The author, therefore, recommends that the phase diagram of the Zr - H₂ system or other metal - gas systems must be compiled in a uniform format as schematically shown in Figs. 1 (a), 1 (b) and 1 (c), where the T - C diagram has been

supplemented with the P - C isotherms and the P - T isochores. This provides not only a better understanding of the various phase relations but also an easy means to readily compute the various thermodynamic quantities from the P - C - T data through equations (1), (2) and the Gibb's - Duhem equation. Some of the author's computed results published elsewhere ⁽⁵⁾ are shown in Fig. 7. The modified phase diagram therefore eliminates the necessity of even a separate compilation of the thermodynamic data.

Conclusions:

1. The phase diagram of a metal - gas system should be represented in the form of T - C diagram supplemented either by the P - C isotherms or the P - T isochores or both.
2. The modified phase diagram may be readily used to compute the various thermodynamic quantities and hence a separate compilation of the latter may not be essential.

Acknowledgement:

The author is grateful to the Director, National Institute of Foundry and Forge Technology for according permission to present the paper.

....

References:

1. M. Hansen and K. Anderko, Constitution of Binary Alloys, Mc Graw - Hill, New York, 1958.
2. R. P. Elliott, Constitution of Binary Alloys, First Supplement, Mc Graw - Hill, New York, 1965.
3. F. A. Shunk, Constitution of Binary Alloys, Second Supplement, Mc Graw - Hill, New York, 1969.
4. V.K. Sinha and K.P. Singh, Trans. Ind. Inst. Metals, 1974, Vol. 27, p. 289.
5. V.K. Sinha, Met. Trans., 1976, Vol.7A, p. 472.
6. R. Speiser, Metal Hydrides, W. M. Mueller, J.P. Blackledge and G.G. Libowitz, eds., p. 51, Academic Press, New York, 1968.
7. V.K. Sinha and K.P. Singh, J. Nucl. Mater., 1970, Vol. 36, p. 211.
8. V.K. Sinha and K.P. Singh, Met. Trans., 1972, Vol.3, p. 1581.
9. V.K. Sinha, J. Chem. Soc. Faraday Trans. 1976, Vol. 72, p. 134.
10. V.K. Sinha, J. Nucl. Mater., 1976, Vol. 59, p. 201
11. Ref. 2, p. 513.
12. K.E. Moore and W.A. Young, J. Nucl. Mater., 1968, Vol.27, p.316.
13. S. Mishra, K.S. Shivaramakrishnan and M.K. Agundi, J. Nucl. Mater., 1972/73, Vol. 45, p. 235.

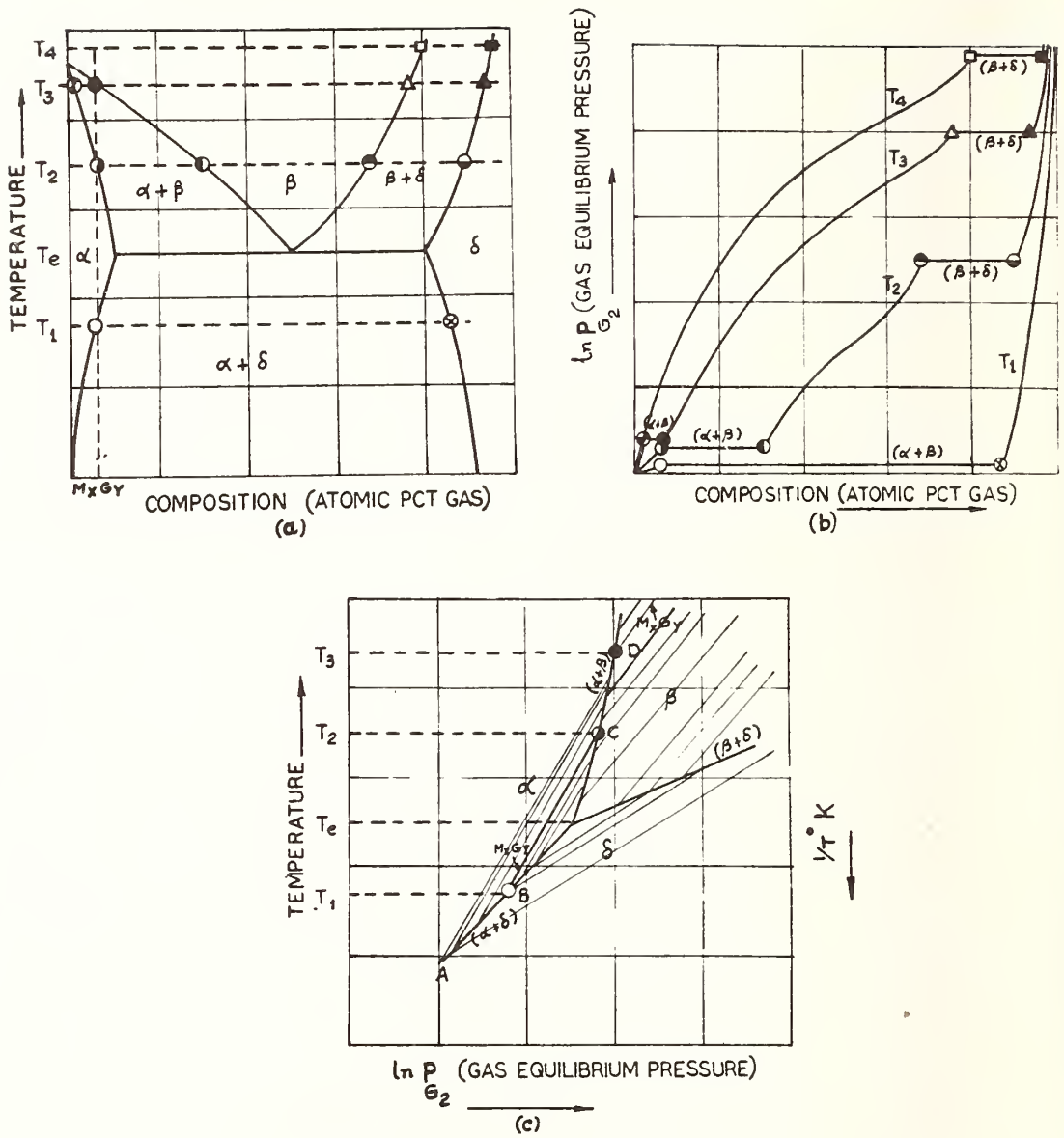


Figure 1. Phase-Diagram of Metal-Gas System (Schematic) (a) Temperature-composition Diagram (b) Pressure-Composition Isotherms (c) Pressure-Temperature Isochores

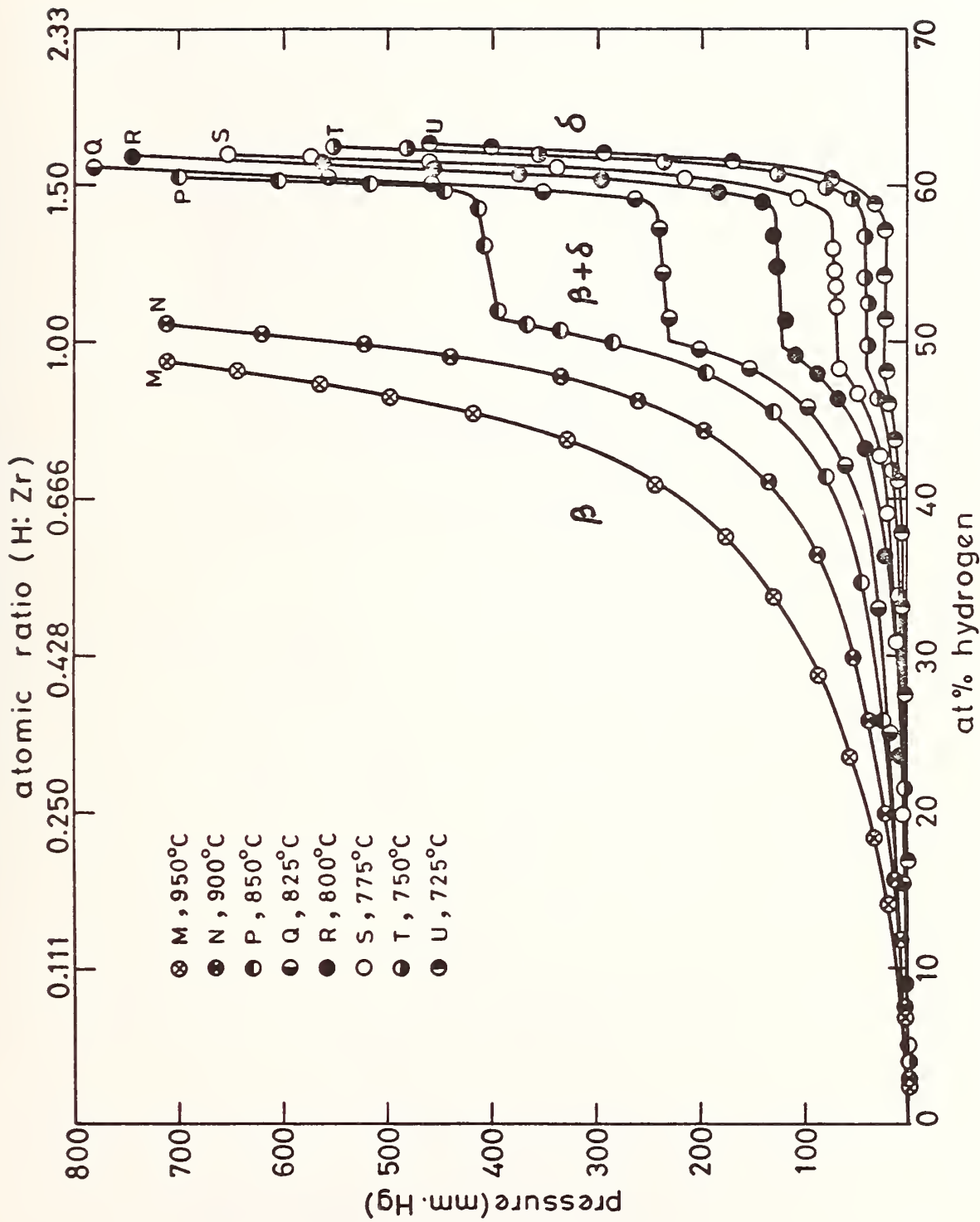


Fig. 2 Isothermal pressure against at% hydrogen for unalloyed Zr in the temperature range 725 to 950°C.

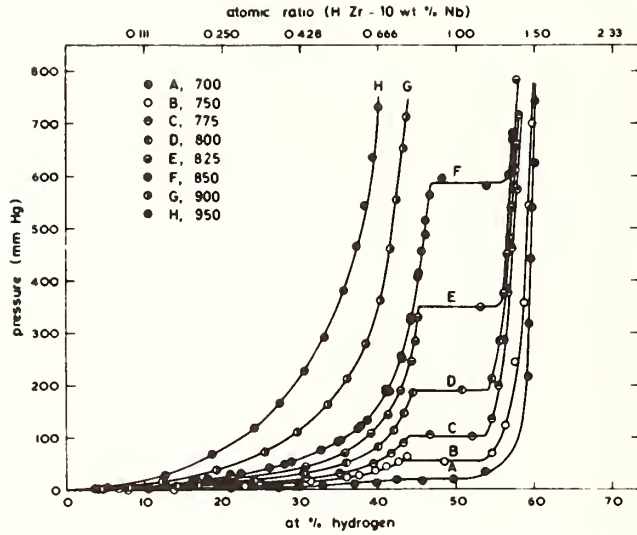


Fig. 3—Isothermal pressure against at. pct H for Zr-10 wt pct Nb alloy in the temperature range 700° to 950° C.

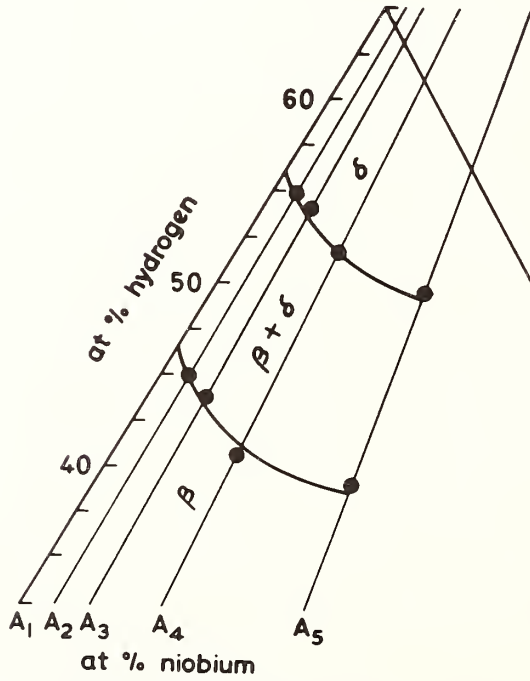


Fig. 4—Isothermal section for the ternary system Zr-Nb-H at 700°C. A₁, 0.0 at. pct Nb; A₂, 2.46 at. pct Nb; A₃, 4.91 at. pct Nb; A₄, 9.84 at. pct Nb; A₅, 19.71 at. pct Nb.

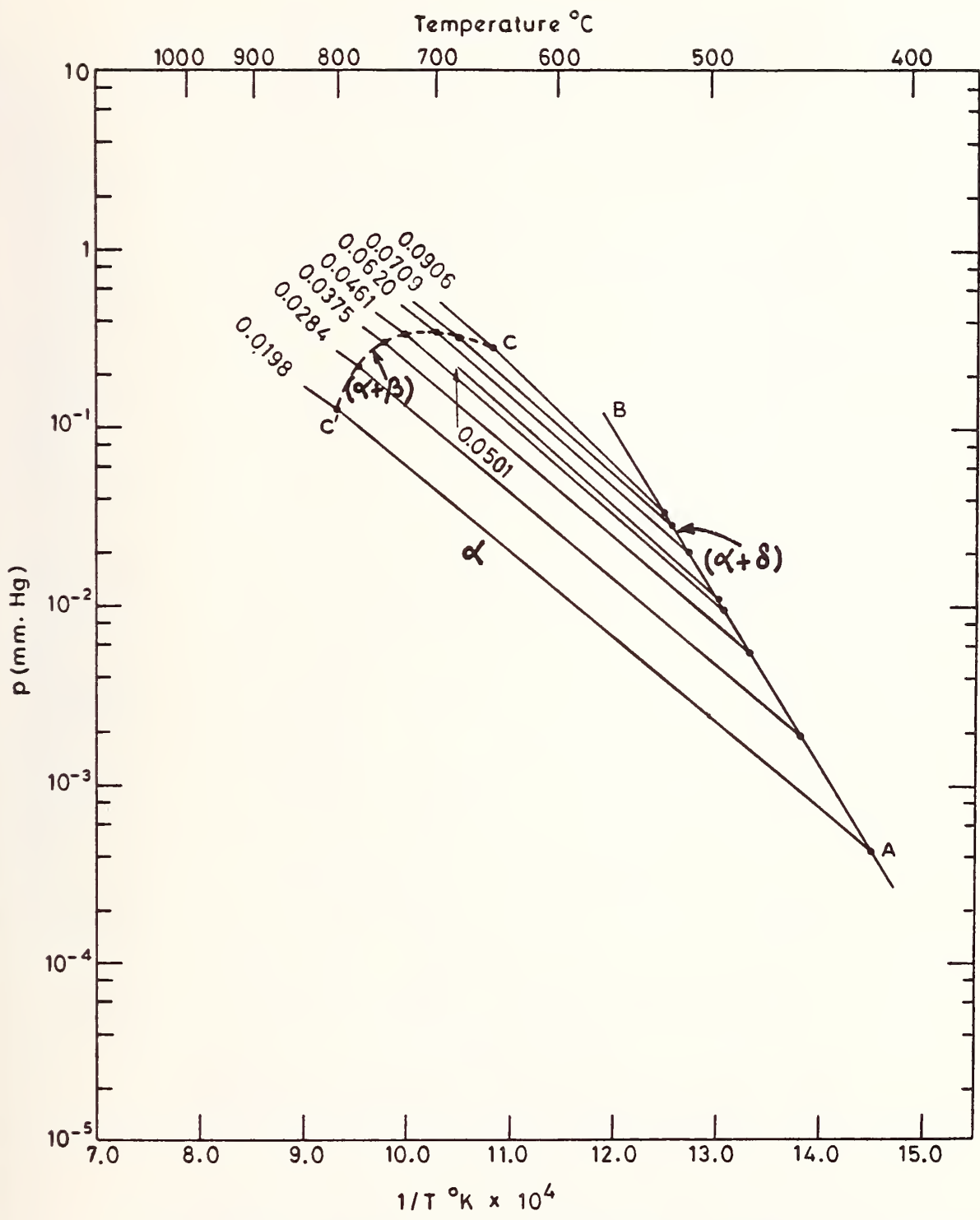


Fig. 5 Summary plot of decomposition pressure vs. reciprocal of temperature for different zirconium-2.5 wt% niobium-hydrogen alloys. The number on a plot represents the H/(Zr-2.5 wt% Nb) atomic ratio

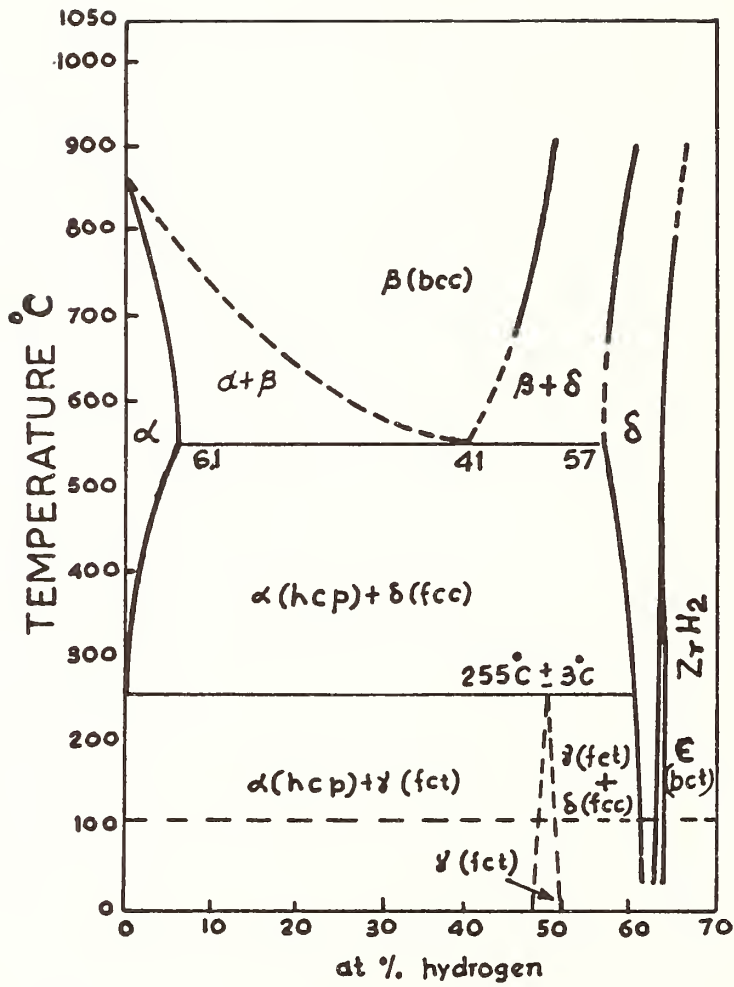


FIG.6. THE EQUILIBRIUM PHASE RELATIONS IN ZIRCONIUM-HYDROGEN SYSTEM

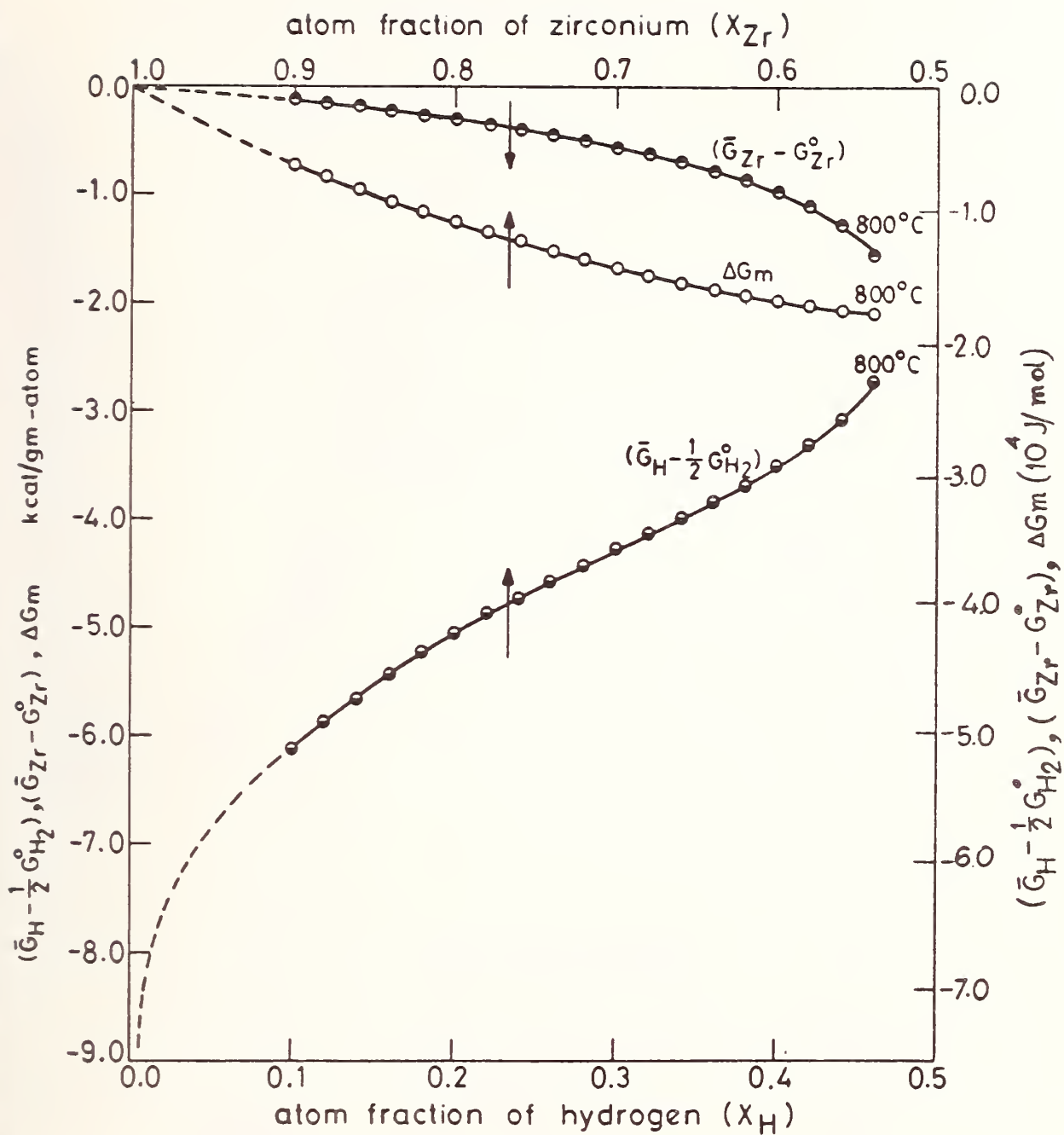


Fig. 7 Free energy against atom fraction of hydrogen plot in the β -phase of Zr- H_2 system at 800°C .

•, $(\bar{G}_H - \frac{1}{2} G_{H_2}^0)$; •, $(\bar{G}_{Zr} - G_{Zr}^0)$; ○, ΔG_m . The arrow indicates the direction in which an isothermal curve shifts with increase in temperature.



THEORY OF ALLOY PHASES

R. E. Watson
Brookhaven National Laboratory*
Upton, NY 11973

H. Ehrenreich†
Harvard University
Cambridge, MA 02138

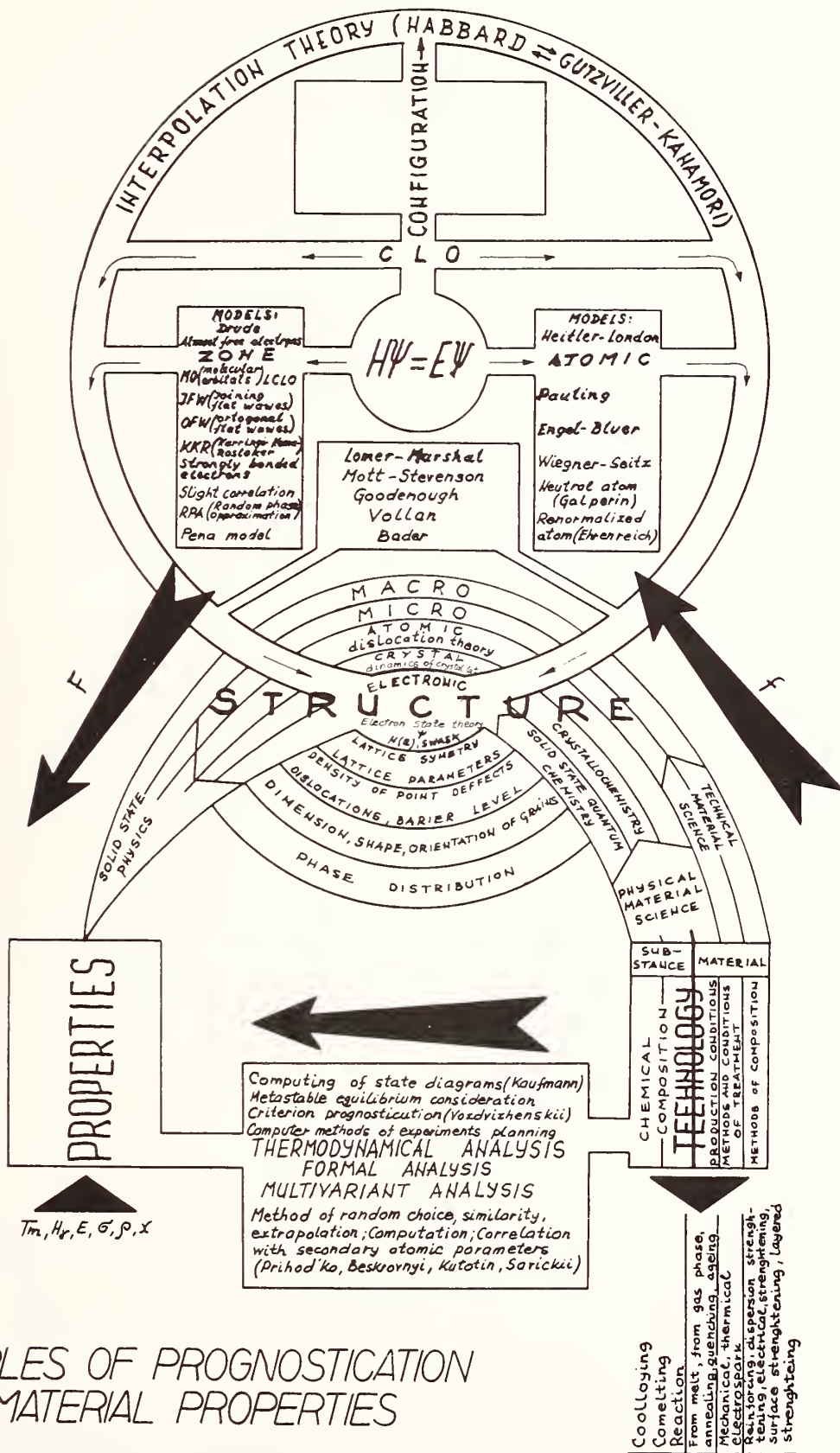
and

L. H. Bennett
Institute of Materials Research
National Bureau of Standards
Washington, DC 20234

I. Introduction

The problem of understanding and predicting phase diagrams may be attacked in a variety of ways ranging from the successful thermodynamic approaches of Kaufman and others to the a priori band theory estimates of the solid-state physicist. In one of his last papers, Samsonov produced¹ a "global map" (Fig. 1) that indicates the dilemma of talking about the subject of this tutorial. The work-horses of this meeting are in the lower part of the diagram, sitting on the ground so-to-speak. In the heavens is Schrödinger's equation, surrounded by a variety of practical and impractical schemes, including faulty transliterations (e.g. Prof. Brewer, who is on the program of the Workshop, is called Bluer). The orderliness of Fig. 1 is only apparent - the real life situation is much more complicated. The purpose of the present article is to explore various non-thermodynamic approaches from the viewpoint of solid-state physics. We will not attempt complete coverage of the subject but will, instead, try to indicate the scope of activity and to indicate some of the progress which has been made.

It appears to be within the means of present day a priori energy



PRINCIPLES OF PROGNOSTICATION OF MATERIAL PROPERTIES

Fig. 1. Samsonov's organization (1) of a variety of schemes for predicting phase diagrams and other properties of solids.

band theory to estimate the phase diagram of a binary system, provided sufficient care is taken in the choice of the system. The computer costs would be high and the results would probably indicate little that wasn't already understood. This type of approach will be of minor concern here. Instead we will ask what solid-state theory, as practiced in either a chemistry or physics department, has to say concerning various model approaches to phase diagram predictions and what physical basis there is for choosing the relevant parameters entering these approaches. We will also consider several classes of questions concerning solubility or tendencies for martensitic transformations, which are appropriate to ask of a band theory calculation. Finally, we will remind the reader of a few of the approximations, which are often used but not always justified, in solid state theory.

Section II will be concerned with transition metal cohesion, magnetic effects and alloying. This will be followed by consideration of potentials and pseudo-potential applications. Section IV will discuss electronegativities and pair-potential approaches. This will be followed by consideration of Madelung effects and the problem of defining atomic size and charge. The final sections will cover some aspects of what can be learned from band theory calculations concerning such matters as alloy solubility, as well as some activities by the solid-state community of which the metallurgist and ceramist should be aware.

As has already been admitted, this will be a broad-brush review. We apologize to those workers whose results are either neglected or, worse, dealt with inadequately.

II. Transition Metals: Cohesion, Magnetic Effects and Alloying

It is useful to begin by considering the cohesion of the pure transition metals. The various factors² contributing to a band theory estimate of cohesion in Ti are indicated in Fig. 2. The atomic ground configuration is $3d^2 4s^2$, (a), whereas the $3d^3 4s$ configuration is more appropriate to the metal. The resulting atomic excitation, (a) \rightarrow (b), is the familiar Brewer promotion energy. The atomic charge

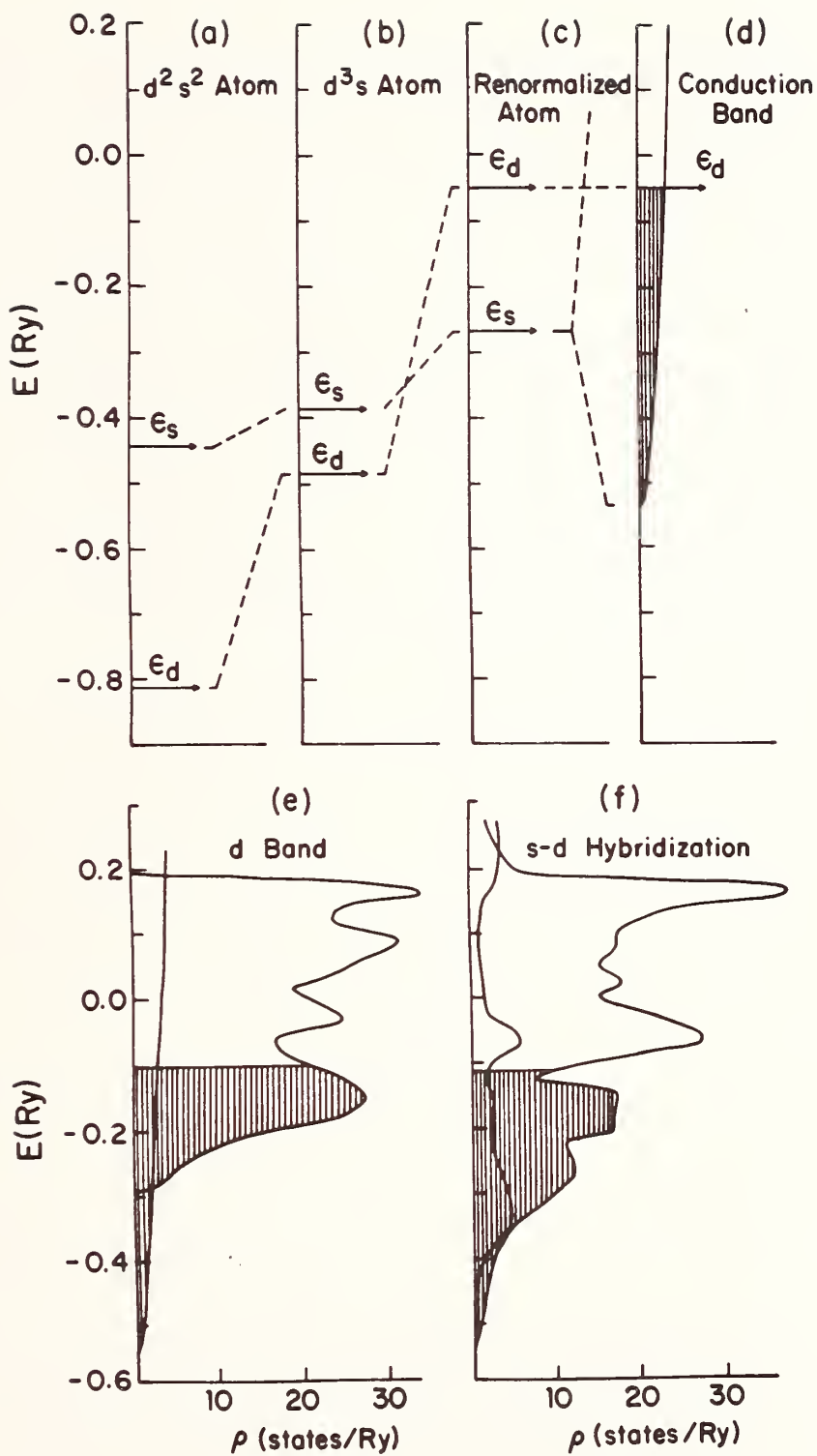


Fig. 2. The various factors contributing to the electron energy structure of a transition metal. As an example of these, Ti is taken from its free atom ground state to the metal. See Ref. 2 for details.

within the metal is constrained to be within the atomic Wigner-Seitz cell whereas some of the charge is considerably outside this volume in the free atom. The resulting compression of charge increases the valence electron contributions to the coulomb potential and raises the one-electron energy levels, ϵ_s and ϵ_d , as is seen in (c). The s level broadens into a non-d conduction band, as in (d). The bottom-most level of this band is determined by the boundary condition that the wavefunction be flat at the Wigner-Seitz radius. This condition lets the electron have a compressed charge density without a severe cost in kinetic energy and, as a result, substantially lower energy than the ϵ_s of the renormalized atom. As was pointed out³ by Wigner and Seitz, this is the essential feature of cohesion in the alkali metals: the center of gravity of the occupied levels in the resulting conduction band lies lower than the free atoms one-electron level, ϵ_s . This does not have to be the case in the transition metals due to more important d-electron contributions. As is indicated in (e), the d level broadens into a band whose center of gravity remains at ϵ_d finally, the conduction and d bands hybridize (the two curves in (f) indicate the relative weights of d and non-d characters in the final density of states). As Friedel and his associates⁴ have emphasized, it is the broadening of the d levels into a band structure which is essential to the variation in cohesion across a transition metal row. Putting one electron per atom in the d bands gains the difference in energy between ϵ_d and the center of gravity of the occupied levels. Putting in a second electron per atom yields less energy than the first, since one must fill states lying closer to ϵ_d . Once the band is half filled, some of the benefits of band broadening are lost since states above ϵ_d are being occupied. Once the band is completely filled, band broadening makes no further contribution to cohesion since the center of gravity of the occupied levels is the equal to ϵ_d . Estimates of the various contributions to cohesion of the 3d and 4d transition metal rows are indicated in Fig. 3 (see ref. 2 for details of these calculations). Agreement with experiments is quite

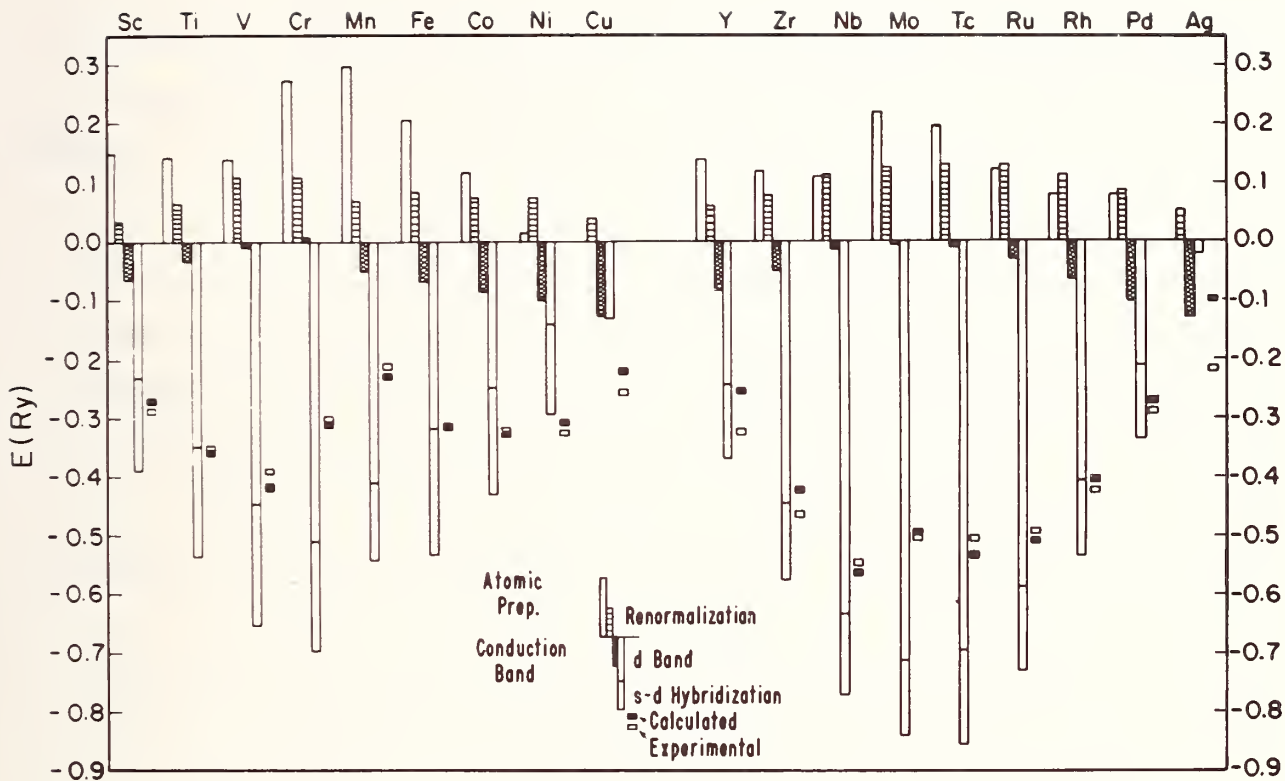


Fig. 3. Theoretical estimates of the various contributions to the cohesion of the 3d and 4d row transition metals. The breakdown of the contributions follows from Fig. 2: These are the preparation of the atom into the proper atomic configuration, renormalization to the metallic volume, conductor and d-band broadenings, and the effects of s-d hybridization. See Ref. 2 for details of the calculation.

good in this set of estimates. The effects of d-band broadening and of promotion of the free atom into the configuration most appropriate to the solid are most important in determining the variation of cohesion across the rows. Cu and Ag with their filled d bands have no d-band broadening contributions. There are significant contributions arising from hybridization between d and conduction bands. For the other metals, the band-broadening contribution depends on the extent to which the d-band is filled and is proportional to the band width of the metal in question. Friedel and Ducastelle⁵ have pointed out that the band width, and hence its contributions to cohesion, does not arise from a sum of atom-atom pair interaction terms.

Band calculations such as these typically yield non-d electron counts of $1 \pm 1/4$ electrons across a transition metal row. This is consistent with Engel-Brewer theory, as it is commonly defined, for the body-centered and hexagonal metals, but not for the face centered cubic metals encountered in the Ni and Cu columns of the periodic table. The Brewer or Pauling view emphasizes the role of non-d electrons in transition metal structures while the band theory view, as exemplified in Fig. 3, suggests that d electrons play the essential role.

The difference in energy on going from one structure to another is, of course, much smaller than the total cohesive energy. Nevertheless band theory has had modest success in predicting the experimental trends. Pettifor, for example, has taken⁷ electron densities of states, $\rho_1(\epsilon)$, such as that plotted for the fcc structure in Fig. 2, and has evaluated the energy differences

$$\Delta E = \Delta \int_{\text{band bottom}}^{\text{Fermi level}} \epsilon \rho_1(\epsilon) d\epsilon, \quad (1)$$

between fcc, bcc and hcp structures. After modest adjustment of parameters (e.g. band width and position), his results reproduce the experimental trends.

It has been recognized for some time that the presence of local magnetic moments sensibly alters a transition metal's lattice constant⁸. These magnetic contributions have been the object of calculations by

Poulsen et al.⁹ and by Janak and Williams¹⁰. The latter's results for the Wigner-Seitz radii and for bulk moduli, calculated for paramagnetic metals, are shown in Fig. 4. Calculation agrees with experiment for the 4d metals which are paramagnetic, but breaks are seen in the middle of the 3d row where magnetic moments occur. Janak and Williams, using exchange polarized band calculations, went on to estimate the derivatives of the plotted quantities with moment and, using the experimentally accepted moment values, obtained the results of Fig. 5. The agreement with experiment is quite good, but perhaps deceptively so in the case of Mn which occurs in four allotropes whose Wigner-Seitz radii do not correlate with the moments which occur. Two of the four allotropes, the γ and δ phases, are close packed and, of the two, the phase with the larger moment has the smaller Wigner-Seitz radius contrary to the model employed in Fig. 5. Poulsen et al.'s calculations were limited to the Fe and Ni columns of the periodic table. They obtained similarly good results and were able to discuss the relative stability of the fcc and bcc phase of iron.

For the case of the properties of disordered transition metal alloys, the coherent potential approximation (CPA) has been developed¹¹. In this scheme, the d-electrons maintain their atomic character, e.g. in Cu-Ni alloys, the d-electrons are Cu-like at Cu sites and Ni-like at Ni sites, in first approximation. Efforts, largely in France, have been made^{12,13} applying CPA and various perturbation schemes to the prediction of phase stability in such alloys. In general these employ model densities of states of the constituent metals. A sample¹² of the results is shown in Fig. 6 where comparison is made with Kaufman's thermodynamic approach¹⁴. This is not the only, or necessarily the best example we could have chosen, but is particularly interesting because of the contact it makes with the thermodynamic predictions methods discussed elsewhere in this workshop. The technology of such calculations is being actively studied and improved. Questions concerning how to improve quantum mechanical models for real alloys, which remain computationally tractable are the object of study. The calculations have reached the stage where the question

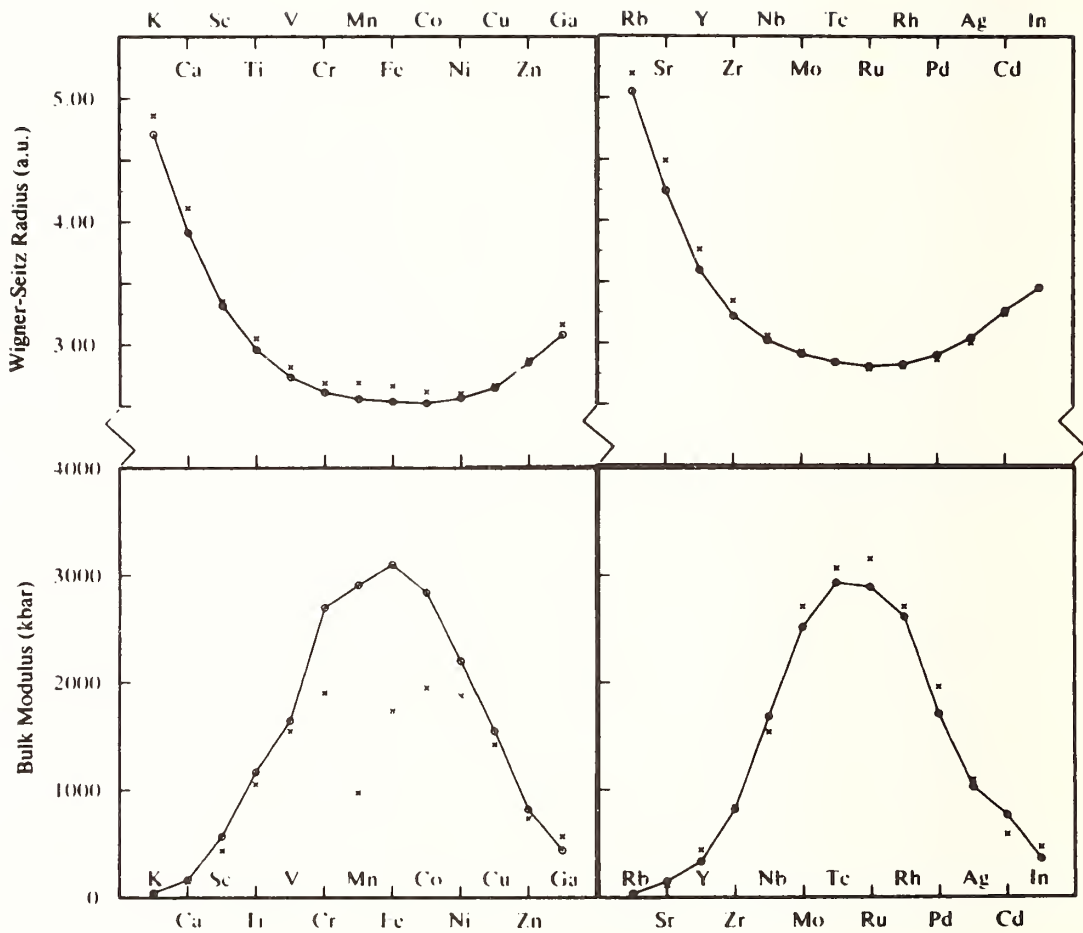


Fig. 4. Janak and Williams' band theory estimates⁽¹⁰⁾ of the Wigner-Seitz radii and bulk moduli of 3d and 4d transition metals in the paramagnetic states. The crosses are experimental values. Note that there are significant deviations for Cr through Ni, which have magnetic moments.

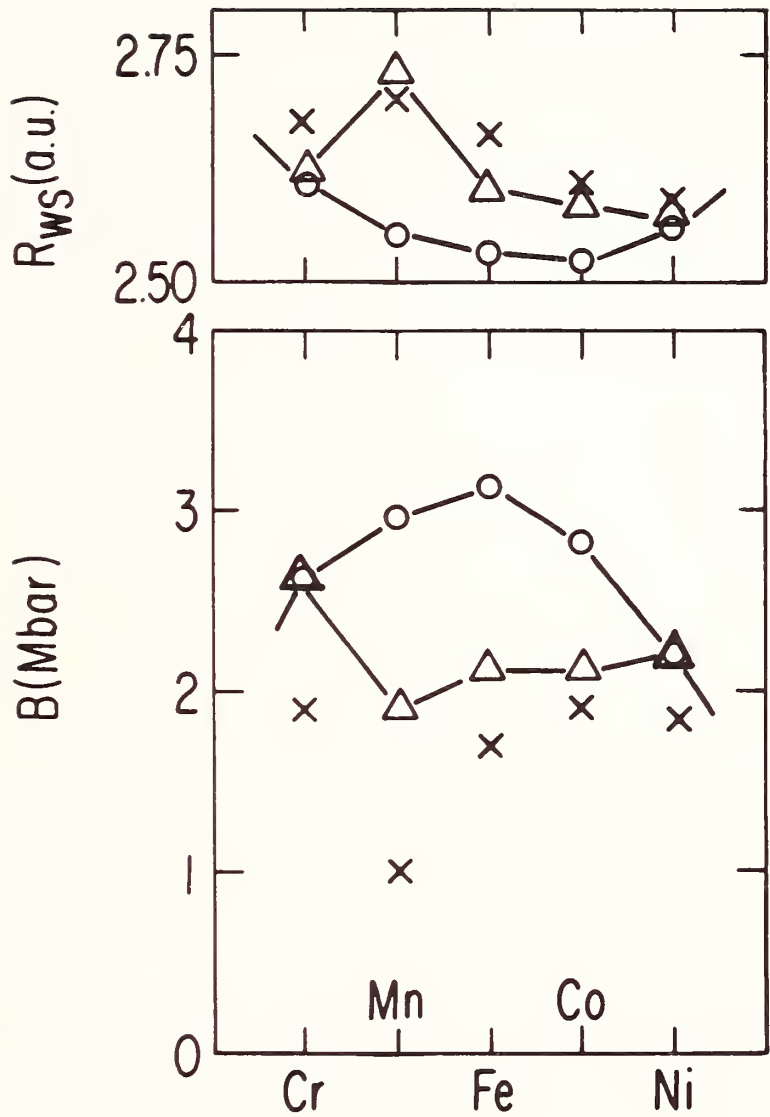


Fig. 5. Janak and Williams' estimates⁽¹⁰⁾ of Wigner-Seitz radii and bulk moduli for the paramagnetic (circles) and magnetized (triangles) transition metals Cr through Ni. The crosses are the experimental values.

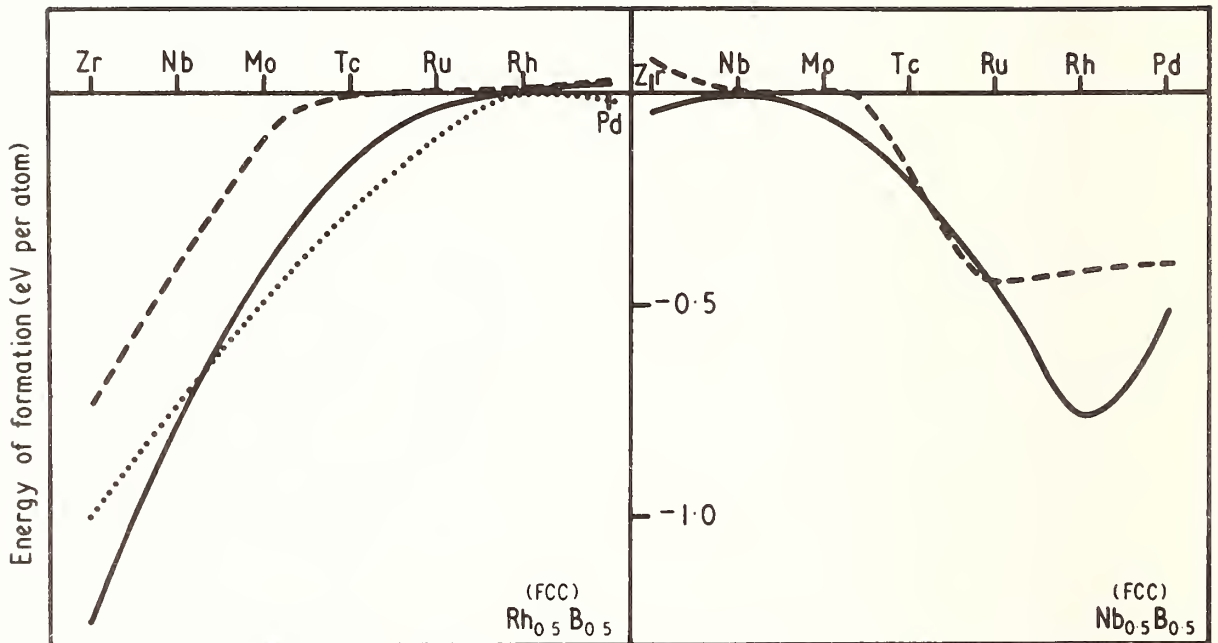


Fig. 6. van der Rest et al.'s estimates¹² of the energy of formation of equiconcentrational rhodium and niobium based alloys with elements of the second transition metal row having the fcc structure. The dashed lines are their standard solutions, the dotted obtained with an improved model density of states. Comparison is made with thermodynamic estimates of Kaufman (solid lines).

of how well theory agrees with experiment is also being addressed. Few, if any, real qualitative contradictions have been found thus far for the relatively small number of alloy systems that have been carefully studied. This indicates that the models used are at least qualitatively adequate and may be used to obtain insight into the physical mechanisms important to alloy formation.

III. Approximations, Potentials and Pseudopotentials

Of the several approximations made in some of the calculations cited here, two deserve special mention. One is associated with estimating total energy differences and the other with potentials. Approximations are often computationally necessary and less frequently quantitatively justifiable. Accordingly one must be alert to their possible implications.

The total energy of a many-electron system having one-electron energies ϵ_i that are characteristic of the interacting system is

$$E = \sum_i^{\text{all electrons}} \epsilon_i - \sum_i^{\text{all electrons}} \sum_{j < i} \left[\left\langle i i \left| \frac{e^2}{r_{ij}} \right| j j \right\rangle - \left\langle i j \left| \frac{e^2}{r_{ij}} \right| j i \right\rangle \right] \quad (2)$$

Since each ϵ_i has contributions from interaction with all other electrons, j , a simple sum of one-electron energies double counts electron-electron interaction terms which thus are subtracted to obtain a correct expression for the total energy E . Now it is normally the difference in total energy which is of concern and usually there is an atomic core common to the states being compared: if so, we may rewrite Eq. (2)

$$E = E_c + \sum_i^{\text{valence electrons}} \epsilon_i - \sum_i^{\text{valence electrons}} \sum_{j < i} \left[\left\langle i i \left| \frac{e^2}{r_{ij}} \right| j j \right\rangle - \left\langle i j \left| \frac{2}{r_{ij}} \right| j i \right\rangle \right] \quad (3)$$

where the sums are limited to the valence electrons and E_c is the core energy involving the kinetic and nuclear potential energies of the

core electrons plus core-core interelectronic terms. There still remains a subtraction of valence electron - valence electron interaction terms which is often computationally inconvenient when calculating an energy difference characteristic of two phases. When taking such energy differences it is often assumed that the differences in the double sum may be neglected, yielding

$$\begin{array}{c} \text{valence} \\ \text{electrons} \end{array} \quad \Delta E = \Delta \sum \epsilon_i \quad (4)$$

which, in its integral form, is Eq. (1). This approximation is frequently valid, though rarely is the justification presented in a published paper. Indeed, there are cases where the approximation is inapplicable. Consider the case of a transition metal where alloying or compound formation has led to an increase (decrease) in d electron count with a compensating decrease (increase) in the number of non-d electrons. Being more compact, the interaction energy between a pair of d electrons is roughly twice that among non-d or between d and non-d electrons. Eqs. (1) and (4) are not applicable if interchange between d and non-d electrons is significant.

Approximations are also involved in the potentials used in calculating energies and wavefunctions of many-electron systems. "Non-local" effects occur because one electron acts to avoid another due to the repulsive e^2/r_{ij} interaction. The potential sampled by electron i depends on that electron's spatial distribution. While exchange (and correlation) terms can be manipulated so that the potential multiplying the wave function ϕ_i is a function only of coordinates i, the resulting potential $V(\vec{r}, i)$ is only appropriate to electron i. In other words, there is a term

$$V(\vec{r}, i) \phi_i(\vec{r})$$

in the one-electron, Schrödinger equation rather than

$$V(\vec{r}) \phi_i(\vec{r})$$

where $V(\vec{r})$ is a "local" potential common to all electrons.

Hartree-Fock theory, for example, includes non-local effects associated with exchange. Calculations employing different potentials for different electrons are computationally inconvenient and normally avoided for solids. Sometimes ℓ -dependent potentials are used where electrons, or more precisely, wavefunction components of differing angular quantum number ℓ , "sample" different potentials. The results of Figs. 2 and 3 are an example in which d and non-d electrons were allowed differing, hence non-local, potentials as is desirable on physical grounds. More specifically, these calculations employed Hartree-Fock-Wigner-Seitz potentials. These potentials differ from Hartree-Fock theory in that they include a self-Coulomb exchange-correlation hole which is centered, and contained within, the atomic site at which the potential is defined. Put another way, the potential is such that each electron in the neutral unit cell samples the potential due to all the others in that cell, excluding the full charge associated with itself. Such potentials are expected to provide a good approximation to correlation effects for d electrons; they are less appropriate for the less localized non-d electrons for which the hole should be centered about the electron in question.

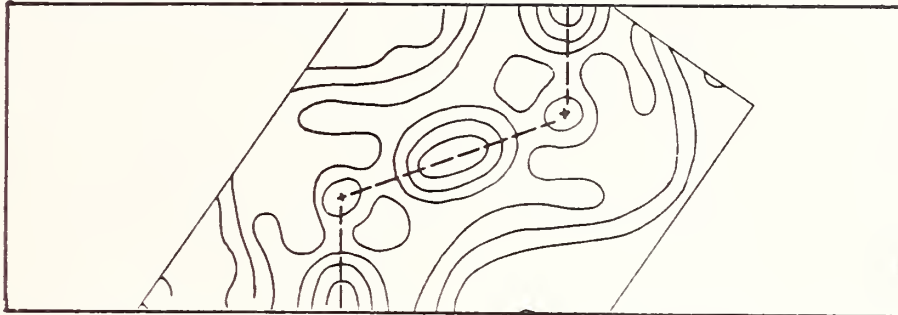
Starting with the work of Slater¹⁵ and of Kohn, Hohenberg and Sham¹⁶, among others, there has been considerable work directed toward defining a single potential to serve all electrons. Hedin and Lundqvist¹⁷ have derived a local potential which incorporates correlation as well as exchange effects. The dielectric response of metallic electrons to an external perturbation was evaluated. This permitted an estimate of their contribution to the potential sampled by an electron. The result is an exchange - correlation potential which is a function of the electron density at the point at which the potential is evaluated. Hedin and Lundqvist's potential is widely used in energy band calculations. This has been extended by von Barth and Hedin¹⁸ to the magnetic case where separate exchange-correlation potentials are constructed for electrons of majority and minority spin. It is likely that someone will

generate an ℓ -dependent variant of this class of potential to differentiate between d and non-d electrons in transition metals. Whatever the gains, the beauty and simplicity of a unified local exchange-correlation potential will have been sacrificed.

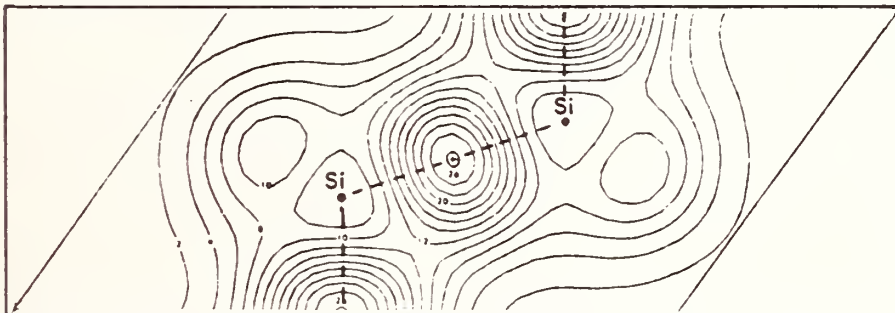
Pseudopotentials are often used, particularly for semiconductors and simple metals. In this constant, a repulsive term is added to the potential which accounts for orthogonalization to the atomic core. This allows one to deal with a wavefunction which does not have the wiggles, associated with core orthogonalization, in the interior of an atom. Both local and ℓ -dependent pseudopotentials are in common usage. Calculations for silicon suggest what can happen. Using a local pseudopotential, Walter and Cohen computed¹⁹ the charge density of the silicon valence electrons, as portrayed by the "contour map" in the middle of Fig. 7. Note the ellipsoids of charge built up between Si atoms. The experimental results appearing at the top of the figure were obtained²⁰ by Yang and Coppens from "forbidden" x-ray reflections - - reflections, which, by symmetry, would be absent if the density were simply a sum of spherical contributions. There are ellipsoids of charge of about the same magnitude as those computed, but with their long axis parallel, rather than normal to the Si-Si line. Using a two term ℓ dependent pseudopotential, Chelikowsky and Cohen obtained²¹ the results at the bottom of the figure. Better agreement is obtained in both the magnitude and the shape of the ellipsoid. In order to get the shape of the bonding charge correct, use of a nonlocal potential was thus required. The importance of this to total energies and, in turn, to the prediction of phase stability has not yet been assessed. Local pseudopotentials are very useful for many problems but one must be alert to their potential shortcomings. The applicability of this method has been extended to transition metals²², but due to technical reasons, its utility appears to be limited.

Stroud and Ashcroft used local pseudopotentials in their estimate²³ of the relative stability of the hcp, bcc and fcc struc-

Experimental
(Yang and Coppens)



Local Pseudopotential
(Walter and Cohen)



Nonlocal Pseudopotential
(Chelikowsky and Cohen)

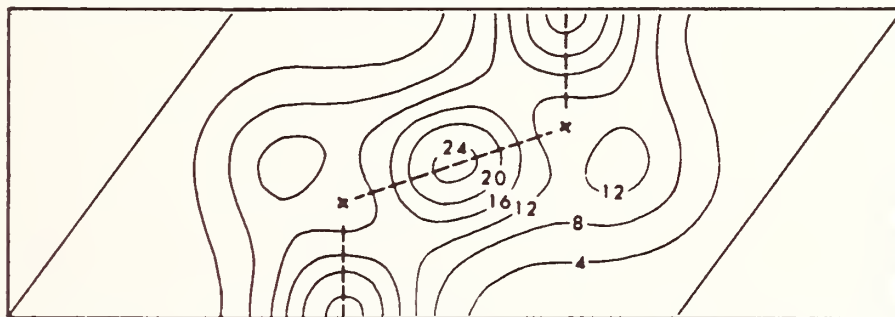


Fig. 7. The valence electron distribution in silicon as inferred experimentally from forbidden x-ray reflection data (top figure); from local pseudopotential theory (middle figure) and from non-local pseudopotential theory (bottom figure). (Refs. 20, 19 and 21 respectively.)

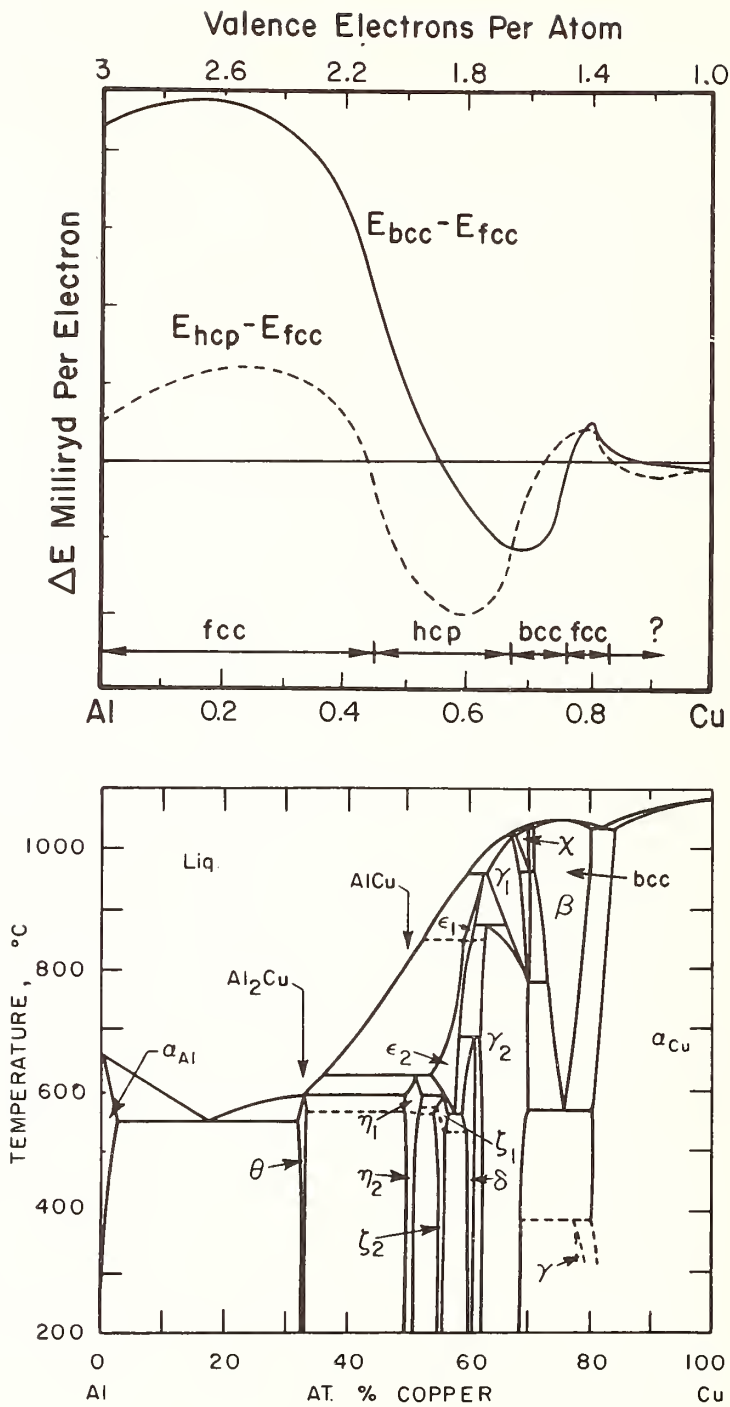


Fig. 8. The relative stability of the fcc, hcp and bcc structures in the CuAl alloy system as estimated by Stroud and Ashcroft²³. The actual phase diagram of the system is shown for comparison. Note that the bcc region (β phase) is correctly predicted for $0.7 < x < 0.8$ and that complex phases, not considered in the calculations occur for $0.45 < x \leq 0.7$ where the hcp structure is predicted. While the hcp is predicted for $x > 0.85$, the results are too close to call in this region.

tures for the Cu-Al system. Their results are shown in Fig. 8. The prediction of stable phases is indicated at the bottom of the plot. At the Cu rich end the computed phase energies are too close to one another to call. It is gratifying that the predicted bcc phase stability falls in just the region where the bcc β phase occurs. The region of predicted hcp stability is one where a variety of complicated structures occur to which the calculations are not relevant (though the η and ϵ phases are hexagonal, approximately close-packed structures). The predictions seen here are rather more successful than is typical for such calculations.

Girifalco has recently noted²⁴ that he can correlate alloy solubility by considering ion core radii, which are basically the radii of the repulsive cores of pseudopotentials instead of atomic sizes. If the core radii of homovalent constituents differ by more than 20%, there will not be mutual solubility. Whether this is more properly viewed as a size effect, or, instead, as a measure of the potential and in turn the electronegativity is difficult to say. We are inclined to the latter view.

Before leaving pseudopotentials, we should note that the machinery has been developed²⁵ to deal with ternary systems. Its much more complicated than the binary case and to our knowledge has not yet been used in actual calculations.

As has been indicated above, there are many classes of potential available to the band theorist. They often yield predictions of Fermi surfaces, optical spectra, and other properties that are consistent with experiment. While the evidence is somewhat limited, it would appear that potentials which yield consistent predictions for other properties do not yield consistent results for the alloy phase stability problem where small differences between large quantities are involved. Attention to this issue by solid-state theorists may yield insight into the problem of understanding alloy formation.

IV. Electronegativities and Pair Potential Approaches

The idea of electronegativity - the tendency for some atomic species to attract or donate electronic charge - is useful and intuitively satisfying. There are some problems associated with its use. First, there is no universal scale. Pauling and others consider Au the most electronegative among the metallic elements. This means that it attracts electrons from sites occupied by other metal constituents more strongly than any other metal. On the other hand most electronegativity scales employed by metallurgists, in connection with solubility or phase structure considerations, have a number of the transition metals such as Pt and Ir more electronegative than Au. On this point we believe the Pauling scale to be the "truer" measure of charge flow. What is more in addition to electronegativity, it appears to be necessary to have at least a second parameter to describe the metallurgical effects of concern to us here. There is, however, considerable difficulty in finding a parameter that is truly independent. Consider, for example, Miedema's scheme²⁶.

Miedema and his associates introduced a metallurgical electronegativity scale which used experimental workfunctions as a starting point. For this scale, Pt is more electronegative than Au. Instead of defining the second parameter, say, in terms of the atomic size, they used the electronic density at the outer part of the atomic cell appropriate to the atom in its elemental solid form. When constructing a compound or alloy of several atomic species there would be density mismatches which must be removed. This would cost energy unlike the electronegativity mismatches which cause charge flow and compound stabilization. The result is a plot for the elements as in Fig. 9: this is not Miedema's most recent set of parameters but serves present purposes well. Miedema's point was that, for alloys, one could draw two lines, in this case through H, thereby producing predictions for the heat of formation of H-metal alloys. The electronegativity dominates in the top and

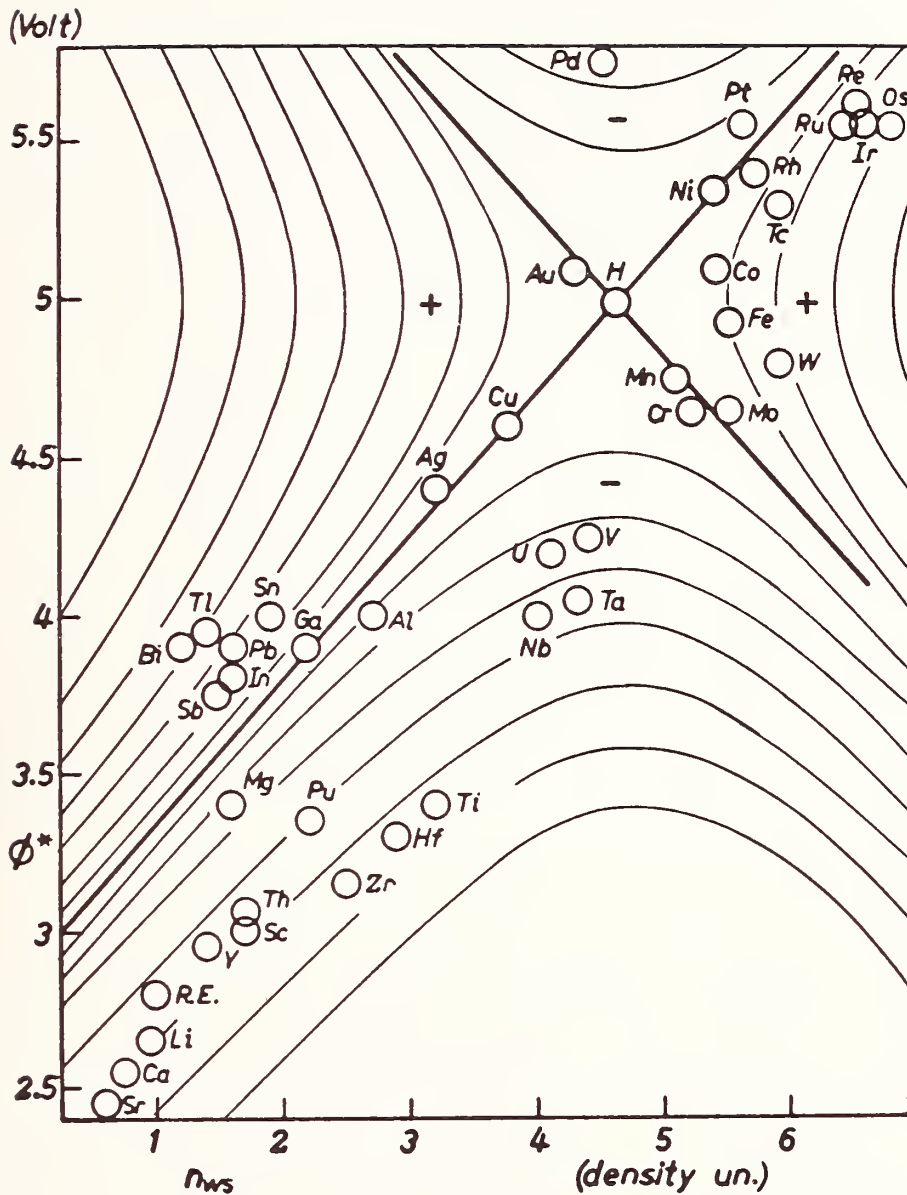


Fig. 9. A plot of Miedema's chemical potential and electron density parameters²⁶ for the purpose of predicting alloy heats of formation. Taking hydrogen alloys as an example, the straight lines divide regions of positive and negative heats of formation. The top and bottom quadrants, where the chemical potential dominates, produce alloys stabilized in energy whereas the left and right quadrants cost energy to form. One can draw contours of constant heat of formation as is done schematically with the light curves.

bottom quadrants leading to gains in energy on alloy formation. The density mismatch dominates in the side quadrants causing energy loss. Only one other factor had to be introduced for the scheme to predict the sign of heats of formation rather satisfactorily: in a case involving the alloying of a polyvalent p band metal such as Sn with a transition metal, a p-d hybridization term, whose value is independent of the particular pair involved, would have to be added. Miedema has drawn energy contour lines going away from the crossed lines, such as seen for the H-metal alloys in Fig. 9, and these types of contours, he reports, quite satisfactorily give the magnitudes of the heats of formation for a variety of alloy systems. Whatever its numerical success, there is one factor bothersome to a solid-state theorist, namely, to the extent that the electronegativity is a function of a single physical parameter, that parameter must be an electron density. No solid-state theorist has really calculated an electronegativity scale from first principles, but Lang and Kohn have calculated²⁷ its near equivalent - namely the work function which is a measure of the Fermi level and hence the chemical potential. Their electron gas results, with the average electron density the only independent variable, are in rather good agreement with experiment. This is suggested by Miedema's parameters plotted in Fig. 9 for the points lie close to a universal curve. One might say that the number of independent parameters involved lies somewhere between one and two, a situation not uncommon to most schemes. Atomic size, core "size", electronegativity, valence and electron density are intimately connected with one another column by column in the periodic table, making it almost impossible to deal with independent or almost independent variables.

Simons, St. John and Bloch²⁸ have dealt with another aspect of electronegativities namely that different valence shells make separate "orbital" electronegativity contributions to the total. This idea is found in Mulliken's concept of electronegativity.

They²⁸ introduced a term which is given approximately by

$$X_{\ell} \sim E_{\ell}/Z \quad (5)$$

where E_{ℓ} is the binding energy of an $n\ell$ valence electron outside the ion stripped to its core and Z is the charge of the stripped ion. This reflects the notion that electronegativity is some measure of the attractive interaction between a valence electron and the atomic core. The total electronegativity becomes

$$X_{\text{tot}} = a \sum_{\ell=0}^2 X_{\ell} + b . \quad (6)$$

The constants a and b are chosen so that X_{tot} reproduces Paulings' values²⁹ for first row elements. Having done this, the resulting electronegativities obtained for all but the transition metals lie between the Pauling and Phillips³⁰ scales - agreeing when these two scales agree and providing a compromise when they do not. St. John and Bloch took as a second parameter a measure of the relative role of s and p bonding with the fraction

$$S \equiv (X_0 - X_1)/X_0 \quad (7)$$

Using this and X_{tot} , they obtained the map of the structures of the non-transition elements displayed in Fig. 10. It has been recognized for some time that the more electronegative elements tend to form covalent structures while the most electropositive such as the alkali metals tend to be bcc. Introduction of S allows one to differentiate between hcp, fcc and covalent structures for the elements of intermediate electronegativity. A similar mapping is seen in Fig. 11 for the so called octet compounds - fifty-fifty compounds with eight valence electrons per molecular unit. Here the independent parameters are the electronegativity difference and the average of the S values. Again boundaries can be drawn between regions apparently favoring different structures. By introducing ℓ dependent orbital electronegativities which are measures of an

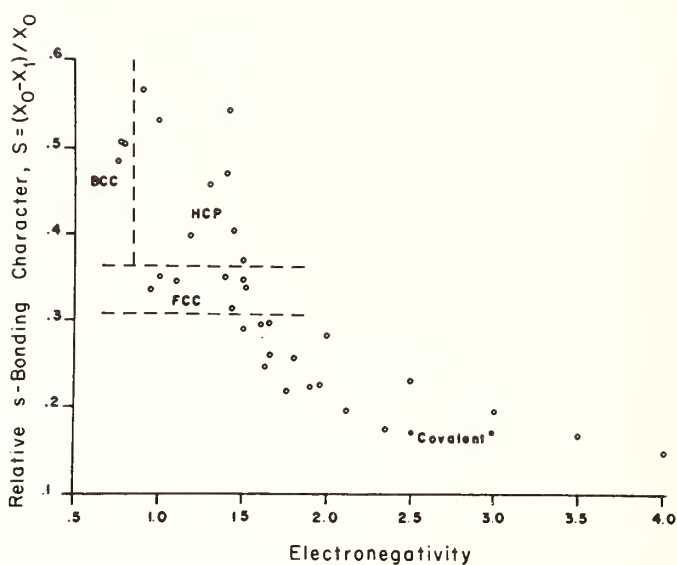


Fig. 10. Correlation of the structures of the non-transition metal elements with electronegativity and fraction of s characters in the bonding as obtained by St. John and Bloch²⁸.

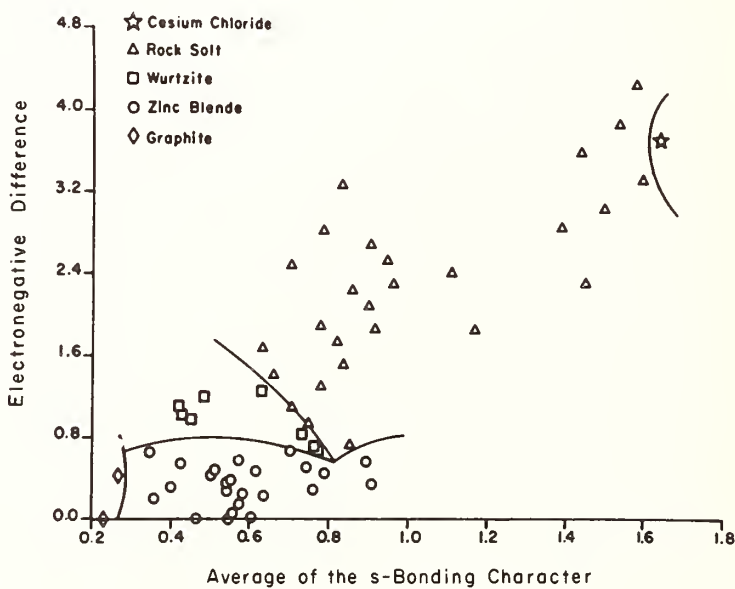


Fig. 11. Mapping of the structures of the AB_{8-N} "octet" compounds as a function of electronegativity difference and average s fraction of bonding as obtained by St. John and Bloch²⁸.

l dependent pseudopotential, Simons, St. John and Bloch have provided a non-local potential description of bonding in those materials. Still needed is theoretical justification for the parameters used.

In the transition and noble metals changes in d, and non-d electron counts, denoted respectively by Δn_d and Δn_{cond} , tend to oppose one another upon alloying. The Mössbauer isomer shift³¹, which measures the charge density at the nucleus, indicates that as much as one non-d conduction electron's worth of charge flows on or off the site of a given atom upon alloying. The flow is always onto the site in the case of Au. However, adding dilute amounts of Ag to Au causes the Au 5d bands to drop relative to the Fermi level as is evident from the more silvery color of the alloy. A lowering of the d bands implies a more attractive potential and hence charge flow off the site, opposite to the isomer shift result. The picture which has emerged³² is that the occupied d bands of Au, which lie beneath the Fermi level, are hybridized with electron states belonging to the other constituent of the alloy causing a reduction (a negative Δn_d) of the 5d count in the bands. This is more than compensation by a flow of non-d charge onto the Au site (a positive Δn_{cond}) producing a small net negative charge on that site. The d electrons, being more, make a larger repulsive coulomb contributions to the potential. Therefore, a decrease in the d count causes a drop in core level and d band energies. While Au has filled d bands and is electronegative, a transition metal such as Ti has almost empty d bands and is electro-positive. Hybridization fills empty d levels causing Δn_d to be positive. The counterflow of conduction electron charge leads to a depletion of charge at the site.

A recent analysis³³ of the available isomer shift data for various transition metals suggests that not only is the ratio $\Delta n_d / \Delta n_{\text{cond}}$ negative but that to a remarkable degree it is a constant independent of the transition metal impurity in question or of the other constituents in the alloy host.

Machlin has recently incorporated³⁴ electronegativity effects

into the traditional pair potential approach to alloying. He took an interaction potential of the form

$$V(r_{ij}) = \frac{-A}{r_{ij}^4} + \frac{B}{r_{ij}^8} \quad (8)$$

where r_{ij} is the distance between an atom pair. The powers of r_{ij} were chosen somewhat arbitrarily: fractional powers would have done a bit better. Such an interaction potential can be related to pseudopotentials, at least for simple metals, and in turn to such parameters as atomic size. Machlin obtained the parameters A and B by fitting to lattice constants and cohesive energies of the pure elements. By assuming that the atomic radius scales with the valence electron screening distance of the ion core and, in turn, employing Gordy and Thomas's view of electronegativity which was related to such screening, Machlin was able to introduce the effect of charge transfer on A and B. In doing this he used enlightened empiricism: if the scheme introduced a systematic error in the prediction of lattice constants for some class of compounds, the electronegativity contribution would be scaled to bring the lattice constants into line. Phase stability problems were considered after this. In regard, for example³⁴, to the competition of the Al₅ and Ll₂ structures for compounds such as Nb₃Sn, the scheme predicted the stable phase correctly in 66 out of 73 cases considered. In subsequent consideration of competition between the Al₅ and A₂ structures it correctly predicted the A₂ structure for V₃Al and the Al₅ for the 21 other compounds considered. The scheme is more precise in its predictions than say, Miedema's. It should be, since the input information is more detailed. Whatever its success or failure there are arguments against its applicability to transition metals. As pointed out in Section II, Friedel and Ducastelle have noted^{4,5} that the d-band broadening contribution to transition metal cohesion, after the manner of Figs. 2 and 3, does not arise from a sum of atom-atom pair interaction terms (it is something more like the square root of a sum of squares). Moreover Krause has recently argued³⁵ that a two-body interaction potential description of the phonons of the noble metals implies that the fcc structure is unstable with respect to a sliding of [111] planes and the hcp structure is favored. Higher order interaction terms appear

in schemes such as that of de Fontaine discussed elsewhere in these proceedings. Such terms are quite small numerically but crucial to his predictions.

V. Charge and Volume

One question which has not been dealt with is the preference for a alloy to form an ordered versus a disordered structure. Perturbation theories exist which should be useful for such a question. The stumbling block is the Madelung term associated with the ordered phase. It requires an assignment of charge to the constituent atoms. One way to assign charge is to integrate the charge density over the volume of an atomic site but this, then, requires the definition of the atomic volumes. Unfortunately there is³⁶ no universally accepted and useful way to define atomic charge and volume. Lacking this, the order-disorder problem becomes difficult.

Consider the case of V_3Si for which Staudemann, Coppens and Muller³⁷ obtained the electron distribution from x-ray diffraction data. Given data throughout the unit cell one can infer the charge associated with V or Si sites as a function of their relative size as is done in Fig. 12. A physically plausible definition of the boundary region, between sites is where the valence charge is a minimum. This would correspond to a flat in the integrated density plot. Staudemann et al. concluded that the structure in the region $R_V/R_{Si} \sim 1.6$ corresponds to such a flattening and therefore to a compound consisting of roughly $Si^{+2.1}$ and $V^{-0.7}$ sites. Although these charges involve flow opposite to conventional electronegativity assignments, the difference in electronegativity between Si and V is not large and changes in the Si electronegativity associated with a metallic environment might well lead to the deduced direction of charge flow. On the other hand, the metallic radii³⁸ of Teatum, Waber and Geschneidner place R_V/R_{Si} at 1.02 and at this ratio V and Si have their atomic valence charge density, i.e. they are neutral. Two reasonable choices of atomic size yield two very different conclusions concerning charging in this system.

It should be noted that ionic charges of $\pm 0.1e$ correspond to Madelung terms of 5-10 kcal/mole. Charging of at least $\pm 0.1e$ is typically inferred from many experimental results. In 1936 Mott showed that a Madelung energy with an effective charge of 0.06e accounts for the order-disorder transition of brass. The situation is particularly difficult for refractory hard metals such as WC. It is generally agreed that these materials have covalent

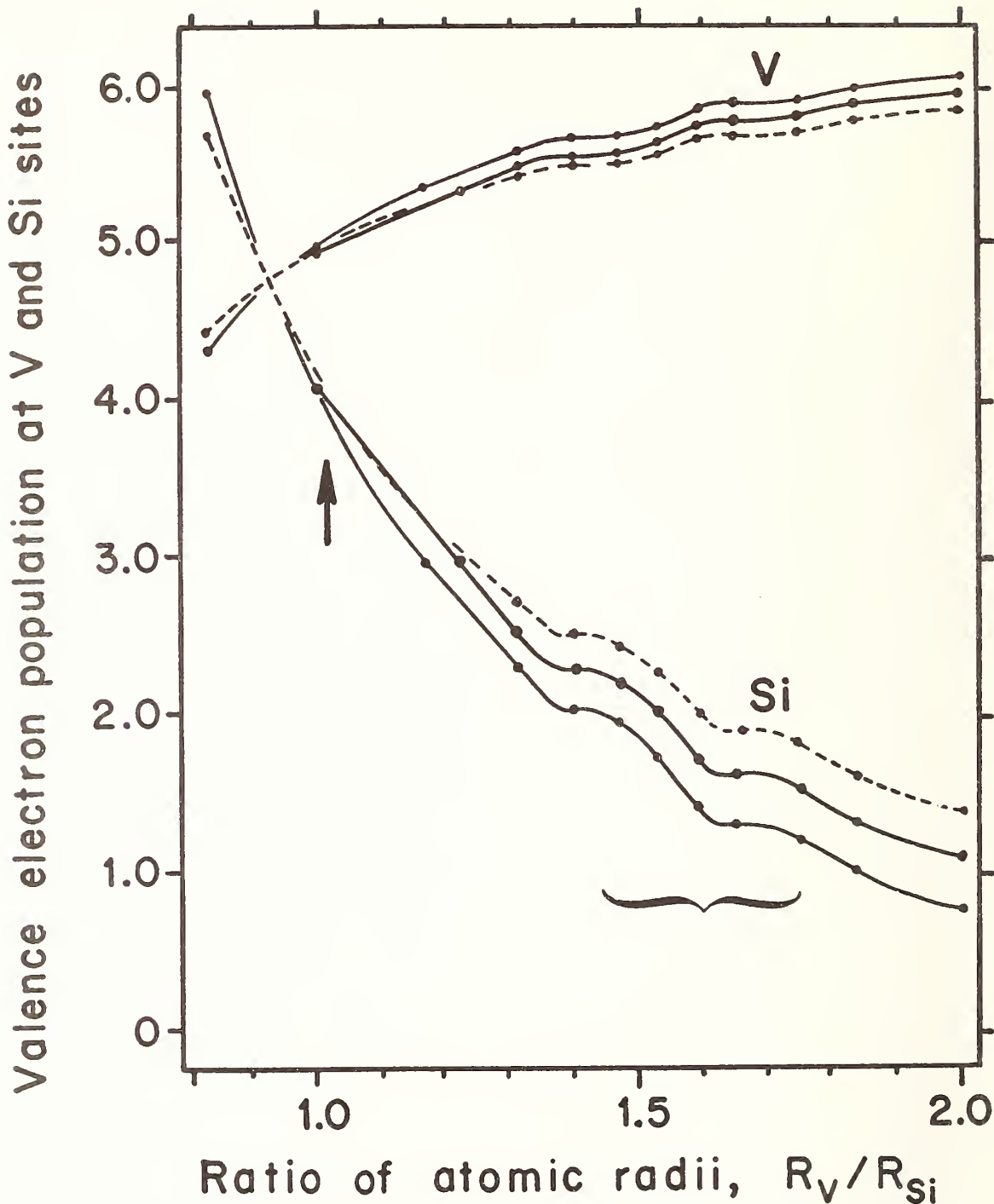


Fig. 12. V and Si site charge in V_3Si as a function of the ratio of V to Si atomic radii³⁷. The spread is associated with various estimates of x-ray extinction coefficients. The bracket marks the region of flattening cited in text, where the boundary between atoms corresponds to some minimum in the average valence electron density. This leads one to infer substantial charging of atomic sites. The arrow at ≈ 1.0 marks the ratio appropriate to a standard choice of atomic radii³⁸: there is little or no charging of the V and Si sites with this definition of site volumes.

and metallic bonding character and it is often argued that there is significant ionic charging as well but there is no general agreement as to the direction in which that charge flows.

VI. Band Theory

The technology of doing energy band calculations has advanced substantially in recent years. Self-consistent results for pure elements and compounds are becoming commonplace as are results for disordered systems where the energy levels have widths associated with finite lifetimes. Wave functions as well as eigenvalues are being obtained and aspherical terms are sometimes incorporated into the potentials. Total energies, however, are not easy to obtain to the accuracy relevant for the purposes of the present meeting. Band theory results are nevertheless very useful in understanding why certain effects occur.

Switendick, for example, has considered³⁹ hydrogen solubility in Ni, Pd and Pt. Pd readily accepts H whereas Pt does not. Switendick has shown that hydrogen solubility in these metals correlates with the presence of d states, above the Fermi level in the pure metal, which have s-like symmetry at the interstitial hydrogen site. Not only are these states available for filling upon addition of a proton into the lattice but the presence of the proton lowers their energy causing them to lie deep in the d-bands.

Gelatt, Weiss and Ehrenreich⁴⁰ have employed band theory in estimates of the heats of formation of 3d and 4d transition metal hydrides. The principal ingredients are (1) the formation of a metal-hydrogen bonding band; (2) the lowering of the d bands due to the presence of the proton and (3) the binding of the extra electron associates with the H atom.

Band structure information can also provide insights into distorted structures or into martensite transitions leading to distorted structures. Often an undistorted structure has degenerate, partially filled levels at the Fermi level. A distortion which splits the degeneracy can often be stabilized by the energy lowering of the one set of sublevels. Switendick has discussed⁴¹ the Ti-V-H phase diagram in such terms.

VII. Other Matters

There are a variety of activities which, as a matter of record, deserve mention in this talk. We will close by citing two.

There has been a beautiful series of work by Wagner and Horner at Jülich concerned with dilute hydrogen in metals⁴². At dilute concentrations the hydrogens interact via strain fields which are long ranged. Classical theory works in such a case and results depend on the shape of the host on a macroscopic scale.

Finally, an area of major activity⁴³ in statistical mechanics has been second order phase transitions and critical points. Whether it be a structural, a superfluid or a magnetic transition, the order parameters involved display universal temperature dependences in the vicinity of the transition temperature. While much work has been done on the tricritical point in the helium system, it is relevant to tricritical points in other phase diagrams including the metal hydrides. Some of the most vigorous intellectual activity in solid-state physics and chemistry is in this area. In contrast, the theory of first-order phase transitions is in poor shape.

In this superficial survey we have tried to give a physicist's view of some of the things that work in metallurgy, of some of the pertinent activities in solid-state theory, and of some of the secrets that we hide.

DISCUSSION

Question - One must introduce temperature dependence. This is a profound problem.

R. Watson - Sorry! I should at the onset have admitted that I was going to legislate entropy out of existence for the purpose of my talk among a variety of other subjects. (Something else I would have liked to discuss are the, what we call, glassy systems. I'm thinking of the transition metal glasses). There are included some efforts but they are an order of two magnitudes more rudimentary in nature. Some solid state theorists do admit temperature exists, in a variety of ways. But for instance a marriage of say some pseudopotentials predictions with a temperature dependence, this type of technology has not yet arrived in a comfortable way.

F. Carter - Many years ago Pauling freely mixed s-p-d orbitals, and physicists at the time said that was wrong. Now they agree that s and d ought to be mixed. What has happened to the p-orbitals? How well do they fit into the renormalization scheme?

R. Watson - In transition metals the p's were always there. They were higher up. In a continuum band picture, you went from pure s-character at the bottom of the band to something which went smoothly into p-character. In fact, when you are interested in the noble metals, it is worth putting a p level on that plot as well, because there are symmetry points in the zone of high p character. For instance, this becomes important in the question of why silver is different from copper or gold. It's the s-d-p separation, that counts if you're dealing with a noble metal. So, when I said s, it was s-p.

Footnotes

*Supported by U. S. Energy Research and Development Administration.

†Supported in part by the National Science Foundation.

- (1) G. V. Samsonov, *Science of Sintering* 8, 5 (1976).
- (2) G. D. Gelatt Jr., H. Ehrenreich, R. E. Watson, *Phys. Rev.* B15, 1613 (1977).
- (3) E. P. Wigner and F. Seitz, *Solid St. Phys.* 1, 97 (1955).
- (4) J. Friedel, *Physics of Metals I*, J. M. Ziman, Ed., (Cambridge Univ. Press, 1969) and F. Ducastelle and F. Cyrot - Lackmann *J. Phys. Chem. Sol.* 32, 285 (1971).
- (5) F. Ducastelle, *J. Physique* 31, 1055 (1970).
- (6) W. Hume-Rothery, *Progress in Materials Science*, 13, 5, "The Engel-Brewer Theories of Metals and Alloys", 1967. L. Brewer, in "High-Strength Materials", edited by V. F. Zackay, (Wiley, New York, 1965), pp. 12-103. L. Brewer, in *Phase Stability in Metals and Alloys*, edited by P. Rudman, J. Stringer, and R. I. Jaffee, (McGraw-Hill), New York, 1967), pp. 39-61, 241-9, 344-6, and 560-8. L. Brewer, *Science*, 161, 115 (1968). N. N. Engel, "Alloy Phase Stability Criteria", *Developments in the Structural Chemistry of Alloy Phases*, edited by B. C. Giessen, (Plenum Press, New York, 1969) pp. 25-40.
- (7) D. G. Pettifor, *J. Phys. C* 3, 367 (1970).
- (8) e.g., See M. Shiga, *AIP Conf. Proc.* 18, 463 (1974).
- (9) U. K. Poulsen, J. Kollar and O. K. Andersen, *J. Phys. F.* 6, L241 (1976).
- (10) J. F. Janak and A. R. Williams, *Phys. Rev.* B14, 4199 (1976).
- (11) P. Soven, *Phys. Rev.* 156, 809 (1967); B. Velicky; S. Kirkpatrick and H. Ehrenreich, *Phys. Rev.* 175, 747, (1968), and H. Fukuyama, H. Krakauer and L. Schwartz, *Phys. Rev.*, B10, 1173 (1974).

- (12) J. van der Rest, F. Gautier and F. Brouers, *J. Phys. F.* 5, 2283 (1975).
- (13) F. Gautier, J. van der Rest and F. Brouers, *J. Phys. F.* 5, 1884 (1975), and M. Cyrot and F. Cyrot-Lackmann, *J. Phys. F.* 6, 2257 (1967).
- (14) L. Kaufman and H. Bernstein, Computer Calculation of Phase Diagrams, (Academic Press, New York, 1970) p. 89-90.
- (15) J. C. Slater, *Phys. Rev.* 81, 385 (1951).
- (16) P. Hohenberg and W. Kohn, *Phys. Rev.* 136, B864 (1964); W. Kohn and L. Sham, *Phys. Rev.* 140, A1333 (1965) and L. Sham and W. Kohn, *Phys. Rev.* 145, 561 (1966).
- (17) L. Hedin and B. I. Lundqvist, *J. Phys. C.* 4, 2064 (1971).
- (18) U. von Barth and L. Hedin, *J. Phys. C.* 5, 1629 (1972).
- (19) J. P. Walter and M. L. Cohen, *Phys. Rev.* B4, 1877 (1971).
- (20) Y. W. Yang and P. Coppens, *Sol. St. Comm.* 15, 1555 (1974).
- (21) J. R. Chelikowsky and M. L. Cohen, *Phys. Rev. Letters* 33, 1339 (1974).
- (22) W. A. Harrison, "Pseudopotentials in the Theory of Metals", W. A. Benjamin, New York, 1966.
- (23) D. Stroud and N. W. Ashcroft, *J. Phys. F.* 1, 113 (1971).
- (24) L. A. Girifalco, *Acta Met.* 24, 759 (1976).
- (25) G. M. Rooney, A. L. Kipling, B. A. Lambos, *J. Phys. Chem. Sol.* 36, 677 (1975).
- (26) A. R. Miedema, F. R. de Boer and P. de Chatel, *J. Phys. F* 3, 1558 (1973); A. R. Miedema, *J. Less Common Met.* 32, 117 (1973); A. R. Miedema, R. Boom and F. R. de Boer, *J. Less Common Met.* 41, 283 (1975) and 46, 54 (1976) and A. R. Miedema, *J. Less Common Met.* 46, 67 (1976).
- (27) N. D. Lang and W. Kohn, *Phys. Res.* B3, 1215 (1971).
- (28) J. St. John and A. N. Bloch, *Phys. Rev. Let.* 33, 1095 (1974) and references therein.
- (29) L. Pauling, The Nature of the Chemical Bond (Cornell Univ. Press, Ithaca, NY (1960) 3rd ed.
- (30) J. C. Phillips, *Phys. Rev. Let.* 20, 550 (1968).
- (31) e.g. See N. N. Greenwood and T. C. Gibb, Mössbauer Spectroscopy (Chapman and Hall, London 1971).

- (32) R. E. Watson, J. Hudis and M. L. Perlman, Phys. Rev. B4, 4139 (1971); R. M. Friedman, J. Hudis, M. L. Perlman and R. E. Watson, Phys. Rev. B 2433 (1973); C. D. Gelatt, Jr., and H. Ehrenreich, Phys. Rev. B10, 398 (1974), and T. S. Chou, M. L. Perlman and R. E. Watson, Phys. Rev. B14, 3248 (1976).
- (33) R. E. Watson and L. H. Bennett, Phys. Rev. B15, 502 (1977).
- (34) E. S. Machlin, Acta Met. 22, 95 (1974); Machlin, Acta Met. 22, 109 (1974), and E. S. Machlin and S. H. Whang, J. Phys. Chem. Sol. 37, 555 (1976).
- (35) C. W. Krause, Phys. Let. 57A, 390 (1976).
- (36) R. E. Watson and L. H. Bennett, Charge Transfer in Alloys: The Blind Men and the Elephant, Charge Transfer/Electronic Structure of Alloys, L. H. Bennett and R. H. Willens, ed. (Metallurgical Society of the American Institute of Mining, Metallurgical, and Petroleum Engineers, 1973).
- (37) J. L. Staudenmann, P. Coppens and J. Muller, Sol. St. Comm. 19, 29 (1976).
- (38) E. T. Teatum, K. A. Gschneidner, Jr. and J. T. Waber, Los Alamos Report LA-4003 (1968) unpublished.
- (39) A. C. Switendick, Proc. Hydrogen Economy Miami Energy Conf., Coral Gables, Florida, paper S6-1 (1974).
- (40) C. D. Gelatt, Jr., J. A. Weiss and H. Ehrenreich, Solid State Comm. 17, 663 (1975).
- (41) A. C. Switendick, J. Less Common Metals 49, 283 (1976).
- (42) H. Wagner and H. Horner, Advances in Phys. 23, 587 (1974).
- (43) e.g. D. P. Landau, Mag. and Mag. Mat'ls-76, AIP Conf. Proc. 34, 373 (1976) and the series Phase Transitions and Critical Phenomena, ed. C. Domb and M. S. Green (Academic Press, NY) vols. 1-6.

PANEL I

COMPUTATION AND PREDICTION OF PHASE DIAGRAMS

(Methods of Phase Diagram Calculations)

Moderator: O. J. Kleppa, The James Franck Institute,
University of Chicago, Chicago, IL

Panel Members:

L. Brewer, Inorganic Materials Research Div.,
Lawrence Berkeley Laboratories, University of
CA, Berkeley, CA

D. de Fontaine, Materials Dept., University of
CA, Los Angeles, CA

R. L. Dreshfield, Materials Processing and
Joining Section, NASA Lewis Research Center,
Cleveland, OH

B. C. Giessen, Dept. of Chemistry and Mechanical
Engineering, Northeastern University
Boston, MA

L. Kaufman, ManLabs, Inc., Cambridge, MA

A. Navrotsky, Chemistry Dept., Arizona State
University, Tempe, AZ

Several of these panel members' texts appear in the poster session "Computational Techniques in Phase Diagram Construction", where there were further presentations by these authors. General remarks follow Dr. Dreshfield's paper, on p. 659.



ESTIMATION OF CONJUGATE γ AND γ' COMPOSITIONS

IN Ni-BASE SUPERALLOYS

by Robert L. Dreshfield

Lewis Research Center

ABSTRACT

To control the formation of unwanted phases, superalloy metallurgists have developed methods of estimating the composition of the matrix phase of alloys. That composition is then used to estimate the alloy's propensity toward sigma and other unwanted phase formations upon prolonged exposure to elevated temperatures in service. This paper reviews two approaches for estimating phase composition from the melt composition. One method is based on assigning essentially fixed stoichiometry to precipitating phases and is typified by "PHACOMP." The second method uses analytical geometry to interpret phase diagrams and is shown to be applicable to a two-phase region of a six-component Ni-base system. The geometric method is also shown to be applicable to commercial Ni-base superalloys.

INTRODUCTION

The nickel-base superalloys used in the hot section of gas turbines have been developed to the point where they have useful strength at approximately 80 percent of their melting point (ref. 1). Over 50 such alloys are commercially available.

Typical nickel-base superalloy contain nickel, aluminum, chromium, titanium, zirconium, carbon, and boron. In addition molybdenum, tungsten, niobium, tantalum, hafnium and other reactive or refractory metals may be added to the melt. The two major phases in the alloys are a face centered cubic matrix, γ , and a dispersed, usually coherent, ordered face centered cubic phase, γ' . Small amounts of carbides and borides (usually <3 percent) and other intermetallic compounds are frequently

present and are responsible for profound changes in mechanical properties. These alloys are clearly described as multicomponent-multiphase alloys typically containing 6 to 13 intentionally added alloy elements and three to five phases.

Since the sigma phase instability was identified in Ni-base superalloys (ref. 2) and the presence of sigma was correlated with a loss of stress rupture life (refs. 3 to 6), the superalloy industry has sought methods to prevent or minimize its occurrence in the alloys. This paper deals with two approaches which have been offered to control the melt compositions to minimize the occurrence of sigma and other undesirable phases in superalloys. The first approach, as exemplified by "PHACOMP" (ref. 7) and the method of reference 8 uses a chemical stoichiometric calculation to estimate the composition of the γ phase. The propensity of the alloy toward phase instability is then determined by calculating the average electron vacancy concentration (\bar{N}_v) of the γ . The second approach is to estimate the composition of the conjugate phases (γ and γ') by applying analytical geometry to existing phase diagrams (refs. 9 to 11). The analysis is continued to determine if the melt composition is likely to fall in a phase field containing unwanted phases. In both methods, an attempt is made to estimate the composition of at least one of the conjugate phases (usually γ) from the melt composition.

This paper will review the stoichiometric and geometric approaches for estimating the compositions of conjugate phases in superalloys. It will also show that the geometric approach can be used to develop a description of a two-phase region of a six-component system and show that the description of the six-component system can be applied to commercial Ni-base superalloys.

STOICHIOMETRIC APPROACH

Methodology. - The first efforts to control sigma phase in superalloys were those of Boesch and Slaney (ref. 8) and Woodyatt and coworkers (ref. 7). These methods made use of a two step computation. In the first

step the melt composition was used to calculate a "residual matrix" or γ -phase composition. In the second, the \bar{N}_v of the γ was compared to an empirically determined value to estimate the propensity of the alloy to form unwanted phases. The procedure is exemplified by the method described in reference 12 which follows:

A. Calculate γ matrix composition in atomic percent:

1. Calculate composition of carbides and borides as follows:

- a. Half the carbon forms mono-carbides in the sequence TaC, NbC, ZrC, TiC, and VC.
- b. Half the carbon forms either Cr_{23}C_6 or $\text{Cr}_{21}(\text{Mo}, \text{W})\text{C}_6$ if Mo or W are present. If Mo + W is greater than 6 weight percent, $[\text{NiCo}_2(\text{Mo}, \text{W})_3]\text{C}$ forms instead of M_{23}C_6 .
- c. A boride, $(\text{Mo}_{0.5}\text{Ti}_{0.15}\text{Cr}_{0.25}\text{Ni}_{0.10})_3\text{B}_2$ forms.
- d. All of the Al, Ti, and Nb remaining following formation of carbides and borides plus 3 percent of the melt's Cr form γ' of the stoichiometry $\text{Ni}_3(\text{Al}, \text{Ti}, \text{Nb}, \text{Cr})$. If there is insufficient Ni, β will also form having a stoichiometry $\text{Ni}(\text{Al}, \text{Ti}, \text{Nb}, \text{Cr})$.
- e. The residual γ matrix resulting from subtracting the amount of compounds in (a) to (d) is scaled to 100 percent.

B. The \bar{N}_v of the residual γ matrix is calculated by

$$\bar{N}_v = \sum_{i=1}^n f_i (N_v)_i \quad (1)$$

where

f_i atomic fraction of the n th element

$(N_v)_i$ 4.66 for Cv, Mo, W; 3.66 for Mn; 2.22 for Fe; 1.61 for Co
0.61 for Ni

($(N_v)_i$ may be taken as 10.66 - group number if no value is known.) If \bar{N}_v is approximately 2.45 or greater the alloy is prone to form σ or other undesirable phases.

Discussion. - This method has been successfully used to control the melt composition of several commercial superalloys (ref. 12). While it would be interesting to review all the additional work in this area, it is considered beyond the scope of this paper and interested readers are referred to references 12 to 17. To summarize the additional work, it should be noted that much of it has been directed at finding a universal critical \bar{N}_v , that is, a value of \bar{N}_v appropriate to all alloys or toward finding a systematic method of defining the critical \bar{N}_v for a particular melt. It has been proposed that for some elements N_v be altered and that the γ' composition be altered from those first proposed. No method has been successful in finding a γ' composition and a series of elements' N_v s which can properly estimate σ and other instabilities at a single value of \bar{N}_v for all alloys.

It should be noted that the methods which rely on a nearly fixed γ' stoichiometry necessarily assume that no Al, Ti, Nb (and perhaps other γ' formers), C and B are soluble in the γ . Mihalisin and Pasquine (ref. 17) suggested that this treatment of γ' was in error and could account for problems observed in predicting the stabilities of alloy 713C and alloy 713LC. They suggested that actual chemical analysis of the γ' phase be made and that a mass balance, also using the measured volume fraction of γ' , be used to calculate the residual γ matrix composition. The propensity toward forming σ phase of that γ was estimated in a manner similar to that described earlier for PHACOMP in that the \bar{N}_v was calculated and compared to an empirically selected value. The presence of significant Al in the γ was also noted in reference 18 for Udimet 700. While the method of reference 17 is likely to better estimate the γ composition than PHACOMP, it suffers from the need for preparing a melt from which the γ' can be analyzed. Therefore the method of reference 17 is of reduced value in alloy development programs.

GEOMETRIC APPROACH

The Ni-Al-Ti-Cr System at 750^o C

Background. - The work of Kriege and Baris (ref. 19) confirmed the presence of significant Al and Ti in the γ phase of 15 commercial Ni-base superalloys. Further, their work showed, while γ' was nearly stoichiometric, that variations in its compositions occur which could affect a PHACOMP calculation.

In an effort to avoid reliance on a fixed or predictable γ' composition to predict γ composition, references 9 to 11 used analytic geometry to interpret the Ni-Al-Ti-Cr phase diagrams of Taylor and co-workers (refs. 20 to 23). The problem addressed that of finding the composition of the γ phase, given the melt composition and assuming the melt lies in the two-phase ($\gamma + \gamma'$) field. The approach was to find the intersection of the tie line on which the two-phase alloy lies and the $\gamma - \gamma'$ solvus surface (the locus of γ compositions saturated with respect to γ').

Methodology. - As a first step the $\gamma - \gamma'$ solvus surface of the Ni-Al-Ti at 750^o C was curve fit using the method of least squares. This equation was then altered to fit the Ni-Al-Ti-Cr $\gamma - \gamma'$ solvus resulting in the equation

$$\text{Al} + 1.5\text{Ti} = 1.33\text{Cr}^2 - 0.566\text{Cr} + 0.12 \quad (2)$$

That equation (2) is a good simulation of the $\gamma - \gamma'$ solvus at low Ti concentrations can be seen in figure 1 by comparing the solid lines surface (eq. (2)) and the double-dashed line from reference 23.

The next step was to deduce the tie line behavior in the alloy systems. Fortunately, Taylor and Floyd showed some tie lines in their ternary diagrams in references 20 to 22. The tie line system in the four component systems has to include the tie lines of the three component systems as a limit and further, the tie lines in the four component systems must not intersect each other in the two-phase field. The details of the system proposed are described in references 10 and 11. The procedure will now be briefly reviewed for the Ni-Al-Ti-Cr system at 750^o C. Three assumptions are made to allow a closed form solution:

1. Assume that for the system Ni-Cr-Al tie lines (for $\gamma + \gamma'$) intersect at (Ni, 0.25Al) (fig. 2).

2. Assume that for the system Ni-Cr-Ti that η and γ' are mutually soluble and tie lines intersect at (Ni, 0.25Ti) (fig. 3).

3. Assume that for the system Ni-Al-Ti that $\gamma + \gamma'$ tie lines intersect at (Ni, -0.05Al) (fig. 4). (Also shown as point S in fig. 1.)

In the specific construction to be used, a tie line is formed by the intersection of two planes. One plane has a zone axis (for this paper defined as a line common to all planes in the set) from the Cr corner to point S in figure 1. The other plane has line U-V as a zone axis (fig. 1). The Al to Ti to Ni ratio of the alloy governs the selection of the plane from the Cr-S set and the Cr concentration selects the plane from the U-V set.

Because U-V and Cr-S are zone axes for the two planes determining the tie line, the only places where the tie line families can intersect are on U-V or Cr-S. Both of these lines are outside of the two-phase field; therefore, Gibbs' phase rule is followed.

The details of the construction by which the composition of the γ phase in a two-phase quaternary alloy is determined from the above analysis follows. In figure 1 the composition of the two-phase quaternary alloy is projected on the Ni-Al-Ti diagram by passing a line from the Cr corner of the quaternary, through the two-phase alloy A to the Ni-Al-Ti ternary. This construction locates a point T in the ternary diagram that has the same relative Ni, Al, and Ti concentration as in the quaternary alloy. This is shown as line Cr-A-T. The intersection of U-V (the line connecting 0.25Al, 0.75Ni, and 0.25Ti, 0.75Ni) and T-S (the tie line in the Ni-Al-Ti ternary) established point X on the tie line (containing the two-phase quaternary alloy A). The tie line on which alloy A lies is X-A-G. The composition of G (γ phase) is determined by finding the intersection of X-A with the solvus surface.

The mathematics of this treatment can be followed in reference 10 or 11. The approach was adapted to commercial superalloys by using a stoichiometric approach to account for carbides, borides, and γ' formed by Nb, Ta, Zr, and V. The Mo and W in γ were treated by analogy to Cr. Comparison of γ predicted by the geometric method for the

alloys in Table I and that determined by references 18 and 19 are shown in Table II. Note that both Co and Ti were in error by a constant amount and factor, respectively.

Discussion. - While the application of the procedure to commercial alloys was encouraging, it required some extra assumptions. It was felt that the general techniques of using analytic geometry to interpret two-phase regions of multicomponent phase diagrams had been demonstrated.

The Ni-Al-Cr-Ti-W-Mo System at 850^o C

Background. - Analysis of the work of references 10 and 11 suggested that a better superalloy phase diagram could be developed by including W and Mo directly in the system's phase diagram. Further, it was clear from references 10 and 11 that to predict conjugate phase compositions it was not necessary to graph a phase diagram, only to describe its significant features by mathematical expressions. These ideas from references 10 and 11 coupled with a quantitative analytical procedure for γ' (ref. 19) encouraged the author to initiate a study to determine the compositional limits of γ and γ' in the Ni-Al-Cr-Ti-W-Mo system at 850^o C (refs. 24 and 25). The temperature of 850^o C was selected as it was thought to be near the temperature at which σ and related phases precipitate rapidly (refs. 4 to 6).

Experimental approach. - The experimental details of the study are available in reference 25. They will only be summarized here. After checking two preliminary alloys, a series of melts were made, the compositions of which were based on a fraction of a three-level factorial design (ref. 26). The experimental design is shown in Table III. The compositions of the two-phase alloys melted are shown in Table IV. The alloys were homogenized for 4 hours at 1190^o C and air cooled to room temperature. They were heated at 850^o C for 1008 hours before being air cooled to room temperature. The γ' was quantitatively extracted from the heat treated two-phase alloys using the method of reference 19. After the γ' residues and the alloys were chemically analyzed, the composition of γ was calculated by a mass balance.

This experimental approach allowed the determination of the conjugate γ and γ' compositions with a single melt. The solvus hypersur-

faces were then described by fitting a third degree equation to the γ and γ' compositions using linear regression analysis (ref. 27).

The average composition and amount of γ' are shown in Table V. The range of composition is consistent with that of other investigations (refs. 17 to 19, and 28 to 30). Also shown in Table V is the sample standard deviation (S) for each element except Ni. The value of S is less than one-third the range of each element observed which suggests the spread in observed compositions is significant when compared to analytical errors.

The average composition of γ is shown in Table VI. The sample standard deviation (S), also shown in Table VI for each element can be seen to be less than one-third the range of each element, again suggesting that the observed spread is greater than would be expected from experimental errors. The range of γ compositions is consistent with the ranges observed in other work (refs. 17 to 19, and 28 to 30).

Gamma-gamma prime relationship. - The compositions of the γ in Table VI and γ' shown in Table V are compositions of the phases from two-phase alloys. These compositions, therefore, represent points on the solvus hypersurfaces, and when considered in pairs (one γ and one γ') from a heat, these are, in fact, the compositions of conjugate phases.

To obtain a more useful description of these solvus hypersurfaces, the data points from each extraction were fitted with curves using a multiple linear regression computer program (ref. 27). The model equation used to fit both sets of data was:

$$\begin{aligned}
 Al = & B_0 + B_1 \times Cr + B_2 \times Mo + B_3 \times Ti + B_4 \times W \\
 & + B_5 \times Cr^2 + B_6 \times Mo^2 + B_7 \times Ti^2 + B_8 \times W^2 \times W \\
 & + B_9 \times Cr \times Mo + B_{10} \times Cr \times Ti + B_{11} \times Cr \\
 & + B_{12} \times Mo \times Ti + B_{13} \times Mo \times W + B_{14} \times Ti \times W \\
 & + B_{15} \times Cr \times Mo \times Ti + B_{16} \times Cr \times Mo \times W \\
 & + B_{17} \times Cr \times Ti \times W + B_{18} \times Mo \times Ti \times W + \text{error}
 \end{aligned}
 \tag{3}$$

where Al, Cr, Mo, Ti, and W are in atomic percent, B_0 is a constant, and B_1, B_2, \dots, B_{18} are coefficients.

For both solvus hypersurfaces, the regression program rejected coefficients with less than a 25-percent significance level. The low significance level was chosen because it is recognized that the independent variables have errors associated with them. Although it is desirable to simplify the equations, the regression analysis assumption that the independent variables are known without error is violated. The low significance level is believed to avoid rejecting significant terms.

The constant and coefficients for both solvus equations are shown in Table VII. The multiple regression coefficient (R^2) for the γ is 0.89 and for the γ' , R^2 is 0.87.

These two equations may be used to plot sections of the hypersurfaces or simply to estimate the amount of a particular element in a phase if four others are known. The usefulness of these equations could be increased if they could be used to estimate the compositions of conjugate phases, given the composition of a two-phase alloy.

The compositions obtained in this investigation for γ and γ' are the compositions of conjugate phases. Therefore a tie line is known to pass through the γ composition, the alloy composition and the γ' composition. Direction numbers for the tie lines were calculated by:

$$DN_i = \frac{I_\gamma - I_{\gamma'}}{Cr_\gamma - Cr_{\gamma'}} \quad (4)$$

where

DN_i direction number for the i th element

I_γ composition of I in γ

$I_{\gamma'}$ composition of I in γ'

Cr_γ composition of Cr in γ

$Cr_{\gamma'}$ composition of Cr in γ'

These direction numbers for each element (Cr being 1) indicate the change in amount of the element along a tie line per unit change in Cr. These, in effect, describe the slope of the tie lines.

To determine the phase compositions from the alloy composition by using the tie lines, the direction number of the tie line needs to be known as a function of the composition of the alloy. The direction numbers were estimated from the alloy compositions by using a multiple linear regression program (ref. 27) to fit the direction numbers for Al, Mo, Ti, and W to equations of the form:

$$\text{DN}_i = B_0 + B_1 \times \text{Al} + B_2 \times \text{Cr} + B_3 \times \text{Mo} + B_4 \times \text{Ti} \\ + B_5 \times \text{W} + \text{error} \quad (5)$$

The full model was used since the uncertainties involved in rejecting terms of low significance seemed large when compared to the small gain obtained in simplifying these equations. The values of the constants and coefficients for these equations are summarized in Table VIII.

The two-phase region of this alloy system can now be described by using the equations for the solvus hypersurfaces and those which relate the direction numbers of the tie lines to the alloy chemistry. In principle, these equations could be solved simultaneously to find the composition of the γ and γ' for an alloy of known composition. This approach was not used because errors resulting from the least squares curve fitting were expected (and did) result in conditions where the tie lines fail to intersect the solvus hypersurfaces. Furthermore, because the solvuses are parabolic in shape, it is possible that two real and positive solutions exist.

The procedure used to find the compositions of the conjugate phases from the composition of a two-phase alloy is described below. It was programmed in FORTRAN IV for a time-sharing IBM 360 computer (ref. 25). First, the composition of the alloy is used to establish direction numbers for Al, Mo, Ti, and W by using the equations from Table VIII. Next, the alloy composition is changed by an increment of Cr and the new values for the other elements are calculated from the direction numbers. The composition is therefore still on the tie line. The new values of Cr, Mo, Ti, and W are used in the solvus equation to calculate the Al for the solvus, if the other four elements were as just estimated. This procedure is repeated until the Al compositions on the tie line and on the solvus agree to within 0.005 percent or until it is obvious

that no intersection will be found. If it appears that a second solution is likely, the procedure is repeated. If no intersection is located, the closest approach of the tie line to the solvus (as defined by the least difference in Al) is displayed as a solution.

To solve for γ composition, the Cr is increased from the alloy composition. To solve for the γ' composition, the Cr is decreased from the alloy composition. The closest approach is taken as a solution if no intersection is found for γ when Al is 0 percent or Cr is 40 percent. The closest approach is used for γ' if Al is 30 percent or Cr is 0 percent. Where two intersections were found, the higher Cr solution for γ and the lower Cr solution for γ' appeared to be closer to the experimental values.

The results of this calculation for the two-phase experimental alloys are compared to the experimental results in Table IX. The experimental compositions and those calculated by the phase analysis procedure are in good agreement. Except for γ composition in two alloys (ref. 25) the agreement was excellent. It is assumed that the two exceptions were the result of accumulated error.

Occurrence of additional phases. - The primary purpose of the investigation reported in references 24 and 25 was to define the $\gamma + \gamma'$ region of the Ni-Al-Cr-Ti-W-Mo system. During the conduct of the investigation, 51 alloys were melted. Two alloys were determined to contain only γ , 27 alloys contained only γ and γ' and the remaining 22 alloys were multiphase alloys containing phases other than γ and γ' . This section will relate primarily to the latter group of multiphase alloys which contained from three to six identifiable phases.

The composition of the multiphase alloys and phases (other than γ and γ') present are listed in Table X. The phases observed were σ , μ , and two body centered cubic phases, one having a lattice constant (A_0) similar to Cr, the other having an A_0 similar to W and Mo. No alloy in Table X contains more than 74.5 percent Ni and only alloys 3 and 44 contain in excess of 70 percent Ni. When one converts the two-phase alloys of Table IV to atomic percent, it is seen that these alloys had greater than 65.5 percent Ni and all but two alloys had greater than 67 percent Ni. This compares well with the $\gamma - \sigma$ boundary of 62 to

64 percent Ni + Co reported in reference 31 and the $\gamma - \alpha$ boundary of 60 percent in reference 20, see figure 5.

While the alloy composition offers a quick check for stability it should be more revealing to examine the γ composition as in PHACOMP. Instead of using an N_v approach, however, a more direct treatment of the phase diagram is proposed here. Reference 31 shows that Mo and W are 1.75 times more potent than Cr in promoting σ formation. By using an analogy to the 67 percent Ni limit for two-phase alloys, it is suggested that the $[Cr + 1.75(Mo + W)]$ for the γ should be less than 33 percent (100 - 67 percent). For the stable alloys in Table VI, only two (alloy 15 and alloy 37) have values of the function $Cr + 1.75(Mo + W)$ which were greater than 33 percent. The maximum value was 36.1 for alloy 15. For the multiphase alloys, the γ composition could only be estimated by use of the computer program previously mentioned from reference 25. The lowest value of the function was 20.2 percent but only three alloys of 14 for which a computation could be made, had values less than 30 percent.

A third parameter which appears capable of assisting in the prediction of additional phases is the rate of change of Al with respect to Cr (Al direction number) along the $\gamma + \gamma'$ tie line. For the two-phase alloys, only two alloys had Al direction numbers which measured greater than -0.30, the maximum value being -0.22. For the multiphase alloys, the minimum value estimated from the computer program of reference 25 was -0.20. Eight of 22 alloys had values greater than 0.0.

The relationship of the direction number of a tie line to a phase boundary is shown in figure 5. The line Q-R is the boundary between a two-phase ($\gamma + \gamma'$) field and a three-phase ($\gamma' + \gamma' + \alpha$) field. It can be seen in the $\gamma + \gamma'$ field as Cr increases from the Ni-Al binary to line Q-R, the Al direction number increases from negative ∞ to -0.74. While the difference between the experimental limit of about -0.30 does not compare too well with that predicted by the Ni-Al-Cr phase diagram, one can see that there is a basis for the concept.

The three parameters for estimating occurrence of multiphase alloys are shown in figure 6. They are shown schematically as a Venn diagram to imply that as more than one of the conditions is satisfied, the probability of occurrence of additional phases increases.

APPLICATION TO COMMERCIAL ALLOYS

Phase diagram. - The alloys studied in reference 19 are typical of current commercial Ni-base superalloys. The heat treatments for these alloys, except for Udimet 700, are typical of the condition in which the alloys may be placed in service. In addition to the six elements studied in the last investigation, the commercial alloys in reference 19 contain C and may have intentional additions of Co, Nb, Fe, Ta, and V. The compositions from reference 19 were used to determine whether the "phase diagram" could be applied to commercial alloys.

The compositions from reference 19 were first converted to atomic percent to test the "phase diagram." The composition was then adjusted for carbide formation by using the procedures suggested in reference 32. The adjusted composition was then treated as an alloy composition using the computer program described earlier. The procedure in effect treated all elements other than Al, Cr, Mo, Ti, and W as if they were Ni. This appears to be a reasonable assumption for Co and Fe, but Ta and Nb are shown in reference 19 to be γ' formers.

The results of these calculations of γ and γ' compositions are compared to the compositions reported in reference 19 in Table XI. The compositions of γ calculated compared well with those reported except for alloys IN 100, Mar M200, Nimonic 115 and Nicrotung. For the γ' compositions, only alloys Inconel X-750 and Unitemp AF 1753 failed to show good agreement between the calculated and observed values. For alloy Unitemp AF 1753, the estimating procedure reported the alloy composition for the γ composition. This can be considered to indicate the alloy to be single phase.

The "phase diagram" of this investigation is capable of describing one phase in all of the commercial alloys examined. Of the six phase analyses which were not in reasonable agreement, four were for the γ phase. This is probably because the γ' composition was directly determined in both this investigation and reference 19 and a greater uncertainty should exist for the composition of the γ phase. The two alloys for which the γ' estimate was poor had the lowest weight fraction γ' of the alloys examined. Errors in estimating the tie line direction numbers would be expected to be magnified in the composition of the phase more

distant from the alloy composition because of a leverage effect.

The results of the above comparisons indicate that the techniques developed in this investigation should be capable of being adapted for use in commercial alloys. It appears that the discrepancies between the estimates based on the current work and reference 19 are partly the result of the fact that the alloys in reference 19 were heat treated for shorter times and at different temperatures than the current work. The other obvious source differences is that the current work made no attempt to account for additional elements, except as they enter into carbide reactions.

Additional phases. - The alloys of reference 19 were also used to test the applicability of the parameters related to formation of additional phases. The three parameters (Ni in alloy; $Cr + 1.75(Mo + W)$ in γ ; and Al direction number on the $\gamma + \gamma'$ tie line) were calculated using the data from reference 19. These parameters are shown in Table XII. Also shown in Table XII are the phases that Collins and Kortovich (ref. 15) observed in these alloys. (It should be noted that the composition of the alloys varied slightly between refs. 15 and 19.) Reference 19 did not report on the stability of the compositions.

While the phase boundary between the two-phase and multiphase alloys is not identical to that of reference 25, it can be seen that the three parameters show similar critical regions. Alloys with less than 67 percent Ni + Co + Fe were multiphase alloys. γ phase with $Cr + 1.75(Mo + W)$ greater than 31.5 formed additional phases. While it is difficult to find a critical value for the Al direction number, the average value for alloys having a high propensity toward forming σ and μ is -0.44 while it is -0.55 for the stable alloys. The difference between the averages is significant at the 95 percent level.

The three parameters identified in reference 25 do appear to be appropriate in determining if commercial alloys are likely to form undesirable phases. The specific composition of IN 100, which is shown from reference 15 as a σ former in Table XII, may have been stable in reference 19. IN 100 is one of the alloys which may be stable or σ forming within its normal composition limits (refs. 3 to 6).

CONCLUDING REMARKS

A review of two methods of estimating conjugate phase compositions in Ni-base superalloys has been presented. Both methods had as an ultimate objective the estimation of a melt's propensity for forming unwanted phases such as σ .

One method as exemplified by PHACOMP uses the chemical stoichiometric approach. This method reduces from the melt composition the elements that are believed to precipitate and arrives at the residual matrix by difference. The stability of the alloy is determined by calculating the average electron vacancy concentration (\bar{N}_v) of the residual matrix and comparing that with an empirically determined critical \bar{N}_v .

The method has been successfully used as a quality control tool for several commercially produced alloys where the range of compositions is limited and the critical \bar{N}_v was empirically determined. However, when used as a research tool, no single γ' composition or elemental \bar{N}_v s could be found to allow one critical \bar{N}_v for sigma formation. One reason for this problem is that γ' has been experimentally shown to have a variable stoichiometry and perhaps of greater significance is that γ' formers are soluble in γ in varying amounts.

It is believed that the stoichiometric approach also can be successfully used in systems where the precipitate is in essence a line compound (solvus independent of composition), has little solubility in the second phase, or is present in small amounts. This may be the case for the carbides and borides in the Ni-base superalloys.

The analytical geometric approach to estimating the composition of conjugate phases has been demonstrated for Ni-base alloys containing up to six components. The work reviewed here has shown that the two-phase region ($\gamma + \gamma'$) of the Ni-Al-Cr-Ti-W-Mo systems at 850^o C can be satisfactorily modeled. If one is given a melt composition the composition of the conjugate γ and γ' can be determined from the model. Furthermore, I believe that the approach that was applied to a six-component Ni-base system can be used in either higher order Ni-base systems and in other alloy bases.

In developing the geometric approach for estimation of conjugate phase compositions, it was observed that the propensity toward formation

of additional phases could be estimated from parameters available from the geometric analysis. Specifically it was observed that the Ni in the alloy, the parameter $Cr + 1.75(Mo + W)$ and the Al direction number along the $\gamma + \gamma'$ tie line, can be used to estimate the propensity of an alloy toward additional phase formation. All three parameters can be related to solvus curves on conventional phase diagrams. It is suggested that additional study in relating phase diagram parameters to solvus surfaces can further refine this approach and make it applicable to different alloy bases, higher order systems and perhaps three or four phase regions. For years the phase diagram literature has touched on mathematical modeling of systems; however, in practice the industry has settled for what it can draw on a plane sheet or model in three-dimensional space.

In closing, I would like to offer that the work reviewed here should encourage more work on multicomponent systems where the computer can allow interpretation of the modeled diagrams. This approach has been demonstrated here and its extension to commercial alloys has been indicated.

REFERENCES

1. Quigg, R. J. and Collins, H. E., Superalloy Development for Aircraft Gas Turbines, ASME Paper 69GT-7, Cleveland, Ohio (March 1968).
2. Wlodek, S. T., Trans. ASM 57 (1), 110 (1964).
3. Ross, E. W., J. Met. 19 (12), 12 (1967).
4. Dreshfield, R. L. and Ashbrook, R. L., NASA TN D-5185 (1969).
5. Dreshfield, R. L. and Ashbrook, R. L., NASA TN D-6015 (1970).
6. Dreshfield, R. L. and Ashbrook, R. L., NASA TN D-7654 (1974).
7. Woodyatt, L. R., Sims, C. T., and Beattie, H. J., Jr., Trans. AIME 236 (4), 519 (1966).
8. Boesch, W. J. and Slaney, J. S., Met. Prog. 86 (1), 109 (1964).
9. Dreshfield, R. L., NASA TM X-52530 (1969).

10. Dreshfield, R. L., NASA TN D-5783 (1970).
11. Dreshfield, R. L., Metall. Trans. 2 (5), 1341 (1971).
12. Sims, C. T., in The Superalloys, Sims, C. T. and Hagel, W. C., eds. (John Wiley & Sons, Inc., New York, N. Y., 1972), Chapter 9.
13. Barrows, R. G. and Newkirk, J. B., Metall. Trans. 3 (11), 2889 (1972).
14. Wallace, W., Nat. Res. Coun. Can. Q. Bull. No. 3, 1 (1974).
15. Collins, H. E. and Kortovich, C. S., J. Mater. 4 (1), 62 (1969).
16. Barrett, C. S., J. Inst. Met. 100, 65 (1972).
17. Mihalisin, J. R. and Pasquine, D. L., in International Symposium on Structural Stability in Superalloys (Metall. Soc. AIME, New York, N. Y., 1968), p. 134.
18. Kriege, O. H. and Sullivan, C. P., Trans. ASM 61 (2), 278 (1968).
19. Kriege, O. H. and Baris, J. M., Trans. ASM 62 (1), 195 (1969).
20. Taylor, A. and Floyd, R. W., J. Inst. Met. 81, 451 (1952-1953).
21. Taylor, A. and Floyd, R. W., J. Inst. Met. 80, 577 (1951-1952).
22. Taylor, A. and Floyd, R. W., J. Inst. Met. 81, 25 (1952-1953).
23. Taylor, A., Trans. AIME 206 (10), 1356 (1956).
24. Dreshfield, R. L. and Wallace, J. F., Metall. Trans. 5 (1), 71 (1974).
25. Dreshfield, R. L. and Wallace, J. F., The Effect of Alloying on Gamma and Gamma Prime in Nickel-Base Superalloys, Case Western Reserve Univ., 135 pages (May 1972); also NASA CR-120940.
26. Connor, W. S. and Zelen, M., Fractional Factorial Experiment Designs for Factors at Three Levels. National Bureau of Standards Applied Mathematics Series No. 54, 12 (May 1959).
27. Sidik, S. M., NASA TN D-6770 (1972).
28. Loomis, W. T., Freeman, J. W., and Sponseller, D. L., Metall. Trans. 3 (4), 989 (1972).

29. Mihalison, J. R., Rev. High-Temp. Mater. 2 (3), 243 (1974).
30. Kishkin, S. T., Kozlova, M. N., and Lashko, N. F., Izv. Akad. Nauk SSSR, 170 Met. (Jan.-Feb. 1972).
31. Kirby, G. N., Sponseller, D. L., and Van Vlack, L. H., Metall. Trans. 5 (6), 1477 (1974).
32. Decker, R. F., Strengthening Mechanisms in Nickel-Base Super-alloys, presented at Steel Strengthening Mechanisms Symposium, Zurich, Switzerland (May 5-6, 1969).

TABLE I. - COMPOSITION OF ALLOYS

Alloy	Refer- ence	Heat treat- ment	Weight percent (balance is nickel)												
			Cr	Co	Al	Ti	W	Mo	Nb	Ta	V	Fe	C	B	
B-1900	19 ↓	1	7.9	9.8	5.9	1.0	----	5.7	-----	4.5	-----	----	0.09	----	
GMR 235		1	15.9	-----	3.5	2.0	----	5.0	-----	---	----	9.8	.15	----	
Inconel 700		2	14.3	28.5	3.0	2.5	----	3.9	-----	---	----	.7	.12	----	
Alloy 713C		1	12.6	-----	6.8 ^a	.8	----	4.7	2.1	---	----	----	.16	----	
Inconel X-750		3	14.6	-----	.8	2.4	----	----	.8	---	----	6.5	.04	----	
IN 100		1	9.8	15.0	5.6	5.7 ^a	----	3.1	-----	---	0.9	----	.19	----	
Mar-M 200		1	8.9	9.5	4.5	1.9	12.3	----	1.1	---	----	----	.16	----	
Nicrotung		1	11.0	9.9	4.4	4.2	8.0	----	-----	---	----	----	.07	----	
Nimonic 115		4	14.8	14.8	4.8	3.9	----	3.5	-----	---	----	----	.14	----	
René 41		5	19.0	10.7	1.5	3.1	----	9.7	-----	---	----	----	.09	----	
TRW 1900		1	10.1	10.3	6.7	1.0	9.2	----	1.6	---	----	----	.14	----	
Udimet 500		6	18.7	19.3	2.9	3.0	----	4.3	-----	---	----	----	.07	----	
Udimet 700		7	15.4	18.8	4.4	3.4	----	5.0	-----	---	----	----	.06	----	
Unitemp AF 1753		8	16.4	7.7	2.0	3.4	8.3	1.5	-----	---	----	9.0	.23	----	
Waspaloy		9	18.6	13.0	1.4	2.9	----	4.2	-----	---	----	----	.05	----	
Alloy 713C		17 ↓	1	13.23	-----	5.86	.79	----	4.46	^b 2.09	---	----	.10	.11	0.01
Alloy 713LC (heat 07)			1	12.32	-----	5.90	.72	----	4.46	^a 2.13	---	----	.20	.06	.01
Alloy 713LC (heat 17)	1		12.52	-----	5.90	.60	----	4.41	^a 2.10	---	----	.15	.03	.01	
IN 731 X	1		9.60	9.72	5.60	4.66	----	2.46	-----	---	.85	.23	.16	.01	

Heat treat- ment	Description
1	As cast
2	2160° F/ 2 hr/air cool + 1600° F/ 4 hr/air cool
3	2100° F/ 2 hr/air cool + 1550° F/ 24 hr/air cool + 1300° F/20 hr/air cool
4	2175° F/1½ hr/air cool + 2010° F/ 6 hr/air cool
5	1950° F/ 4 hr/air cool + 1400° F/ 16 hr/air cool
6	1975° F/ 4 hr/air cool + 1550° F/ 24 hr/air cool + 1400° F/16 hr/air cool
7	2140° F/ 4 hr/air cool + 1800° F/136 hr/air cool
8	2150° F/ 4 hr/air cool + 1650° F/ 6 hr/air cool
9	1975° F/ 4 hr/air cool + 1550° F/ 24 hr/air cool + 1400° F/16 hr/air cool

^aValue higher than AMS specification for alloy.

^bReported in ref. 17 as Nb + Ta.

TABLE II. - COMPARISON OF
 PROPOSED METHOD AND
 ANALYZED DATA

Element	Average difference, \bar{d} , wt % ^a	Sample standard deviation of difference, S_d
Cr	1.1	2.05
Al	.007	.57
Ti ^b	.007	.28
Co ^b	.017	2.74
Mo	.136	1.36
Fe	1.38	1.10
W	-3.73	3.52

$$\bar{d} = \sum_{i=1}^n \frac{\text{literature} - \text{calculated}}{n}$$

^b \bar{d} was forced to be essentially zero.

TABLE III. - EXPERIMENTAL DESIGN

Element	Level	Alloying addition, at.%, Ni is balance, heat number	
		1-36	37-49
Al	Low	4.0	4.0
	Medium	9.0	8.0
	High	13.0	12.0
Ti	Low	0.25	0.25
	Medium	1.75	1.75
	High	4.75	3.75
Cr	Low	6.5	6.5
	Medium	13.5	12.5
	High	20.5	18.5
W	Low	0	0
	Medium	2.0	1.5
	High	4.0	3.0
Mo	Low	0	0
	Medium	3.0	2.0
	High	6.0	4.0

TABLE IV. - COMPOSITION OF
TWO-PHASE ALLOYS

Heat	Composition, wt %					
	Al	Cr	Mo	Ni	Ti	W
98	2.9	9.4	0	76.9	1.5	9.3
99	3.9	11.2	9.3	73.9	1.7	0
2	4.1	12.5	4.8	78.4	.2	0
5	1.5	5.9	4.2	75.7	1.3	11.2
7	3.9	6.8	0	80.0	3.3	6.0
12	3.7	5.5	4.6	72.4	.1	13.7
14	6.4	5.7	0	81.0	1.4	5.5
15	2.2	20.0	5.1	65.1	1.5	6.1
16	1.9	6.5	10.2	77.4	3.9	0
^a 21	1.7	6.2	0	85.9	.2	5.9
22	1.8	12.1	5.2	79.4	1.5	0
23	4.8	6.3	10.8	76.6	1.5	0
28	7.4	6.3	0	74.3	.2	11.9
31	4.7	17.7	0	70.6	1.2	5.8
33	1.9	5.9	9.6	75.7	1.2	5.7
34	2.1	13.3	0	80.7	3.9	0
35	4.7	5.4	4.8	81.4	3.6	0
37	3.9	13.2	6.8	70.2	1.3	4.6
38	6.5	12.8	4.0	73.5	3.2	0
39	5.4	6.6	6.8	81.1	.1	0
40	5.9	11.2	0	72.6	1.6	9.0
41	1.8	12.3	6.7	72.2	3.0	4.0
42	4.1	18.9	3.7	68.9	.1	4.3
46	4.1	10.9	7.9	68.6	.3	8.2
47	5.6	11.5	3.5	73.2	1.3	4.8
48	3.6	17.5	0	75.2	3.8	0
49	5.5	17.2	0	75.6	1.7	0

^aAlloy contain less than 1 percent γ' - no analysis of γ' could be made.

TABLE V. - COMPOSITION AND AMOUNT OF GAMMA PRIME

Heat	Element, at. %						Amount of γ' , wt%
	Ni	Al	Cr	Mo	Ti	W	
98	78.0	12.5	2.7	---	3.7	3.1	40.1
99	76.1	13.8	2.6	2.9	3.9	---	39.4
2	74.5	17.3	5.1	2.4	.7	---	29.3
5	75.7	13.3	2.1	1.1	5.1	2.7	^a 5.6
7	76.9	11.7	2.4	---	7.1	1.9	39.2
12	77.8	14.6	1.9	1.5	.3	3.9	31.9
14	73.3	15.9	4.2	---	2.8	3.8	18.4
15	74.3	11.3	4.9	1.1	6.3	2.1	16.8
16	75.6	10.3	1.5	2.3	10.3	---	20.3
22	76.2	7.8	8.9	2.2	4.9	---	8.5
23	74.2	15.9	2.7	3.9	3.3	---	44.5
28	72.1	16.9	3.5	---	.3	7.2	32.1
31	74.3	16.0	4.0	---	3.3	2.4	41.3
33	77.1	10.8	2.4	2.4	5.9	1.4	^a 1.4
34	73.1	10.1	2.9	---	13.9	---	21.5
35	77.3	12.1	2.3	1.7	6.6	---	54.5
37	74.7	15.7	2.7	1.7	3.5	1.7	35.3
38	74.7	15.1	3.5	1.6	5.1	---	34.2
39	77.5	15.5	3.2	3.5	.3	---	44.7
40	76.0	15.1	3.3	---	2.3	3.3	55.7
41	72.4	10.6	2.1	2.9	9.5	2.5	23.9
42	73.6	17.5	4.6	1.3	.3	2.7	27.1
46	76.6	14.9	2.9	1.7	.4	3.5	29.3
47	75.8	15.3	3.2	1.3	2.4	2.0	55.6
48	76.1	13.1	3.9	---	6.9	---	38.7
49	75.9	15.3	6.1	---	2.7	---	51.9
S		0.851	0.336	0.573	0.502	0.852	

^aElectrolyte was H_3PO_4 - extraction not quantitative in amount of γ' .

TABLE VI. - COMPOSITION OF GAMMA

Heat	Element, at.%, balance is Ni				
	Al	Cr	Mo	Ti	W
98	2.1	16.4	---	0.5	2.9
99	4.3	19.1	7.5	.8	---
2	4.7	17.2	3.0	0	---
7	6.1	10.9	---	1.7	1.9
12	5.5	8.9	3.7	.1	5.0
14	12.7	6.6	---	1.5	1.2
15	3.5	26.5	3.6	.9	1.9
16	2.1	9.2	7.5	3.1	---
22	3.4	13.9	3.2	1.5	---
23	5.1	10.7	8.7	.5	---
28	15.4	8.5	---	.1	2.2
31	5.5	29.9	---	.1	1.3
34	2.5	17.7	---	1.9	---
35	6.9	10.3	4.2	1.2	---
37	4.3	21.8	5.5	.5	1.3
38	11.9	18.5	2.7	2.9	---
39	7.6	10.5	4.3	0	---
40	9.5	23.3	---	1.5	2.1
41	1.9	17.8	4.5	1.9	.9
42	5.5	25.7	2.5	.1	.8
46	6.7	16.7	6.3	.4	2.3
47	7.5	24.4	3.1	.5	.8
48	3.5	27.7	---	2.5	---
49	6.2	30.7	---	1.1	---
S	0.640	0.391	0.224	0.256	0.374

TABLE VII. - REGRESSION ANALYSIS OF
GAMMA AND GAMMA PRIME

$$\left[\text{Equation: Al} = \sum_{n=0}^{n=18} B_n \times F_n \right]$$

n	Phase		Factor, F _n
	γ Coefficient, B _n	γ' Coefficient, B _n	
0	13.3992	7.42647	Constant
1	-1.07392	3.59713	Cr
2	1.80069	0	Mo
3	0	.849058	Ti
4	15.3168	-.589230	W
5	.0318507	-.292157	Cr ²
6	.0455815	.149930	Mo ²
7	1.53473	-.0256415	Ti ²
8	-2.59870	-.0398181	W ²
9	-.100793	-.127831	Cr × Mo
10	-.204796	-.310730	Cr × Ti
11	-.504191	.290021	Cr × W
12	-2.12721	-.245979	Mo × Ti
13	.598921	.876515	Mo × W
14	-7.75600	-.155343	Ti × W
15	.153165	.0675603	Cr × Mo × Ti
16	0	-.275617	Cr × Mo × W
17	.486625	0	Cr × Ti × W
18	-1.43936	.0226054	Mo × Ti × W
R ²	.89	.87	

TABLE VIII. - LEAST SQUARES ANALYSIS OF
DIRECTION NUMBERS

$$\left[\text{Equation: Direction number} = \sum_{n=0}^{n=5} B_n \times F_n. \right]$$

n	Element				Factor, F _n
	Al coefficient, B _n	Mo coefficient, B _n	Ti coefficient, B _n	W coefficient, B _n	
0	-2.4316	-0.0032572	-1.04691	-0.52841	Constant
1	.066096	-.0010339	.046595	-.054240	Al
2	.059819	-.013136	.030941	.030041	Cr
3	.0088685	.087981	.026712	.020858	Mo
4	.14622	.021598	-.070565	.054511	Ti
5	.090661	.024404	.040548	.14031	W
R ²	.64	.72	.76	.37	
^a T	.35	.09	.96	.29	

^aT is the significance level of the least significant coefficient.

TABLE IX. - COMPARISON OF ANALYZED DATA AND
CALCULATION FOR EXPERIMENTAL ALLOYS

Element	Phase	Average difference, \bar{d} , ^a at. %	Sample standard deviation of difference, S_d
Al	γ	-0.50	1.6
	γ'	.59	1.5
Cr	γ	.93	4.8
	γ'	.90	1.8
Mo	γ	.18	.54
	γ'	-.09	.72
Ti	γ	.12	.82
	γ'	.12	1.28
W	γ	.23	.95
	γ'	-.66	1.6

$$^a \bar{d} = \sum_{i=1}^{i=n} \left(\frac{\text{observed} - \text{calculated}}{n} \right).$$

TABLE X. - OCCURRENCE OF PHASES

Alloy	Element, at. %						Phase			
	Al	Cr	Mo	Ti	W	Ni	Cr	^a Mo, W	σ	μ
3	14.6	8.4	5.5	0.2	---	71.2				×
4	12.9	11.9	---	1.3	4.1	69.8		×		
6	7.3	21.6	5.6	1.4	3.6	60.5		×	×	
8	13.1	21.9	2.8	4.3	1.8	56.1	×	×	×	
9	4.0	14.8	5.4	5.1	2.1	68.6		×		×
10	9.7	23.5	6.4	.4	4.6	55.4		×	×	
13	8.8	15.2	5.5	1.6	1.8	67.1				×
17	8.6	23.4	---	4.3	---	63.7	×			
18	15.3	14.0	3.0	4.9	---	62.9	×		×	
19	9.9	17.8	3.1	.1	2.1	67.0		×		×
20	15.7	13.1	5.4	.2	2.0	63.5		×	×	
24	14.2	20.7	---	1.4	---	63.6	×			
25	13.3	7.1	2.9	4.6	3.4	68.6		×	×	
26	3.9	21.8	5.6	4.5	3.6	60.6		×	×	×
27	7.1	17.0	---	4.6	4.0	67.2	×	×		
29	4.1	22.7	3.2	.1	3.8	66.1		×		
30	9.8	14.8	5.8	.1	3.8	65.7		×		×
32	14.7	13.7	3.1	1.7	1.9	65.3	×	×	×	
36	14.8	21.0	6.4	4.5	---	55.3	×	×	×	
43	12.9	12.5	4.1	4.9	1.3	64.2				×
44	10.9	6.4	2.0	3.3	2.9	74.5		Unidentified		
45	3.6	19.6	4.1	3.9	2.6	66.2		×		

^aMo and W cannot be differentiated by X-ray diffraction.

BCC phase with A_0 at approximately 3.15 Å.

TABLE XI. - COMPARISON OF OBSERVED AND ESTIMATED PHASE COMPOSITIONS

IN COMMERCIAL ALLOYS

Alloy	Phase	Element, at. %									
		Al		Cr		Mo		Ti		W	
		Obs ^a	Est ^b	Obs	Est	Obs	Est	Obs	Est	Obs	Est
B-1900	γ	5.1	1.8	18.3	20.5	5.4	5.7	0	0	---	---
	γ'	17.2	16.4	3.0	4.4	2.3	2.6	1.9	1.7	---	---
GMR 235	γ	3.8	3.5	20.6	22.5	3.2	3.3	.6	.4	---	---
	γ'	17.6	14.3	2.3	6.0	1.4	2.2	5.1	4.4	---	---
Inconel 700	γ	4.0	4.8	19.4	16.9	2.4	2.3	1.0	1.7	---	---
	γ'	13.6	13.0	4.3	5.7	1.2	1.8	6.7	6.4	---	---
Inconel 713C	γ	8.1	5.4	24.3	27.2	3.9	3.6	.1	.6	---	---
	γ'	19.2	18.0	3.5	6.5	1.5	2.3	1.3	.6	---	---
Inconel X-750	γ	.6	.5	17.9	16.9	---	---	1.2	2.0	---	---
	γ'	6.9	15.5	2.3	1.5	---	---	12.8	12.5	---	---
IN 100	γ	4.8	10.4	24.0	14.8	3.1	2.4	.5	3.0	---	---
	γ'	14.0	13.4	3.4	1.2	.7	.6	8.6	10.7	---	---
Mar M 200	γ	3.2	.5	20.4	29.4	---	---	0	0	4.2	2.1
	γ'	14.8	13.5	3.1	3.4	---	---	3.7	3.6	4.0	4.9
Nicrotung	γ	.9	8.4	26.1	18.3	---	---	1.0	1.8	2.9	2.1
	γ'	14.9	10.6	3.3	4.9	---	---	7.6	8.2	2.3	3.0
Nimonic 115	γ	4.6	8.8	26.5	19.1	2.9	2.1	.6	2.6	---	---
	γ'	15.7	12.8	4.1	3.6	.6	1.4	7.2	8.4	---	---
Rene 41	γ	1.3	.5	26.8	27.6	7.0	8.2	.7	1.1	---	---
	γ'	9.2	9.3	3.5	5.3	1.3	1.0	10.9	9.2	---	---
TRW 1900	γ	7.6	7.4	24.1	27.3	---	---	.4	.9	3.0	1.8
	γ'	17.4	17.5	3.9	3.9	---	---	1.4	.9	2.6	6.6
Udimet 500	γ	2.3	3.7	28.6	26.7	3.0	2.6	.6	1.0	---	---
	γ'	13.5	10.7	2.9	5.6	1.0	2.1	7.9	8.3	---	---
Udimet 700	γ	5.3	6.8	24.3	24.0	3.9	3.8	1.5	1.3	---	---
	γ'	13.9	12.5	2.7	4.0	.9	1.5	8.1	7.6	---	---
Unitemp AF 1753	γ	2.4	4.4	22.5	18.1	1.1	.9	1.1	2.7	2.7	3.4
	γ'	11.6	7.9	1.3	8.0	.3	.9	11.6	5.9	1.8	0
Waspaloy	γ	1.1	.5	25.0	24.6	3.2	2.6	.7	1.2	---	---
	γ'	9.5	11.2	2.4	4.3	.7	2.1	12.5	10.6	---	---
\bar{d}^c	γ	-0.82		0.99		0.15		-0.69		0.85	
	γ'	.83		-1.5		-.60		.55		-.95	
S _d	γ	3.1		4.8		.56		.75		1.2	
	γ'	3.1		2.1		.49		1.7		2.4	

^aObs is the experimentally observed value (ref. 19).

^bEst is the value estimated by the calculation.

$$\bar{d}^c = \sum_{i=1}^n \left(\frac{\text{observed} - \text{calculated}}{n} \right)$$

TABLE XII. - PHASE OCCURRENCE IN COMMERCIAL ALLOYS

Alloy	Parameters			Phase ^b
	Alloy Ni + Co + Fe, ^a at. %	Gamma Cr + 1.75 × (Mo + W), ^a at. %	Al DN ^a	
Inconel X-750	78.9	17.9	-0.40	n
Mar M 200	73.1	27.4	-.67	n
Inconel 700	72.6	23.6	-.64	n
B-1900	72.5	27.0	-.79	n
Nicrotung	70.7	31.2	-.61	n
Waspaloy	70.5	30.6	-.37	n
GMR 235	69.9	26.2	-.75	--
TRW 1900	69.1	29.4	-.49	n
IN 100	68.7	29.4	-.45	σ
Unitemp AF 1753	68.4	29.2	-.43	n
Nimonic 115	67.7	31.6	-.50	σ
Udimet 500	67.6	33.9	-.44	σ
Udimet 700	67.5	31.1	-.40	σ
Inconel 713C	67.5	31.1	-.53	σ
Rene 41	65.6	39.1	-.34	μ

^aFrom Kriege and Baris (ref. 19).

^bFrom Collins (ref. 15).

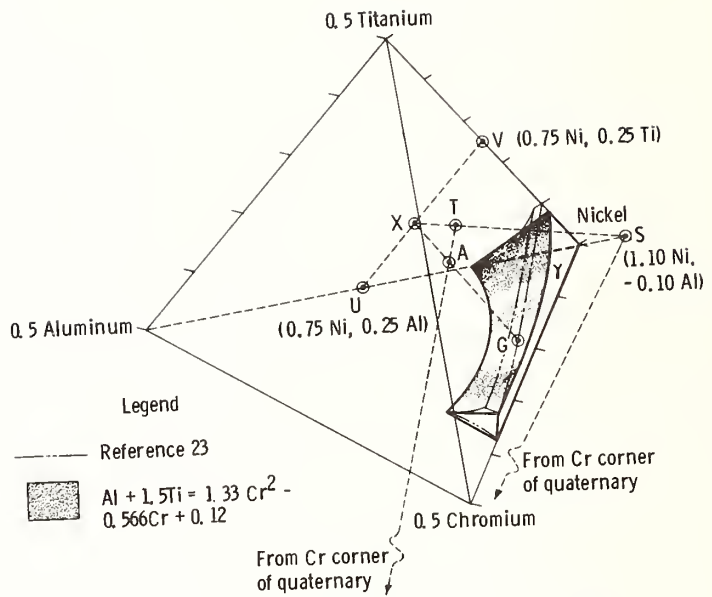


Figure 1. - Nickel-rich region of Ni-Al-Cr-Ti system at 750° C.

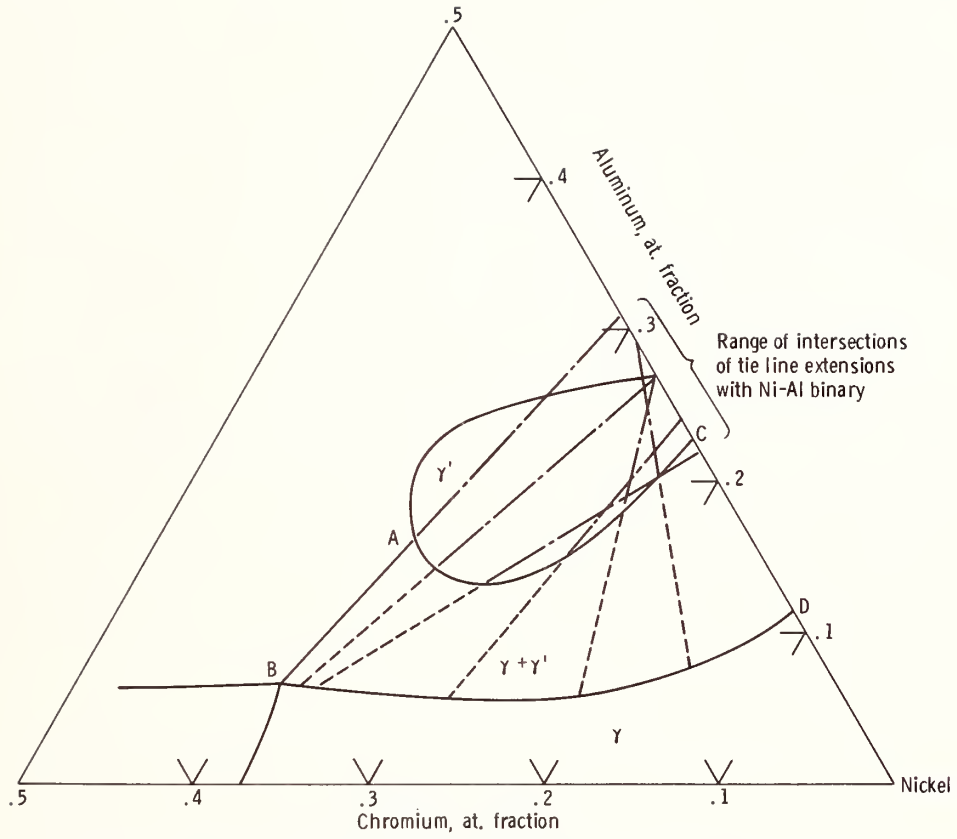


Figure 2. - Nickel-rich region of Ni-Cr-Al system at 750^o C (after Taylor and Floyd (ref. 20)).

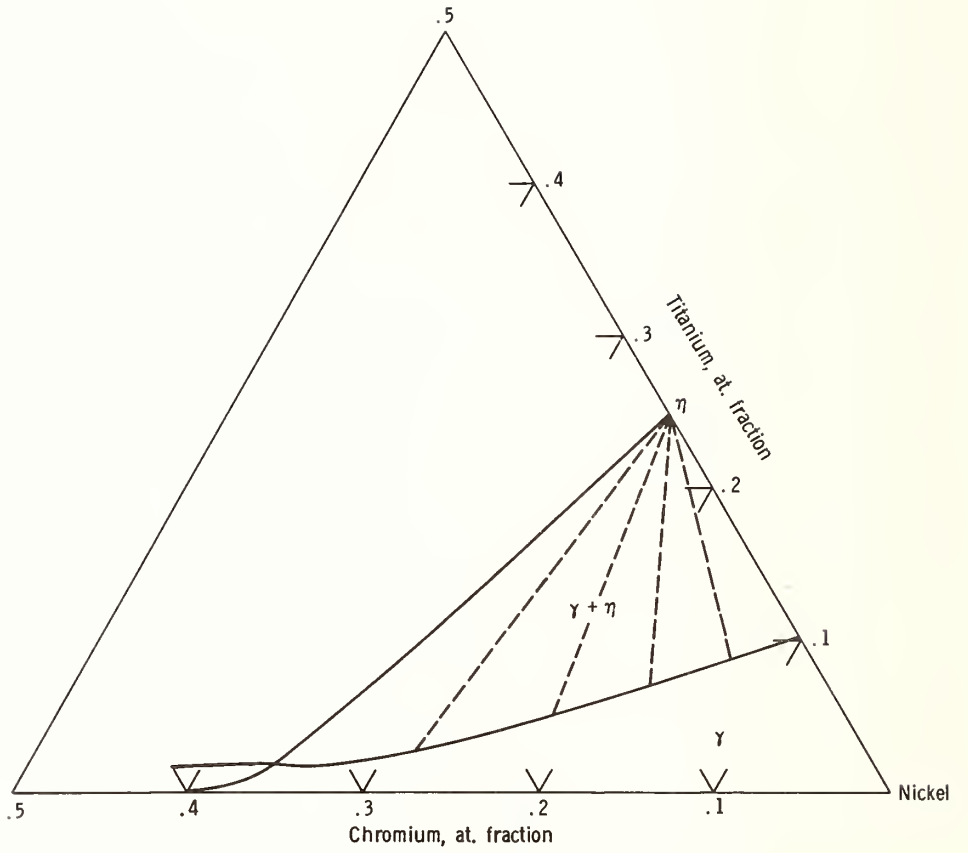


Figure 3. - Nickel-rich region of Ni-Cr-Ti system at 750° C (after Taylor and Floyd (ref. 21)).

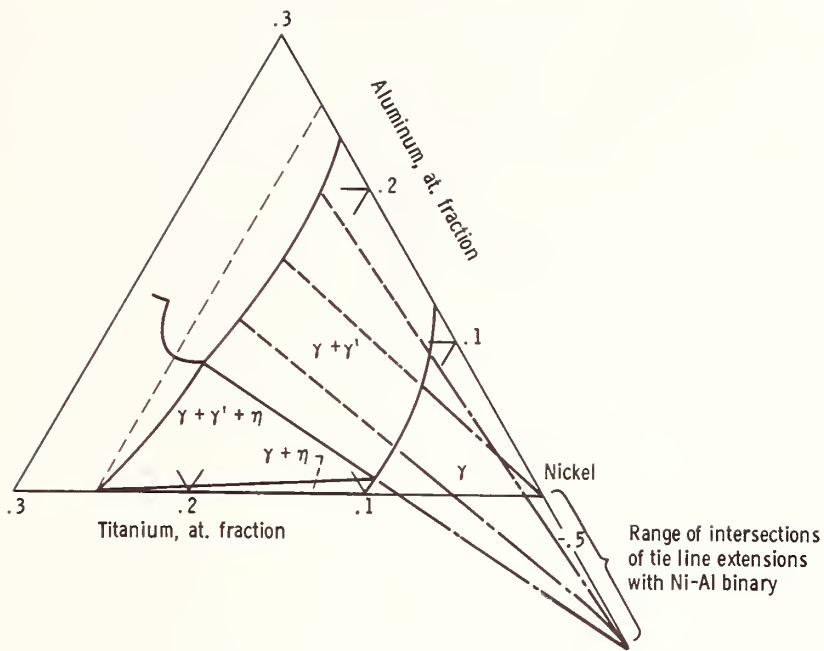


Figure 4. - Nickel-rich region of Ni-Ti-Al system at 750^o C (after Taylor and Floyd (ref. 22)).

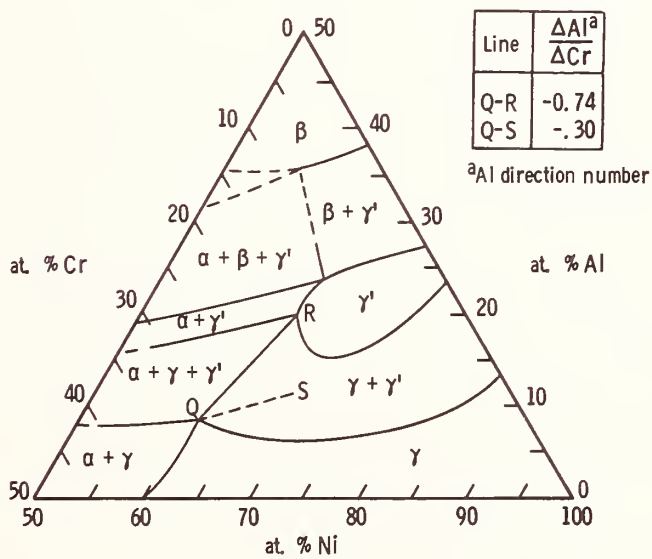


Figure 5. - The Ni-Cr-Al phase diagram at 850^o C from reference 20.

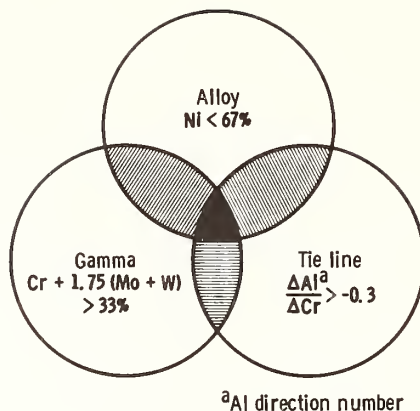


Figure 6. - Occurrence of BCC and TCP phases in experimental alloys.

Discussion following the Panel I presentations on Tues Jan 11.

George Armstrong - I am pleased to see Prof. Brewer is going to publish his solvus curves in a numerical form, because as I will attempt to show later, one of my beliefs is that one does not have to be able physically to look at a phase diagram to extract useful information, but only be able to massage it numerically.

J. Elliott - I have a comment I would like to make: we're going to have to do some experiments. We are interested in what constitute the phases in equilibrium in a number of systems of technological importance; the Fe-Cr-Ni-C for example. What we would like, is to do a few measurements and do a lot of calculations. The trouble is that we have a complicated set of interactions. We have written down a complicated program similar to that which Larry Kaufman has, and have compared experimental liquidus results in the Fe-Cr-Ni-C system with these calculations and there is quite a difference. Adjusting the data and going through another calculation improves certain features, but it depends on your taste as to whether this gives a better fit. We have not used ternary and higher order coefficients in our calculations. These would then give a better fit. The trouble then arises: when do we use such a "better" set of data for other calculations such as for the Fe-Cr-Mn-C system or Fe-Ni-Mn-C system. And the result of this is that we are not quite as optimistic as we were at the outset that we would be able to do a limited set of experimental points to be able to rapidly predict what the liquidus surfaces are.

L. Kaufman - It depends on your viewpoint. Your calculation seems to indicate that we could be out by as much as 2 to 3 percent. For most practical kinds of applications you are really not interested in this close detail, as, for example, in an application like Bob Dreshfield's where you want to know roughly where the liquidus surfaces are. It depends on what you want. We are not trying to imply that you shouldn't do the experiment.

F. L. Carter - My question is to Dr. Kaufman as well as the others: Are the x-ray parameters and distances used in the calculations and do the calculations predict lattice parameters or compositions of phases?

L. Kaufman - Not on the ones that we are currently doing. In the kind of considerations that Leo Brewer does, volumes can be important.

L. Brewer - Yes. They are very important because, particularly in solid solubility, the strain energies are very important term.

A. Navrotsky - Volume considerations certainly are important in the high pressure oxide work and the crystallography is important in choosing appropriate forms of equations in complicated silicate systems. For example, questions of how many sites are involved in mixing, and things of this sort, are to be considered.



The Representation of Phase Equilibria

Alan Prince
(The General Electric Co. Ltd.,
Hirst Research Centre, Wembley, England)

In two years we will see the 150th anniversary of the first investigations of alloy phase equilibria. F. Rudberg⁽¹⁾ of Sweden produced a tabular representation of what we would call nowadays the inverse-rate cooling curves of the Pb-Sn alloy series. The importance of this early work is not so much the fact that Rudberg tabulated his data on the familiar temperature-concentration axes, but the detailed conclusions he drew from his work⁽²⁾. The Russian A. Ya. Kupfer in examining the specific gravity of Pb-Sn alloys also determined the liquidus temperatures of these alloys⁽³⁾. Over the past century and a half there has been a great increase in our knowledge of alloy phase equilibria, especially of binary systems. Multicomponent systems have been less well studied. To the end of 1973 some 6223 ternary systems had been examined, 1237 quaternary systems, 149 quinary systems, and 27 senary systems. This represents a minute percentage of possible systems and it must be remembered that very few of the systems studied have been investigated in any detail.

In terms of phase equilibria it is important to consider the representation of binary, ternary, and quaternary systems. Methods need to be available for the representation of more complex systems but little experimental data exists on which to apply these methods.

Phase diagrams are graphical representations of the phase relationships in heterogeneous systems. The phase diagram can be considered to consist of a coordinate framework enclosing geometrical elements (the phase complex) representative of the phase relationships. The coordinate framework is based on a concentration simplex, which is equated to the concentration diagram of the system, combined with other geometrical elements representing such additional externally variable parameters as temperature and pressure, figure 1. This terminology appears unduly academic at first glance. However its introduction by the Russian metallurgist Kurnakov⁽⁴⁾ paved the way for a consideration of multicomponent systems by topological techniques.

Representation of Concentration - The Concentration Simplex

A ternary system with components A, B, and C is represented by two concentration axes. This follows from the relation

$$X_A + X_B + X_C = 100$$

where X_A , X_B , X_C are the molar, weight, or atomic percentages of components A, B, and C respectively. The concentration diagram is a two-dimensional simplex, figure 2a, containing three vertices, three edges, and one surface. It contains no internal diagonals and all lines and surfaces connecting the vertices of a simplex coincide with its edges and surfaces. The number of vertices of a simplex exceeds by one the dimension of the space in which it exists.

Simplexes can have edges of equal or unequal length. A two-dimensional regular simplex with equal edges is normally used to represent concentrations in ternary systems. It is the well-known Gibbs triangle or concentration triangle, figure 2b. Any alloy with a composition defined by a point within this triangle has the concentrations of its components defined by dropping perpendiculars from the point to the three sides of the triangle. Alternatively concentrations of any component can be equated to the area of the triangle including the alloy and the edge containing the other two components.

This elementary preamble leads to a consideration of the Kurnakov method for representing concentrations in multicomponent systems. For n-component systems

$$\sum_{i=A}^n X_i = 100$$

Concentrations are represented in n-component systems by (n-1)-dimensional simplexes with n vertices. The concentrations X_i ($i = A, B, \dots, n$) for any alloy in the n-component system are defined by the lengths of the perpendiculars dropped from the point representing the alloy on to the (n-2)-dimensional hyperfaces of the concentration simplex. Alternatively the concentrations X_i are given by the ratio of the hypervolume of the simplex containing the point representing the alloy and all the vertices of the concentration simplex except vertex i to the hypervolume of the concentration simplex :-

$$X_i = \frac{V_i}{V}$$

In ternary systems the hypervolumes of the simplexes are the areas of appropriate triangles. In quaternary systems four vertices, A, B, C, D, in three-dimensional space define the concentration simplex. The normal representation is by means of an equilateral tetrahedron, as first suggested by Roozeboom⁽⁵⁾, figure 3. The concentration of any component in alloy M is the ratio of the volume of the tetrahedron opposite the vertex of the component to the volume of the concentration tetrahedron, e.g.

$$X_A = \frac{V_A}{V} = \frac{\text{Volume MBCD}}{\text{Volume ABCD}}$$

It is not possible to visualise or graphically represent a quinary concentration diagram since this would require four-dimensional space. Since the number of geometrical elements in any simplex is determined by the relation

$$\sum_{1}^n S(n) = 2^n - 1 = {}^n C_1 + {}^n C_2 + \dots + {}^n C_n$$

we can deduce that for a quinary system with $n = 5$ there will be

${}^n C_1 = 5$ vertices, ${}^n C_2 = 10$ edges, ${}^n C_3 = 10$ surfaces, ${}^n C_4 = 5$ volumes, and ${}^n C_5 = 1$ hypervolume. The vertices correspond to the components, edges to the constituent binary systems, surfaces to the ternary systems, volumes to the quaternary systems and the hypervolume to the quinary system itself. All we can now do is to project such a quinary simplex, a pentahedroid, as a three-dimensional figure, figure 4 or, as will be noted later to consider two-dimensional projections of the simplex.

Representation of Concentration - Secondary Methods

In most compilations of constitutional data concentrations have been expressed in weight percentages or atomic percentages of the components. The industrial metallurgist normally works in weight percentages. He recognises the eutectoid point in the Fe-C system as containing 0.80 weight percentage carbon not as containing 3.61 atomic percentage carbon.

Notwithstanding this practice there are cogent scientific reasons for considering alternative methods for representing concentrations. The historic paper by W. Hume-Rothery and co-workers⁽⁶⁾ introduced the concept of electron concentrations - the ratio of valency electrons to atoms - as a powerful tool in understanding phase relationships in binary alloys. For Cu and Ag alloys with favourable size-factors it was shown that the maximum solid solubilities of B - subgroup elements corresponds to an electron concentration of about 1.4. The electron compounds were shown to occur at specific electron concentrations, corresponding to electron: atom ratios of 3:2, 21:13, and 7:4. Later workers⁽⁷⁾ have used electron concentrations in studying ternary alloy systems to show how the interplay of size-factors and electronic structure influence the formation of ternary solid solutions based on binary electron compounds at constant e:a ratios.

Electron concentration effects also apply to some solid solutions in binary transition metals. Difficulties in assigning a valency to the transition metals led Hume-Rothery to describe concentrations in terms of average group numbers (AGN) of the alloys. Group numbers from 1 to 10 are allotted to the elements of Groups 1A to VIIIC respectively. If all the electrons outside the rare-gas shell are counted the AGN is identical with the electron concentration.

Another method of representation, used extensively in researches on superalloys, uses the electron-vacancy number, N_v , which is related to the electron concentration by the relation $N_v = 10.66 - e/a$, where N_v represents the electron vacancies in the 3d subshell. In the series V, Cr, Mn, Fe, Co, Ni the electron vacancy numbers assigned are 5.66, 4.66, 3.66, 2.66, 1.71, 0.66 respectively. Elements in the same group have identical values of N_v , e.g. Mo = 4.66. One of the major aims in the superalloy field is the constitutional avoidance of topologically close-packed phases, particularly the sigma phase. The basic problem addressed by the PHACOMP method is to calculate the solubility limits in terms of an average N_v for the fcc residual matrix phase in multicomponent alloys. This requirement has led to novel methods for representing constitutional data⁽⁸⁾ in terms of polar diagrams. One of the refractory metals Cr, Mo, W

is placed at the centre of the plot and the elements of the first long period are sequentially displayed on the perimeter, figure 5. The binary systems of Mo with the transition elements are represented by the radial segments Mo-Ni, Mo-Co, etc. Ternary systems are represented by the sectors Fe-Mo-Mn, Mn-Mo-Cr, etc. They can also be represented by more than two radial segments. For example the system Fe-Mo-Cr can be regarded as the summation of Fe-Mo-Mn and Mn-Mo-Cr since the radial segment Mo-Mn can be regarded as the line joining Mo to an Fe-Cr alloy with an electron vacancy equal to 3.66 (the 50 atomic percent Fe-Cr alloy). Iso-electron vacancy lines can be drawn which spiral outwards in a counter-clockwise direction. The solid solubility limits for the fcc phase follow this pattern of behaviour.

In their later form⁽⁹⁾ polar diagrams have been stacked on each other to give a three-dimensional representation.

The Coordinate Framework

The coordinate framework normally considered in alloy systems is the concentration-temperature diagram. Pressure is not one of the external parameters often used. For binary systems a two-dimensional diagram suffices. Ternary systems are represented by a three-dimensional diagram, a right triangular prism. Quaternary systems require four-dimensional space for representation of the concentration-temperature diagram. Assuming constant pressure conditions quaternary systems can be represented by a series of isothermal sections which are individual tetrahedra. To represent such systems in three or two dimensions it is necessary to use projections of the four-dimensional diagram. For higher component systems projections are obligatory. Emphasis will be placed on quaternary systems with some reference to quinary systems.

Projection Methods

Ternary diagrams are frequently represented by two-dimensional projections of the space model (i.e. the coordinate framework and the phase complex) on to the Gibbs triangle. Nothing further need be said about such systems.

There is no difficulty in projecting any point in a ternary space model on to the concentration triangle since the concentration coordinates of the point do not change on projection. The position is more difficult in quaternary systems. We will consider the projection of any point within the tetrahedron so as to establish a relationship between the coordinates of the point, representing a quaternary alloy, and the coordinates of its projection on one of the concentration triangles of the tetrahedron. Two general methods have been used, the perspective projection and the parallel projection.

Perspective Projections

Projections are made from one of the vertices of the tetrahedron to the opposite triangular face. In figure 6 an alloy of composition X is projected from vertex B on to the triangle ACD. The coordinates of the

quaternary alloy are a, b, c, d where a is the content of component A etc. The coordinates of the projected point x_1 are a_1, c_1, d_1 i.e. alloy x_1 is a ternary alloy with a content a_1 of component A etc.

Since any point on a line from a vertex to the opposite face of a tetrahedron contains the same ratio of the components associated with that face, then

$$a : c : d = a_1 : c_1 : d_1$$

But $a + b + c + d = 100$

and $a_1 + c_1 + d_1 = 100$

Knowing the composition of the quaternary alloy X the composition of the projected point x_1 can be obtained. In alloy x_1 the relative concentrations of A, C, and D ($a_1 : c_1 : d_1$) are known. The absolute values are given by the relations

$$a_1 = \frac{100 a}{a + c + d}$$

$$c_1 = \frac{100 c}{a + c + d}$$

$$d_1 = \frac{100 d}{a + c + d}$$

The reverse problem, that of finding the quaternary alloy composition from the projected point, requires the use of two projections. If the two projections are x_1 ($a_1 = 60, c_1 = 30, d_1 = 10$) and x_2 ($b_2 = 71^{3/7}, c_2 = 21^{3/7}, d_2 = 7^{1/7}$) then

$$a_1 : c_1 : d_1 = 60 : 30 : 10 = a : c : d$$

$$b_2 : c_2 : d_2 = 500 : 150 : 50 = b : c : d$$

or $b_2 : c_2 : d_2 = 100 : 30 : 10$

whence $a : b : c : d = 60 : 100 : 30 : 10$

As $a + b + c + d = 100$ it follows that $a = 30, b = 50, c = 15, d = 5$.

The perspective method of projection has been used extensively for the examination of quaternary phase equilibria. G. Phragmen's extensive publication on Al-base alloys uses perspective projections throughout⁽¹⁰⁾ and the recent textbook by L.F. Mondolfo also uses this type of projection⁽¹¹⁾. In each case the projection is made from the Al vertex of the tetrahedron.

Parallel Projections

In perspective projections all alloys within the tetrahedron are projected from lines radiating from a vertex of the tetrahedron. If the vertex were removed to infinity the lines would be parallel. We can differentiate two basic types of parallel projections. The first uses projections parallel to one of the edges of the tetrahedron; the second uses orthogonal projections (perpendicular to specific faces).

In figure 7 x_3 is the parallel projection of quaternary alloy X (a, b, c, d) on to the concentration triangle ACD. The direction of the projection is parallel to edge BD of the tetrahedron. The advantage of this type of projection is that two of the coordinates of alloy X remain the same in the projected point x_3 . In this case the coordinates a and c are identical in alloy X and its projection x_3 .

$$Da_3 = a_3 = Ba = a$$

$$Dc_3 = c_3 = Bc = c$$

$$d_3 = Ae = Ad_3 + d_3e = d + d_3e$$

$$AD = a + b + c + d = Da_3 + b + a_3e + Ad_3$$

$$\text{i.e. } b = d_3e$$

$$\text{Hence } d_3 = b + d$$

A second projection parallel to the edge AB on to the concentration triangle BCD gives a projected point x_4 . The c and d coordinates of quaternary alloy X and projected point x_4 are identical. The third coordinate for x_4 (b_4) = a + b. The two projections give the a, c, and d values for alloy X. They define the composition of X.

Orthogonal projections involve projecting any point within the tetrahedron at right angles to the plane of the projection. This plane is usually one of the concentration triangles or it can be a plane parallel to two mutually perpendicular, but not intersecting, edges of the tetrahedron. In the former case a quaternary alloy X (a, b, c, d) is projected on to triangle ACD as x_1 (a_1, c_1, d_1), figure 8a. From X draw planes XX_1X_2 , XX_1X_3 , and XX_2X_3 parallel to the faces ABC, ABD, and BCD respectively. Triangle $X_1X_2X_3$ has at its centre of gravity point x_1 .

From figure 8b

$$EX_1 = JL = d; Jx_1 = d_1. Lx_1 = d_1 - d$$

$$GD = MK = a; Kx_1 = a_1. Mx_1 = a_1 - a$$

$$FX_1 = ON = c; Ox_1 = c_1. Nx_1 = c_1 - c$$

In any equilateral triangle $Lx_1 = Mx_1 = Nx_1$

$$\text{i.e. } d_1 - d = a_1 - a = c_1 - c.$$

$$\text{But } a + b + c + d = 100 \text{ and } a_1 + c_1 + d_1 = 100.$$

$$\text{Hence } a_1 - a + c_1 - c + d_1 - d = b.$$

It follows that $a_1 - a = c_1 - c = d_1 - d = \frac{b}{3}$

In other words the coordinates a_1, c_1, d_1 of the projected point x_1 are related to the coordinates a, b, c, d of the quaternary alloy X by the relations

$$a_1 = a + \frac{b}{3} \quad c_1 = c + \frac{b}{3} \quad d_1 = d + \frac{b}{3}$$

If the coordinates of two projected points, x_1 and x_2 , are known one can determine the coordinates of alloy X. This follows from the previous relations and a similar set of relations for projection x_2 on, say triangle BCD.

$$b_2 = b + \frac{a}{3} \quad c_2 = c + \frac{a}{3} \quad d_2 = d + \frac{a}{3}$$

Alternatively it is possible to take a second projection parallel to the basal concentration triangle on to one of the side triangles. G. Petzow and A.O. Sampaio⁽¹²⁾ used the parallel orthogonal projection method in work on the U - UMn_2 - UAL_2 - UFe_2 system. Projecting the T phase at the 760°C invariant reaction on to the U - UAL_2 - UMn_2 , figure 9a, produces a composition of 6.87%U, 50.84% UAL_2 , 42.29% UMn_2 or 37.92% U, 33.89% Al, 28.19% Mn. Projecting parallel to the U - UMn_2 - UAL_2 face on to the U - UMn_2 - UFe_2 face allows the % UFe_2 in phase T to be read directly as 7.63%. The % Fe = 5.09. The T phase therefore has a composition

$$37.92 = U + \frac{5.09}{3}, \quad 33.89 = Al + \frac{5.09}{3}, \quad 28.19 = Mn + \frac{5.09}{3}$$

leading to T (36.2 U, 32.2 Al, 26.5 Mn, 5.1 Fe).

A second type of orthogonal projection is the square orthogonal projection⁽¹³⁾. This is formed by rotating the tetrahedron about an edge, say AC, until the edge BD is horizontal and orthogonally projecting the rotated tetrahedron on to a plane parallel to both non-intersecting edges of the tetrahedron. The projection plane is a square with the two edges, AC and BD, of the tetrahedron as its diagonals, figure 10b. A quaternary alloy X (a, b, c, d) lies on plane $A_1 B_1 C_1 D_1$, figure 10a, parallel to edges AC and BD. Let point O represent the intersection of AC and BD in the projection, figure 10b. The x axis is taken from O along OC, the y axis from O along OB. The coordinates of X in the projection are

$$Ox_1 = \frac{a_1 X + Xc_1}{2} - Xc_1 = \frac{a_1 X - Xc_1}{2}$$

$$Oy_1 = \frac{d_1 X + Xb_1}{2} - Xb_1 = \frac{d_1 X - Xb_1}{2}$$

The lengths $Xa_1, Xb_1, Xc_1,$ and Xd_1 are equal to the concentrations of components A, B, C, and D (a, b, c, d) in alloy X. Therefore

$$Ox_1 = \frac{c - a}{2} \quad \text{and} \quad Oy_1 = \frac{b - d}{2}$$

A second square orthogonal projection is produced by rotation about edge AD until edge BC is horizontal, figure 8c. On this projection

$$Ox_2 = \frac{b - c}{2} \quad \text{and} \quad Oy_2 = \frac{a - d}{2}$$

The coordinates of quaternary alloy X can be derived from the coordinates of the two projections. Since $100 - (b + c + d) = a$

$$100 - (2x_1 \ 0 + 2y_1 \ 0 - 4y_2 \ 0) = 4a$$

$$a = \frac{50 - x_1 \ 0 - y_1 \ 0 + 2y_2 \ 0}{2}$$

The remaining coordinates follow from the previous relations.

In an extensive study of quaternary systems Cayron⁽¹⁴⁾ makes use of an orthogonal projection of the tetrahedron on to one of the faces, say ACD figure 11b, linked with a second projection along a plane perpendicular to one edge of face ACD, say edge AD, figure 11c.

F.M. Perel'man has developed what she calls "optimal projections", these being the most convenient projections of multidimensional figures for the quantitative determination of phase equilibrium relationships. As applied to quaternary systems the optimal projection of a regular tetrahedron is obtained by turning say triangle BCD about the edge CD on to the adjoining triangle ACD. Triangle BCD is thereby projected on to triangle ACD without any distortion of scale. Triangles ABC and ABD, figure 12, project as line segments on edges AC and AD respectively, and vertex B coincides with vertex A. An optimal projection of this type can be used to consider the phase relationships in alloys rich in components C or D. A second optimal projection derived by projecting triangle ABC on to triangle ACD can be used to consider phase relationships in alloys rich in components A or C. From two such parallel projections the compositions of such invariant points as M or points on the monovariant curves WM, XM, YM, and ZM can be determined quantitatively. The standard text by Perel'man⁽¹⁵⁾ discusses the method of optimal projections and applies it to a variety of problems, such as the estimation of the liquidus temperatures of multicomponent alloys. According to Palatnik and Landau⁽¹⁶⁾ the optimal projection method has not found extensive application in the analysis of multicomponent systems since "this is a consequence of the complexity of the geometrical constructions, and of the fact that substantial distortions of shape, and even complete omission of whole regions of coexistence of phases and the interfaces between them, as well as of certain important details of the phase diagrams of multicomponent heterogeneous systems often occurs".

The projection methods outlined above do not exhaust the subject. Ricci⁽¹⁷⁾ considers other methods and the inter-relation of various projections. Which method is used will depend to a large extent on the region of the system that is being investigated and the preference of the authors in choosing a projection method that presents the data in the clearest possible manner.

Quaternary systems have been dealt with at some length. This is justifiable on the grounds that the conceptually simple ternary systems, together with quaternary systems, are those on which experimental data exists. Little experimental data is available on quinary and higher-component systems.

Projection techniques for the graphical representation of quinary systems have been published by Perel'man^(15, 18) and in Chapter 4 of Cayron's book⁽¹⁴⁾. Phragman has also dealt with the perspective projection of quinary Al alloys on to a concentration tetrahedron⁽¹⁰⁾. The complexity of these projections methods makes one doubt whether sectioning techniques do not provide a better method of representation of the equilibria. The next section considers this topic.

Sectioning Methods

As previously noted no difficulty is experienced in representing the temperature - concentration diagrams of binary and ternary systems. For quaternary and higher-component systems some form of sectioning is required to allow a graphical representation of the system in two- or three-dimensions. Assuming isobaric conditions sections of phase diagrams are $(n - \alpha)$ -dimensional, where α is the number of external factors assumed constant in the given section of the n -component phase diagram.

In quaternary systems the application of one constraint to the system gives three-dimensional sections. If the temperature is assumed constant the isothermal section appears as a three-dimensional tetrahedron. A series of such tetrahedra relating to various temperatures provides a useful, if laborious, means for tracing the variation of the equilibria as a function of temperature⁽¹⁹⁾. F.N. Rhines has made extensive use of isothermal sections combined with an exploded representation of each phase region⁽²⁰⁾. Figure 13 is an example of an isothermal section at a temperature equal to the binary BD eutectic temperature. Liquid whose composition is represented on the surfaces 4-5-6 or 5-7-8 is in equilibrium with solid β or solid α whose compositions are represented by corresponding points on surfaces 1-2-3 and 9-10-11 respectively.

If a series of isothermal sections are projected on to the concentration tetrahedron a three-dimensional polythermal projection of the quaternary system is produced. Each triangular face represents a polythermal projection of the appropriate ternary system whilst the interior of the tetrahedron represents the polythermal projection of the quaternary system. Such projections are useful in tracing the course of freezing of quaternary alloys. However not many systems have been studied in sufficient experimental detail to allow this type of representation.

Another type of three-dimensional section is produced if, instead of assuming constant temperature, the content of one component is maintained constant. A section at a constant %B is a triangular plane acd parallel to the basal triangle ACD , figure 14. Temperature-concentration diagrams are drawn for each of the three ternary systems at the constant %B - sections ac for the system ABC , cd for BCD , and ad for ABD . From these the quaternary section at constant %B is produced. The method has been advocated by A. Schrader and M. Hanemann⁽²¹⁾. It provides information on the sequence of phase fields through which any quaternary alloy on the section acd passes through on cooling or heating. It does not indicate the compositions of coexisting phases since these lie outside the plane of the section.

If two constraints are applied to a quaternary system ($P = \text{constant}$) the resulting sections will be two-dimensional. Referring to figure 9, a section at a constant $\%UFe_2$ through an isothermal tetrahedron will be a triangle⁽¹²⁾. A similar result would obtain if an isothermal section were taken through the temperature-concentration diagram of figure 14. Alternatively one may take a section at a constant percentage of one component through a polythermal section of the quaternary system, to produce a polythermal representation of the equilibria. Examples are given in the paper by G. Petzow and F. Aldinger⁽²²⁾.

Finally two-dimensional sections are produced if two of the component concentrations are assumed constant. This is equivalent to sectioning the three-dimensional temperature-concentration diagram, figure 14, at a constant percentage of component A, B, or C. In experimental work it would be normal to determine two-dimensional sections at constant concentrations of two components. It is not necessary to assume this restriction since temperature-concentration sections can be produced for any line segment through a quaternary system. L.S. Palatnik and A.I. Landau⁽¹⁶⁾ have described a variety of methods for producing two-dimensional temperature-concentration sections of multicomponent systems. These have been summarised in a review by the author⁽²³⁾.

The combinatorial method of number chains relies on the description of the indices of the individual hypervolumes intersected by a one-dimensional concentration axis passing through a polythermal projection of the n -component system. As a simple example consider the polythermal projection of a ternary eutectic system. It is required to construct the temperature-concentration section ab , figure 15. The components are denoted 1,2,3; binary eutectics as 12, 13, 23; the ternary eutectic as 123 or E; the liquid phase as 0. The section ab intersects the projected areas (1)(12)(123), (1)(13)(123), (3)(13)(123) and (3)(23)(123). The sequence of indices produced is called a numerical chain. It provides a representation of the phase composition and the sequence of phase regions in the required section. To construct the section a table of phase compositions must be produced from the numerical chain. The first area cut by the section ab is tabulated in full. Each succeeding area is tabulated only insofar as the one number which distinguishes it from the preceding area. The last area cut by the section ab is tabulated in full. This gives a table of phase compositions of the form:

1	3	3
12	13	23
123		123

The numeral 0, representing the liquid phase, is added to all indices and those indices underlined by which an area differs from its preceding area:

01	<u>03</u>	03
012	<u>013</u>	<u>023</u>
0123		0123

A lattice is constructed to represent the number of columns and rows in the table. All underlined indices are denoted by a point on the lattice:

01		03	03
012	<u>013</u>		<u>023</u>
0123			0123

The points are now joined together so that they conform to the rule of adjoining phase regions and the cross rule. The rule of adjoining phase regions states that the dimension of the phase diagram or regular section, R , is related to the dimension of the boundary between neighbouring phase regions, R_1 , by the relation:

$$R_1 = R - D^- - D^+$$

where D^- and D^+ represent, respectively, the number of phases that disappear and the number of phases that appear in a transition from one phase region to the other. The cross rule concerns the phase distribution in the four phase regions meeting at a point in a two-dimensional phase diagram or regular section. Of the four phase regions one will have the minimum number of phases; neighbouring phase regions will each have an additional phase; the fourth phase region is joined to the phase region with the minimum number of phases through the central point and it contains the maximum number of phases, figure 16. Inspection will show that the rule of adjoining phase regions is obeyed for all transitions from one phase region to another in figure 16.

We can now complete the construction of the temperature-concentration section ab of figure 15. This leads to the

01		<u>03</u>	03
012	<u>013</u>		<u>023</u>
0123			0123

well-known section illustrated in figure 17. The area 0123 represents the coexistence of the liquid phase with the three components. It is the invariant ternary eutectic. When all liquid is consumed all alloys would be represented by the index 123.

The utility of the combinatorial method of numerical chains for constructing two-dimensional sections is only evident when quaternary and higher-component systems are considered. An alternative method proposed by A.I. Landau, the shadow method, involves casting a shadow of the concentration axis of the required two-dimensional section on to the coordinate simplex of the system. In quaternary eutectic systems it is assumed that a light is placed at the quaternary eutectic point in the concentration tetrahedron and that the light casts a shadow of the concentration axis on to the side faces of the tetrahedron. The concentration axis passes through individual volumes in the three-dimensional polythermal projection of the quaternary system and its shadow passes through the corresponding areas on the side faces of the projection in the same sequence. For simplicity the concentration tetrahedron is unfolded about its base triangle into four planar

triangles, figure 18. The shadow of the concentration axis ab lays in areas that produce the numerical chain (1)(12)(124), (1)(12)(123), (1)(13)(123), (3)(13)(123), (3)(23)(123), (3)(23)(234). The corresponding table of compositions is therefore:

01		<u>03</u>		<u>03</u>
012		<u>013</u>	<u>023</u>	<u>023</u>
0124	<u>0123</u>			<u>0234</u>

The corresponding phase diagrams of section ab is illustrated in figure 19.

Reciprocal Systems

Reciprocal systems involve double decomposition reactions of the type $AB + CD \rightleftharpoons AD + CB$. Such systems are met when dealing with salt systems such as $KF + NaCl \rightleftharpoons KCl + NaF$. The system is ternary since all compositions can be expressed in terms of any three of the compounds (components), i.e. in terms of NaCl, KCl, and NaF since $KF = KCl + NaF - NaCl$. By appropriate choice of components it is possible to express any composition in terms of positive percentages of three-components. Figure 20 illustrates the graphical representation of a reciprocal system. Two triangles are placed together to form a square. The composition X is a ternary eutectic mixture of KCl + KF + NaF. If it is assumed that the side of the square is equal to 100% of the three components, $aX = \% KCl$, $bX = \% NaF$ and $cX = \% KF$. The composition Y is similarly derived as $fY = \% KCl$, $ey = \% NaF$ and $hY = \% NaCl$. Alternatively Y can be referred to the three components outside the triangle in which it is placed. In figure 20 Y would then have a composition $dY = \% KCl$, $gY = \% NaF$ and $hY = -\% KF$. The negative sign for the $\% KF$ indicates that this component does not enter the phase composition of Y in reality. It also ensures that the total $\%$ of the three components adds to 100% since $dY + gY - hY = dY + gh = de$. Ricci⁽¹⁷⁾ gives an extensive treatment of reciprocal systems to which those interested in pursuing the topic are recommended.

Systems with Variable Valency of a Component

Probably the most important system to consider is the Fe-O system. Figure 21a gives the phase stability diagram in relation to the temperature and partial pressure of the oxygen. As its name implies this diagram indicates the ranges of temperature and P_{O_2} under which condensed phases are stable. Within the magnetite field the Phase Rule indicates that the temperature and P_{O_2} are independent variables. ($P + F = C + 2$. $F = 2 + 2 - 2 = 2$). There are two degrees of freedom since two phases are involved - the magnetite and the gas phase. The boundary curves, such as that between magnetite and wustite represent conditions for the coexistence of these phases - magnetite, wustite and the gas phase - implying a monovariant equilibrium. A particular temperature is associated with a fixed P_{O_2} .

If we choose to maintain a large gas reservoir at $P_{O_2} = 10^{-8}$ atmospheres and slowly heat a sample of hematite in this reservoir the phase stability diagram indicates the temperature ranges over which the condensed phases are stable. Hematite is stable to point 1; at this

temperature it is in equilibrium with magnetite; from 1 to 3 magnetite is stable etc. The drawback to this method of representation is that the compositions of the condensed phases are not shown. To overcome this objection one may represent the Fe-O phase diagram as a normal-temperature concentration diagram but with a series of curves showing identical values of partial pressures of oxygen in the gas phase in equilibrium with the condensed phases. In figure 21b one such curve is drawn at $P_{O_2} = 10^{-8}$ atmospheres. If the sample of hematite is slowly heated in an atmosphere with $P_{O_2} = 10^{-8}$ atmospheres, the hematite will remain unchanged until 875°C is reached. At this temperature hematite of composition 1 is in equilibrium with magnetite of composition 2 in accordance with the reaction $3Fe_2O_3 = 2Fe_3O_4 + \frac{1}{2}O_2$. Increase of temperature involves the completion of the reaction with disappearance of the hematite phase. With increasing temperature the oxide composition changes slightly across the magnetite field, 2-3, until at 1275°C magnetite of composition 3 is in equilibrium with wustite of composition 4 in accordance with the reaction $Fe_3O_4 = 3FeO + \frac{1}{2}O_2$. Subsequently the oxide is converted wholly to wustite whose composition then changes along the curve 4-5. At 1400°C solid wustite, 5, is equilibrated with liquid oxide, 6. Further increase in temperature moves the liquid composition to saturation with Fe at 1635°C at point 7. At 1635°C liquid oxide is in equilibrium with O_2 -saturated liquid Fe according to the reaction $FeO(\text{liquid}) = Fe(\text{liquid}) + \frac{1}{2}O_2$. Beyond 1635°C the liquid oxide phase disappears and the liquid Fe is reduced in dissolved oxygen content.

The relation between the two representations are indicated in figure 21 by dotted lines at the invariant reaction temperatures.

A.D. Pelton and H. Schmalzried⁽²⁴⁾ have considered the generalised geometrical representation of phase diagrams, particularly with the aim of optimising thermodynamic information for multicomponent systems in two-dimensional diagrams. Three types of phase diagrams were studied:

1. diagrams whose coordinate framework consisted of two thermodynamic functions. Temperature, pressure, and chemical potential are the defined thermodynamic functions. Such diagrams would include T-log P_{O_2} diagram, figure 21a, T-P diagrams, and the log PCl_2 -log P_{O_2} diagram for the U-O-Cl system⁽²⁵⁾
2. diagrams whose coordinate framework consists of one thermodynamic function and a ratio of conjugate extensive variables. Typical of such diagrams are plots of $T - X_O/X_{Fe} + X_O$, figure 21b, and plots of $\log P_{O_2} - X_{Cr}/X_{Fe} + X_{Cr}$ for an isotherm of the Fe-Cr-O system
3. diagrams whose coordinate framework consists of two ratios of conjugate extensive variables. In the Fe-Cr-O system an isotherm could be plotted with coordinates $X_O/X_{Fe} + X_{Cr} - X_{Cr}/X_{Fe} + X_{Cr}$ ⁽²⁴⁾.

Analytical Representation of Phase Equilibria

The complexity of most quaternary and higher-component systems makes their graphical representation a difficult task for all concerned. For this reason increasing interest is being taken in analytical methods for representing phase equilibria. O.S. Ivanov⁽²⁶⁾ has considered this technique using the polythermal projection of the Al-Mg-Zn system to illustrate the applicability of the approach. It was found that quadratic

equations of the form

$$T = k_0 + k_1 a + k_2 b + k_3 a^2 + k_4 ab + k_5 b^2$$

(T = liquidus temperature; a = Al content in weight %; b = Mg content in weight %)

were adequate to describe the liquidus surface in this ternary. Expressions for the monovariant curves could be derived by appropriate computer programming and indeed the computer could be used, with peripheral devices, to construct projections and sections and to generate the space model of the ternary system.

N.N. Sobolev and colleagues have considered the analytical representation of the solidus surface of the Mo-Nb-Ti-V quaternary system⁽²⁷⁾. They used the method of simplex lattice designs, devised by H. Scheffé⁽²⁸⁾ to investigate the properties of multicomponent systems as a function of composition and extended by J.W. Gorman and J.E. Hinman⁽²⁹⁾. The basis of this method is the selection of compositions on a lattice arrangement and determination of some corresponding property at each composition. In the present case solidus temperatures were determined for each alloy composition on the lattice. The solidus surface, or hypersurface for the Mo-Nb-Ti-V system, is then represented by a polynomial equation relating the solidus temperature to composition. Coefficients in the polynomial are functions of the measured temperature at the lattice points.

To obtain a uniform distribution of alloy compositions in the quaternary system a quadratic, cubic, or quartic lattice is selected, figure 22. The proportion of any component in the quadratic lattice is either 0, $\frac{1}{2}$, or 1 since each edge of the concentration simplex has one lattice point at its centre. Similarly the proportion of any component in the cubic and quartic lattices are 0, $\frac{1}{3}$, $\frac{2}{3}$, 1 and 0, $\frac{1}{4}$, $\frac{1}{2}$, $\frac{3}{4}$, 1 respectively.

The polynomials relating the solidus temperature, t , to the alloy composition ($x_1 + x_2 + x_3 + x_4 = 1$) are:-

quadratic model

$$t = \sum_{1 \leq i \leq 4} \beta_i x_i + \sum_{1 \leq i < j \leq 4} \beta_{ij} x_i x_j$$

cubic model

$$t = \sum_{1 \leq i \leq 4} \beta_i x_i + \sum_{1 \leq i < j \leq 4} \beta_{ij} x_i x_j + \sum_{1 \leq i < j \leq 4} \gamma_{ij} x_i x_j (x_i - x_j) + \sum_{1 \leq i < j < k \leq 4} \beta_{ijk} x_i x_j x_k$$

quartic model

$$\begin{aligned}
 t = & \sum_{1 \leq i \leq 4} \beta_i x_i + \sum_{1 \leq i < j \leq 4} \beta_{ij} x_i x_j + \sum_{1 \leq i < j \leq 4} \gamma_{ij} x_i x_j (x_i - x_j) \\
 & + \sum_{1 \leq i < j \leq 4} \delta_{ij} x_i x_j (x_i - x_j)^2 + \sum_{1 \leq i < j < k \leq 4} \beta_{iijk} x_i^2 x_j x_k \\
 & + \sum_{1 \leq i < j < k \leq 4} \beta_{ijjk} x_i x_j^2 x_k + \sum_{1 \leq i < j < k \leq 4} \beta_{ijkk} x_i x_j x_k^2 \\
 & + \sum_{1 \leq i < j < k < l \leq 4} \beta_{ijkl} x_i x_j x_k x_l
 \end{aligned}$$

The coefficients in the polynomials are functions of the experimentally determined solidus temperatures at the lattice compositions selected in the model used. In Scheffé's nomenclature the solidus temperature of a pure component, i , is denoted by t_i ; the solidus temperature of a binary alloy containing $\frac{1}{2} i$ and $\frac{1}{2} j$ is denoted by t_{ij} where i and j are integers and $i < j$. Designating the components as 1, 2, 3 and 4 a 50:50 alloy of components 1 and 2 would have a solidus temperature t_{12} . The number of distinct numbers in the subscript indicates how many components are involved in the alloy, and the number of times a specific number appears indicates the relative proportions of the components. A binary alloy with $\frac{2}{4} x_1$ and $\frac{1}{4} x_4$ would have a solidus temperature designated as t_{1114} ; a ternary alloy with $\frac{1}{4} x_2$, $\frac{1}{2} x_3$, $\frac{1}{4} x_4$ would have a solidus temperature designated as t_{2334} . Figure 23 illustrates the nomenclature for the solidus temperatures of the 35 alloys in the quartic model of a quaternary system. If the solidus temperatures of these 35 alloys are determined experimentally the coefficients in the fourth-order polynomial can be calculated (see Appendix). It will be noted that all the coefficients are functions of the experimentally determined solidus temperatures.

Having determined the coefficients it remains to test the particular model used for the system under study. The fourth-order polynomial for a quaternary system has 35 coefficients, the same as the number of alloy lattice points. The polynomial will exactly match the value of temperature for each alloy. To test the model additional alloy compositions are necessary. A number of arbitrary alloys, whose compositions do not coincide with the regular lattice of compositions, are checked for solidus temperature and these experimental results are compared with those calculated from the polynomial. If the t -test as used in statistics indicates no significance in the difference between experimental and calculated results the model is acceptable. Sobolev and co-workers fitted their data for 35 alloys in the Mo-Nb-Ti-V system, only one alloy of which was a quaternary, to a fourth-order polynomial. Ten arbitrary alloys were used as a check on the applicability of the model with the calculated coefficients. Of these, three were quaternary alloys. The differences in solidus temperatures were negligible for two;

the third alloy was quoted as having an experimentally determined solidus of 1930°C as against the calculated value of 1980°C. This latter alloy was included in a section of the quaternary system studied by R.S. Polyakova⁽³⁰⁾ whose value of 2000°C for the solidus is close to the calculated value.

The difficulty with this method of representation is the need to decide which model is appropriate to the system under consideration. The simplest model, involving a quadratic model, requires only 10 experimental alloys to be examined in order to derive the coefficients of the polynomials for a quaternary system. As the complexity of the model increases or as the number of components in the system increases so does the number of experimental observations increase. This point is illustrated in the table below.

	MODEL		
	Quadratic	Cubic	Quartic
Quaternary	10	20	35
Quinary	15	35	70
Senary	21	56	126

The Mo-Nb-Ti-V system is a simple system in that the constituent binaries and ternaries all show complete solid solution series. Complicated hypersurfaces for the solidus are not anticipated. As Sobolev and his co-workers have shown it is feasible to produce an analytical expression for the solidus surface in this quaternary system which accords well with limited experimental data. The equation of the solidus surface can then be used to compute sections of the quaternary system. Sections at constant % Ti are given in the original paper.

Experimental data on phase equilibria could well be stored in the memory of a computer. With sufficient data and suitable programmes the computer could be used to produce analytical representations of phase boundaries. Three-dimensional diagrams and two-dimensional sections or projections could be computed and presented in graphical or tabular form. This extension of the traditional techniques for graphical representation of phase equilibrium data will mainly apply to multicomponent systems, in particular to the more complex quaternary systems and to all higher-order systems when experimental data begins to accumulate.

References

1. F. Rudberg, K. Svenska Vet. Akad. Handl., 1829, 157; Pogg. Ann., 1830, 18, 240
2. A. Prince, Annals Sci., 1955, 11, (1), 58
3. A. Ya. Kupfer, Ann. chim. phys., 1829, 40, 285
4. N.S. Kurnakov, "Collected Works", Vol. 1, 1961, Moscow (Acad. Sci. U.S.S.R.)
5. H.W.B. Roozeboom, Z. physikal. Chem., 1894, 15, 145
6. W. Hume-Rothery, G.W. Mabbott, and K.M. Channel-Evans, Phil. Trans. Roy. Soc., 1934, (A), 233, 1
7. T.B. Massalski and J.H. Perepezko, Z. Metallkunde, 1973, 64, 176
8. C.T. Sims, J. Metals, 1966, 18, (10), 1119
9. C.S. Barrett, J. Inst. Metals, 1972, 100, 65
10. G. Phragmen, J. Inst. Metals, 1950, 77, 489
11. L.F. Mondolfo, "Aluminium Alloys : Structure and Properties", Butterworths, London, 1976
12. G. Petzow and A.O. Sampaio, Z. Metallkunde, 1966, 57, 625
13. F.A.H. Schreinemakers, Z. physikal. Chem., 1909, 65, 553
14. R. Cayron, "Etude Theorique des Diagrammes D'Equilibre dans les Systemes Quaternaires", Institut de Metallurgie, Louvain, 1960
15. F.M. Perel'man, "Phase Diagrams of Multicomponent Systems. Geometric Methods", Consultants Bureau, New York, 1966
16. L.S. Palatnik and A.I. Landau, "Phase Equilibria in Multicomponent Systems", Holt, Rinehart and Winston Inc., New York, 1964
17. J.E. Ricci, "The Phase Rule and Heterogeneous Equilibrium", Chapter 16, D. Van Nostrand Co., New York, 1951 ; Dover Publications Inc., New York, 1966
18. F.M. Perel'man, "Methods for the Representation of Multicomponent Systems. Five-Component Systems", Moscow, Acad. Sci. U.S.S.R., 1959
19. A. Prince, "Alloy Phase Equilibria", Chapter 15, Elsevier, 1966
20. F.N. Rhines, "Phase Diagrams in Metallurgy", McGraw-Hill, New York, 1956

21. A. Schrader and M. Hanemann, Z. Metallkunde, 1945, 35, 185
22. G. Petzow and F. Aldinger, Z. Metallkunde, 1968, 59, 145
23. A. Prince, Metallurgical Rev., 1963, 8, (30), 213
24. A.D. Pelton and H. Schmalzried, Metall. Trans., 1973, 4, 1395
25. O. Knacke, "Metallurgic l Chemistry", Proc. Symposium N.P.L./Brunel Univ., July 1971, H.M.S.O. (London), 1972, p. 549
26. O.S. Ivanov, Izvest. Akad. Nank SSSR., Metally, 1969, (1), 204
27. N.N. Sobolev, V.I. Levanov, O.P. Eliutin and V.S. Mikheev, Izvest. Akad. Nauk SSSR., Metally, 1974, (2), 217
28. H. Scheffé, J. Roy. Statistical Soc., 1958, 20B, 344
29. J.W. Gorman and J.E. Hinman, Technometrics, 1962, 4, 463
30. R.S. Polyakova, Izvest. Akad. Nank SSSR., Metally, 1970, 3, 199

APPENDIX

Solutions for the coefficients in the fourth-order polynomial

$$\beta_i = t_i$$

$$\beta_{ij} = 4t_{ij} - 2t_i - 2t_j$$

$$\gamma_{ij} = \frac{8}{3} (-t_i + t_j + 2t_{iiij} - 2t_{ijjj})$$

$$\delta_{ij} = \frac{8}{3} (-t_i - t_j + 4t_{iiij} + 4t_{ijjj} - 6t_{ij})$$

$$\begin{aligned} \beta_{iijk} &= 32 (3t_{iijk} - t_{ijjk} - t_{ijkk}) + \frac{8}{3} (6t_i - t_j - t_k) \\ &\quad - 16 (t_{ij} + t_{ik}) - \frac{16}{3} (5t_{iiij} + 5t_{iiik} - 3t_{ijjj} - 3t_{ikkk} \\ &\quad - t_{jjjk} - t_{jkkk}) \end{aligned}$$

$$\begin{aligned} \beta_{ijjk} &= 32 (3t_{ijjk} - t_{iijk} - t_{ijkk}) + \frac{8}{3} (6t_j - t_i - t_k) \\ &\quad - 16 (t_{ij} + t_{jk}) - \frac{16}{3} (5t_{ijjj} + 5t_{jjjk} - 3t_{iiij} - 3t_{jkkk} \\ &\quad - t_{iiik} - t_{ikkk}) \end{aligned}$$

$$\begin{aligned} \beta_{ijkk} &= 32 (3t_{ijkk} - t_{iijk} - t_{ijjk}) + \frac{8}{3} (6t_k - t_i - t_j) \\ &\quad - 16 (t_{ik} + t_{jk}) - \frac{16}{3} (5t_{ikkk} + 5t_{jkkk} - 3t_{iiik} - 3t_{jjjk} \\ &\quad - t_{iiij} - t_{ijjj}) \end{aligned}$$

$$\begin{aligned}
\beta_{ijkl} = & 256_{ijkl} - 32(t_{iijk} + t_{iijl} + t_{iikl} + t_{ijjk} \\
& + t_{ijjl} + t_{jjkl} + t_{ijkk} + t_{ikk1} + t_{jkk1} + t_{ijl1} \\
& + t_{jkl1} + t_{ikl1}) + \frac{32}{3}(t_{iiij} + t_{iiik} + t_{iiil} \\
& + t_{ijjj} + t_{jjjk} + t_{jjj1} + t_{ikkk} + t_{jkkk} + t_{kkk1} \\
& + t_{i111} + t_{j111} + t_{k111}).
\end{aligned}$$

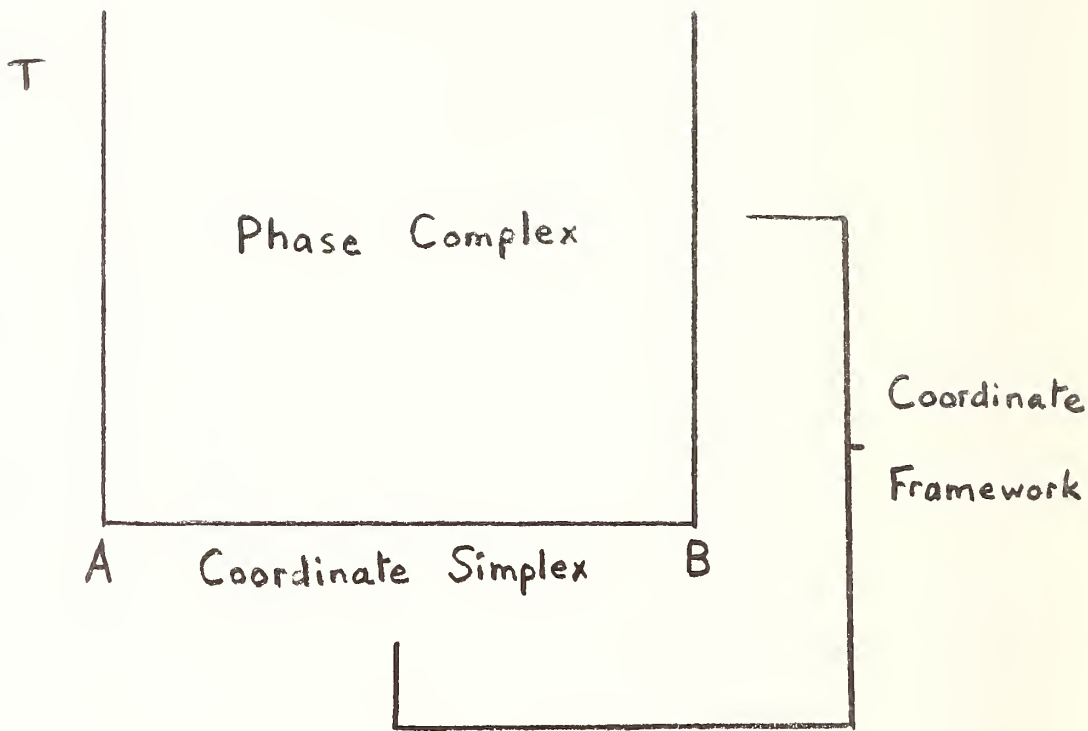


FIGURE 1. BINARY PHASE DIAGRAM WITH T-X
COORDINATE FRAMEWORK

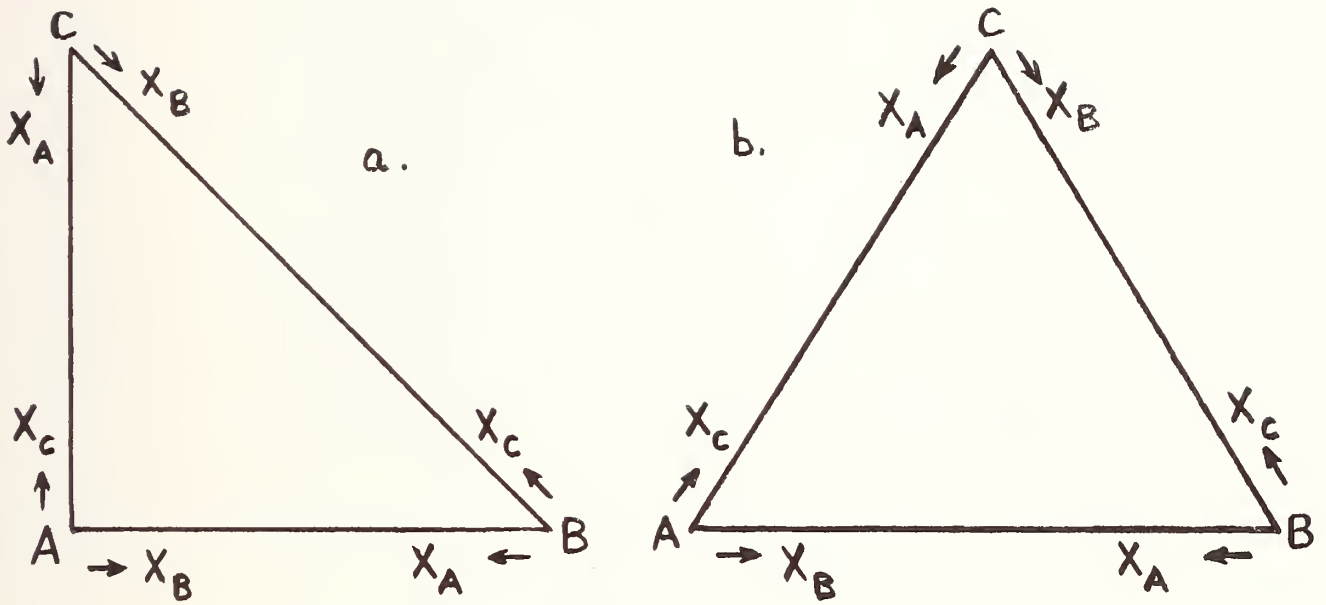


FIGURE 2. a) Ternary System Concentration Diagram
 b) The Gibbs Triangle

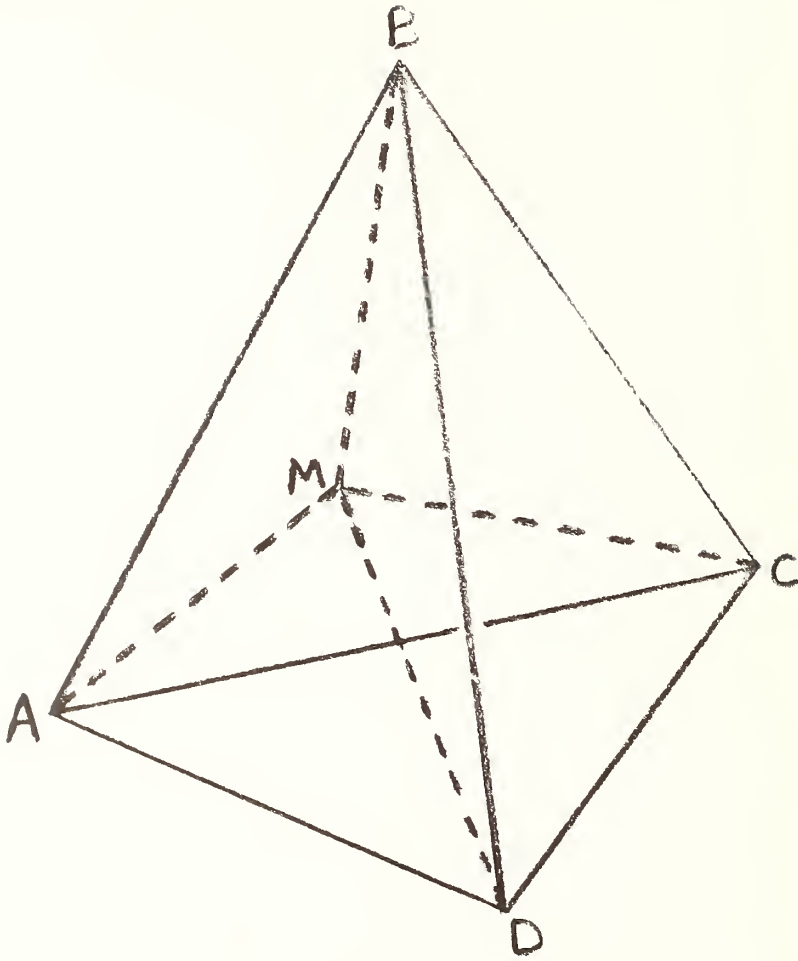


FIGURE 3. Quaternary System Concentration Diagram

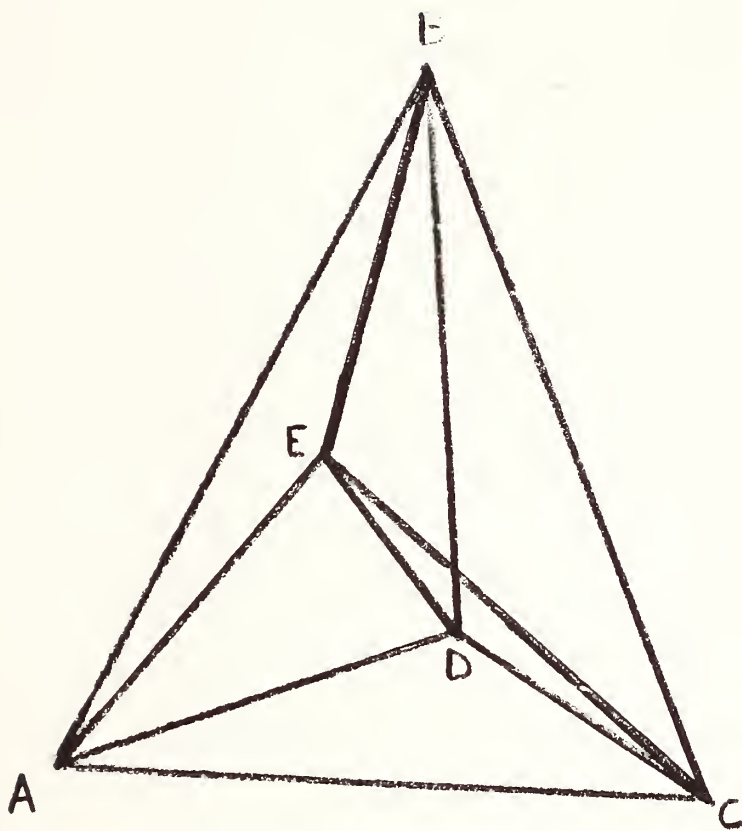


FIGURE 4. Three-dimensional projection of a Quinary System Concentration Diagram

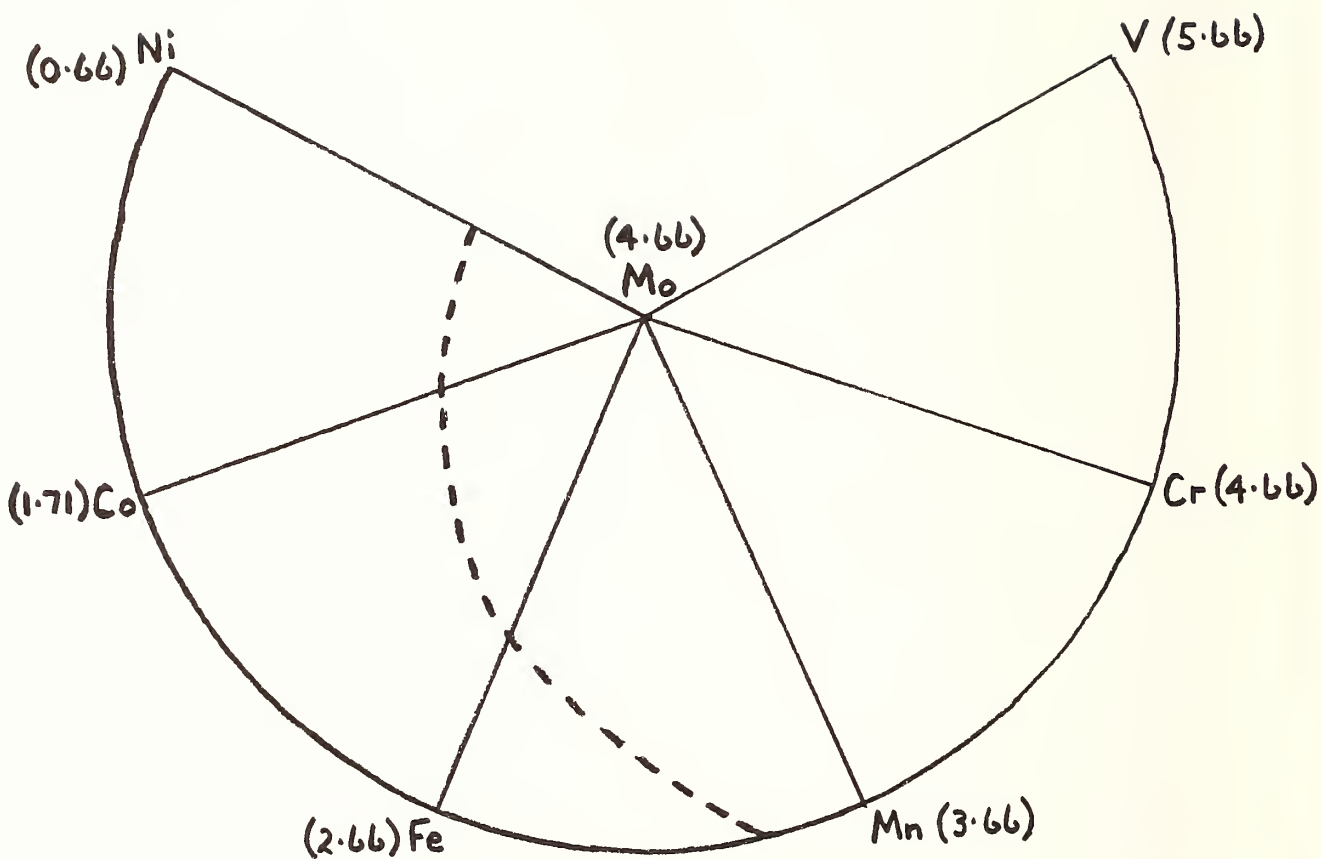


FIGURE 5. Polar Diagram for Mo Alloys
 (--- $N_v = 3.5$)

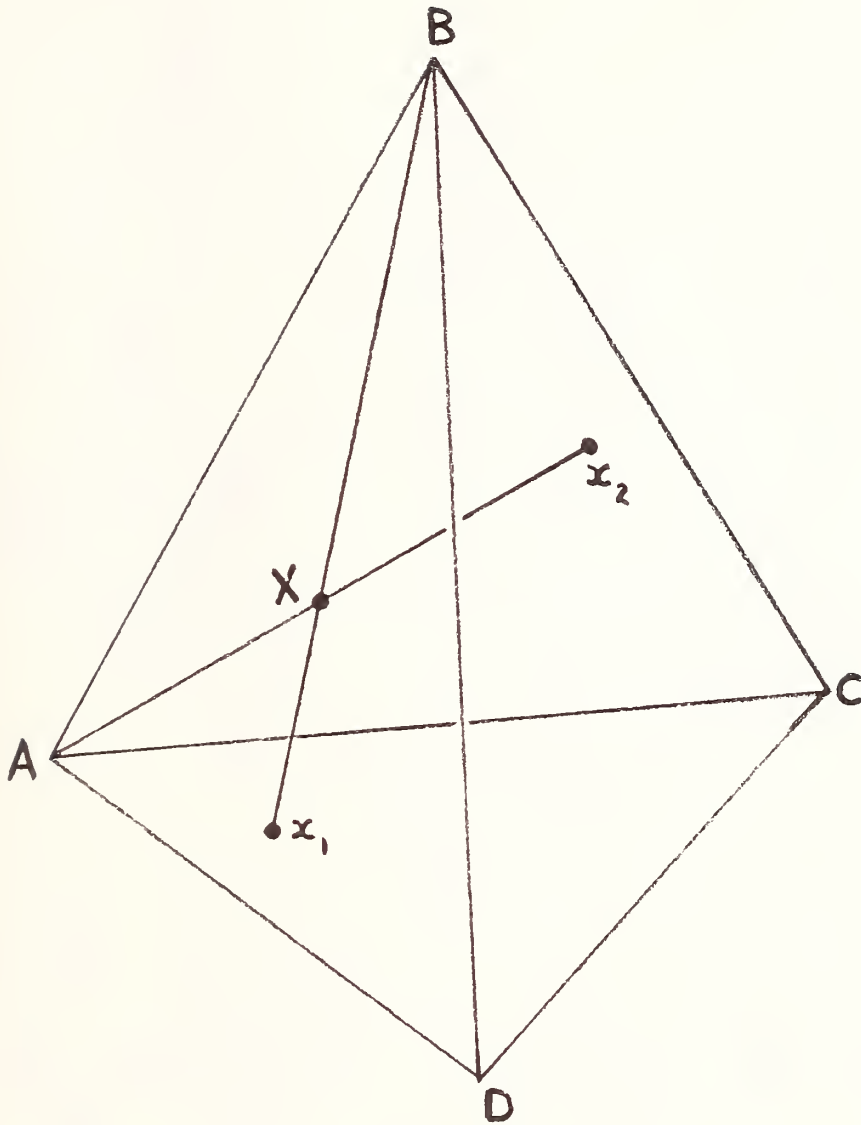


FIGURE 6. Perspective Projection of Quaternary Alloy X

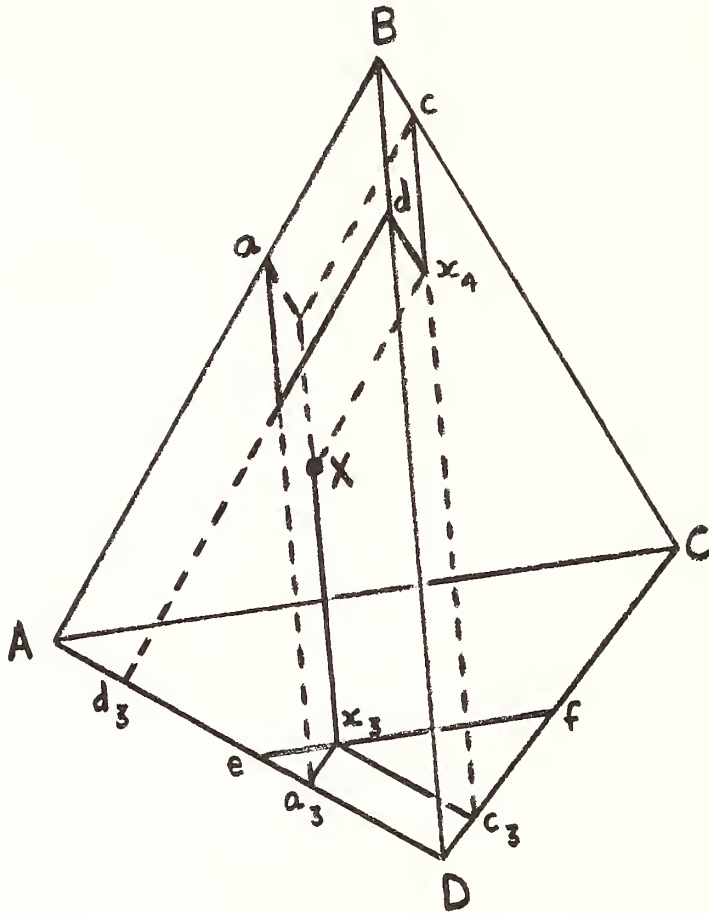


FIGURE 7. Parallel Projection of Quaternary Alloy X

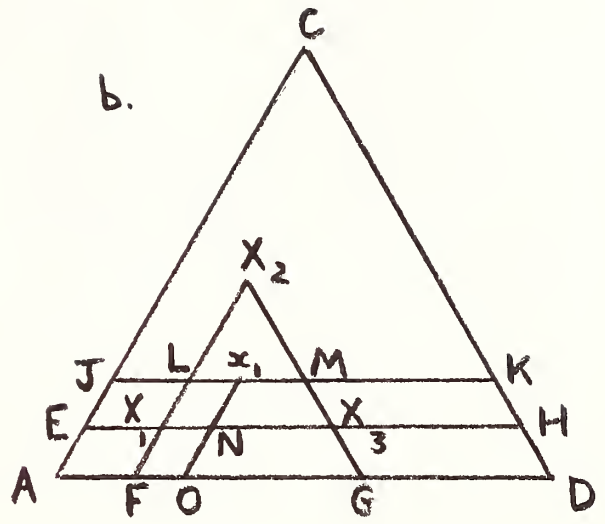
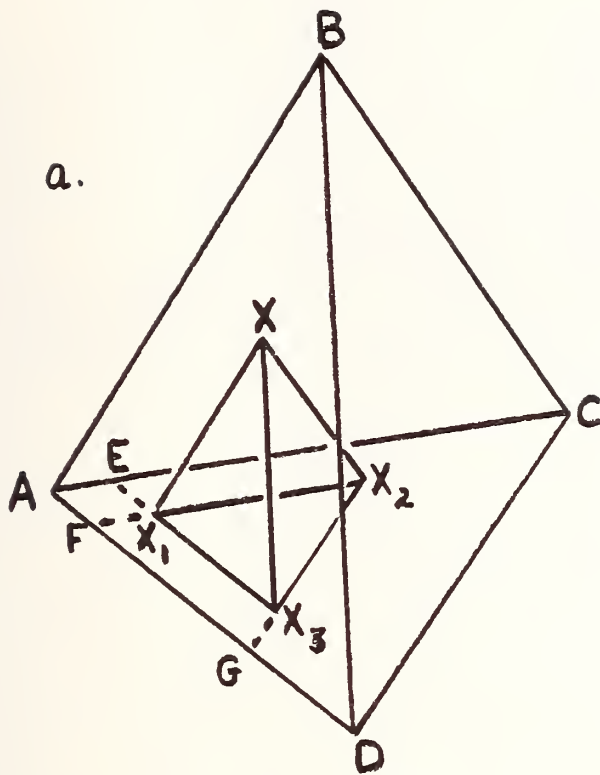


FIGURE 8. Orthogonal Parallel Projection of Quaternary Alloy X

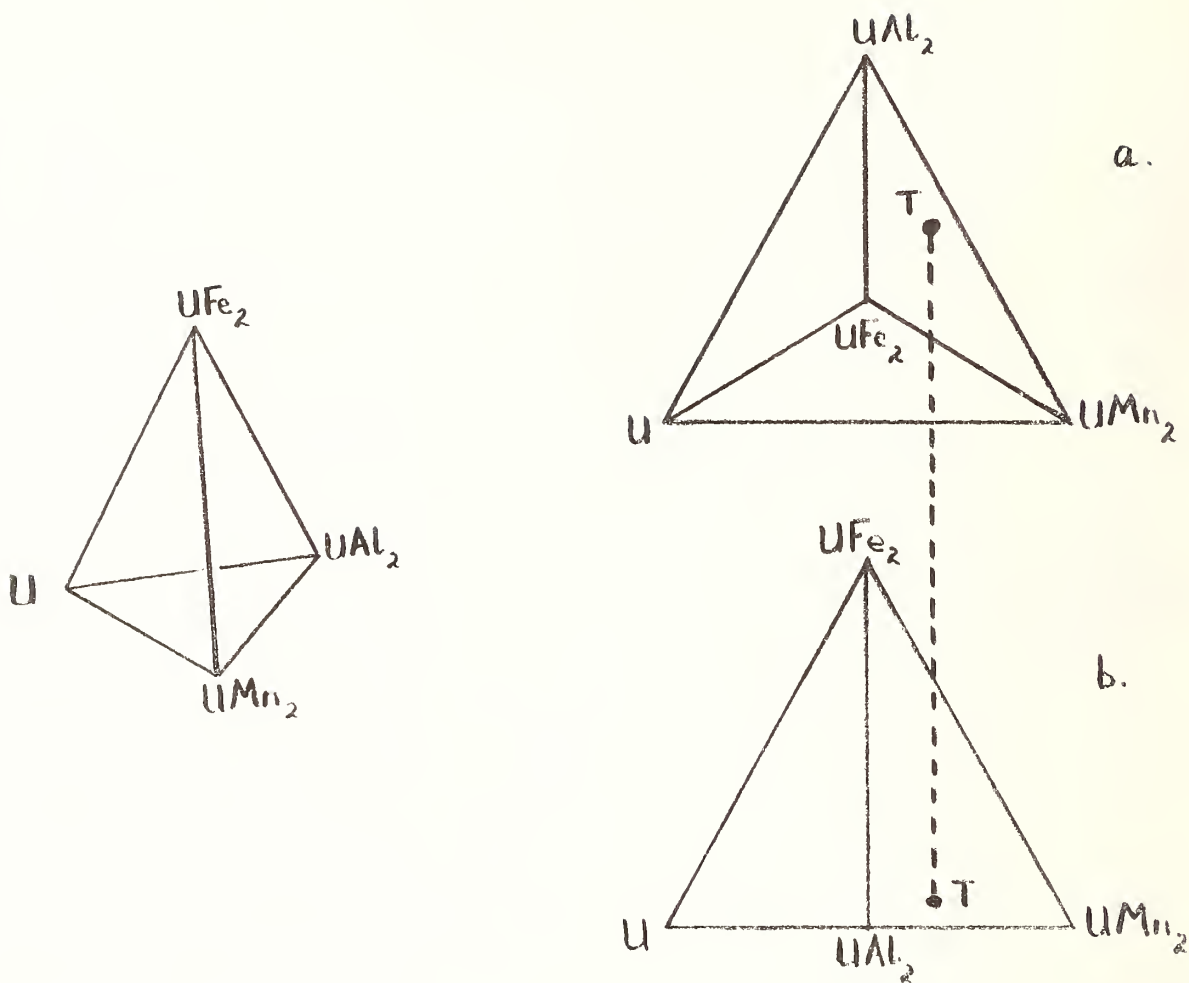


FIGURE 9. Projection of the U-UMn₂-UAl₂-UF_e₂ System

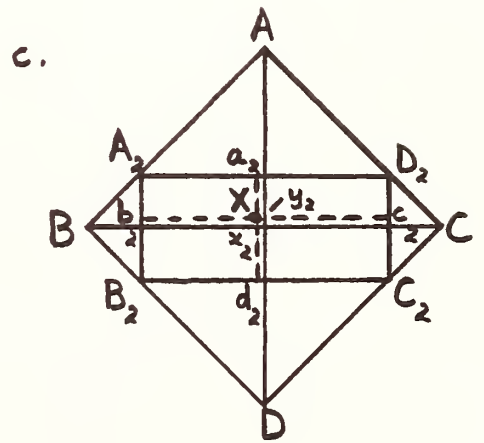
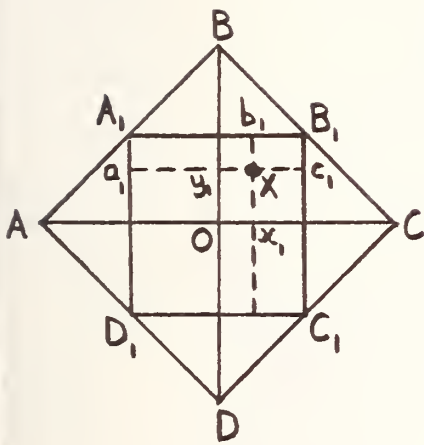
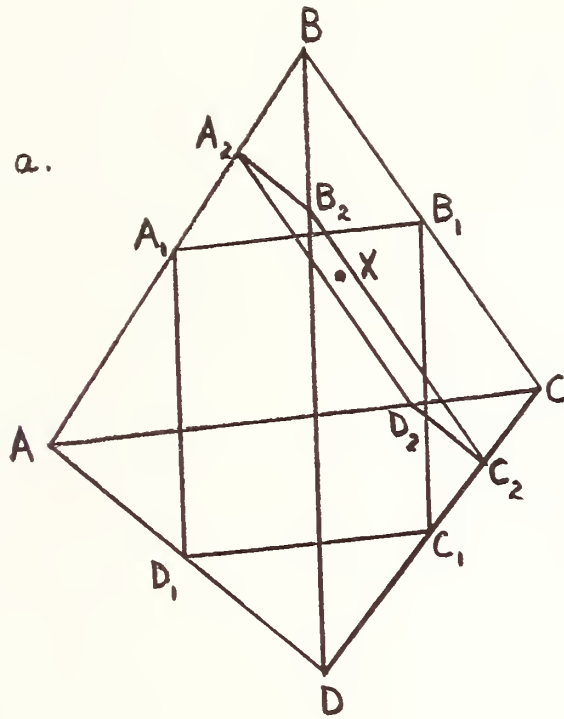
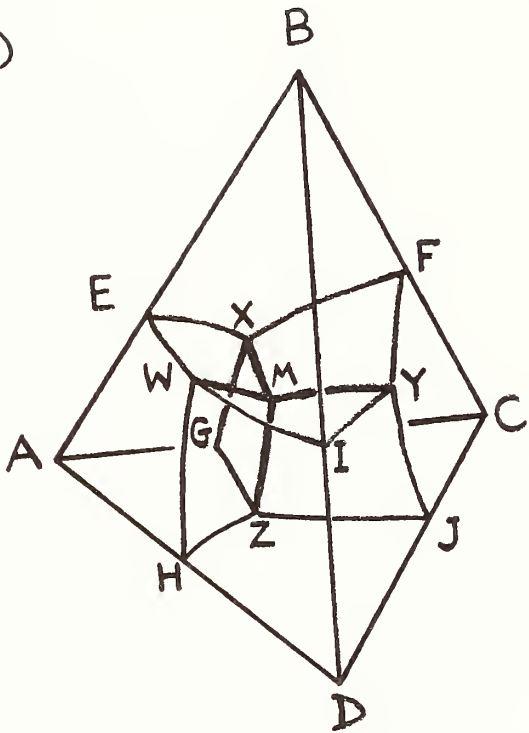
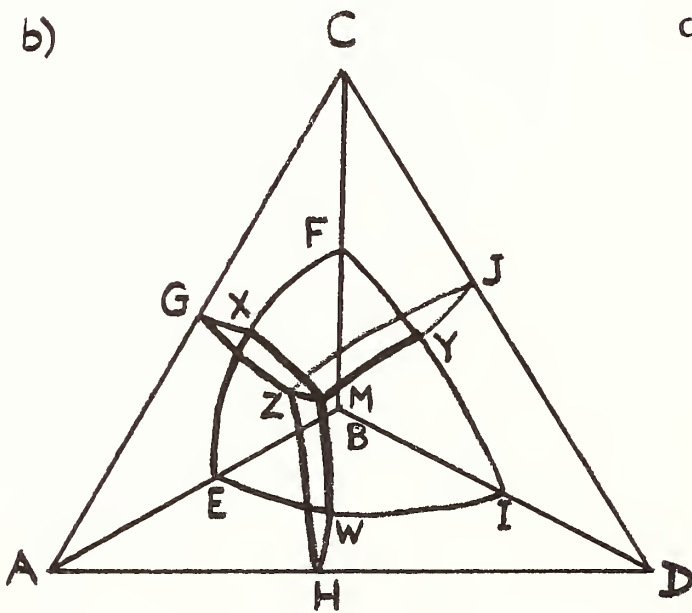


FIGURE 10. Square Orthogonal Projection of Quaternary Alloy X

a)



b)



c)

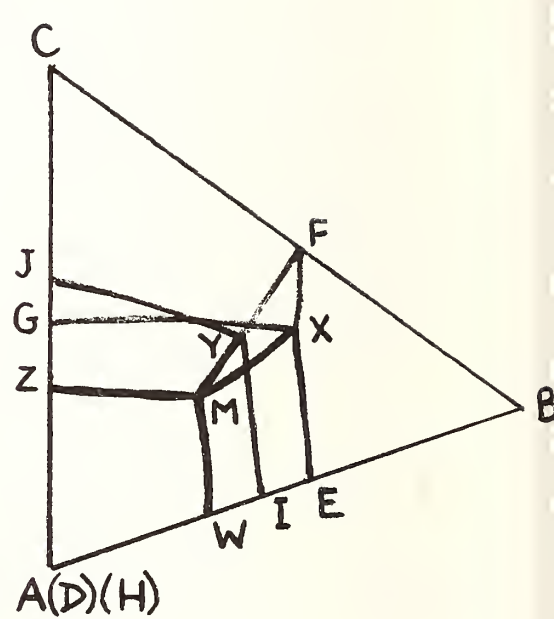


FIGURE 11 CAYRON ORTHOGONAL PROJECTION OF A SIMPLE QUATERNARY EUTECTIC SYSTEM

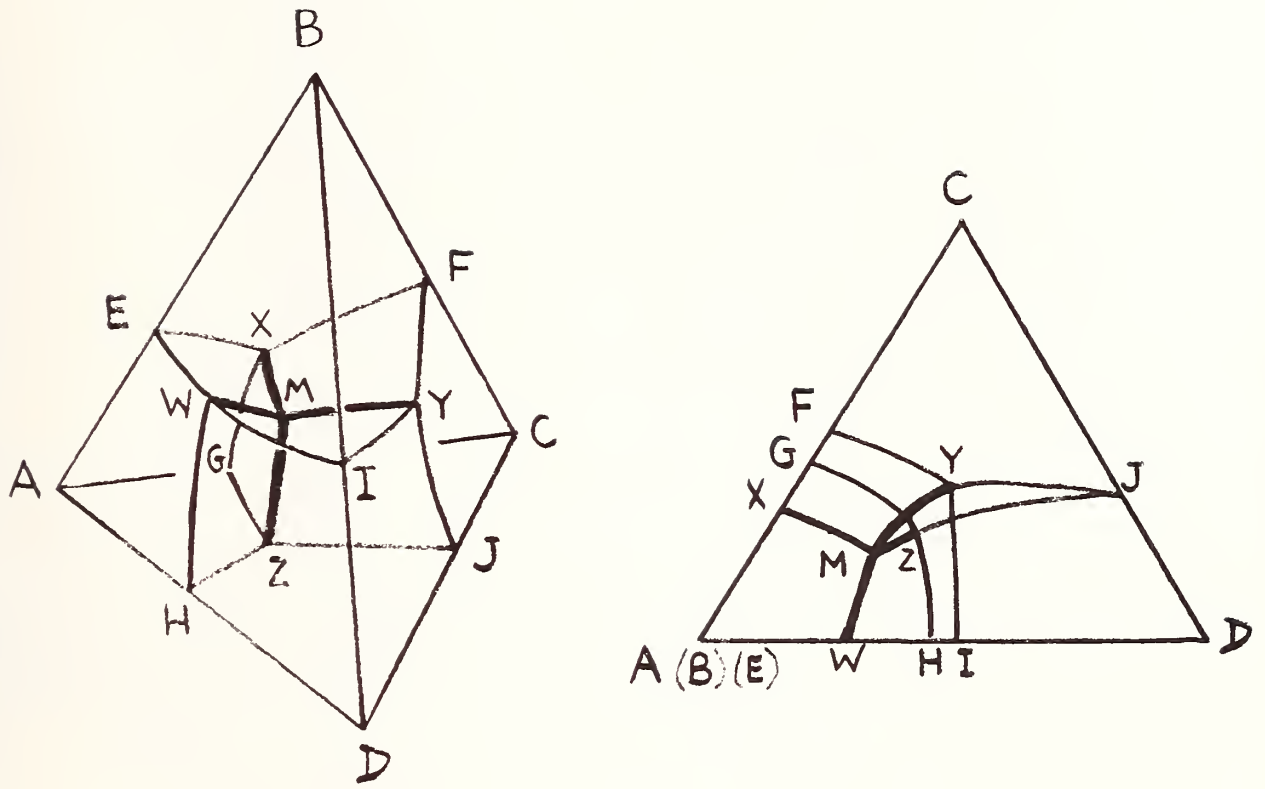


FIGURE 12. PEREL'MAN OPTIMAL PROJECTION OF A SIMPLE QUATERNARY SYSTEM.

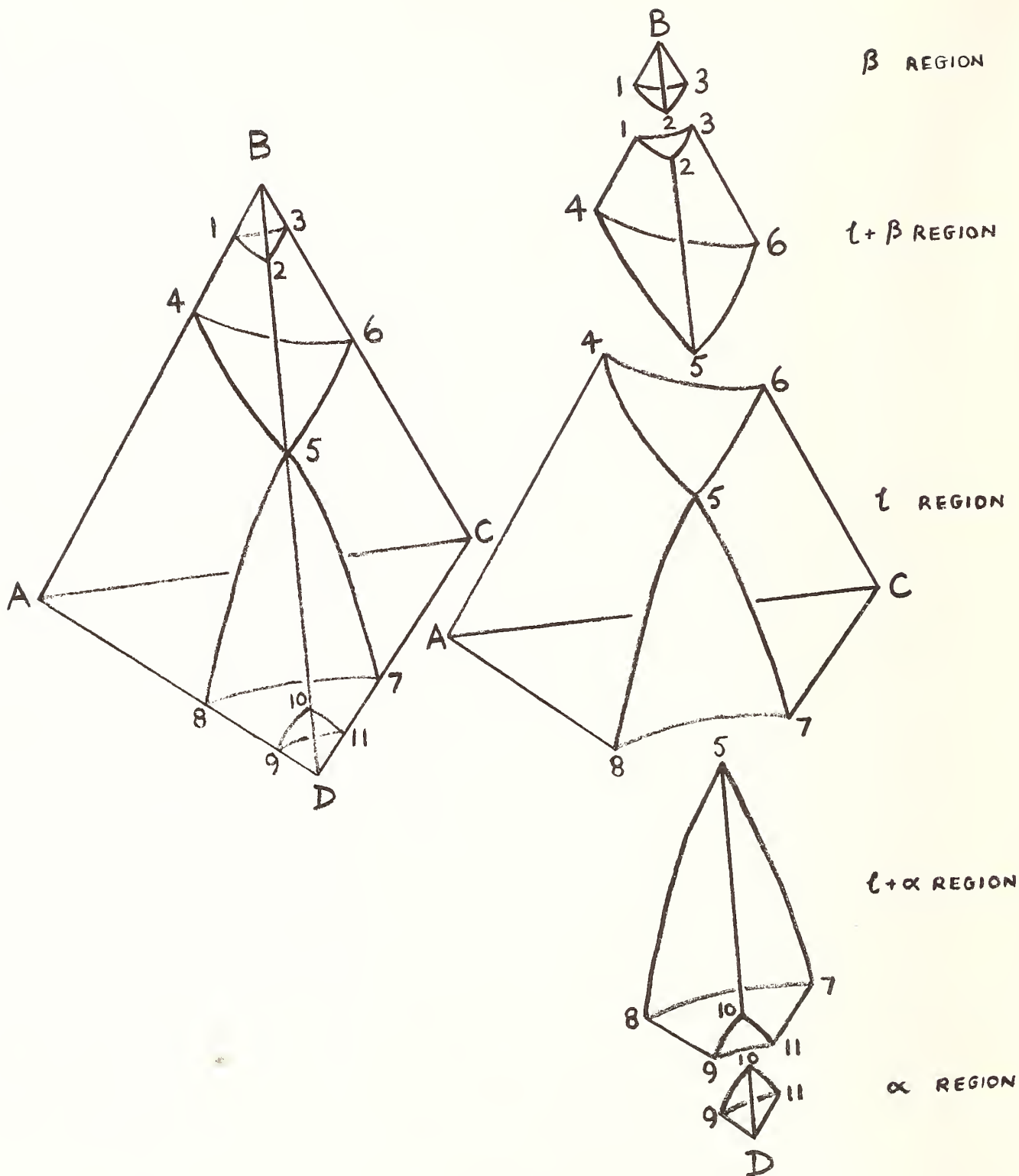


FIGURE 13. ISOTHERMAL SECTION WITH EXPLODED MODEL OF PHASE REGIONS.

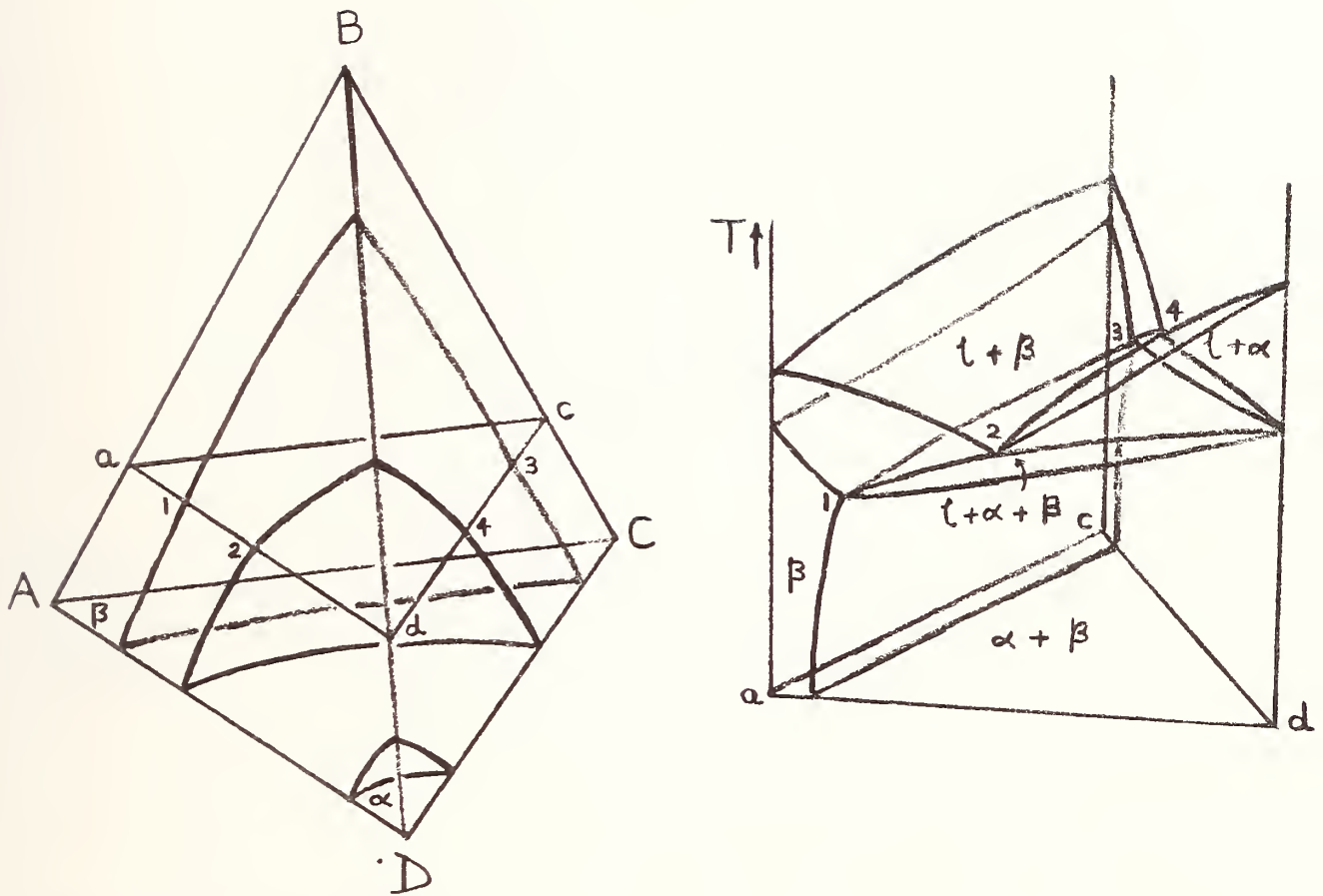


FIGURE 14. THREE - DIMENSIONAL TEMPERATURE -
 CONCENTRATION SECTION OF A QUATERNARY
 SYSTEM AT CONSTANT % B.

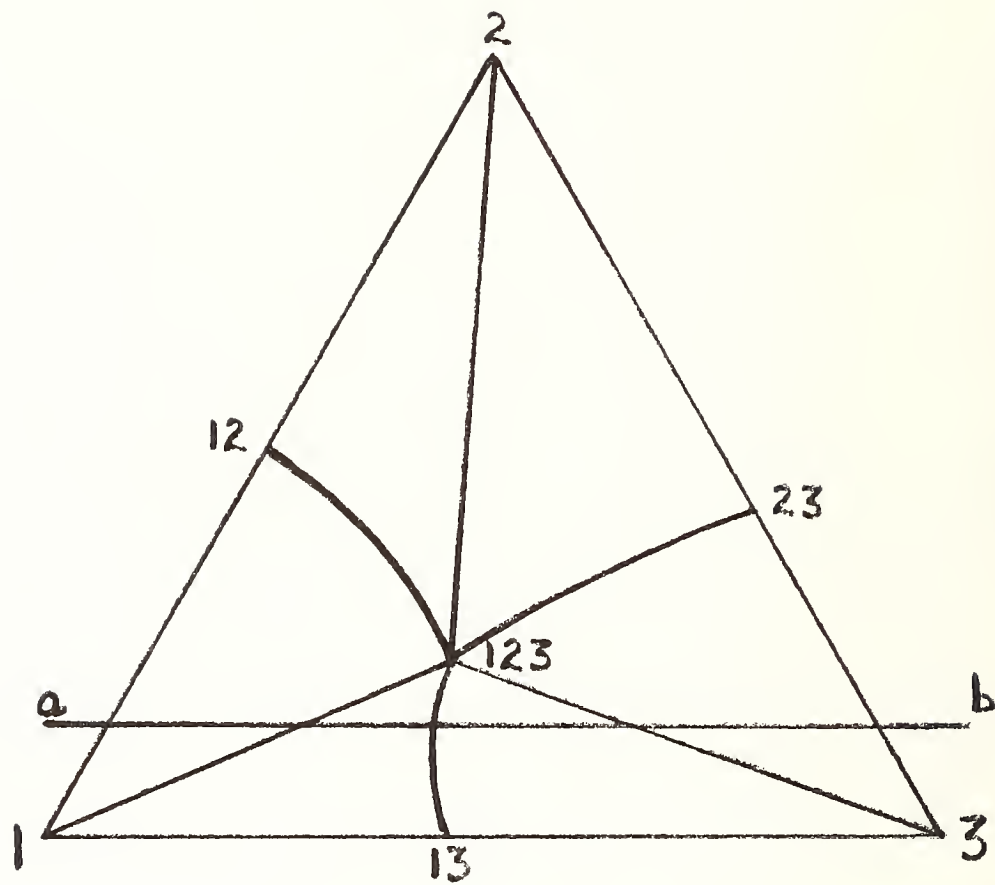


FIGURE 15. Section ab of the Ternary Polythermal Projection 234

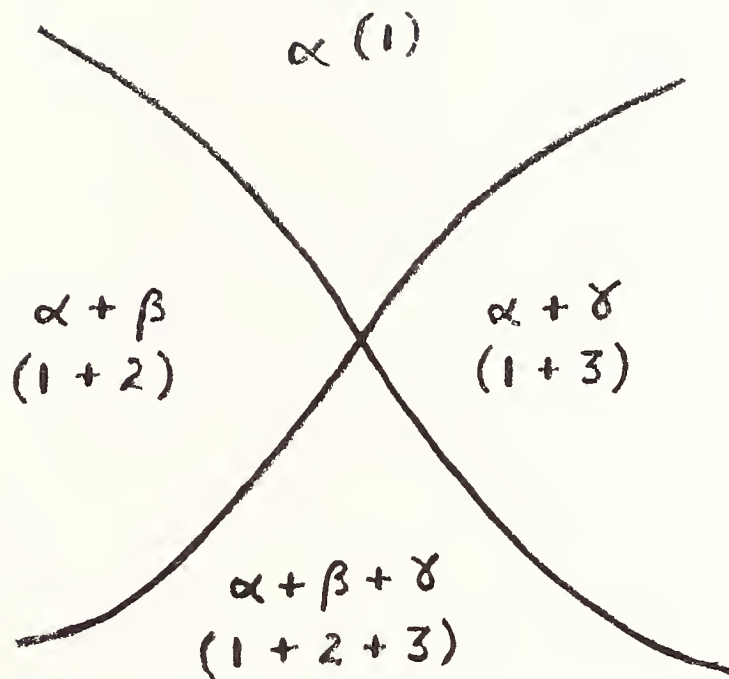


FIGURE 16. Illustration of the Cross Rule

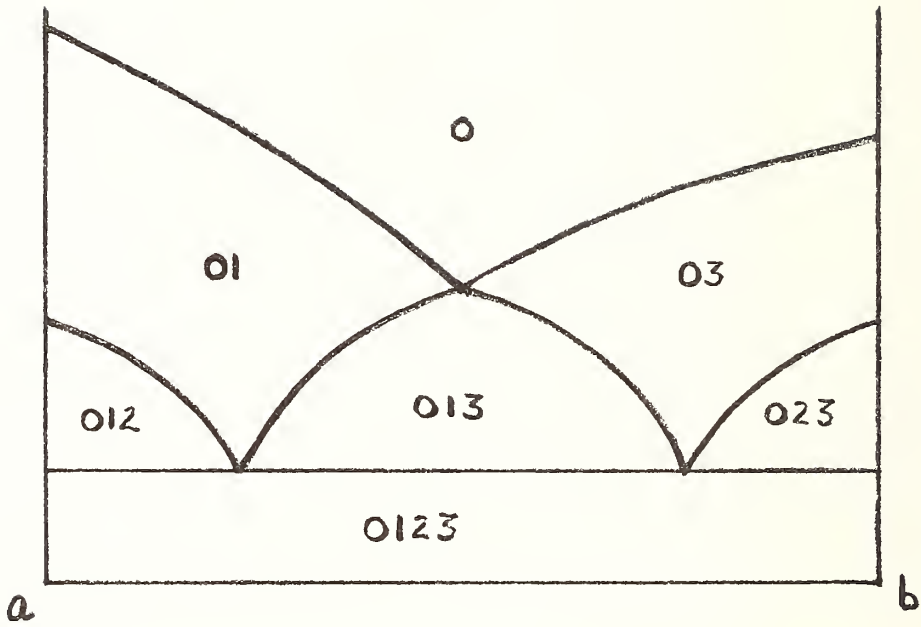


FIGURE 17. Two-dimensional Section along ab

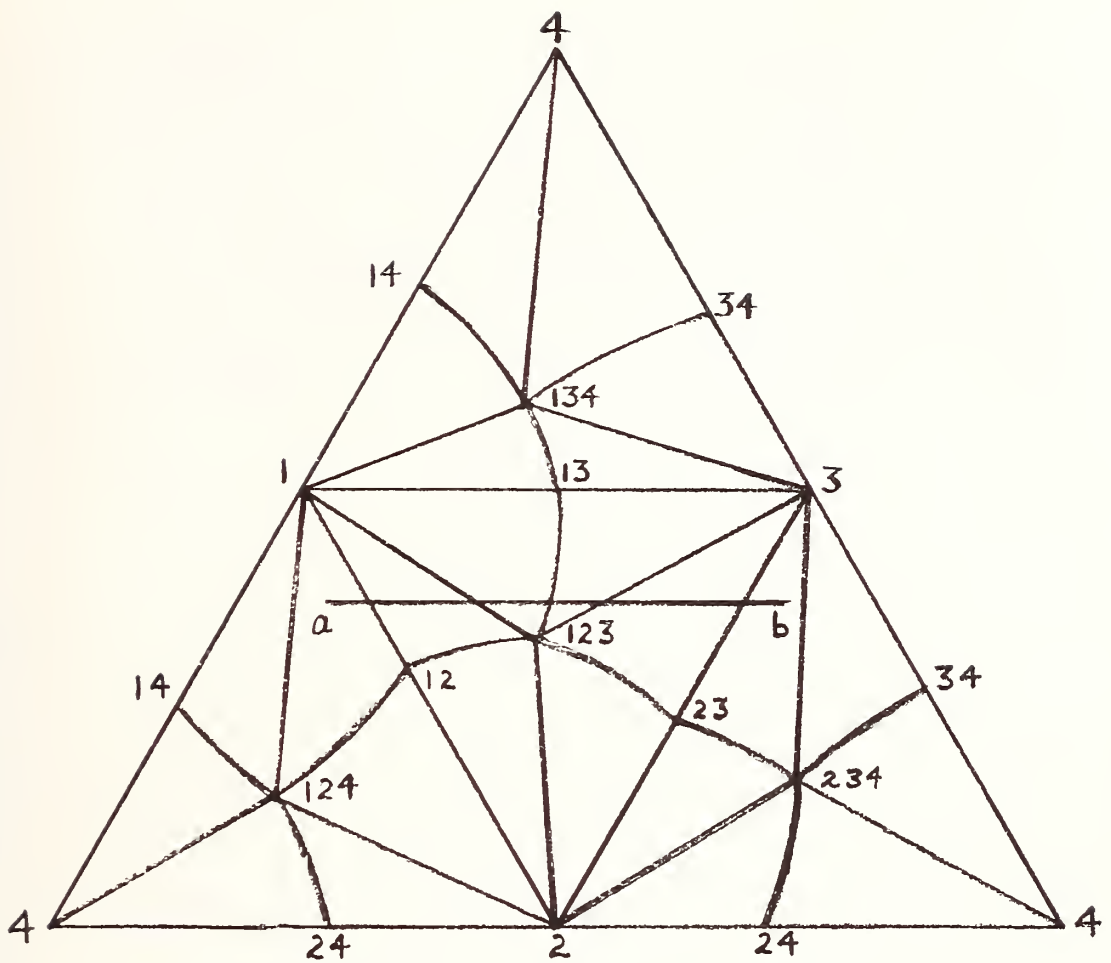


FIGURE 18. The Concentration Tetrahedron
Unfolded About the Basal Triangle

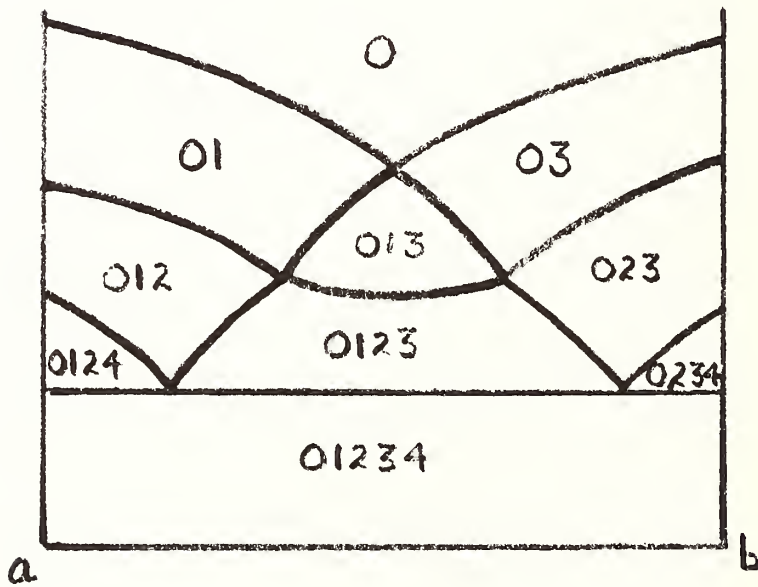
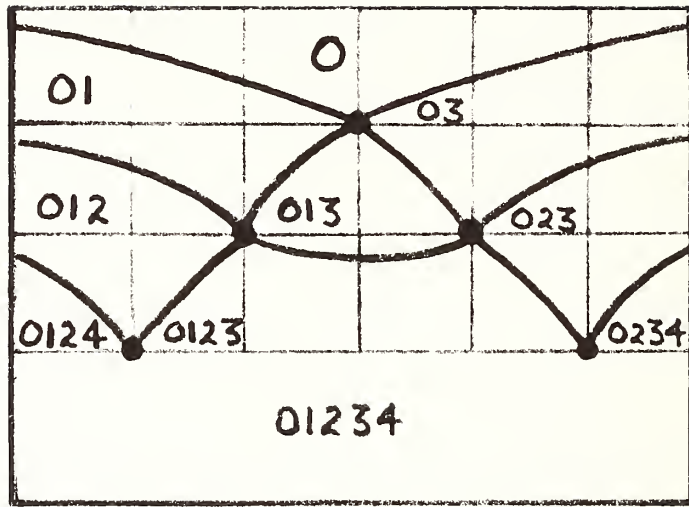


FIGURE 19. Two-dimensional Section Along ab

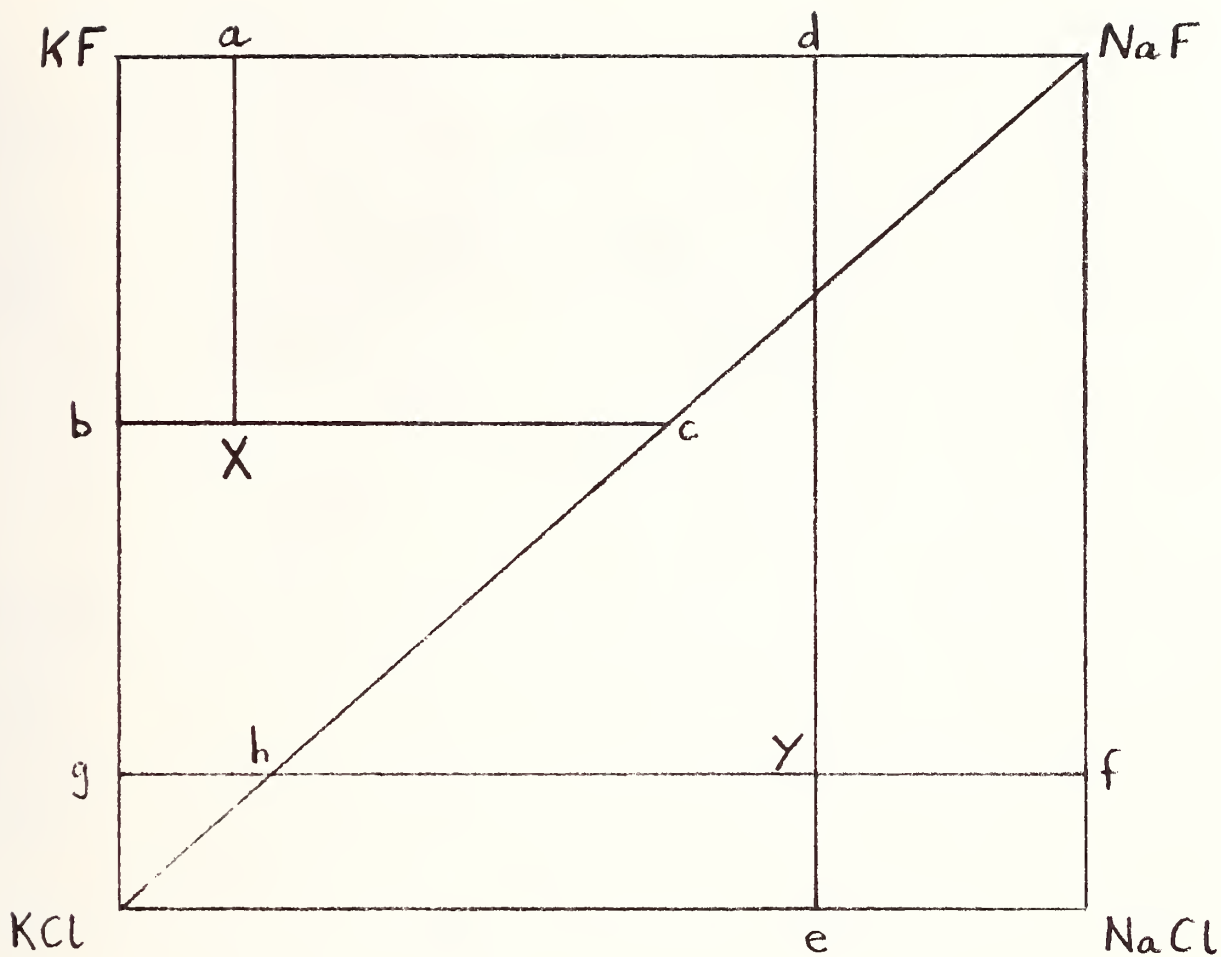


FIGURE 20. Representation of a Reciprocal System

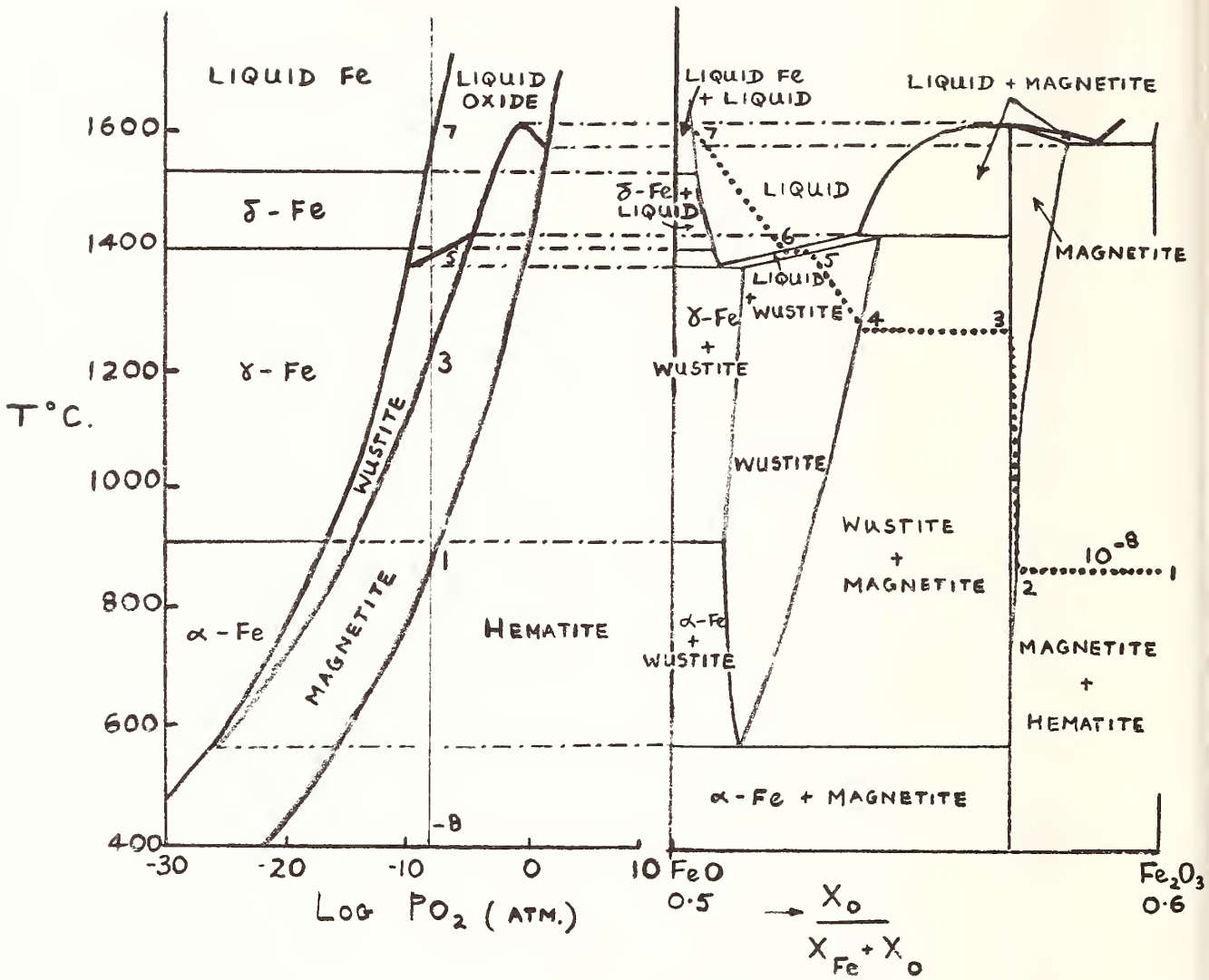
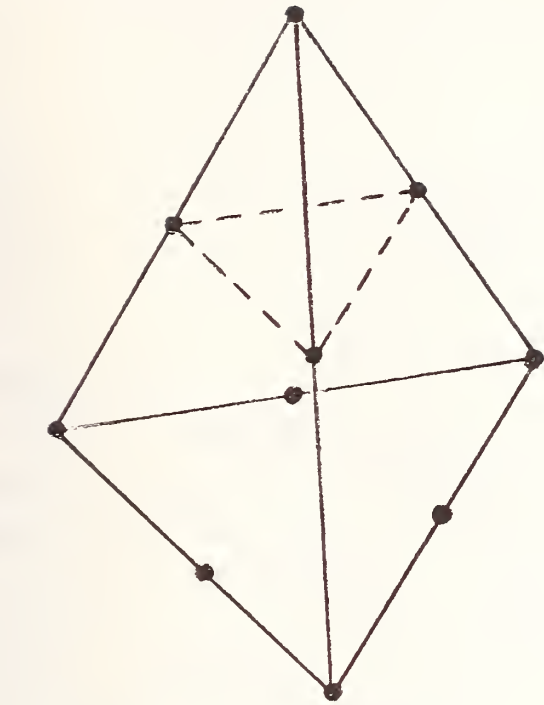
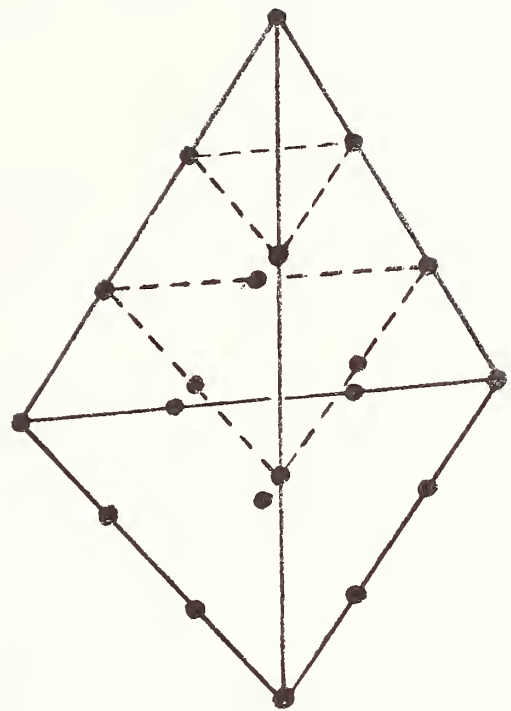


FIGURE 21a) PHASE STABILITY DIAGRAM FOR THE Fe-O SYSTEM.

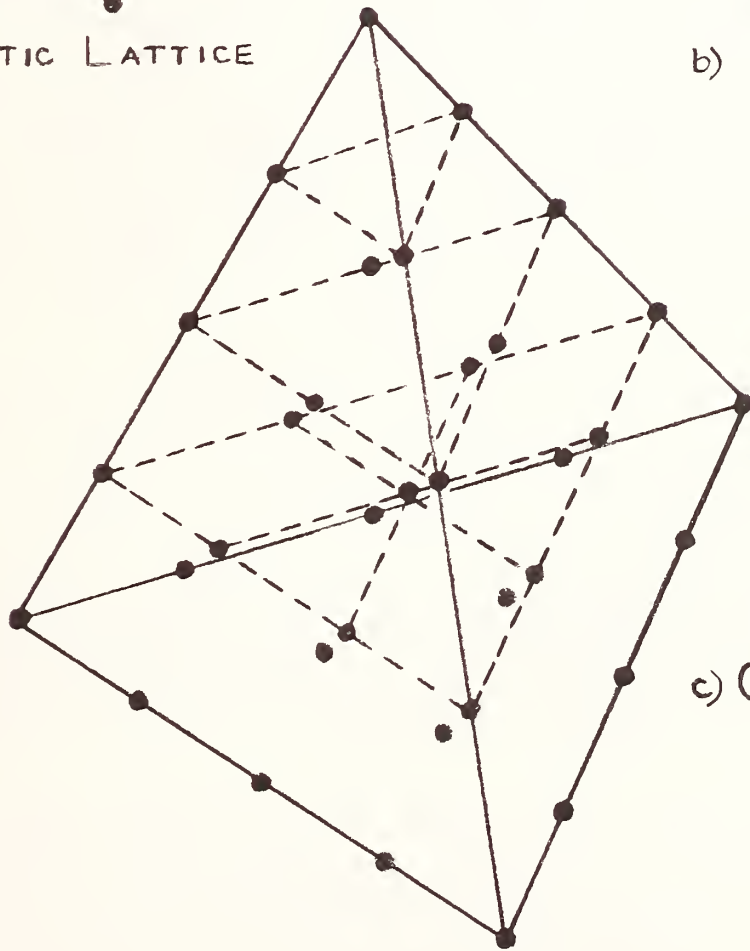
b) PHASE DIAGRAM OF THE Fe-O SYSTEM.



a) QUADRATIC LATTICE



b) CUBIC LATTICE



c) QUARTIC LATTICE

FIGURE 22. LATTICE TYPES FOR A QUATERNARY SYSTEM

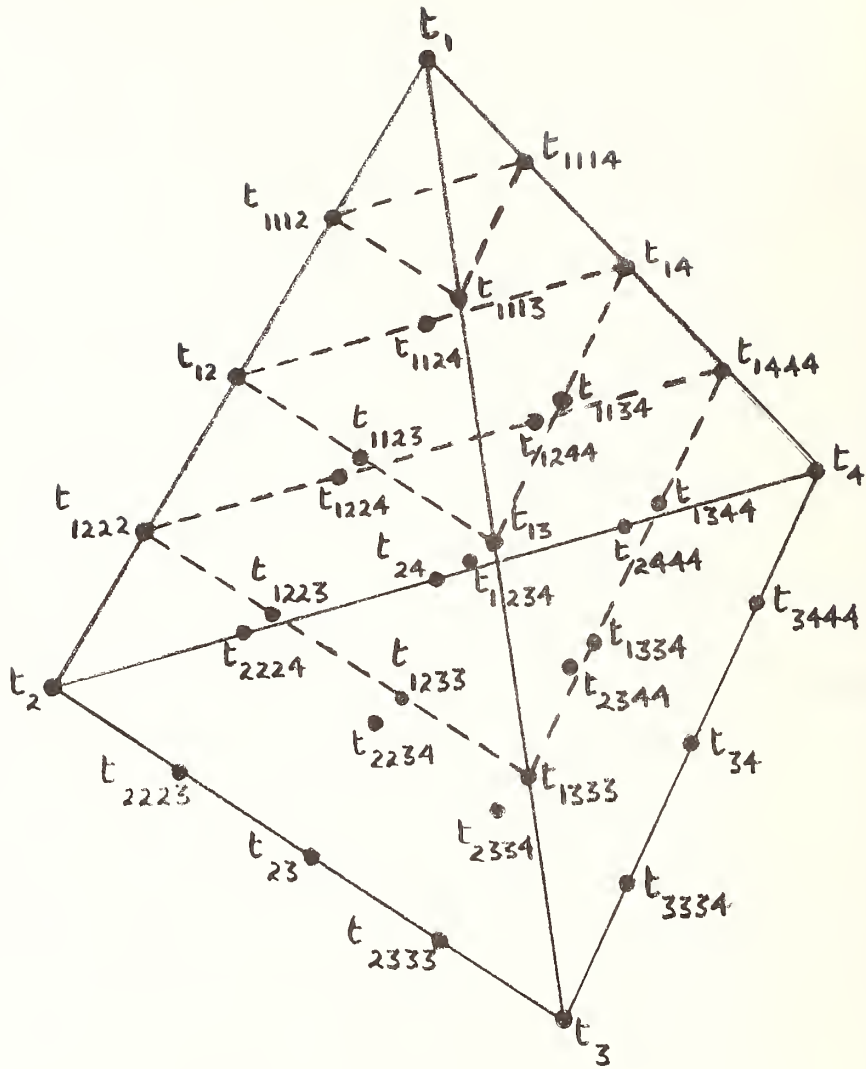


FIGURE 23. Nomenclature for Solidus Temperatures in a Quaternary System According to the Quartic Model



Phase-Diagram Compilations - A User's View

J. D. Livingston
General Electric Company
Corporate Research and Development
Schenectady, New York

INTRODUCTION

A major goal of this Workshop is to assess the current status of phase-diagram compilations in metallurgy and ceramics, and users' needs for such information, in order to assist the NBS Alloy Data Center in setting priorities for their newly-initiated efforts in this area. I was asked to present for discussion a user's view of the type of format and means of distribution most desirable for phase-diagram information. The views presented will represent my own bias, that of a research metallurgist in an industrial laboratory. However, they also have been influenced by discussions with many others, and by the results of two recent questionnaires, one sent to registrants of this Workshop, and one sent to a group of prominent metallurgists in the United Kingdom by Dr. A. Prince.

TYPES OF USE

User needs for phase-diagram information vary considerably in their breadth and depth. On the one extreme, a worker initiating a research program on a particular alloy system is usually willing to devote considerable time to a study of past results. In such a case of in-depth need, a phase-diagram compilation serves only as a starting point for entry into the literature, and the worker will go to the original references for most of his information. Papers more recent than the compilation will be located through abstract journals and Citations Index.

On the other extreme, many metallurgists must often find quick answers to such questions as, "What's the minimum melting point in the Pb-Sb system?", "How much Ni dissolves in Cr at 1000°C?", "What intermetallics form between Au and Sn?". Here the need is for quick access to a compilation as broad and as up-to-date as possible, preferably available on his own bookshelf. Between these two extremes ranges an entire spectrum of phase-diagram needs of varying depth.

In my own research, I have often found phase-diagram compilations useful in surveying alloy systems to select a suitable alloy for an experimental program. For example, when starting a research program on eutectoid reactions several years ago, I used phase-diagram compilations to tabulate known eutectoid reactions, their temperatures, phases, etc., prior to selecting a few systems for specific experiments. For such a use, breadth and currency of coverage, and compactness of format, were of prime importance.

In industrial research, the alloys of interest usually contain many components. Binary phase-diagram information, although helpful, goes only part of the way towards providing the necessary answers. Ternary phase-diagram information can be extremely useful in unraveling such complex problems. For quaternary, quinary, and higher-order systems, however, the difficulty of representation and interpretation of phase-diagram information becomes so great that a compilation of published information becomes of doubtful value.

TYPES OF DISTRIBUTION

There are many ways in which data compiled at an information center can be distributed to potential users. On a limited scale, information can be directly supplied in response to individual telephone requests. If the data are appropriately computerized, a user with access to an appropriate terminal can conduct an on-line search for the information he needs. However, it seems very clear that for the immediate future most materials scientists and engineers will prefer phase-diagram compilations in book form.

For alloys, the best-known source of phase-diagram information is the Hansen-Elliott-Shunk series.⁽¹⁾ These books present critically-evaluated phase diagrams for binary alloys and considerable crystallographic and other information, and are extremely useful. However, the explosive growth in metallurgical literature made this task increasingly difficult, time-consuming, and expensive. The latest supplement, prepared by Shunk, required over 700 pages to cover only the three-year period 1962 to 1964. A later attempt to continue this series and consolidate the earlier volumes eventually was discontinued because of the magnitude of the necessary effort and the lack of sufficient funding. Thus this series, which has been of great value to the metallurgical profession, is now 12 years out of date.

In addition to the problems of time and expense, the preparation of critical evaluations a la Hansen has another problem - a critical evaluation may be wrong. For example, Shunk's supplement devotes over four pages to the Nb-Sn system*, and one of the most clearcut conclusions reached was the following: "That Nb₃Sn is stable only at high temperatures is well established." This "well established" conclusion is now known to be completely wrong.

A less expensive, less time-consuming, and less subjective approach to compiling the literature on metallurgical phase diagrams is that which has been taken by the Institute of Scientific Information of the USSR Academy of Sciences. On an annual basis, they compile phase diagrams direct from the literature, with no attempt at evaluation or correlation with earlier results. In addition, in a prescribed format, they present considerable additional information describing the work. This series now includes 20 volumes, covering the literature from 1955 through 1974.⁽²⁾ An important feature of this series is that it includes ternary and higher-order systems, making this the most extensive compilation of ternary phase-diagram information available. Use of this series was cumbersome in the past, because they lacked a cumulative index and the annual indices were alphabetized in Russian. However, volume 20, which recently appeared, contains a cumulative index for all 20 volumes and is alphabetized by the standard chemical symbol. A similar index for volumes 1-19 was recently published by NASA.⁽³⁾

An approach involving even less time and expense is that of simply compiling phase diagrams in compact form, with little or no evaluation or further information beyond a bibliographic reference. Such an approach was used for the 1964 and 1969 editions of Phase Diagrams for Ceramists.⁽⁴⁾ Each of these editions compiled over 2000 diagrams in about 600 pages, sometimes including as many as six diagrams on a single page. Despite the limited information presented, these handbooks have been found to be extremely useful by workers in the field. The 1975 supplement to this series now accompanies the diagram with a brief descriptive text, but as a result this volume contains only about 800 diagrams. For metals, similar but much less comprehensive compilations can be found in such handbooks as Smithells' Metals Reference Book⁽⁵⁾ and ASM's Metals Handbook.⁽⁶⁾ Since these handbooks are aimed more at metallurgical engineers than research scientists, diagrams are presented in weight percent rather than atomic percent.

*Actually, this diagram appears in Shunk as Cb-Sn. Elliott's supplement also spelled niobium with a C, a mistake that Hansen did not make.

A very recent compilation is Moffatt's Handbook of Binary Phase Diagrams⁽⁷⁾, which covers the literature since 1954, and hence supplements the Hansen-Elliott-Shunk series. Diagrams, which are presented with no explicit evaluation, are presented in loose-leaf format. This allows annual updating to be interpolated into alphabetical order when supplements arrive. Another interesting feature is a double-entry index, with each diagram indexed for both elements. This can be much more convenient than the usual single-entry system when surveying, for example, the binary alloys of Zn or Zr. The index also integrates the indices of Hansen, Elliott, and Shunk.

For workers with easy access to a good technical library, a simple bibliography on phase-diagram information can be very useful. Houghton and Prince⁽⁸⁾ compiled a bibliography of phase-diagram literature through 1954, and Spengler⁽⁹⁾ reviewed the literature from 1949 to 1960. Prince⁽¹⁰⁾ has prepared a bibliography on ternary and higher-order systems covering the literature from 1955 through 1973. Containing 18,000 references, this will be published this year.

The Alloy Data Center of NBS has prepared a comprehensive list of all existing phase-diagram compilations and of current data centers active in this area. They are also preparing a comprehensive index by alloy system incorporating 12 major phase-diagram compilations. Such lists and indices can guide the individual researcher to the appropriate compilations or data centers.

As we move from indices and bibliographies to simple diagram compilations (like Moffatt and the early volumes for ceramists) to diagram compilations including additional information (like the Russian series) to compilations of critical evaluations (a la Hansen), the product becomes increasingly useful but the time and expense required for preparation increases substantially. Because user needs vary so greatly in breadth and depth, no single format will be best for all needs. However, any decisions on future projects must clearly balance the information desired by the users - which is often "as much as possible" - against the time and expense involved in preparing the compilation.

CURRENT STATUS AND NEEDS

The current status of phase-diagram compilation in English is poor,

but it is improving. For binary alloys, the Hansen-Elliott-Shunk series is now 12 years out of date, but the recent appearance of Møffatt's Handbook partly fills this gap. Although a critically-evaluated compilation of all binary systems has now become an impractical task, evaluations limited to particular metals of industrial importance are feasible and desirable. A recent example is that of Mondolfo⁽¹¹⁾ dealing with aluminum-base systems.

A more serious gap exists in the compilation of ternary phase-diagram information, which is of particular importance to industrial researchers dealing with complex alloys. The bibliography by Prince⁽¹⁰⁾, which will appear this year, will be a very welcome tool for locating such information. A comprehensive compilation of evaluated ternary diagrams has been proposed to Gmelin by a group at Stuttgart under Petzow.⁽¹²⁾ However, this proposed work is estimated to require about 18,000 pages, and, when it finally appears, will probably be priced beyond the reach of individuals and small libraries.

There would be considerable utility to a book on ternary phase diagrams falling between Prince's bibliography and Petzow's proposed compendium. A format similar to the early volumes of Phase Diagrams for Ceramists would allow the presentation of one to two thousand of the most important diagrams in a single handy volume. Alternatively, a looseleaf format such as Møffatt's might be the most practical approach, since it easily incorporates updating. The 20 volumes of Russian compilations would provide many of the necessary diagrams without the need for consulting all of the original literature. Thus the task could be accomplished with modest requirements of time and money. In my view, such a compilation would be of considerable value to industrial metallurgists.

ACKNOWLEDGMENTS

I am grateful to A. Prince for the results of his questionnaire, and for a preprint of his paper on multicomponent alloy constitution data compilations. I am grateful to G. C. Carter for the results of the questionnaire sent to workshop registrants. Also of great help were conversations with many colleagues, especially W. G. Møffatt and J. H. Westbrook.

References

1. M. Hansen and K. Anderko, Constitution of Binary Alloys, 2nd Edition, McGraw-Hill, New York, 1958; R. P. Elliott, 1st Supplement, 1965; F. A. Shunk, 2nd Supplement, 1969.
2. Phase Diagrams of Metallic Systems, N. V. Ageev, ed., Russian Institute for Scientific and Technical Information, Moscow, 20 annual volumes.
3. NASA Technical Translation NASA TT F-17296, C. M. Scheuermann, Lewis Research Center, 1976; reproduced in these proceedings as paper TPSII-1.
4. E. M. Levin, C. R. Robbins, and H. F. McMurdie, Phase Diagrams for Ceramists, American Ceramic Society, 1964; Supplement, 1969; 2nd Supplement, 1975.
5. Metals Reference Book, C. J. Smithells, ed., Butterworths, U.K., 5th ed., 1976.
6. Metals Handbook, Vol. 8, Metallography, Structures, and Phase Diagrams, American Society for Metals, Metals Park, Ohio, 1973.
7. W. G. Moffatt, Handbook of Binary Phase Diagrams, General Electric Co., Schenectady, N.Y., 1976.
8. J. L. Haughton and A. Prince, The Constitution of Alloys: A Bibliography, The Institute of Metals, London, 2nd ed., 1956.
9. H. Spengler, Metall. 15, 883, 1004 (1961).
10. A. Prince, A Bibliography of the Constitution of Multicomponent Alloy Systems (1955-1973), to be published.
11. L. F. Mondolfo, Aluminum Alloys: Structure and Properties, Butterworths, U.K., 1976.
12. F. Aldinger, E.-Th. Henig, H. L. Lukas, and G. Petzow, paper MPSI-1, this workshop.



Some Thoughts on the Distribution of Reference Data

Dr. Howard J. White, Jr.
Office of Standard Reference Data
National Bureau of Standards
Washington, D.C.

ABSTRACT

Some of the characteristics of the existing methods of distributing reference data are discussed. Strengths and weaknesses of the various methods are pointed out. There does not appear to be one superior method, but rather various methods or combinations of methods are indicated for individual cases. The problem of distributing reference data on phase diagrams is considered specifically.

KEY WORDS

Distribution of phase diagrams; distribution of reference data; formats for reference data.

I. INTRODUCTION

The generation of phase diagrams and their utilization to solve technological and scientific problems are covered in other sessions of this Workshop. This paper is focussed on the format and distribution of phase diagrams; that is, on the advantages and disadvantages of the various methods that might be considered for transferring phase diagrams from their generators to their users. After a general consideration of the possible methods of transferring data, the problem of phase diagrams is taken up specifically and some recommendations for the future are made.

II. METHODS OF TRANSFERRING DATA

The following listing would appear to cover the principal methods that are currently used for transferring data.

- a) Personal conversations and letters
- b) Lectures
- c) Loose-leaf data sheets
- d) Technical papers in journals
- e) Monographs
- f) Computer tapes and card decks
- g) Responsive computer programs available
 - i) for query by batch method
 - ii) for interactive query via terminal
- h) Handbooks

The methods listed above will be considered in some detail. However, two conclusions can be cited immediately. First, none of the above is the universal solution to the data distribution

problem. Each has its strengths and weaknesses. Secondly, the suitability of each of the above depends on the nature of the data and the nature of the interest group involved.

III. INTEREST GROUPS

An interest group can be defined as those individuals with a direct, immediate, or continuing interest in the data in question because they generate them or need to use them. An interest group may be small, medium-sized, or large; and its properties will vary accordingly.

1. The Small Interest Group

There appear to be several reasons why an interest group may be small. However, the basic properties of the group seem to be the same whatever the reason.

First of all, the data may represent a field that is blossoming. As yet, only a few appreciate the value of the data. It is probable that each member of the interest group knows the work of the other members and may know a number of them personally. The users and generators of the data tend to be the same people. There is no one else involved. A small interest group may also result from a field that is so narrow that only a few can profit from the availability of the data. The users and generators of the data are often linked by a public or private mission-oriented agency which supports the effort for its own purposes. Alternatively, a narrow portion of a large field might be developed rapidly for a specific purpose. Again, users and generators may be linked by a mission-oriented agency which provides support. An example might be the JANAF Project which

originally provided thermodynamic data for purposes of rocket design. Finally, generators and users of the data may be closely coordinated because of unusual constraints in the field. Again, there is often a common support agency. High-energy accelerator physics with its extremely expensive equipment can be cited as an example.

In all of the cases mentioned, the members of the interest group can be expected to know of one another and know how to obtain the pertinent literature in the field.

2. Medium-Sized Interest Group

The data of interest to such a group have proved their worth over a range of problems. The members of the group are no longer closely connected. Few know or know of all members of the group. The members have several reasons to want the data. However, the members in general have the same technical background, know about the same journals and books, and hear of and attend the same lectures.

3. Large Interest Groups

If the interest group is large, the data have proved their worth in many fields. The members of the group do not know one another and may not have similar backgrounds. Potential users do not necessarily know all sources of data, and generators are not aware of all possible uses for their data.

The above brief characterizations of the interest groups can serve to establish some of their properties and the differences between them. It is clear that the problem of reaching

the members of an interest group will change with the size of the group. The large interest group is different from the small one not only in size but also in nature.

IV. PROPERTIES OF METHODS FOR TRANSFERRING DATA

The various methods for transferring data have been listed in a previous paragraph. Some properties of these methods will now be considered. These properties have been stated from the standpoint of a user's needs and refer to advantages or disadvantages a given method may have with respect to fulfilling the user's needs. The properties to be considered may be listed as follows:

- a) Rapidity of response to perceived need
- b) Degree of responsiveness to need
- c) Permanence, suitability for reference, and transferability
- d) Restrictions on the audience
- e) Restrictions on data
- f) Restrictions on use

Cost is an obvious property which has not been mentioned. It will be considered along with the properties which are listed. Each of the methods for transferring data cited in the first section of this paper will now be considered in terms of these properties.

A. Personal Communication

The response is generally very rapid. Since personal communication, whether verbal or by letter, is interactive, it is fully responsive. In other words, the prospective user can

obtain the data he needs and any collateral information about it which is necessary to substantiate its suitability. However, the results of personal communication are essentially unsuitable for reference or transfer. There is no information other than the name of the source that can be used by a third person to substantiate the data for his own purposes. Personal communication is essentially limited to a small audience. It is inexpensive when provided as a professional service, but may become expensive when provided as a consulting service. It is limited to small amounts of data and the user and producer of the data must make direct contact.

B. Lectures

Although a lecture requires more formal preparation, it is still quite a rapid method for transferring information. It is reasonably responsive and some interaction in the form of questions and answers is often possible during or after the lecture. Unless converted into a technical paper, it is ephemeral and unsuited to reference. It is limited to quite small amounts of data, and the user and producer must make direct contact.

C. Loose-Leaf Data Sheets

These represent a reasonably rapid method of transferring data. Changes can be made in a short period of time by substitution of individual data sheets. The format is fixed and non-interactive. As a result, responsiveness depends on the design of the data sheet. Loose-leaf data sheets are permanent as a collection although individual sheets may be replaced from time to time.

In principle, they are suitable for reference although the organization, indexing, replacement, etc. of the individual sheets open the way to multiple errors in filing and the inadvertent use of obsolete sheets. Collections of loose-leaf data sheets are heartily disliked by librarians. In theory there is no limit to the audience that can be served; in practice the method is limited to a moderate audience by the cost and complexity of the dissemination procedures. Again, there is no limit in principle on data content although cost and complexity increase with size. The user must contact the distributor and remain in contact with him.

D. Technical Papers

These are slower. The more formal method of presentation and the details of the publication process limit the rapidity of response. It is also necessary to find a journal willing to publish the data in question. The format is fixed and non-interactive, and the responsiveness depends on the nature of the paper. They are subject to unrecognized obsolescence. Technical papers are permanent, easily referenced, and transferrable. Technical journals have a larger audience and, in fact, are too expensive for a smaller one unless they are subsidized. The feasibility of presenting data through papers in a journal again depends on the availability of a journal willing to accept the papers. There are essentially no restrictions on the data and no direct connection between the user and author is required.

E. Monographs

The characteristics of monographs are essentially the same

as those of technical papers. They tend to be more massive and slower in coming out. The problem of finding a publisher may be a serious one.

F. Computer Tapes and Card Decks

The initial response may be slow because the development of software may be needed to produce the tapes. Updating can be quite rapid. These, too, are of fixed format and non-interactive, and the responsiveness depends on the design of the product. They are permanent and can be transferred, but no systematic reference system is currently available. There is no inherent restriction on the size of the audience, but the use may require a substantial investment in equipment and probably software. These costs tend to limit applicability to sophisticated, high-volume users. There are no restrictions in principle on the data. In fact, tapes are excellent for very large files. Use requires the availability of suitable hardware and software.

G. Responsive Computer Programs

These are rapid, once established. Batch systems are fixed in format; limited flexibility is often provided with interactive systems. Again, no systematic reference system is available. There are a few restrictions on the use of batch systems. The user of an interactive system must have access to a terminal. They are good in principle for all sizes of fields. Large files are expensive to maintain on the computer and may be expensive to search unless very carefully designed. Someone must pay for software-development costs and for up-time on the computer.

H. Handbooks

These are slow in being generated, and in general are preceded by one or several of the other methods. They are fixed in format, non-interactive, and responsiveness depends on design of the handbook. A handbook is permanent, transferrable, and easily referenced in itself. However, unless it is carefully put together, it may present difficulties to those who wish references to a definitive source of the data. Handbooks tend to be widely available and are often designed to assist in data transfer between different groups. They are strongly advertised and marketed. There is no restriction on the amount of data contained. The limitations on the quality of the data are often difficult to determine.

V. APPLICATIONS TO DATA ON PHASE DIAGRAMS

The phase-diagram field is a mature field with a large interest group. There are many sources for data which must be incorporated into phase diagrams, and there are many practical engineering applications of phase diagrams. In fact, phase diagrams are among the most pervasive data there are with uses ranging from metallurgy and the formation of ceramic materials through an entire spectrum of applications in the materials field. As a result, formal mechanisms for finding, transferring, and providing references are needed. Although the more ephemeral methods of transferring data may have uses in specific instances, the more permanent mechanisms must clearly play the major role.

The monograph has been the historic method of choice with such classical examples as Hansen's "Constitution of Binary Alloys"

and "Phase Diagrams for Ceramists." It seems probable that the monograph will continue to be extensively used for distributing phase diagrams.

An article in a journal is also an attractive possibility. Such an article could cover a smaller area than the comprehensive monographs and would be published more rapidly. At the same time, the needed permanence and ease of reference would be obtained. The problem, of course, is in finding a journal to publish such compilations. Standard research journals are usually unwilling to publish compilations of phase diagrams. In this regard, the Journal of Physical and Chemical Reference Data should be considered. This relatively new Journal is devoted to the publication of reference data. Thus, a compilation of phase diagrams, if prepared to the editorial specifications of the Journal, would be a suitable article for publication. In fact, one compilation of phase diagrams has already been accepted for publication. I would recommend that serious thought be given to publication of suitable compilations of phase diagrams in this Journal on a systematic basis.

Finally, some consideration should be given to the data center. A data center as a formal entity is a relatively new concept. It consists of a group or "groups" who have accepted responsibility for compiling and evaluating data in a given field. Examples are the Alloy Data Center in the field of metals and the group producing phase diagrams for ceramists in the non-metallic field. The data center has the potential to provide any of the techniques for transferring data which

have been discussed above along with a degree of institutional permanence. Thus, it can be personal and interactive and still provide a stable, recognizable reference point.



Remarks on Producing and Publishing Critically Evaluated Data

W. B. Pearson
Faculty of Science, University of Waterloo
Waterloo, Ontario, Canada

As somebody who has been concerned for nearly thirty years with critical compilations of phase equilibria and structural data on metals and alloys in particular^(1 - 5), I offer some thoughts on "how to get the job done". This may be valuable since my experience runs through the days of "bits of paper" to "quick-sort" filing cards with the 102 perimetrically punched holes, to the advent of Xerox copying, and finally into the computer age. Secondly it encompasses various organization systems from the "do it yourself" to the international "moonlighting" system of Structure Reports and, by observation, to fully (though perhaps inadequately) funded systems, based either on government grant financing, or on commercial sales. In all I have directly written or edited over 19,000 pages of critically evaluated data.

My general conclusions are as follows: a fully computer-based operation, is by far the most elegant, since with appropriate programming it can lead to books printed directly from magnetic tapes, but such a system requires very considerable financial backing, even if it goes no further than data handling and storage and does not proceed to the ultimate step of book production direct from the data files. Although computer programmes can be readily used to calculate and check data, the use of computers in no way obviates the need for experts to find the data in the literature and to critically evaluate it. In contrast to computer-based operations, a system of data handling by hand, using part-time typists as required, although far less elegant, is still workable and gives the final product at less cost.

Secondly, in order to get a critical data compilation prepared (unless there is sufficient money available to employ as many full-time assessors as is necessary), it is much better to support a single person (or possibly two) full-time for the two or three years that may be required for the project, than to

organize a team of many people on a "moonlighting" basis for nominal honoraria, each of whom is expected to complete a portion of the compilation. In the latter case the work is likely to become indefinitely delayed due to some members of the "team", for various reasons, not completing their assignments.

Perhaps some recollections of the works that I have undertaken will give substance to these conclusions, and the experience apparent therein will be useful to those contemplating undertaking and publishing critical assessments of data.

In preparing the first volume of "The Lattice Spacings and Crystal Structures of Metals and Alloys"⁽²⁾ (1044 pp.), I read all of the relevant literature and transcribed the pertinent data onto "quick-sort" cards with the 102 perimeteral holes assigned to the elements by atomic number. This handled cross-referencing satisfactorily and although shaking out the required cards from a wire was clumsy, it was just adequate for the job that existed at that time. However, rewriting all of the data and typing and checking the ms. in preparation for the publisher proved to be very time consuming and inefficient.

My choice of the method of producing Volume 2 of this work⁽³⁾ (1446 pp.) was more fortunate than I realized at the time, and indeed in retrospect, had I not adopted that method, it is very doubtful whether I would ever have been able to complete the work. As I read each paper that contained pertinent data, I wrote it up immediately in a form suitable for publication, and also constructed a running tabulation of data. These portions of ms. were then immediately typed, checked and set aside for final processing. When the total literature survey was completed and treated in this way, Xerox copying machines were just becoming generally available. Therefore, all that I did in constructing the final ms. for the publishers, was to assemble all of the written reports on any particular alloy system. I then cut out the parts that I selected from any of these reports, pasted them in the required order on a sheet of paper, together with the required references at the bottom of the page, and finally copied the synthesized page by

Xerox to give a flat page for the publisher. In this way construction of the final ms. was exceedingly rapid requiring only scissors, glue and a Xerox copying machine. The amount of connecting material that had to be written and typed at this stage turned out to be negligibly small, as also did the number of reports that had to be completely rewritten. Generally they could be assembled by a sentence cut from this, and a sentence from that report. The assembly of the extensive tables of structural data (490 pp.) in appropriate alphabetical order was handled in a similar manner.

Whether such a method could be now used to assemble a third volume of the same work is a good question, but I think it could if the person had his full time to devote to it and the help of one other person. However, I doubt that as an alternative, a committee of say ten people on a part-time basis would be too successful; data would probably accumulate more rapidly than it could be processed.

As a general editor of Structure Reports for some 15 years⁽⁴⁾, I have further experience of organizing numerous co-editors. Structure Reports is a series of annual volumes, which report in critical fashion all crystal structure determinations published in the year to which the volume is attributed. It is divided into three sections: Metals, Inorganic and Organic, each having its own co-editor assigned for the year in question. The work of a section co-editor thus comprises reading the appropriate literature, checking data and producing critical reports thereon which, when appropriately combined and edited, constitute the ms. The general editor is responsible for producing lists of structural papers to be read and for general coordination and checking of the different ms., reading proofs, etc. The trouble with this organization, where each editor takes on the work out of a sense of goodwill to the crystallographic community and in exchange for a relatively small honorarium, was that due to accidents or personal problems, one section of a volume frequently delayed the publication of the whole for several years. At one point the situation was so bad that Structure Reports volumes were

only being published some 10 years after the year whose work was critically reported. Recently this back-log has been eliminated and Structure Reports now are appearing in the shortest possible time; only 2-3 years after the work that they report is published. Thus all volumes and up to and including 1973 were published by the end of 1975.

This changed state of affairs resulted from three factors - the first two are mentioned for completeness although they are trivial in the present context; the third is more interesting. First, only those section co-editors were assigned volumes whose record indicated that they could produce ms. rapidly. Secondly, the general editor no longer covered the world literature and produced lists of papers to be reported: the main subject journals were reported by the co-editors as they were received and Bulletin Signalétique abstracts #161, "Cristallographie" were used simultaneously as a source of references of papers containing structural data.

The third reason for the rapid publication transpired to be a switch to direct photo-offset printing of typed ms. instead of having printers set the ms. in monotype, as was the earlier practice. This change was adopted primarily because the cost of typesetting the volumes was making them too expensive for individuals to purchase. At the time of the change, using any typing service to produce pages with justified lines was as expensive as setting the ms. in monotype, so "moonlighting" typists were engaged to type the pages of ms. in a standard format. The general editor then read the pages in proof and had corrections done before the ms. was assembled and sent to the publisher for photo-offset printing. It so happened that this process turned out to be very much more rapid than the original one where the ms. was sent to the publisher who then went through it marking it for the printer, who set it in print. Thereafter the general and section editors went through up to four proofs to ensure correctness of the data. From this, one may conclude that unless a continuous data-bank operation is to be established at the same time as the production of ms., hand-typing operations may still be cheaper and as rapid as computer-based operations, unless these are fully funded to provide

day workers necessary for the operation. These observations are very cogent to the production of volumes of critically assessed data on phase equilibria, since computer handling of such operations is likely to require the development and successful operation of special programmes.

Finally a remark or two on comparative costs may be interesting. When I first became general editor of Structure Reports producing volumes in the early 1960s, a consumer buying the volumes obtained an average of 7 pages per Dutch florin (D fl) spent, whereas critically evaluated data on a similar subject produced by a commercial company ran at one page only per D fl., if my recollection is correct. Nevertheless, the production of Structure Reports was unsubsidized, and over the years they were self-financing and made a modest profit. In more recent years the costs of typesetting volumes of Structure Reports began to increase alarmingly so that the price per page doubled. However, the changeover from typesetting to photo-offset printing of hand-typed ms. pages again halved the cost of a printed page. A certain loss of elegance results from the change from typeset pages to typed pages with unjustified lines, but as far as I am aware this has not produced adverse comments, the users finding that any moves to reduce costs are welcome.

References

1. Vanadium and its Alloys. J. Iron and Steel Inst., 1950, Vol. 164, pp. 149-159.
2. Lattice spacings and structures of metals and alloys. Pergamon Press, London, 1958, pp. 1044.
3. Lattice spacings and structures of metals and alloys. Vol. 2, Pergamon Press, Oxford, 1967, pp. 1446.
4. Structure Reports. International Union of Crystallography, Oosthoek, Utrecht. Volumes 17, 18, 19, 20, 21, 22, 23, 24, 25, 26, 27, 28, 29, 30A, 30B, 31A, 31B, 32A, 32B, 33A, 33B, 34A, 34B, 35A, 35B.
5. The Crystal Chemistry and Physics of Metals and Alloys, Wiley & Sons, New York, 1972, pp. 806.

Discussion Following the Tuesday Afternoon Session on Representations,
Format, and Distribution

K. Gschneidner - In our compilation of binary cerium diagrams, we have given the diagram in atomic percent for the researcher, and on the opposite page in weight percent for the industrial user.

T. Livingston - You can do that if you have the luxury of the space available. Usually there is a financial limitation. The question is, "What is the minimum acceptable depth?" The way I view it, if you plot increasing information, starting from bibliographies increasing to evaluated compendia, the value probably goes up monotonically, but I feel it has a decreasing slope and the cost may go up, but it may have an increasing slope.

L. Brewer - But what do you do if there are six or more contradictory diagrams, do you give them all in your compendium?

T. Livingston - There is always *some* evaluation involved. Moffat does some evaluation too. For example, if a melting point is obviously off, this gets taken care of. But, how many man-hours can you spend? Another question is, how good is the person doing it? There is some optimum there in man-hours you can spend. It may come to the point where you may want to put - maybe not all 6... (you can throw out some of them because maybe they violate the phase rule or something!) - but several in your compilation.

J. Cahn - There is a danger with evaluated data. The melting point of manganese sulfide just went up over 100 degrees and it was recorded as early as the 1930's that it was higher. All the weight of the evaluated phase diagrams came down on the wrong figure. You can't always rely on the evaluators.

D. Kahan - A full evaluation is going to be costly not only in money, but also in time and delay in getting it to the users.

J. Livingston - In loose leafing you can update periodically, but you may still be a few years behind. Dr. Pearson and a few other people suggested that maybe there would be a market for some sort of a current awareness journal, something like the Diffusion and Defect Data Journal, or Structure Reports.

B. Rosof - The participants here know a lot about phase diagrams, but many metallurgists (not only PhD's, but also bachelor's degrees), can't evaluate phase diagrams for themselves. For them, I think, evaluated compendia are far more important than for people here who are researchers in the field.

J. Livingston - There is obviously a whole range of user needs and we are trying to get a feeling for what the priorities are. Maybe we should go after the best evaluated product, but I think that many people I speak to in industry, at least, would rather have a compendium of a thousand diagrams, some of which may not be right, or many of which may be wrong. They're not all interested in the third decimal.

Author Index

- Ageev, N. V., 90
 Ageeva, D. L., 90
 Aldinger, F., 164
 Ammann, P., 1334
 Ansara, I., 121
- Badie, T. M., 550
 Bailey, D. M., 1027
 Balakrishna, S. S., 1200
 Bale, C. W., 1077
 Beam, J. E., 1428
 Bennett, L. H., 261, 450, 592
 Bilimoria, Y., 1047
 Blander, M., 1093
 Boreni, R., 259
 Boyle, M. L., 726
 Brebrick, R. F., 1220
 Brown, J. J., Jr., 272
- Cameron, T. B., 566
 Carter, F. L., 763
 Carter, G. C., 36, 261, 450
 Cassidy, R. T., 272
 Chang, L. L. Y., 165
 Chang, Y. A., 229, 774
 Chart, T. G., 1186
 Choudary, U. V., 229, 774
 Cleek, G. W., 1, 257
 Cook, L. P., 1, 257, 440
 Craig, D. F., 272
- Davison, J. E., 1428
 de Fontaine, D., 967, 999
 Dew-Hughes, D., 1411
 Doman, R. C., 1378
 Dreshfield, R. L., 624
- Ehrenreich, H., 592
 Eliezer, I., 803, 846, 1440
 Elliott, J. F., 1332, 1453
 Evans, B. L., 226
- Fine, H. A., 355
 Fisher, J. R., 909
 Fivozinsky, S. P., 1325
 Flukiger, R., 375
 Fopiano, P. J., 567
- Gaye, H., 907
 Giessen, B. C., 1161
 Gittus, J. H., 1065
 Glasser, F. P., 407
 Goldstein, J. I., 462
 Gulya, V. B., 1139, 1151
 Gschneidner, K. A., Jr., 226
- Haas, J. L., Jr., 909
 Hasebe, M., 911
 Henig, E.-Th., 164, 955
 Hirano, S., 508
 Howald, R. A., 803, 846, 1440, 1470
 Hsu, C. C., 1109
- Jackson, M. R., 423
 Jaffee, R. I., 1420
 Johnson, J. R., 483
 Jorda, J.-L., 375
- Kagan, E. K., 346, 351
 Kahan, D. J., 261
 Kaufman, L., 1065
 Khanna, K. M., 575
 Kikuchi, R., 967, 999
 Kiseleva, N. N., 1139, 1151
 Kolesnikova, T. P., 90
 Kreidler, E. R., 1307
 Kubaschewski, O., 1027
- Larson, H., 1354
 Livingston, J. D., 703
 Lukas, H. L., 164, 955
 Lupis, C. H. P., 907
- Mallik, A. K., 1200
 McCormick, S., 1047
 McNally, R., 1378
 Merrill, L., 100
 Mighell, A., 259
 Minor, D. B., 440
 Miodownik, P. A., 1065, 1479
 Mlavsky, A. I., 1426
 Mondolfo, L., 1382
 Morral, J. E., 566
 Myers, S. M., 516

Nakamura, K., 508
Negas, T., 1, 257
Neumann, J. P., 229
Nishizawa, T., 911

Ondik, H. 259

Pehlke, R. D., 1360
Pelton, A. D., 1077
Petrova, L. A., 90
Petzow, G., 164, 955
Prince, A., 660
Prochazka, S., 1409

Rairden, J. R., 423
Reilly, J. J., 483
Reno, R. C., 450
Rhines, F. N., 142
Romig, A. D., Jr., 462
Rosof, B. H., 1090
Roth, R. S., 1, 257

Saboungi, M.-L., 1093, 1109
Saito, S., 508
Sandrock, G. D., 483
Savitskii, E. M., 1139, 1151
Scheuermann, C. M., 1237
Selle, J. E., 1471
Sherwood, G. B., 1325
Sinha, V. K., 578
Slick, P., 1427
Smith, J. F., 1027
Smugeresky, J. E., 516

Sōmiya, S., 508
Spear, K. E., 744
Stalick, J., 259
Stein, V.S., 1506
Swartzendruber, L. J., 450

Tarby, S. K., 726
Thompson, W. T., 1077
Thurmond, C. D., 23
Tulupova, I. V., 1506

Van Tyne, C. J., 726
Verkade, M. E., 226
VerSnyder, F. L., 1418
Vol, A. E., 346, 351

Wachtman, J. W., 1
Wang, F. E., 545
Watkin, J. S., 1065
Watson, R. E., 592
White, H. J., Jr., 709
White, W. B., 251

Zimmermann, B., 955

SUBJECT INDEX

Each paper has been indexed under one or more of these entries for ease of retrieval. This index is cursory rather than exhaustive. Those papers giving numerical phase diagram data or phase diagrams on specific systems are listed in the Materials Index.

- Acceptor solubilities 26-27
- Activity coefficients 726-727, 774, 777-786, 803-845, 1047-1048, 1052-1055
- Additive systems (salts) 1093, 1098-1108
- Ageev, translated cumulative index 1237-1306
- Aircraft industry 262, 1396, 1418-1419
- Allen and Cahn 1012, 1017
- Alloy physics 84-89, 592-623
 - (Also see under specific terms)
- Alloys (see under Metallic systems)
- Amorphous materials 261-268, 1161-1185
- Analytical representations 672-675
- Angular correlation 450-461
- Applications (see under Needs and Applications, under main headings of Ceramics systems, Semiconductor systems, High pressure diagrams, or specific terms)
- Atomic deposition methods 151, 516-544
 - summary 1172
- Autoradiography 566

- Bale-Pelton polynomials and coefficients 846-847, 874-875, 902-903, 1445
- Band theory 619
- Batteries 262, 1109-1138
- Bonding, chemical (see also Crystal chemistry) 612-614, 763-773
 - , transient liquid phase (TLP) 1418-1419
- Bonnier and Caboz 956
- Bragg-Williams 978, 1000, 1008
- Brouwer diagrams 27

- Calculations of phase diagrams (see under Theories of phase diagrams, specific topics, and see Tuesday's poster session on this subject, pp 726-1236)
- Calphad 37, 49, 1188
- Calorimetry (including differential scanning calorimetry, DSC) 1171, 1173
- Capsule bursting method 508-515
- Ceramic systems (see also under specific systems, Materials Index)
 - compilation activities, review 2-5, 12-22, 121-122, 165, 252-256, 257-258, 1327-1331, 1460-1471
 - compilations, review 1-2, 14-22, 256, 407, 1326, 1374
 - needs and applications (see also under Panels II, III, and IV on User Needs, pp 1332-1452) 9-22, 121, 703-708, 1352, 1356-1357, 1361-1366, 1371, 1375-1377, 1378-1381, 1409-1410, 1427, 1442-1450, 1451-1452, 1455-1457, 1471, 1475
 - questionnaire review 5-22

Charge distribution, transfer 607, 615-619, 766
Chatillon-Colinet 141
Chemical analysis 143, 552, 1379
Chemical scan (isothermal) 151
Cluster variation (theory) 967-998, 999-1026, 1474
Coatings of materials 262, 423-439
Coherent phase diagrams 999-1026
Cohesion, cohesion energy 594-603, 616
Compilations (see under Ceramic systems, Semiconductor systems,
Metallic systems, High pressure diagrams)
Compilation methods 22, 163, 658, 720-725, 1475-1478
Composites 1378-1381
Compounds (see also the Materials Index) 100-200, 763-773, 1378-1381
Compound prediction 763-773, 1112, 1139-1150, 1151-1160, 1220-1236, 1473
Computerized data banks (see under Crystallography and under
Thermodynamics)
Concentration simplex 660-662
Concorde, alloys in use 1396
Coordination numbers, 1479-1491
- generalized 767
Crystal chemistry 84-89, 101, 545-547, 620-621, 745-746, 763-772, 1139-1150,
1479-1491
Crystallography
- compilations 82-83, 259-260, 720-725, 1326
- computerized data bank 259-260
- theory and prediction of phases 100-109, 659, 763-773, 1139-1150, 1151-1160
Data banks, computerized
- crystallography 259-260
- thermodynamics and thermochemistry 37, 40, 41, 43, 45, 49,
121-124, 1077-1089, 1186-1199
Data compilations (see under Ceramic systems, Semiconductor systems,
Metallic systems, High pressure diagrams, under the subtopic "compilations")
Density of states (esp Ti) 595
Differential thermal analysis, DTA (see under Thermal analysis)
Diffusion couple analysis 142, 149-151, 465, 522-524, 913
Dilatometry 142, 151, 517
Dip sampling 143
Distribution and publication of phase diagrams 262-264, 703-708,
709-719, 720-725, 1325-1326
Donor solubilities 26-27
Electrical conductivity (experimental phase change det.) 143, 517
Electrochemical probe 148
Electron densities 611
Electron diffraction 148
Electron distribution 607, 615-619, 766
Electron energies 594-609

Electron microprobe 148, 156, 462-471
 - microscope, reflecting, transmission, scanning (SEM, STEM) 146, 148, 440-449, 462, 471-474
 Electronegativity 610-613, 766
 Electronic density of states (esp Ti) 595
 Electronic materials (see under narrower term, Semiconductor systems, or specific topics)
 Ellingham diagrams (see also Metal-gas phase diagrams Solid-vapor diagrams and Pourbaix diagrams) 1077-1088, 1428
 Emf measurements in galvanic cells 517
 Energy storage/conversion 262, 1109-1138, 1426, 1428-1439, 1440-1450, 1458
 Experimental techniques of phase diagram determination (see under specific techniques)

F*A*C*T (Facility for the Analysis of Chemical Thermodynamics) 1077-1089
 Field ion microscope 146
 Format of phase diagrams
 - representation 16-18, 262-264, 265-271, 578-591, 658, 660-702, 1093-1108, 1315-1324, 1458-1460, 1506-1519
 - distribution and publication 262-264, 703-708, 709-719, 720-725, 1325-1326
 - publication standards 1307-1324

Geometric description of superalloys 628-658
 Gibbs energy function, generation of 1027-1046
 Glasses (see also specific glasses in the Materials Index)
 - ceramic 1378-1381
 - metallic 261-268, 1161-1185
 - needs 1378-1381
 Graphical methods 45, 265-271, 628-658, 1077-1089, 1506-1519

Hardy-type power series 141
 High pressure phase diagrams
 - compilation activities, review 100-120
 - compilations, review 101-108
 - needs and applications 261-268, 703-708
 - P-T, P-T-X diagrams 121-122, 153, 578-591
 Hillert 956
 History of data compilations 2, 36, 90, 100
 Hot stage microscopy 1310
 Hot wire microscopy 355-374
 Hume-Rothery 662
 Hyperfine techniques (see also under nuclear magnetic resonance, Mossbauer effect, perturbed angular correlation) 450-461

Industrial needs and applications

- ceramics 1378-1381, 1409-1410, 1427, 1440-1450, 1455
- composites 1378-1381
- glasses 1378-1381
- intermetallics 1378-1381
- ionic systems (see salt systems)
- iron and steelmaking 567-574, 1360-1377, 1378-1381, 1421-1423
- non-ferrous 567-574, 1334-1353, 1354-1359, 1378-1381, 1382-1408, 1418-1419, 1423-1425, 1427
- salt systems 1426, 1428-1439
- superconductors 1411-1417

Interaction parameters 1210-1214

Intermetallics (see also under Compounds, or see under specific systems in the Materials Index)

- needs 1378-1381

Internal pressure 1210-1214

International Atomic Energy Agency (IAEA) 38, 45, 60-61, 78-79

Ion backscattering methods 151, 516-544

- implantation methods 151, 516-544

Ionic systems (see also Salt systems, and also specific systems in the Materials Index) 115-120, 165-225, 251-256, 272-345, 1093-1108

Iron and steelmaking (needs) 1360-1377, 1378-1381, 1421-1423

Irradiation effects 1065-1076

Kaburagi and Kanamori 1012, 1017

Kohler 141, 956

Least squares method of optimizing phase diagrams 955-966

Lever rule, enhanced 454

Magnetic effects 594-603

Margules 848, 872, 874, 876, 903

Matte 1356-1357, 1456

Metal-gas phase diagrams (see also Solid-vapor, Pourbaix-, Ellingham diagrams, etc) 1047-1064, 1077-1088, 1090-1092, 1332-1333

Metallic-nonmetallic component diagrams 1047-1064, 1077-1088, 1090-1092

Metallic radii 763

Metallic systems (see also under specific systems, Materials Index)

- compilation activities, review 37-38, 40-48, 49, 92-94, 122, 164, 226-228, 229-250, 751, 1186-1199, 1327-1331, 1460-1471
- compilations, review 36-38, 50-74, 90-94, 122, 227, 234, 346-350, 351-354, 744-762, 1237-1306, 1326, 1374, 1406
- needs and applications (see also under Panels II, III, and IV on user needs, pp 1332-1452) 121, 261-262, 567, 703-708, 725, 1109, 1180-1182, 1352, 1355-1357, 1361-1366, 1371, 1375-1377, 1378-1381, 1382-1408, 1411-1417, 1427, 1447-1448, 1451-1452, 1455-1457, 1471, 1475
- questionnaire review 261-266

Metallographic analysis 142-143, 156, 517

Metastable phases 261-266, 1161-1185, 1421, 1457
Mossbauer effect 152, 450-461, 615
Microanalysis 913, 1379
Microchemical analysis 148, 440
Micro-furnace 357
Micro-indent hardness 148
Micro x-ray diffraction 148
Microscopy (see under specific type, e.g. optical, electron, etc.)

Natural iteration (theory) 967, 974-978
Needs and Applications (see under Ceramics systems, Semiconductor system, Metallic systems, High pressure, etc., and see under Industrial needs).
Newton-Raphson iteration method 967, 976-977, 1017
Non-ferrous phase diagram industrial needs 1334-1353, 1354-1359, 1378-1381, 1382-1408, 1418-1419, 1423-1425, 1427
Non-stoichiometry prediction 770
Nuclear Magnetic Resonance (NMR) 121, 152, 450-461

Olson 730-731
Optical microscopy (color, reflectivity, other) 148, 411-413
Order-disorder 984-998, 999-1026

P-T, P-T-X, diagrams 28, 121-122, 153, 253, 578-591, 1421, 1456
Pair approximation (theory) 968-973, 1009-1010, 1017
Pair potentials 610, 616, 1424
Pauling 620, 763-773, 1479-1491
Perturbed angular correlation (PAC) 450-461
Phacomp 37, 624-627, 1423
Phase rule 143-144, 162
Physical chemistry and metallurgy, general 84-89
Potential-composition diagrams 1077-1088
Potential-potential diagrams 1077-1088
Potentials (see also under specific potentials) 603-609, 1011-1015
Polar diagrams 662-663, 684
Pourbaix diagrams (see also Metal-gas diagrams, Solid-vapor diagrams, Ellingham diagrams, Stability diagrams, etc.) 1090-1092, 1428
Predictive methods (see under Theories of phase diagrams, Thermodynamics theories, or under specific topics)
Predominance area phase diagrams 1077-1088
Pressure scan 152
Projection methods
- parallel 664-668
- perspective 663-664
Pseudopotentials 603-609, 1014
Publication and distribution 262-264, 703-708, 709-719, 720-725, 1325-1326
Publication standards 1307-1324

Quenching (see also spat-cooling) 1310
- argon jet 383
- rapid quenching methods, summary 1172

Quenched phase plots 1166

Questionnaire, reviews
- ceramic system 5-22
- metallic systems 261-268

Radioactive techniques 148

Raoultian activity coefficient 726-727

Reciprocal systems, representations of 671
- salt systems 1093-1108

Redlich-Kister 803-845, 846-906, 1445

Representations of phase diagrams 16-18, 262-264, 265-271,
578-591, 660-702, 1093-1108, 1315-1324, 1507-1520

Russian literature 44, 46, 50, 51, 92-99, 346-350, 351-354, 1237-1306

Salt systems (see also Ionic systems and see specific systems
in the Materials Index) 1093-1108
- needs 1426, 1428-1439

Scratch hardness 148

Second order phase transitions 620

Sectioning methods for phase diagram representations 668-671

Selective chemical solution 148

Semiconductor systems
- compilations, review 23, 346-350, 351-354
- needs and applications (see also under Panels II, III, and
IV on User Needs, pp 1332-1452) 27-28, 121, 703-708, 1426, 1471, 1475

Semiconductor compounds, predictive methods 1220-1236

Sigma phase 625-658, 916, 1065

Slags (see also under Materials Index for specific systems) 362-366,
908, 1334-1353, 1356, 1361, 1368-1369, 1374, 1440, 1456

Smelting
- copper 1336-1339, 1342-1349, 1354
- lead 1354
- nickel 1339-1340, 1350-1352
- zinc 1354

Solid state physics (see under Alloy physics or under specific topics)

Solid-vapor diagrams (see also Metal-gas phase diagrams Pourbaix-
Ellingham diagrams, etc.) 28, 121-122, 362-374, 1047-1064, 1077-1088,
1090-1092, 1332-1333

Solubilities, donor, acceptor 26-27

Speiss 1357

Splat cooling 383, 1171

Stability diagrams (see also under Pourbaix, Ellingham)
1047-1064, 1077-1088, 1428, 1456

Standards of publication 1307-1324

Stoichiometric description of superalloys 625-627

Strain energy 1210-1214
Strain fields 620
Stress, phase diagrams under external tensile -, or shear stress
575-577
Structural instabilities 769
Sulfur: desulfurization 1372, 1456
Superalloys 37, 262, 423-439, 624-658, 1186
- stoichiometric description 625-627
- geometric description 628-658
- phacomp 37, 624-627, 1423
Superconductivity as technique in phase diagram determination
384-386
Superconductors 262, 375, 387-392, 401, 545-549, 616-618, 770
1148, 1158, 1326, 1411-1417
- needs 1411-1417
Surface phases 262, 268, 1459-1460
Surrounded atom model 141

Temperature scan method 151
Tetrahedron approximation 968, 978-983, 1008
Theories of phase diagrams (see review article pp 592-623, Tuesday's
poster session on the topic pp 726-1236, and see under specific topics)
- listing of treatments of the subject 84-89
Thermal analysis, including differential thermal analysis, (DTA) 121, 142
377-382, 407, 417-419, 517, 1171, 1310
Thermal gravimetric analysis 517
Thermochemistry (see Thermodynamics)
Thermodata 37, 122
Thermodynamics
- compilations 37, 53, 75-81, 196, 228, 229-250
- computerized data banks 37, 49, 121-124, 1077-1089, 1186-1199, 1451
- theory, including computerized methods (see also Tuesday's poster
session on the topic pp 726-1236; and see under specific topics)
37, 121-128, 143-144, 163, 803-845, 846-906, 1077-1089, 1100,
1457-1458, 1472-1475
- listing of treatment of theory 84-89
Toop 141, 730-731, 956
Transient Liquid Phase (TLP) bonding 1418-1419

Variable valency in representation of phase diagrams 671-672
VINITI (see under Russian literature)

Wiederkehr 960

X-ray analysis 143, 156, 407-422, 440-449, 517, 551
- synchrotron light 163

MATERIALS INDEX

This index represents a listing of pages on which quantitative information is given for specific systems: 1) all pages are noted on which phase diagram figures appear; 2) generally, those pages are noted on which data evaluation is discussed; 3) generally, those pages are noted on which related thermodynamic data, or sometimes related crystallographic data appear. A few summarizing data tables occur in these proceedings. No attempt has been made to list these under each individual material. Rather, these are noted under the general material category (e.g. "rare earths", etc.). Alloys have been listed with their components in alphabetical order under the component of lowest alphabetical occurrence. For compounds, the formulas have been alphabetized, but compounds forming components of salt systems are not broken up to further alphabetize, in order to preserve chemical meanings (e.g. $\text{CaF}_2\text{-AlF}_3\text{-Al}_2\text{O}_3$ is listed under $\text{AlF}_3\text{-Al}_2\text{O}_3\text{-CaF}_2$, rather than Al-Ca-F-O).

A-15 compound formation prediction	1148, 1158
$\text{A}_2^{\text{III}}\text{B}^{\text{IV}}\text{O}_7$ compound formation prediction	1149-1150, 1159-1160
Ac-B	762
Ag laves phase prediction	1147, 1157
Ag-B	770
Ag-Cu	780
Ag-Cu-S	774-797
Ag-Cu-Se	774-802
Ag-Cu-Zn (several temps)	237-246
Ag-Pd	1218
Ag-S	779-780
Ag-Si	219
Al	1407
Al-Au-In	455
Al-B	749, 753-757
Al-Be-Fe	544
Al-Ca-O-Si	1370
Al-Co-Cr-Ni	438
Al-Co-Fe-Si	1392, 1405
Al-Cr-Fe-Ni	438
Al-Cr-Fe-Si	1392, 1405
Al-Cr-Mo-Ni-Ti-W	630-635

Al-Cr-Nb	1189-1190, 1199
Al-Cr-Ni	628-630, 655, 658
Al-Cr-Ni-Pt	439
Al-Cr-Ni-Ti	628-630, 654
Al-Cr-Zr	1189-1190, 1194-1189
Al-Cu	608
Al-Cu-Mg-Si	1389-1390, 1402
Al-Fe-Mn	1391, 1403
Al-Fe-Mn-Si	1392, 1405
Al-Fe-Ni-Si	1392, 1405
Al-Fe-Si	1392, 1394, 1404, 1407
Al-Ge-Nb	1415
Al-Li	1115-1118, 1128-1131
Al-Li-Mg	1109-1138, 1134-1138
Al-Mg	1118-1119, 1128-1129, 1132
Al-Mg-Zn	1385-1386, 1399
Al-Mn	134
Al-Ni-Ti	628-630, 657
Al-Sn	1219
Al-Ti-V (Ti-6Al-4V)	567-574
Al-Zn	1393, 1406
AlCa ₂ F ₇ , and related cpds.	283-285
AlCaF ₅ -FNa	318
Al ₂ CaF ₉ Na	320
AlF-CaF ₂	280-285
AlF ₃	278
AlF ₃ -AlF ₆ Li ₃ -AlF ₆ Na	329, 331
AlF ₃ -AlF ₆ Na ₃ -CaF ₂	314, 317-324
AlF ₃ -AlF ₆ Na ₃ -Al ₂ O ₃	322-326
AlF ₃ -AlF ₆ Na ₃ -Al ₂ O ₃ -CaF ₂	333, 335-337

$\text{AlF}_3\text{-AlF}_6\text{Na}_3\text{-Al}_2\text{O}_3\text{-CaF}_2\text{-FLi}$	272-354
$\text{AlF}_3\text{-AlF}_6\text{Na}_3\text{-Al}_2\text{O}_3\text{-CaF}_2\text{-FLi}$	336, 338
$\text{AlF}_3\text{-AlF}_6\text{Na}_3\text{-FLi}$	229, 332
$\text{AlF}_3\text{-Al}_2\text{O}_3\text{-CaF}_2$	328
$\text{AlF}_3\text{-FLi}$	300-305
$\text{AlF}_6\text{Li}_3\text{-AlF}_6\text{Na}_3$	306-311
$\text{Al}_6\text{Li}_3\text{-AlF}_6\text{Na}_3\text{-Al}_2\text{O}_3$	228-330
$\text{AlF}_6\text{Li}_3\text{-Al}_2\text{O}_3$	310, 312
$\text{AlF}_6\text{Li}_3\text{-CaF}_2$	314, 316
$\text{AlF}_6\text{Li}_3\text{-CaF}_2\text{-FLi}$	329, 333-334
AlF_6Na_3	277
$\text{AlF}_6\text{Na}_3\text{-AlF}_3$	289-296
$\text{AlF}_6\text{Na}_3\text{-Al}_2\text{O}_3$	296-299
$\text{AlF}_6\text{Na}_3\text{-Al}_2\text{O}_3\text{-CaF}_2$	325-328
$\text{AlF}_6\text{Na}_3\text{-CaF}_2$	285-290
$\text{AlF}_6\text{Na}_3\text{-FLi}$	305-308
$\text{AlKO}_2\text{-O}_2\text{Si}$	442
Al_2O_3	279
$\text{Al}_2\text{O}_3\text{-AlF}_3$	300
$\text{Al}_2\text{O}_3\text{-CaF}_2$	299-300
$\text{Al}_2\text{O}_3\text{-CaO-MgO-Na}_2\text{O-O}_2\text{Si}$	362-366, 374
$\text{AlO}_{1.5}\text{-KO}_{0.5}$	884
$\text{Al}_2\text{O}_3\text{-WO}_3$	221
Alloy 713 and 713LC	642
Am-B	752-756, 762
As-Ga	1233-1234
As-In	1233-1234
Au laves phase prediction	1147, 1157
Au-B	771
Au-Cu	726-743, 984-985, 988, 997-998, 1007-1011, 1020-1024

Au-Cu-Ni	726-743
Au-Mn	1013, 1025
Au-Ni	726-743
Au-Sb (including metastable diagram)	1173
Au-Si	1219
Au-Si (including metastable data)	1178
Au-Te	271
B-Ba	748, 753-757
B-Be	748, 752-757
B-C-Fe	566
B-Ca	748, 753-757
B-Co	749, 752-756, 761
B-Cr	749, 753-756, 759, 768
B-Fe	749, 753-756, 760
B-Fe (including metastable data)	1177, 1178
B-Hf	749, 753-756, 758
B-Ir	749, 753-756, 761
B-La	749, 753-756, 758
B-Mg	748, 753-757
B-Mn	749, 753-756, 760, 768
B-Mo	749, 753-756, 759
B-Nb	749, 753-756, 759, 768
B-Ni	750, 753-756, 761
B-Np	752-756, 762
B-Os	749, 753-756, 760, 770
B-Pa	762
B-Pd	750, 753-756, 761
B-Pt	750, 752-756, 761
B-Pu	752-756, 762
B-Re	749, 753-756, 760

B-Rh	749, 753-756, 761
B-rich systems	752
B-Ru	749, 753-756, 760, 770-771
B-Sc	749, 753-756, 758
B-Sr	748, 753-757
B-Ta	749, 753-756, 759, 768
B-Tc	749, 753-756, 760
B-Th	752-756, 762
B-Ti	749, 753-756, 758
B-transition metal	751
B-U	752-756, 762
B-V	749, 752-756, 759
B-W	749, 753-756, 759, 771
B-Y	749, 753-756, 758
B-Zr	749, 753-756, 758
B-1900	642, 652-653
B_2O_3 - WO_3	220
BaO- WO_3	206
Be-Cu	539, 543
Be-Cu-Ne	543
Be-Fe	541
Be-Si	1219
Be-Ti (including metastable data)	1177
Be-Ti-Zr	1174
BeO- WO_3	202
Bi-Nb	1219
Bi_2O_3 - WO_3	225
Brasses	1383-1385, 1398

C	857
C-Cr-Fe	1058
C-Cr-Fe-O	1048, 1060
C-Fe	155, 572, 885, 1368
C-Fe (metastable data)	1367
C-Fe-H-O-S	1081
C-Fe-Ni	470, 480, 880
C-Fe-Sb	573
C-H-Ni-O-S	1081
C-Ni (at three pressures)	111
C-Ni	891-901, 904
C-W	770
CO ₃ -HO-Li-Na	1098, 1108
Ca-Cu-Mg (several temps)	247-250
Ca-Fe-O-Si	1368
CaF ₂	279
CaF ₂ -FLi	310, 313-315
Ca-O-Si	1369
CaO-WO ₃	204
CdO-WO ₃	219
Cl-F-K-Li	1095, 1107
Cl-F-Li-Na	1095, 1105-1106
ClK-(HO) ₂ Mg-MgO	511, 514-515
ClLi-(HO) ₂ Mg-MgO	511-512, 515
ClNa-(HO) ₂ Mg-MgO	511, 513, 515
Co-Fe-Ni	479
Co-Gd (including metastable data)	1177
Co-Sm	769
Cr-Fe	916, 935

Cr-Fe-Mg-O	1062
Cr-Fe-Ni	911-954
Cr-Fe-Ni (including irradiation effects)	1066-1069, 1071, 1074-1075
Cr-Fe-O	1059, 1061
Cr-Ni	916, 939
Cr-Ni-Ti	628-630, 656
Cr-O-S	1424
Cr-U (including metastable data)	1177
$\text{Cs}_2\text{O}\cdot\text{WO}_3-\text{WO}_3$	201
Cu-Fe	916, 924, 938, 1027-1046
Cu-Fe-Mn	911-954
Cy-Fe-Ni	911-954
Cu-Fe-O-SiO ₂	1333
Cu-Fe-O-S-Si	1343
Cu-Fe-S	1333, 1343
Cu-Ge-Nb	1417
Cu-Mn	916, 940
Cu-Nb-Sn	1416
Cu-Ni	726-743, 916, 941
Cu-Ni-S	1350
Cu-O-S	1090-1092
Cu-S	779
Cu smelting	1336-1339, 1342-1349, 1354
Cu ternary alloys	229-250
Cu-Zn	1383-1385, 1398
Cu-Zr (including metastable data)	1177, 1178
$\text{Dy}_2\text{O}_3-\text{O}_3\text{Sc}_2$	553-565
$\text{Dy}_2\text{O}_3-\text{WO}_3$	211

F-Li	280
Fe-H-O-Ti	503
Fe-H-Ti	456, 498, 500, 506-507
Fe-Mn	916, 936
Fe-Mn-Ti	490-492, 504-505
Fe-Ni	916, 937, 1082, 1084
Fe-Ni (including irradiation effects)	1065, 1068-1069
Fe-Ni-Mn (including irradiation effects)	1065, 1068, 1072-1073
Fe-Ni-O	1078, 1082-1086
Fe-Ni-O-S	1077-1089
Fe-O	700, 909-910, 1080, 1084
Fe-O-S	1080, 1424
Fe-O-Si	1343
Fe-O-Ti	488-489, 501
Fe-Sb	573
Fe-Ti	486-488, 499
Ga-In-Sb	137, 138, 139
Ga-Nb	387-389, 397, 402-404
Ga-Sb	1233-1234
Ga-Sn-Zn	136
GaO ₃ -WO ₃	222
Ge-Nb	389-392, 405-406
GMR 235	642, 652-653
graphite	857
H-Zr	587, 590-591
HfO ₂ -WO ₃	214
H-Nb-Zr	588-589
H ₂ O-(HO) ₂ Mg-MgO	511, 515
Ho ₂ O ₃ -O ₃ Sc ₂	552-565

In-Sb	1233-1234, 1236
$\text{In}_2\text{O}_3\text{-WO}_3$	223
IN 100	642, 652-653
IN 731 X	642
Inconel 700	642, 652-653
Inconel 713 C	642, 652-653
Inconel X-750	642, 652-653
Ir laves phase prediction	1147, 1157
$\text{KO}_{0.5}\text{-O}_2\text{S}$	902, 906
$\text{K}_2\text{O}\cdot\text{WO}_3\text{-WO}_3$	199
$\text{La}_2\text{O}_3\text{-WO}_3$	208
Li-Mg	1119-1120, 1128, 1133
$\text{Li}_2\text{O}\cdot\text{WO}_3\text{-WO}_3$	197
M 316 stainless (including irradiation effects)	1065
Mar - M 200	642, 652-653
Metal hydrides	610-612
Mg-Pb	1388, 1401
Mg-Si	1386, 1400
Mg-Zn (including metastable data)	1177, 1178
MgO-WO_3	203
Mn-O-S	1424
Mo-P	770
Mo-V	1218
Mo-W	1218

$\text{Na}_2\text{O} \cdot \text{WO}_3 - \text{WO}_3$	198
Nb-Ni (including metastable data)	1177
Nb-Ti	1218
Nb-W	1218
$\text{Nb}_2\text{O}_5 - \text{WO}_3$	215
$\text{Nd}_2\text{O}_3 - \text{WO}_3$	210
Ni-based (superalloys)	624-658
Ni-O-S	1078-1080, 1424
Ni smelting	1340-1341, 1350-1352
Ni-Ti	135, 769
Nicrotung	642, 652-653
Nimonic 115	642, 652-653
O-Si	882
Os laves phase prediction	1147, 1157
Oxide systems	165-225, 251-256, 257-258, 272-345, 355-374, 410-422, 440-449, 508-514, 550-562, 909
PbO-WO_3	224
Pb-Sn (including metastable data)	1175
Pb-Te	1235
Pd laves phase prediction	1147, 1157
Pd-Si (including metastable data)	1177, 1178
Pt laves phase prediction	1147, 1157
Pt-V	549

Rare earths	110, 226-228, 751-752, 763
- tabulation of structure vs pressure	110, 112-120
$Rb_2O \cdot WO_3 - WO_3$	200
René 41	642, 652-653
Re-W (including irradiation effects)	1066, 1068-1069, 1076
Rh laves phase prediction	1147, 1157
Ru laves phase prediction	1147, 1157
$Sm_2O_3 - WO_3$	209
Sn-V	770
$SrO - WO_3$	205
Steels: 43XX steel	571-572
$Ta_2O_5 - WO_3$	216
$TiO_2 - WO_3$	212
Ti-rich, commercial (Ti-6Al-4V)	567-574
Tool steels	572-573
TRW 1900	642, 652-653
Udimet 500	642, 652-653
Udimet 700	642, 652-653
Unitemp AF	642, 652-653
$UO_3 - WO_3$	217
V-W	1218

Waspaloy 642, 652-653

$Y_2O_3 - WO_3$ 207

$ZnO - WO_3$ 218

$ZrO_2 - WO_3$ 213

U.S. DEPT. OF COMM. BIBLIOGRAPHIC DATA SHEET	1. PUBLICATION OR REPORT NO. NBS SP-496	2. Gov't Accession No.	3. Recipient's Accession No.
4. TITLE AND SUBTITLE Applications of Phase Diagrams in Metallurgy and Ceramics—Volume 1 Proceedings of a Workshop Held at the National Bureau of Standards, Gaithersburg, Maryland, January 10-12, 1977		5. Publication Date March 1978	
		6. Performing Organization Code	
7. AUTHOR(S) G. C. Carter, Editor		8. Performing Organ. Report No.	
9. PERFORMING ORGANIZATION NAME AND ADDRESS NATIONAL BUREAU OF STANDARDS DEPARTMENT OF COMMERCE WASHINGTON, D.C. 20234		10. Project/Task/Work Unit No.	
		11. Contract/Grant No.	
12. Sponsoring Organization Name and Complete Address (Street, City, State, ZIP) National Bureau of Standards; National Science Foundation; Defense Advanced Research Projects Agency; Office of Naval Research; National Aeronautics & Space Administration; Energy Research & Development Administration; U.S. Army Research Office		13. Type of Report & Period Covered	
		14. Sponsoring Agency Code	
15. SUPPLEMENTARY NOTES Library of Congress Catalog Card Number: 78-2201			
16. ABSTRACT (A 200-word or less factual summary of most significant information. If document includes a significant bibliography or literature survey, mention it here.) The proceedings of a Workshop on Applications of Phase Diagrams in Metallurgy and Ceramics, held at the National Bureau of Standards, Gaithersburg, Maryland, on January 10-12, 1977, is presented in this NBS Special Publication. The Workshop was co-sponsored by the Institute for Materials Research and the Office of Standard Reference Data, NBS, and the National Science Foundation, the Defense Advanced Research Projects Agency, the Office of Naval Research, the National Aeronautics and Space Administration, the Energy Research and Development Administration, and the U. S. Army Research Office. The purpose of the Workshop was to assess the current national and international status of phase diagram determinations and evaluations for alloys, ceramics and semi-conductors; to determine the needs and priorities, especially technological, for phase diagram determinations and evaluations; and to estimate the resources being used and potentially available for phase diagram evaluation. These proceedings reflect the detailed contents of the Workshop for both the tutorial and review sessions as well as four poster sessions and four panel sessions covering the subjects; critical phase diagram availability, user needs of phase diagrams, experimental methods of determination, theoretical methods of calculation and prediction, methods of phase diagram representations of calculation and prediction, methods of phase diagram representations (especially multicomponent) and distribution to the user. Three of the panels addressed the subject of phase diagram needs in industrial applications. Cont.			
17. KEY WORDS (six to twelve entries; alphabetical order; capitalize only the first letter of the first key word unless a proper name; separated by semicolons) Ceramics; computer predictions; critical evaluations; data compilations; electronic materials; industrial needs; metallurgy; phase diagrams; theory of phase diagrams; thermodynamics.			
18. AVAILABILITY <input checked="" type="checkbox"/> Unlimited <input type="checkbox"/> For Official Distribution. Do Not Release to NTIS <input checked="" type="checkbox"/> Order From Sup. of Doc., U.S. Government Printing Office Washington, D.C. 20402, SD Stock No. 003-003-01895-3 <input type="checkbox"/> Order From National Technical Information Service (NTIS) Springfield, Virginia 22151		19. SECURITY CLASS (THIS REPORT) UNCLASSIFIED	21. NO. OF PAGES 767
		20. SECURITY CLASS (THIS PAGE) UNCLASSIFIED	22.

16. ABSTRACT (A 200-word or less factual summary of most significant information. If document includes a significant bibliography or literature survey, mention it here.)

These proceedings represent documentation of this assessment, and constitute a valuable resource to workers in these areas, especially those planning to initiate phase diagram programs. Most subjects within the overall scope have been dealt with substantially in these proceedings; a few specialized topics such as surface and small particle phases, needed for the study of catalysis, have not been treated in detail. As the Alloy Data Center maintains a continuing phase diagram program, we would like to receive suggestions for similar topics of current and future interest, descriptions of new needs, or addenda and corrigenda to these proceedings. A tear-off sheet has been provided at the end of these proceedings for this purpose to be sent to the NBS Alloy Data Center.

If you wish to send us your suggestions for additional topics of current and future data compilation needs, or if you have any other addenda or corrigenda to these proceedings, please note them on this page and return to the

Alloy Data Center
National Bureau of Standards
Bldg. 223, Room B-150
Washington, DC 20234

Name _____

Affiliation _____

Address _____

City _____ State _____ Zip Code _____

Suggestions:

(cut here)

NBS TECHNICAL PUBLICATIONS

PERIODICALS

JOURNAL OF RESEARCH—The Journal of Research of the National Bureau of Standards reports NBS research and development in those disciplines of the physical and engineering sciences in which the Bureau is active. These include physics, chemistry, engineering, mathematics, and computer sciences. Papers cover a broad range of subjects, with major emphasis on measurement methodology, and the basic technology underlying standardization. Also included from time to time are survey articles on topics closely related to the Bureau's technical and scientific programs. As a special service to subscribers each issue contains complete citations to all recent NBS publications in NBS and non-NBS media. Issued six times a year. Annual subscription: domestic \$17.00; foreign \$21.25. Single copy, \$3.00 domestic; \$3.75 foreign.

Note: The Journal was formerly published in two sections: Section A "Physics and Chemistry" and Section B "Mathematical Sciences."

DIMENSIONS/NBS

This monthly magazine is published to inform scientists, engineers, businessmen, industry, teachers, students, and consumers of the latest advances in science and technology, with primary emphasis on the work at NBS. The magazine highlights and reviews such issues as energy research, fire protection, building technology, metric conversion, pollution abatement, health and safety, and consumer product performance. In addition, it reports the results of Bureau programs in measurement standards and techniques, properties of matter and materials, engineering standards and services, instrumentation, and automatic data processing.

Annual subscription: Domestic, \$12.50; Foreign \$15.65.

NONPERIODICALS

Monographs—Major contributions to the technical literature on various subjects related to the Bureau's scientific and technical activities.

Handbooks—Recommended codes of engineering and industrial practice (including safety codes) developed in cooperation with interested industries, professional organizations, and regulatory bodies.

Special Publications—Include proceedings of conferences sponsored by NBS, NBS annual reports, and other special publications appropriate to this grouping such as wall charts, pocket cards, and bibliographies.

Applied Mathematics Series—Mathematical tables, manuals, and studies of special interest to physicists, engineers, chemists, biologists, mathematicians, computer programmers, and others engaged in scientific and technical work.

National Standard Reference Data Series—Provides quantitative data on the physical and chemical properties of materials, compiled from the world's literature and critically evaluated. Developed under a world-wide program coordinated by NBS. Program under authority of National Standard Data Act (Public Law 90-396).

NOTE: At present the principal publication outlet for these data is the Journal of Physical and Chemical Reference Data (JPCRD) published quarterly for NBS by the American Chemical Society (ACS) and the American Institute of Physics (AIP). Subscriptions, reprints, and supplements available from ACS, 1155 Sixteenth St. N.W., Wash., D.C. 20056.

Building Science Series—Disseminates technical information developed at the Bureau on building materials, components, systems, and whole structures. The series presents research results, test methods, and performance criteria related to the structural and environmental functions and the durability and safety characteristics of building elements and systems.

Technical Notes—Studies or reports which are complete in themselves but restrictive in their treatment of a subject. Analogous to monographs but not so comprehensive in scope or definitive in treatment of the subject area. Often serve as a vehicle for final reports of work performed at NBS under the sponsorship of other government agencies.

Voluntary Product Standards—Developed under procedures published by the Department of Commerce in Part 10, Title 15, of the Code of Federal Regulations. The purpose of the standards is to establish nationally recognized requirements for products, and to provide all concerned interests with a basis for common understanding of the characteristics of the products. NBS administers this program as a supplement to the activities of the private sector standardizing organizations.

Consumer Information Series—Practical information, based on NBS research and experience, covering areas of interest to the consumer. Easily understandable language and illustrations provide useful background knowledge for shopping in today's technological marketplace.

Order above NBS publications from: Superintendent of Documents, Government Printing Office, Washington, D.C. 20402.

Order following NBS publications—NBSIR's and FIPS from the National Technical Information Services, Springfield, Va. 22161.

Federal Information Processing Standards Publications (FIPS PUB)—Publications in this series collectively constitute the Federal Information Processing Standards Register. Register serves as the official source of information in the Federal Government regarding standards issued by NBS pursuant to the Federal Property and Administrative Services Act of 1949 as amended, Public Law 89-306 (79 Stat. 1127), and as implemented by Executive Order 11717 (38 FR 12315, dated May 11, 1973) and Part 6 of Title 15 CFR (Code of Federal Regulations).

NBS Interagency Reports (NBSIR)—A special series of interim or final reports on work performed by NBS for outside sponsors (both government and non-government). In general, initial distribution is handled by the sponsor; public distribution is by the National Technical Information Services (Springfield, Va. 22161) in paper copy or microfiche form.

BIBLIOGRAPHIC SUBSCRIPTION SERVICES

The following current-awareness and literature-survey bibliographies are issued periodically by the Bureau:

Cryogenic Data Center Current Awareness Service. A literature survey issued biweekly. Annual subscription: Domestic, \$25.00; Foreign, \$30.00.

Liquified Natural Gas. A literature survey issued quarterly. Annual subscription: \$20.00.

Superconducting Devices and Materials. A literature survey issued quarterly. Annual subscription: \$30.00. Send subscription orders and remittances for the preceding bibliographic services to National Bureau of Standards, Cryogenic Data Center (275.02) Boulder, Colorado 80302.

U.S. DEPARTMENT OF COMMERCE
National Bureau of Standards
Washington, D.C. 20234

POSTAGE AND FEES PAID
U.S. DEPARTMENT OF COMMERCE
COM-215



OFFICIAL BUSINESS

Penalty for Private Use, \$300

SPECIAL FOURTH-CLASS RATE
BOOK

1298

